

28TH ANNUAL PRECISE TIME AND TIME INTERVAL (PTTI) APPLICATIONS AND PLANNING MEETING



*Proceedings of a meeting held at
The Hyatt Regency Hotel
at Reston Town Center
Reston, Virginia
3 — 5 December 1996*

DISTRIBUTION STATEMENT A
Approved for Public Release
Distribution Unlimited

20040121 102

*The U.S. Naval Observatory
Washington, DC*



NONPRINT FORM

1. Type of Product: Softback book	2. Operating System/Version:	3. New Product or Replacement: New	4. Type of File:
5. Language/Utility Program:			
6. # of Files/# of Products: 1/1	7. Character Set:	8. Disk Capacity:	
	9. Compatibility:	10. Disk Size:	
11. Title: Proceedings of the 28th Annual Precise Time and Time Interval (PTTI) Applications and Planning Meeting			
12. Performing Organization: U.S. Naval Observatory 3450 Massachusetts Ave., NW Washington, DC 20392-5420	13. Performing Report #:	14. Contract #:	
		15. Program Element #:	
16. Sponsor/Monitor: U.S. Naval Observatory 3450 Massachusetts Ave., NW Washington, DC 20392-5420	17. Sponsor/Monitor # Acronym:	19. Project #:	
	18. Sponsor/Monitor #:	20. Task #:	
		21. Work Unit #:	
22. Date: 1997		23. Classification of Product: Unclassified	
24. Security Classification Authority: DOD		25. Declassification/Downgrade Schedule: none	
26. Distribution/Availability: A Approved for public release; distribution is unlimited.			

NONPRINT FORM

27. Abstract: This document is a compilation of technical papers presented at the 28th Annual Precise Time and Time Interval (PTTI) Applications and Planning Meeting held 3-5 December 1996 at the Hyatt Regency Hotel at Reston, Virginia. Papers are in the following categories:

- Recent developments in rubidium, cesium, and hydrogen-based atomic frequency standards, and in trapped-ion and space clock technology;
- National and international applications of PTTI technology with emphasis on GPS and GLONASS timing, atomic time scales, and telecommunications;
- Applications of PTTI technology to evolving military navigation and communication systems; power systems; pulsars; and relativity;
- Dissemination of precise time and frequency by means of GPS, geosynchronous communication satellites, and computer networks.

28. Classification of Abstract:

Unclassified

29. Limitation of Abstract:

Unclassified Unlimited

30. Subject Terms: time, atomic time, time scales, precise time, frequency standards, precision oscillators, cesium, rubidium, hydrogen masers, trapped ion, time transfer, frequency transfer, synchronization, GPS, navigation, telecommunications, communication satellites, computer networks, power systems, pulsars, relativity

30a. Classification of Subject Terms:

Unclassified

31. Required Peripherals:**32. # of Physical Records:****33. # of Logical Records:****34. # of Tracks:****35. Record Type:****36. Color:**

No

37. Recording System:**38. Recording Density:****39. Parity:****40. Playtime:****41. Playback Speed:****42. Video:**

No

43. Text:

Yes

44. Still**Photos:**

No

45. Audio:

No

46. Other:**47. Documentation/Supplemental Information:**

Bound hardcopies are available from POC. Hardcopies may also be ordered via <http://tycho.usno.navy.mil/ptti/orderform.html>. Table of contents available at <http://tycho.usno.navy.mil/ptti/index.html>.

48. Point of Contact and Telephone Number: Lee A. Breakiron

Time Service Department, U.S. Naval Observatory, 3450 Massachusetts Ave., NW, Washington, DC 20392-5420

(202) 762-1092

breakiron.lee@usno.navy.mil

28TH ANNUAL PRECISE TIME AND TIME INTERVAL (PTTI) APPLICATIONS AND PLANNING MEETING

Editorial Committee Chairman
Lee A. Breakiron
U.S. Naval Observatory

Proceedings of a meeting sponsored by
the U.S. Naval Observatory
the NASA Goddard Space Flight Center
the NASA Jet Propulsion Laboratory
the Space and Naval Warfare Systems Command
the U.S. Naval Research Laboratory
the U.S. Air Force Space Command
and the Air Force Office of Scientific Research

and held at
The Hyatt Regency Hotel
at Reston Town Center
Reston, Virginia
3 — 5 December 1996



United States Naval Observatory
Washington, DC 20392-5420

1997

ORDER FORM FOR PROCEEDINGS

You can order back issues of the Proceedings from either PTTI or NTIS

Year	PTTI Price	NTIS Number	NTIS Price subject to change without notice
1 - 1969*		unavailable	
2 - 1970**	\$ 25.00	AD-881014 (incl. Vols. 1 and 2)	\$ 44.00
3 - 1971**	\$ 25.00	AD-758739	\$ 71.50
4 - 1972**	\$ 25.00	AD-A010785/4	\$ 61.50
5 - 1973**	\$ 25.00	AD-A010786/2	\$ 84.00
6 - 1974	\$ 25.00	AD-A018192/5	\$ 84.00
7 - 1975	\$ 25.00	AD-A040774/2	\$ 115.00
8 - 1976**	\$ 25.00	AD-A043856/4	\$ 115.00
9 - 1977**	\$ 25.00	AD-A123920/1	\$ 84.00
10 - 1978	\$ 25.00	N79-24731/8	\$ 125.00
11 - 1979	\$ 25.00	N80-29096/8	\$ 115.00
12 - 1980	\$ 25.00	N81-27467/2	\$ 125.00
13 - 1981	\$ 25.00	N82-20494/2	\$ 125.00
14 - 1982**	\$ 25.00	N83-35351/6	\$ 106.00
15 - 1983**	\$ 25.00	AD-A149163/8	\$ 115.00
16 - 1984	\$ 25.00	N85-29221/7	\$ 71.50
17 - 1985	\$ 25.00	unavailable	
18 - 1986	\$ 25.00	unavailable	
19 - 1987**	\$ 25.00	unavailable	
20 - 1988	\$ 35.00	AD-A217145/2	\$ 61.50
21 - 1989	\$ 65.00	unavailable	
22 - 1990	\$ 70.00	N91-25755/0	\$ 106.00
23 - 1991	\$ 85.00	AD-A255837/7	\$ 57.00
23 - Tutorial	included	AD-A254745/3	\$ 39.00
24 - 1992	\$ 85.00	AD-A267301/0	\$ 57.00
25 - 1993	\$ 85.00	N94-30639/6	\$ 67.00
26 - 1994***	\$ 95.00	N95-32319/2	\$ 57.00
27 - 1995	\$ 115.00	unavailable	
28 - 1996	\$ 115.00	unavailable	
28 - Tutorial	\$ 35.00	unavailable	

*The Proceedings of the 1st PTTI meeting consists of an 8-page report.

**Original Proceedings no longer available for sale; however, copies made from the original can be purchased from PTTI.

***Includes an Errata volume

When ordering from PTTI, return order form with payment to:
PTTI Executive Committee
U.S. Naval Observatory
3450 Massachusetts Avenue, NW
Washington, DC 20392-5420
Tel: 202-762-1414, Fax: 202-762-1511

When ordering from NTIS, contact:
U.S. Department of Commerce
Technology Administration
National Technical Information Service
Springfield, VA 22161
Tel: 703-487-4630

Make checks payable to "Treasurer, PTTI." Do not send cash. We cannot accept credit card orders. When you register for the PTTI meeting or order the Proceedings, your name is added to the PTTI mailing list to receive future meeting information.

EXECUTIVE COMMITTEE

MRS. SHEILA FAULKNER, CHAIRMAN
U.S. Naval Observatory

COMMANDER MARK M. ATKISSON, USN
U.S. Naval Observatory

MR. RONALD L. BEARD
U.S. Naval Research Laboratory

DR. LEE A. BREAKIRON
U.S. Naval Observatory

LIEUTENANT COLONEL MICHAEL CIMAFONTE, USAF
U.S. Air Force Space Command

MR. RAYMOND L. GRANATA
NASA Goddard Space Flight Center

DR. HELMUT HELLWIG
Air Force Office of Scientific Research

DR. WILLIAM J. KLEPCZYNSKI
U.S. Naval Observatory

MR. PAUL F. KUHNLE
Jet Propulsion Laboratory

MR. JOHN R. RUSH
NASA Headquarters

COMMANDER TIMOTHY F. SHERIDAN, USN
Space and Naval Warfare Systems Command

DR. RICHARD L. SYDNOR
Jet Propulsion Laboratory

MS. FRANCINE M. VANNICOLA
U.S. Naval Observatory

DR. JOHN R. VIG
U.S. Army Research Laboratory

DR. JOSEPH D. WHITE
U.S. Naval Research Laboratory

MS. NICOLETTE M. JARDINE
Administrative Assistant
U.S. Naval Observatory

OFFICERS

GENERAL CHAIRMAN
DR. SAMUEL R. STEIN
Timing Solutions Corporation

TECHNICAL PROGRAM COMMITTEE CHAIRMAN
MS. FRANCINE M. VANNICOLA
U.S. Naval Observatory

TECHNICAL PROGRAM COMMITTEE
DR. HENRY F. FLIEGEL
The Aerospace Corporation

MR. PAUL F. KUHNLE
Jet Propulsion Laboratory

DR. SAMUEL R. STEIN
Timing Solutions Corporation

DR. RICHARD L. SYDNOR
Jet Propulsion Laboratory

MR. S. CLARK WARDRIP
AlliedSignal Technical Services Corporation

EDITORIAL COMMITTEE CHAIRMAN
DR. LEE A. BREAKIRON
U.S. Naval Observatory

CONSULTANT TO THE EDITORIAL COMMITTEE
DR. RICHARD L. SYDNOR
Jet Propulsion Laboratory

EXHIBITS AND PUBLICITY COMMITTEE CHAIRMAN
MR. DONALD H. MITCHELL
TrueTime, Inc.

TECHNICAL ASSISTANCE
MR. JEFFREY S. INGOLD
MR. S. CLARK WARDRIP
AlliedSignal Technical Services Corporation

PTTI AWARD COMMITTEE

DR. LEONARD S. CUTLER, CHAIRMAN
Hewlett-Packard Company

DR. HENRY F. FLIEGEL
The Aerospace Corporation

DR. RICHARD L. SYDNOR
Jet Propulsion Laboratory

PAST RECIPIENTS OF THE DISTINGUISHED PTTI SERVICE AWARD

1994

DR. GERNOT M. R. WINKLER
U.S. Naval Observatory
(Retired)

1995

DR. JAMES A. BARNES
National Institute of
Standards and Technology
(Retired)

SESSION CHAIRMEN

SESSION I

DR. SIGFRIDO LESCHIUTTA
Politecnico di Torino
Istituto Elettrotecnico Nazionale
G. Ferraris

SESSION V

MR. R. MICHAEL GARVEY
Frequency and Time Systems, Inc.

SESSION II

DR. JOSEPH D. WHITE
U.S. Naval Research Laboratory

SESSION VI

MR. MARTIN B. BLOCH
Frequency Electronics, Inc.

SESSION III

DR. SAMUEL R. STEIN
Timing Solutions Corporation

SESSION VII

DR. ANDREAS BAUCH
Physikalisch-Technische Bundesanstalt

POSTER SESSION

MR. JEFFREY S. INGOLD
AlliedSignal Technical Services
Corporation

SESSION VIII

DR. GERRIT DE JONG
NMI Van Swinden Laboratorium

SESSION IV

COMMANDER MARK M. ATKISSON, USN
U.S. Naval Observatory

SESSION IX

DR. MARC A. WEISS
National Institute of
Standards and Technology

SESSION X

MS. ANGELA D. MCKINLEY
U.S. Naval Observatory

ARRANGEMENTS

**MRS. SHEILA FAULKNER
MR. PAUL F. KUHNLE
DR. RICHARD L. SYDNOR**

FINANCE COMMITTEE

**DR. WILLIAM J. KLEPCZYNSKI
MRS. SHEILA FAULKNER**

THE RECEPTIONISTS AT THE 28TH ANNUAL PTTI MEETING WERE:

**MS. BRENDA HICKS
MS. NICOLETTE JARDINE
MRS. ALINE KUHNLE
MRS. KAY TALLEY
MRS. BETTY WARDRIP**

ADVISORY BOARD MEMBERS

MR. S. CLARK WARDRIP, CHAIRMAN
AlliedSignal Technical Services Corporation

Mr. David W. Allan
Allan's TIME

Professor Carroll O. Alley
University of Maryland

Dr. James A. Barnes
Consultant

Mr. Martin B. Bloch
Frequency Electronics, Inc.

Mrs. Mary Chiu
The Johns Hopkins University
Applied Physics Laboratory

Dr. Leonard S. Cutler
Hewlett-Packard Company

Dr. Henry F. Fliegel
The Aerospace Corporation

Mr. Jeffrey S. Ingold
AlliedSignal Technical Services
Corporation

Mr. Robert H. Kern
KERNCO, Inc.

Mr. Pete R. Lopez
TRAK Microwave

Mr. Jack McNabb
TRAK Microwave

Mr. Donald H. Mitchell
TrueTime, Inc.

Mr. Jerry R. Norton
The Johns Hopkins University
Applied Physics Laboratory

Mr. Allen W. Osborne, III
Allen Osborne Associates

Mr. Terry N. Osterdock
Absolute Time

Dr. Bradford W. Parkinson
Stanford University

Mr. Harry E. Peters
Sigma Tau Standards Corporation

Dr. Victor S. Reinhardt
Hughes Aircraft

Mr. William J. Riley
EG&G, Inc.

Dr. Henry Robinson
Duke University

Mr. Ronald C. Roloff
FTS/Austron
(Datum Companies)

Dr. Samuel R. Stein
Timing Solutions Corporation

Mr. Michael R. Tope
TrueTime, Inc.

Mr. James L. Wright
Computer Sciences Raytheon

TABLE OF CONTENTS

PTTI OPENING ADDRESS	1
-----------------------------------	----------

**Admiral Paul Tobin
Oceanographer of the Navy**

PTTI DISTINGUISHED SERVICE AWARD	7
-----------------------------------------------	----------

**Presented by
Dr. Leonard S. Cutler
Hewlett-Packard Company
to
Dr. Sigfrido Leschlutta
Politecnico di Torino and
Istituto Elettrotecnico Nazionale G. Ferraris**

KEYNOTE ADDRESS	11
------------------------------	-----------

**Impact of Atomic Clocks on Navigation, Communication, and Science
Dr. Giovanni Busca
Observatoire de Neuchâtel**

SESSION I

INTERNATIONAL TIMEKEEPING ACTIVITIES

**Dr. Sigfrido Leschiutta, Chairman
Politecnico di Torino and
Istituto Elettrotecnico Nazionale G. Ferraris**

Impact of International Decisions on TAI Generation	25
C. Thomas, Bureau International des Poids et Mesures	

IEN Time and Frequency Metrological Activity and Support to User Needs	37
F. Cordara, V. Pettiti, and P. Tavella, Istituto Elettrotecnico Nazionale Galileo Ferraris	

Time and Frequency Keeping and Its Distribution System at CRL	51
M. Imae, M. Hosokawa, Y. Hanado, K. Imamura, A. Otsuka, and T. Morikawa, Communications Research Laboratory	
Frequency Standards, Timekeeping, and Traceable Services at the National Research Council of Canada	65
R. J. Douglas, J.-S. Boulanger, S. Cundy, M.-C. Gagné, W. Cazemier, B. Hoger, R. Pelletier, J. Bernard, A. A. Madej, L. Marmet, K. Siemsen, and B. G. Whitford, Institute for National Measurement Standards	
Time and Frequency Activities at NIST	75
J. Levine and D. B. Sullivan, National Institute of Standards and Technology	
European PTI Report	83
F. Cordara, Istituto Elettrotecnico Nazionale G. Ferraris; A. De Marchi and M. Serafino, Politecnico di Torino; and S. Leschiutta, Istituto Elettrotecnico Nazionale G. Ferraris and Politecnico di Torino	

SESSION II

NEW PRODUCTS FOR THE TIMING COMMUNITY

Dr. Joseph D. White, Chairman
U.S. Naval Research Laboratory

**Presentations were made by representatives of Absolute Time Corporation; Allen
Osborne Associates, Inc.; Datum, Inc.; Sigma Tau Standards Corporation;
Telecom Solutions; 3S Navigation; TRAK Systems; and TrueTime, Inc.**

SESSION III

TELECOMMUNICATIONS APPLICATIONS

Dr. Samuel R. Stein, Chairman
Timing Solutions Corporation

The Network Computer as Precision Timekeeper	97
D. L. Mills, University of Delaware	
On the Shipboard Application of Network Time Protocol (NTP, RFC 1305) ..	109
M. E. Bautista, Lockheed Martin Advanced Technology Labs	

- The Range Covered by a Random Process and the New Definition of MTIE . 119**
P. Tavella, A. Godone, Istituto Elettrotecnico Nazionale G. Ferraris; and S.
Leschiutta, Istituto Elettrotecnico Nazionale G. Ferraris and Politecnico di Torino

POSTER SESSION

Mr. Jeffrey S. Ingold, Chairman
Allied Signal Technical Services Corporation
(papers have been reassigned to Sessions VI, VII, IX, and XI)

SESSION IV

MILITARY APPLICATIONS

Commander Mark M. Atkisson, USN, Chairman
U.S. Naval Observatory

- Military Applications of Time and Frequency 125**
R. L. Beard and J. D. White, U.S. Naval Observatory; and J. A. Murray, SFA, Inc.
- The Alternate Master Clock and Precise Time Requirements; Why An Alternate Master Clock? 141**
W. V. Bollwerk, U.S. Naval Observatory Alternate Master Clock

SESSION V

OPERATIONAL PTTI

Mr. R. Michael Garvey, Chairman
Frequency and Time Systems, Inc.

- Experience at the CENAM with Time and Frequency Standards Signals Received by the Global Positioning System (GPS) 151**
V. Molina-López, Centro Nacional de Metrología and Centro de Investigación y Estudios Avanzados del Instituto Politécnico Nacional; H. Jardón-Aguilar, Centro de Investigación y Estudios Avanzados del Instituto Politécnico Nacional; and J. T. Vega-Durán and J. M. López-Romero, Centro Nacional de Metrología
- Stabilization of a Fiber-Optic Link Using a Temperature-Controlled Fiber Segment 163**
R. L. Sydnor, M. Calhoun, J. Lopez, and W. Diener, Jet Propulsion Laboratory

Demonstration of Synchronization Between Two Geosynchronous Satellites Without Ground Intervention	169
J. C. Camparo, R. P. Frueholz, and A. P. Dubin, The Aerospace Corporation	
PTTI: Utilizations and Experimentations at Hydro-Québec	179
G. Missout, Hydro-Québec Research Institute	

SESSION VI

THEORETICAL ASPECTS OF TIMING

Mr. Martin B. Bloch, Chairman
Frequency Electronics, Inc.

GPS and Relativity: An Engineering Overview	189
H. F. Fliegel and R. S. DiEsposti, The Aerospace Corporation	
Operational Use of the Hadamard Variance in GPS	201
S. T. Hutsell, U.S. Naval Observatory Alternate Master Clock; W. G. Reid, U.S. Naval Research Laboratory; 1Lt J. D. Crum, USAF, and 1Lt H. S. Mobbs, USAF, 2d Space Operations Squadron; and J. A. Buisson, Antoine Enterprises, Inc.	
A Simple Algorithm for Approximating Confidence on the Modified Allan Variance and the Time Variance	215
M. A. Weiss, National Institute of Standards and Technology, and C. A. Greenhall, Jet Propulsion Laboratory	
Pulsar-Appropriate Clock Statistics	225
D. N. Matsakis and F. J. Josties, U.S. Naval Observatory	

SESSION VII

ATOMIC FREQUENCY STANDARD PERFORMANCE

Dr. Andreas Bauch, Chairman
Physikalisch-Technische Bundesanstalt

PTB's Primary Clock CS1: First Results After Its Construction	237
A. Bauch, H. Brand, T. Heindorff, B. Fischer, and R. Schröder, Physikalisch-Technische Bundesanstalt	
The JPL Hg+ Extended Linear Ion Trap Frequency Standard: Status, Stability, and Accuracy Prospects	245
R. L. Tjoelker, J. D. Prestage, and L. Maleki, Jet Propulsion Laboratory	

NIST-7, The U.S. Primary Frequency Standard: New Evaluation Techniques	255
R. E. Drullinger, J. H. Shirley, and W. D. Lee, National Institute of Standards and Technology	
A Derivation of the DICK Effect from Control-Loop Models for Periodically Interrogated Passive Frequency Standards	265
C. A. Greenhall, Jet Propulsion Laboratory	
Temperature Control for Hydrogen Maser Frequency Standards	273
Y. Fu, Z. Xhou, and X. Liu, Beijing Institute of Radio Metrology and Measurement	
First Commercial Prototype of an Optically Pumped Cesium-Beam Frequency Standard	281
M. L. Baldy, Tekelec Telecom	
Ultrasensitive High Resolution Laser Spectroscopy and Its Application to Optical Frequency Standards	289
J. Ye, L.-S. Ma, and J. L. Hall, JILA, University of Colorado and National Institute of Standards and Technology	

SESSION VIII

CONFERENCE/WORKING GROUP UPDATES

Report from the ITU-R Working Party 7A on Time Signals and Frequency Standard Emissions	305
G. de Jong, NMi Van Swinden Laboratories	
The Selection and Use of Precise Frequency and Time Systems	313
R. L. Sydnor, Jet Propulsion Laboratory	
The IEEE Frequency Control Symposium	323
J. R. Vig, U.S. Army Research Laboratory	
The CCDS Working Groups	327
C. Thomas, Bureau International des Poids et Mesures	
Conference and Working Group Updates: The European Frequency and Time Forum	331
S. Leschiutta, Politecnico di Torino and Istituto Elettrotecnico Nazionale G. Ferraris, and M. Serafino, Politecnico di Torino	
Status Report on Radionavigation Systems and the Institute of Navigation ..	335
L. G. Charron, U.S. Naval Observatory	

SESSION IX

TIME TRANSFER TECHNIQUES

Dr. Marc A Weiss, Chairman
National Institute of Standards and Technology

Precision Time and Frequency Transfer Utilizing SOMET OC-3 339
M. Calhoun, P. Kuhnle, and R. Sydnor, Jet Propulsion Laboratory; S. Stein, Timing Solutions Corporation; and G. A. Gifford, U.S. Naval Observatory

A Comparison of the Highest Precision Commonly Available Time Transfer Methods: TWSTT and GPS CV 349
J. DeYoung, F. Vannicola, and A. D. McKinley, U.S. Naval Observatory

First Results from GLONASS Common-View Time Comparisons Realized According to the BIPM International Schedule 357
W. Lewandowski and J. Azoubib, Bureau International des Poids et Mesures; A. G. Gevorkyan and P. P. Bogdanov, Russian Institute of Radionavigation and Time; J. Danaher, 3S Navigation; G. de Jong, NMi Van Swinden Laboratorium; and J. Hahn, Deutsche Forschungsanstalt fuer Luft und Raumfahrt

A Contribution to the Standardization of GPS and GLONASS Time Transfers 367
W. Lewandowski and J. Azoubib, Bureau International de Poids et Mesures; A. G. Gevorkyan and P. P. Bogdanov, Russian institute of Radionavigation and Time; W. J. Klepczynski, ISI Corporation; M. Miranian, U.S. Naval Observatory; J. Danaher, 3S Navigation; N. B. Koshelyaevsky, Russian National Time and Frequency Service; and D. W. Allan, Allan's TIME

Testing Motorola Oncore GPS Receiver and Temperature-Stabilized Antennas for Time Metrology 387
W. Lewandowski and P. Moussay, Bureau International de Poids et Mesures; P. Guerin, F. Meyer, and M. Vincent, Observatoire de Besançon

SESSION X

TIMING SYSTEMS PERFORMANCE

Mrs. Angela D. McKinley, Chairman
U.S. Naval Observatory

Continuous Observation of NAVSTAR Clock Offset from the DoD Master Clock Using Linked Common-View Time Transfer 397
W. G. Reid, U.S. Naval Research Laboratory

1996 GPS Time Transfer Performance	409
1Lt J. D. Crum, USAF, 2d Space Operations Squadron	
Performance Analysis of the GPS Monitor Station Timing Subsystem Enhancement Program at the Naval Research Laboratory	417
I. J. Galysh, D. M. Craig, and W. G. Reid, U.S. Naval Research Laboratory	
The End of an Era: SVN 10 End-of-Life Frequency Standard Testing	429
1Lt Gary L. Dieter, 2d Space Operations Squadron, and M. J. Van Melle, Rockwell Space Operations Company	
Performance Evaluation of the GPS Block IIR Time Keeping System	441
A. Wu, The Aerospace Corporation	
GLONASS Onboard Time/Frequency Standards: Ten Years of Operation ...	455
A. B. Bassevich, P. P. Bogdanov, A. G. Gevorkyan, and A. E. Tyulyakov, Russian Institute of Radionavigation and Time	

SESSION XI

CLOCKS IN SPACE (originally part of the Poster Session)

Design of a Hydrogen Maser for Space	463
E. M. Mattison and R. F. C. Vessot, Smithsonian Astrophysical Observatory	
Spacecraft-Spacecraft Doppler Tracking as a Xylophone Interferometer Detector of Gravitational Radiation	471
M. Tinto, Jet Propulsion Laboratory	
PHARAO: A Space Clock with Cold Cesium Atoms	477
Ph. Laurent, E. Simon, G. Santarelli, and A. Clairon, BNM-Laboratoire Primaire du Temps et des Fréquences; Ch. Salmon and P. Lemonde, Laboratoire Kastler Brossel; N. Dimarcq and C. Audoin, Laboratoire de l'Horloge Atomique; and F. Gonzalez and F. J. Changeart, Centre National d'Études Spatiales	
List of Attendees	487

PTTI OPENING ADDRESS

**Admiral Paul Tobin
Oceanographer of the Navy
Washington, DC 20392, USA**

CAPTAIN KENT FOSTER (USNO): Good morning, ladies and gentlemen. Again, welcome to the 28th Annual PTTI Meeting. This is only my second time at one of these meetings, but I'm sure that there are at least a few of you out there today that have been present at all or most of the prior 27 sessions. I must say that your commitment, your dedication, and your expertise are most commendable.

Before going any further into this meeting, I would like to identify, and then let us all acknowledge, the hard work of some folks who have arranged these facilities and services that we will be enjoying here for the next few days, and for the overall organization of the entire sessions. First of all, from NASA JPL, Dr. Richard Sydnor and Mr. Paul Kuhnle; from AlliedSignal, Mr. Clark Wardrip and Mr. Jeff Ingold. I'm told that are a couple uncompensated folks of a purely volunteer spirit who have spent much time this year, as in the previous years, working the registration desk. They are Betty Wardrip and Aline Kuhnle, who I assume are in some capacity associated with Clark and with Paul.

From the Hyatt Regency side of the team, the very accommodating efforts of Helene Williams and Jean Messick are very much appreciated. And from the Naval Observatory, Ms. Francine Vannicola, the Technical Program Chairperson for the PTTI Executive Committee; Dr. Lee Breakiron; and of course our all-around brochure and graphics mechanic, Nikki Jardine, have been very busy planning for the success of this meeting. Lastly, even though she said she has retired "not just from the Observatory," she is still doing her thing as the overall ramrod of style, class, and smoothness that characterize these annual PTTI sessions – at least the last 14, I'm told – Mrs. Sheila Faulkner. If you would please join me in expressing some appreciation for the hard work of all these folks.

[Applause]

As a sponsor for the PTTI meeting, I feel somewhat at liberty at making minor adjustments to the program as it's printed here in your brochure. And I am going to deviate from that tradition this morning by not presenting the PTTI opening address. Thank you, I was afraid that would draw a standing ovation from the crowd. I am even more pleased, however, that Admiral Paul Tobin, the Oceanographer of the Navy, has accepted my invitation to present the opening address. Besides being my boss, Admiral Tobin is the Resource Sponsor for the Naval Observatory's operation mission as well as for all operational meteorology, oceanography, and mapping, charting, and geodesy programs carried out by the Navy.

As a resource sponsor, he and his staff provide the Observatory with the mother's milk of sustained operations: money and people. However, Admiral Tobin's most prestigious credentials for speaking to us today are not his present duties or the fact that he happens to be my boss.

They are, rather, his career experience and success as a surface warfare officer. As such, he has been in many situations in which reliable precise time capabilities were critical to his operational responsibilities involving navigation, communications, and putting weapons on target. He has commanded two surface combatants, a guided missile destroyer, and a guided missile cruiser, as well as a battle group staff in the Western Pacific.

While not at sea, Admiral Tobin has held many key staff leadership positions ashore, including Director of Naval Communications and Information Systems and Director of Navy Information Resources Management. He holds a Master of Science Degree from the Naval Post Graduate School in Computer Systems Management, and he is a distinguished graduate of the Industrial College of the Armed Forces where, quite a few years ago, I had the pleasure to first meet the Admiral as a classmate.

Ladies and gentlemen, if you would please welcome Admiral Paul Tobin.

[Applause]

ADMIRAL PAUL TOBIN: Good morning. I'm delighted that my schedule allowed me to spend a little time with you today to tell you how much I support your work, and how important I think it is, and how important it is to the United States Navy. I'm delighted to see this large turnout. I didn't realize that the PTTI conference really had this large a turnout from industry, other government agencies, and, of course, from the Navy as well. So I'm delighted to be here today and I'd like to give you a little view into how I feel about what you're doing and the future of your work certainly in relation to the Navy.

About a year ago, I didn't know what PTTI meant. I was vaguely aware that the Navy had some association with the Master Clock up at the Observatory, and that was about it. A few things have happened since then that have heightened my awareness. First of all, when I left my last job at the Chief of Naval Education and Training down in Pensacola, Florida, the staff gave me a wonderful going away gift; it was a Garmon GPS hand-held navigation instrument.

I'm a boater, and I've been boating for years – that's what most surface warfare officers do when they take their ships away from them, we buy a boat and continue to go to sea in one form or another. But I got this little device and I walked around my back yard trying to get it to work, and it was seeking out stations; and after about 8 or 9 minutes, it shut itself off; that was a feature to save the batteries – it actually consumes quite a bit of battery power. And I was very frustrated because I couldn't get it to work.

So finally I went back, as a last resort, and read the manual. And it indicated that you had to tell this device roughly where you were and you could fire it up and see where it thought roughly where you were. I did that, and at the initial starting point it thought I was somewhere in the Indian Ocean; and I was in Pensacola, Florida. So I was giving it a hard challenge. So I roughly put in the latitude and longitude of Pensacola and then about 3 minutes later it acquired all the stations and I began to see the magic of GPS.

That kind of made me ask: How does this thing work? Well, I found out that the key to GPS, as you all know, is very precise time; the more precise, the more accurate it is. But, I've become a great GPS believer. Having had commands before the advent of GPS, where I've been stuck around the Equator with bad weather, not being able to get sun lines, no Omega, no Loran, literally D-R-ing with a \$500 million warship out in the ocean trying to find a little island called "Diego Garcia," I now appreciate the significance of having these instrument that really make navigation a much simpler job – and also make it a lot safer. We're working now with digital nautical charts where we can actually have a small representation of a ship on a digital nautical chart, and rather than wait 3 minutes for the navigator to take his lines of

variance, make the fix and report it to the commanding officer, the commanding officer or the counting officer can see the position of the ship in a matter of 2 or 3 seconds, every 2 or 3 seconds. And it's going to certainly simplify the navigation process and help us avoid some of the accidents that unfortunately we still have.

The second thing that heightened my awareness is that I received a new job. Quite unexpectedly, I was called and asked if I would like to be the Oceanographer of the Navy. I immediately said yes because I knew it was something that I would want to do and I knew that it would give me an opportunity to learn a great deal. During the last 9 months, I have learned a great deal, thanks to Ken Johnston and Kent and all his folks; I've learned a great deal about astronomy, or astrometry, as it's correctly called; and I've also learned a great deal about oceanography and meteorology and know how come complex a subject it is; and I've also learned what an important part precise time plays in all of these domains.

Navigation, we have talked a little bit about that. Extremely important for navigation to know where you are in your own ship, to also know where you are from the standpoint of the initial launch point of a weapon system. Also, we are now incorporating GPS systems into long-range gun projectiles, and that's really saying something when you think about the electronics in a gun system has to withstand initial setback of around 2 to 3 thousand g's when it's fired; so not only does it have to be small and light, it has to be resilient to these tremendous physical forces. But the chips are now available, the capability to do that. And we're also incorporating GPS in our long-range cruise missile programs.

Precise time is also an important part of our crypto-systems, synchronizing systems – it's fundamental to that. It's also fundamental to most of our communications systems where time multiplexing is a very important part of what we do; and without precise time, it just wouldn't happen.

I'm not going to talk too much about technology this morning because there are really too many experts here in the audience for me to even risk getting into that area. But it does remind me of a story of an individual who was involved in the great Johnstown flood in Pennsylvania, a very serious event in our history. Unfortunately, he was overcome by the flood, but not before he had performed a number of heroic feats and gone through many experiences.

So when he got to Heaven, he spent a lot of time going around telling everybody about his experiences with the Johnstown flood. And I can kind of relate to that because I was in the Philippines during the eruption of Mount Pinatubo; and we were about 5 miles too close; and I learned a lot about volcanoes and I learned a lot about the frailty of human life. And my wife told me I talk too much about it and in every opportunity when people asked me about it, I would go into a long discussion. So finally she said, "How about knocking off the Mount Pinatubo stories?"

Well, this fellow up in Heaven was getting on everybody's nerves with these stories about the Johnstown flood, and he just wouldn't stop. But he went to St. Peter, and he wasn't getting a large enough audience; and he said, "I'd like to talk to the town council and make a presentation on the Johnstown flood." St. Peter said, "Really don't think we're ready for that, and we don't want you to do that." He said, "No, I really would like to do that." And St. Peter said, "Well, I think I have to warn you that Noah's going to be there."

Well, I feel like there are a lot of Noahs here in the audience, so I'm not going to get very technical this morning. But I do want to talk to you about a revolution in oceanography. Believe it or not, knowing where we are has really opened the door to a whole new world in oceanography. There are lots of twin peaks that are out there that are charted that are now

suddenly being realized are not twin peaks at all, there was only one peak. And we found out that we really didn't know exactly where we were, and in terms of all of our hydrographic surveys, all the work we had done over the past 200 years, there is an awful lot of catching up to do, an awful lot of refinement. And now we truly have a capability to know exactly where we are; and we have the tools to do precise surveys of the ocean bottom, and it's opened up a whole new world.

I've been amazed at how inaccessible oceanography is. There is just an explosion of interest in meteorology – and astronomy, for that matter, tremendous interest. If you go to the Nature Company or any of the big book stores, you'll see books and books on that, not to mention personal computers where half the stores are tied up with that. But when it comes to oceanography, there is very little. And usually it's because it's so inaccessible; it's hard to see what's on the ocean bottom and hard to get a feel for it. I think now with GPS and precise navigation, that's all changing. We're beginning to paint very accurate pictures of the ocean bottom, have a much better appreciation of what's down there; it has great implications for us in the Navy for submarine navigation; it has implications in mine warfare. It's very important for us to know the difference between a high-explosive mine and a refrigerator. Those are the kinds of distinctions we're having to make on the ocean bottom, but we have the tools now that can tell the difference between a car and a refrigerator. And also, we can create databases that actually go into areas and chart all the stuff that's on the bottom, and then we can go back and do computer surveys and figure out what has changed over a period of time. So if some new large physical object has entered into that particular area, that certainly would be the basis of a more detailed search for mine hunters. It's very important technology that we're spending a lot of time on now and we're very interested in.

As I mentioned before, GPS plays a big role in our weapon systems and will play a greater role – that little problem I had in my backyard in Pensacola acquiring was a stumbling block now; but now we have new GPS systems that can acquire very rapidly or can be preprogrammed with station data before they're fired. So they literally can acquire correct positions in a matter of seconds rather than in the 4 to 5 minutes that I'm used to.

So truly, the ability to accurately predict time and time interval is a national asset. The work that you're doing, I think, is a national asset. And anybody who doesn't appreciate it should just get on the Internet like I did yesterday – I thought I'd start looking around on our Home Page and see what's available – to be able to go up and check out the performance of all the clocks and all 24 of the GPS satellites; that's kind of incredible that that kind of technology's available; and it's open to the general public and certainly is a national asset.

At one of my budget hearings earlier in the job, someone suggested that we start selling time. Of course, we jumped up and down and said, "You know, you're missing the point. That's one of the great things that we do, and we wouldn't want to do that." But there are actually people who are thinking that we ought to be selling precise time. I don't think the Navy is certainly intending to that, but that was one of the types of things that came up, because people put a lot of value on it; but it is a resource that we are glad to provide and we certainly value our role in doing that.

So, in short, it's not hard for me to understand how important your work is. I am very supportive. I know that you are thinking about new technologies, we are in the Navy; it's time probably to replace our hydrogen masers and cesium clocks with new technology. Dr. Johnston has talked to me about that a number of times. I'm a supporter of it; I'm going to support the effort, and certainly going to support continued research in this field. I thought precise time down to a microsecond was fine, but I soon learned that we're really talking about nanosecond accuracy, and we would like to do better than that. I thought 5-meter accuracy

for GPS was fantastic; but now with differential GPS and what's called "kinematic GPS," we're talking about accuracies in a matter of centimeters. Incredible stuff, and it's all based on an accurate knowledge of time. And that's what you do, and certainly we appreciate the work that you're doing.

I hope you have a very productive conference. I'm going to be here this evening, and I hope I have an opportunity to meet and visit with you this evening. And I appreciate the opportunity to talk with you a short period this morning. Thank you very much.

[Applause]



Sigfrido M. Leschiutta

PTTI DISTINGUISHED SERVICE AWARD

Presented by
Dr. Len S. Cutler
Hewlett-Packard Co.

to

Dr. Sigfrido M. Leschiutta
Istituto Ellettrotecnico Nazionale Galileo Ferraris
and Politecnico di Torino

It's a great honor and pleasure for me to help recognize at this time past achievements in the time and frequency arena. I'm very happy that I can do this for my friend Sigfrido Leschiutta, whom I've known for about 28 years. I'm sure everyone agrees that he's very well qualified to receive this award, as evidenced by a long list of important accomplishments. Those who know Sigfrido well are always impressed with the number of projects with which he has been involved in a leading way and with his energy and enthusiasm.

He was with the LASSO project. He was chairman of the URSI Commission A on Electromagnetic Technology and vice chairman of the CCIR UIT Commission 7 on Time and Frequency and was also involved with the BIPM. He was chairman of the scientific council of the Italian space agency and member or chairman of several URSI working groups. He organized a number of international conferences, particularly on laser-ranging instrumentation and measurement of both G and g , and he organized two experiments on the Equivalence Principle of relativity using clocks. He helped set up a course on metrology and fundamental constants. And this is, of course, by no means a complete listing.

Sigfrido was the chief of the Time Section of the IEN, the national standards laboratory in Italy at Torino, and was active in atomic and piezoelectric frequency standards, as well as in the computation of the UTC(IEN) timescale. He set up dissemination services using TDN satellite comparisons. He has been president of the IEN for the last several years. He is a full professor of electronic measurements at the Politecnico di Torino and a joint professor of time and frequency metrology.

He has published more than 100 papers in various fields and written several books. He has a very broad range of interests and talents, as we all know. Dr. Gernot Winkler says, "Sigfrido is one of the most educated people I have ever met." Winkler talks about Sigfrido's collections of musical instruments and the books that he has written on harpsichords. He also mentions that Sigfrido is an excellent tour guide, particularly in Florence, Italy, where Gernot had the pleasure of being squired around by Sigfrido. Gernot says, "I have very great regard for him as a wonderful human being full of esprit, patience, tolerance, and humor."

Prof. Andrea De Marchi mentions a number of things, both technical as well as personal. One time a number of people, including Sigfrido's wife, couldn't piece together the scarce information available well enough to be able to decide in which continent Sigfrido was, let alone where he was. He also talks about Sigfrido's interest in music and musical instruments of all kinds. Not only does he collect the instruments and write about them, but he also builds them. He collects antique radios and, a few years back, had about 40 of them stolen, but he still has plenty. He also collects mopeds and has a very large number of books. Andrea says, "He is a really remarkable man."

Dr. Franco Cordara has had a long association with Sigfrido and remembers many of the important technical contributions he made. He talks about the great enthusiasm that Sigfrido had for the annual USNO flying clock visits. He also mentions the joint program that Sigfrido was involved in in 1983 between IEN, the U.S. Naval Research Lab, and the Italian Navy to test out a synchronization system based on GPS. That's a long time ago. He tells of a joke letter that Sigfrido helped prepare to send from India to the IEN about the "discovery in an Indian research institute of a new clock based on the Adam's apple movement stimulated by the drinking of a particular kind of whiskey."

I remember first meeting Sigfrido in the late 1960s when he came to visit our lab in Beverly, Massachusetts. We were all very impressed with his knowledge of frequency and time technology and his great enthusiasm. His visit is deeply imprinted in my memory.

Clearly Sigfrido has made many valuable contributions to the time and frequency community as well to physics and electronics in general. He is indeed a very capable individual with great breadth and depth in his knowledge and his ability to apply it. He is also a fine human being.

With great pleasure we now give him his award and express our congratulations and appreciation for his outstanding contributions and service to our community. Sigfrido, will you please come up?

DR. SIGFRIDO LESCHIUTTA: Len Cutler was so kind as to give a list of some things I have done. I think the list is too wide. I don't think I have performed all the things you have said. But let me put the things in another way. The honor I am receiving is a big one, and I think it is my duty, since you are giving me this award, to say a few words about two groups of people that were instrumental in my activities. One group of people was here in the United States when I visited the U.S. Naval Observatory about 30 years ago. I met Dr. Winkler. From that visit I took the impression of how important it is, when a task is given, to be concentrated on and devoted to the task.

The second part of my stay was at the National Bureau of Standards, where I met Jim Barnes, another recipient of this award. And at NBS I learned the importance of the dignity of a national standards laboratory as the backbone of the research for the industry of the country. In that laboratory I met Dave Allan, who became a friend of many, many occasions. He was also with us for a period of about a month.

And finally, Len, my first visit to a factory in the United States was to you in Beverly about 30 years ago at the old BOMAC Factory. And of you and your group, I remember Bob Vessot and Jacques Vanier. From you and your coworkers I learned the importance that also a factory has to devote to fundamental research. And the 5060 was really a good accomplishment for science and technology.

This is the first group of people I have to thank. The second one are the people that are working with me in Torino. Some of them were named. I am relying continuously on the help of all my coworkers.

So thank you again, Len, and thanks again to this community.

IMPACT OF ATOMIC CLOCKS ON NAVIGATION, COMMUNICATION, AND SCIENCE

Giovanni Busca
Observatoire de Neuchâtel
CH-2000 Neuchâtel, Switzerland

Abstract

An analysis of the development of atomic clocks during the last decade shows that the applications, particularly where related to GPS, have grown at a rate much faster than the clock development itself. However, improved clock performances and reliability are expected to be determinant for future applications in navigation, communications, and science. This problem is illustrated considering five basic topics. The first is the relevance of space atomic clock, a subject certainly noncontroversial in the Time and Frequency (T&F) community. The second and third topics are more provocative and concern, respectively, the alternative to the use of space atomic clocks in satellite navigation systems and the associated important issue of the atomic clock lifetime. The fourth topic is an ideal program towards the realization of high performances and reliable space atomic clocks. Finally, the last topic is a review of the flight opportunities for atomic clocks around the year 2000.

1 RELEVANCE OF SPACE ATOMIC CLOCKS

It is not difficult to recognize the relevance of space atomic clocks in the framework of GPS. The GPS market is growing exponentially thanks to civil applications, which will account for 90% of the overall applications around the year 2000.^[1] The economical importance of GPS is recognized worldwide and also in Europe^[2], not without some concerns, GPS being a totally American system. Even if the T&F community as always been aware of the fact that the space atomic clocks are at the heart of GPS, this awareness was not common outside this community and only recently has touched the policy makers and managers, as illustrated in the following short review.

The Space Agency of Japan in September 96^[3], referring to the development of a local contribution to GPS and to the four main technical obstacles identified, commented that "the onboard atomic clock is the technology giving the biggest headache." This comment contains two concepts: 1) the atomic clock technology is important, 2) the technology is difficult. The same agency in November 1996, while scaling down plans for an immediate local contribution to GPS, recommended that "Japan continue to develop related satellite navigation technology such as atomic timing standards."^[4]

In Europe, the recent activity of the Observatory of Neuchâtel (ON), as external support laboratory of the European Space Agency (ESA) focusing essentially on the development of space atomic clocks, has contributed to the award of a first industrial contract for the

development of a space rubidium clock in connection with the European Global Navigation Satellite System (GNSS-2) program.

In the USA, the NAPA report charting the future of GPS^[5] proposes to "reduce satellite clocks errors through use of improved clocks" and also suggests the development of a suitable space hydrogen maser. From the industrial side, important and exciting plans have been made public for adding navigation payloads containing space atomic clocks aboard 12 ICO communication satellites.^[6] In conclusion, the relevance of the space atomic clocks seems presently well recognized.

2 ALTERNATIVES TO THE USE OF SPACE ATOMIC CLOCKS

Alternatives to the use of space atomic clocks have been considered in the past and are still considered today. An ESA study in 1983 in connection with the navigation system NAVSAT, similar to GPS, proposed replacing the space atomic clocks by a continuous uploading of timing and navigation signals to transparent transponders on the satellites. The signals were generated by an ensemble of suitably synchronized ground stations (five stations and fifty antennas required without considering the redundancy problem).

Today, the European Geostationary Navigation Overlay Service (EGNOS), presently under implementation, is realizing such a philosophy. The NAPA report^[5] also suggests replacing, at least partially, the space atomic clocks with high-performance quartz oscillators. However, a study by the Observatory of Neuchâtel (ON) for ESA in 1993, based upon the assumption of a space atomic-clock lifetime of 7.5 years, showed clearly that, contrary to the conclusion of the previous NAVSAT report, the onboard atomic clocks could reduce the overall system complexity and cost and improve the system performance and reliability.

The same report showed also that the availability of more performers and more reliable clocks could reduce further the overall system cost and increase the number of applications, including possibly the precision landing of aircraft.

All the previous considerations are dominated by the assumption made about space atomic clock lifetimes; this is the real central issue of the problem.

3 SPACE ATOMIC CLOCK LIFETIME

The lifetime is defined as the time period during which the clocks perform according to the given specifications. The lifetimes of GPS clocks reported in the following are based on the very recent data furnished by Dr. R. Beard of Naval Research Lab, whose contribution is acknowledged.

Block II rubidium clocks:

No. of clocks: 11 Average lifetime: 1.1 years

Block II cesium clocks:

No. of clocks: 35 Average lifetime: 2.9 years

Current rubidium clocks:

No. of clocks: 4 Average lifetime: 1.04 years

Current cesium clocks:

No. of clocks: 21 Average lifetime: 3.14 years

The GLONASS cesium clocks' average lifetime, as given by Dr. Gevorkian of the Russian Institute of Radionavigation and Time (RIRT), whose contribution is also acknowledged, is approximately 1 year. With three cesium clocks onboard, a GLONASS satellite has by consequence an average lifetime of 3 years.

It is clear that using atomic clocks with a lifetime of the order of 1 year makes the overall system very costly. A logical question is then why the space clocks' lifetime is so much shorter than the lifetime of the ground clocks of the same type. It would be strange that a solution of this problem could not be found, within the capability of the present technology, in the near future.

4 PROGRAM TOWARD THE REALIZATION OF RELIABLE SPACE ATOMIC CLOCKS

The realization of reliable space clocks, ideally and historically, appears as the conclusion of a complex process involving five phases:

- 1) R&D accompanied by the prototyping of ground clocks
- 2) Production in small quantities of ground clocks
- 3) Production in large quantities of ground clocks
- 4) Prototyping of space clocks
- 5) Industrial production of space clocks.

This process should involve ideally the continuity of the personnel and the continuity in time through all the process. The phases 3 and 5 are typical industrial tasks. The other phases are suitable also for research institutes. Referring to the GPS rubidium and cesium clocks, all the phases of the process have been realized; however, the continuity of the personnel was not always preserved.

In Europe, with respect to the rubidium clock, the phase 5 (industrial production of space clock) has started recently. All the previous phases have been performed and the continuity of the personnel assured from the development work at ON to the production phase in a spin-off company.

With respect to the space hydrogen maser (SHM), the phase 4 is under completion, in the USA at the Smithsonian Astrophysical Observatory, and in Europe at the ON, without industrial involvement. However, the phase 3 of the SHM process is missing, being unrealistic for this device. Tables 1 to 5 illustrate in more detail the present or recent activity for each one of the five phases.

Commenting on the recent development of new microwave frequency standards presented in Table 1, we can surely predict that the future space clocks will be derived from the new developments described in this table. We can already anticipate today that more new clocks will be certainly be performing than the actual space clocks now. However, we cannot predict today their reliability, which depends strictly upon the evolution of the technology, particularly laser technology, during the next few years. As shown in Table 5, the most important effort is related to the laser-cooled clocks. A significant effort is also present in ion traps and laser-pumped

devices. The reasons of the success of laser-cooling are outlined in Table 1.1. We think we are in the presence of a technical revolution of historical significance. The technique gives high line Q, high line homogeneity, and a relatively good S/N, which is expected to improve further with transverse cooling of the atomic beams. The microgravity clock, operating on a satellite in the absence of gravity, is expected to be the "ultimate" clock of the future.

Table 1.2 shows the particular contribution of the industry to the R&D.

Tables 2 to 5 illustrate the present international situation relating to the corresponding phases.

Table 5.1 is a summary of recommendations that we are trying to implement in the European programs.

5 FLIGHT OPPORTUNITIES IN THE YEAR 2000

Flight opportunities exist for demonstrating new technology and improved lifetime. Table 6 illustrates some of these opportunities.

6 CONCLUSION

In conclusion, the development of space atomic clocks is still an active process which has perhaps a bottleneck in the final phase of the process: the industrial production of reliable space clocks.

Some general reflections on how to solve this problem have been presented and flight opportunities for proving new concepts and clocks reliability have been reviewed.

In a period of shrinking budgets, a way for obtaining better results at lower cost can be through increased international cooperation. We hope that this will be the case, particularly in relation to technical and scientific experiments onboard of the International Space Station and in connection with the GPS II F Reserve Auxiliary Payload opportunities.

8 REFERENCES

- [1] D. Allan 1994, Proceedings of ION GPS-1994, pp. 25-32.
- [2] *Interavia*, July 1994.
- [3] *Space News*: 9-15 September, 1996.
- [4] *GPS World*, November 1996.
- [5] "*The Global Positioning System: Charting the Future*," May 1995 (NASA and NRC).
- [6] *Space News*, 11-17 March 1996.
- [7] A. Clairon, et al.1996, Proceedings of the 10th European Frequency and Time Forum (EFTF), 5-7 March 1996, Brighton, UK (IEEE Conference Publication 418).
- [8] These Proceedings and G.A. Costanzo, et al.1997, Proceedings of the 11th European Frequency and Time Forum (EFTF), 4-6 March 1997, Neuchâtel, Switzerland, to be published.

- [9] These Proceedings and M. Zucco, et al. 1997, Proceedings of the 11th European Frequency and Time Forum (EFTF), 4-6 March 1997, Neuchâtel, Switzerland, to be published.
- [10] These Proceedings.
- [11] These Proceedings and J.S. Boulanger, et al. 1997, Proceedings of the 11th European Frequency and Time Forum (EFTF), 4-6 March 1997, Neuchâtel, Switzerland, to be published.
- [12] C. Mandache, et al. 1997, Proceedings of the 11th European Frequency and Time Forum (EFTF), 4-6 March 1997, Neuchâtel, Switzerland, to be published.
- [13] Y. Wang, et al. 1996, "*Some considerations on the cesium atomic fountain standard*," Proceedings of the 5th Symposium on Frequency Standards and Metrology (ed. J.C. Bergquist), 15-19 October 1995, Woods Hole, Massachusetts, USA (World Scientific, Singapore), pp. 74-80.
- [14] P. Berthoud, et al. 1997, Proceedings of the 11th European Frequency and Time Forum (EFTF), 4-6 March 1997, Neuchâtel, Switzerland, to be published.
- [15] C. Valentin, et al. 1997, Proceedings of the 11th European Frequency and Time Forum (EFTF), 4-6 March 1997, Neuchâtel, Switzerland, to be published.
- [16] These Proceedings.
- [17] E. Clerq, et al. 1994, Proceedings of the 8th European Frequency and Time Forum (EFTF), 9-11 March 1994, Weihenstephan, Germany, p. 497.
- [18] R.L. Tjoelker, J.D. Prestage, and L. Maleki 1996, "*Record frequency stability with mercury in a linear ion trap*," Proceedings of the 5th Symposium on Frequency Standards and Metrology (ed. J.C. Bergquist), 15-19 October 1995, Woods Hole, Massachusetts, USA (World Scientific, Singapore), pp. 33-38.
- [19] G. Mileti, and P. Thomann 1995, Proceedings of the 9th European Frequency and Time Forum (EFTF), March 1995, Besançon, France, p. 271.
- [20] P.J. Chantry, et al.: 1992, "*Towards a miniature laser-pumped cesium cell frequency standard*," Proceedings of the IEEE International Frequency Control Symposium, 27-29 May 1992, Hershey, Pennsylvania, USA, pp. 114-122.
- [21] C. Thomas (BIPM), private communication.
- [22] P. Laurent, et al. 1996, Proceedings of the CPEM, June 1996, Braunschweig, Germany, and Proceedings of the ESA Symposium on Space Station Utilization, 30 September-2 October 1996, Darmstadt, Germany (ESOC), in press.
- [23] R.C.F. Vessot, et al. 1996, "*High precision time transfer to test an H-maser on Mir*," Proceedings of the 5th Symposium on Frequency Standards and Metrology (ed. J.C. Bergquist), 15-18 October 1995, Woods Hole, Massachusetts, USA (World Scientific, Singapore), pp. 39-45.
- [24] H.S. Schweda, et al. 1996, "*Hydrogen maser frequency standard for scientific experiments in space*," Proceedings of the 5th Symposium on Frequency Standards and Metrology (ed. J.C. Bergquist), 15-18 October 1995, Woods Hole, Massachusetts, USA (World Scientific, Singapore), pp. 522-524, and L. G. Bernier et al. 1997, Proceedings of the 11th European Frequency and Time Forum (EFTF), 4-6 March 1997, Neuchâtel, Switzerland, to be published.

- [25] R. Kohl, and M. Bird: Proceedings of the 11th European Frequency and Time Forum, 4-6 March 1997, Neuchâtel, Switzerland, to be published.
- [26] C. Couplet, et al.1995, "*Miniaturized rubidium clocks for space and industrial applications*," Proceedings of the 1995 IEEE International Frequency Control Symposium, 31 May-2 June 1995, San Francisco, California, USA, pp. 53-59.
- [27] G. Busca, and P. Thomann 1997, "*CRONOS, a redshift experiment*," Proceedings of the COSPAR General Assembly, 17-20 July 1996, Birmingham, England, UK, in press.
- [28] G. Busca, and P. Thomann 1997, Proceedings of the ESA Symposium on Space Station Utilization, 30 September-2 October 1996, Darmstadt, Germany (ESOC), in press.

TABLE 1: RESEARCH ON NEW ATOMIC CLOCKS: Phase 1

Institutes	Country	Status	Ref
Laser-Cooled Cs Clocks			
Fountains			
LPTF in collaboration with ENS, LHA	France	operational	[7]
CRL	Japan	work in progress	[8]
NRLM		" "	
PTB	Germany	" "	
NPL	England	" "	[9]
NIST	USA	" "	[10]
NRC	Canada	" "	[11]
IFTAR	Romania	" "	[12]
Beijing Univ.	P.R. China	" "	[13]
IEN	Italy	" "	
Continuous Beam			
ON	Switzerland	first clock signal obtained	[14]
LHA	France	work in progress	[15]
Other Microwave Standards			
Laser-Pumped Cs Beams			
NIST	USA	operational	[16]
LPTF	France	operational	[17]
Ion Traps			
JPL	USA	operational	[18]
PTB	Germany	work in progress	
Laser-Pumped Cs, Rb Gas Cells			
Several institutions	USA, Japan China, Europe	work in progress	[19]

TABLE 1.1: WHY LASER COOLING ?

The Magnetic Optical Trap (MOT)

MOT: appears as the historical conclusion of process dealing with a basic physics problem: the confinement of atoms for the interrogation: (buffer gas, bulb Teflon coating, Ramsay cavity with thermal beams)

MOT: allows cooling from gas phase:

Potentials: - Relatively compact clock
 - Relatively high density of atoms
 - Low velocity beams (see below)

Inconvenient: - Acceleration sensitivity

Velocity dependent effects:

	Fountain or continuous beam	Conventional Cs (including laser pumped) clocks
- Average velocity	~1M/s	100 ÷ 200 M/s
- Velocity distribution width	~cm/s	10 ÷ 100 M/s
- 2nd order Doppler effects reduced by 4 orders of magnitude		
- High line Q potential	10^{10} (microgravity clock 10^{11})	$2 \times 10^7 \div 10^8$
- High atomic signal potential	$10^5 - 10^6$ atoms/s	$10^5 \div 10^8$ atoms/s
- High accuracy potential	3×10^{-15} REF [7]	$\leq 1 \times 10^{-14}$

**TABLE 1.2: CLASSICAL MICROWAVE ATOMIC CLOCKS.
NEW INDUSTRIAL DEVELOPMENT : Phase 1**

	Manufacturer	Country	Main characteristics	Ref
Laser pumped gas cell Cs	Westinghouse	USA	miniaturized, low power, low cost	[20]
Laser pumped Cs beam	Tekelec Telecom	France	presented at this meeting	

TABLE 2: NEW INDUSTRIAL PRODUCTS : Phase 2

Hydrogen Maser	Various companies or institutions	RUSSIA, USA, Switzerland	Utilization in time keeping. ~50% of masers reported to BIPM show a low frequency drift $\leq 1 \times 10^{-16}$ /day	[21]
-------------------	-----------------------------------------	--------------------------------	--------------------------------------------------------------------------------------------------------------------------------	------

TABLE 3: NEW INDUSTRIAL PRODUCTS : Phase 3

Cs beam	Hewlett-Packard High Performances	USA	low flicker floor: 6×10^{-15}	[21]
Rubidium gas Cell	Tekelec Neuchâtel Time	Switzerland	magnetron resonator 0.25 liter 0.47 kg 8 w drift $\leq 1 \times 10^{-11}$ /month	

TABLE 4: SPACE ATOMIC CLOCKS DEVELOPMENTS : Phase 4

Device	Institute	Characteristics	Ref
Microgravity laser cooled, Cs clock: PHARAO		$\phi = 30$ cm $L = 80$ cm Length of interaction = 20 cm	[22]
	CNES - LPTF - LKB - LHA - LPMO France	Stability goal $\sigma_y(\tau) = 3 \times 10^{-14} \tau^{-1/2}$ $1 \leq \tau \leq 10^5$ s.	
Space Hydrogen Maser	SAO USA	Physics Package 70 kg Flicker floor $< 1 \times 10^{-15}$	[23]
Radioastron SHM	ON Switzerland	35 kg Flicker floor $\leq 2 \times 10^{-15}$	[24]
Space Rubidium			
DWE / Cassini-Hugens	Dornier satellites system, Germany	1.8 kg 2.3 liters 12 watts 40 g	[25]
Radioastron S-RUSO	ON	1.2 kg 1.2 liter $w = 8$ w $\sigma_y(\tau) = 1 \times 10^{-11} \tau^{-1/2}$ $1 \leq \tau \leq 100$ s drift 4×10^{-11} /month	[26]

TABLE 5: SPACE ATOMIC CLOCKS. NEW INDUSTRIAL PRODUCTS : Phase 5

GPS / GLONASS	Business as usual	
ESA GNSS-2 S-RUSO - GPS compatible	Tekelec Neuchâtel Time Switzerland	Specs ≤ 1 kg ≤ 0.6 liters ≤ 10 watts Flicker ≤ 5×10^{-14} Drift ≤ 1×10^{-13} /day

**TABLE 5.1: IMPROVING THE SPACE ATOMIC CLOCKS
RELIABILITY AND LIFETIME**

Establishing a better connection between the space clock production and the industrial production of ground clocks.

- ☐ Use of same critical physics package hardware for space and ground clocks.
- ☐ Space electronics derived from the industrial electronics package for ground clocks.

Scientific study of the clock lifetime limitation factors.

- ☐ Identification of the problem areas.
- ☐ Study of the phenomena (normally related to the physics package).
- ☐ Solution of the problems (typical example: the GPS Rubidium lamp aging problem successfully solved).

Extensive long term ground testing prior to launch.

**TABLE 6: OPPORTUNITIES FOR SPACE CLOCKS UTILIZATION
IN THE YEARS 2000**

	Ref
<input type="checkbox"/> Radioastron S-VLBI mission 2 S-RUSO + 1 SHM	[27]
<input type="checkbox"/> GPS II F Flexibility Reserve	
<div>Allocation:</div> <div>154 kg</div> <div>465 W thermal power</div> <div>350 W DC power</div>	
<input type="checkbox"/> International Space Station	
<div>- EXACT (<u>E</u>xperiment on <u>A</u>tom<u>i</u>c <u>C</u>locks and <u>T</u>iming)</div>	[28]
<div>- ACES (<u>A</u>tom<u>i</u>c <u>C</u>lock <u>E</u>nsemble in <u>S</u>pace)</div> <div>Microgravity clocks, SHM, Ion Traps, Laser Time Transfer</div>	[22]
<input type="checkbox"/> NASA Research Announcement	
<div>Proposals: Fundamental physics in μ-gravity:</div> <div>Laser cooling, atomic physics, gravitational and relativistic physics</div>	

Questions and Answers

SAMUEL STEIN (TIMING SOLUTIONS CORP.): Which is really better, do you think, clocks in space or to do synchronization from the ground clock continuously?

GIOVANNI BUSCA: The answer is very simple. As far as the atomic clock is working, it's much better to have the atomic clock in space. Cheaper, more performance, more reliability. But it has to work, of course.

ROBERT DOUGLAS (NRC, CANADA) : I would just like to comment. It's dangerous to believe someone unreservedly has a vested interest in clocks in space. I have a vested interest in clocks on the ground and not in space, and I agree with Giovanni.

RICHARD GRIFFIN (TEXAS INSTRUMENTS) : On the short lifetime in space clocks, has there been any correlation worked out between space environment effects, particular proton belts, and the short lifetimes?

GIOVANNI BUSCA: I think this question should probably be answered by Ronald Beard. From what I know myself, it's just an impression, the lifetime limitation is associated more to electronic problems than anything else.

RONALD BEARD (NRL) : Thank you. It's a complicated answer to the lifetime issue that's an average lifetime of operation. As far as we can tell, and many people have looked at it, there is a radiation effect on them *per se*. It's a complicated interaction within the system. And, say, the average lifetime is so long, a number of them failed early, but quite a few of them have operated for a long period of time, except for the rubidiums, which seem to be consistently of short duration.

IMPACT OF INTERNATIONAL DECISIONS ON TAI GENERATION

Claudine Thomas
Bureau International des Poids et Mesures
Pavillon de Breteuil, 92312 Sèvres Cedex, France

Abstract

Under the terms of the Convention du Mètre, the Bureau International des Poids et Mesures (BIPM) operates under the supervision of the Comité International des Poids et Mesures (CIPM). The CIPM has created a number of consultative committees which bring together the world's experts in their specified fields as advisers on scientific and technical matters. Among them, the Comité Consultatif pour la Définition de la Seconde (CCDS) deals with the definition and realization of the second, and the establishment and diffusion of International Atomic Time (TAI) and Coordinated Universal Time (UTC).

The CCDS held its 13th meeting in March 1996. It made a number of recommendations and addressed requests to its Working Groups, some of which have a direct impact on the work carried out at the BIPM Time Section. The most important recommendation is Recommendation S2 (1996), which concerns the application of the correction for the blackbody radiation shift to the results of all primary frequency standards. As this has direct consequences for the accuracy of TAI, immediate action was necessary. Another example is the creation of a CCDS Working Group on the expression of uncertainties in primary frequency standards. Evidence of the need for such a group became clear during discussions of how uncertainties should be presented and interpreted when combining measurements of the SI second produced by primary frequency standards. Finally, the Recommendation S4 (1996), which asks for coordination of the GPS and GLONASS timing systems, may lead to a worldwide network of time links using GPS and GLONASS in a complementary way. The aim of this paper is to present these international decisions to the timing community, to show how they influence the work of the BIPM Time Section, and to figure out the consequences for TAI.

INTRODUCTION

Worldwide agreement on units of measurement and practical provision of accurate measurement standards are assured under the diplomatic treaty of the Convention du Mètre through the activities of the Bureau International des Poids et Mesures (BIPM) and the national metrology institutes. Under the terms of the Convention, the BIPM operates under the exclusive supervision of the Comité International des Poids et Mesures (CIPM), which itself comes under the authority of the Conférence Générale des Poids et Mesures (CGPM).

The CGPM receives the report of the Comité International on work accomplished; it examines the arrangements required to ensure the propagation and improvement of the Système International d'Unités (SI) and endorses scientific resolutions of international scope.

The CIPM oversees and directs the work of the BIPM and proposes its future program to the Conférence Générale. It created a number of consultative committees which bring together the

world's experts in their specified fields as advisers on scientific and technical matters. Among the tasks of the consultative committees is the preparation of recommendations for discussion at the CIPM. The membership of a consultative committee is decided by the CIPM in consultation with the President of the consultative committee, who is normally a member of the CIPM, and the Director of the BIPM. Laboratories invited to be members are national metrology institutes of a member state of the Convention du Mètre already recognized internationally as most expert in the field. In addition to laboratory members, a consultative committee may include as members international unions, or other international organizations, and named individuals (members by appointment) whose knowledge and competence in the field are such that they can provide valuable assistance even though they do not come from a member laboratory. The President may also invite experts (invited guests) for a specified meeting of the consultative committee for advice on a particular item considered at the meeting. In addition, studies on specified subjects are dealt with by permanent or temporary working groups which report their conclusions to their consultative committee. Recommendations proposed by a consultative committee to the CIPM represent a consensus among members and serve to define the work of the BIPM and national laboratories. Among them, the most important become CIPM Recommendations, and eventually Resolutions of the CGPM.

The Time Section of the BIPM is responsible for the establishment and diffusion of International Atomic Time (TAI) and Coordinated Universal Time (UTC). For issues concerning time, the CIPM takes advice from the Comité Consultatif pour la Définition de la Seconde (CCDS). Although the name of this consultative committee appears to constrain its work to the definition and realization of the SI second, CCDS sessions are forums in which most of the scientific and technical problems encountered in time metrology are addressed.

In recent years, the CCDS has been chaired by Prof J. Kovalevsky and its membership has included twenty-one institutions, four international unions, one member by appointment, Prof. B. Guinot (formerly Head of the BIPM Time Section), and the Director of the BIPM, Dr. T.J. Quinn. The CCDS is helped in its work by four CCDS Working Groups:

- * the Working Group on TAI, chaired by Dr P. Pâquet (ORB, Brussels, Belgium),
- * the Working Group on Two-Way Satellite Time Transfer, chaired by Dr W.J. Klepczynski (ISI, Washington D.C., USA),
- * the Working Group on Application of General Relativity to Metrology, chaired by Prof. B. Guinot, and
- * the Working Group on the Expression of Uncertainties in Primary Frequency Standards, chaired by Dr. R. Douglas (NRC, Ottawa, Canada).

In addition, the Working Group on TAI has created a Sub-group on GPS and GLONASS Time Transfer Standards, chaired by D.W. Allan (Allan's TIME, Fountain Green, Utah, USA).

In general, the CCDS meets every third year. The last meeting (the 13th) was held at the BIPM on 12 and 13 March 1996, and attracted representatives from all but one institution and from all international unions. The President of the CCDS also invited four experts: D.W.

Allan, Dr. G.M.R. Winkler (ISI, Washington D.C., USA), Prof. A. De Marchi (Polytechnico de Torino, Turin, Italy), and Dr. V.A. Brumberg (IPA, St. Petersburg, Russia); the physicists of the BIPM Time Section also attended. Dr. P. Fisk (NML-CSIRO, Sydney, Australia) was appointed secretary for this meeting.^[1] Twenty-five working documents, sent to the CCDS before the meeting, were examined during the session.^[2] Consensus was reached on four Recommendations (see Appendix I) and these were proposed to the CIPM in September 1996, one of them, Recommendation S4 (1996), becoming CIPM Recommendation 1 (CI-1996). The CCDS also addressed a formal request (see Appendix II) to the Sub-group on GPS and GLONASS Time Transfer Standards. It should be noted that the CCDS Working Group on the Expression of Uncertainties in Primary Frequency Standards was created during this 13th meeting.

The impact on the establishment of TAI and UTC of some of the recommendations and decisions of the CCDS taken during its last meeting is examined below. The chosen examples concern the estimation and improvement of the accuracy of TAI and the use of GLONASS as a complementary technique for high accuracy time transfer between clocks contributing to TAI.

BLACKBODY FREQUENCY SHIFT

The definition of the SI second ideally requires the observation of the ground-state hyperfine transition of an unperturbed cesium atom. Corrections for perturbations should, thus, be estimated together with their respective uncertainties, and applied to the results of measurements provided by primary frequency standards. The largest corrections (greater than a few parts in 10^{14}) compensate for the quadratic Zeeman effect, the quadratic Doppler effect, and the cavity phase difference.^[3] These bring uncertainties ranging from a few parts in 10^{15} to a few parts in 10^{14} for the most accurate primary standards. Other effects, such those related to cavity detuning, microwave leakage, Majorana transitions, asymmetry of the microwave spectra, and the electronic equipment do not induce a global shift in the measurement, but contribute to the uncertainty budget of the standard by some parts in 10^{15} .^[3]

TAI is defined as a coordinate time scale in a geocentric reference frame, with the SI second as realized on the rotating geoid as the scale unit. It follows that, if the primary frequency standard is used to evaluate the duration of the TAI scale unit, it is also necessary to apply a correction compensating for the difference in gravitational potential between the standard site and the rotating geoid. This correction is about 1×10^{-13} for a standard at 1,000 m above the rotating geoid and can be calculated with an uncertainty of 1 to a few parts in 10^{16} .

Another important shift is due to alternating electric fields in the thermal radiation of a cesium atomic standard. This was explained for the first time in a paper by Itano, Lewis, and Wineland^[4] published in 1982. Under the influence of the radiation from the walls surrounding the atoms inside the clock at temperature T , the clock transition frequency is reduced with respect to its value at $T = 0$ K. From the formula provided by Itano *et al.*, the amplitude of the effect is 1.7×10^{-14} for $T = 300$ K. Its uncertainty is conservatively estimated at 1×10^{-15} , taking into account the fact that the radiation involved is not emitted by a perfect black body.

In the past the blackbody radiation shift was not taken into account. It appeared for the first time in 1994 when the optically pumped primary frequency standard NIST-7 was first evaluated.^[5] The amplitude of the effect made it negligible for primary standards presenting an uncertainty of order 1×10^{-13} , but not for those showing uncertainties of a few parts in 10^{14} or below. At the time no uniform procedure was applied by the laboratories which reported data from primary frequency standards, with the consequence that it was discussed at

a formal meeting of the CCDS Working Group on TAI in March 1995.^[6] There was unanimous agreement that a correction, by which the clock frequency is transferred at 0 K, should be made. The conclusion of the Group that the blackbody correction should be applied to all primary standards was incorporated in a draft recommendation that the CCDS approved in March 1996 as Recommendation S2 (see Appendix I).

The CCDS Working Group on TAI also made the statement that "all laboratories keeping primary frequency standards evaluate the blackbody correction (to 0 K) for their standards and communicate the values, with their uncertainties, to the BIPM stating whether or not the correction has been applied, and that the BIPM study the implications for TAI of the uniform application of the correction."^[6] Since the end of 1995, the BIPM has been in a position to apply the blackbody correction to all the measurements provided by the most accurate primary frequency standards since they came into operation. It follows that the duration of the scale unit of TAI shows a departure from the SI second on the rotating geoid which is larger than before by an amount of about 2×10^{-14} s. Although the accuracy of TAI is degraded, it is important to note that the appearance of new primary frequency standards, such as the BNM-LPTF cesium fountain FO1^[7], which have outstanding accuracy (uncertainty of the LPTF-FO1 estimated at 3×10^{-15} , makes it possible to improve our knowledge of the departure of the TAI scale unit from the SI second on the rotating geoid.

Compensation for the discrepancy of the TAI scale unit was initiated in May 1995. This takes the form of cumulative frequency steering corrections, each of relative amplitude 1×10^{-15} , which are applied on dates separated by intervals of 60 days, a procedure which does not degrade the medium-term stability of the time scale. In mid-1996, we observed that the discrepancy had not yet been decreased by this procedure, which, in fact, has only compensated the natural drift of the scale. It was, thus, decided to increase the relative amplitude of the corrections to 1.5×10^{-15} , starting September 1996.

UNCERTAINTIES IN PRIMARY FREQUENCY STANDARDS

During the 13th meeting of the CCDS, held in March 1996, the President opened a general discussion on how uncertainties are expressed in primary frequency standard measurements.

According to the *International Vocabulary of Basic and General Terms in Metrology* (VIM entry 3.9^[8]), the uncertainty of a measurement is defined as a "parameter, associated with the result of a measurement, that characterizes the dispersion of the values that could reasonably be attributed to the measurand." The *ISO Guide to the Expression of Uncertainty in Measurement* (GUM^[9]) states that the standard uncertainty (entry 2.3.1.) is "the uncertainty of the result of a measurement expressed as a standard deviation" and recommends that uncertainty be expressed as a combination of a Type A and a Type B uncertainties. The Type A uncertainty (GUM entry 2.3.2.) is obtained "by the statistical analysis of series of observations" and the Type B uncertainty "by means other than the statistical analysis of series of observations."

In time and frequency applications, the data which are analyzed are in the form of time series. This leads to the question of what is intended when an uncertainty is calculated. Is it the expected variation of the quantity over a period of time, or is it merely the uncertainty of a single measurement? When a primary frequency standard is in operation in a laboratory, both are investigated. Take the example of the BNM-LPTF cesium fountain FO1.^[7]

* The stability of the device is characterized by an Allan deviation curve obtained from the

comparison of LPTF-FO1 with a local hydrogen maser. The result is expressed in the form $\sigma_y(\tau) = 2 \times 10^{-13} \tau^{-1/2}$, thus giving the evidence of white frequency noise, for averaging times τ between 1 s and 10^4 s. For longer averaging times, the value of $\sigma_y(\tau)$ reaches a limit, equal to 2×10^{-15} , due to the hydrogen maser performance. This is a statistical analysis and, thus, corresponds to a method of evaluation of a Type A uncertainty.

- * A measurement of the frequency of LPTF-FO1 is made relative to the local hydrogen maser over an averaging time τ of a few hours. This corresponds to the full white frequency noise of the primary standard not yet degraded by the maser noise. A number of corrections applied to the measurement result are evaluated, together with their standard uncertainties. Finally a corrected result is delivered, together with a standard uncertainty obtained by quadratic sum of individual uncertainties. This uncertainty is designated as the Type B uncertainty of the LPTF-FO1 standard.

Similar procedures are in use for all primary frequency standards and this calls for a few remarks.

The Type A uncertainty, as described above, is not characterized by one simple value of standard deviation resulting from white and Gaussian noise as in other metrological measurements, but by the variation of a standard deviation versus an averaging time, possibly showing non-white noise.

The type B uncertainty, as described above, applies to a measurement carried out over a given averaging time which must be indicated. This is a practice which is not often made in other metrological measurements.

The hypothesis of complete independence of the different components of the uncertainty budget is implicitly made when they are computed using a quadratic sum. This hypothesis may not be justified^[10] and some authors prefer to increase the value resulting from the quadratic sum in order to take into account suspected correlations.

An evaluation of the different corrections and of their uncertainties should rigorously be made for each measurement provided by a primary standard. The accuracy characterizing a standard can change during its life, as is the case for NIST-7 for which the Type B uncertainty was found to be 1×10^{-14} in 1994 and was updated to 5×10^{-15} in September 1996 after an upgrade of the system. This leads to the question of what is meant by the Type B uncertainty of a continuously operating primary frequency standard such as the classical standards PTB CS2 and CS3, for which the complete evaluation may be carried out only once.

The corrections to apply may be estimated with different methods. They may result from application of a formula, as is the case for the blackbody correction, and the corresponding uncertainties depend on the degree of validity of a theory. Corrections may also be derived from measurements, as is the correction for the quadratic Zeeman effect, and the corresponding uncertainties result from statistical analysis of the measurement results. Here, the separation between Type A and Type B evaluation method is not obvious.

The Type B uncertainty determination, as described above, is helpful for comparing the accuracy of the different primary frequency standards only if the different operators agree on the set of corrections which should be applied. This has already been discussed in the preceding section for what concerns the blackbody radiation shift. It is also important to note the particular case of the gravitational correction. Since the SI second is a proper unit, valid in a space domain surrounding the laboratory where the primary standard is located^[11], there is no reason to apply a correction due to the gravitational field experienced in the laboratory. The corresponding

uncertainty should, thus, not be taken into account. However, if the second produced by the primary standard is transferred to TAI, it is necessary to take into account the differential gravitational field between the standard site and the rotating geoid. This is exemplified in the publication of the uncertainty budget for the BNM-LPTF cesium fountain FO1^[7], where the gravitational correction appears as an additional line after a first quadratic sum of the other uncertainties involved.

The CCDS considered the questions summarized above to be of sufficient importance that a Working Group on the Expression of Uncertainties in Primary Frequency was formed. The membership of the working group is Dr. R. Douglas, Chairman, D.W. Allan, Dr. A. Bauch (PTB, Braunschweig, Germany), Dr. A. Lepek (INPL, Jerusalem, Israel), Prof. A. De Marchi, and Dr. C. Thomas (BIPM, Sèvres, France), and it is still largely open to other experts from timing laboratories. The main question this group must address is how to apply the recommendations of the ISO guide on uncertainty to the specific case of primary frequency standards. The answer to this question should clarify the way the different measurements reported to the BIPM from primary frequency standards should be used to evaluate the accuracy of TAI.^[12, 13]

USE OF GLONASS, AND GPS AND GLONASS STANDARDS

Since the beginning of 1995, the GPS common-view technique has been the sole means of time transfer used for TAI computation. Twice a year the BIPM distributes GPS international common-view schedules to laboratories contributing to TAI. The collection and treatment of the rough data are effected by the BIPM according to well-established procedures. The international network of GPS time links used by the BIPM is organized to follow a pattern of local stars within a continent, together with two-distance links, NIST-OP and CRL-OP, for which data are corrected to take account of on-site ionospheric measurements and postprocessed precise satellite ephemerides. Only strict common views are used in order to overcome effects due to the implementation of Selective Availability on satellite signals. If GPS time receivers in operation in timing laboratories are differentially calibrated, the accuracy of one common-view measurement is characterized by a standard uncertainty of a few nanoseconds. In addition, the measurement noise in time comparisons between distant clocks is smoothed out by averaging over a few days, an averaging period which remains shorter than the 5-day interval between two TAI updates. It follows that the resulting time scale is no longer affected by white phase noise, which results in an improvement in its short-term stability.

Although the GPS common-view method currently gives full satisfaction for the computation of TAI, improvements in the quality of clocks and the need for redundancy in time transfer methods have led the BIPM to take a particular interest in the GLONASS common-view method. The first commercial GLONASS time receivers specifically designed for fully automatic common-view observations appeared on the market in early 1995 and tests began immediately. Following Recommendation S 3 (1993) of the CCDS at its 12th meeting^[14], the BIPM issued the first official international GLONASS common-view schedule in December 1995 for implementation in January 1996. By spring 1996, six time laboratories already observed GLONASS in common view and this number is expected to increase rapidly.

A GLONASS common-view time transfer between California, the East Coast of the United States, and the BIPM has been under way since the end of July 1995. Results show a level of noise over one GLONASS common-view measurement slightly larger than for GPS.^[15] However, the internal delays of GLONASS equipment have not yet been calibrated, so a complete estimation of the accuracy remains to be carried out.

It would be highly interesting for the time community to use both systems, GPS and GLONASS, in an interchangeable way: this would provide robustness, redundancy, and reliability. However, there exist some differences which should be worked out. The most important concerns the coordinate reference frames in which the positions of the Earth stations and satellites are expressed, WGS 84 for GPS and SGS 90 for GLONASS. The reference frame which is internationally agreed for positions on the Earth is the IERS Terrestrial Reference Frame (ITRF) produced by the International Earth Rotation Service (IERS). The WGS 84 is very close to the ITRF, but conversion formulae are needed to transform data expressed in the SGS 90 into the ITRF and introduce an uncertainty of several meters. A standard procedure using the ITRF for both systems would, thus, be desirable. Another point concerns the differences between the time scales broadcast by the satellite systems, GPS time and GLONASS time, and UTC. A constant effort is maintained to keep GPS time very close to UTC, within a few tens of nanoseconds, and to ensure that this difference is accurately known. If Selective Availability were not implemented, the GPS satellites would distribute a close approximation to UTC in real time. The offset between GLONASS time and UTC, however, reaches 30 μ s and is not accurately known (an error as large as 1 μ s is suspected). The effect is that, although GLONASS signals are not intentionally degraded, they do not provide access in real time to a good approximation to UTC.

These different issues were discussed during the 13th meeting of the CCDS and were addressed in Recommendation S 4 (1996) (see Appendix I), which was approved in September 1996 as CIPM Recommendation 1 (CI-1996), entitled "Coordination of satellite systems providing timing." In this, system operators are recommended to use ITRF as the sole reference frame and to synchronize satellite times closely with UTC.

Besides this formal recommendation, it is clear that some standardization work is required to make time receivers able to observe indifferently GPS and GLONASS satellites, for instance software problems such as treatment of short-term data and data file format. This is relevant to the activities of the Sub-Group on GPS and GLONASS Time Transfer Standards, which was formally requested by the CCDS to contact manufacturers in order to design new time receivers able to match the requirements of time and frequency metrology. The BIPM is working hard on this item^[16, 17] through tests of new devices and suggestions to manufacturers.

CONCLUSIONS

The meetings of the Comité Consultatif pour la Définition de la Seconde gather world experts on the different theoretical and technical problems encountered in time metrology. The recommendations which are developed during these meetings represent a consensus among the members and serve to define the work of the Time Section of the BIPM and national timing laboratories. Two of the latest and most important decisions of the CCDS concern the uniform application of a correction to compensate for the blackbody radiation shift experienced by cesium atoms in primary frequency standards and encouragement of the use of the GPS and GLONASS satellite systems in a complementary way for international time transfer. In addition, a discussion on how uncertainties should be expressed to describe primary frequency standards has been initiated inside a newly created CCDS working group.

ACKNOWLEDGMENTS

The author is grateful to Malcolm Lawn (NML-CSIRO, Sydney, Australia) and Gérard Petit (BIPM, Sèvres, France) for helpful discussions.

REFERENCES

- [1] Comité Consultatif pour la Définition de la Seconde 1996, *Report of the 13th Meeting*, BIPM, Sèvres, France, in press.
- [2] Comité Consultatif pour la Définition de la Seconde 1996, Working documents submitted to the 13th Meeting, BIPM, Sèvres, France.
- [3] A. Bauch, T. Heindorff, R. Schröder, and B. Fischer 1996, "The PTB primary clock CS3: type B evaluation of its standard uncertainty," *Metrologia*, **33**, 249-259.
- [4] W.M. Itano, L.L. Lewis, and D.J. Wineland 1982, *Physical Review*, **A25**, 1233-1235.
- [5] W.D. Lee, J.H. Shirley, J.P. Lowe, and R.E. Drullinger 1995, *IEEE Transactions on Instrumentation and Measurement*, **IM-44**, 120-123.
- [6] G. Petit 1995, "Report on the discussions and decisions of the meeting of the CCDS Working Group on TAI, 13 and 14 March 1995," BIPM, Sèvres, France, 13 pages.
- [7] A. Clairon, S. Ghezali, G. Santarelli, P. Laurent, S.N. Lea, M. Bahoura, E. Simon, S. Weyers, and K. Szymaniec 1996, "Preliminary accuracy evaluation of a cesium fountain frequency standard," Proceedings of the 5th Symposium on Frequency Standards and Metrology, 15-19 October 1995, Woods Hole, Massachusetts, USA, ed. J.C. Bergquist (World Scientific, Singapore), pp.45-59.
- [8] "International Vocabulary of Basic and General Terms in Metrology," 1993, International Organization for Standardization, second edition, 59 pages.
- [9] "Guide to the Expression of Uncertainty in Measurement," 1993, International Standardization Organization, 101 pages.
- [10] A. De Marchi 1994, "Different schemes and structure of the accuracy budget in cesium frequency standards," Proceedings of the 5th Russian Symposium on Metrology of Time and Space, pp. 102-109.
- [11] B. Guinot 1996, "Application of General Relativity to Metrology," *Metrologia*, International Reports, in press.
- [12] C. Thomas 1996, "Stability and accuracy of the International Atomic Time TAI," Proceedings of the 10th European Frequency and Time Forum (EFTF), 5-7 March 1996, Brighton, UK (IEEE Conference Publication 418), pp. 520-527.
- [13] J. Azoubib, M. Granveaud, and B. Guinot 1977, "Estimation of the scale unit duration of time scales," *Metrologia*, **13**, 87-93.
- [14] Comité Consultatif pour la Définition de la Seconde 1993, Report of the 12th Meeting, BIPM, Sèvres, France, 74 pages.
- [15] W. Lewandowski, J. Danaher, and W.J. Klepczynski 1996, "GLONASS common-view time transfer between North America and Europe and its comparison with GPS," Proceedings of the 10th European Frequency and Time Forum (EFTF), 5-7 March 1996, Brighton, UK (IEEE Conference Publication 418), pp. 388-392.
- [16] W. Lewandowski, P. Moussay, P. Guérin, F. Meyer, and M. Vincent 1997, "Testing the Motorola Oncore GPS Receiver and temperature-stabilized antennas for time metrology," these Proceedings.

- [17] W. Lewandowski, J. Azoubib, A.G. Gevorkyan, P.P. Bogdanov, W.J. Klepczynski, M. Miranian, J. Danaher, and D.W. Allan 1997, "*A contribution to the standardization of GPS and GLONASS time transfers,*" these Proceedings.

Acronyms

BIPM	Bureau International des Poids et Mesures, Sèvres, France
BNM-LPTF	Bureau National de Métrologie, Laboratoire Primaire du Temps et des Fréquences, Paris, France
CCDS	Comité Consultatif pour la Définition de la Seconde
CGPM	Conférence Générale des Poids et Mesures
CIPM	Comité International des Poids et Mesures
CRL	Communications Research Laboratory, Tokyo, Japan
GLONASS	Global Navigation Satellite System
GPS	Global Positioning System
IERS	International Earth Rotation Service, Paris, France
INPL	National Physical Laboratory of Israel, Jerusalem, Israel
IPA	Institut d'Astronomie Appliquée, St. Petersburg, Russia
ISI	Innovative Solutions International, Washington D.C., USA
ISO	International Standardization Organization
ITRF	IERS Terrestrial Reference France
LPTF-FO1	Fontaine No. 1 du LPTF (Cs fountain No. 1 of the LPTF)
NIST	National Institute of Standards and Technology, Boulder, Colorado, USA
NIST-7	Primary frequency standard No. 7 developed at the NIST
NML-CSIRO	National Measurement Laboratory, Commonwealth Scientific and Industrial Research Organization, Sydney, Australia
NRC	National Research Council, Ottawa, Canada
OP	Observatoire de Paris (Paris Observatory), Paris, France
ORB	Observatoire Royal de Belgique, Brussels, Belgium
PTB	Physikalisch-Technische Bundesanstalt, Braunschweig, Germany
SI	Système International d'Unités (International System of Units)
TAI	Temps Atomique International (International Atomic Time)
UTC	Coordinated Universal Time

Appendix I
RECOMMENDATION S 1 (1996)
Primary frequency standards

The Comité Consultatif pour la Définition de la Seconde,
considering

- the importance of maintaining an adequate number of primary frequency standards to assure the accuracy and long-term stability of TAI,
 - that new primary standards are being developed using new technology,
 - that these new standards are significantly more accurate than the traditional primary standards upon which TAI and UTC have been based in the past,
 - that in consequence, the accuracy of TAI and UTC will rapidly become dependent on these new standards,
 - that considerable resources are required to maintain primary frequency standards as operational facilities to assure the accuracy of TAI,
- recalling* its Recommendation S 1 (1993) on the accuracy of primary frequency standards,
requests national metrology institutes and other laboratories developing new primary standards, to make every effort to provide the human and other resources necessary to maintain as operational facilities these new standards upon which the accuracy of TAI and UTC is based.

RECOMMENDATION S 2 (1996)
Blackbody frequency shift

The Comité Consultatif pour la Définition de la Seconde,
considering

- that the relative uncertainty of some primary frequency standards is now below 5×10^{-15} and that even smaller uncertainties are expected in the near future,
 - that the relative frequency shift due to blackbody radiation may be as large as -1.7×10^{-14} at 300 K,
 - that there is a growing need for more accurate comparisons of the frequencies of primary standards,
 - that, even though no measurement has yet been made of the cesium blackbody radiation frequency shift, there is consistency between the theoretical understanding and experimental verification of AC Stark shift measurements in other systems,
 - that there is a need for uniformity in reporting the frequency and the corresponding uncertainty of primary standards, and
 - that there is a need for improved accuracy in TAI,
- recommends* that a correction for blackbody radiation be applied to all primary frequency standards.

RECOMMENDATION S 3 (1996)
Correlations among clocks contributing to TAI

The Comité Consultatif pour la Définition de la Seconde,
considering

- that there have been reports of correlations among clocks operating at a given site,
 - that the basis upon which TAI is calculated assumes that such correlations do not exist,
 - that correlated behavior of clocks contributing to TAI can lead to a degradation of TAI,
 - that there is insufficient evidence to warrant taking any specific action at this time,
- requests*
- that laboratories contributing to TAI perform clock-data studies as well as experiments aimed

at developing a better understanding of correlations among clocks and quantifying these effects,
— that the results of such work be shared with all laboratories contributing to TAI and be sent to the Bureau International des Poids et Mesures.

RECOMMENDATION S 4 (1996)¹
Coordination of satellite systems providing timing

The Comité Consultatif pour la Définition de la Seconde,
considering

- the international value of having both Global Positioning System (GPS) and Global Navigation Satellite System (GLONASS) operational with a composite contribution of 48 satellites,
- the desirability of using either or both systems interchangeably,
- that currently significant time differences exist between the two systems,
- that significant differences exist in the coordinate reference frames used for each,
- that other important satellite timing systems are now being designed and developed,

recommends

- that the reference times (modulo 1 second) of satellite navigation systems with global coverage² be synchronized as closely as possible to UTC, — that the reference frames for these systems be transformed to be in conformity with the terrestrial reference frame maintained by the International Earth Rotation Service (ITRF), — that both GPS and GLONASS receivers be used at timing centers.

Appendix II

Section 7 of the Report of the 13th Meeting of the CCDS, 1996:

[...] A formal request from the CCDS to this sub-group [Sub-group on GPS and GLONASS Time Transfer Standards] was written with the objective of strengthening contacts between the manufacturers of GPS and GLONASS time receivers and the community.

The Comité Consultatif pour la Définition de la Seconde,
noting the marked improvements in the quality of both primary frequency standards and commercial atomic clocks,

recognizing that the performance of commercially available GPS and GLONASS receivers currently used does not meet time transfer requirements,

asks the CCDS Sub-group on GPS and GLONASS Time Transfer Standards

- to contact manufacturers of receivers and request them to adapt the hardware and software of their systems to match the requirements of time and frequency laboratories so that their receivers can record the signals of GPS and GLONASS satellites in dual-frequency mode, in multi-channel mode and, in a data format defined by the sub-group, can provide internal calibration and be as insensitive as possible to environmental conditions,
- to keep time and frequency laboratories informed of its actions.

¹This Recommendation was adopted by the CIPM as Recommendation 1 (CI-1996) at its 85th meeting in September 1996.

²Such as Global Positioning System (GPS), Global Navigation Satellite System (GLONASS), International Maritime Satellite Organization (INMARSAT), Global Navigation Satellite System 1 (GNSS1), Global Navigation Satellite System 2 (GNSS2).

Questions and Answers

DAVID ALLAN (ALLAN'S TIME): I think you make an excellent point. For example, you can show that in order to evaluate many of the systematics in clocks, you need to know the noise types before you do that. And so you have to bring the two together to estimate each other. So to bring these two different types of uncertainties and to bring them under one hat I think is an extremely important step. I commend you for what you're bringing out to us.

IEN TIME AND FREQUENCY METROLOGICAL ACTIVITY AND SUPPORT TO USER NEEDS

F. Cordara, V. Pettiti, and P. Tavella
Istituto Elettrotecnico Nazionale Galileo Ferraris
Corso M. d'Azeglio, 42 - 10125 Torino, Italy
Tel. +39 11 39191, Fax +39 11 346384, e-mail: metf@tf.ien.it

Abstract

The increased importance of time and frequency metrology in scientific and industrial applications has raised a request of a wider spectrum of services from the national standard laboratories. On the metrological side, a new generation of frequency standards and the worldwide availability of extremely accurate time dissemination systems have opened new perspectives of research and applications. The IEN Time and Frequency Laboratory, charged with the realization and dissemination of the Italian standard time, in order to meet the requests of different users has been engaged in different activities that are reviewed in this paper, where also the future possibilities are discussed.

INTRODUCTION

The IEN Time and Frequency Laboratory, which has been charged by law in 1991 with the research, realization, and dissemination of the SI unit of time for Italy, has been involved since the seventies in the realization of a local UTC time scale, known as UTC(IEN), and has been contributing with its cesium clocks to the ultimate reference of time UTC established by BIPM. The traceability of UTC(IEN) to the international time scale is realized by two GPS receivers, following the complete BIPM common-view schedule for Europe, and with the software updated according to the technical directives of the CGGTTS Working Group. The dissemination of UTC(IEN) to the real-time user is performed in different ways, as described in the following, with accuracies ranging from 0.05 s to 100 μ s.

As regards a major issue coming from the industrial market, that of traceability of secondary standards to the national standard of time and frequency, a variety of solutions are offered through different synchronization techniques, namely coded time signals, passive TV, GPS comparisons, and clock transportation, with uncertainties, at the 1σ level, ranging from 1×10^{-9} to 5×10^{-14} . Another means of dissemination is the accreditation activity performed by IEN for the Italian Calibration Service (SIT) that has been a response of the National Metrology Institutes (NMI) to the hugely increased request of traceability to the SI units coming from the calibration and test laboratories as a consequence of the implementation in industries of Quality Assurance Standards, such as ISO 9000 series and EN 45001. In this framework, interlaboratory comparisons are organized to check the competence level of the laboratories accredited for frequency and to ensure the traceability to the national standard, therefore completing the Regional Metrological scheme, foreseen to be extended worldwide in the near future, establishing a reliable comparability of measurements, results that will be of great help in removing the technical barriers to the international trade.

Training courses for technicians, consultation on the development of calibration procedures, and studies on the implementation of the ISO *"Guide to the Expression of Uncertainty in Measurement"* in the field of frequency calibration are also part of the dissemination activity performed. In connection with the implementation of the digital synchronization networks in telecommunications, studies devoted to the statistical characterization of the phase noise effects and of the transferred instabilities in slaved clocks have also been performed.

UTC(IEN) AND TA(IEN) REALIZATION

The national time scale UTC(IEN) is currently realized with five commercial cesium standards, two of which are Hewlett-Packard 5071A of the High Performance type, and the rate of the selected Master Clock is steered to UTC(BIPM), using the internal microstepper, in order to maintain the national reference of time well within $\pm 0.5\mu\text{s}$ of UTC and to hold the average frequency within $\pm 1 \cdot 10^{-13}$ of the same reference. A noticeable improvement in the compliance to these limits has been obtained since the introduction in 1994 of the new HP cesium clocks in the generation of the IEN time scale. To improve the long-term stability and the reliability of UTC(IEN), an ensemble time algorithm^[1] has been implemented since 1995 and the data of the independent atomic time scale TA(IEN) are regularly sent to BIPM.

To evaluate the performances of these two time scales, in Fig. 1 are reported the time differences UTC - UTC(IEN) and TAI - TA(IEN), from BIPM Circulars T, for the period May 1995 - October 1996, with additional information about the Master Clock used and the microstepper correction applied to steer it to UTC. Up to MJD 50169 (27 March 1996), the HP5071 #219 and the HP5061B cesiums were maintained in the clock room with tight temperature and humidity control; the room was abandoned after that date for technical problems of the conditioning system. Since that date, all the clocks have been operating in the Time and Frequency Laboratory, where the environmental changes are more consistent. The mean frequency departures of UTC(IEN) computed from these data were found to be equal to $+0.6 \cdot 10^{-14}$ for 1995 (MJD 49839 to 50079) and to $-1.6 \cdot 10^{-14}$ for 1996 (MJD 50084 to 50384). In Figs. 2 and 3 are shown the frequency instabilities (ADEV) of the two IEN time scales versus UTC and TAI, for observation times from 5 to 160 days, computed with the overlapping sample technique, and in Fig. 4 are reported the mean rates of the IEN clocks versus UTC computed using the Circular T data smoothed with a 30-day moving filter.

Looking at the results obtained in the IEN time scales, the following considerations can be made. Even if the new cesium clocks give a significant improvement on the long-term stability, instabilities of a few units in 10^{-14} can still be detected, causing trouble in achieving the goal of a synchronization at 100 ns with respect to UTC. By an inspection of Fig. 4, it appears that in the second half of 1996, in correspondence with the removal of the clocks from the dedicated room, a small but appreciable increase of the instability is observable, mostly due to the variation of temperature, which causes also a certain correlation among clocks. But some sudden frequency variations were detected on a 5071A cesium even in the controlled environmental situation, as seen in the first part of Fig. 4. Similar anomalies have been observed also by other laboratories. This makes difficult the modelling of clock performances and, thus, their correct prediction. Such aspect requires further investigation.

The following improvements in the time scale realization are expected. First, the move of the clocks in a new temperature-controlled room near to the Time and Frequency Lab, and the addition of a third HP5071A cesium in the ensemble. Second, an optical fiber link is foreseen connecting with the Italian telecommunication research center (CSELT), located about 10 km from IEN. This connection would guarantee the safe introduction of the two HP5071A

clocks available at CSELT, thus increasing the number of new generation clocks realizing the national time scale. Due to these changes in the ensemble, also some modification in the algorithm seems advisable. Particularly the weighting procedure, now based on the observation of one year of data to detect the largest seasonal fluctuation, is probably to be changed by the introduction of an exponential moving average, better suited to estimate the current clock behavior and giving less importance to older data. By the modelling of the long-term frequency variations, also the adaptation of the frequency prediction techniques will be investigated.

INTERNATIONAL TIME TRANSFERS

An average of 45 GPS common-view comparisons are routinely performed daily to relate UTC(IEN) to the international time scale UTC, and the IEN results are also compared weekly with those of the Physikalisch-Technische Bundesanstalt (PTB) - Germany and of the Institute of Radio Engineering and Electronics (IREE-TP) - Czech Republic. The availability of two GPS receivers of different manufacturers in these laboratories has given us the chance to investigate in 1995 the noise limits of this synchronization system and the long-term stability of the equipment used, both using the BIPM regular common-view schedule and a special one featuring equally spaced tracks with high-elevation-angle satellites.

The results, reported in [2], showed a time deviation over 1 hour of less than 2 ns for the link between IEN and IREE, but also the presence of daily variations of several nanoseconds that could be related to the sensitivity of the receiving antennas and down-converters to outdoor temperature variations, and also to the use of a rough model for the computation of the ionospheric correction inside the receivers. The long-term behavior of the two receivers at IEN had been already investigated over more than one year, in 1993 and in 1994, averaging the daily synchronization results versus GPS time of each receiver and computing their differential delay; a peak-to-peak variation of 5 ns and a correlation between the differential delay and the outdoor temperature was found.

On the other end, the delay of the NBS/GPS reference receiver of IEN, calibrated by BIPM at the end of January 1995 by means of a portable reference GPS receiver, was found in good agreement (-20 ns vs. -18 ns) with a previous calibration performed in 1986.^[3]

From October to December 1995, IEN joined the international synchronization experiment based on INTELSAT satellites at 307° , using a Direct Broadcasting Satellite receiving station and a MITREX modem, to test the frequency and time transfer capability of such systems used in a one-way mode.^[4] In the final setup, the satellite beacon frequency was used as a reference to lock an oscillator of the conversion chain to compensate for the Low Noise Converter oscillator drift that would have exceeded the tight input frequency tolerances of the modem used. The one-way synchronization measurements were performed during the 300 s range phase that preceded the European two-way sessions, using the range data from three laboratories to correct for the satellite position delays.

As a sample of the receiving system performances, in Fig. 5 are reported for the link IEN-NPL the frequency and time instability estimators MDEV and TDEV, for integration times between 1 s and 2000 s, after the satellite movement has been modelled with a fifth-order polynomial regression. In Fig. 6 we have reported the comparisons between the time scales of IEN and of the Technical University of Graz (TUG) from 6 to 29 November 1995, as obtained by the one-way INTELSAT measurements corrected with the range data, and by GPS common view. The standard deviation of the residuals between the two synchronization systems is 4 ns.

In order to join the two-way network, that will start its regular schedule again next year, a VSAT

(Very Small Aperture Terminal) RF Transceiver designed for a two-way satellite communication system and operating in the whole Ku-band frequency range (14.0 - 14.5 GHz Tx, and 10.95 - 12.75 GHz Rx) has been installed in September 1996 near the Time and Frequency Laboratory. The system is equipped with a 1.8 m dish antenna, a 4 W High Power Amplifier, and a Low Noise Amplifier with a noise temperature of 110 K and a frequency agility of 1 kHz in the transmitting and receiving chains. A bench testing, using MITREX codes, of the delay instabilities of this equipment (Tx plus Rx) for different signal-to-noise ratios (C/N), supplying to the receiving part the transmitted RF signal converted by a local mixer and synthesizer, has been performed and the results are reported in Fig. 7. For the three typical simulated C/N values, a $\tau^{-3/2}$ slope is shown for MDEV and an uncertainty limit of the order of $1 \cdot 10^{-13}$ over 500 s is reached by the system. It is planned to have this station operative in the first half of 1997, after receiving approval from the national INTELSAT signatory.

UTC(IEN) DISSEMINATION SOURCES

The dissemination in real time of UTC(IEN) to the Italian users is performed by means of dedicated services available through the reception of the regular programs broadcasted by the national broadcasting company (RAI), by a time-coded information distributed on the telephone network, and by the synchronization of two NTP (Network Time Protocol) primary servers. The coded time signals generated by IEN and broadcasted 15-25 times per day by the RAI FM and AM transmitters, apart from being the most common source of the time of the day information in Italy, can be used both for the synchronization of remote clocks with a precision of the order of 0.1 ms and for disciplining the frequency of quartz oscillators at the level of $1 \cdot 10^{-9}$.^[5] Also, the time of the day announcement service made by the Italian Telecom is synchronized by these signals.

Fig. 8 shows the format of the RAI time code (SRC), updated in 1995 to include the information on the current year and warnings about the switching from standard to daylight saving time and the introduction of a leap second on UTC time scales. The coded time signals transmitted from the RAI studios in Rome are continuously monitored at IEN to check the propagation delays and to compare the controlled clocks of some users. A sample of the long-term behavior of this delay is given in Fig. 9, reporting the results obtained from August to October 1996, where it can be seen that the majority of the data is within a range of 0.1 ms. The coded time and date information (CTD) service on telephone lines, following the format agreed in 1991 among some European laboratories, is addressed mainly to the synchronization of PC clocks and has been operative at IEN since 1991.^[6] This service is operated by several European timekeeping laboratories, mostly with the capability of round-trip delay determination, a feature that has not been implemented in our case. A set of three time-code generators provides the redundancy of the system that cannot be accessed from abroad.

To provide an average compensation of the delay at the user side, the 1 pps reference in the code (transition from carriage return to line feed characters) is anticipated by 70 ms. An investigation on the effective propagation delays at different distances and on the synchronization precision obtainable has been recently performed using a Time Code Generator and an On Time Marker (OTM) monitor, both developed at the Technical University of Graz. To estimate the half-round trip delay, the GDM (Generator Delay Measurement) function of the generator and dedicated software were used and, when possible, the time of arrival of the code time reference (OTM) has been measured versus UTC(IEN) with an external time-interval counter. The GDM results are averaged over 8 consecutive measurements, while the OTM ones are averaged over 50 samples. The tests were performed in different laboratories: at IEN, receiving the signal back

through the local telephone exchange or connecting to the services of other countries (Austria - TUG, Germany - PTB, the Netherlands - VSL, Portugal - IPQ, and Switzerland - OFMET) and in other Italian institutions (Cagliari Observatory in Sardinia, Hewlett-Packard Italy - Milan, Vitrociset - Rome) that are synchronized to the IEN time scale.

In Fig. 10 are reported the half-round trip results obtained in the GDM mode and, in the case of the IEN local link and of the Hewlett-Packard one, also the calibration of the one-way (OTM) delay. For the other connections, where only 4 synchronizations were available; the results are reported in Table 1. One can observe in all cases a residual time offset between the OTM and the GDM evaluation ranging from 2 to 7 ms inside the national network, with outliers of more than 10 ms for international calls. The standard deviation over different calls from the same location has been of the order of 1-2 ms. Looking to the average delays found, the 70 ms advance given to the IEN CTD time marker allows synchronization inside the country, even without a calibration of the path delay, within ± 20 ms.

A final consideration that can be made is that the modem delays and their asymmetry are more influential than the geographical distance in the synchronization error. The time of the day, synchronized by the IEN standard signals, and general information about the activity of the Time and Frequency Lab can be accessed via the World Wide Web at the address "www.iен.it". Moreover, two NTP primary servers located in the IEN buildings are directly synchronized by the CTD time reference previously described. This last service can be accessed via the Internet at the following server addresses: "time.iен.it" and "tempo.cstv.to.cnr.it".

TRACEABILITY TO UTC(IEN)

In the framework of the Italian Calibration Service SIT, the IEN has already accredited 16 laboratories for frequency and performs the remote calibration of their reference oscillators using a variety of synchronization methods, depending on the uncertainty level requested. In a similar way, the traceability to the national time scale is also guaranteed to some 15 other metrological laboratories. The uncertainty levels recognized to the accredited centers can range from $1 \cdot 10^{-9}$ to $3 \cdot 10^{-13}$, depending on the reference oscillator and on the synchronization system used. In Fig. 11 is shown a sample over a three-month period of the calibration data of a remote disciplined quartz oscillator. In this case, the synchronization and disciplining system used, based on the IEN/RAI coded time signals, ensures the removal of the frequency drift and a traceability to UTC(IEN) within a few parts in 10^{-10} . The traceability to the IEN time scale is also obtainable using the GPS signals, either with the common-view technique or using a kind of "melting pot" technique that is especially suited to the multichannel receivers found in disciplined devices.^[7]

The characterization of this type of receiver is of particular interest also for its possible use in the primary laboratories as an alternative to the more expensive and not very reliable timing receiver presently on the market. A sample of the uncertainty obtained in the frequency calibration of a remote HP5071A clock using a GPS multichannel receiver on the user side, and the reference receiver at IEN, can be seen in Fig. 12. The daily time differences between UTC(IEN) and UTC(Lab), obtained computing a mean value from the 24 series of 100 s measurements at the remote site and from the average of all the measurement collected at IEN according to the common-view schedule, have been used to compute each data point. The standard deviation level obtained, using a 5-day moving average filter, is of the order of $5 \cdot 10^{-14}$. Finally, concerning the well-known passive television method that is still used in 50% of the Italian laboratories, an example of the capability (ADEV) of the system used in common view between IEN and CSELT laboratories (10 km) to compare two HP5071A High

Performance standards is shown in Fig. 13. These results, that have been obtained computing the time differences between 60 measurements one second apart, repeated at both sides every 2 minutes, with improved TV receivers and sync separators developed by CSELT, demonstrate that the noise level of such arrangement after 1 day reaches the nominal noise level due to the clocks compared.

STATISTICAL PROBLEMS IN TELECOMMUNICATIONS AND INDUSTRIAL APPLICATIONS

The expertise gained in statistics and mathematical modelling in time and frequency metrology has found some important applications for different industrial needs. Firstly, IEN has been charged by the Italian telecommunication research center (CSELT) to investigate on the stability characteristics of clocks to be used in the Synchronous Digital Hierarchy. The investigation, either on theoretical aspects or in experimental evaluations, allowed the clarification of the relationships among the different families of statistical tools used to specify clock stability (power spectra, variances, peak-to-peak behavior) and the evaluation of the transfer of noises along a chain of phase-locked clocks.^[8,9]

A second activity concerned the implementation of the ISO *"Guide to the Expression of Uncertainty in Measurement."* Recently IEN was charged by the EAL Task Force revising WECC Doc. 19 to prepare some examples of uncertainty evaluation in time and frequency. Therefore, two procedures taken among the typical measurement problems of time and frequency calibration laboratories were developed^[10] and will be used also in support to the Italian calibration service. On such a subject IEN launched also a EUROMET proposal (#382/1996). On a contract given by an Italian high-technology industry, IEN studied also the possibility of estimating the optimal calibration interval of a measuring instrument by using suitable stochastic models. Calibration error may be in fact one of the most important sources of measurement errors but, on the other hand, calibrations have an overall cost and may imply an interruption of the production process. Using the theory of stochastic processes and time series analysis, some suitable models have been developed that seemed promising after a preliminary experimental validation.^[11] Due to the qualification gained in this field, an IEN researcher was called to work as expert in the ISO Technical Committee 176 dealing with standardization of suitable procedures (also in measurements) to assure quality programs.

CONCLUSIONS

The IEN time and frequency metrological activities cover a wide range of the needs of Italian users in research, traceability, and standardization. To improve the accuracy, stability, and reliability of UTC(IEN) realization and dissemination, a number of actions are going to be undertaken, such as the research on a cesium fountain primary standard, the increase of the number of new cesium standards, and the realization of new standard signals distribution links and equipment. The use of higher resolution measurement systems, more frequent clocks intercomparisons, and security systems on the reference frequency and time signals are also foreseen. Concerning the time comparisons systems, the two-way station will be put in operation and studies on the accuracy of GPS receivers will be carried out. A very consistent increase of the accreditation activity is also expected in the near future and, finally, a database of the relevant measurement results performed will be made available to the user through electronic mail.

mail.

ACKNOWLEDGMENTS

The authors wish to thank the following people and institutions for their very helpful cooperation: D. Kirchner and H. Ressler (Technical University of Graz, Austria), D. Beretta (Hewlett-Packard, Italy), L. Mureddu (Cagliari Observatory, Italy), D. Tonti (Vitrociset, Italy), and the colleague S. Denasi.

REFERENCES

- [1] F. Cordara, G. Vizio, P. Tavella, and V. Pettiti 1994, "*An algorithm for the Italian atomic time scale*," Proceedings of the 25th Annual Precise Time and Time Interval (PTTI) Applications Applications and Planning Meeting, 29 November-2 December 1993, Marina del Rey, California, USA (NASA CP-3267), pp. 389-400.
- [2] J. Cermák 1996, "*A GPS parallel common-view experiment*," Proceedings of the 10th European Frequency and Time Forum (EFTF), 5-7 March 1996, Brighton, UK (IEEE Conference Publication 418), pp. 296-301.
- [3] W. Lewandowski, and P. Moussay 1995, "*Determination of the differential time correction between GPS time equipment located at the Observatoire de Paris, France, and at the Istituto Elettrotecnico Nazionale, Torino, Italy*," BIPM Report 95/07.
- [4] G. Brida, F. Cordara, V. Pettiti, and A. Godone 1996, "*One-way frequency and time transfer in the frame of INTELSAT two-way experiment*," Proceedings of the 10th European Frequency and Time Forum (EFTF), 5-7 March 1996, Brighton, UK (Conference Publication 418), pp. 423-429.
- [5] F. Cordara, V. Pettiti, and P. De Giorgi 1994, "*Time and frequency traceability sources in the Italian Calibration Service*," Proceedings of the 8th European Frequency and Time Forum (EFTF), 9-11 March 1994, Weihenstephan, Germany, pp. 1029-1038.
- [6] F. Cordara, V. Pettiti, R. Quasso, and E. Rubiola 1993, "*Performances of a date dissemination code on telephone lines using commercial modems*," Proceedings of the 24th Precise Time and Time Interval (PTTI) Applications and Planning Meeting, 1-3 December 1992, McLean, Virginia, USA (NASA CP-3218), pp. 243-254.
- [7] F. Cordara, and V. Pettiti 1996, "*GPS disciplined oscillators for the traceability to the Italian time standard*," Proceedings of the 27th Precise Time and Time Interval (PTTI) Applications and Planning Meeting, 29 November-1 December 1995, San Diego, California, USA (NASA CP-3334), pp. 113-124.
- [8] R. Bonello, A. Manzalini, A. Godone, C. Novero, and P. Tavella 1995, "*Stability characterization of stand alone synchronisation equipments*," in Proceedings of the 9th European Frequency and Time Forum (EFTF), March 1995, Besançon, France, pp. 220-225.
- [9] P. Tavella, A. Godone, and S. Leschiutta 1997, "*The range covered by a random process and the new definition of MTIE*," these Proceedings.

- [10] P. Tavella 1996, "*Uncertainty evaluation in T&F calibrations*," submitted to EAL Task Force revising WECC Doc. 19-1990.
- [11] P. Tavella, A. Bobbio, S. Costamagna, and A. Montefusco 1996, "*Stochastic drift models for the determination of calibration intervals*," Proceedings of Advanced Mathematical Tools in Metrology, September 1996, Berlin, Germany.

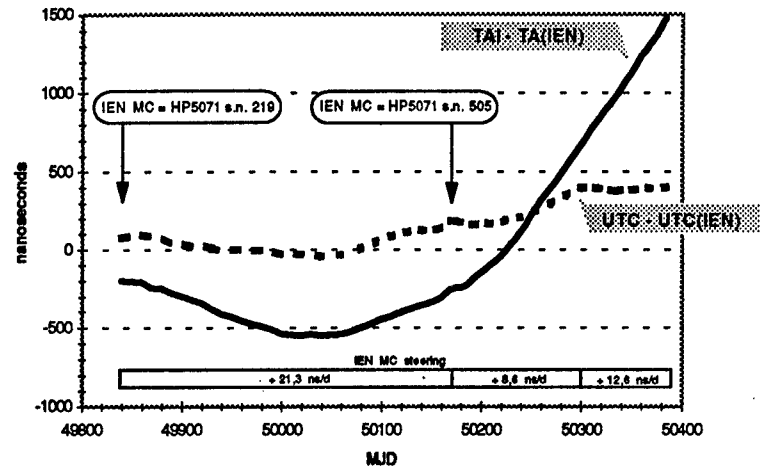


Fig. 1 - UTC(IEN) and TA(IEN) from May 1995 to October 1996 (MJD: 49839 - 50384) - BIPM Circular T

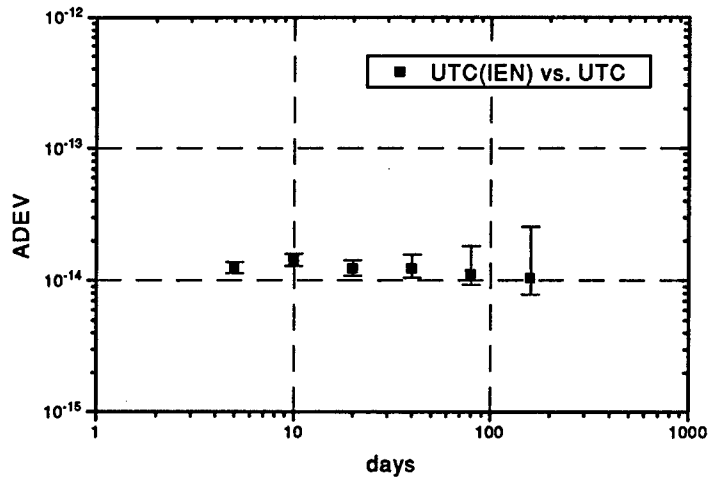


Fig. 2 - Frequency instability of UTC(IEN) vs. UTC from May 1995 to October 1996 - BIPM Circular T

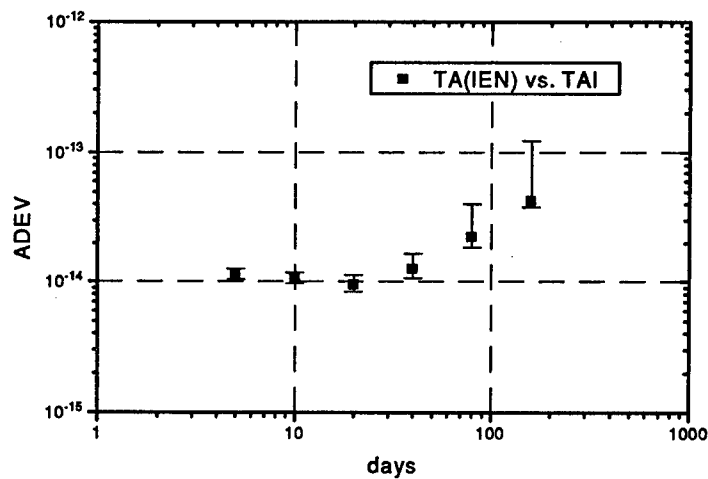


Fig. 3 - Frequency instability of TA(IEN) vs. TAI from May 1995 to October 1996 - BIPM Circular T

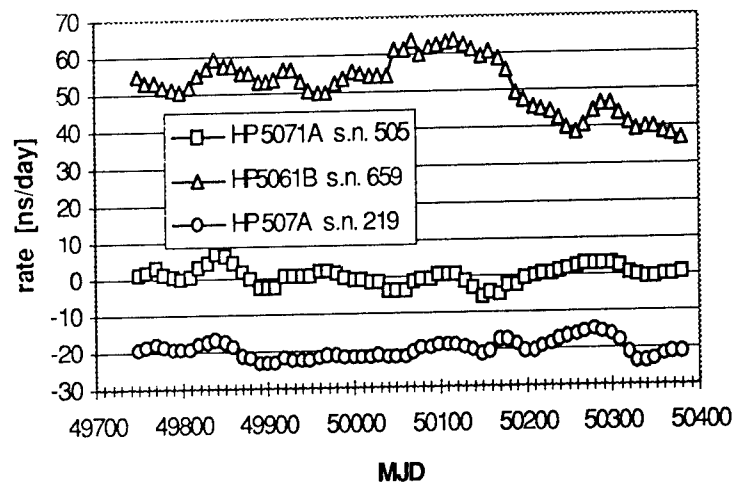


Fig. 4 - Rates of the IEN cesium clocks vs. UTC from January 1995 to October 1996

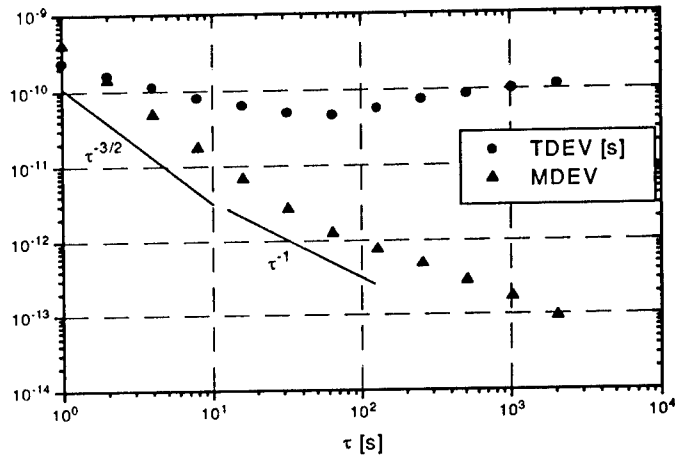


Fig. 5 - IEN / NPL synchronization link instabilities

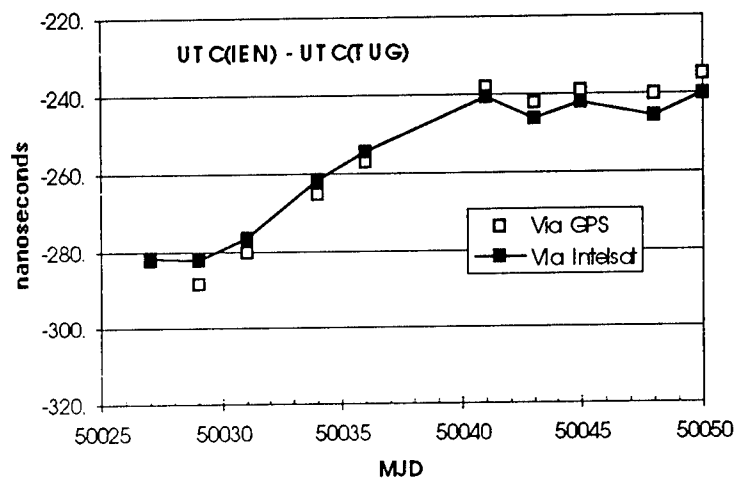


Fig. 6 - IEN / TUG time scales comparisons

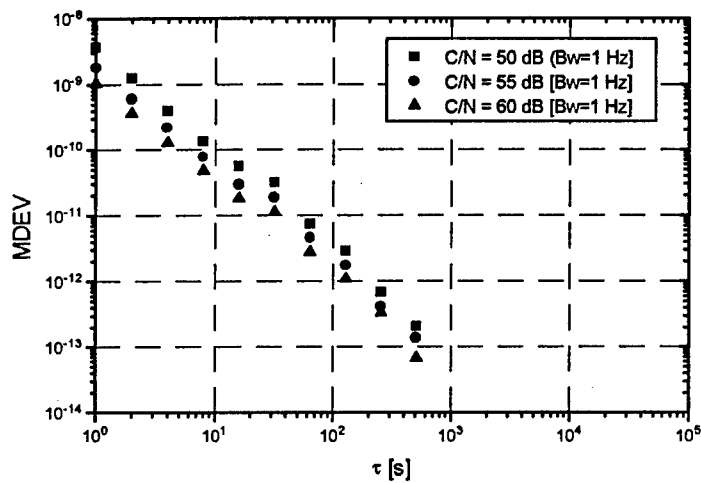


Fig. 7 - IEN two-way station instability for different signal to noise ratios

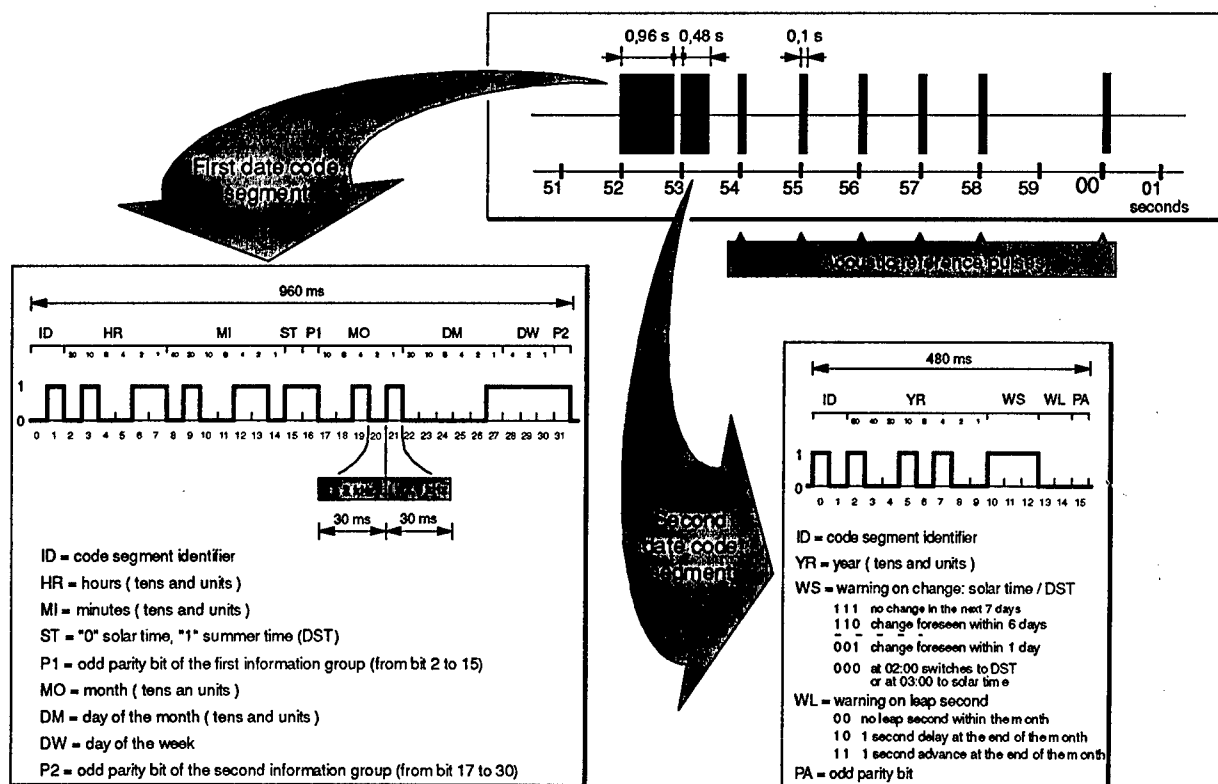


Fig. 8 - IEN / RAI Time Code format

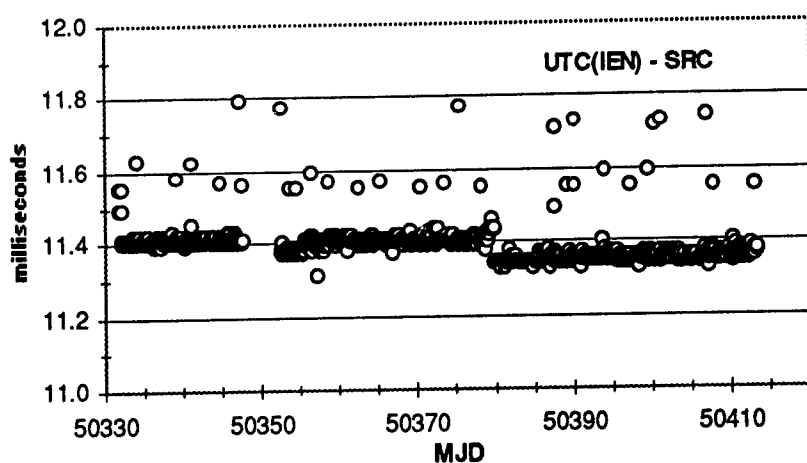


Fig. 9 - Long term delay variations of the SRC signals received at IEN

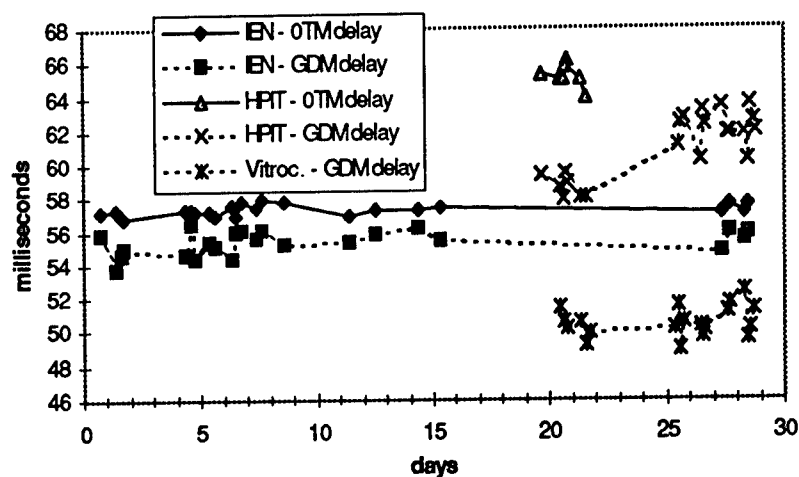


Fig. 10 - Telephone time code half-round trip and calibration delays

Lab.	OTM	$\sigma(\text{mean})$	$\sigma(\text{single})$	GDM	$\sigma(\text{mean})$	$\sigma(\text{single})$	OTM-GDM	Distance
	[ms]	[ms]	[ms]	[ms]	[ms]	[ms]	[ms]	[km]
IEN(I)	57.3	0.3	2.4 - 2.6	55.3	0.5	0.9 - 1.5	2.0	-
CAO(I)	-	-	-	83.8	1.5	1.3 - 1.8	-	650
OFMET(CH)	55.3	0.4	0.3 - 0.4	67.2	0.4	0.2 - 0.4	-11.9	330
TUG(A)	69.1	0.5	2.5 - 2.8	66.9	0.9	1.2 - 1.6	2.2	649
PTB(D)	45.0	0.6	0.1 - 0.3	51.5	0.9	0.1 - 0.2	-6.5	835
VSL(NL)	47.0	0.3	0.2 - 0.4	49.5	0.5	0.1 - 0.3	-2.5	813
IPQ(P)	68.3	0.9	0.3 - 0.4	81.9	0.4	0.2 - 0.3	-13.6	2195

Table 1 - Telephone time code half-round trip and calibration delays

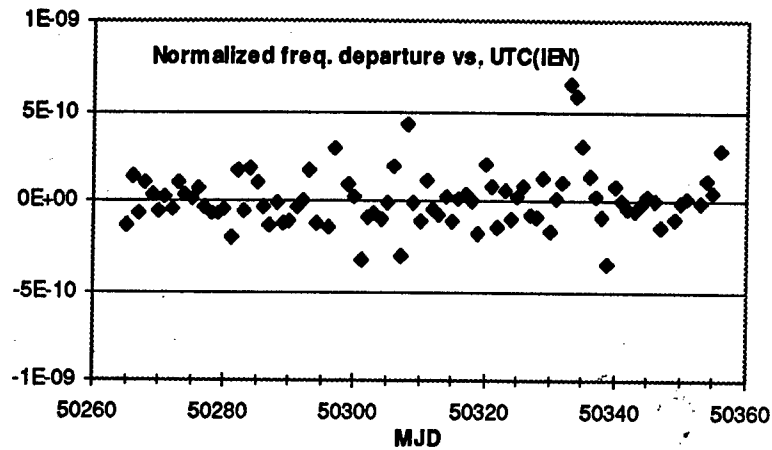


Fig. 11 - Ovenized quartz oscillator disciplined by IEN / RAI time signals

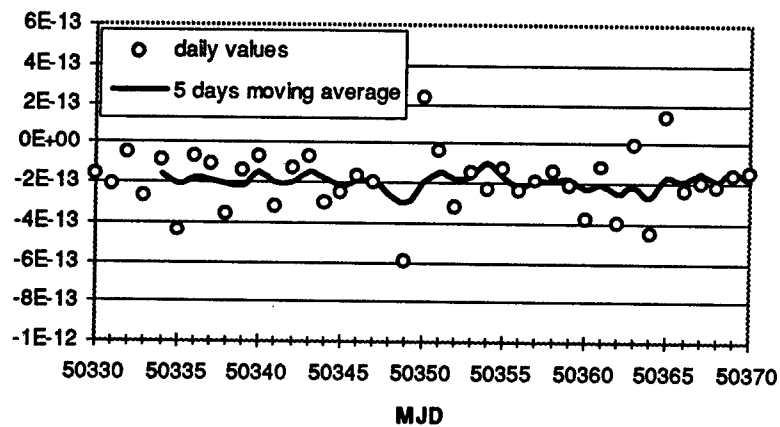


Fig. 12 - Frequency calibration of a remote cesium using a GPS multichannel receiver

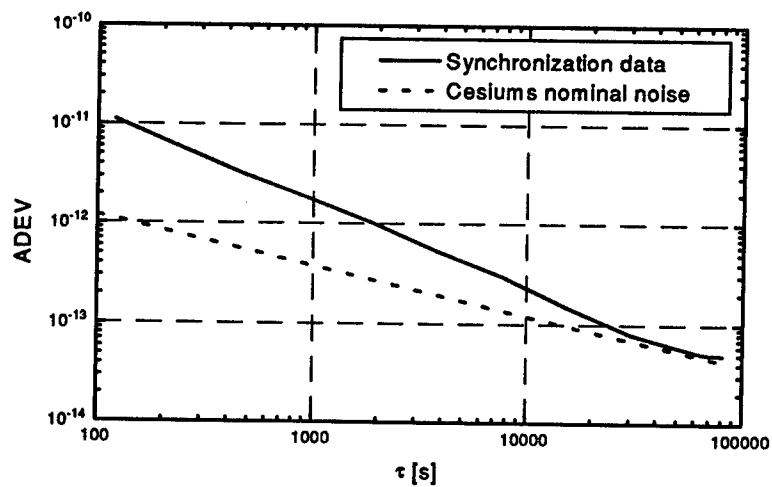


Fig. 13 - Frequency instability of two cesium clocks compared via the passive TV method in common-view

Questions and Answers

DAVID ALLAN (ALLAN'S TIME): Two quick questions on the chart you have showing the frequency performance of the 5071s. Can you show that chart quickly?

FRANCO CORDARA: Yes.

DAVID ALLAN: First question is what is the reference? Second question, there appears to be the correlation of the two, has that been correlated with an environmental parameter? Temperature, humidity, pressure?

FRANCO CORDARA: The reference chosen has been UTC, because I think it was the best reference in our case. And the correlation that can be seen here on the three standards is due to the fact that the temperature in the normal time and frequency lab has been changed this summer and fall by 3 degrees. And it has seasonal changes which are voluntarily performed in the lab. And, of course, the temperature is not stable within 1 degree and they have 2 degrees.

We have noticed from the temperature recordings that these were corresponding to about 3-degree variations. And here to lowering of the same temperature.

TIME AND FREQUENCY KEEPING AND ITS DISTRIBUTION SYSTEM AT CRL

Michito Imae, Mizuhiko Hosokawa, Yuko Hanado,
Kuniyasu Imamura, Atsushi Otsuka, and Takao Morikawa
Communications Research Laboratory
4-2-1, Nukuikita-machi, Koganei, Tokyo, 184 Japan
tel: +81-423-27-7566, fax: +81-423-27-6686
e-mail: imae@crl.go.jp

Abstract

As a national frequency standards laboratory in Japan, Communications Research Laboratory (CRL) is doing research and development work on a primary frequency standard. Besides the primary standard, CRL is in charge of the generation of local UTC, UTC(CRL), and its time and frequency distribution via HF and LF radio signals, telephone line, and computer network. CRL contributes to TAI not only atomic clock data, but also as one of the node laboratories of the international GPS time transfer network of the BIPM. For this purpose CRL is studying the GPS ionospheric measurement system and two-way time transfer using communication satellites. In this paper we will present activities on time and frequency standards at CRL.

1 INTRODUCTION

Communications Research Laboratory (CRL) has a long history, more than 50 years, involving time and frequency standards, and several remarkable results were achieved. But after around the epoch when its name was changed from RRL (Radio Research Laboratory) to CRL, the number of researchers in time and frequency were reduced because of several reasons. One of them was that CRL shifted and expanded its research area to communication and information engineering. Another one was that CRL performed research and development on applications of time and frequency standards.

At present we are considering how to do basic research work and service on time and frequency standards to contribute to science, engineering, and social life. In this paper we describe the present and near future activities in the field of time and frequency at CRL. Work in this field falls into following areas:

- developing primary frequency standards,
- determining and keeping frequency and time standards,
- disseminating frequency and time standards, and
- comparing standards to those established by organizations in foreign countries. And the following basic research activities will support the above items:
 - research and development of technology for precisely measuring frequency and time,
 - theoretical research.

2 TIMEKEEPING AT UTC(CRL)

2.1 Primary Atomic Frequency Standard^[1-5]

(1) Optically Pumped Cesium Standard

Research on Cs standards at CRL has been inactive in the last few years due to several reasons. In order to reactivate and prompt the research, a joint research project on an optically pumped cesium-beam-type frequency standard was contracted with National Institute of Standards and Technology (NIST) of the USA in January 1996. In this project, we aim to establish a primary frequency standard with accuracy of several parts in 10^{-15} until 1998 and will contribute to the accuracy of TAI at the level of 10^{-15} .

The standard is based on NIST-7 and several important improvements will be made. One of them is the adoption of an anti-resonance mode ring cavity, which is expected to have very low dimensional sensitivity of end-to-end phase difference and to result in high accuracy. It has never previously been adopted in primary Cs standards and its performance is anticipated with great interest.

(2) Cesium Fountain Standard

The recent progress in laser cooling and trapping technology has enabled a cesium-fountain-type frequency standard using very cold atoms to be developed. It is very promising as a future primary standard with an accuracy of $10^{-15} \sim 10^{-16}$, since the use of low-velocity atoms and a single cavity reduces or eliminates most of the frequency shifts such as second order Doppler shift or cavity end-to-end phase shift, which limit the accuracy of the Cs-beam-type standard. Due to this great advantage in accuracy evaluation, many institutes of time and frequency standards have recently started researching fountain standards. Indeed, LPTF in France has developed a fountain-type standard and succeeded in achieving an accuracy of 3×10^{-15} .

We have also started preliminary experiments in order to establish the basic technologies required for a fountain standard, and succeeded in trapping and cooling cesium atoms down to several microkelvins in a gas cell. As a next step, we plan to launch cold atoms upward in 1996.

After establishing these technologies, we will start designing and developing a fountain standard in 1997.

2.2 Timekeeping Using Commercial Clocks^[6-8]

About 10 cesium atomic clocks are working to generate UTC(CRL) at CRL. The TA(CRL) calculation algorithm was established for generating a time scale at CRL in 1978. The algorithm requires that the short-term and long-term fluctuations of each clock be separated with a digital filter. Each clock is then weighted for short- and long-term stability to average out the fluctuations. And the evaluation method of unbiased Allan variances from biased ones was also studied. These results were applied to calculation of the TA(CRL) as a paper time scale.

In 1985, a real-time UTC(CRL) generation method, illustrated in Figure 1, was developed from the conventional master clock method for generating UTC (CRL). This method uses a weighted-average technique which incorporates microphase steppers. With the current UTC(CRL), a time difference of less than 100 ns and a frequency difference of better than 1×10^{-14} is kept against UTC.

3 TIME AND FREQUENCY DISSEMINATION

3.1 HF and LF Standard Time Emission

At CRL, one of the main methods of disseminating frequency and time standards is time signal emission using the shortwave band, JJY, and the longwave band, JG2AS. JJY has been used ever since transmissions were started in 1940. These signals are currently transmitted from NTT's Nazaki Station (located in Sanwa-machi Sashimagun, Ibaraki Prefecture). Since there had been problems with the accuracy of the disseminated frequency and with interference, CRL's inner committee was organized to discuss the future plan of standard time and frequency dissemination during 1993 and 1994. The following steps were proposed as a result of this committee's work.

- (a) Strengthen emission power of the standard long-wave band and establish it as the proper standard frequency station.
- (b) Gradually decrease the use of the standard shortwave band, and eventually abolish its use as a standard.
- (c) Establish a dissemination method for frequency and time standards that is suitable for the multimedia age.

In response to item (b), of the conventional five standard shortwave bands (2.5, 5, 8, 10, and 15 MHz), two were eliminated (2.5 and 15 MHz) in 1996.

As for item (a), although JG2AS is still in an experimental stage, the number of radio-controlled watches and clocks that receive JG2AS in Japan already exceeds 300,000. Its dissemination accuracy is on the order of 10^{-11} or 10^{-12} . CRL has requested funds to construct a new longwave station. This new station will have more than 5 times stronger emission power compared with the present one. If CRL can obtain the funds, the new station will begin operation in 1999.

3.2 Telephone Line Service of Standard Time^[9]

As for item (c) of the previous section, several dissemination methods are currently being researched, such as Telephone JJY, Network Time Protocol, and FM radio broadcasting. The most representative of these is a time information service using telephone lines, called the Telephone JJY, which started public service in August 1995. Telephone JJY was started after basic experiments had been conducted over several years. It uses commercial telephone lines and has a loop-back function which enables compensation of the line and circuit delay on the user side. Users can calibrate clocks to the Japanese Standard Time within an accuracy of 1 ms using the loop-back function. Telephone JJY is used by various broadcasting stations to

calibrate master clocks and for disseminating time as a replacement for JJY. Because the number of PC networks is expanding, uses per month as of October 1996 reached as much as 21,000. The number of uses is increasing at a rate of almost 2,000 a month. Figure 2 shows the number of users of Telephone JJY since August, 1995.

3.3 NTP Server of UTC(CRL)^[10]

Since the rapid spread of computer networks such as the Internet, time synchronization among the computers connected to the network is very important. The NTP (Network Time Protocol) is an excellent technique to the computer network such as the Internet. However, there are several problems when a UNIX workstation is used as a server: the time resolution, the nature of multi-tasking, the I/O port problem, and the property of asymmetry of I/O path delays.

CRL's NTP stratum-1 server connected to UTC(CRL) under development is based on an IBM-compatible PC with a specially designed ISA bus board for a time code generator, and modified NTP protocol, which works for MS-DOS. Some of the problems described above are improved by this server. This work is being cooperatively performed with one of the Internet providers in Japan and it will be in service in 1997.

4 TIME TRANSFER

4.1 GPS Time Transfer^[11-12]

In order to contribute the atomic clocks of CRL to TAI and UTC and to clarify the relationship between UTC(CRL) and UTC, CRL is conducting routine time transfer using GPS satellites according to the BIPM observation schedule which is used by major world time and frequency research institutes.

During 1987 and 1988, a CRL researcher conducted cooperative research at BIPM on an ionospheric total-electron-content measurement receiver based on the GPS dual-frequency P-code signal cross-correlation (this device is GTR-2, which is commercially available as TECmeter). The device is used to compensate for ionospheric delays in time comparisons.

As shown in the Figure 3, CRL is operated as one of three major nodes of the international GPS time transfer network for BIPM, and plays an important role in TAI computations. Thus, CRL contributes to TAI not only by atomic clock data, but also as one of the node laboratories of the international GPS time transfer network of the BIPM.

4.2 Two-Way Satellite Time Transfer^[13-14]

Two-way satellite time transfer (TWSTT) using a communications satellite (ATS-1) was achieved in 1975 at a precision of 1 ns between Japan and the United States. This involved the successful detection of the relativistic Sagnac effect caused by the earth's rotation. In 1983, TWSTT experiments were conducted in Japan on the

Ka-band (20/30 GHz band) using an experimental communications satellite (CS).

These experiments, however, were interrupted for some time by problems in securing international satellite links due to problems in the facilities in the partner country. Beginning in 1992, however, international TWSTT experiments were resumed using the INTELSAT satellite. With CRL taking the initiative, experiments were conducted between Japan and Taiwan (Telecommunications Laboratory), and Japan and Korea (Korean Research Institute of Standards and Science). CRL has a Mitrex modem 2500A and an original one which is compatible with the Mitrex modem developed at CRL, and two Ku (12/14 GHz) band ground stations with 1.8-m dish antennas. The experiments were conducted at a precision of 1 ns.

The preparation work is currently underway for a joint experiment between Japan and Australia (CSIRO-NML) during 1996-1997. We will also conduct TWSTT experiments with the United States, and try to establish a key time transfer station in the Asian region.

4.3 Time Transfer Using High-Speed Digital Network

Under cooperative study with Nippon Telegram and Telephone Co. (NTT), precise time transfer experiments are being performed. This research is using a high-speed digital network, which has a data transmission rate of 2.4 Gbps. It uses a physical layer of SDH level and has a possibility of time transfer precision of ns level using the two-way method. A time-transfer experiment is being made between CRL Koganei headquarters and NTT Optical Network Systems Laboratories; the distance is about 70 km. We are planning to make simultaneous time-transfer experiments using this method and two-way satellite time transfer beginning in 1997.

5 RELATED RESEARCH WORK

5.1 Pulsar Timing Observation^[15-17]

Many researchers are now paying close attention to pulsars, especially millisecond pulsars, which have a millisecond rotation rate. These pulsars are believed to be even better than the atomic frequency standard on earth in terms of long-term stability on the order of a year. As a research application of the 34-meter antenna constructed at the Kashima Space Communication Center in 1988, CRL initiated a project in 1989 with the main objective of developing applications to time scales of the properties of these pulsars.

Currently, the most accurate pulsar timing measurements are performed by the 305-meter ground-fixed antenna at the Arecibo Observatory in Puerto Rico. Since the 34-meter antenna at CRL collects 1/80th the amount of light as the Arecibo antenna, we are studying the development of measurement equipment that will compensate for this low light collection capability by broadening the observation frequency band and extending the observation time.

We started out with measurement equipment based on a total bandwidth of 4 MHz which has a 16-channel filter bank, before developing 50 MHz, 256-channel obser-

vation equipment which uses an acoustic optical spectrometer (AOS) along with a dedicated averaging device. A schematic diagram of the measurement system using AOS is shown in Figure 4. We are currently evaluating the capability of this equipment. If it performs to its full design potential, we think we will be able to make observations with an accuracy of 1 microsecond or less for PSR-1937+21.

5.2 Theoretical Research the Relativistic Effects^[18-20]

The relativistic effects due to the earth's orbital motion and solar gravity that affect the earth's proper time and frequency standards can be as large as 10^{-8} . Even near the earth, the velocity of a satellite and the effects of the earth's gravity can cause frequency fluctuations on the order of about 10^{-10} . Therefore, in order to use stable frequency standards that are as accurate as 10^{-14} , we have to consider relativistic effects.

In 1990, CRL conducted a theoretical investigation of time geostationary orbits, where a flying body will have the same proper time as the bodies on the earth's geoid surface. Since then, we have been engaged in theoretical research concerning the precise measurement of time and space. We have also been conducting collaborative research with the National Astronomical Observatory and Tohoku University, resulting in the development of a formula which simultaneously determines the mass and distance of a single star by considering the gravitational lens effect and the effects of gravitational delay on the arrival time of pulse signals from a pulsar due to massive interstellar bodies.

The following projects are part of ongoing theoretical research on relativistic effects:

1. A study of the effects of interstellar gravitational fields on the construction of reference frames and pulsar time scales.
2. A study of relativistic effects on two-way satellite time transfer, lunar geodesy, and planetary geodesy.

5.3 Basic Research and Development of the Future GNSS^[21]

According to a statement of the President of the United States in March 1996, the use of GPS after 2005 is guaranteed. Since the main purpose of GPS system is for the military, the next-generation GNSS (Global Navigation Satellite System) should be constructed independently of the military under international cooperation. We will start to develop several key technologies to contribute this next-generation GNSS:

- A spaceborne hydrogen maser. The development of a spaceborne hydrogen maser requires the size and weight of the maser to be reduced considerably. We plan to develop a maser that weighs 50–100 kg and has a stability at the 10^{-15} level. There are two approaches to satisfying the requirements; one is to use a full-sized microwave cavity, which is being developed at the Smithsonian Astronomical Observatory, and the other is to use a small-sized cavity such as a sapphire-loaded cavity or a loop-gap-type cavity.
- Precise time and frequency transfer between a spaceborne hydrogen maser and a ground-based clock at the 10^{-15} and 0.1–0.01 ns levels.

6 APPLICATION OF TIME AND FREQUENCY STANDARDS^[22]

For the application area of the time and frequency standards, CRL is doing research and development in VLBI (Very Long Baseline Interferometry) and SLR (Satellite Laser Ranging). One of the biggest projects in this field is the Crustal Deformation Monitoring System in the Tokyo Metropolitan Area. It has four sets of VLBI and SLR stations around the Tokyo metropolitan area to monitor the geodetic movement precisely. The station locations are illustrated in Figure 5. We already finished the VLBI facilities and started the observations. Precise time and frequency is one of the most important technologies for this project. We are also studying a real time VLBI using high-speed digital communication links in cooperation with NTT.

7 CONCLUSION

The situation of time and frequency standards at CRL has not been very active for at least the past few years. Meanwhile, the accuracy of the top level of the frequency standards is reaching the order of 10^{-15} . In addition, needs of the society and industry for the time and frequency standards are expanding into various areas. Considering this situation of time and frequency standards, CRL is trying to contribute to the time and frequency domain. Figure 6 shows the projection of research on time and frequency standards at CRL.

8 REFERENCES

- [1] T. Maeno, H. Saito, J. Umezu, Y. Ohta, M. Kajita, and R. Hayashi 1990, "*Characteristics of a frequency stabilized and spectral narrowed laser diode system*," Conference on Precision Electromagnetic Measurements, June 1990.
- [2] T. Maeno, H. Saito, J. Umezu, Y. Ohta, R. Hayashi, and P. Thomann 1991, "*The expansion of optical locking range of a spectral narrowed laser diode system using a current feedback technique*," Proceedings of the 5th European Frequency and Time Forum (EFTF), 12-14 March 1991, Besançon, France, pp. 249-251.
- [3] T. Maeno, H. Saito, J. Umezu, Y. Ohta, M. Kajita, and R. Hayashi 1991, "*Characteristics of a laser diode system for an optically pumped cesium atomic clock*," IEEE Transactions on Instrumentation and Measurement, IM-40, 146-148.
- [4] M. Kajita 1994, "*A novel interpretation of collision cross sections between Cs and rare gas atoms*," Proceedings of the 8th European Frequency and Time Forum (EFTF), 9-11 March 1994, Weihenstephan, Germany, pp. 939-943.
- [5] M. Kajita 1996, "*Collisional effect with optically pumped atomic clock*," Proceedings of the 10th European Frequency and Time Forum (EFTF), 5-7 March 1996, Brighton, UK (IEEE Conference Publication 418).
- [6] M. Shibuki, K. Sebata, M. Aida, and K. Nakagiri 1993, "*Increase of accuracy for the TA (CRL) time scale*," Proceedings of the International Symposium on Atomic Frequency Standard and Coherent Quantum Electronics, August 1993.

- [7] M. Shibuki, K. Sebata, M. Aida, and K. Nakagiri 1994, "*Improvement of the accuracy of the atomic time scale at CRL*," **Japanese Journal of Applied Physics**, **33**, No. 3B.
- [8] K. Yoshimura 1989, "*Degrees of freedom of the estimate of the two-sample variance in the continuous sampling method*," **IEEE Transactions on Instrumentation and Measurement**, **IM-38**, 1044-1049.
- [9] N. Moritani, T. Akatsuka, T. Satoh, and M. Aida 1992, "*Standard time dissemination system using public telephone line*," **Japan Clock Association Journal**, September 1992.
- [10] T. Gotoh, and K. Imamura 1995, "*Development of the UTC (CRL) time dissemination server for computer networks*," Proceedings of the 9th European Frequency and Time Forum (EFTF), March 1995, Besançon, France.
- [11] M. Imae, E. Kawai, and M. Aida 1993, "*Long term and long distance GPS time transfer results corrected by measured ionospheric delay*," **IEEE Transactions on Instrumentation and Measurement**, **IM-42**, 490-493.
- [12] W. Lewandowski, M. Imae, C. Thomas, and M. Aida 1993, "*Determination of the differential time correction between GPS time receivers located at the CRL and the Observatoire de Paris*," Report BIPM-93/4.
- [13] F. Takahashi, K. Imamura, E. Kawai, C. B. Lee, D. D. Lee, N. S. Chung, et al. 1993, "*Two-way time transfer experiments using an INTELSAT Satellite in an inclined geostationary orbit*," **IEEE Transactions on Instrumentation and Measurement**, **IM-42**, 498-504.
- [14] B. S. Engelkemier, K. Imamura, F. Takahashi, T. Yoshino, and N. S. Chung 1995, "*INTELSAT Two-way time transfer experiments among Japan, Korea, and Taiwan*," **IEEE Transactions on Instrumentation and Measurement**, **IM-44**, 98-102.
- [15] Y. Hanado, M. Imae, H. Kiuchi, S. Hama, and A. Kaneko 1992, "*Millisecond pulsar observation system at CRL*," Proceedings of the 23rd Annual Precise Time and Time Interval (PTTI) Applications and Planning Meeting, 3-5 December 1991, Pasadena, California, USA (NASA CP-3159), pp. 377-384.
- [16] Y. Hanado, M. Imae, M. Sekido, H. Kiuchi, and S. Hama 1994, "*New millisecond pulsar observation system at CRL*," **Japanese Journal of Applied Physics**, **33**, No. 3B.
- [17] Y. Hanado, M. Imae, and M. Sekido 1995, "*Millisecond pulsar observation system using acousto-optic spectrometer*," **IEEE Transactions on Instrumentation and Measurement**, **IM-44**, pp. 107-109.
- [18] M. Hosokawa, and F. Takahashi 1992, "*Time geostationary orbits in the solar system*," **Publications of the Astronomical Society of Japan**, **44**, 159-162.
- [19] M. Hosokawa, K. Ohnishi, T. Fukushima, and M. Takeuti 1993, "*Parallactic variation of gravitational lensing and measurement of stellar mass*," **Astronomy and Astrophysics**, **278**, L27-L30.
- [20] K. Ohnishi, M. Hosokawa, T. Fukushima, and M. Takeuti 1995, "*Variation of gravitational delay in pulsar timing observation due to proper motion of foreground stars and measurement of stellar mass*," **Astrophysical Journal**, **448**, 271-280.
- [21] Y. Ohta, H. Saito, and J. Umezu 1991, "*Development of a very small hydrogen maser using a loop-gap resonator*," **Transactions of the Institute of Electronics, Information and Communication Engineers**, **J74-C-I**, No. 6 (in Japanese).

- [22] F. Takahashi, M. Imae, T. Yoshino, Y. Takahasi, K. Heki, T. Miki, T. Kondo, Y. Kunitomi, N. Kurihara, T. Othubo, H. Takaba, T. Iwata, H. Kiuchi, Y. Koyama, Y. Hanado, M. Sekido, K. Imamura, J. Nakajima, and A. Sugiura 1994, *"The plan of Metropolitan Crustal Deformation Monitoring System by Communications Research Laboratory," Journal of the Geodetic Society of Japan* (CRCM'93 Proceedings special issue).

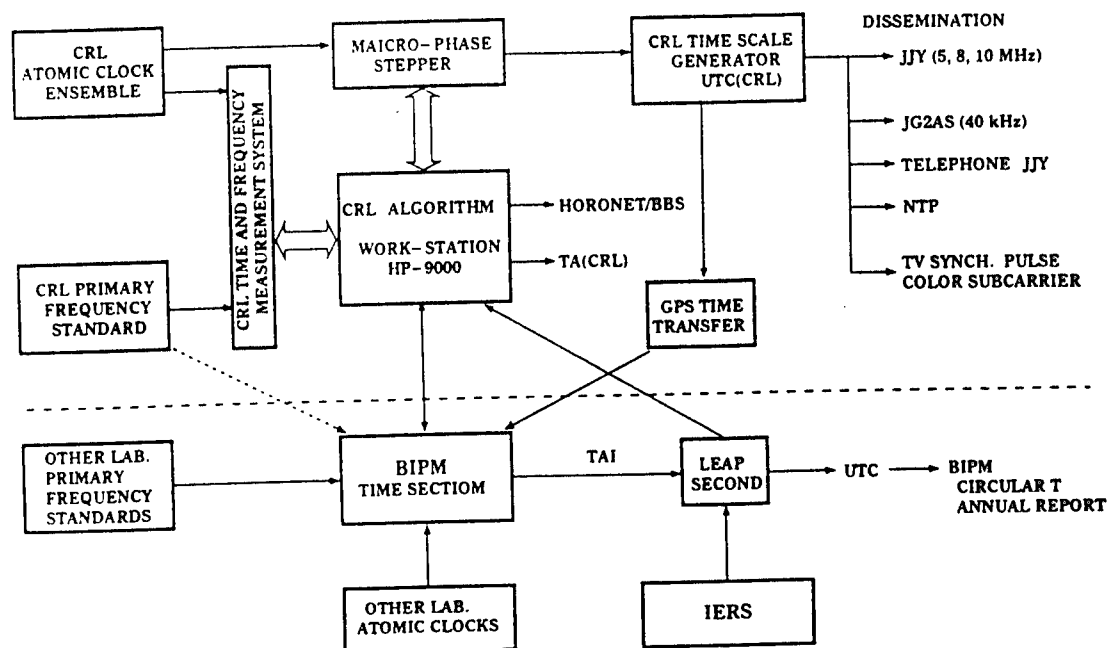


Figure 1 Real-time UTC(CRL) Generation System and Relation between TAI and UTC.

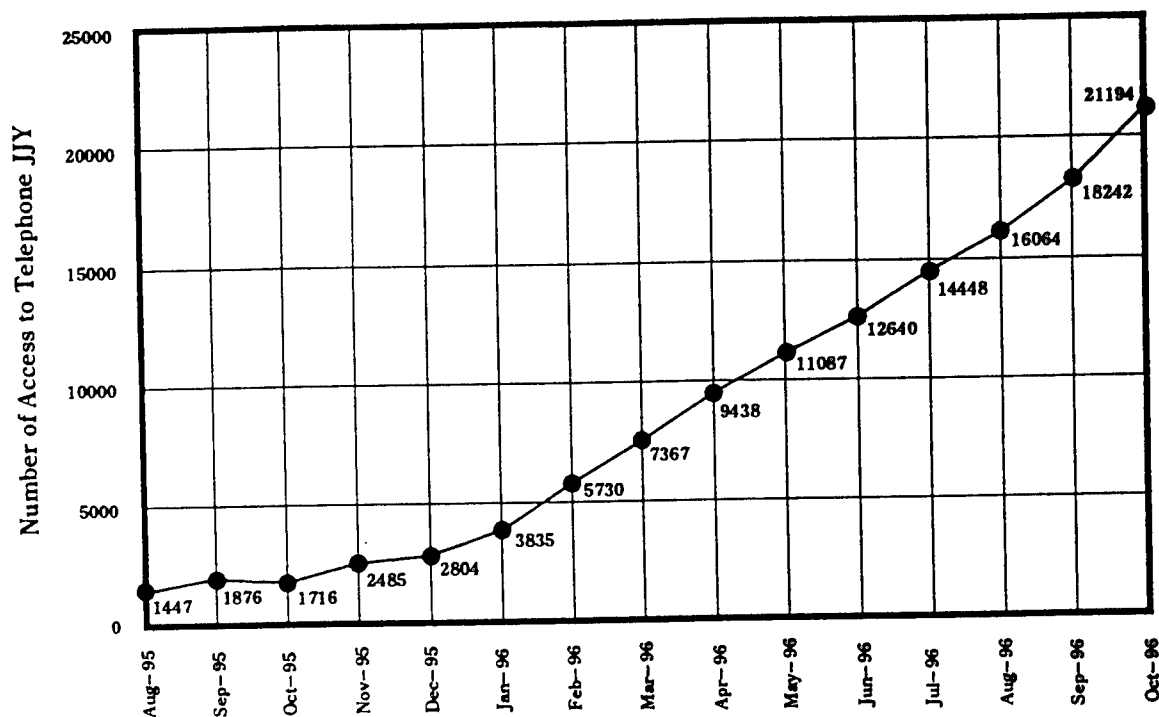


Figure 2 Number of Access to Telephone JJY System

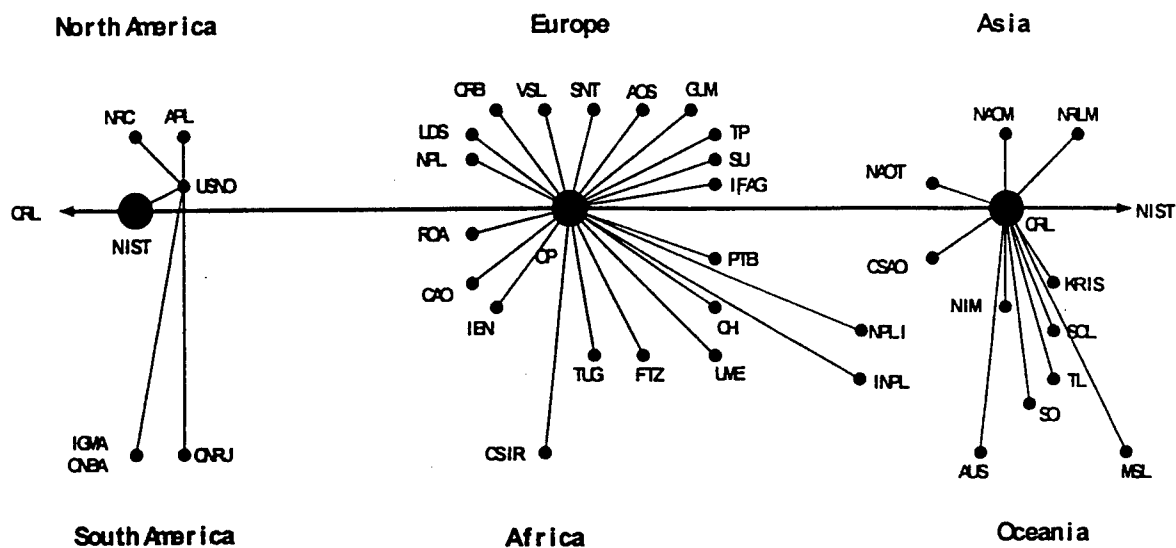


Figure 3 GPS Time Transfer Network for TAI Calculation (from brochure of BIPM).

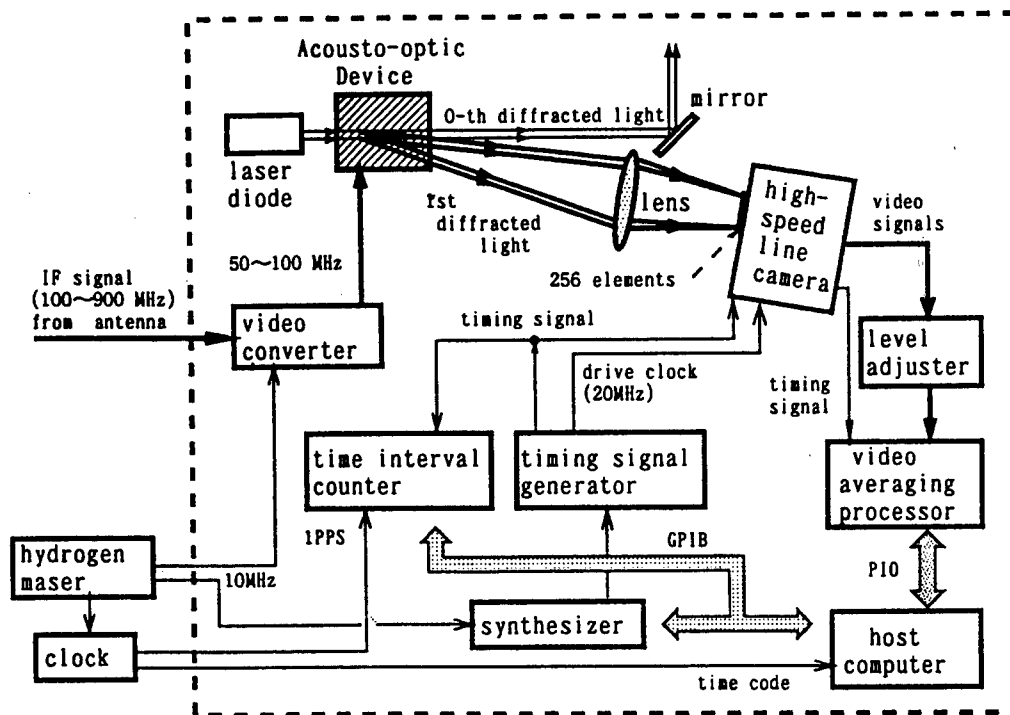


Figure 4 Schematic Diagram of the Pulsar Timing Measurement System using AOS.

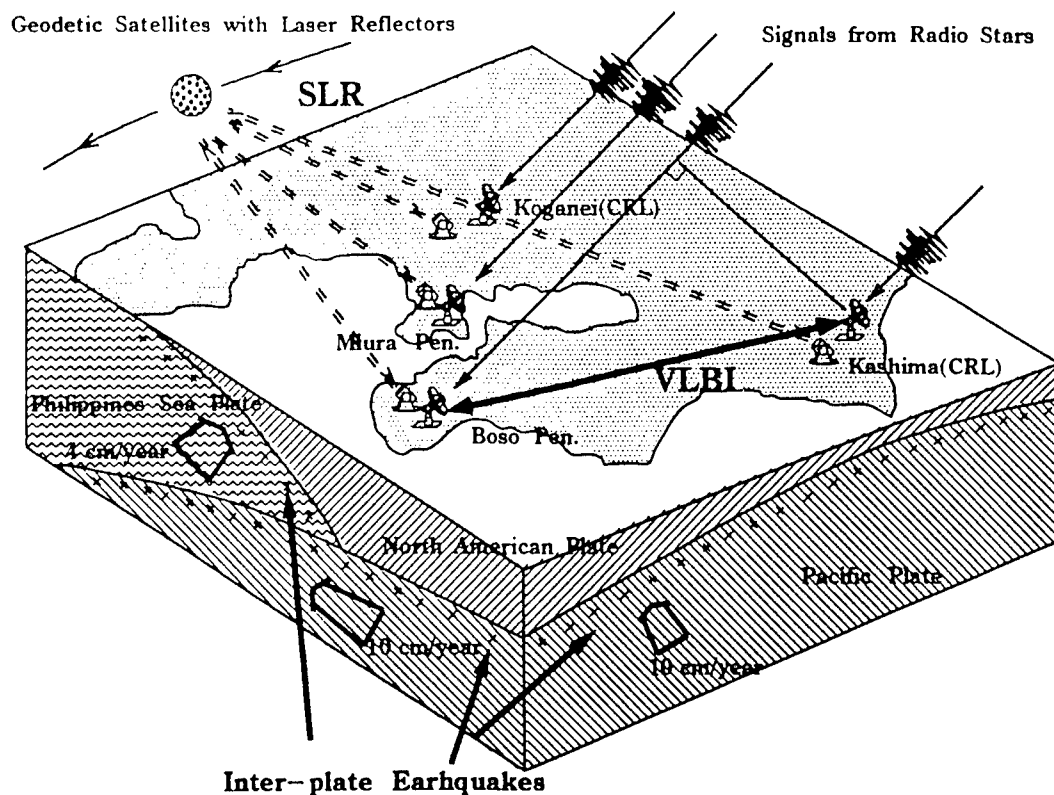


Figure 5 Crustal Deformation Monitoring System for the Tokyo Metropolitan Area.

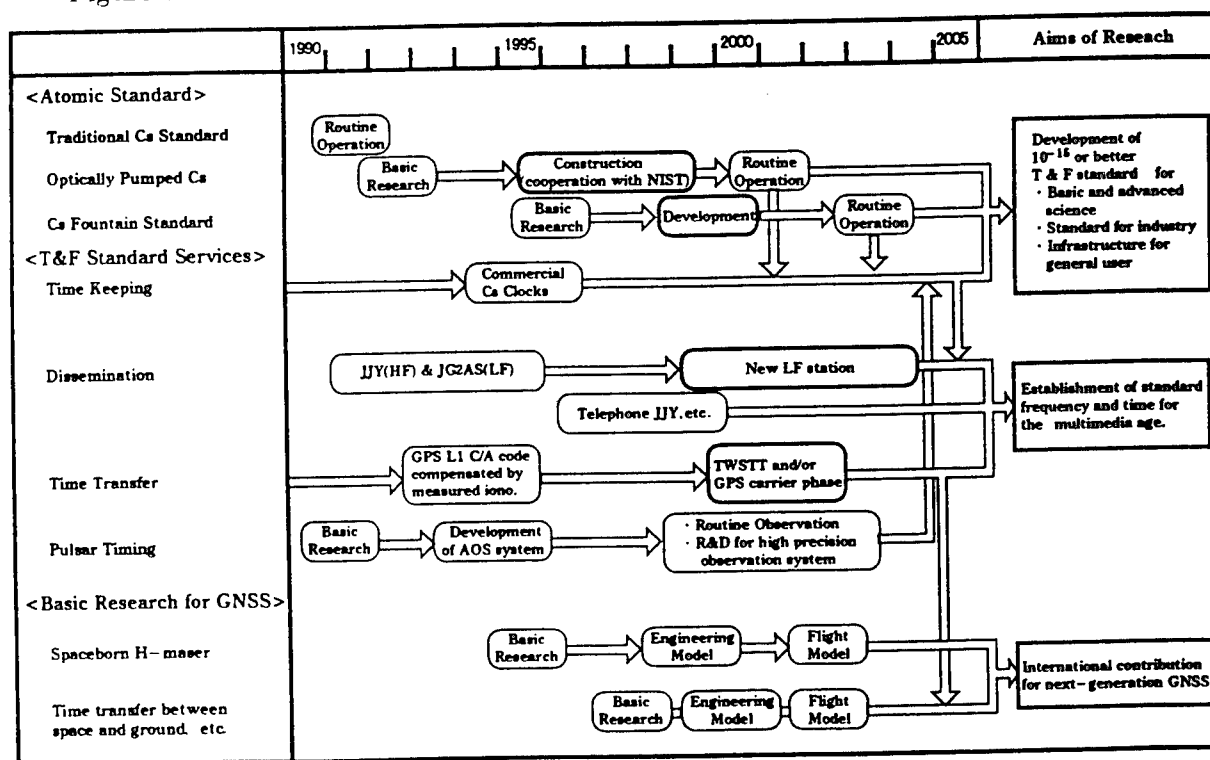


Figure 6 Projection of Research on Time and Frequency Standards at CRL.

Questions and Answers

SIGFRIDO LESCHIUTTA (IEN, ITALY): Your communication research laboratory is a laboratory belonging to a ministry as a public laboratory?

MICHITO IMAE: The Ministry of Post and Telecommunication.

SIGFRIDO LESCHIUTTA: Concerning the LF station on 40 kHz, what kind of signals are you planning to radiate? Also, time codes.

MICHITO IMAE: On the present LF station, we also transmit a time code. But the transmission power is not strong enough to cover all of Japan.

RICHARD KEATING (USNO): The Japanese Communication Satellite, the JC-SAT, as you call it, I notice has a wide footprint over Eastern Australia and New Zealand. Is the down link a spread-spectrum technique and, if so, who makes the modems?

MICHITO IMAE: It is only a communication satellite which has a transponder and we transmit such a signal. It can operate in spectrum mode.

SIGFRIDO LESCHIUTTA: I have a third question. Could you please present the last slide? You were speaking about your research on a spacebourne H-maser. Could you elaborate a bit since the problem arose this morning?

MICHITO IMAE: In Japan, as Dr. Busca mentioned this morning, there are several plans to construct a new generation of the GNSS by the Agency of Science and Technology, NASADA, and our ministry. The Japanese Committee for Space Development decided to gather all of these plans and discuss how Japan can contribute to this domain. So at present we are discussing within the committee the basic technology for an onboard clock and research work. We will start next year in my laboratory.

FREQUENCY STANDARDS, TIMEKEEPING, AND TRACEABLE SERVICES AT THE NATIONAL RESEARCH COUNCIL OF CANADA

R. J. Douglas, J.-S. Boulanger, S. Cundy, M.-C. Gagné,
W. Cazemier, B. Hoger, R. Pelletier, J. Bernard,
A. A. Madej, L. Marmet, K. Siemsen, and B. G. Whitford
Frequency and Time Standards Group
Institute for National Measurement Standards
National Research Council of Canada, Ottawa K1A 0R6, Canada
Phone: (613) 993-5186, fax: (613) 952-1394, e-mail: rob.douglas@nrc.ca

Abstract

Canadian frequency metrology services and Canada's official time services are both provided by the National Research Council of Canada (NRC). NRC designs, builds, and operates a group of laboratory frequency standards, both primary cesium clocks and hydrogen masers. It disseminates the results as both time and traceable frequency. NRC has an active research and development program in time and frequency technology: on frequency standards (microwave and optical) and on calibration and dissemination techniques with complete uncertainty budgets. Its present and planned capabilities are presented and discussed.

INTRODUCTION

The National Research Council of Canada provides accurate time and frequency services for Canada, which are also available to interested parties in Mexico and the United States under the terms of the North American Free Trade Agreement. The services are based on the capabilities within NRC's time laboratory, on its capabilities to intercompare and coordinate with other laboratories, and on its ability to deliver those services to clients.

CESIUM CLOCKS

One major difference between PTTI work at NRC compared to many other time laboratories is the presence of three continuously operated laboratory cesium-beam standards designed and built at NRC 20 to 25 years ago. They are large, classical magnetic-dipole cesium clocks, 2 to 5 m in overall length, with provision for beam-reversal (to evaluate the microwave cavity phase shift). The larger clock, CsV, has a Ramsey interaction length of 2.1 meters and a linewidth (FWHM) of 60 Hz^[1] and an independent standard uncertainty in SI average frequency of 5×10^{-14} for times longer than 1 day. The two smaller clocks (CsVI-A and CsVI-C) each have an interaction length of 1 meter and a linewidth of 90 Hz^[2] with an independent standard uncertainty in SI average frequency of 7×10^{-14} for times longer than 1 day. These standards

are operated to be dominated by white frequency noise of $3 \times 10^{-12} \tau^{-1/2}$, which suffices to characterize directly most frequency standards, except hydrogen masers.

The past year has been one of major building reconstruction and CsV has been assaulted by each of the "elements" identified by ancient Greece: air, earth, water, and fire. We have taken this time to build (and rebuild) an environmental chamber for CsV which should control the temperature and temperature gradients. We expect CsV to be capable of a flicker-frequency noise floor well below the 10^{-14} level that we commonly observed when the room temperature was not well controlled.

In addition to these primary cesium clocks, there are experimental systems. CsVI-B was withdrawn from service as a primary clock and dismantled. Some of its parts likely will be recycled in the future in an NRC cesium-fountain frequency standard. CsVII was an optically pumped short (20 cm interaction length) frequency standard which did not meet its optimistic design goals for frequency stability. A magneto-optic trap and optical molasses system has been in operation for 2 years^[3] and has developed the ability to trap 10^7 cesium atoms per second, confine them in a 1 mm ball, cool them to less than 5 microkelvin, and re-accelerate them (at 4000 m/s^2) to speeds of 7 m/s—all with an optical power low enough (6 mW per beam) to be easily compatible with cryogenic operation. This work is aimed at a tall cesium fountain (2.5 m overall trajectory height, with 1.2 m above the microwave interaction region to give a 1-second Ramsey interaction time or a 0.5 Hz linewidth).

Our laboratory uses two HP5071A "high performance" commercial Cs clocks, one in the main time laboratory and one in the adjunct laboratory 22 km distant at CHU, the NRC shortwave radio station that continuously broadcasts its time and frequency references.

HYDROGEN MASERS

NRC operates three home-built hydrogen masers. One is 30 years old and is operated largely to allow three-cornered-hat measurements of the short-term stability of the two more modern masers^[4], which are operated in the cavity auto-tuning mode as clocks. Their stability at 10 days is generally less than 2×10^{-15} . One (H3) is fitted with a cavity coated with FEP-120 Teflon and the other (H4) is coated with Fluoroplast F-10 with a wall shift about half that of the FEP-120 Teflon. The masers have proved useful in evaluating the time and frequency transfer characteristics of the Geodetic GPS measurement systems, in some optical frequency measurements^[5], and evaluating hydrogen masers for clients. They are planned for use in frequency intercomparison from cesium fountains.^[6,7,8]

PHASE COMPARATORS

The short-term phase stability of clients' frequency standards can be evaluated at 5 MHz using our multichannel phase comparator. Averaging for 1 s, it is dominated by a white phase noise, having a modified Allan deviation of less than $3 \times 10^{-12} \tau^{-1.5}$ between any two channels. Redundant computers record the data stream from the phase comparator. Shorter-term and higher-stability intercomparisons (such as for hydrogen masers) are measured separately. Longer-term phase comparisons are routinely made in a fully automated way by counting down to 1 pps and comparing with 1 pps signals from other clocks.

LASER-COOLED TRAPPED SINGLE-ION OPTICAL FREQUENCY WORK

A single, trapped $^{138}\text{Ba}^+$ ion was laser-cooled to 15 mK and measurements were made of the linewidth of several Zeeman components and the center frequency of the $5d\ ^2D_{3/2} - 5d\ ^2D_{5/2}$ clock transition (with a wavelength of 12 m). The best value for the FWHM of a Zeeman component and the center frequency of the transition were 5.8 kHz and $24,012,048,317,170 \pm 440$ Hz (1.8×10^{-11}), respectively. The frequency measurements were made by direct comparison to cesium using the NRC frequency chain.

Recently, similar work on the 674 nm $5s\ ^2S_{1/2} - 4d\ 2D_{5/2}$ clock transition of an $^{88}\text{Sr}^+$ ion has yielded 500 Hz for the FWHM of a Zeeman component. The local oscillator used to interrogate the single ion is a cavity-locked laser which is predictable relative to the Sr^+ clock transition to within 2×10^{-12} over many hours. The ion temperature is near 10 mK. Frequency measurements $444,779,043,984 \pm 28$ kHz (6.3×10^{-11}) for the transition center have been made with respect to an iodine stabilized HeNe laser at 474 THz, with absolute measurements relative to Cs planned. The Sr^+ single-ion frequency reference at 445 THz and the link to 474 THz is planned to be developed and maintained as a simplified calibration tool for the iodine-stabilized He-Ne lasers at 474 THz, which are commonly used in length metrology. Part of the chain exploits a 2022 nm laser (whose third harmonic is beat with the laser interrogating the Sr^+ resonance), which will be used to develop frequency standards at other frequencies of interest for telecommunications technology.

COMMON-VIEW GPS

NRC's major international time intercomparison link is through a common-view GPS receiver, operated on the tracking schedule prescribed for Eastern North America by the Bureau International des Poids et Mesures. Some of NRC's clients also use this tracking schedule.

Antenna and receiver failures have necessitated unit substitutions. Whenever possible, relative calibrations of replaced antenna components were checked using a Mitrex modem, upconverting to the GPS L1 frequency. Since the Mitrex chipping rate is 2.5/1.023 times the GPS C/A chipping rate, a simple GPS code simulator was built and tested. With a data modulator (driven from an appropriate 50 bps GPS navigation message), we feel that this should evolve into a useful calibration tool.

GEODETIC GPS FREQUENCY TRANSFER

NRC has been collaborating with the geodesists of Canada's Department of Natural Resources on the frequency-transfer characteristics of their carrier-phase-smoothed techniques. In these tests we have been using 8- and 12-channel, dual-frequency, Turborogue GPS receivers. Both code pseudoranges and the integrated carrier phase are recorded in the "geodetic" mode, where each receiver's 20.456 MHz sampling clock is phase-locked to a 5 MHz frequency reference (at many sites from H masers), and the absolute timing is measured from a 1 pps gated out from the receiver's clock. This mode seems to avoid limitations that have been reported for timing receivers exploiting the same technology. The stability of the timing behavior of some of these receivers has been criticized, and after power-down (and at random other times at some sites) the relative phase of the receiver clock and the reference is lost. In an attempt to avoid the difficulties associated with determining the relative phase of the 20.456 MHz and the

reference 5 MHz (in hard-to-resolve steps of 78.2 ps), we have designed and built an external 20.456 MHz synthesizer which can be phase-reset by an external 1 pps clearing the synthesizer registers. If the 1 pps is phased correctly with respect to the reset, in a 200-ns window, we expect the only phase ambiguities left in a receiver using this system will be 48.885-ns steps, which are much simpler to resolve with the GPS receiver itself.

In this mode, we have performed zero-baseline tests using two Turborogue SNR-8000 receivers sharing a single antenna and separately locked to two outputs of a single maser. The differential noise level and stability are quite satisfactory^[9] without any special measures having been taken.

Until recently, full receiver measurements have been recorded every 30 seconds. They are preprocessed into a set of carrier-smoothed pseudorange measurements every 7.5 minutes. The global solution was done using GIPSY software (developed at JPL) in a postprocessing mode. Unlike many other geodetic analyses, the fitting was done independently for each 24-hour period, fitting observations from 24 stations around the world selected from the shared database of the International GPS Service for Geodynamics (IGS). An unconstrained discontinuity is allowed from one day's clock intercomparison solution to the next day's solution. The histogram of discontinuities is best described by identifying the end-of-day rms deviation of the solution as 310 ps (i.e. a end-of-day jump size of 440 ps), with occasional outliers.

The daily global solution has a wide-open timing filter (1 ms white phase noise allowance), and yet the fitted time differences between two maser-equipped receiver stations show excellent post-fit stability. If the day-to-day discontinuities are discounted as being in some sense "fixable," then the Allan deviation of the residuals for the short term (7.5 minutes to 1 day) is $8 \times 10^{-13} \tau^{-1/2}$ (white FM noise, τ in seconds— $\sigma_y(\tau = 1 \text{ day}) = 2.7 \times 10^{-15}$), or 10 times more stable than a high-performance-option HP5071A. If all the discontinuities are included for the same data, the Allan deviation of the residuals is about five times worse: $4 \times 10^{-12} \tau^{-1/2}$ (from 7.5 minutes to 1 day), and $\sigma_y(\tau = 1 \text{ day}) = 1.4 \times 10^{-14}$. For times beyond one day, even well-maintained masers cannot be relied upon to give a negligible contribution to the measured stability of the receiver clock differences, and so we have not continued our stability analysis beyond 1 day.

Likely, somewhere between these two limits is the frequency stability of this geodetic methodology. The traditional stability analysis, used above, does not cope well with the solution discontinuities. We use caution in interpreting these results, and we are more comfortable with two other statistical measures which exploit the nearly complete independence of the daily fitting procedures (the previous day's prediction only provides the initial estimates of the satellite orbits for the following day's solution).

Each day's solution also gives a 24-hour average frequency difference between any two stations, and rms averages of the first difference of these can be used to give the Allan deviation at 24 hours, $\sigma_y(\tau = 24 \text{ h})$, completely rigorously. The Allan deviations are shown for several different baselines in Table 1. It is quite encouraging to find Allan deviations at one day of 5×10^{-15} for baselines of 4,000 and 6,000 km, and of 7×10^{-15} for a 17,000 km (great-circle) baseline, with no common-view satellites.

As part of the Canadian Active Control System, a wide-area differential GPS system under development at the Geodetic Survey for use across Canada, we have started collecting full Turborogue data at 1-second intervals (up to 12 channels of C/A code pseudorange, C/A carrier phase, L1/L2 delay and—if available—the L1 and L2 P-code pseudoranges and integrated carrier phase data...). The objective is a real-time Canada-wide differential GPS overlay. Subsets of the full receiver data (e.g. RINEX) are not sufficient for the preprocessing that is normally done. We plan to use the same 1-second observations for reporting to BIPM with their common-view tracking schedule. We believe that absolute GPS calibration is important, and plan to work on

the more important influence parameters: multipath, filter, and correlator variations.

GEOSYNCHRONOUS SATELLITE TWO-WAY TIME TRANSFER

Two-way time transfer at 14/12 GHz is done routinely with USNO and NIST. Data acquisition was begun in 1989, and has continued three times per week. The data acquisition is largely automated, but the subsequent data analysis is not, and full analysis is not used routinely at NRC. In our plans, it is a technique with promise for the inter-laboratory intercomparisons expected with cesium-fountain frequency standards, but we believe that the currently identified needs of most Canadian clients can likely be met more economically with development of geodetic GPS techniques.

STANDARD UNCERTAINTIES FOR TIME AND FREQUENCY METROLOGY

We have developed and used a rigorous analytic method for calculating the noise contribution to the standard uncertainty of a time or average frequency in the presence of non-white noise (white PM + flicker PM + white FM + flicker FM + random walk FM) which can be used for many interpolation or extrapolation procedures that are common in time and frequency applications. The method is easier to use than simulations, and unlike simulations the new method can converge to an extent which allows it to be used for optimizing weights in fitting procedures.^[10] We have used this procedure to analyze the standard uncertainty associated with the crystal and maser oscillators which are associated with a pulsed frequency standard that is intermittently operated.^[11,6,7,8] We have extended this work to develop a simple procedure for converting stability measures into the standard uncertainty for transferring average frequency between two general time intervals.

OBTAINING STANDARD UNCERTAINTY FROM THE ALLAN DEVIATION

In metrology, the average frequency is often calibrated at one time interval and used at another interval often shorter than the first interval, and perhaps much later than the first. The transfer of average frequency from one interval to another is a process that is closely related to the stability of the frequency standard used to effect the frequency transfer. The Allan deviation or the modified Allan deviation is commonly used to characterize the stability, but there has been no easy way of converting this knowledge into a rigorous estimate of the standard uncertainty in the general case. Clients of average frequency (including almost all metrology) want to have the standard uncertainty^[12] in the value of their average frequency to allow them to claim rigorous traceability to SI, in keeping with their understanding of the *Guide to the Expression of Uncertainty in Measurement*.

The frequency difference measurements made in the calibration are generally combined linearly, and the expected standard uncertainty at a user interval can be calculated for the general case in a way similar to that outlined for least-squares fitting.^[10] The calibration data have a specific structure, and there is a "structure factor" which will independently affect each noise type of the usual sum of power-law noises, with the noise amplitude given by the Allan deviation or

modified Allan deviation. There will be no cross-terms of mixed noise types. The structure factors will also depend on the effective bandwidths for the Allan deviation determination, the calibration interval, and the end-use interval. Boulanger^[11,6,10] has developed a convenient analytic form of the required cross-correlations, but the problem has appeared rather too messy for most tastes. Using Boulanger's methods, the "AB structure factors" (the correction factor by which to multiply the Allan deviation to obtain the standard deviation) might be determined for specific calibration types and holdover times. If it is important to distinguish the effects of white phase noise, we would expect to have to use the modified Allan deviation and use a "MAB structure factor."

Recently we have derived, and plan to use a practical method (simple enough for hand calculator use) for converting the Allan variance $\sigma_y^2(\tau)$ measure of stability into a rigorous estimate of the standard uncertainty of average frequency due to the transfer process from one general time interval to another. The method is applicable when the measured $\sigma_y^2(\tau)$ reveals that the stability can be modelled by a sum of phase noise (white and flicker phase noise), white frequency noise, flicker frequency noise, and random-walk frequency noise.

The simple method applies to the commonly used endpoint, or strict average frequency transfer without frequency drift. (Although the standard uncertainty with drift and/or with least-squares fits could be estimated in the same general way, they would still be intricate to use.) The first simplification is to consider what will commonly be possible to arrange: to keep the effective noise bandwidths the same for the Allan deviation characterization, for the calibration interval $[t_1, t_2]$, and for the end-use interval $[t_3, t_4]$. The ratio of the (standard uncertainty)² to Allan variance is calculated for each noise type, and the limit is taken as the low-frequency cutoff tends to zero and the high-frequency cutoff tends to infinity.

We had expected to have to discriminate between the white phase and flicker phase noise, and so use the modified Allan deviation. We were pleasantly surprised to find that this is not required in most cases. As long as the accuracy required for an estimate of the standard deviation is in the normal metrological range of 10-20%, and if no endpoint of the calibration and end-use intervals are closer to any other than 10 times the high-frequency bandwidth, then the expressions in Figure 1 may be used with the Allan deviation, and we may avoid the minor difficulties sometimes encountered in determining the modified Allan deviation from a data set with missing values.

In using the four expressions in Figure 1, one need only decompose the Allan deviation graph for the standard (measured against a standard, and by a measurement system, each having at least a 2-3 times lower Allan deviation). The decomposition gives four numbers (the intercept of four lines τ^{-1} , $\tau^{-1/2}$, τ^0 , and $\tau^{1/2}$ on the log-log graph with the vertical line with τ equal to the calibration interval τ_1), each is squared and each is multiplied by its AB structure factor specified in Figure 1. The four products are summed, and the square root is taken to obtain the standard deviation in the average frequency over the interval τ_2 , after a holdover time of t , due to the random instability of the frequency standard. Of course, all other sources of average frequency uncertainty must still be added in quadrature to this frequency-transfer uncertainty to obtain the final answer desired by the client. The method also works rigorously for negative t , corresponding to postprocessing of the calibration data.

As one example of postprocessing, we have considered the effect of different local oscillators for average-frequency transfer in field-calibrating GPS-disciplined oscillators, transferring the common-view or wide-area differential GPS 24-hour frequency average to a shorter, centered interval. The results are graphed, in the common way in metrology as the $2\text{-}\sigma$ uncertainty, in Figure 2 as the dashed lines. The local oscillators considered are modelled conservatively:

- Cs HP5071A (PM 1.5×10^{-10} at .01 s or 1.7×10^{-17} at 24 h, white FM of 2.3×10^{-13} at 24 h, flicker FM of 2×10^{-14} , and random walk FM of 10^{-16} at 24 h),
- Cs HP5071A (high performance: PM 1.5×10^{-10} at .01 s or 1.7×10^{-17} at 24 h, white FM of 3.8×10^{-14} at 24 h, flicker FM of 0.8×10^{-14} , and random walk FM of 10^{-16} at 24 h),
- a good Rb HP5065A (PM 1.5×10^{-10} at .01 s or 1.7×10^{-17} at 24 h, white FM of 5×10^{-13} at 100 s or 1.7×10^{-14} at 24 h, flicker FM of 1×10^{-13} , and random walk FM of 10^{-13} at 24 h), and
- H maser Kvarz CH1-75 (PM 3×10^{-13} at 1 s or 3.5×10^{-18} at 24 h, white FM of 5.1×10^{-16} at 24 h, flicker FM of 6×10^{-15} , and random walk FM of 10^{-16} at 24 h).

The Cs standards are in their white frequency noise regime, and so their standard uncertainty for frequency transfer from 24 hours to short time intervals could have been estimated easily without the AB structure factors, but only by using the AB structure factors could we form a reasonable estimate for the capabilities of the Rb standard and the H maser, which are dominated by non-white frequency noise at 24 h.

This example is simple enough so that field calibration might be done by an energetic client, using a local oscillator certified for frequency transfer, or by a system comprised of a travelling phase-comparator, a frequency standard, and a GPS receiver used in the common-view mode. It would give to clients the means to calibrate, as a function of end-use time interval and time of day, the standard uncertainty $u_y(\tau_2, \text{time of day})$ in the average frequency of a GPS-disciplined oscillator at their own site, accounting for the site-dependent and time-dependent variation due to multipath, cabling, temperature, positioning, the ephemerides, the ionosphere, the troposphere, and SA compensation. The competing route is a shorter-term frequency transfer using a real-time wide-area differential GPS network, such as the Canadian ACS, with one or more nodes being a national metrology laboratory responsible for average frequency.

LOW-LEVEL SERVICES

As with many time and frequency groups, our highest public profile is as the identifiable national experts on time. We provide official time for Canada: disseminating it by telephone, radio networks, and short-wave radio. Radio station CHU broadcasts continuously at 3.33 MHz, 7.335 MHz, and 14.67 MHz. Our only long-term plans concerning CHU note the requirement that by the year 2007, the 7.335 MHz frequency allocation will be reserved for broadcast only.

These services provide English voice announcements, French voice announcements, and Bell 103 decodeable FSK signals at 300 bps, both by telephone and short-wave radio. These services provide traceable time (when the receiver and decoder are calibrated) and time interval or frequency (when the stability of the decoder is known). They are being used ever more heavily as companies undertake the documentation of traceable calibration as part of their quality control (or ISO-9000) procedures. CHU's Bell 103 readable code also provides one of the cheapest ways for network administrators to access time and date data for implementing a Network Time Protocol (NTP) server. We plan to install NTP servers which are generally accessible, and for the general public not using NTP we would prefer to develop methods to deliver time along with the uncertainty (bounded by the loop time of a time request).

TRACEABLE SERVICES

At a higher level of accuracy than outlined above, we assess client calibration laboratories for average frequency as part of the formal Canadian Laboratory Assessment Service (CLAS). For average frequency, as for all other metrological quantities, client laboratories are expected to maintain an independent local standard and both the means and the practice of establishing and documenting proper statistical control and calibrations relative to a national metrology laboratory. At present, our view is that GPS-disciplined oscillators of the present designs cannot serve both roles. Remote calibration is done by common-view TV line-10 measurements in the metropolitan areas of the NRC time laboratory, by common-view LORAN-C in the vicinity of the Great Lakes LORAN-C chain, by common-view GPS across Canada, and by travelling artefact of known frequency and stability. The Canadian Active Control System is not yet used for average frequency calibrations or stability measurements relative to Canada's national standards. The remote calibration service for short-term average frequency calibration, outlined above, is still in the planning stages, but would be a satisfactory means of establishing the statistical control for present-day GPS disciplined oscillators.

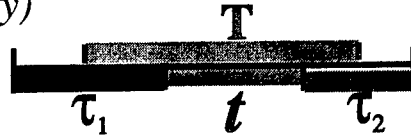
For clients wishing to calibrate time and frequency standards for time, or for average frequency, or for stability, NRC offers calibration services in its laboratory relative to its internal standards or to international time scales. With the stability measurement made at NRC comes the possibility of certifiable capability for average frequency transfer from one time interval to another. At present this can only be done economically if the client's standard has a stability (Allan deviation) which can be decomposed into a sum of power-law noise types. The AB structure factors then would give an analytic form for the expected standard uncertainty for average frequency transfer from one time interval to any other.

REFERENCES

- [1] A.G. Mungall, R. Bailey, H. Daams, D. Morris, and C.C. Costain 1973, "*The new NRC 2.1 metre primary cesium frequency standard CsV*," *Metrologia*, **9**, 113-127.
- [2] A.G. Mungall, H. Daams, and J.-S. Boulanger 1981, "*Design, construction and performance of the NRC CsVI primary cesium clocks*," *Metrologia*, **17**, 123-139.
- [3] J.-S. Boulanger, M.-C. Gagné, and R.J. Douglas 1996, "*Cold atoms and cesium fountains at NRC*," Proceedings of the 1996 IEEE International Frequency Control Symposium, 5-7 June 1996, Honolulu, Hawaii, USA, pp. 1089-1096.
- [4] J.-S. Boulanger, D. Morris, and R.J. Douglas 1994, "*Hydrogen masers and cesium fountains at NRC*," Proceedings of the 25th Annual Precise Time and Time Interval (PTTI) Applications and Planning Meeting, 29 November-2 December 1993, Marina del Rey, California, USA (NASA CP-3267), pp. 345-356.
- [5] A.A. Madej, K.J. Siemsen, J.D. Sankey, R.F. Clark, and J. Vanier 1993, "*High-resolution spectroscopy and frequency measurement of the mid-infrared $5d^2D_{3/2}$ - $5d^2D_{5/2}$ transition of a single laser-cooled barium ion*," *IEEE Transactions on Instrumentation and Measurement*, **IM-42**, 234-241.
- [6] R.J. Douglas, J.-S. Boulanger, and C. Jacques 1994, "*Accuracy metrics for judging time scale algorithms*," Proceedings of the 25th Annual Precise Time and Time Interval (PTTI) Applications and Planning Meeting, 29 November-2 December 1993, Marina del Rey, California, USA (NASA CP-3267), pp. 249-266.

- [7] D. Morris, R.J. Douglas, and J.-S. Boulanger 1994, "*The role of the hydrogen maser for frequency transfer from cesium fountains,*" **Japanese Journal of Applied Physics**, **33**, 1659-1668.
- [8] J.-S. Boulanger, and R.J. Douglas 1994, "*Frequency control of hydrogen masers using high-accuracy calibrations,*" Proceedings of the 1994 IEEE International Frequency Control Symposium, 1-3 June 1994, Boston, Massachusetts, USA, pp. 695-708.
- [9] R.J. Douglas, and J. Popelar 1995, "*PTTI applications at the limits of GPS,*" Proceedings of the 26th Annual Precise Time and Time Interval (PTTI) Applications and Planning Meeting, 6-8 December 1994, Reston, Virginia, USA (NASA CP-3302), pp. 141-152
- [10] R.J. Douglas and J.-S. Boulanger 1995, "*Metafitting: weight optimization for least-squares fitting of PTTI data,*" 26th Annual Precise Time and Time Interval (PTTI) Applications and Planning Meeting, 6-8 December 1994, Reston, Virginia, USA (NASA CP-3302), pp. 347-360.
- [11] R.J. Douglas 1992, "*Local oscillator requirements for timekeeping in the $10^{-14}\tau^{-1/2}$ Era,*" Proceedings of the 1992 IEEE International Frequency Control Symposium, 27-29 May 1992, Hershey, Pennsylvania, USA, pp. 6-26.
- [12] "*Guide to the Expression of Uncertainty in Measurement,*" first edition, Technical Advisory Group on Metrology, Working Group 3 (International Organization for Standardization, 1992). Published in 1993 in final form in the name of the Bureau International des Poids et Mesures, the International Electrotechnical Commission, the International Federation of Clinical Chemistry, the International Organization for Standardization, the International Union of Pure and Applied Chemistry, the International Union of Pure and Applied Physics, and the International Organization of Legal Metrology.

AB Structure Factors: *converting Allan variance $\sigma_y^2(\tau_i)$ into (standard uncertainty)² in Average Frequency Transfer across gap t , from τ_1 to τ_2*



1). Decompose and multiply the $\sigma_y^2(\tau_i)$ terms

White / Flicker phase noise by $2(\tau_1^{-2} + \tau_2^{-2}) / (3\tau_1^{-2})$

White frequency noise by

$$[|t+\tau_1| + |t+\tau_2| + \tau_1 + \tau_2 - |t| - |t+\tau_1+\tau_2|] / \tau_2$$

Flicker Frequency noise by

$$\left[\ln \left[\frac{(\tau_1+t+\tau_2)^2}{\tau_1\tau_2} \right] + \frac{2t+\tau_1}{\tau_2} \ln \left| \frac{\tau_1+t+\tau_2}{t+\tau_1} \right| + \frac{2t+\tau_2}{\tau_1} \ln \left| \frac{\tau_1+t+\tau_2}{t+\tau_2} \right| + \frac{t^2}{\tau_1\tau_2} \ln \left| \frac{t(\tau_1+t+\tau_2)}{(t+\tau_1)(t+\tau_2)} \right| \right] / [2\ln 2]$$

Random walk frequency noise by

$$[|t|^3 - \tau_1^2\tau_2 - \tau_1\tau_2^2 - |t+\tau_1|^3 - |t+\tau_2|^3 + |t+\tau_1+\tau_2|^3] / [2\tau_1^2\tau_2]$$

2). Add and take the square root to get the standard uncertainty due to the transfer.

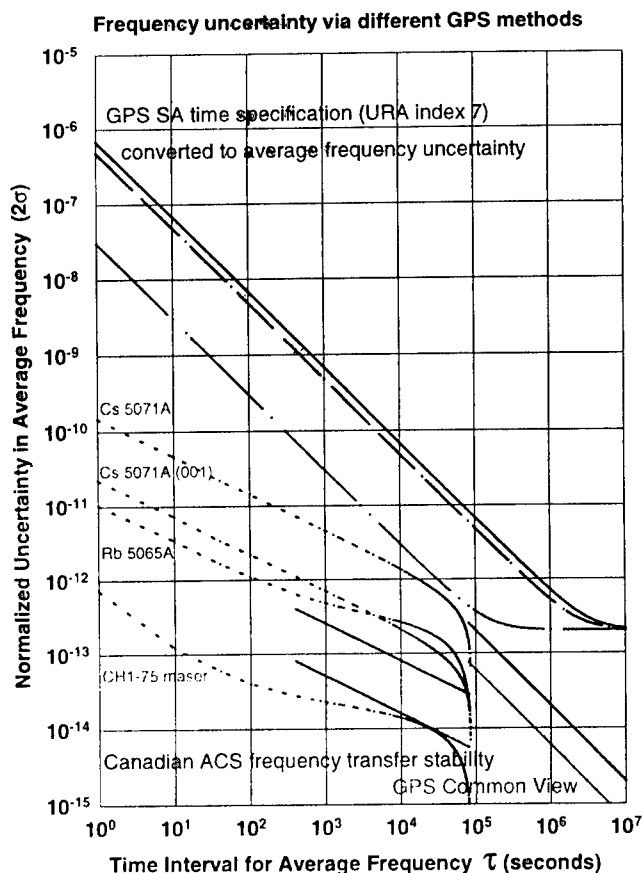


Fig. 1. (above) The simplified method for converting the Allan deviation of an oscillator into its standard uncertainty for the transfer of average frequency from one general time interval to another by decomposition into power law terms and multiplying by the Allan-Boulanger structure factors.

Fig. 2. 2-σ Uncertainty in Average Frequency vs Time Interval.

Top: normal SA worst-case correlation
: normal SA uncorrelated
: SA off, medium multipath
: Common view - SA on, daily average
: ACS - SA on, ionosphere measured, carrier phase smoothed, 8 channels.
Dashed curves: standard uncertainty in average frequency from a one-day calibration interval to an end-use interval centered in the calibration interval, of length τ .

TIME AND FREQUENCY ACTIVITIES AT NIST

J. Levine and D. B. Sullivan
Time and Frequency Division
National Institute of Standards and Technology
325 Broadway, Boulder, Colorado 80303, USA

Abstract

The mission, organization, and activities of the Time and Frequency Division of the National Institute of Standards and Technology are described. Topics covered include frequency standards, time scales, time transfer, optical frequency standards, spectral-purity measurements, synchronization for telecommunications, and time and frequency broadcast services.

INTRODUCTION

During the last decade, two other reports on the activities of the Time and Frequency Division of NIST^[1,2] have been presented at PTTI Meetings. This paper provides a very general update to that material with specific mention of some of our most recent activities. This introduction briefly describes the mission and organization of the Division, while the remaining sections offer a bit more information on activities of the Division.

The mission of the Time and Frequency Division is to support U.S. industry and science through provision of measurement services and research in time and frequency and related technology. To fulfill this mission the Division engages in:

- the development and operation of standards of time and frequency and coordination of them with other world standards;
- the development of optical frequency standards supporting wavelength and length metrology;
- the provision of time and frequency services to the United States; and
- basic and applied research in support of future standards, dissemination services, and measurement methods.

The work supporting length metrology derives from the definitional dependence of the meter on the second. This work contributes to a larger program in the Precision Engineering Division of NIST's Manufacturing Engineering Laboratory, which has primary responsibility for length and its dissemination.

The Division is organized into eight technical Groups: Time and Frequency Services, Time Scale & Coordination, Cesium Standards, Ion Storage, Spectral Purity Measurements, Laser Spectroscopy, Optical Frequency Measurements, and Network Timing. The Groups are necessarily small, and the Group Leaders are, thus, able to function primarily as technical leaders within their areas. The unifying theme of time and frequency measurement runs through each of these Groups, bringing strong interaction among the Groups.

NEW FREQUENCY STANDARDS

The accuracy of NIST's time scale is derived from primary frequency standards which provide the practical realization of the definition of the second. To meet advancing needs, the Division has constructed a new frequency standard, NIST-7, which went into operation in early 1993. This atomic-beam standard^[3,4] is based on optical pumping (using diode lasers) rather than the traditional magnetic methods used for state selection and detection. The current uncertainty for this standard is 5×10^{-15} , but further improvements in evaluation methods should allow for improvement perhaps to 1 or 2×10^{-15} . The Division is constructing a new cesium-fountain frequency standard^[5], which should be in operation within the next year. This work is a collaboration with the Atomic Physics Division of the Physics Laboratory at NIST, the Politecnico di Torino, and the Istituto Elettrotecnico Nazionale Galileo Ferraris. Looking toward still higher accuracy, the Division is studying standards based on trapped, laser-cooled ions^[6,7]. Ion standards offer promise of accuracy improvements of many orders of magnitude. While the ion studies continue to involve demonstrations of prototype clocks, the work is treated as basic research, providing the knowledge base for future standards.

IMPROVED TIME SCALES

The NIST time scale is the stable clock system which provides accurate signals for services and applications and which serves as a reference for research on new standards and measurement methods. The reliability and stability of this time scale is based on the use of an ensemble of frequency standards combined under the control of a computer-implemented algorithm. The key internal time scale used by NIST is called AT1. Recent improvements to the scale^[8] involve the addition of new commercial hydrogen masers and cesium-beam standards and the development of new reset procedures in the AT1 algorithm. The drift rate of the scale has been reduced from 1×10^{-16} /day to 3×10^{-17} /day. The random fluctuations of AT1 were also reduced by a factor of 2 to 2×10^{-15} at 100 days. Further improvements are expected as two additional hydrogen masers are added to the scale. Improvements are also being made in the electronic systems which read the clock outputs. All of these improvements are critical to the successful evaluation and use of the next generations of primary frequency standards now being developed by the Division.

IMPROVED METHODS OF TIME TRANSFER

Since the world operates on a unified time system, Coordinated Universal Time (UTC), highly accurate time transfer (to coordinate time internationally) is a critical ingredient in the operation of time scales and primary frequency standards. The Division is working to further improve the GPS common-view time transfer method, which is the key method now used for international time coordination.^[9] The Division is also working with others (including USNO) to improve the two-way time transfer method. While the simplicity and reliability of common-view time transfer makes it the current method of choice, the two-way method offers good potential for improved performance. A two-way link between North America and Europe has been studied, and another two-way link to the Pacific region is under development. Recent NIST work has focussed on errors in the earth stations.^[10]

IMPROVED OPTICAL FREQUENCY STANDARDS

The Division is also engaged in developing improved optical frequency measurements important for primary frequency standards, secondary wavelength standards based on atomic and molecular transitions, advanced optical communication, analytical instrumentation, and length measurement. The most obvious interest is in the development of future primary frequency standards using optical transitions, since, in general, higher frequency transitions yield a better fractional-frequency uncertainty. Another area of effort is on diode lasers, which can have very high spectral purity, tunability, simplicity, and low cost.^[11] The approach taken in this work is to prove concepts through demonstration of working systems. The Division also develops and characterizes accurate optical frequency and wavelength references such as the carbon dioxide laser^[12] and the calcium-stabilized diode laser.^[13] Such frequency references serve as standards in making accurate spectroscopic measurements in industrial and scientific programs. The program has recently been expanded to include a responsibility for the development of advanced optical-frequency standards to support improved length measurement and standards.

IMPROVED SPECTRAL-PURITY MEASUREMENTS

The Division's development of new spectral-purity measurements supports sound specifications for aerospace systems such as radar systems and special communication systems. Systems capable of making highly accurate measurements of both phase-modulation (PM) and amplitude-modulation (AM) noise have been developed for carrier frequencies in the RF and microwave regions.^[14] Portable systems have also been developed^[15], and these are being used to validate measurements made in industrial and government laboratories. Further work will broaden the spectral coverage and simplify comparison of measurement accuracy among standards laboratories. New PM and AM calibration services have been brought into operation over the last several years.

SYNCHRONIZATION FOR TELECOMMUNICATIONS

The Time and Frequency Division has been actively engaged with the telecommunications industry in issues relating to synchronization of advanced generations of telecommunications networks. NIST has made useful contributions to emerging telecommunications systems, particularly in the area of phase noise measurement and the statistical measures used to characterize the noise in telecommunications synchronization systems. Over the last five years, the Division has offered annual workshops (jointly with industry) on synchronization in telecommunications systems.

TIME AND FREQUENCY BROADCAST SERVICES

The Division provides time and frequency broadcasts from stations WWV and WWVB in Fort Collins, Colorado, and from WWVH in Hawaii and a time code broadcast from NOAA's GOES weather satellites.^[16] Last year, the Division initiated a project to increase the power output and reliability of the WWVB broadcasts at 60 kHz. At somewhat higher output power, these LF broadcasts could become substantially more useful for mobile and consumer applications, because the antenna/receiver cost and size would be very small and line of sight to the transmitter is not required. The Division also operates a Network Time Service and

a telephone service, the Automated Computer Time Services (ACTS)^[17], designed for setting clocks in digital systems.

These broadcasts serve applications in a broad range of systems in business, telecommunications, science, transportation, and radio/TV broadcasting. Industry calibration laboratories are served by the Division's Frequency Measurement Service, which provides these laboratories with continuous assurance of the accuracy of their frequency measurements.

APPLICATION OF TIME AND FREQUENCY TECHNOLOGY

Finally, the Division applies time and frequency technology to important problems in high-resolution spectroscopy^[18] and quantum-limited measurements.^[19]

DISCUSSION

We are witnessing a broad resurgence in the development of high performance time and frequency systems. This is the result of two key factors. First, satellite methods for time transfer now allow synchronization/syntonization of even the best atomic standards. Today's best standards simply could not be compared using the time transfer methods of the 1970s. The second factor involves the development of methods for controlling the states and motions of atoms using lasers. These new methods provide the means for circumventing the limitations inherent in the thermal-beam standards of the past. They make possible entirely new standards with a potential for reducing uncertainties by orders of magnitude.

Past advances in atomic timekeeping have opened up opportunities for advancing technologies requiring high-accuracy timing. Notable examples include satellite navigation, telecommunications, and electrical power distribution. If this history is any guide, we should expect similar technological advances to follow the development of the next generations of atomic standards. Program planning in the Time and Frequency Division of NIST is certainly based on that expectation.

REFERENCES

- [1] D.B. Sullivan 1987, "*Activities and plans of the Time and Frequency Division of the National Bureau of Standards*," Proceedings of the 18th Annual Precise Time and Time Interval (PTTI) Applications and Planning Meeting, 2-4 December 1986, Washington, D.C., USA, pp. 1-9.
- [2] D.B. Sullivan 1994, "*Time and frequency technology at NIST*," Proceedings of the 25th Annual Precise Time and Time Interval (PTTI) Applications and Planning Meeting, 29 November-2 December 1993, Marina del Rey, California, USA (NASA CP-3267), pp. 33-37.
- [3] R.E. Drullinger, D.J. Glaze, J.P. Lowe, and J.H. Shirley 1991, "*The NIST optically pumped cesium frequency standard*," *IEEE Transactions on Instrumentation and Measurement*, IM-40, 162-164.

- [4] R.E. Drullinger, W.D. Lee, J.H. Shirley, and J.P. Lowe 1995, "*The accuracy evaluation of NIST-7*," **IEEE Transactions on Instrumentation and Measurement**, IM-44, 120-123.
- [5] C.R. Ekstrom, W.M. Golding, R.E. Drullinger, F.L. Walls, A. DeMarchi, S.L. Rolston, and W. Phillips 1996, "*The design of an atomic fountain frequency standard prototype at NIST*," Proceedings of the 5th Symposium on Frequency Standards and Metrology, 15-19 October 1995, Woods Hole, Massachusetts, USA, ed. J.C. Bergquist (World Scientific, Singapore), pp. 411-412.
- [6] D.J. Wineland, J.C. Bergquist, D. Berkeland, J.J. Bollinger, F.C. Cruz, W.M. Itano, B.M. Jelenkovic, B.E. King, D.M. Meekhof, J.D. Miller, C. Monroe, M. Rauner, and J.N. Tan 1996, "*Application of laser-cooled ions to frequency standards and metrology*," Proceedings of the 5th Symposium on Frequency Standards and Metrology, 15-19 October 1995, Woods Hole, Massachusetts, USA, ed. J.C. Bergquist (World Scientific, Singapore), pp. 11-19.
- [7] M.E. Poitzsch, J.C. Bergquist, W.M. Itano, and D.J. Wineland 1996, "*Cryogenic linear ion trap for accurate spectroscopy*," **Reviews of Scientific Instrumentation**, 67, 129-134.
- [8] T.E. Parker, and J. Levine, "*Impact of New High Stability Frequency Standards on the Performance of the NIST AT1 Time Scale*," **IEEE Transactions on Ultrasonics, Ferroelectrics, and Frequency Control**, to be published.
- [9] W. Lewandowski, G. Petit, and C. Thomas 1993, "*Precision and accuracy of GPS time transfer*," **IEEE Transactions on Instrumentation and Measurement**, IM-42, 474-479.
- [10] F.G. Ascarunz, S.R. Jefferts, and T.E. Parker 1996, "*Earth station errors in two-way time transfer*," Proceedings of the 1996 IEEE International Frequency Control Symposium, 5-7 June 1996, Honolulu, Hawaii, USA, IEEE Catalog No. 96CH35935, pp. 1169-1172.
- [11] R.W. Fox, C.S. Weimer, L. Hollberg, and G.C. Turk 1993, "*The diode laser as a spectroscopic tool*," **Spectrochimica Acta**, 15, 291-299.
- [12] C.C. Chou, A.G. Maki, S.J. Tochitsky, J.-T. Shy, K.M. Evenson, and L.R. Zink 1995, "*Heterodyne frequency measurements and analysis of CO₂ 0002-[1001,0201]I,II sequence band transitions*," **Journal of Molecular Spectroscopy**, 172, 233-242.
- [13] A.S. Zibrov, R.W. Fox, R. Ellingsen, C.S. Weimer, V.L. Velichansky, G.M. Tino, and L. Hollberg 1994, "*High-resolution diode-laser spectroscopy of calcium*," **Applied Physics B**, 59, 327-331.
- [14] F.L. Walls 1993, "*Secondary standard for PM and AM noise at 5, 10, and 100 MHz*," **IEEE Transactions on Instrumentation and Measurement**, IM-42, 136-143.

- [15] F.G. Ascarrunz, and F.L. Walls 1996, "*A standard for PM and AM noise at 10.6, 21.2 and 42.4 GHz,*" Proceedings of the 1996 IEEE International Frequency Control Symposium, 5-7 June 1996, Honolulu, Hawaii, USA, IEEE Catalog No. 96CH35935, pp. 852-853.
- [16] R.E. Beehler, and M.A. Lombardi 1991, **NIST Time and Frequency Services**, NIST Special Publication 432 (Revised 1990) (available from the Superintendent of Documents, U.S. Government Printing Office, Washington, D.C. 20402-9325 USA).
- [17] J. Levine, M. Weiss, D.D. Davis, D.W. Allan, and D.B. Sullivan 1989, "*The NIST Automated Computer Time Service,*" **Journal of Research of the National Institute of Standards and Technology**, **94**, 311-321.
- [18] K.M. Evenson 1995, "*Laser spectroscopy in the submillimeter and far infrared region,*" **Atomic, Molecular, and Optical Physics Reference Book**, ed. G.W.F. Drake (AIP Press, New York, New York, USA), pp. 473-478.
- [19] J.J. Bollinger, W.M. Itano, D.J. Wineland, and D.J. Heinzen, "*Optimal frequency measurements with maximally correlated states,*" **Physical Review**, **A54**, R4649-R4652.

Questions and Answers

CLAUDINE THOMAS (BIPM, FRANCE): The oscillation we see in UTC - UTC(NIST) is due to your steering process? Or is it a seasonal variation or something which has to do with humidity variations?

JUDAH LEVINE: I don't know. I think it is a little of both. The steering loop which we use for controlling UTC(NIST) has a 1-year time constant to it. And that could very well amplify an underlying annual term, or at least not attenuate an underlying annual term.

I think it is a little of both. I think there is an annual term either in our timescale or in the distribution process, and our algorithm did not completely remove it.

CLAUDINE THOMAS: I have a second comment. I really appreciate seeing the uncertainty budget from NIST-7. In fact, I must say that it's the first time I've seen it.

JUDAH LEVINE: I think Dr. Drullinger is sitting back there. You ought to hassle him.

CLAUDINE THOMAS: Is it published somewhere?

JUDAH LEVINE: I don't know.

CLAUDINE THOMAS: I mean, the uncertainty budget with a 5 part in 10 to the 15th.

JUDAH LEVINE: I refer you to Dr. Drullinger.

GERNOT WINKLER (INNOVATIVE SOLUTIONS INT'L): I note with interest that you're increasing the power on 60 kHz. This is going to be an improvement, but it will not cure the basic problem on the East Coast, which is the nighttime interference from MSF, England. I wonder what wisdom is there to spend so much money on improving the power instead of changing the frequency.

JUDAH LEVINE: In the first place, thanks to the United States Navy, the cost of improving the power is not as much as you think, because the transmitters were free. The Navy gave them to us.

That's a difficult issue. Our hope is that the electric field at the East Coast will exceed 100 microvolts per meter after the upgrade is finished; and we think that's going to be enough that the receivers can lock. I think changing the frequency - well, to be perfectly honest, I would guess that it's politically unthinkable. There is an enormous install base of WWVB receivers. I would hesitate to suggest it. My guess is that I'd be run out of town on a rail. I just don't think it's possible, I think we're too far into it now. I mean, it's something to consider, but I would guess it just can't be done.

SIGFRIDO LESCHIUTTA (IEN, ITALY): Excuse me, the frequency is still at 60 kHz?

JUDAH LEVINE: Yes, it's exactly 1,000 times the power line frequency, exactly.

EUROPEAN PTTI REPORT

Franco Cordara
Istituto Elettrotecnico Nazionale G. Ferraris
Corso Massimo d'Azeglio, 42, Torino 10125, Italy

Andrea De Marchi
Politecnico di Torino, Torino, Italy

Michele Serafino
Politecnico di Torino (guest researcher)

Sigfrido Leschiutta
Politecnico di Torino and Istituto Elettrotecnico Nazionale

Abstract

Time and Frequency Metrology in Europe presents some peculiar features in all its four main components: research on clocks and time scales, comparisons and dissemination methods, and dissemination services. Apart from the usual and traditional tasks of the national metrological laboratories, an increasing number of cooperation activities between the European Countries are promoted inside some European organizations, such as the EC, EAL, and EUROMET, that will be dealt with in what follows. The present situation is evolving in four directions: national authorities strive to reduce nationally provided funds and suggest that their national laboratories compete in Brussels for community-provided funds, some trends toward a "privatization" of metrological and standardization activities, the upsurge of new labs and organizations, and the availability in some European countries of well-trained researchers coming from Eastern Europe. There are two additional problems, similar, as far we can presume on both sides of the Atlantic: the shrinking of defense-driven markets and the economical crisis of space agencies.

1 INTRODUCTION

Time and frequency activities are alive and well in Europe, in all its four components: research on clocks and time scales, comparisons and dissemination methods, and dissemination services. European laboratories are more and more confronted with the ubiquitous GPS and are forced to explore new avenues. The scope of this paper is to present a report on these activities, pointing out practices or solutions that are peculiar to a developed continent such as Europe, that has to cope with a host of issues, political, economic, and also technical, such as GPS. Also, some technical or organizational aspects that are different from the practices followed in the United States will be pointed out. Some of the new developments and problems are presented and commented in the second section.

In the third section, with charts and graphs the distribution of all these activities over Europe is considered, along the selection criteria adopted to form the database.

Research on atomic clocks and related devices is presented in the fourth section, following two guide lines, the kind of institution involved, and the type of research performed.

Section 5, dealing with research on dissemination systems, describes two major items: a relevant series of *one-way* and *two-way* experiments and research on the so-called marginal effects on GPS time comparisons, such as the instrumentation or the ionospheric and tropospheric effects.

Dissemination activities and their consequence, traceability, are presented in Section 6; two items are of interest, one in the realm of well known distribution services – frequency standard and time signal emissions, time codes, and so on – and the other in the certification of “external” or industrial laboratories.

Finally, in the last section, an exercise in summarizing the situation and in forecasting the future will be attempted, also taking into account the political changes occurring on the Continent.

Since this paper is a general survey, relevant bibliography will not be appended. The reader interested in the various technical topics is referred to some Transactions or Proceedings of a number of devoted Symposia or Meetings, quoted in what follows. This paper is an update of a similar effort presented during the 23rd PTTI Meeting; consequently information still valid is not repeated here.

2 NEW DEVELOPMENTS AND PROBLEMS

2.1 Situation

In presenting a report on the PTTI activities in Europe, the concept of Europe itself has to be defined. For the recent political and economical changes, also the organization aspects have changed dramatically or are in the process of being modified.

While for the Western countries general information is available or can be guessed, for Eastern Europe the past and the present situation is known to a far lesser extent. This fact is obviously reflected in this report. Data presented here were mostly deduced by personal acquaintances, visits, or, as will be seen, inspection of the literature. Omissions, errors, or faulty guesses, of which the authors only will be responsible, will be undoubtedly detected.

The acronyms used are spelled out in the Annex to this paper, but some, more important, will be now introduced:

EC European Commission, an organization with economical and political scopes; most of the Western European countries are members of EEC. It is planned that the political implications of EEC will increase with time, a major step, with profound resonance, being the adoption of a common currency in a few years time.

EUROMET European Collaboration in Measurement Standards, secures a common metrological basis for all the activities on a regional basis.¹

EAL European cooperation for the Accreditation of Laboratories.

¹There is an upsurge of metrological organizations with regional basis: NORAMET (Canada, Mexico, United States), APMP (Asia-Pacific Metrology Program), SIM (Sistema Iberoamericano de Metrologia), and COOMET (Cooperation among national Metrology institutes of Central and Eastern European states); similar organizations are active in Central-South Africa and in North Africa.

This somewhat complicated structure is needed in order to assure the uniformity of calibration criteria and standards. The running of these machineries is a formidable task; in history-laden Europe, there are twelve principal languages and six others have a recognized status, even if EC has only four official working languages.

There is a growing pressure from the 24 new states originating from the breakup of the communist area to join European organizations, with the risk of introducing big changes in the existing structures. This explains the struggle among EC members to find new criteria to stabilize the process.

2.2 Privatize or Not

Profound changes in the organization of metrology are under way, such as the "privatization" of the metrological activities, completed in the Netherlands and in progress in the United Kingdom. Another trend along with the privatization is the stress on these institutions to devote their activities to a research nearer to industrial needs or the demands coming from the world market.

Since these new approaches in some extent disrupt a century-long tradition, it seems interesting to provide some details as regards the privatization of NPL—the National Physical Laboratory—the standards Laboratory for the UK.

In 1992 the UK Government launched a study of possible changes in NPL's status. This included, but rapidly rejected, its sale or the creation of a "non-profit distributing" company. This was because these structures could fail financially and this was not acceptable to the Government. The solution they adopted, therefore, was that of a "Government-Owned Contractor-Operated" (GOCO) body modelled on similar American management arrangements for some of its own national laboratories, such as Los Alamos. Under GOCO, the Government owns NPL's equipment, buildings, and land, but the staff have formed a company "NPL Management Ltd.," which is a subsidiary of its management contractors (Serco plc) for the current 5-year contract. Key features of the new organization are:

- The Government has guaranteed a very high proportion of NPL's income throughout the contract. This stability (not available within the civil service structure) gives the Laboratory a sound base on which to plan its future development;
- costs have been reduced and the UK Government has reinvested these savings in new activities at NPL. As a result of this and other new contracts, NPL has taken on over 100 new staff in the last year; and
- as NPL remains constrained from taking unfair advantage of its "monopoly" position, it does not compete with accredited laboratories. In addition, it does not market its services outside the UK if these are available from the country's own national laboratory. This maintains NPL's previous operational policies.

2.3 The Impact of the European Community

The European Community (EC), now the European Union, is supporting a number of research programs, on competitive basis. In particular, the Standards, Measurements, and Testing (SMT) research program (1994-1998) is now underway, under the so-called IV Framework Programme for Research, Technological Development, and Demonstrations.

The objectives of the program are:

- to improve the position in all sectors of European industry,
- to promote research in support of the European standardization bodies,
- to support the further development of the European measurement infrastructure, and
- to promote the dissemination and application of good measurement practice.

Priorities are on:

- measurement in support of the research,
- measurement and testing in the industrial development phase,
- measurement and testing for the control of production
- technical support to total quality in measurement, and
- written standards for industry.

The indicative Community founding available in total for the 5-year period is 173 MECU (million ECU). ECU is the name adopted for the accounting unit, to become, hopefully, a currency. The quoted founding is equivalent to about 220 million dollars.

The development of common primary standards (devices) is included in these programs.

2.4 Regional Metrological Organizations – EUROMET

The need for establishing a consistency of measurements worldwide, as required by increased industrial competitiveness, has been producing some changes in the traditional roles of the international bodies, namely the BIPM and the Consultative Committees of the CIPM, responsible for the uniformity of measurements, and is pushing toward the foundation of regional organizations for metrology.

If the main role of BIPM is the keeping and dissemination of the units of the International System, and the Consultative Committees are now concerned with the definition of key comparisons in the different fields among the national metrology institutes (NMI) to establish the equivalence of units, the regional groupings are going to take the responsibility for the consistency of measurements in a more limited (continental) area. This task is done by means of interlaboratory comparisons extending the traceability to the SI units at a larger number of laboratories.

The first of such organizations, EUROMET, was established in 1989 on a voluntary basis and its structure has been reproduced in other areas (APMP, NORAMET, SIM) and is going to be developed also in Africa. The membership of the NMI of Western Europe in EUROMET has been a way to coordinate researches and intercomparisons on measurement standards, to transfer metrological expertise among the members and to provide information about the resources and services available. Other important tasks of EUROMET are also the cooperation with the European calibration services and that of legal metrology. The framework for these activities has been provided by specific projects (cooperation, comparison, traceability, and consultation) activated in the 10 basic subject fields, each one coordinated by a Rapporteur. For any subject field, every NMI can appoint a Contact Person who takes part to the meeting organized by the Rapporteur, usually once per year.

In 1996, the EUROMET Committee accepted the first "associated members," namely the national metrology institutes of the Czech Republic, Slovak Republic, Poland, and Hungary, and there is a growing interest in joining the organization from other Eastern European countries. A new feature of the comparisons performed in this context between the national laboratories is publication in *Metrologia* of the final results to document the equivalence in measurements.

The projects agreed and running to date in the time and frequency field deal with: a) satellite time and frequency intercomparisons using PRN codes, b) research on new cesium primary standards, and c) stability characteristics of measurement systems. A new project on the uncertainty evaluation in time and frequency calibration has been proposed recently.

Updated information on proposed, agreed upon, and completed EUROMET projects in the different fields is available on World Wide Web at the following address: <http://www.dfm.dtu.dk>. A good occasion to exchange information on the activities performed at the NMI is given by the yearly Contact Persons meeting organized by the Rapporteur; for example, the last meeting held in March 1996 at NPL gave the chance to get detailed information on the structure and planned activity of the new Swedish time and frequency laboratory at the Swedish National Testing and Research Institute.

3 EUROPEAN TIME AND FREQUENCY LABORATORIES

In the quoted report presented in 1993, a survey of the existing laboratories was given. The laboratories and institutes listed in that report are still active², some with names or affiliations changed, but a large number of new institutions were formed in the last three years for three reasons :

- to reflect the political changes,
- to satisfy new needs of testing and calibrations in countries in which previously no sizable T/F activities were present, and
- to take profit from the emergence of traceability needs.

A special case in Europe is that of the BIPM, the Bureau International des Poids et Mesures, with seat in Paris; because this bureau belongs to an international organization based on the international treaty signed in 1875 during the "Conference Diplomatique du Mètre," its researchers and activities are not dealt with much in what follows. The relevant and continuous level of activity of BIPM in our field can be estimated anyway from the high number of contributions in the PTTI Meetings.

An attempt has been made to deduce, at least approximately, the "workforce" engaged in time and frequency activities in Europe, with the additional exception of the researchers working in military institutions, in industry, and in Russia and eastern countries.

The total number is about 170 people. About 50 are active in France (LPTF, LHA, LPMO, OCA, CNET, CNES, and universities); about 35 are estimated to operate in Germany (PTB, FTZ, Max-Planck Institute, DARA [the German space agency], and a host of universities). About 30 are in Italy (IEN, IMGC, ISPT, Cagliari Observatory, Matera laser ranging station,

²F. Cordara, S. Grimaldi, and S. Leshiutta 1994, "European PTTI Report," Proceedings of the the 25th Annual Precise Time and Time Interval (PTTI) Meeting, 29 November-2 December 1993, Marina del Rey, California, USA (NASA CP-3267), pp. 39-54.

and some universities) and about the same figure can be credited to the UK. The remaining people are working in Austria, Belgium, the Netherlands, the Nordic countries, Portugal, Spain, and Switzerland. A far larger number of experts in PTTI technologies are engaged in the calibration centers, at the moment 193 labs are active in Western Europe only, as will be shown in Table II.

To investigate "productivity" and types of interest, a bibliographical research was performed by examining all the papers that appeared in the last 10 years, from 1987 to 1995 and, whenever possible, 1996. Papers considered are those presented in oral or poster form at :

- EFTF - the European Forum on Time and Frequency,
- FCS - the Frequency Control Symposium, and
- PTTI - the Precision Time and Time Interval Meeting,

or that appeared in:

- Metrologia and
- IEEE Transactions on Instrumentation and Measurement.

For these two latter sources, the analysis was limited to the available printed material. For all the five sources, a referee committee is active.

The total number of papers prepared in European labs in the 10 years considered, in the domain of time and frequency and following the above-mentioned selection criteria, is some 700. Trends about the number of papers and the conference of presentation are presented in Fig. 1.

4 RESEARCH OF FREQUENCY STANDARDS AND CLOCKS

Using the database of the previous section, an inquiry was made about the subject of the research and the kind of laboratory involved, national metrological institute, national research laboratory dedicated to one specific topic – astronomical observatories included –, universities, and industries.

The results are gathered in Fig. 2. In the last 10 years, European labs have produced about 280 papers, 110 of which devoted to cesium devices (traditional, optically pumped, fountains, etc.). This figure reflects the strong and traditional European involvement in the standard that embodies the SI definition of the second. Nearly 35 papers deal with hydrogen masers. Since 1993 remarkable interest in the frequency stabilization of lasers, not so much as frequency standards, but as length standards or references, can be observed.

In more detail regarding the national laboratories, in the UK the cesium fountain is being studied. In France, in addition to the fountain research, an evaluation of an optically pumped cesium-beam was recently performed, and a factory started the production of an optically pumped cesium-beam standard. Future activities are planned toward atomic clocks to be operated in microgravity conditions. Germany has built two vertical cesium beams and some ion traps. Finally, in Italy, the final evaluation of the magnesium-beam standard was recently

presented and a research activity was initiated on an unconventional cesium-beam frequency standard.

Of some interest is an effort of support and coordination launched by the European Community in the field of cesium devices. The responsibility of this activity was given to Politecnico di Torino. The aim of this effort is a coordination of the European laboratories, also via a support of researcher mobility. Labs in England, France, Germany, Italy, and Switzerland joined in this effort.

5 RESEARCH ON SYNCHRONIZATION SYSTEMS AND DISSEMINATION METHODS

Using the same database introduced in Section 3, a survey was performed about the papers on comparison, dissemination, and similar topics. The results are given in Fig. 3. The papers are over 430; the interest is evenly divided between comparison, dissemination, and applications of time and frequency technology. Differences between synchronization, comparison, and dissemination are indeed faint ones, since the same basic methods or technologies can be used for all three operations. Research and experiments on these topics are widespread and devoted to four major lines: satellite time transfer (two-way and one-way), GPS, broadcasting from special dedicated transmitters, and the use of modems on telephone lines.

5.1 Satellite Time and Frequency Transfer

Two-way

In this field, most of the activities performed by European laboratories have been related to the two-way intercomparisons on INTELSAT satellite 5-13 at 307°E using the PRN codes generated by MITREX modems. Six European laboratories (TUG, NPL, PTB, FTZ, OCA, and VSL) regularly performed three measurement sessions per week during 1994 and 1995 and were joined by two U.S. laboratories (NIST and USNO).

The huge amount of data collected has been analyzed by the participants and the results have been compared with those obtained from the GPS common-view technique, showing that further studies and characterization of the equipment used are necessary to reach the accuracy of 10^{-15} over one day, obtained in common clock experiments, that makes the method so interesting for the comparison of the new primary standards.

Of particular importance is the measurement of the station delays by means of a satellite simulator, possibly at each synchronization session, and the knowledge of the long-term stability of the delays of the instrumentation used for time scale generation and distribution, in addition to that of the time interval counter used. In 1997 one more station (IEN) will be able to join the existing network that is expected to resume the normal comparisons schedule in January 1997.

Again using a two-way method, experiments of time and frequency dissemination by means of spread-spectrum coded signals, used for satellites tracking and transmitted with normal programs by ASTRA Direct TV broadcasting satellites, have been performed by Time Tech (Germany) with the aim to establish a very accurate dissemination system, usable by disciplined secondary standards at a level approaching that of hydrogen masers for integration times of about one day.

The modification of the SATRE modem, used in this experiment, to make it compatible with the MITREX codes, has also been nearly completed by the same source. Among the interesting features of this device we can quote the ± 15 MHz frequency agility, very helpful using V-SAT ground stations, the availability of codes with higher chip rates, fast acquisition times even at low signal levels, and the capability of remote control. The availability of such a device on the market is instrumental for the development of the two-way network.

As regards to the two-way time transfers using laser techniques, a new experiment called T2L2 (Time Transfer by Laser Link) has just been proposed by OCA, CNES, and the European and Russian Space Agencies. The payload will be put on the Russian space station Mir (380-410 km altitude, 51.6° inclination) in 1999 and is the first experiment scheduled after LASSO; the expected accuracy is 50 ps, ideal for comparing the cesium fountains clocks that should be in operation by the end of the century in a number of laboratories. Timing centers need to be connected with a laser station where the start time of the lasers pulses carrying the clock information and the time of arrival of the reflected photons are measured in the reference clock time scale. Special timers have been designed and the stability of the payload ranges from 1 ps over 300 s to 10 ps over 10 days.

One-way

Coming to one-way systems based on geostationary satellites, further activities have been performed in France and Italy using different techniques. The TV signals of the Direct Broadcasting Satellite (DBS) TDF2 has been used by four labs in France to synchronize clocks, correcting the results for the satellite movement by means of different techniques, e.g. averaging over one sidereal day and correcting for the longitude drift by one calibrated link, etc. The possibility of determining the satellite position from the synchronization data has also been tested comparing the results with the data supplied by the satellite control center, but the short baselines limited the precision. Frequency comparisons with Allan deviations of a few parts in 10^{14} have been obtained over a period of 10 days.

The test performed by IEN in the frame of the INTELSAT 5-13 experiment was based on the reception of the MITREX codes transmitted by the other European labs by means of a DBS receiving station that had been frequency-stabilized to cope with the locking range requirement of the modem. The measurement results, after the correction for the satellite movement obtained from the pseudorange data of the two-way stations, showed that frequency transfer capabilities at the $3 \cdot 10^{-14}$ for observation times greater than 2 days are achievable.

5.2 GPS SYSTEM

The error budget of a time comparison or time dissemination via GPS or GLONASS satellites has a large number of entries that can be gathered in a number of classes. For a time-minded user's standpoint, the most important classes are the way to collect and treat the data, position of the antenna, equipment delays and their variations with time and temperature, and propagation effects.

GPS for Comparisons

Apart from the research performed at the BIPM on both GPS and GLONASS receivers behavior and on the obtainable accuracy of carrier-phase and P-code measurements, experiments have been performed to characterize the long-term stability of the GPS receivers delays and the noise of common-view time transfers (IREE-Czech Rep.) and on the use of modified geodetic receivers for time transfer (Astronomical Institute, Berne University, Switzerland). In this

last case, the results obtained from carrier-phase measurements and P-code observations, also compared with the common-view results, have shown a factor of 10 improvement of the precision with the carrier-phase comparisons over the code measurements, but also that relevant phase changes due to temperature effects on the receivers are present. Frequency comparisons at 10^{-14} over 3 hours seem possible.

To get the utmost accuracy from the GPS comparisons, the need to use a more sophisticated model to compute the corrections for the tropospheric and the ionospheric delays, taking into account the local meteorological parameters, the position of the satellite observed, and the time of the day, has also been demonstrated.

GPS for Dissemination

The dissemination service scene in Europe has registered a high increase in the use of GPS signals both as time references at the microsecond level and to discipline quartz and rubidium standards, thanks to the availability of unexpensive multichannel receiving cards. No competition for the time being has come from European countries, but programs for the implementation of a global navigation system for the civilian market (GNSS - Global Navigation Satellite System) are entering the implementation (GNSS1) or the study phase (GNSS2).

The development of a system called EGNOS (European Global Navigation Overlay System) is promoted by the Commission of the European Union (CE), the European Space Agency (ESA), and EUROCONTROL and will include geostationary satellites to complement the existing satellite navigation systems (GPS and GLONASS) to meet the integrity requirements of civil aviation for all phases of flight and those of maritime, inland navigation, and rail transportation in the European Region. To these users one has to add the potential market (20 million) of the Intelligent Vehicle Highway Systems, that should offer in-car navigation facilities. What matters more for the time and frequency community is that EGNOS geostationary satellites, if the program is eventually approved, will also disseminate accurate time, synchronized to UTC, to the users, as will be done by the other augmentation systems under study in the United States (WAAS) and Japan (MTSAT).

Much reliance on this research comes from the BIPM, the Bureau International Poids et Mesures, in Paris and a great deal of research and experiments was performed at the BIPM itself in recent years. The development of this research was well covered in past PTTI Meetings, mostly about the treatment of data and the influences of poorly known antenna coordinates. These problems having been solved or identified, the interest is now in the propagation phenomena, both in the ionosphere and troposphere, and in the study of the equipment delays. A better knowledge of ionospheric delay variations was promoted by the possible use of the GPS system for the "precise" navigation of scientific satellites. Since the common-view method, on which at the moment the formation of TAI time scale is based, is a one-way method, studies and experiments are under way in Europe on the effects of the ionospheric delay.

6 DISSEMINATION AND TRACEABILITY

6.1 LF Dissemination Systems

A major difference between Europe and the USA lies in the fact that in Europe a large share of the dissemination services is performed via dedicated or broadcasting stations operating in the LF and MF bands, between 50 kHz and about 1600 kHz.

Coming back to these traditional dissemination systems, the situation of the broadcasting stations in the LF and MF band is nearly unchanged from the last report (1993). Nevertheless, an

increased use can be observed of such transmissions for the automatic synchronization of cheap electronic devices like wrist watches and wall clocks that address the wider consumer market. To give an example, the production of integrated circuits to decode DCF 77 emissions operated by PTB (Germany) has reached to date a total of 25 million units.

6.2 Time Dissemination via Modems and Telephone Lines

These telephone services were first implemented at the Technical University of Graz, Austria, in 1988 and subsequently in Sweden (1990), in Italy (1991) and are planned, using the same code, to be in operation in the near future in Germany, the Netherlands, and the UK.

The European telephone time code dissemination services, designed for the synchronization of computer clocks and following a common format, have been activated in a relevant number of countries as shown in the Table I, where also some international telephone numbers can be found.

Table I - European Time Code Services

Country	Laboratory	Telephone No.	Link Delay Measurement
Austria	TUG	+43 316 472 366	yes
Belgium	ROB	+32 237 303 20	no
Germany	PTB	+49 531 512 038	yes
Italy	IEN	(*)	no
Netherlands	VSL	+31 152 617 181	yes
Portugal	IPQ	+35 112 940 425	yes
Switzerland	OFMET	+41 313 233 225	yes
Sweden	SP	(*)	yes
United Kingdom	NPL	(*)	yes

(*) service not available from abroad

Most services that use a time code generator, developed at the Technical University of Graz (Austria) have the capability to measure the round-trip delay and to correct the 1 pps markers for the one-way delay, allowing one to trace a local clock to the national time scale with an uncertainty of a few milliseconds. In the near future, the service will be operative also in Spain, Poland, and Turkey.

6.3 Traceability

The heavily increased demand of measurement and test equipment traceability to the national measurement standards, stimulated by the application of ISO 9000 Quality Standards and by the need of removing the technical barriers to the international trade agreements, has been faced in Western Europe by establishing in each country accreditation services for both calibration and test laboratories.

Since 1994 these activities, mostly related to interlaboratory comparisons, proficiency testing of accredited centers, and the development of guidance documents, have been coordinated by EAL (European cooperation for the Accreditation of Laboratories) that reached at the end of 1995 an overall membership of 20 countries. The calibration and testing bodies of 12 of these countries are signatories of the Multilateral Agreement of mutual equivalence and acceptance of calibration certificates and test reports involving 5,000 labs. There are of course strong connections between EAL and the national metrological institutes, as they guarantee

the vertical traceability to the SI units in each country, the European Commission, and the international organizations charged with scientific and legal metrology.

In 1995 the first accreditation bodies from Eastern Europe, namely from the Czech Republic, the Slovak Republic, and Hungary, joined EAL. As regards to the time and frequency field, the Table II reports the number of calibration centers accredited for each member country, updated to early 1996:

Table II - European Calibration Centers Accredited for Time and Frequency

Country	Calibration Service	Number of Accredited Centers	
		Frequency	Time Interval
Denmark	DANAK	8	5
Finland	FINAS	6	2
France	COFRAC	32	4
Germany	DKD	16	8
Ireland	ILAB	3	3
Italy	SIT	16	1
Netherlands	NKO	19	12
Portugal	IPQ	5	-
Spain	ENAC	2	2
Sweden	SWEDAC	8	7
Switzerland	SAS	13	3
United Kingdom	UKAS	64	15

The total number of accredited centers for frequency is 193, with an increase of about 40% versus the 1993 data, and the uncertainty levels are within 10^{-6} and 10^{-13} .

7 FINAL REMARKS

A general remark is the fact that the research developed in the European countries finds no adequate industrial counterpart. A great deal of the research performed in the universities remains at academic level. The manpower and the allocated funds appear adequate to the size of the populations and industries to be served, but the necessity to respect national priorities involves sometimes a duplication of efforts.

One must be aware of the fact that in the past the "technical standards" were a "polite" form of protection for the factories of a country. In other words, the "acceptable technical standards" played the role of customs. Speaking of "duplication," a word of prudence is of order. While, in calibration and applied metrology services, the amount of resources to be dedicated at the end must be proportional to the market to be served, the situation is quite different as regards fundamental metrology. In this realm, where the accuracy of a device can be only estimated and not measured, "duplication" of efforts is needed for two reasons: the search of systematic unknown effects from one side and of new avenues to reach a specific goal from the other. These facts are not usually appreciated by the administrators for whom there is no need of research on something already existing on the market.

One could wonder why there are so many metrological laboratories in Europe, having a population of the same order of that of the United States. The answer it is not an easy one,

but the situation can be justified by the strong specialization of the individual labs, the different needs and levels of industries, the different priorities given by each country, and also – why not – psychological factors such as national pride.

What can be done, and has been done, is a painstaking effort of coordination. In the realm of standards (not the devices, the calibration and testing procedures), much has been achieved. But two major problems, one economical, the second political, stand in front of the research on time and frequency in Europe; the first is in the limited amount of money that will be allocated in the future, at least in some nations. The second one, a major task indeed, awaits the European laboratories in establishing cooperation plans with the 20-odd metrological laboratories or institutions of East Europe. Western European labs were and are, to some extent, technologically minded, whereas in Eastern labs the ingenuity was sometimes limited only by the available technology. A lot can be learned from both sides in this cooperation and amalgamation process.

In a previous PTTI meeting, another point was raised concerning an additional effort of organization to be attempted toward a possible coordination between the three annual symposia: EFTF, FCS, and PTTI. All three are very vital enterprises, but in a period of general shortage of resources, some considerations should be made about this topic, leading toward a sort of sharing in frequency or in time domain. An encouraging step was recently announced with a decision from IEEE-Frequency Control Symposium and the EFTF (European Frequency and Time Forum) to check the advantages of holding alternatively two events on both sides of the Atlantic.

ANNEX

Acronyms Used in the Text

CNES	Centre National Études Spatiales, Toulouse, France
CNET	Centre National Études Télécommunication, Bagneux, France
COFRAC	National calibration service of France
DANAK	National calibration service of Denmark
DKD	National calibration service of Germany
ENAC	National calibration service of Spain
FINAS	National calibration service of Finland
FTZ	Forschung und Technologiezentrum, Darmstadt, Germany
IEN	Istituto Elettrotecnico Nazionale, Torino, Italy
ILAB	National calibration service of Ireland
IMGC	Istituto di Metrologia G. Colonnetti, Torino, Italy
IPQ	Institut Português de Qualidade, Monte de Caparica, Portugal
IREE	Ustav Radiotechniky a Elektroniky CSAV, Praha, Czech Republic
ISPT	Istituto Superiore Poste e Telecomunicazioni, Roma, Italy
LHA	Laboratoire de l'Horloge Atomique, Orsay, France
LPMO	Laboratoire Physique Mesure Oscillateurs, Besançon, France
LPTF	Laboratoire Primaire Temps et Frequences, Paris, France
NIST	National Institute of Standards and Technology, Boulder, Colorado, USA
NKO	National calibration service of the Netherlands
NPL	National Physical Laboratory, Teddington, UK
OCA	Observatoire Côte d'Azur, Grasse, France
OFMET	Swiss Federal Office of Metrology, Wabern, Switzerland
ORB	Observatoire Royal de Belgique, Brussels, Belgium
PTB	Physikalisch-Technische Bundesanstalt, Braunschweig, Germany
SAS	National calibration service of Switzerland
SIT	National calibration service of Italy
SP	Sveriges Provnings - och Forskning Institut, Borås, Sweden
SWEDAC	National calibration service of Sweden
TUG	Technische Universität, Graz, Austria
UKAS	National calibration service of the United Kingdom
USNO	U.S. Naval Observatory, Washington, D.C., USA
VSL	Van Swinden Laboratorium, Delft, the Netherlands

THE NETWORK COMPUTER AS PRECISION TIMEKEEPER*

David L. Mills
Electrical Engineering Department
University of Delaware
Newark, Delaware 19716, USA
mills@udel.edu; URL:www.eecis.udel.edu/~mills

Abstract

This paper describes algorithms to discipline a computer clock to a source of standard time, such as a GPS receiver or another computer synchronized to such a source. The algorithms are designed for use in the Network Time Protocol (NTP), which is used to synchronize computer clocks in the global Internet. They have been incorporated in the NTP software for Unix and Windows and, for the highest accuracy, in the operating system kernels for Sun, DEC, and HP workstations. Rms errors on LANs are usually less than 10 μ s and on global Internet paths usually less than 5 ms. However, rare disruptions of one kind or another can cause error spikes up to 100 μ s on LANs and 100 ms on Internet paths.

1 INTRODUCTION

General purpose workstation computers are becoming faster each year, with processor clocks now operating at 300 MHz and above. Computer networks are becoming faster as well, with speeds of 622 Mbps available now and 2.4 Gbps being installed. Using available technology and existing workstations and Internet paths, it has been demonstrated that computers can be reliably synchronized to better than a millisecond in LANs and better than a few tens of milliseconds in most places in the global Internet.^[1] This technology includes the Network Time Protocol (NTP), now used in an estimated total of over 100,000 servers and clients in the global Internet. Over 220 primary time servers are available in this network, each connected to an external source of time, such as a GPS radio clock or ACTS telephone modem.

Reliable network synchronization requires crafted algorithms which minimize jitter on diverse network paths between clients and servers, determine the best subset of redundant servers, and discipline the computer clock in both time and frequency. The Network Time Protocol (NTP) is designed to do this in Unix and Windows operating systems. The NTP architecture, protocol, and algorithms have evolved over almost two decades, with the latest NTP Version 3 designated an Internet (draft) standard^[2]. Among the goals of this design are:

*Sponsored by: DARPA Information Technology Office Contract DABT 63-95-C-0046, NSF Division of Network and Communications Research and Infrastructure Grant NCR 93-01002, Northeastern Center for Electrical Engineering Education Contract A303 276-93, Army Research Laboratories Cooperative Agreement DAA L01-96-2-002, and Digital Equipment Corporation Research Agreement 1417.

1. Optimize the computer clock accuracy and stability, subject to constraints of network overheads and/or telephone toll charges, relative to local and/or remote sources of time.
2. Enhance the reliability by detecting and discarding misbehaving local and/or remote sources and reconfigure network paths as necessary.
3. Automatically adjust algorithm parameters in response to prevailing network delay/jitter conditions and the measured stability of the computer clock.

At the heart of the NTP design are the algorithms that discipline the computer clock to an external source, either an NTP server elsewhere in the Internet or a local radio or modem. A key feature in this design is improved accuracy to the order of a few microseconds at the application program interface (API). The need for this becomes clear upon observing that the time to read the computer clock via a system call routine has been reduced from 40 μ s a few years ago on a Sun Microsystems SPARC IPC to less than 1 μ s today on an UltraSPARC.

The computer clock discipline algorithm, which is at the heart of the design, is described in this paper. It is implemented as an adaptive-parameter, type-II, hybrid phase/frequency-lock loop. Portions of the algorithm are implemented in the NTP software that runs the protocol and provides the computer clock corrections. The remaining portions have been implemented in this software and in the operating system kernel. For greater accuracy, a stable oscillator and counter delivering a pulse-per-second (pps) signal can be used to steer the computer clock frequency, while an external NTP server or local radio provides the UTC time. For the highest accuracy, a pps signal synchronized to UTC can be used directly to discipline the frequency and time within the second, while an external source, such as an NTP server or radio, provides the UTC seconds numbering.

2 NETWORK TIME PROTOCOL

While not in itself the subject of this paper, an overview of the NTP design will be helpful in understanding the algorithms involved. As described in [3], a *synchronization subnet* is a hierarchical set of time servers and clients organized by *stratum*, in much the same way as in digital telephone networks. The servers at the lowest stratum are synchronized to national standards by radio or modem. In order to provide the most accurate, reliable service, clients typically operate with several redundant servers over diverse network paths.

The NTP software operates in each server and client as an independent process or *daemon*. At designated intervals, a client sends a request to each configured server and expects a response at some later time. The exchange results in four clock readings, or *timestamps*, one at the sending time (relative to the sender) and another at the receiving time (relative to the receiver), for the request and the reply. The client uses these four timestamps to calculate the clock offset and roundtrip delay relative to each server separately. The *clock filter algorithm* discards offset outliers associated with large delays, which can result in large errors. As a by-product, a statistical accuracy estimate called *dispersion* is produced which, combined with the stratum, is used as a metric, called *synchronization distance*, to organize the NTP subnet itself as a shortest-path spanning tree.

The clock offsets produced by the clock filter algorithm for each server separately are then processed by the *intersection algorithm* in order to detect and discard misbehaving servers called *false tickers*. The *true chimers* remaining are then processed by the *clustering algorithm* to discard outliers on the basis of dispersions for each server as compared to the

ensemble dispersion. The *survivors* remaining are then weighted by dispersion and combined to produce a correction used to discipline the computer clock.

A clock correction is produced for each round of messages between a client and a survivor. Corrections less than 128 ms are amortized using the NTP clock discipline algorithm, which is the main topic of this paper. Those greater than 128 ms cause a step change in the computer clock, but only after a sanity period of 15 minutes while these large values persist. Corrections of this magnitude are exceedingly rare, usually as the result of reboot, broken hardware, or missed leap second event.

Primary servers sometimes operate with more than one synchronization source, including multiple radios and other primary servers, in order to provide reliable service under all credible failure scenarios. The same NTP algorithms are used for all sources, so that malfunctions can be automatically detected and the NTP subnet reconfigures according to the prevailing synchronization distances.

3 COMPUTER CLOCK OSCILLATOR CHARACTERIZATION

The time-of-day (TOD) function in modern workstations is commonly implemented using an uncompensated quartz crystal oscillator and counter, which delivers a pulse train with period ranging from 10 ms to less than 1 ms. Each pulse causes a timer interrupt, which increments a software logical clock variable by a fixed value *tick* scaled in microseconds or nanoseconds. Conventional Unix systems represent the TOD as two 32-bit words in seconds and microseconds/nanoseconds from UTC midnight, 1 January 1970, with no provision for leap seconds. Thus, the clock reading precision is limited to the tick interval; however, many systems provide an auxiliary counter with reading precision of a microsecond or less, which can be used to interpolate between timer interrupts.

That typical computer clocks behave in ways quite counterproductive to good timekeeping should come as no surprise. There are no explicit means to control crystal ambient temperature, power level, voltage regulation, or mechanical stability. For instance, in a survey of about 20,000 Internet hosts synchronized by NTP, the median intrinsic frequency error was 78 ppm, with some hosts as much as 500 ppm. Since the clock oscillator is not temperature stabilized, its frequency may vary over a few ppm in the normal course of operation.

In order to correct for an intrinsic frequency error, adjustments must be made at intervals depending on the accuracy and jitter requirements. At a typical clock period of 10 ms and a frequency tolerance of 500 ppm, for example, the TOD function must add or subtract 5 μ s at each timer interrupt and complete the entire 500- μ s adjustment within a 1-s adjustment interval. The residual error, thus, has a sawtooth characteristic with maximum amplitude 500 μ s, which can be reduced only by reducing the intrinsic frequency error or by reducing the adjustment interval as described later in this paper.

Assuming the clock discipline can learn the nominal frequency error of each clock oscillator separately and correct for it, the primary characteristic affecting the clock accuracy is the oscillator stability. The traditional characterization of oscillator stability is a plot of *Allan variance*^[4], which is defined as follows. Consider a series of time offsets measured between a computer clock and some external standard. Let x_k be the k th measurement and τ_k be the interval since the last measurement. Define the *fractional frequency*

$$y_k \equiv \frac{x_k - x_{k-1}}{\tau_k}, \quad (1)$$

which is a dimensionless quantity. Now, consider a sequence of N independent fractional frequency samples $y_k (k = 0, 1, \dots, N - 1)$. If the interval between measurements t is the same as the averaging interval, the two-sample Allan variance is defined

$$\sigma_y^2(\tau) \equiv \langle (y_k - y_{k-1})^2 \rangle = \frac{1}{2(N-2)\tau^2} \sum_{k=2}^{N-1} (x_k - 2x_{k-1} + x_{k-2})^2 \quad (2)$$

and the *Allan deviation* as the square root of this quantity. Figure 1 shows the results of an experiment designed to determine the Allan deviation of a typical workstation (Sun SPARC IPC) under normal room-temperature conditions over about five days. The data used to generate this plot were obtained using the PPS signal of a GPS receiver captured by a special interface described in [5].

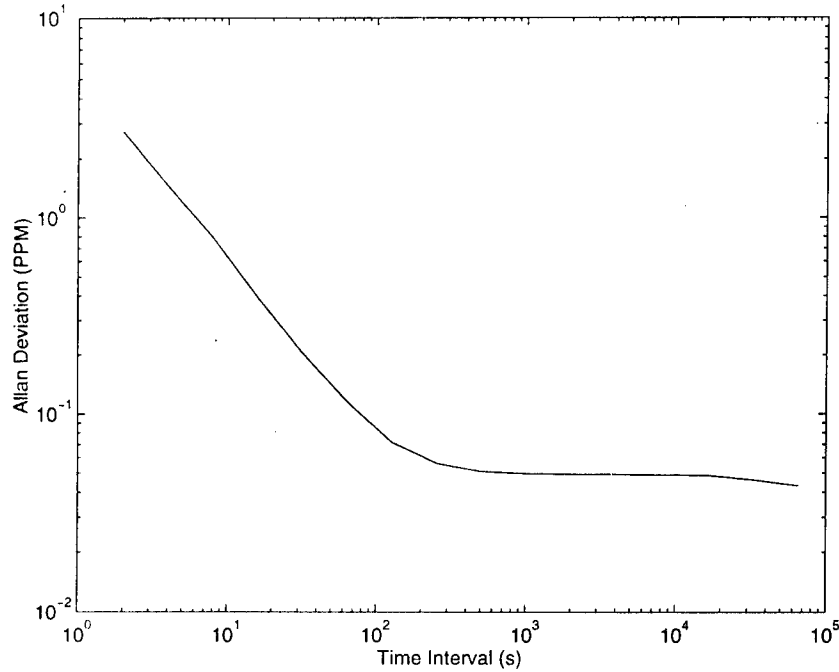


Figure 1. Allan Deviation Plot

It is important to note that both the x and y scales of Figure 1 are logarithmic, but the axes are labelled in actual values. Starting from the left at $\tau = 2$ s, the plot tends to a straight line with slope near -1, which is characteristic of white phase noise.^[6] In this region, increasing τ increases the frequency stability in direct proportion. At about $\tau = 1000$ s the plot flattens out, indicating that the white phase noise becomes dominated first by white frequency noise (slope -0.5), then by flicker frequency noise (flat slope). In other words, as τ is increased, there is less and less correlation between one averaging interval and the next. The inflection point between these two regions is important in the design of the clock discipline algorithm, as described later.

4 THE NTP CLOCK DISCIPLINE

The clock discipline algorithm adjusts the computer clock time as determined by NTP, compensates for the intrinsic frequency error, and adjusts the server update interval and loop time constant dynamically in response to measured network jitter and oscillator stability. A comprehensive description of the algorithm is given below (an outline of the algorithm appeared previously in [1]). The algorithm is implemented as the feedback loop shown in Figure 2. The variable θ_r represents the reference phase provided by NTP and θ_c the control phase produced by the variable frequency oscillator (VFO), which controls the computer clock. The phase detector produces a signal V_d representing the instantaneous phase difference between θ_r and θ_c . The clock filter functions as a tapped delay line, with the output V_s taken at the sample selected by the algorithm. The loop filter, with impulse response $F(t)$, produces a correction V_c , which controls the VFO frequency ω_c and, thus, its phase. The characteristic behavior of this model, which is determined by $F(t)$ and the various gain factors, is studied in many textbooks and summarized in [7].

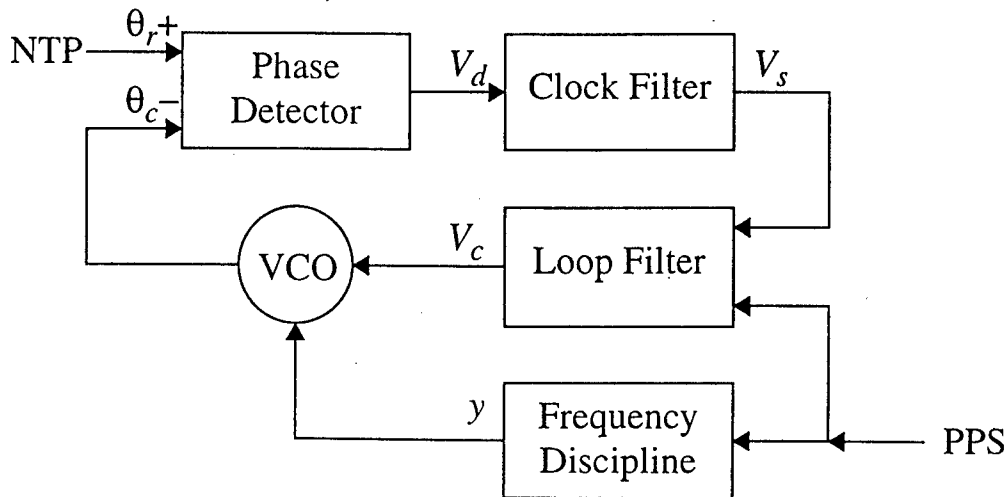


Figure 2. NTP Clock Discipline

The new clock discipline differs from the one described in the NTP specification and previous reports. It is based on an adaptive-parameter, hybrid phase-lock/frequency-lock loop (PLL/FLL) design which gives good performance with update intervals τ from a few seconds to tens of kiloseconds, depending on accuracy requirements and acceptable network overheads. In the most general formulation, an algorithm that corrects for clock time and frequency errors computes a prediction $\hat{x}_k = x_{k-1} + y_{k-1}\tau_k$ and then a correction $x = x_k - \hat{x}_k$. As each correction is determined, the clock is adjusted by $-x$, so that it displays the correct time, and the frequency y_k is adjusted to minimize the corrections in future. Between updates, which can range from

seconds to hours, the algorithm amortizes x in small increments at adjustment intervals t_A . At each adjustment interval the value

$$ax + y_k t_A \quad (3)$$

is added to the clock time and x is multiplied by $1 - a$, where a is a constant between zero and one. In the NTP daemon for Unix and Windows, t_A is one second; while, in the modified kernel described later, t_A is one clock tick. This model provides rapid adjustment (fast convergence) when x is relatively large, together with fine adjustment (low jitter) when x is relatively small. In PLL mode, the first term in eq. (3) is necessary for stability; in both PLL and FLL modes, it is also necessary in order to prevent monotonicity violations when the magnitude of adjustment is large.

The PLL mode is used in configurations with remote NTP servers or local radios, where the averaging interval is usually below the knee of the Allan deviation plot. In this mode the frequency at the k th update is determined directly from the summation

$$y_k = b \sum_{i=1}^{k-1} x_i \tau_i, \quad (4)$$

where b is a constant between zero and one. In order to understand the PLL dynamics, it is useful to consider the limit as τ_i approaches zero. From eqs. (3) and (4), the oscillator frequency is adjusted by

$$y(t) = ax(t) + b \int_0^t x(\tau) d\tau. \quad (5)$$

Since phase is the integral of frequency, the integral of the right hand side represents the overall open-loop impulse response of the feedback loop. Taking the Laplace transform,

$$\theta(s) = x(s) \frac{1}{s} \left(\frac{a+b}{s} \right) = x(s) G(s), \quad (6)$$

where the extra pole $\frac{1}{s}$ at the origin is due to the integration which converts the frequency $y(s)$ to phase $\theta(s)$. After some rearrangement, the transfer function $G(s)$ can be written

$$\frac{\omega_c^2}{s^2} \left(1 + \frac{s}{\omega_z} \right), \quad (7)$$

where $\omega_c^2 = b$ is the loop gain and $\omega_z = \frac{b}{a}$ is the corner frequency. From elementary theory, this is the transfer function of a type-II PLL which can control both time and frequency. The averaging interval is determined by the loop time constant, which depends on the choice of a and b ; however, these constants must be chosen so that the damping factor $\xi = \frac{\omega_c}{2\omega_z} = \frac{a}{2\sqrt{b}} = 2$, in order to preserve good transient response. For good stability, the time constant should be at least eight times the total loop delay which, because of the clock filter delay, is eight times the update interval. For values of $a = 2^{-10}$, $b = 2^{-24}$ and $\tau = 64$ s for instance, the PLL has a risetime in response to a phase step of about 53 minutes and a 63% response to a frequency

step of about 4.25 hours, which is a useful compromise between stability and network overhead on a LAN. Values of τ as low as 64 s are necessary to achieve the required capture range of 500 ppm; however, much larger values are appropriate on long paths in the Internet. For other values of τ , a varies as $\frac{1}{\tau}$, while b varies as $\frac{1}{\tau^2}$.

The FLL mode is used in configurations with modem services, such as those operated by NIST, USNO, PTB, and NPL, where the averaging interval (τ in this case) is usually above the knee. The FLL, adapted from [8], operates in the same way as the PLL, except that the frequency y_k is determined indirectly from the exponential average

$$\bar{y}_k = \bar{y}_{k-1} + w(y_k - \bar{y}_{k-1}), \quad (8)$$

with $w = 0.25$ determined by experiment. The goal of the clock discipline is to adjust the clock time and frequency so that $x_k = 0$ for all k . To the extent this has been successful in the past, we can assume corrections prior to x_k are all zero and, in particular, x_{k-1} . Therefore, from eqs. (1) and (8) we have

$$y_k = \bar{y}_k + \frac{x_k}{\tau_k}, \quad (9)$$

In PLL mode, eq. (4) is used for y_k in eq. (3); while, in FLL mode, eq. (9) is used instead.

A key feature of the NTP design is the automatic selection of τ in response to measured network jitter and oscillator stability. The ensemble dispersion is used as a measure of oscillator stability in both the PLL and FLL modes. If the correction exceeds this value, the oscillator frequency is deviating too fast for the clock discipline to follow, so τ is reduced in stages to the minimum. If the opposite case holds for some number of updates, τ is slowly increased in steps to the maximum. Under typical operating conditions, τ hovers close to the maximum; but, on occasions when the oscillator frequency wanders more than about 1 ppm, it quickly drops to lower values until the wander subsides.

5 OPERATING SYSTEM KERNEL MODIFICATIONS

Previous experience has justified the claim that an ordinary workstation running the algorithms described above can reliably maintain time accurate to a millisecond or two relative to a server on the same LAN. However, with a 1-s adjustment interval, 500-ppm frequency tolerance, and τ at the knee of the Allan deviation plot, it is not possible to improve the accuracy much better than this, primarily due to the instability of the clock oscillator and also due to the sawtooth error. Both of these problems can be addressed in the form of operating system kernel modifications, which in effect move the clock discipline algorithm to the kernel, as described in [5]. This provides a smaller adjustment interval, which reduces the sawtooth error and also provides more precise phase and frequency control. Without the kernel modifications, the adjustment interval is limited by practical considerations to 1 s; with the kernel modifications, the adjustments occur at every timer interrupt.

The modifications have been implemented and tested on Sun, DEC, and HP workstations. They are distributed in Digital Unix 4 for the DEC Alpha and planned for early release in Solaris 2 for the Sun SPARC. They include two system functions, one to read the system clock and related status indicators and error bounds, and another to adjust the clock phase and frequency. The clock discipline algorithm operates as shown in Figure 2, with phase corrections

provided at each NTP update. The oscillator frequency is preset when the NTP daemon is first started, in order to reduce the start-up transient, after which the frequency is controlled by the algorithm.

The pps signal is connected using a pulse generator and level converter. Each on-time transition causes an interrupt to the serial port driver, which latches the current seconds offset and disciplines the clock oscillator, as shown in Figure 2. The signal can be used in two ways, to discipline the oscillator frequency and to discipline the phase. Frequency discipline is used when a stable pps signal is available, but not synchronized to UTC time. In this case, the floor of the Allan deviation plot moves downward and the knee moves to the right. Thus, τ can be made much larger, increasing the averaging time and improving the accuracy. Frequency and phase discipline is used when a pps signal synchronized to UTC time is available.

Since noise problems on the pps signal could lead to serious errors, the kernel routines carefully grade and groom the data. Three-stage median filters are used to discard outliers and provide quality metrics for jitter and wander. The nominal frequency offset is computed from the time difference between the beginning and end of a calibration interval and added directly to the frequency variable, as shown in Figure 2. These operations are complicated by the requirement that all values must depend only on the clock hardware. When relatively small tick values are involved, less than a millisecond with DEC Alpha, and large frequency errors, as much as 500 ppm, this requires the initial calibration interval to be not more than 4 s. If the stability metric exceeds a threshold, the length of the calibration interval is reduced by half. If this is not the case for several consecutive intervals, the interval is doubled up to a maximum of 256 s, which corresponds to a frequency resolution of a few parts in 10^9 .

The NTP daemon performs a number of sanity checks to insure the integrity of the radio or modem ASCII timecode and the pps signal itself. The sanity checks are implemented by a suite of mitigation algorithms which identify improperly operating hardware or software, cast out the truants, and continue operating with the remaining sources, even if this means casting out a radio or modem and demoting the stratum. For instance, before the pps signal can be considered valid, the computer clock must be within 128 ms of the offset associated with the source of the signal. In addition, the source must remain among the survivors of the intersection and clustering algorithms. In practice, failures of this kind are not uncommon with WWVB radio clocks in our part of the country, since a combination of poor signal strength and local interference sometimes cause relatively large receiver errors.

Considerable effort was made in the implementation of the NTP software and kernel modifications to reduce hardware and operating system delay variations; however, not all machines make good timekeepers. Unpredictable delay variations occur in the hardware, interrupt routines, buffering operations, and system scheduling policies. In the case of a network interface, the network driver captures a receive timestamp in the interrupt routine. In the case of a radio or modem, this is done using a *line discipline*, which is invoked by the serial port driver. It inspects for one of a designated set of intercept characters, usually the one designated *on-time* in the ASCII timecode string sent by the radio. Upon finding an intercept character, it captures a receive timestamp and stuffs the bits in the input buffer following the intercept character. The NTP daemon captures a transmit timestamp before computing the cryptographic message digest used to verify the server authenticity. Fortunately, the MD5 algorithm used for this purpose has an almost constant running time independent of the message contents. The daemon measures this time and then advances the transmit timestamp by a like amount in the following message.

6 PERFORMANCE ANALYSIS

In order to assess the performance of the NTP algorithms in the global Internet, recordings of raw timestamp data were made over an 11-day period involving three paths selected to represent extreme cases with presumed large delays and delay variations. The three paths are between the University of Delaware (pogo.udel.edu) and (WUSTL) Washington University in St. Louis (navobs1.wustl.edu, 15 router hops), (IEN) IEN Galileo Ferraris in Torino, Italy (time.iien.it, 19 hops), and (OZ) University of Melbourne in Australia (ntp.cs.mu.oz, 22 hops). Each server is synchronized to GPS, although only pogo has the modified kernel and pps support.

A common assumption is that network delays are reciprocal; that is, the statistics exploited by the various NTP algorithms on each direction of transmission are the same. In order to test this assumption, the raw data collected on all three paths were processed by a simulator program which faithfully models the NTP algorithms and includes provisions to adjust the various parameters and graph the results. The propagation delay can be estimated as the mean of the ten lowest delays on each direction. The IEN outbound path delay was 93.0 ms and the return 97.9 ms, while the figures for the OZ path were 124.6 and 138.4 ms, and for the WUSTL path are 19.6 and 19.5 ms. The offset errors due these nonreciprocal delays are half the differences, 2.45, 6.9, and 0.05 ms, respectively. These errors are surprisingly small, considering the number of router hops and the great distances involved.

In addition to the fixed propagation delays, there are variable delays due to queueing in routers along the path. For instance, the mean roundtrip delays on the IEN, OZ, and WUSTL paths are 345.4, 359.9, and 65.4 ms, respectively, leaving 154.5, 96.9, and 26.3 ms as the mean queueing delays. Thus, between a quarter and a half of the mean roundtrip delays are due to queueing delays. However, after processing by the NTP algorithms, the degree to which the NTP algorithms clean up the raw data can be seen in representing the before and after for the WUSTL path. The mean offset errors for the raw data are 15.2, 9.8, and 4.8 ms for the IEN, OZ, and WUSTL paths, respectively, while the RMS errors are 64.0, 470.0, and 19.5 ms. However, after processing by the NTP algorithms, the mean offset errors are reduced to .045, .004, and .003 ms, respectively, while the RMS errors are reduced to 2.9, 3.0, and 0.15 ms. These values should be added to the nonreciprocal path errors in the total error budget. Figure 3 shows the results for the WUSTL path; the other paths behave in similar ways.

The graph has a spiky characteristic shared by the other paths and suggests further processing might eliminate most or all of the spikes, especially if the pps signal were used to stabilize the clock oscillator and the length of the clock filter increased a substantial amount. While the emphasis in this paper is on heroic paths in the Internet, a similar experiment involving pogo and another machine on the same Ethernet LAN shows negligible mean error, rms error .007 ms, and maximum error .078 ms, the latter due to a single spike of unknown origin during a run of 15 days.

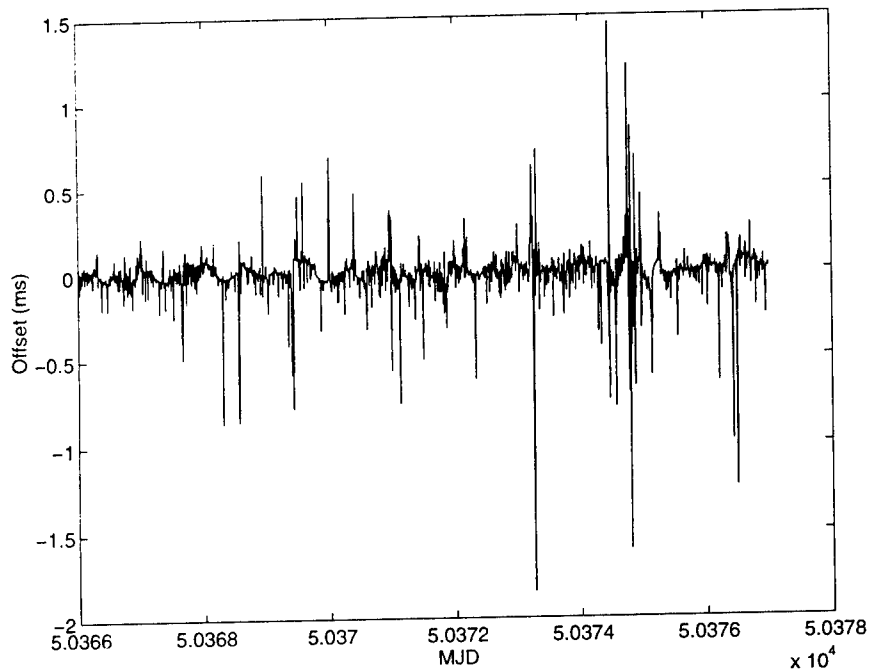


Figure 3. Processed Data Offsets

7 SUMMARY AND CONCLUSIONS

The significance of this work is confirmation that general purpose workstations with appropriate software support can deliver timekeeping accuracies in the low millisecond range over global distances using the Internet shared with many other users and applications. This may be especially useful for astronomy, oceanography, manufacturing, and process control applications.

The key to achieving accuracies of this order is through carefully crafted algorithms and the use of a stable external oscillator and counter to produce a PPS signal. The signal is processed by algorithms embedded in the operating system kernel and used to discipline the frequency of the computer clock at every timer interrupt.

The package of NTP software and kernel modifications has been implemented for several families of Unix and Windows workstations and is available for public distribution. The kernel modifications have been incorporated in the standard Digital Unix operating system and are planned for early release in the Solaris operating system.

8 REFERENCES

References [1, 2, 3, 5, 7] are available from Internet archives in PostScript format. Contact the author for location and availability.

- [1] D.L. Mills 1995, "*Improved algorithms for synchronizing computer network clocks*," **IEEE/ACM Transactions on Networks**, 245-254.
- [2] D.L. Mills 1992, "*Network Time Protocol (Version 3) specification, implementation and analysis*," Network Working Group Report RFC-1305, University of Delaware, March 1992, 113 pp.
- [3] D.L. Mills 1991, "*Internet time synchronization: the Network Time Protocol*," **IEEE Transactions on Communications**, COM-39, 1482-1493. Also in: **Global States and Time in Distributed Systems**, ed. Z. Yang and T.A. Marsland (IEEE Press, Los Alamitos, California, USA), pp. 91-102.
- [4] D.W. Allan 1987, "*Time and frequency (time-domain) estimation and prediction of precision clocks and oscillators*," **IEEE Transactions on Ultrasound, Ferroelectrics, and Frequency Control**, UFFC-34, 647-654. Also in: **Characterization of clocks and oscillators**, ed. D.B. Sullivan, D.W. Allan, D.A. Howe, and F.L. Walls 1990, NIST Note 1337, National Institute of Standards and Technology/U.S. Department of Commerce (U.S. Government Printing Office, Washington, D.C., USA), pp. TN121-TN128.
- [5] D.L. Mills 1994, "*Unix kernel modifications for precision time synchronization*," Electrical Engineering Department Report 94-10-1, University of Delaware, October 1994, 24 pp.
- [6] S.R. Stein 1985, "*Frequency and time—their measurement and characterization*" (*Chapter 12*). In: **Precision Frequency Control**, Vol. 2, ed. E.A. Gerber and A. Ballato (Academic Press, New York, New York, USA), pp. 191-232 and 399-416. Also in: **Characterization of Clocks and Oscillators**, ed. D.B. Sullivan, D.W. Allan, D.A. Howe, and F.L. Walls 1990, NIST Technical Note 1337, National Institute of Standards and Technology/U.S. Department of Commerce (U.S. Government Printing Office, Washington, D.C., USA), pp. TN61-TN119.
- [7] D.L. Mills 1992, "*Modelling and analysis of computer network clocks*," Electrical Engineering Department Report 92-5-2, University of Delaware, May 1992, 29 pp.
- [8] J. Levine 1995, "*An algorithm to synchronize the time of a computer to universal time*," **IEEE Transactions on Networks**, 3, 42-50.

ON THE SHIPBOARD APPLICATION OF NETWORK TIME PROTOCOL (NTP, RFC 1305)

Melanie E. Bautista

Lockheed Martin Advanced Technology Labs

1 Federal Street, M.S. A&E3W, Camden, New Jersey 08102, USA

Phone: (609)338-3987, fax: (609)338-4144, email: mbautist@atl.lmco.com

Abstract

The rapid evolution of naval combat system computing platforms is inspiring novel approaches in the design of shipboard time distribution systems. The Network Time Protocol (NTP) is being considered as a component in some of these new models. This paper presents studies conducted to evaluate the viability of NTP, in general, as a shipboard timekeeping mechanism, and in particular, as a non-mission critical timekeeping mechanism for the AEGIS Weapon System.

1 INTRODUCTION

The AEGIS Weapon System (AWS) is a complex system of systems. It is deployed on U.S. Navy cruisers and destroyers, and is capable of engaging enemy ships, planes, and submarines simultaneously. Defense Secretary William Perry has described the AEGIS Weapon System as providing "...thorough and accurate battlefield awareness by drawing intelligence about the battlefield from many sources and speeding it to the commander fighting the battle."

Traditionally, the computing base of the AWS consisted of military standard computers. These computers were programmed to perform a single function and communicated with other computers through direct connections, implemented as military standard low-level serial links. The traditional architecture utilized shadow processors, with primary and alternate computers, to provide fault tolerance. A dedicated military standard time distribution network enabled coordination among the various computers.

Today, the combined effect of changing threat scenarios, modification of doctrine to address these threats, injection of commercial-off-the-shelf (COTS) technologies, and diminishing defense spending is changing naval system computing architectures.

A migration towards a COTS network of high-powered COTS processing nodes, which hosts a suite of fully distributed application programs, is currently taking shape. In this new type of environment, by its very definition, the need to achieve system wide time synchronization still exists. The U.S. Navy is considering a number of novel solutions, some of which include the Network Time Protocol (NTP) as a component.

This paper presents a series of experiments conducted to evaluate the performance of NTP in a shipboard environment, as part of the fifth Engineering Development Model (EDM5) AEGIS Weapon System (AWS) communications benchmarking effort.

2 EDM5 LABORATORY CONFIGURATION

A laboratory test-bed network was constructed to support AWS EDM5 communications testing. The network was designed to simulate key processing elements, interconnected via candidate local area network (LAN) technologies and capable of generating representative levels of AWS communications traffic. The network provided the infrastructure and hardware to conduct a variety of computer communication benchmarks, including those for NTP. It consisted of nine Hewlett Packard (HP) workstations, three of which were Tactical Advanced Computer 3 (TAC3) HP-750 machines running the HP-UX version 9.05 operating system. The remaining six machines were TAC4 HP-J210's running HP-UX 10.01. All nodes supported two interfaces: an Ethernet interface to a file server and a Fiber Distributed Data Interface (FDDI) to a router backbone. The router backbone consisted of four Cisco 7513 routers interconnected in a fault-tolerant FDDI configuration.

3 SHIPBOARD TIME SYNCHRONIZATION REQUIREMENTS

The requirements for time synchronization in a heterogeneous, diverse, networked collection of computers take added dimension when the target operating environment is aboard a battle-ready ship. Whereas a land-based commercial application network might concern itself primarily with the accuracy, portability, and scalability of a timekeeping mechanism, a sea-based tactical application network must also guarantee the settling time, stability, and survivability, as well as more stringent synchronization requirements, of its timekeeper.

Synchronization describes the ability of NTP to make a system of clocks agree in both frequency and time. Settling time describes the elapsed time required for NTP to reach nominal synchronization. Stability describes the ability of NTP to regulate the clocks, such that measured time offsets do not climb or descend too far or too often. Survivability describes the ability of NTP to be robust in face of system failures or degraded system states.

4 EXPERIMENTAL OBJECTIVE

Performance requirements in each of these categories are derived from the AWS A-level Specification, and differ for mission critical versus non-mission critical elements. The goal of EDM5 NTP testing was to evaluate NTP against these performance criteria in the non-mission critical configurations currently planned, and to gain insight into how NTP might perform in a mission critical configuration.

5 NTP EXPERIMENTS

Because NTP offers a dynamic clock correction mechanism, its behavior is expected to vary with time. Because it is significant to understand such behavior over both the short- and the long-term, two experiments were designed and conducted.

5.1 NTP Stability Experiment

5.1.1 Objective

The NTP Stability Experiment was designed to measure the long-run synchronization and stability of a system of clocks disciplined by NTP. The experiment was also designed to allow a measurement of initial settling time. The first part of this experiment configured a timekeeping subnetwork from the EDM5 test-bed equipment, establishing NTP communications over 10 megabit-per-second (Mbps) Ethernet. The second part of this experiment utilized the same configuration, but, instead, established communications over 155 Mbps FDDI. Figure 1 shows the NTP synchronization subnet topology exercised for both parts of the experiment.

5.1.2 Configuration

As shown, host wil13429 was designated as a stratum 10 NTP server, "master." Host wil13428 was designated as a backup NTP server, "backup master," at stratum 12. The master and backup master were then designated as peers. All other hosts in the test-bed were designated NTP clients to both masters. The master and backup master employ their own local clocks as time references. Therefore, this NTP configuration attempts to slave all clocks in the test-bed to the local clock of wil13429, and to wil13428 in case of failure.

5.1.3 Implementation

Automated statistics collection was enabled to capture NTP system state variables for the duration of each test; and the NTP synchronization subnet was permitted to free run relatively undisturbed. Part I examined clock behavior for 11 days. Part II studied behavior for 7.

5.2 NTP Load Experiment

5.2.1 Objective

The NTP Load Experiment was designed primarily to study the survivability aspects of NTP performance. It does this by subjecting NTP host computers to a harsh environment, and comparing clock synchronization and stability before and after stress conditions are applied. The experiment also tests for the impact of host computer crash failures and recoveries, which are simulated by abruptly terminating and re-initiating the NTP software on the NTP hosts under test.

The harsh environment consists of two components: contention for communication resources and processing resources. Communications resource drain was simulated by injecting a bursty traffic pattern into the network. Processing resource drain was accomplished by running CPU-intensive applications on the NTP hosts under test.

A series of test scenarios composes the experiment. These scenarios attempt to model conditions that might occur during shipboard operations. For example, it is conceivable for a situation to arise, in which NTP is able to run for only 15 minutes after start-up, before being terminated during a failed system state. It then remains inactive for 10 minutes before being re-instantiated. Yet, throughout its activity, NTP must compete for network and/or central processing unit (CPU) resources, due to the stress associated with system failure and recovery. How NTP will perform under these and similar conditions is of significant interest. Therefore, scenarios were carefully constructed to benchmark NTP as part of this experiment, as shown in Figure 3.

Because of the short duration of each test, the NTP Load Experiment also provided an opportunity to study short-run performance against synchronization, stability, and settling time

requirements.

5.2.2 Configuration

This experiment configured a basic timekeeping subnetwork consisting of a single client and single server from the EDM5 test-bed equipment. Communications were established over FDDI. Figure 2 illustrates the basic NTP synchronization subnet topology used. A TAC3 and a TAC4 versions of this configuration were implemented. In the TAC3 version, wil13428 acted as an NTP server to NTP client wil13427, with the local clock of wil13429 providing a time reference to both. In the TAC4 version, wil13430 acted as an NTP server to NTP client wil13435, with the local clock of wil13434 providing the time reference.

5.2.3 Implementation

The experiment was conducted as follows: First, NTP configuration files were modified to implement either the TAC3 or TAC4 synchronization subnet. Second, each scenario was executed in series as listed in Figure 3, constituting an iteration of a test suite. Third, the levels of network and processor activity were altered and the test suite rerun. Figure 4 outlines the NTP configurations and corresponding platform activity levels used for each iteration of a test suite. Completion of the experiment was signified by exhausting the list.

To implement the experiment, several UNIX scripts were developed. A high-level description of each is provided. The main script manages the initiation and termination of the NTP client and server as needed to match the sequence defined by the test suite. It invokes a separate script to calibrate the NTP client and server at the start of each test scenario. It also invokes the NTP query utility, "ntptime," periodically to collect and record time offset statistics. The script was designed to execute a single iteration in 9 hours, at 1 hour per scenario, including 20 minutes for calibration.

The calibration script simply instantiates the NTP client and server together, lets them run for an amount of time, then terminates each just before the test scenario begins. The calibration phase attempts to equalize NTP performance in the client and the server hosts.

The network load scripts generate bursty traffic over the network by invoking an AWS communications simulation tool, developed in-house, in a predetermined sequence. In an attempt to affect the maximum network-related stress on NTP, this sequence specifies parameters which cause the tool to create different levels of network utilization approximately every minute for the duration of an iteration. Because the NTP algorithms choose an optimal source of timekeeping information partially as a function of past statistics on path delays, creating an environment in which path delays vary each time NTP communicates increases the likelihood that NTP makes a nonoptimal decision for the current network state. A FDDI Network Advisor was used to measure and record traffic traces during each loaded network iteration to verify the test conditions. Note that the network load scripts were executed manually on separate hosts from the NTP hosts under test.

Two versions of CPU load scripts were utilized for the experiment. One script, again, exercised the AWS communications simulation tool. This time the tool was invoked on each of the NTP hosts under test, such that the processors were constantly polling for a control message scheduled never to arrive. The other script simply repeatedly invoked a recursive UNIX "find" command. Both scripts drained approximately 96% of CPU resources, as measured by the UNIX utility, "top."

6 ASSUMPTIONS

A series of assumptions limit the scope of the experiments as designed:

The standard distribution of NTP is tested. This version of NTP is tuned for networks expecting to synchronize to clock references over the Internet. Note that the Naval Surface Warfare Center, Dahlgren Division (NSWC-DD), is studying which NTP parameters are tunable and how to tune them in order to optimize performance in an AEGIS-like network. Such a network is isolated from the Internet, is more geographically compact, and utilizes clock references local to the ship. An independent validation of the NSWC-DD findings is planned, as well as rerunning of the experiments described herein to characterize NTP when it has been appropriately tuned.

Only TAC3 and TAC4 NTP performance is characterized. Because the quantity and quality of synchronization achievable via NTP is ultimately determined by the hardware and operating system it attempts to discipline, the scope of any characterization of NTP is limited to the platform in question, and cannot necessarily be extrapolated to other host platforms. Specifically, mission critical elements are not being hosted in either the TAC3 or the TAC4 platforms. Therefore, it is not fully accurate to compare NTP performance, as measured by the experiments reported herein, against mission critical requirements.

Only the symmetric active mode of NTP operation is evaluated. This mode enables the maximum exchange of time information in the subnet and, therefore, theoretically produces the most reliable synchronization. Properties and performance of other NTP modes will not be studied in these tests.

Sufficient aging of the NTP drift files has occurred. The NTP algorithms are implemented as a software daemon, "xntpd." Because xntpd attempts to discipline time by regulating the oscillator aboard each processor, its performance enhances with increased understanding of the idiosyncrasies of the hardware. Thus, xntpd records drift data to a file, which is continually updated during runtime. A more veteran drift file provides better information to xntpd.

NTP accurately reports synchronization performance. The xntpd software distribution delivers two query utilities, "xntpd" and ntpdate, for examining NTP system state variables. These variables include time offset between pairs of NTP nodes. NSWC-DD determined that xntpd reports more dated information than ntpdate, but concluded that NTP does accurately measure its own performance. Based on these findings, it is most accurate to utilize ntpdate when conducting short-duration tests, whereas for long-duration tests, xntpd still provides an accurate depiction of performance. This study makes an assumption that xntpd automated statistics collection employs techniques similar to xntpd. This is a reasonable assumption, based on a cursory examination of the code.

7 STATUS

To date, all experiments described in this paper have been completed. The data have been collected, and much of them have been reduced, plotted, and analyzed. However, a full analysis, to produce measures of synchronization, settling time, stability, and survivability, is pending completion and will be published as a separate document.

8 PRELIMINARY CONCLUSIONS

As of the date of initial data analysis, AEGIS EDM5 system requirements were continuing to evolve towards final definition. Therefore, it was not possible to conclude with certainty whether NTP, when hosted on the TAC3 and TAC4 platforms, can satisfactorily perform the non-mission critical time synchronization function for an EDM5 incarnation of AEGIS. However, preliminary data suggest that, as expected, in the configurations tested, NTP cannot meet mission critical performance requirements. It is believed that adding a highly reliable time reference to these configurations might enhance performance enough to reverse this conclusion.

The suite of tests and evaluation did indicate that the movement in time and frequency of clocks, disciplined by NTP, occurs in a coordinated fashion. Furthermore, it was determined that when xntpd is terminated on a host, its local clock begins to drift immediately until the daemon is re-initiated. It is significant to note that NTP performance degraded when introduced onto the TAC4 platform. This confirms that operating system upgrades do not necessarily imply NTP performance upgrades. Instead, xntpd should be benchmarked for all candidate hardware platforms, operating system revisions, and synchronization subnet topologies.

Perhaps, the most important conclusion drawn from these experiments is that NTP performance can be significantly enhanced by tuning xntpd. By customizing user-definable parameters for an isolated, geographically localized synchronization subnet, it is expected that synchronization, settling time, stability, and survivability numbers will drop. It has been demonstrated that reducing the polling interval, from a 64 to 1024 second range to a 16 to 64 second range, trims client-to-server offsets by an order of magnitude. Continued testing using actual EDM5 hardware and introducing mission critical synchronization subnet topologies are recommended.

9 REFERENCES

M.E. Bautista, S. Dempsey, W.J. Reilly, M. Teter, and L. Weinberg, "*EDM5 network communications testing status report, February 1996*," NS-C-ADV-T-2001, April 1996.

"*High performance distributed computing program: engineering testbed one report*," Naval Surface Warfare Center/Dahlgren Division, and Johns Hopkins University Applied Physics Laboratory, November 1995.

D.L. Mills, "*Network Time Protocol (version 3) specification, implementation and analysis*," RFC 1305, March 1992.

K.F. O'Donoghue, and T.R. Plunkett 1996, "*Development and validation of network clock measurement techniques*," Proceedings of the 4th International Workshop on Parallel and Distributed Real-Time Systems (IEEE Computer Society Press).

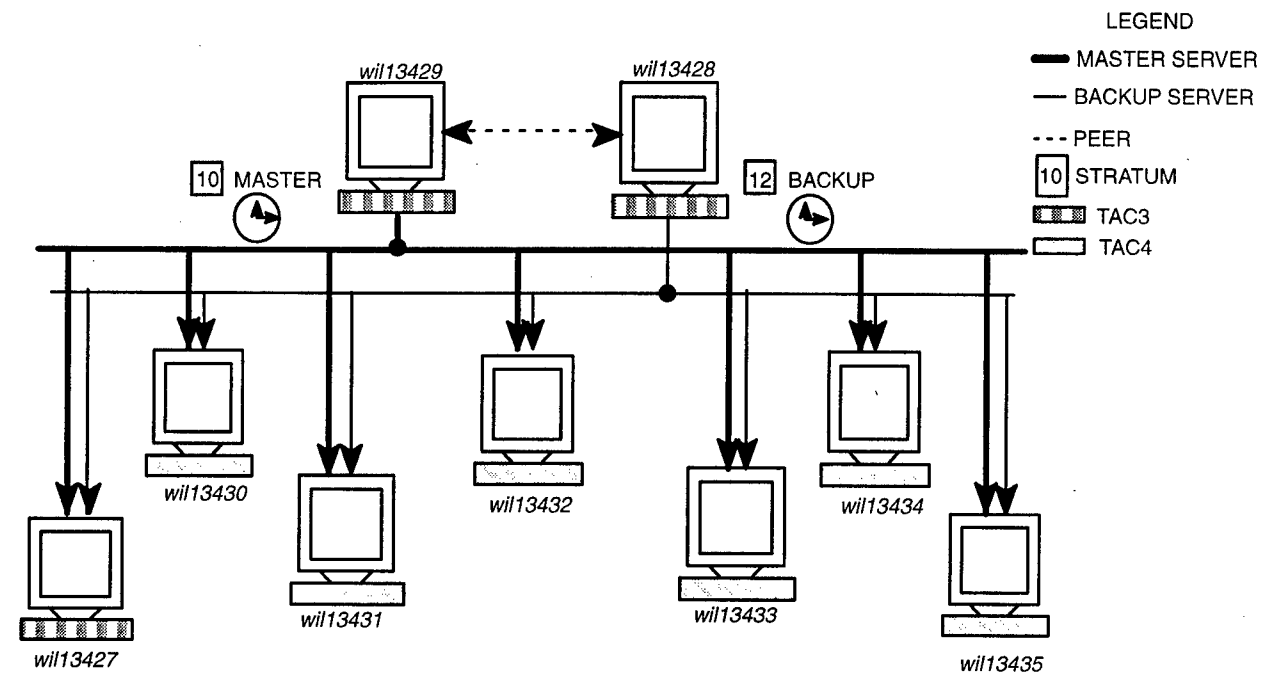


Figure 1. NTP Stability Experiment Synchronization Subnet Topology

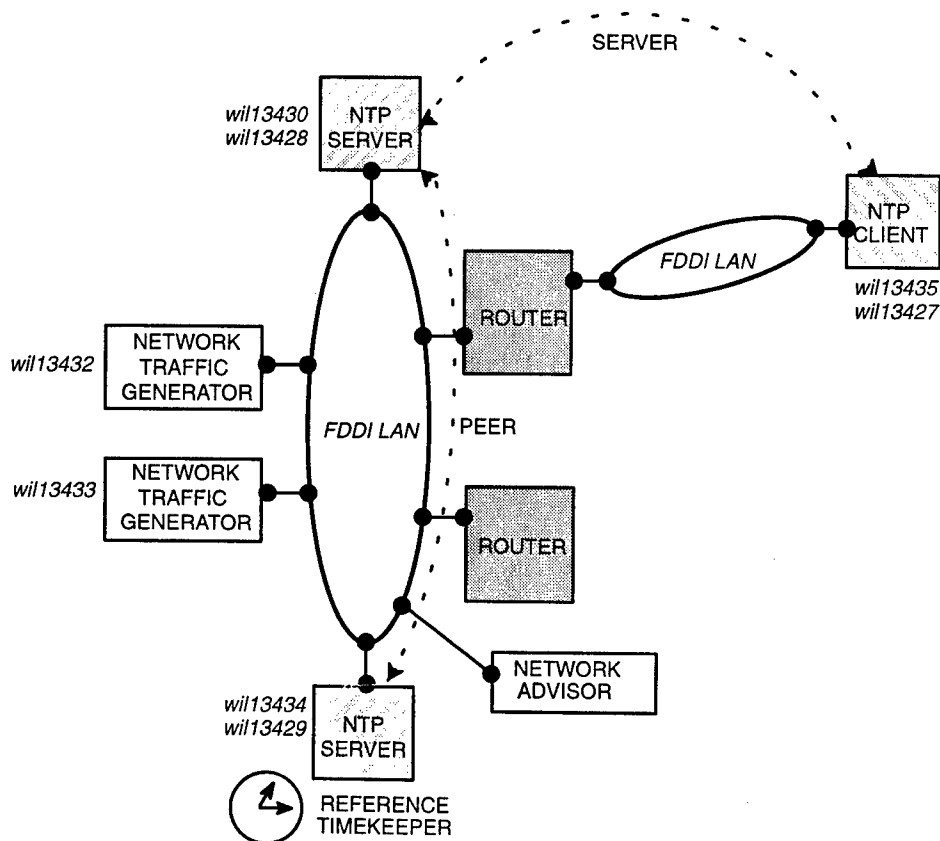


Figure 2. NTP Load Experiment Synchronization Subnet Configuration

NTP Client and Server Active Period Profiles Specified in Minutes	Reference Name
Client/Server Up Continuously	csuc
Client Up 10 Down 30	c1030
Client Up 20 Down 20	c2020
Client Up 15 Down 10 Up 15	c151015
Server Up 10 Down 30	s1030
Server Up 20 Down 20	s2020
Server Up 15 Down 10 Up 15	s151015
Client/Server Up 10 Down 15 Up 15	cs101515
Client/Server Up 15 Down 10 Up 15	cs151015

Figure 3. Scenarios Composing a Single Test Suite

	[64 1024] second NTP polling interval	[16 64] second NTP polling interval
TAC-3	no load	no load
TAC-3	network load	network load
TAC-3	CPU load	CPU load
TAC-3	network and CPU load	network and CPU load
TAC-4	no load	no load
TAC-4	network load	network load
TAC-4	CPU load	CPU load
TAC-4	network and CPU load	network and CPU load

Figure 4. NTP Configurations and Platform Conditions During Iteration of a Test Suite

Questions and Answers

RICHARD SCHMIDT (USNO): What version of NTP were you doing this test on?

MELANIE BAUTISTA: 3.4.

RICHARD SCHMIDT: And did you do any tests – it wasn't quite clear to me what was the effect of disabling the servers, letting the clients freewheel on NTP from their last known drift rates?

MELANIE BAUTISTA: Actually there were several iterations that were tried. The main iterations were actually disabling NTP on the client machines as well. So it was done in both directions. We disabled the daemon on just the client and then re-initiated and we observed how synchronization was affected. We also did the reverse.

RICHARD SCHMIDT: But I guess my question was we know if you kill NTP on the client, the client's going to run away. There's nothing controlling it. But if you disable access to the server, after some period of time it should have learned what its frequency errors were and it should freewheel fairly accurately. But that depends on how long NTP had been running before you kill that access. Have you done any tests showing that dependency, how long it needs to be running before the client can run fairly successfully without a server?

MELANIE BAUTISTA: Actually, we didn't extend the experiment to that extent. However, these experiments were designed to study short-run characteristics of NTP. So the tests were very short.

The first experiment examined NTP synchronization over a number of days. The NTP load experiment conducted nine trials in series, each trial lasting one hour. So it would be something like the client/server was on for 15 minutes together; client/NTP daemon was terminated for 10 minutes; then both came back on for 15 minutes. And then we recorded the time offsets and studied whether in that short time period we could learn anything worthwhile, because this is the type of environment we would be expecting in an AEGIS environment.

JUDAH LEVINE (NIST): I wouldn't want to talk anybody out of using NTP, but it seemed to me that most of the machinery that is built into NTP is really not needed in your environment. And most of the problems in your environment are things that NTP is not going to help with, in that you have a network and it is what it is. So that its delays are going to be whatever they're going to be. I mean, right, you have some topology and it is what it is. I guess the whole idea of estimating the network every time – I mean, you could just do it, right? It's your closed network. You own the whole thing. It's not like you have to go through anybody else's router.

Let me ask why did you choose NTP as opposed to all the other choices that were available?

MELANIE BAUTISTA: Well, the reason NTP was chosen is because it's automatic, it's something that you can turn on in your workstation, you never have to worry about it. It's true that you could do your own simple implementation of measuring the network delay and doing the simple calculation that NTP does without the additional overhead that NTP builds in in order to support an Internet environment. However, it's implemented; you can just turn the daemon on in your workstation and not worry about it.

The initial concept was not chosen for the mission-critical elements. It's more for all of the workstations on the ship performing non-mission-critical functions.

WILLIAM BOLLWERK (USNO): I have a question for you about the requirements. You say

that there were requirements, and you broke them down into four areas. Those came out of Operations Requirements Document for AEGIS, or where did they come from? The ORD – or what are the actual timing requirements and are they for the critical shipboard operations? You just mentioned that the system is set up for the nonessential, like the supply functions and other things on the ship. Are the requirements broken out into that type of category or what do you have there?

MELANIE BAUTISTA: Because this is really a new feature that's going to be introduced in future baselines of AEGIS, requirements for non-mission-critical time synchronization do not currently exist. However, the concepts being developed for future AEGIS have a different concept of operations, and many of these requirements are being derived from that. A lot of them, however, are based on the AWS top-level specifications such as first start-up times; you have a fixed amount of time that you have to be able to get the whole system up and running by "x" amount of time; if the system goes down, you have to come back alive, everything has to be running within "x" amount of time. Requirements on that level help to define the fault tolerance in fault recovery requirements for NTP.

In terms of synchronization, to date when we are testing, we are testing against old synchronization requirements, in other words, requirements made of the time distribution system in past AEGIS baseline designs. So what the previous system had to perform, we have to at least be able to meet those requirements and perhaps ...I'm not at liberty to say; that's classified information.

KAREN O'DONOGHUE (NAVAL SURFACE WARFARE CENTER): I just wanted to add a couple of things to what Melanie has already said. The question about why NTP might be useful onboard ship – first of all, I don't believe that we see the shipboard network being quite as static as might have been indicated. There are a number of routers onboard ship; there are a number of various subsystem networks; and I think we see the need to be able to – especially in a fault scenario where you're losing networks and various routers might be going down that we might need more flexibility then – we don't have a static network, I guess is what I'm trying to say.

One of the second motivations for looking at NTP is since we are moving towards using COT space workstations onboard ship, we are very interested in the capability of the frequency – being able to modify the phase and the frequency. Because, on COT space workstations you get the capability to figure out what the frequency offset is and to possibly make some correction for that is very attractive.

On the question of requirements, one of the things I'd like to refer to is that there were a number of efforts done by the Navy in the Next Generation Computer Resources Program, which has recently ended, looking at what the timing requirements were for networks, in particular, in the Safenet Program; and some of the earlier requirements documents that came out of that that were made public is that they wanted the synchronization between processors to be within 1 millisecond; and that you needed – I believe the term you used was "settling time," I'm not sure – to be within 5 seconds. So from the time the machine boots, within 5 seconds we need to be synchronized to within 1 millisecond and then maintain that level of stability. Thank you.

THE RANGE COVERED BY A RANDOM PROCESS AND THE NEW DEFINITION OF MTIE

P. Tavella, A. Godone
Istituto Elettrotecnico Nazionale G. Ferraris
Strada delle Cacce 91, 10135 Torino, Italy
tel +39-11-3919235 fax +39-11-3487046
e-mail tavella@tf.ien.it

S. Leschiutta
Istituto Elettrotecnico Nazionale G. Ferraris and
Politecnico di Torino, Dipartimento di Elettronica
Corso Duca degli Abruzzi 24, 10129 Torino, Italy

Abstract

The paper is devoted to the study of the range covered by the time deviation of a clock with respect to a reference one, in a certain observation time interval. In case of a clock affected by Gaussian white phase noise, it is possible to infer the probability law of the covered range and, in particular, the probability that the time deviation exceeds a particular threshold level. The application to telecommunication as related to the Maximum Time Interval Error (MTIE) is discussed.

INTRODUCTION

In the last few years, mostly for the telecommunication community, it became necessary to estimate the possible range spanned by a random process, also without having observed and measured any realization of it. The problem may be illustrated as follows: suppose one has a clock to be used as synchronization unit somewhere in a telecommunication network and knows that the clock signal is mostly affected by a random noise of known spectrum. What is the "time error," i.e. the phase deviation, that such a clock may accumulate in a certain time interval? Apart from deterministic trends, the answer regarding the random component may only be a probabilistic one, the nature of the process being stochastic. So the problem can be better expressed as: knowing the spectral density of phase fluctuations, what is the probability law of the range spanned by such phase fluctuations? In this paper, the case of Gaussian white phase modulation is considered and the range probability law is inferred. This study gives also an indication on the possible "maximum" range by the identification of a certain percentile in the range distribution, i.e. the range value that is not exceeded more than a certain percentage of times. The application to telecommunication is immediate because the range spanned by the phase dictates the correct dimensioning of memory buffers and it is what is contained in the quantity MTIE (Maximum Time Interval Error) largely used and discussed

in the telecomm community and recently redefined as a percentile quantity. The study here presented supports such new definition and provides some materials for its understanding and its practical implementation.

THE RANGE PROBABILITY

Let's consider a Gaussian white process, i.e. a sequence of uncorrelated (white) samples whose probability law is described by a Gaussian density function $f(x)$ with zero mean and variance σ^2 :

$$f(x) = \frac{1}{\sqrt{2\pi}\sigma} e^{-\frac{x^2}{2\sigma^2}} \quad (1)$$

The range spanned by a sequence of such n samples is defined as the difference between the maximum and the minimum value:

$$z = \max \text{ value} - \min \text{ value} \quad (2)$$

The study of the range thus requires the evaluation of the probability of the maximum and minimum values. The density function $g(w)$ of the maximum, i.e. the probability that the larger value falls in between w and $w + dw$ is estimated as the probability that one sample lies in between w and $w + dw$ while all the other $(n - 1)$ samples lie below w , still multiplied by the n possible configurations. In case of independent samples, this is just the product of single probability, thus leading to:

$$g(w) = n[F(w)]^{n-1} f(w) dw \quad (3)$$

where $F(w)$ represents the cumulative distribution function defined as:

$$F(w) = \int_{-\infty}^w f(\xi) d\xi \quad (4)$$

With a similar procedure the density function of the minimum value is found. As a successive step, the density function $h(z)$ of the range z (Eq. 2) is found by means of the composition law of density functions.^[1] In case of a Gaussian parent distribution, it is possible to write an analytical expression for $h(z)$ ^[2] that becomes:

$$h(z) = \frac{n(n-1)}{2\pi\sigma^2} \left(\frac{1}{2}\right)^{n-2} \int_{-\infty}^{\infty} dy \cdot e^{-\frac{(z+y)^2}{2\sigma^2}} e^{-\frac{y^2}{2\sigma^2}} \left[\operatorname{Erf} \left(\frac{z+y}{\sqrt{2}\sigma} \right) - \operatorname{Erf} \left(\frac{y}{\sqrt{2}\sigma} \right) \right]^{n-2} \quad (5)$$

where $\operatorname{Erf}(x)$ stands for the error function:

$$\operatorname{Erf}(x) = \frac{2}{\sqrt{\pi}} \int_0^x e^{-t^2} dt \quad (6)$$

This expression of $h(z)$ is for positive range values and may be estimated, for example, by fixing n and evaluating Eq. (5) for some different values of z . Some results are illustrated in Fig. 1.

It may be noted that, as n increases, the possibility that the n observed samples extend over a larger range becomes more and more likely.

The n Gaussian samples may be interpreted as the result of sampling a clock signal affected by white phase noise. The n samples represent the n measures of the time deviation of the clock (with respect to a reference) repeated with an observation interval τ_0 . At the growing of n , the observation time increases as $\tau = (n - 1)\tau_0$. Fig. 1 indicates, thus, the most probable values for the time deviation of a clock detectable over an observation time τ .

PERCENTILE LEVELS AND THE MAXIMUM TIME INTERVAL ERROR (MTIE)

In the last few years, in the telecommunication community increasing attention has been paid to the development of mathematical tools suitable to characterize clock behaviors in telecommunication networks. An important information is the maximum range spanned by the phase deviation $x(t)$ of a clock because it determines the correct dimensioning of memory buffers. To this aim, the Maximum Time Interval Error (MTIE) was defined as:

$$\text{MTIE}(\tau) = \max_{-\infty \leq t_0 \leq \infty} \{ \max_{t_0 \leq t \leq t_0 + \tau} [x(t)] - \min_{t_0 \leq t \leq t_0 + \tau} [x(t)] \} \quad (7)$$

Nevertheless, this original definition gave some problems because it refers to the maximum range ever spanned, i.e. during the entire life of the clock. From the analysis of data reported in Fig. 1, it appears that, in case of pure Gaussian white phase noise, the maximum spanned range may reach infinitely large values. It is only a matter of time: the larger values are less probable, but not impossible, and after a long period of operation they may be observable. It became, thus, apparent that the original definition (Eq. 7) needed to be better refined and recently, a percentile definition to be interpreted as the maximum range, not to be exceeded more than a certain percentage of times, was adopted.^[3]

How to estimate the percentile of the distribution $h(z)$, i.e. a threshold level a which is expected to be exceeded only a certain percentage $(1 - p)$ of times? To this aim, it is necessary to identify the range value a delimiting an area equal to p to its left, i.e.:

$$H(a) \equiv \int_0^a h(z) dz = p \quad (8)$$

The evaluation of Eq. (8), via Eq. (5), requires some numerical integrations and depends on the values of n and p . An example of some evaluations are reported in Fig. 2, where threshold levels a are individualized as a function of the number of samples n for three different percentile levels p . As the number of samples n increases, the probability that the spanned range is large increases also. Therefore, the threshold that guarantees the p th percentile of the range possibilities moves towards larger values. To be sure of covering 99 out of 100 cases, we must be ready to accept also relatively large values for the range. For example, with $10^4 \div 10^5$ data, we should also accept range values reaching ten times the standard deviation σ of the parent distribution.

ESTIMATING THE PERCENTILE MTIE

The reported study of the probability law of the spanned range is, thus, supporting the estimation of the quantity MTIE in its percentile definition. In the case of white phase noise, it is possible to assess the percentile threshold values for the spanned range only by the knowledge of the standard deviation σ of the Gaussian noise and by the aid of Eq. (8) or of Fig. 2. It appears that the percentile MTIE may be written as:

$$\text{MTIE}_{p-\text{perc}}(\tau) = c(p, \tau) \cdot \sigma \quad (9)$$

where the function $c(p, \tau)$ is a suitable function of the percentile level and of the observation time and has to be estimated by the evaluation of Eq. (8) or by the aid of Fig. 2. The problem may be how to know σ . It may be estimated, for example, by the aid of the relationships between the Allan deviations and the spectral densities^[4] and by exploiting the relationships among those and the standard deviation σ of the Gaussian phase noise. This leads to the following equivalent relationships:

$$\sigma(\tau_0) = \frac{\tau_0}{\sqrt{3}} \sigma_y(\tau_0) = \sqrt{\int_0^{f_h} S_x(f) df} = \sqrt{\frac{h_2}{4\pi^2} f_h} \quad (10)$$

where the introduced symbols are well known: $\sigma_y(\tau)$ is the Allan deviation, $S_x(f)$ is the spectral density of the phase deviation $x(t)$, f_h is the high-frequency cutoff, and h_2 is the constant that determines the amount of white phase noise^[4] in the polynomial model of the frequency spectral density $S_y(f)$. Eq. (10) introduces, thus, a relationship between the amount of phase noise (stated as Allan deviation or spectral density level) and the percentile MTIE. Some examples of experimental validation of the study reported in this paper are presented in [5]. Some experimental measurement data were used to evaluate the original MTIE, as well as the percentile one, through the described procedure, and results are compared and discussed.

FURTHER COMMENTS AND CONCLUSION

The study here presented was devoted to the case of Gaussian white phase noise (white PM). The assumption of Gaussian noise was experimentally checked in [6]. The white PM is certainly not the only noise affecting clock signals. Nevertheless, it is an important case, particularly in the characterization of telecommunication units^[7], where a behavior due to white phase noise is observed also for longer observation intervals. Moreover, the output of a clock locked to a good reference signal presents a behavior similar to the white phase even if the underlying noise may be of a different nature.^[8] The extension of the above theoretical analysis to other kinds of noises usually appearing on clock signals is under development.

The study of the threshold levels reached by a random process is not only interesting for characterizing clocks or telecommunication apparatuses, but also in the determination of calibration intervals of measuring instruments of industrial interest.^[9]

In conclusion, through the estimation of the probability law of the range spanned by a random process, it has been possible to determine the threshold range expected not to be exceeded more than a certain percentage of times. This led to an evaluation of the percentile definition

of MTIE and of its relationship with the noise power spectrum level in the case of clocks affected by white phase noise.

REFERENCES

- [1] A. Papoulis 1965, **Probability, Random Variables, and Stochastic Processes**, McGraw-Hill Book Company, New York, New York, USA, pp. 187-232.
- [2] P. Tavella, and A. Godone, "*The new definition of Maximum Time Interval Error as a percentile in clock stability assessing*," submitted for publication.
- [3] International Telecommunication Union 1995, "*Definition and terminology for synchronisation networks*," ITU-T Recommendation G.810, Geneva, Switzerland.
- [4] International Telecommunication Union 1992, "*Frequency and time (phase) instability measures*," ITU-R Recommendation TF 538-2, Geneva, Switzerland.
- [5] S. Bregni, and P. Tavella, "*Estimation of the Percentile Maximum Time Interval Error of Gaussian White Phase Noise*," submitted to IEEE ICC97 International Conference on Communications, 1997, Montreal, Canada.
- [6] P. Lesage, and C. Audoin 1973, "*Characterization of frequency stability: uncertainty due to the finite number of measurements*," **IEEE Transactions on Instrumentation and Measurement**, IM-22, 157-161.
- [7] R. Bonello, A. Manzalini, A. Godone, C. Novero, and P. Tavella 1995, "*Stability characterization of stand alone synchronisation equipments*," in Proceedings of the 9th European Frequency and Time Forum (EFTF), March 1995, Besançon, France, pp. 220-225.
- [8] A. Godone, E. Bava, and C. Novero 1989, "*Phase lock of submillimetric backward-wave-oscillators*," **IEEE Transactions on Instrumentation and Measurement**, IM-38, 794-798.
- [9] P. Tavella, A. Bobbio, S. Costamagna, and A. Montefusco, "*Stochastic drift models for the determination of calibration intervals*," to appear in Proceedings of Advanced Mathematical Tools in Metrology, September, 1996, Berlin, Germany.

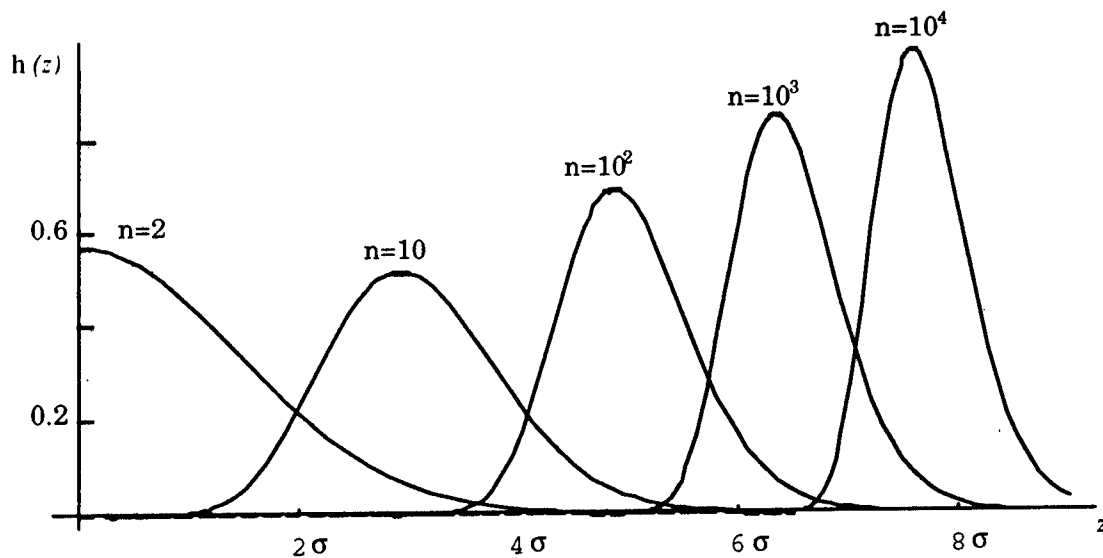


Fig. 1: Probability density function $h(z)$ of the range spanned by a sequence of n uncorrelated Gaussian samples. The values of the range z are normalized to the value of the standard deviation σ of the parental distribution.

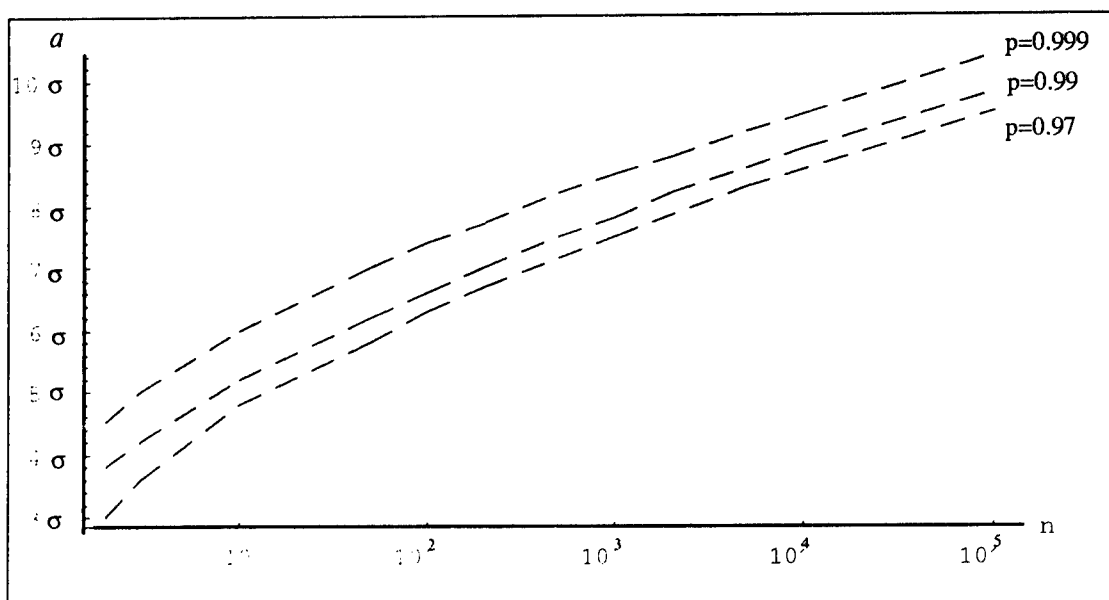


Fig. 2: Threshold levels delimiting the maximum range spanned by the phase deviation at the percentile level p , versus the number n of samples (the threshold level a is normalized to the standard deviation of the Gaussian parental distribution)

MILITARY APPLICATIONS OF TIME AND FREQUENCY

R. L. Beard, J. D. White
U.S. Naval Research Laboratory
4555 Overlook Avenue, SW, Washington, DC 20375, USA

J. A. Murray
SFA, Inc.

Abstract

The introduction of the NAVSTAR Global Positioning System (GPS) to the military community is having an lesser known, but highly significant, impact on those systems requiring dissemination of precise time and frequency. Precise time/frequency and their uses could have a wider ranging influence on military electronic systems than the positioning/navigation aspects. The implications are not as well known or recognized. Time and Frequency (T/F) are a fundamental function needed by all military electronic equipment. From generation of frequencies for communications to remote sensing of geophysical quantities with time-tagged data requires oscillators, T/F standards, and/or clocks. The application and requirements for these standards and their maintenance of them onto a common timescale is a specialist's area often overlooked in the development and deployment of these systems, only to be addressed later as a operational problem area. The wide spectrum of applications and uses for timing devices within military systems can be categorized into different system types: (1) navigation, (2) communications, (3) identification, (4) remote sensing, (5) intelligence, and (6) weapons.

In addition to using T/F devices and technology, military electronic systems are on diverse platforms, which operate most effectively in a highly coordinated, interactive environment. This requires all units and elements of the operating forces to be referenced to the same time. U.S. military systems are required to be referenced to Universal Coordinated Time (UTC) maintained by the U.S. Naval Observatory (USNO), designated UTC(USNO). From this central reference, time is disseminated through various existing military and scientific systems. Navigation systems are the most immediate and well-known users of T/F, and from this fact are the primary systems used for T/F dissemination. Heretofore, a single system has not had the capability of widely disseminating precise time; consequently, many different systems with different capabilities have been used. Today the NAVSTAR GPS provides a general purpose, highly precise means of disseminating time and has been used operationally since the first technology satellites of the system were launched.

This paper summarizes the areas and application of precise time and frequency uses in military systems with specific examples.

INTRODUCTION

The Precise Time and Frequency (PT&F) utilization within military forces encompasses four major areas: (1) timescale generation and coordination, (2) dissemination systems for PT&F, (3) distribution system within platforms and for local areas, and (4) users in platforms and

systems. As used in this paper, the term "user platform" includes ships, submarines, aircraft, land mobile units, and fixed-site installation (e.g. airfields). Within the overall generation, dissemination, distribution, and use of PT&F, a variety of interfaces exist for the transfer or use of PT&F. A standardized interface to determine a common interface between military equipment or systems would provide increased interoperability. The use within the overall context of PT&F, as well as specific examples for equipment, will be discussed in this paper.

US DoD TIMESCALE

The timescale adopted for military systems is Coordinated Universal Time (UTC). UTC is founded on the SI second defined on the period of the frequency between two hyperfine levels of the ground state of the cesium atom. Thus, a cesium-beam standard can be considered as a primary frequency standard, and is used extensively in military systems. Coordinated Universal Time (UTC) was adopted with the advent of atomic time (AT); UTC is the approximation of UT generated by atomic clocks, and since it is approximate, corrections known as "leap seconds" are introduced periodically to keep UT1 and UTC to within 0.9 seconds of one another. International Atomic Time (TAI) is a continuous timescale generated by atomic clocks located in timing centers distributed around the world and coordinated by the International Bureau of Weights and Measures (BIPM), located near Paris, France.

UTC and TAI differ by an integer number of seconds; the rates are the same. UTC itself is a composite of the measurements made at numerous time observatories and centers around the world. It is the basis of legal and scientific measurements maintained by local or national timing centers as the output of their physical clocks, as distinguished from the international value determined as a "paper" or theoretical timescale. The local or national time is identified as UTC(XYZ), where XYZ is the center generating and coordinating the timescale. This quasi-uniform and universal timescale presents particular problems for the military user, in that it is not continuously uniform. The introduction of leap seconds to keep UTC allows the timescale to be used as an approximation to UT1 only for those users with a time accuracy requirement of about ± 0.9 seconds. Alignment of inertial systems, for example, requires knowledge of UT1. Aside from introducing significant jumps in the timescale periodically, the dissemination of the time and value of the leap-second occurrence has posed significant problems for the operating forces.

ALLIED/NATO REFERENCES

For U.S. Allied or NATO operations, the availability of a common timescale poses additional problems. Each participating member nation or ally has, or refers to, an observatory or laboratory that is charged with the establishment and maintenance of their national UTC timescale. These master references are coordinated internationally, and the international UTC timescale forms the basis of timekeeping and time-interval measurements for NATO military forces. Via primary and backup dissemination systems, each equipment/system onboard the various user platforms are provided with time and frequency signals which are directly traceable to the nation's master UTC reference. The accuracy and availability of UTC reference sources differ from nation to nation. The maintenance of UTC is coordinated, but the individual nation's sources and availability for military bases and systems may well have widely varying values. For joint or NATO operations with mixed forces, the capability to be synchronized can be a significant problem. The addition of leap seconds and the communication to operating forces compound the problem.

DISSEMINATION SYSTEMS

Time-dissemination systems are typically military systems developed for navigation and communications and often have their own time basis or timescale. In the case of GPS, the system internal synchronization time basis is determined and known as "GPS Time." This is the time determined by the ground tracking system for maintaining the operation of GPS. GPS time's continuous nature is needed by the system to synchronize the satellites for navigational operation and consistency. The known relation of GPS Time to UTC(USNO) makes GPS a global, continuously available, general-purpose time-dissemination system with much greater precision than previous global systems.

From the time reference through the dissemination system, a platform or user requiring precise time or frequency is at the bottom of a timing hierarchy that gives it traceability to the adopted timescale. In practice, the timescale must be associated with a physical clock, although the true timescale may be a "paper" clock or internal system time base. Figure 1 illustrates this representative timing hierarchy. There may be other routes to traceability, and the hierarchy may even change during a mission. If, for example, the dissemination system were GPS and the platform were an aircraft whose platform clock is not operating until just before a mission, time would be obtained initially from the site clock, which operates continuously. Then, if GPS were using its Selective-Availability/Anti-Spoof (SA/AS) mode, precise time would be needed to acquire its code quickly. However, the platform clock would not be accurate enough for direct access to GPS and might later be updated by it.

Figure 1 also illustrates the overall PT&F resources and systems within the timing hierarchy. There are many communication and navigation systems presently in use which have an inherent capability to disseminate PT&F signals on a non-interference basis with the systems' primary missions. While some of these systems have the capability to disseminate both time and frequency, e.g. GPS and LORAN-C, many systems can be used to disseminate either precise time or frequency. The U.S. Navy Navigation Satellite System (NNSS) or Transit, for example, has only a precise time dissemination capability, and current VLF broadcasts can be used only as a precise frequency reference.

In general, each clock in the hierarchy, depending on its mission, must operate autonomously for some period of time. For a hand-held clock that carries time from a site clock to mobile platforms, autonomy may prevail for only minutes or a few hours. For submarines, the clocks might run autonomously for some months. For survivability, a clock may need to operate autonomously for the time required to restore a failed link with the next higher clock, to establish a different hierarchy, or to finish the overall mission.

SYSTEM PT&F INTERFACES

PT&F interfaces are a secondary and important link in the timing hierarchy. These two-way interfaces between individual systems form a vital link in the dissemination and coordination of PT&F within platforms and between systems. The use within the equipment and the operational requirement the equipment is required to meet are usually tailored to the needs of individual systems, without consideration of the variety of systems on the platform. Consideration for an overall architecture needs to be developed to take advantage of developing universally synchronized military systems.

An important interface issue that needs consideration is that all systems, regardless of how they acquire the reference, should use the same basic timescale, UTC. By accepting it as

the reference, inter- and intra-system interoperation can be supported. These interfaces are generally designed to communicate the time base that the system it serves uses. Traceability between system time bases to UTC can vary widely from one user system to another because of their different requirements and operating methods.

Interfacing of systems beyond use of a common timescale should be aided through a common platform-level timing facility, which could provide time, and perhaps frequency, signals to serve all the users. Beyond time maintenance, little other information would be of common interest. However, not all timing facilities can easily provide all the information needed. If a standard time code is to be used, other considerations are needed: the local distribution medium to be used; the time resolution to be supported by the code itself; the need for and ability to support information about leap seconds; the detail needed to resolve ambiguities of seconds, minutes, hours, days, days of years, and years of centuries; and Time Figures of Merit (TFOMs), if needed. The need to provide TFOMs might depend upon how the accuracy of the service is expected to vary. Users may elect to use TFOMs internally, whether or not the service provides them. Current interfacing time-code considerations have involved the adoption of a code that has provisions for all the information, most of which would be optional. It does place a burden on the users to maintain all the required information to support the interface itself, even though the user may not need the information himself.

TIME FIGURE OF MERIT (TFOM)

A Time Figure of Merit (TFOM) developed for use within a PT&F time code is intended to describe the accuracy of the time reference that is being supplied by the time code to a unit or system. If the TFOM is a credible index of accuracy, a user might assess the accuracy of the reference before accepting a time update from it. In order to accomplish this, the TFOMs would represent an accumulation of timing uncertainties through the chain of time dissemination and distribution operations from the primary reference, e.g., UTC(USNO), to the ultimate user. These uncertainties accrue from measurement errors and uncertain clock performance during periods between direct comparisons with the reference or from "flywheeling" to maintain the reference for continuous operation. The evolution of the errors is illustrated in Figure 2. This method requires that each node in the chain add its uncertainty to that of its reference. While some uncertainties might be considered random and a smaller TFOM might be justified, a more elaborate TFOM is needed to convey all the required information. Obviously, the TFOM can be kept small by keeping the number and uncertainty of measurements low and using better clocks and shorter periods of autonomous operation. The relationships of the timing errors and TFOM values should be managed by some fixed plan for the particular system involved to reduce the amount of information that may need to be transmitted and to ensure equal treatment of the errors as the values propagate through the system and its various nodes. Time management from reference to user can be managed in two principal categories: fixed and fluid hierarchies.

FIXED TIMING HIERARCHIES

In a fixed timing hierarchy, an established chain of timing references is used, as in Figure 1. Normally, fixed chains are designed for a specified accuracy, so the end user can generally rely on the final time reference he receives as being within the system tolerance. There is generally little use for a TFOM in this situation, although an alarm may be used if there is a failure. An alarm received through the chain might be cause for a user to revert to independent

timekeeping with the local clock or to use an available backup reference.

Most fixed hierarchies employ relatively short paths or few nodes to the ultimate UTC reference. The chain in many cases is simply an established time-dissemination service, such as GPS, and the local clock is occasionally or regularly updated via that service. However, the major dissemination services do not ordinarily provide TFOMs, because they have the resources to maintain advertised accuracy with high confidence. An alarm may be issued (e.g., by LORAN-C or GPS), however, if certain equipment is not performing properly. Some other dissemination services involve larger uncertainties than GPS. Although very-low-frequency, low-frequency, and high-frequency transmissions may be very accurate at the source, the error in estimating propagation time to the receiver may be in the order of a millisecond if not within line-of-sight or groundwave range. One-way transmissions from geostationary satellites may involve uncertainties of some tens of microseconds. All of these transmission errors may be considered measurement uncertainties, and appropriate TFOMs might be assigned if the errors can be measured or otherwise quantified. If the information to quantify exists at the node in question, the accuracy of the measurement is then known and could be used to upgrade the TFOM to the users; there is little or no need to transmit it in a time code.

Some fixed hierarchies contain distribution media, such as microwave links, fiber-optic cables, dedicated telephone lines, etc. Their contributions to time error generally consist of fixed delays, which may be compensated by two-way transmissions or simply taken into account by the user. Only the variability of the path would be of concern to the user. However, the range of variability usually is known to the user and cannot be determined by the sender. Therefore, inclusion of a TFOM in the transmitted signal would be of little interest, although an alarm might be useful if the system becomes defective.

FLUID HIERARCHIES

In a fluid hierarchy, part of the timing hierarchy is not fixed. Although the upper levels may be fixed, some at the lower level, especially aircraft and other mobile clocks, may be disconnected from the fixed chain for the length of a mission. To meet their accuracy requirements during these periods of autonomous operation, other links with other systems or equipment traceable to the primary reference are used. Updates then might be obtained from another clock within communication range whose TFOM was lower than their own. Thus, new sub-hierarchies are created, whose structure is based on an hierarchy of TFOMs.

Operation of a fluid hierarchy could depend critically upon the validity of the TFOMs. The TFOM of a platform clock would then be determined from the sum of the following: the uncertainty represented by the TFOM of the last clock used as a reference, the measurement uncertainty with which the last time update was made, and the added time uncertainty contributed by the platform clock since the last update. The second and third terms could cause each lower level of the hierarchy to declare a higher (poorer) TFOM than the previous one. The measurement uncertainty for each time transfer might be a specified number of milliseconds or microseconds, based on nominal values for the technique used. However, there is no good basis for self-determination of the third term if the platform has only one clock and no means to check it against a more accurate reference. "Semi-worst-case (SWC)" clock performance could be assumed since the last update, but the means to determine or calibrate the actual performance is needed to insure performance. SWC performance could assume that the clock has run at the manufacturer's maximum specified rate error since the last update, although experience has shown a significant variability in performance, especially in severe environmental conditions. Success of this operation depends strongly on availability of clocks with better

TFOMs at key distribution nodes. A squadron of aircraft from one location and using the same type of clock, for example, could not update each other, because their TFOMs would be identical.

For platforms using TCXOs or MCXOs, the SWC bound must include the effects of the entire environmental range. The SWC method of determining TFOMs can easily result in having one clock updated by a less accurate clock, although the maximum error is still generally limited by the SWC bound. Some TFOM increments in the more elaborate TFOM schemes are as small as about 10%, a trivial increment considering the coarseness of knowledge of the clock's actual rate. However, in a long daisy chain of updates, a sum of these small increments can reflect a substantial loss of accuracy which would be need to be accounted for. A defective clock under these conditions could badly contaminate the system if protective measures are not used.

THE NAVSTAR GLOBAL POSITIONING SYSTEM (GPS)

The NAVSTAR GPS is a navigation satellite system that provides continuous worldwide three-dimensional position, velocity, and time information to properly equipped systems. This system will be the primary dissemination system for U.S. and cooperating NATO forces. All user systems are synchronized to GPS system time for navigation, and the precise time output is UTC as maintained by the U.S. Naval Observatory (USNO). GPS system time is maintained by the Master Control Station (MCS) through the use of the cesium standards deployed throughout the GPS system and the Alternate Master Clock ensemble of atomic clocks co-located at the MCS by the USNO. The capability of GPS user equipment (UE) to disseminate UTC(USNO) worldwide is to an accuracy of approximately 100 nanoseconds.

GPS UE has several versions that are tailored for the specific user platforms, as described in the Interface Control Document (ICD) for the GPS program, GPS-ICD-060. The various models of GPS UE are assembled from several integral components designed to satisfy the requirements of the variety of user platforms. The receivers of the GPS air and sea UE are each equipped with a common Precise Time and Time Interval (PTTI) module specifically designed to exchange time-related information with other systems. A variety of user equipment for use specifically in PT&F systems has been developed. Most common are equipment for use with the Standard Positioning Service (SPS), but for military systems a few receivers utilizing the Precision Positioning Service (PPS) are also available.

LORAN-C

LORAN-C is a ground-based radio navigation system that broadcasts on a frequency of 100 kHz using a bandwidth from 90 to 110 kHz. At this low frequency, the radio waves follow the earth's curvature, are relatively undisturbed by the earth's ionosphere, and are very stable. The signals propagate in two forms, the "skywave" signals reflected from the ionosphere and the "groundwave" signals following the earth's surface. Groundwave signals provide the more accurate results and skywave somewhat less accurate.

The system consists of many synchronized chains or networks of stations. These stations provide groundwave coverage of most of the United States, Canada, Europe, the North Atlantic, the islands of the Central and West Pacific, the Philippines, and Japan. One station in each chain is designated as a Master Station, and the remaining stations are slave stations. The Master Station transmits groups of pulses that are received by the slave stations. The slave stations receive the master pulse groups and, at a later time, transmit similar groups of synchronized

pulses.

On a user platform, the constant time difference between the reception of the master pulses and the corresponding slave pulses establish a line of position that is used for navigation. Signals from three separate LORAN transmissions are needed to determine a line of position. For PTFS applications only, a single LORAN station is needed if the user accurately knows their position. The LORAN-C system is synchronized by and compared to UTC(USNO) to maintain precise time throughout the system. Except for very long overland paths, LORAN-C groundwaves have a precision of $0.2 \mu\text{s}$ and an accuracy of $0.8 \mu\text{s}$, with the published corrections applied. Cycle identification errors could add $\pm 10 \mu\text{s}$ to these figures. Efforts are now underway to keep the LORAN chains to within 100 ns of UTC(USNO).

DCF-77

DCF-77 is a low-frequency radio transmission system operated by the German government. This system transmits UTC as maintained by the Physikalisch Technische Bundesanstalt (PTB) in Braunschweig, Germany. The transmitter signals are amplitude-modulated BCD time code at a rate of 1 bit/s, with a 1 minute time frame. A user receiver can expect an time accuracy of $50 \mu\text{s}$ to 1 ms, depending upon propagation effects. Frequency measurements can be expected on the order of 5×10^{-13} .

PRECISE TIME REFERENCE STATIONS (PTRSs)

A PTRS is defined here as a remote station employing clocks and measurement systems to independently maintain precise time and frequency references for other users or calibration purposes. Often in these PTRSs the intent is to maintain a timescale synchronized to UTC. The clock systems used may be an ensemble of clocks, multiple clocks tied together with a data acquisition system to produce a combined or improved output, or highly stable high technology clock systems such as hydrogen masers. These clock systems are then compared to the UTC source by several independent time comparison techniques, such as GPS, LORAN-C, and/or Two-Way Satellite Time and Frequency Transfer systems.

A type of PTRS is used in the satellite communications networks of the Defense Satellite Communications System supporting syntonation of the stations and active timing comparison through the system. This employs a special modem to generate and receive precise timing pulses transmitted through the system. By this means very precise time or frequency comparisons can be made to support a spread-spectrum synchronous communications system. Other strategic communications systems employ similar means for maintaining overall system synchronization.

ELECTRONIC TRANSFER DEVICES (ETDs)—PORTABLE CLOCKS

A common means of precise time comparison and dissemination that was extensively used is portable-clock time transfer or so-called traveling clocks. These systems usually consisted of a portable cesium frequency standard that would operate on batteries, and was physically moved from one site to another for time comparison. Accuracies obtainable from this technique have been reported on the order of a few nanoseconds, and it was used for high-precision intercontinental time transfer. Use of this technique currently is limited to short distances

for the most demanding requirements, but a analogous technique is being considered for new systems. This new technique is to use small self-contained Electronic Transfer Devices (ETDs) for short distances, within a limited time of operation, and for distributing between larger numbers of users, e.g. aircraft on a flight line getting ready for takeoff. These small self-contained ETDs are highly dependent upon the type and quality of oscillator used, since it determines the quality of time information available. Implementation of these devices has been significantly hampered by the oscillators required.

USER SYSTEMS/PLATFORMS

Tactical communications systems require PT&F for their operation. The frequency-hopping nature of the Havequick system requires that the participating units be synchronized, and to address this requirement the users are organized into local area nets. Each local area net is controlled by a net master located at a centralized ground site. The net master then distributes net time as the local time reference directly to the users or the users exchange time over the air among themselves to maintain their communication capability. This relationship is shown generically in Figure 3. The net master (HQ Ground Equipment) maintains itself in time globally by some external means, such as through GPS or to a PTRS. Other tactical communications systems operate in a similar manner.

IFF systems, such as the Mark XII, the canceled Mark XV, and the proposed NATO Identification System (NIS), are currently query-respond-type systems. Operating in encrypted mode, the systems rely upon being highly synchronized. They are in principle very similar to tactical communications systems. These systems are also organized to operate in tactical area nets. The operation can then be described in terms of the generic diagram of Figure 3, and interchange of timing information is directly from the local area master or interchanges between units over the air. The definition of accuracy and a suitable interface for the interchange of timing information have been particular problems with the development of the systems. The Mark XV system implementation depended heavily upon the development of a hand-held ETD capable of updating aircraft on the flight line or carrier deck. This development was extremely difficult, given the quality of small oscillators, and was a major factor in the cancellation of the program.

These systems are good representatives of the fluid hierarchy timing systems and the dependence on a suitable PT&F interface that can meet the needs of PT&F information interchange.

PLATFORM DISTRIBUTION SYSTEMS

These systems are a means of providing a precise time and frequency reference at the platform level. These platform levels are typically airbases or ships which have a combination of user systems requiring PT&F resources. These platform-level systems would require survivability and redundancy to meet their military missions. They would be capable of providing PT&F signals for some period, and would not require continuous contact with the time-dissemination systems. The design of these systems combines the primary and backup dissemination systems with precise clocks capable of running independently. An example for airbase use is shown in Figure 4. This system can reduce the individual requirements of the participating user systems and, in turn, provide an increased level of accuracy at the base level.

In Figure 5 an example is shown of a shipboard distribution system. A system of this type would normally employ at least three reference standards. All the standards in the system would contribute to the time and frequency measurements and one is selected to be the master

reference. The output of the master reference could be steered to reflect the combined results of the composite results and, thereby, provide an even more stable time and frequency reference. The distribution of the system could also refer to the physical isolation of the frequency standards from user equipment and from one another. The distribution system survivability and availability are enhanced by the components' physical separation and the ability of any standard in the system to become the overall system reference.

If a platform timing facility were to be provided, it must be decided whether or not the facility would accept time updates from any of its user systems. If TFOMs would be the basis for the facility to accept such updates, their meanings should also be standardized. This would be difficult. Systems use a wide variety of techniques for time transfers, and their criteria for estimating the degradation in timekeeping may also vary. Manufacturers' specifications are probably an insufficient guide to estimate uncertainty, because some are much more conservative than others. Other factors of importance are how often and accurately oscillators are calibrated in frequency, how well the systems are maintained, what the mean time is between (undetected) failure of clocks and measurement systems, and what overall management is used to assure accuracy. A conclusion that might be reached about accepting time updates from the users is that it should be an extraordinary measure that is resorted to only in an emergency.

SUMMARY

This brief paper has touched on a number of issues in the use of PT&F information by military forces. These issues have generally been overlooked in the development of individual systems because those developments rightly focus on the individual system's requirements. Coordination of PT&F for synchronized multi-service and multi-national forces requires that a systems approach be applied to PT&F. The implications of maintaining these services, especially in wartime, are deserving of closer study.

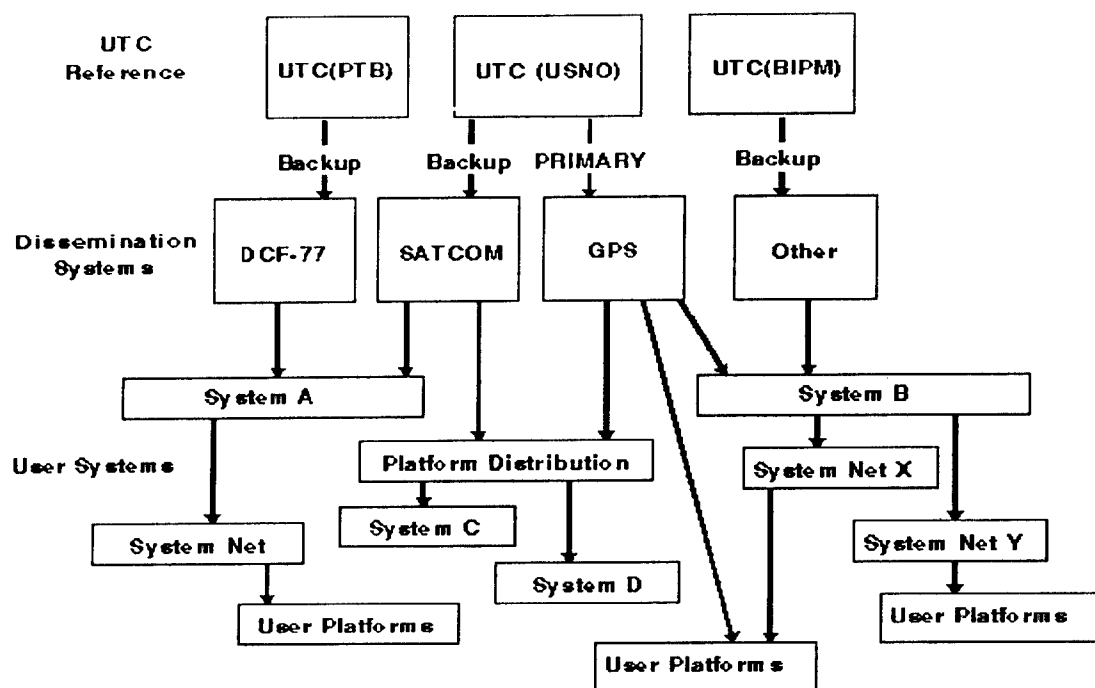


Figure 1, The Timing Hierarchy

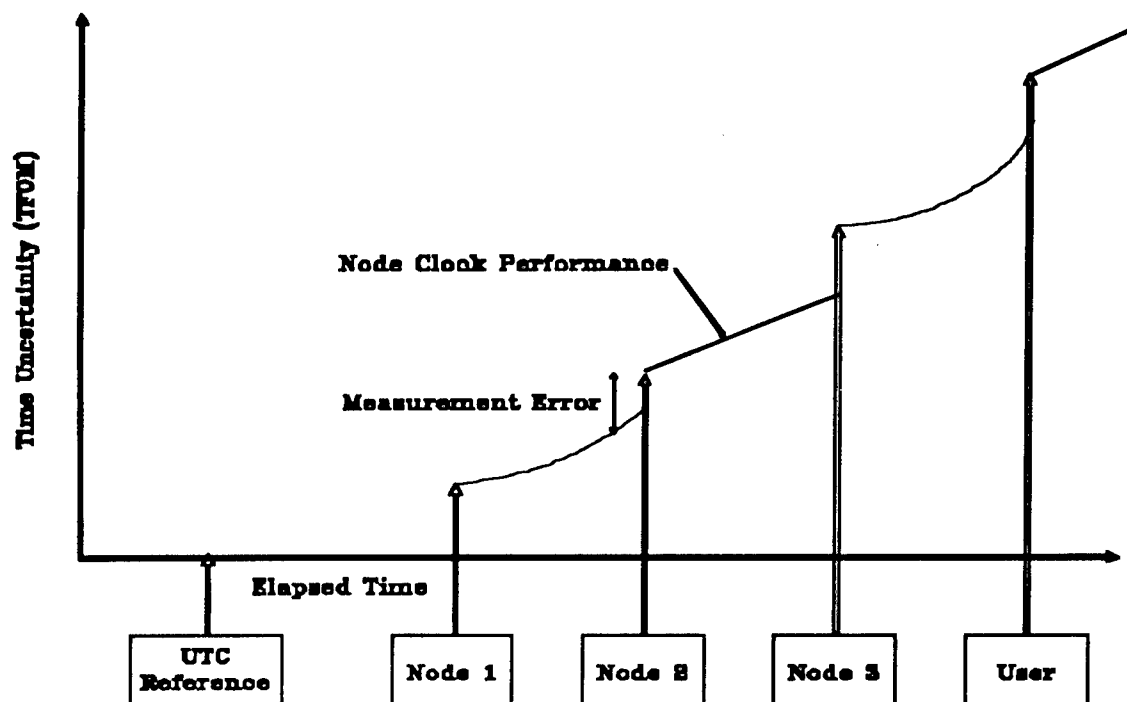


Figure 2, Time Figure of Merit

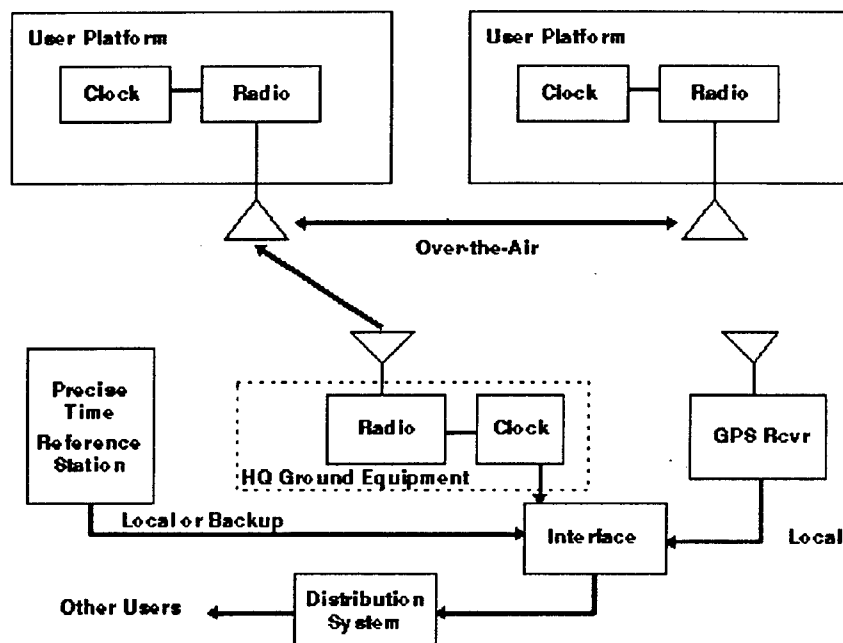


Figure 3, Generic User System

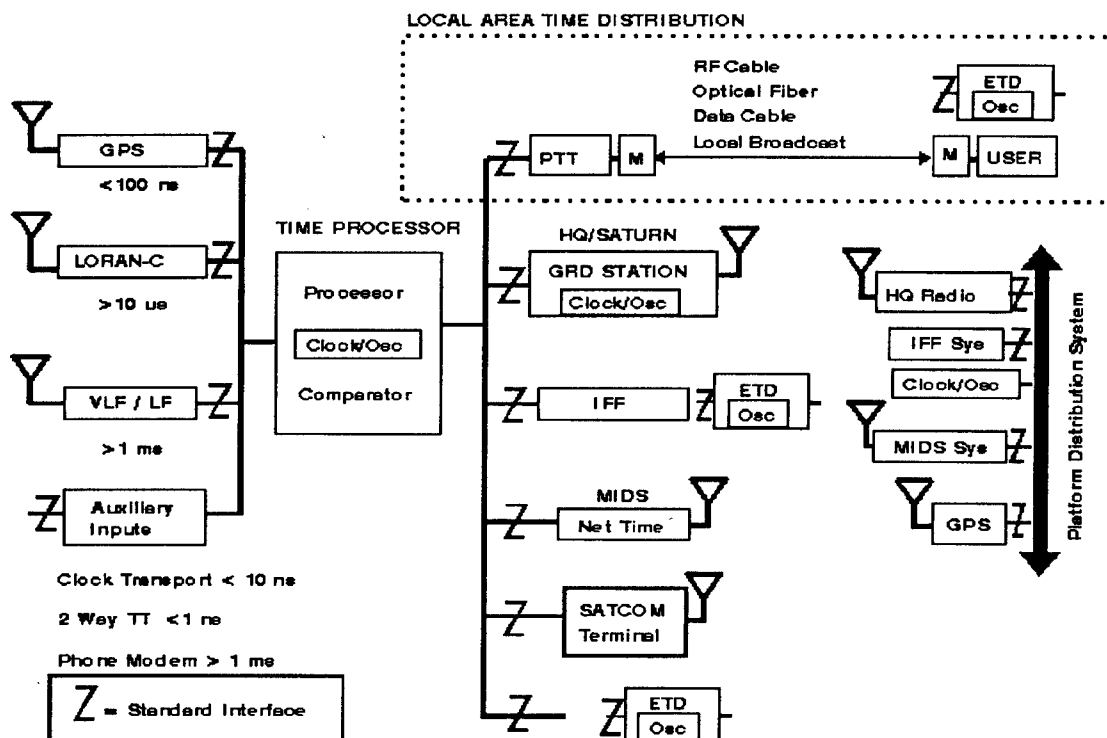


Figure 4, Example Airfield Distribution System

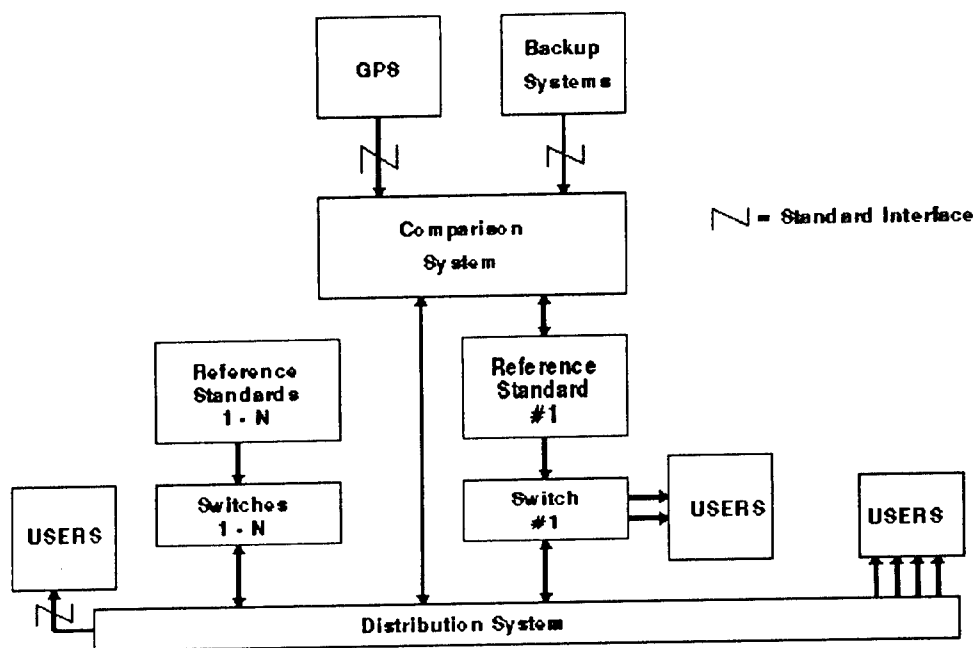


Figure 5, Example Shipboard Distribution System

Questions and Answers

GERNOT WINKLER (INNOVATIVE SOLUTIONS INT'L): In view of the fact that the subject is central to this conference, we should spend maybe three more minutes on that in a general way. The rule of time and specification for the needs for time are unique, not only because time is pervasive and goes into every operation which we know, but also because there is a great confusion about it. Many people who specify accuracy should be aware of why they are using clocks at all. You mentioned, for instance, the fact that in these communication satellites there is a clock. Well, yesterday we had a discussion about the systems, the coming improvements or additions to the Global Navigation System, as envisioned by the Europeans, which do not propose to put clocks into the satellites. I remember Dr. Busca's discussion where he said that clocks will simplify that. So the question of requirements is extremely complex.

In addition, I suggest distinguishing two concepts: a requirement in the sense of minimum tolerance or a requirement without which the system cannot operate or get into trouble. And between the benefits from doing better than that, you mentioned that we're going to upgrade requirements in the future. Well, if you want to do that, why not contract with incentives for operation which is better than the required minimum specifications?

The incentives are extremely important. And they are extremely important for another reason. Because today, our civilization, not only in this country but everywhere in civilization, suffers from what I call the "sufficiency syndrome." Once a requirement is set and people do accomplish the requirement, they feel that's sufficient. We don't need to do any better, because nobody has told us that we have to do better. You see, I'm coming back to these incentives, so these are very important additions.

In addition, there's another point. When you talk about requirements, in the military we have the concept of validated requirements. A command authority, possibly even at the highest levels in DoD for expensive systems, goes through a review; and a requirement is finally specified, because by specifying it, you commit your money. And that has an interesting side aspect because nobody who would have benefits from doing better than a specific requirement can get these requirements known because he will be hit immediately with the question, "Are you willing to pay for it?" So that's a very complicated thing. And I think in the requirement issue, because it is central to the conference, we ought to spend more time on these aspects. Thank you.

ROBERT VESSOT (SMITHSONIAN ASTROPHYSICAL OBSERVATORY): I'd like to comment on the need for short-term stability for possible multi-static radars and tracking systems where you need, in fact, in real time a measure of the position and velocity of that object so that you can do something about it. And I am despairing at the level of support that one can even imagine getting in the near future to keep a group of people alive and well in this direction, because I feel that if we are going to consider this as any form of our national defense system, this short-term stability and the ability to make these determinations of position and velocity depend on time, as Gernot has explained before.

JOHN VIG (ARL): I would like to comment on how we get requirements. Several years ago, my lab director, at a time we were short on money, which is not unusual, had a bright idea that we should have teams going out to do marketing. And I and a couple of colleagues decided to go see program managers. For example, we went to see the program manager of a radio system for the Special Operations Forces. I went in to see a Colonel, and I said, "Sir, we're here to help you. We want to find out what your requirements are so that we can develop a better oscillator for your system." I said, "Could you tell us a little bit about your requirements?" And the guy said, "Not only do I not know what clock we're using, I don't care what clock

And the guy said, "Not only do I not know what clock we're using, I don't care what clock we're using. What I specify is I want a radio for my guys to go into – and he named a country in the Middle East – and I want those guys to be able to stay there for awhile without being discovered. And when the time comes, I want them to be able to turn the radios on and be able to communicate without being discovered and then be extracted from the territory. Those are my requirements. What clock we use is totally up to the contractor." I said, "Okay, can I have the name of the program manager?" So I called the program manager at the contractor and the guy says, "I don't know what clock we're using nor do I care. That's up to Joe Schmoe at Building So-and-so."

It turned out to be a junior engineer who was making the decision as to what clock this system was going to use, which is a system on which the Special Operations Forces are depending. So it's very difficult for one to get the requirements from program officers. The program officers usually don't have the expertise and oftentimes they don't care what the requirements are for the clock or the timing system.

RONALD BEARD (NRL): Right, I think that's the point. It's a system level; a lot of these program managers don't even know they're using time in most cases. They don't care until they get out in the field, the guy plugs in the radio and he can't talk. And then after significant study, a lot of other effort, they find out that the oscillator is not remaining synchronized with the system on the other one; then there is a major problem.

CAPT. KENT FOSTER (USNO): [inaudible]

KEN PERRY (AEROSPACE CORP.): I guess some of what this is saying – this seems to be saying that it's up to us to understand the system requirements so that we can translate those into timing requirements; because, I think it's – I don't know if "unreasonable" is a proper word – but it's not going to happen that this junior engineer is going to understand timekeeping enough to be able to translate timekeeping abilities into requirements. So it's up to us to understand the system requirements and do the translating for the rest of the community.

RICHARD GRIFFIN (TEXAS INSTRUMENTS): A lot of the discussion of requirements is focused on requirements with respect to UTC. The areas we're interested in are more like stability for local between a small number of platforms, but where we need precision timing between platforms. We don't really care how we relate to UTC; we need to be able to have timing standards that we can have among a small number of units to coordinate specific activities, but at a very high precision. So we're concerned with the stability of the clock, not necessarily with its accuracy with respect to the UTC.

RONALD BEARD: That's part of the complexity of the situation, it's that many systems look at it that way. They require precise time for a particular application and radar or something like that.

GERNOT WINKLER: I would like to say that you are not alone. Every timing system has started with the same position, every one. I remember Omega, LORAN – not GPS – but certainly Transit, they all started with the idea that they were not interested in anybody else. And yet, they completely forgot that there are interfaces and that they can get tremendous benefits from making sure that these interfaces are part of the system right from the beginning.

RONALD BEARD: Part of the solution to your particular problem, without trying to be presumptive, may be getting time from another part of the platform that already has a highly stable clock, for example.

MARTIN BLOCH (FEI CORP.): In all of this discussion, there is one major problem which

hasn't really been addressed; and one is to generate precise time or precise frequency at low phase noise. And the second, in my experience in 35 years in this industry, is that the environmental effect of maintaining this under real operational conditions is usually being ignored by those junior people. And the problem is not addressed until after the systems are built and then a lot of money and a lot of effort are poured in and really wasted on this.

So a part in 10 to the 15th sounds ideal when you are at NIST or at USNO, but a part in 10 to the 10th when you are on operational aircraft or in a helicopter or in a moving vehicle is a bear. And we have to find a better way of addressing it in early design of systems rather than fixing it. We can fix anything, but it's very expensive. And we haven't come up with a solution on how to do it yet. But maybe at next year's PTTI, we'll do better.

RONALD BEARD: I think part of the answer to the Captain's question is that this conference provides this kind of information and provides a forum for people to be able to understand the awareness of how this affects their systems. I don't know that we can come up with a particular solution *per se*.

JOHN VIG: One of the reasons that these problems get repeated over and over again is that we have a great deal of difficulty documenting what problems have occurred in the past. Usually when there's a problem, nobody wants to admit to it; it's swept under the rug and it's forgotten as quickly as possible rather than being documented so that people can learn from it. Is there any documentation of the GPS story, for example, as to how the clock development for GPS has progressed over the years and how much money has been spent?

GERNOT WINKLER: What do you expect if you have professors and leaders of all levels who say the past is of no interest to us? "We don't want to hear about the past!"

ROBERT VESSOT: Well, I am part of that past. And I think the issue that I see that is central to this whole discussion is this question of sufficiency. Once the specification is met, everybody says "Yes, amen, things are going to go on forever this way." The problem is that, when an advance was made in the ability to do timekeeping and frequency stability, I've never seen it happen that that advance hasn't been eagerly accepted and implemented. And I think that this is clearly the case now. And if we stop doing advanced research on clocks, we're headed for trouble.

THE ALTERNATE MASTER CLOCK AND PRECISE TIME REQUIREMENTS; WHY AN ALTERNATE MASTER CLOCK?

W. V. Bollwerk

U.S. Naval Observatory Alternate Master Clock
Colorado Springs, Colorado 80902-4238, USA

Abstract

The U.S. Naval Observatory (USNO) Alternate Master Clock (AMC) became fully operational on 23 July 1996. The AMC was relocated to Falcon Air Force Base (AFB) from Richmond, Florida, commencing 24 October 1995. By placing the AMC at Falcon AFB, the clock is co-located with the GPS Master Control Station and, thus, the primary means of global time dissemination. The AMC is in a key position to provide significant improvements to the various space systems operated by the Air Force from Falcon AFB. Efforts are underway to enhance the timing of GPS, the Air Force Satellite Control Network, and some TALON programs within the Space Warfare Center. The AMC will be able to provide a more reliable and robust timing source for all users at Falcon. This will eventually lead to reduced navigation errors, increased communications capability, and improvements in C4I. The areas in which the AMC will be used to enhance worldwide military operations are highlighted.

INTRODUCTION

The U.S. Naval Observatory (USNO) Alternate Master Clock (AMC) is the backup for the Master Clock maintained at USNO. The move of the AMC to Falcon Air Force Base (FAFB) occurred between October 1995 and July 1996. The AMC was previously located in Richmond, Florida. The clock was relocated for several reasons:

1. Richmond, Florida, was highly susceptible to natural occurring problems, such as hurricanes
2. Co-locate with the Global Positioning System (GPS)
3. Place in a more secure environment
4. Provide a greater, more robust backup capability.

The AMC is designed to provide precise time, on the order of 2-3 ns accuracy a day to the military commands located at FAFB. The primary user of AMC data is GPS. Additionally, the system provides timing reference signals to the 50th Space Wing communications squadron and the Air Force Technical Applications Center detachment. Plans are in place to provide precise timing reference signals to the Air Force Satellite Control Network, Space Warfare Center, and other satellite control systems.

This project was coordinated with the Air Force and serves to support the interest of both services. The AMC obtained initial operational capability in November 1995 and was made fully operational on 23 July 1996. The next major step in the development and operational use of this system occurred on 12 September 1996. On this date, the AMC provided a 5 MHz signal to the GPS Monitor Station located at the Master Control Station (MCS).

WHAT COMPRISES THE ALTERNATE MASTER CLOCK

The AMC primary equipment consists of 11 cesium atomic clocks, 2 hydrogen masers, 2 Auxiliary Output Generators (AOGs), data analysis equipment, two-way satellite time-transfer systems, and distribution systems. The two master clocks at the AMC are the AOGs, with each AOG referenced to a hydrogen maser. The master clocks are named AMC #1 and AMC #2.

Data on all AMC clocks are gathered using two separate data analysis systems: the Data Acquisition System (DAS) and the Timing Solutions Corporation Measurement System (TSCMS). The DAS compares all AMC and GPS clocks to AMC #1 and AMC #2 every 20 minutes, while the TSCMS compares the 5 MHz frequency of all AMC clocks to AMC #2 every 20 seconds. These data are used both in the time scale and for analysis of clock performance.

The AMC has three GPS receivers: two Precise Positioning Service (PPS) keyed and one Standard Positioning Service (SPS) unkeyed timing receiver. The PPS receivers are made by Stanford-Telecom and the SPS receiver is made by Allen Osborne Associates. The PPS receivers are used to monitor the GPS satellite clock performance and provide a steering reference to AMC. The SPS receiver is used to conduct common-view time transfer between the AMC and USNO in Washington, DC.

The AMC maintains the highest precision reference to UTC(USNO) using Two-Way Satellite Time Transfer (TWSTT). The means of distributing AMC to users is via a 5 MHz, 1 pps, or IRIG B distribution amplifier. Additionally, many outside users connect into the AMC using a fiber-optic cable. The AMC also has a redundant telephone voice announcing system. The phone number is (719) 567-6742. In the future, the AMC will have a computer modem capability.

The AMC #1 has maintained time to within two nanoseconds of the USNO Master Clock in Washington, DC. This is made possible using the TWSTT system. Hourly the AMC and USNO establish communications via a commercial Ku-band satellite to exchange timing data. AMC #1 is then steered towards the Master Clock using a steering algorithm developed by Paul Koppang (USNO). AMC #2 is steered to USNO(GPS) using the data provided by a keyed Stanford-Telecom receiver.

WHO NEEDS PRECISE TIME?

Many users rely heavily on precise time and precise time intervals. For instance, GPS uses time at the nanosecond level for precise navigation and positioning of military units and weapon systems. The military communication system needs precise time at this same level for the synchronization of secure communications.

Time is disseminated to Department of Defense (DoD) users by many means. USNO primary time dissemination means is using GPS, with over 95% of military users relying on this means of dissemination. GPS provides nanosecond level accuracy to users on a continuous global basis. Other methods of time dissemination and their accuracies include:

1. Two-way Satellite Time Transfer (TWSTT) (nanosecond)
2. IRIG-B (microsecond)
3. Internet (millisecond)
4. Computer modem (millisecond)
5. Voice (second)
6. PTTI Advisory Service (bulletins-postprocessed data).

BENEFITS OF THE ALTERNATE MASTER CLOCK

In the event of a loss of the USNO Master Clock, the AMC will be the time standard for DoD and will operate using an independent time scale. This time scale will be based on the 11 cesium atomic clocks and 2 hydrogen masers. The AMC time scale is automatically computed hourly and manually computed twice per week. Many of the functions of the USNO Master Clock will be performed by the AMC; however, some may be conducted at a reduced level of support.

The installation of the AMC has enabled the direct monitoring of the Falcon GPS Monitor Station cesium clock. The hydrogen masers located at the AMC allow for special testing with classified users. The hydrogen masers will maintain an accuracy of close to 80 picoseconds over a period of one week. Plans already exist to conduct a special timing test between the AMC and the Space Warfare Center. This testing should be completed within the next calendar year, with data available in 1998.

Eventually, USNO plans to establish a distributed master clock. This distributed master clock will consist of the AMC time scale integrated into the USNO Master Clock. This will result in a more robust system and should improve the overall stability of the Master Clock.

TIMING REQUIREMENTS

The discussion of requirements must be addressed when referring to precise time and its uses. The needs within the DoD include, at a minimum, the following:

- 1) Communications
 - a) Secure and Crypto
 - b) Increased bandwidth utilization
- 2) Geo-location
 - a) Remote sensors
 - b) Combat ID
 - c) Cooperative Engagement Capability (CEC)
- 3) Navigation

- 4) Computers
 - a) Data recording
 - b) Network Time Protocol (NTP)
 - c) ATM/SONET

The impact of improved timing for GPS in the future is significant. The integration of timing, from GPS, will significantly enhance the war fighters capability to meet the challenges faced by the increased operations tempo. GPS in the cockpit will allow the pilot to not only improve his navigation picture, but also improve the quality and accuracy of his intelligence picture. Improved timing on the battlefield will reduce the likelihood of friendly fire or collateral damage. Remote sensors will realize the ability to provide precise intelligence data and to communicate these data to the war fighter with greater speed and accuracy.

With the integration of good internal clocks for the GPS receivers, more reliable tracking during periodic loss of the GPS signal will be realized. These internal clocks will significantly improve the Y-code acquisition time for authorized users and require fewer satellites in view to maintain a good position.

THE PTTI MEETING AND ITS PURPOSE

Following this talk on the AMC, a significant discussion arose regarding the need for precise time and the focus of the PTTI Meeting in general. The requirement for precise time transcends many levels within DoD and the commercial market. The impact of computers on everyday life is well known; however, the need for precise time is not as well understood. For instance, the speed of a computer is directly tied to time. A 100 MHz computer will perform an internal operation every 10 nanoseconds. This is not as critical in a stand-alone mode as it is when operating within a distributed system or in a virtual engineering environment. Here remotely located computer systems must rely on accurate timing between the various systems in order to efficiently perform operations and transfer data. For commercial power companies, precise timing at the nanosecond level allows for the accurate location of a power line fault in times unimaginably short in the past.

For the military, more accurate timing translates into putting ordnance on target and minimizing or even preventing collateral damage. In order to make this a reality, time must be known and transferred at the nanosecond level. The fact that light travels at 186,000 miles per second means a nanosecond equates to about one foot in linear distance. Thus, if two or three remote sensors identify the precise time of the occurrence of a unique event, relative to their location, then the exact position of this event will be realized and effective countermeasures may be launched. This assumes the sensors are all referenced to the same time. In terms of mine warfare, precise timing and navigation will prevent the damage or destruction of a ship as it transits a mine field. Why? Because the exact location of the enemy mines will be precisely known and units will then be able to avoid this area.

In the case of ships at sea, timing is critical to communication and combat systems. For a given threat, the ship may have less than 30 seconds to detect the threat and provide the necessary response prior to suffering damage. The program manager responsible for developing this system provides the overall time line from detect to engagement to the contractors. But in many cases, the exact breakdown of the three major components in this scenario is not known or defined. Three major systems are key to the success and all rely on computers and distributed processing systems to operate properly: 1. Detection, 2. Command and Control,

3. Engagement. If each contractor designs their system to meet the overall time line (for instance, 30 seconds), then the ability of the system to counter the threat will not be realized. This problem, coupled with the additional ability to receive threat data from external sources, compounds the processing capabilities of today's computer systems. Therefore, as stated earlier, the ability of a ship to respond to the threat may very well depend on the timing accuracy of the entire detect to engage system down to the nanosecond level.

For the PTTI Meeting to be a success, the right people need to be in the audience. Today's state-of-the-art equipment and high-speed weapons demand the attention of program managers, engineers, and system designers, both in government and industry. These people are not present. After all, what is the purpose of the PTTI conference?

Questions and Answers

ROBERT VESSOT (SMITHSONIAN ASTROPHYSICAL OBSERVATORY): I share your concern about the program management; I've lived long enough to work with NASA for the last 30 years. And I find that the deterioration of program management has gone to a level now where there is more concern with the PERT and the GANTT charts and the budgets than any conceivable interest, even, or understanding technically what is going on. Program managers in the bad old days – or I should think the good old days – used to be engineers that were working in the lab. And they managed outside contractors, but they had a very clear perception of what the goals were and how to get there.

Now program management has been relegated to the MBA; and even though I'm at Harvard, I admire the school, but these are not the kind of people you want to manage technical programs. They have to be engineers at least somewhere along the line, or have access and appreciation for engineering.

WILLIAM BOLLWERK: That's correct. And that's one of the problems we do face. When I was a program manager, I had GS-13s, 14s, and 15s who had no knowledge of the engineering that they were dealing with, much less how to manage it.

JAMES CAMPARO (AEROSPACE CORP.): It seems we keep talking around this issue of a disconnect between high-level system requirements and lower-level PTTI requirements. And I guess one thought that came to me as you were speaking, would it be beneficial at future PTTI meetings to invite program managers and have a session on system requirements? Let them tell us what the overall system requirements are; and that would put us in a better position to try to translate those into lower-level PTTI requirements for them.

WILLIAM BOLLWERK: That would be ideal because then you would get the same people in the room to be able to communicate. It would have to be a classified session. But the other thing we would have to face is, what program managers do we need to invite? We need to know what systems are coming down the line. So we would need assistance from several sectors, because I know I've stood in the same spot Commander Atkinson has here and have tried to find out the requirements. I went through all these operational requirement documents, these joint operational requirement documents and none of them addressed timing. Timing was a given; it's going to be there; but none of them specifically stipulated that I have a timing requirement and I have a timing requirement in the nanosecond or picosecond or microsecond or millisecond level.

So I think if we do get the program managers in here and we get some sponsors from the Pentagon in here, then maybe we can see some of these things put into some of these documents; and then maybe we can start heading in the right direction.

LT. OMAR NAMOOS (USAF): I'll just be brief. I come from the program management community. The thing about putting requirements on timing is – somebody mentioned it earlier – timing is really a derived requirement. I as a program manager have users, war fighters who do a task in the field. And I build my requirements – at least we're trying to do it and we think it's a smarter way – is to say, "build me a box that does this." And that's specified at the performance level.

Timing is then the contractor's responsibility to say, "In order to perform this function for you, I have the following derived timing requirement." The military shouldn't be in the business of doing that.

CAPT. KENT FOSTER (USNO): As a career oceanographer and weather guesser, I'm used

to being in a lot of places where people don't like me a lot because of what I have to say and the information I bring to them. That is true no place more so than it is in dealing with program managers that are building systems that are susceptible to the elements of weather in the ocean and combined effects. And after having dealt with these people for several years, I'm convinced that the big problem is that weather guessers don't make life easier for operators or for people who design systems; they make life more difficult for them because they bring them problems that they need to overcome.

And I think that's the problem that we're coming to grips with here with timing. We don't make life easier for program managers, and it's very, very easy and very desirable for them to ignore us to the extent that they possibly can and get away with it. And that's a mindset that you really have to come to grips with and to reconcile and overcome. And I think that's probably why there are not a lot of program managers here.

PHILLIP TALLEY (RETIRED, AEROSPACE CORP.): In 1992, I made a rather sustained effort to organize a session for this PTTI that would bring in various major contractors like G.E. and Lockheed and so forth to let them explain how they went about through their systems engineering to specify time and frequency, not necessarily by a specific systems, but as a corporation how they went about doing this. And I got some early indication of cooperation, but absolutely no one actually participated. And I tried rather hard.

WILLIAM BOLLWERK: It's not going to be easy to get the program managers or those type of people in here, but that doesn't mean that we should stop trying. We need to make it happen somehow.

GERNOT WINKLER (INNOVATIVE SOLUTIONS INT'L): I think the core problem is that timing is an embedded requirement. And as you said, it is left to the contractor; that means that every contractor is going to solve it in his own way. This is a very expensive procedure; duplication is a consequence of that. And that is the reason why there is a PTTI instruction – or has been – in order to take it out and make sure that there is some coordination between all these individual embedded requirements which otherwise would solve the problem of bringing time to Hawaii or Kwajalein or wherever. We have to have a concentrating, coordinating center for that.

CAPT. KENT FOSTER: I think the solution is embedded; there's no doubt about it. But I don't think that that's a reason why the stated requirement should stay embedded.

GERNOT WINKLER: No, no, I agree.

RICHARD GRIFFIN (TEXAS INSTRUMENTS): A couple comments. We're using the phrase "program managers." I think the working people who do what you're talking about are systems analysts, systems engineers. They're the ones that provide the actual working interface between requirements that come down from operational command and the technologies that exist. That's why I was asked to come to this program by my company, because that's the interface area that I work.

And the way we do it is with error budgets. As the Captain said, one of the biggest problems we face within companies and, frankly, with respect to the government, there is today a great horror about hearing about problems. If you go into a meeting and do an error budget and say, "We're going to have a problem with this," you're going to get hit hard and fast because they don't want to hear about problems; they don't want anything that they feel will jeopardize the budget cycle, will jeopardize the political acceptability of a program, they're not willing to listen to it. And, of course, it's complicated by the fact, as we pointed out, that many of them don't have the technical expertise, either because they are MBAs or they were engineers 30

years ago; and that's the technology they remember, they haven't kept up.

But I think the people you need to bring in would be for a session on systems engineering associated with time. Because in my work what I have to do is take the overall requirements, derive an error budget, and then look at what the technology capabilities are to meet that error budget and go back. But often what I go back with is bad news or poor news. And you need support from there.

RANDOLPH CLARKE (USNO): I have a thought on the idea of program managers here. I think any program managers we could get here probably don't need to come here because they've already got the idea. So we should turn it around and try to determine where the program managers are in the first place, where do they meet, and send our people to their meetings and start opening this up. Eventually, then, we will get program managers here. But we have to make an outreach to where they are. They must have meetings like this.

WILLIAM BOLLWERK: Actually, they don't. There's no central meeting of program managers. Program managers are enmeshed in their own programs to make sure that their programs are executable, as is pointed out, with the budgetary and other cycles.

And also there's the big picture of meeting with their sponsor in the Pentagon, who is the resource sponsor for their funds. And try to then coordinate meetings with the contractors in industry and the Fleet, in some cases, to make sure that everything kind of comes together.

Program managers, though you said they probably shouldn't be here – I tend to disagree with that because they're going to help come up with the solutions; they're going to force their people to come with the solutions one way or another. And if you don't include them, then they may not appreciate the detail to which people have to go through to derive some of these requirements; because, they all are derived. And if we don't derive them properly, a little nanosecond here, as you translate up into the big picture, gets lost, and pretty soon you don't meet your threat or your requirement.

HELMUT HELLWIG (USAF): Try to bridge this. I think I would ask this audience to listen to some of the comments, because if I look at the sequence of the discussion, it is as if one of the discussants hasn't listened to the previous discussant. And I wanted to endorse what you said, it's a systems engineering thing that we're talking about, not a program management thing. Let's have the definitions clear. There are meetings of program managers, and I'm participating in those; you don't talk about this kind of thing, whether it's time or any other technical detail. Time and frequency and clocks are tools of systems engineering, and in a big system they are, yes, an important tool, but one of many, many, many. And you need to get together a systems engineering forum, as you said, and try to bridge the gap between a tool of the systems engineer and the systems engineering community. Most of you are experts in the tool, and you need a link to the systems designer; that's not the program manager, a program manager is not the systems designer.

And in the future, by the way, as a consequence of acquisition from DoD, more and more of the requirements – in fact, the current goal is all requirements, as I think the Lieutenant pointed out – are performance requirements as seen by the war fighter. And it's up to the contractor and the systems engineer to translate those into their particular system. And we will not, and DoD will refrain from specifying, what clock, what time system, what interface, except if it's an interface that matters.

DARRELL ERNST (MITRE CORP): I think I can only support what this gentleman just said. I've worked in this area for many, many years, and it's not the program managers. Program managers' eyes glaze over even when they're directly affiliated with the problem.

I feel that the problem is a lack of education at the engineering level. Many of the engineers that work these problems, these systems engineers, go to a catalog and they find a number of different off-the-shelf items that meet their requirements; if they don't, they call around until they find somebody who's willing to modify their equipment to make it work. And then they plug it together and they run their tests and they go on. And Joe White [NRL] can support me, I think he watched me try to fight a problem in the AFSCN back in the '80s when we were building Falcon Air Force Base. For years, they didn't know it, but they were operating at the half a millisecond error in their timing systems because they were transmitting their IRIG-B code upside down. Engineers looked at it almost every day and didn't know what they were looking at.

It's at the technical level that we have to solve this problem. Program managers are doing their job, they fight Congress and they fight all the different people that are forcing requirements creep on their projects; they don't have time to worry about something to them that's a tiny little part of a huge system. We did a requirements analysis on some comm protocols, and you go ask program managers, or even their systems engineers, and say, "What are your comm protocol requirements?" And they say, "What are you talking about, what's a protocol?"

And the same thing with time. We've got the problem here, not at the program manager level. You go to these contractors; the contractor is going to take a junior engineer and put him on this because we're talking about one rack of equipment; he goes to the TRAK microwave catalog and he picks out his timing equipment; and he's solved the problem, he thinks.

JOHN VIG (ARL): Maybe what we need is a product liability law for military systems. Because when General Motors builds a car and gas tanks start exploding five years later, General Motors is still responsible, and gets sued, and they know it gets very expensive if they design a defective product. Unfortunately, in military systems it doesn't work that way. After a system is delivered and things start going wrong, guess who pays? It's always the taxpayer who pays, not the contractor who delivered that system.

So, in an ideal world, I agree with Lt. Namoos that the government should not be specifying how a system should be implemented; they should be specifying only what the system should do. That's absolutely the correct way of doing things. But if you do it that way, then you also have to have much better specifications for the system; and that specification probably should include lifetime beyond delivery of the system and incentives for ...

CAPT. KENT FOSTER: Not being one to shy away from controversy, I'll add one comment to this. I hear all that about the systems engineers, and I don't disagree with it. But again, system engineers are the solvers of the problem.

In my mind, there clearly has to be some accountability maintained over the systems engineers. And the person who is going to stand up and explain why the end performance level doesn't match the requirement isn't going to be the systems engineer, it's going to be the program manager. And, therefore, the program manager needs to get more involved in addressing the requirement to the performance level.

WILLIAM BOLLWERK: And to complement what the Captain just said, I think a clear example of that is Block IIR and the satellite that's going up in a couple months. It's going up with one set of clocks on it; it was specified to have two different types of clocks: rubidium, cesium. And the fact is that it's going up with only rubidiums.

So if we have a problem with those clocks and that one set of system, then we've completely thrown away a satellite in space, it's completely useless for navigation if those clocks were to fail. And that's where if the program manager was probably more aware of the implications

between rubidiums/cesiums and having two different types of clocks on one satellite so that you don't suffer a manufacturing defect failure or something else, then probably we wouldn't be in that situation. We'll have to see what happens when the satellite goes up, but that's a potential problem with doing something like that.

EXPERIENCE AT THE CENAM WITH TIME AND FREQUENCY STANDARDS SIGNALS RECEIVED BY THE GLOBAL POSITIONING SYSTEM (GPS)

Victoria Molina-López^{1,2}, Hildeberto Jardón-Aguilar²,
José T. Vega-Durán¹, and J. Mauricio López-Romero¹

¹Time and Frequency Division, Centro Nacional de Metrología, CENAM
Apdo. Postal 1-100 Centro, C. P. 76900, Querétaro, Qro. México
km 4.5 Carretera a los Cués, Municipio del Marqués C.P. 76900
Phone: (42) 16-65-76; fax: (42) 15-39-04; e-mail: vmolina@cenam.mx

²Telecommunications Section, Centro de Investigación y Estudios Avanzados
del Instituto Politécnico Nacional (CINVESTAV-IPM), Av. IPN No. 2508
esq. Av. Ticomán, Col. S.P. Zacatenco, C.P. 07000, México, D.F. México
Phone: (5) 747-70-00 ext. 3405; fax: (5) 747-70-02;
e-mail: hjardon@mvax1.red.cinvestav.mx

Abstract

The Time and Frequency Division of the Centro Nacional de Metrología (CENAM) in Mexico has been working along two years with two high-stability signals reception systems: GPS and LORAN-C. We have determined the frequency stability of these systems using a cesium standard as the national reference. In Mexico this kind of research had not been done until now.

In this paper a general review about advantages and disadvantages of different frequency and time dissemination systems is given. Then we expose the results of experimental research on frequency stability of GPS and LORAN-C for an averaging time of from 1 s to 1 day for different observation days. Finally we present the results of experimental research on electromagnetic interference around GPS receiver antenna, delay, and attenuation introduced by the transmission line. A time difference measurement system developed by staff of CENAM at the National Research Council (NRC) in Canada is used in order to calculate the frequency stability. Time domain measurements to calculate frequency stability for GPS and LORAN-C systems are employed.

1 INTRODUCTION

In recent times high-precision and high-stability oscillators, combined with modern techniques of communications systems, make possible the generation of common time and frequency reference signals and their dissemination via radio frequencies (RF). This is the responsibility for any time and frequency primary lab, which has two main activities. The first one is the generation

and maintenance of the frequency and time national standards and the second one is the dissemination of these national standards to all potential users. Time and frequency metrology has a great importance in a multitude of essential services like high-speed communications systems, navigation systems, digital telecommunication networks, telephone, TV, and broadcast services. Also, it is of concern to the efficient use of the electromagnetic spectrum to warn about possible interference conditions, e.g. in geophysics, geodesy, radioastronomy, spacetracking, etc. Specifically the fundamental roles of high-stability time and frequency signals in our country are actually in the communications field. But in general the number of very demanding users in these and others fields in all of the world increase continuously. In this sense accuracy and precise means for dissemination of time and frequency standard signals traceable to national and international standards have assumed great importance recently.^[1]

We can distinguish three general methods to disseminate frequency and time standard signals: (1) using portable clocks, (2) using some communication systems which employ a physical medium as the transmission medium, and maybe the most important dissemination method (3) using any communication system which employs free space as the transmission medium.

The third general method can be sub-classified according to the electromagnetic spectrum division realized by the ITU. Each band in the electromagnetic spectrum is identified by its name and its number. The bands dedicated to broadcast frequency and time services have been numbered from 4 to 9. But some other signals intended for some established systems like navigation can be included in this classification. So we have the following broad subdivisions:

1. High Frequency, HF (band 7: 3 MHz - 30 MHz), standard time and frequency broadcast services. The typically gotten frequency stability in this band is 1×10^{-7} per day. This is mainly due to several factors such as ionospheric reflections from E, F1, or F2 layers, depending on distance, frequency, time of day, and conditions of the ionosphere.^[1]

2. Low Frequency, LF (band 5: 30 kHz - 300 kHz), standard frequency broadcast services and the Long Range Navigation, LORAN-C system. LF signals propagate between the bounds of the ionospheric D layers and earth and are, thus, guided around the curvature of the earth to great distances with low attenuation and excellent stability. But several factors such as propagation over water or dry land, solar activity, atmospheric disturbances, and daily ionospheric height changes, besides other factors, considerably limit the attainable accuracy of time transfer and frequency stability, except in the case of groundwave propagation for short distances from the transmitter where the ionosphere is not involved; in this case typical frequency stability is 1×10^{-11} per day.

In this classification we also consider LORAN-C system, which is an accurate navigation system that is maintained by the U.S. Coast Guard in the U.S. A receiver that measures the arrival times of the signal from three LORAN stations can determine its position with an accuracy of about 100 feet at a range over 1,000 miles. Because of the desire for good long-range position accuracy, the frequency and transmission time of each LORAN transmitter is controlled by a set of cesium clocks or hydrogen masers whose frequency accuracy is maintained by the U.S. Naval Observatory. Because the timing characteristics of the LORAN transmission are so tightly controlled, a receiver measuring the signal from a single LORAN station can produce a very accurate frequency output that is traceable to the U.S. Naval Observatory and NIST. LORAN-C stations transmit a pulsed signal at a carrier frequency of 100 kHz. Transmissions of the various stations are differentiated by the timing of their pulses. The LORAN transmitters in a specific geographical region are arranged in groups of at least three to at most six stations called chains, which are differentiated by the repetition rate of the pulses transmitted by the stations in the chain. This rate is called the Group Repetition Interval or GRI. For example, the South Central USA chain has a GRI of 96,100 microseconds and each station in that chain

(six stations in total) will transmit its signal once every 96,100 microseconds. If the receiver synchronizes its timing with the desired GRI, only stations in that GRI will produce a stable signal.^[7]

3. Very Low Frequency, VLF (band 4: 3 kHz - 30 kHz), communication transmissions and the OMEGA system. VLF propagation is similar to that of LF signals which propagate between the bounds of the ionospheric D layer and earth. Typical frequency stability in this band is 1×10^{-11} per day or better.^[1]

4. Ultra High Frequency, UHF (band 9: 300 MHz - 3 GHz), communication transmissions and the Global Positioning System (GPS).^[1] UHF signals are very stable. Most of the limitations described above for the HF, VLF, and LF bands are overcome by satellite-based dissemination. The atmospheric radio noise in the UHF band is almost negligible so the signal-to-noise ratio is dictated by the receiver thermal noise, although multipath distortion and fading may be present. Relatively low power of transmission is required for hemispheric coverage of satellite signals with excellent stability. Directional antennas are advisable; both antenna and equipment complexity tend to increase, especially at the higher frequencies. The obtained precision is comparable or better than that gotten by using ground-based dissemination systems.

The users which use satellite-based dissemination can operate in one-way and two-way modes. In the first case the user operates in a passive mode, simply receiving the time information directly from the satellite. There are currently five regularly operational satellite broadcasts that can be considered as one-way satellite time dissemination systems; these are briefly described in [3]. The Global Positioning System is considered as being in the one-way category. A complete description of this system can be reviewed in [5].

2 FREQUENCY STABILITY OF STANDARD FREQUENCY SIGNALS

Frequency stability is a term used to characterize the variations in frequency exhibited by high-stability frequency signals and it is also employed when two oscillators are compared. In the IEEE standard (No. 1139-1988) for "*Standard Terminology for Fundamental Frequency and Time Metrology*" are defined the Allan variance (AVAR) and the modified Allan variance (MVAR) as the time-domain stability measures. AVAR is a useful means of characterizing a clock's frequency stability and MVAR is an accepted measure of the performance of time and frequency transmission systems and telecommunication networks.^[6] The Allan variance for overlapping samples is defined as^[9]:

$$\sigma_y^2(\tau) = \frac{1}{2\tau^2(N-2m)} \sum_{i=1}^{N-2m} (\chi_{i+2m} - 2\chi_{i+m} + \chi_i)^2 \quad (1)$$

where χ represents phase measured in time units^[10], N is the total number of phase measurements or time interval difference spaced by a sampling time, τ_0 , and there is no dead time between measurements. The averaging time, τ , is given by $m\tau_0$, where m is the number of measurements that will be considered. Analogously, the modified Allan variance is defined as follows:

$$\text{mod } \sigma_y^2(\tau) = \frac{1}{2\tau^2 m^2 (N - 3m + 1)} \sum_{j=1}^{N-3m+1} \left[\sum_{i=j}^{m+j-1} (\chi_{i+2m} - 2\chi_{i+m} + \chi_i)^2 \right] \quad (2)$$

There are several methods by which to measure frequency stability for frequency standards and their signals received from a radio dissemination system. One of them is the so-called Dual Mixer Time Difference System (DMTD).^[8] And this is the measurement technique used in this experimental research. DMTD was constructed by staff of CENAM at the NRC in Canada; it has 32 channels for 5 MHz high-stability signals compatible with generated signals by cesium or rubidium frequency standards and GPS or LORAN-C receiver outputs. The DMTD is used with a 4.9995 MHz offset oscillator to have a 500 Hz beat frequency and get a resolution improving factor of 1×10^4 with respect to direct measurements taken with a time interval counter. The noise level is as low as 1×10^{-13} for an averaging time of 1 s and the bandwidth is 500 Hz; acquisition is continuous and automatic with an RS-232 communication interface. No dead time between measurements is present.

3 FREQUENCY STABILITY OF STANDARD FREQUENCY SIGNALS RECEIVED BY GPS AND LORAN-C SYSTEM AT THE CENAM

In the GPS the carrier phase and pseudorange are affected by Selective Availability (SA), ionospheric and tropospheric effects, frequency instability in satellites' clocks, frequency instability in receiver clocks, relativistic effects, multipath, potential interference conditions, and random phase noise, and in general there are aging, drifts, and frequency instabilities in all oscillators, amplifiers, and electronic devices used in any communication system, for example frequency up/down converters.

On the other hand, instabilities in frequency standards signals from LORAN-C are linked to subionospheric radio propagation and interference conditions between sky wave and ground wave, and in general there are aging, drifts, and frequency instabilities in all oscillators, amplifiers and others electronic devices involved in any radio dissemination system.

We can have very slow and/or fast phase variations present in GPS and LORAN-C frequency standard signals. The effect of each factor that degrades the high frequency stability present in the origin station can be considered as one of the five types of noise present in a frequency standard signal.^[10]

Prior to measuring the frequency stability of the frequency standard signal with GPS and LORAN-C, measurements were made of delay and attenuation in the transmission line which was used with the receiver equipment. So the electromagnetic environment surrounding the GPS receiver antenna was characterized using the ground magnetic North as reference to stand the antenna. Several antennas were used in different frequency ranges: From 200 MHz to 1300 MHz both a conical log spiral antenna and log periodic dipole antenna were used; from 1000 MHz to 1500 MHz a double-ridged guide horn antenna was used. The implemented system is showed in Figure 1 and in the worst case the obtained level at the input of the antenna was lower than -50 dBm.

Day-by-day reception of frequency standards signals from GPS at CENAM has been excellent. So it has been possible to calculate the frequency stability for these signals for an averaging time of from 1 s to 1 day using a Dual Mixer Time Difference System. But LORAN-C reception

was interrupted every day; better reception was obtained usually at nights, after 20:00 hrs, and seldom in the mornings. The GRI programmed was 96,100 microseconds and the frequently received station was Raymondville, Texas. So we have no time interval difference or phase shifts measurements for continuous days; it was possible to calculate only frequency stability for averaging times less than one day. The system shown in Figure 2 was implemented to measure frequency stability for GPS and LORAN-C.

Typical GPS frequency standard signals are shown in Figures 3-5 for several elapsed times. And typical LORAN-C frequency standard signals are shown in Figures 6-8 for the same elapsed times taken into account for GPS, but on different days. These graphs show the reconstructed phase signals from the original data files obtained from DMTD. After reconstructing the phase signals we applied algorithms to calculate AVAR and MVAR for several averaging times. The obtained results for an averaging time of from 1 s to less than 1 day are shown in Table 1. And the results of frequency stability for GPS for an averaging time of from 1 day to 8 days are illustrated in Figure 9. In this figure ranges of several days are shown: the graph titled "A" means frequency stability from MJD 50365 to MJD 50394 and the graph titled "B" is from MJD 50289 to MJD 50313.

Table 1. Frequency stability for GPS and LORAN-C for an averaging time of from 1 s to 170 minutes.

Averaging Time [s]	LORAN-C		GPS	
	AVAR	MVAR	AVAR	MVAR
1	1.52×10^{-11}	1.52×10^{-11}	8.52×10^{-11}	8.52×10^{-11}
2	2.18×10^{-11}	2.04×10^{-11}	1.01×10^{-10}	8.67×10^{-11}
4	3.24×10^{-11}	2.97×10^{-11}	1.15×10^{-10}	9.46×10^{-11}
8	4.62×10^{-11}	4.09×10^{-11}	1.45×10^{-10}	1.23×10^{-10}
16	6.11×10^{-11}	5.24×10^{-11}	2.10×10^{-10}	1.66×10^{-10}
32	6.92×10^{-11}	5.87×10^{-11}	2.63×10^{-10}	1.95×10^{-10}
64	9.10×10^{-11}	8.33×10^{-11}	3.12×10^{-10}	2.58×10^{-10}
128	1.35×10^{-10}	1.23×10^{-10}	3.97×10^{-10}	2.78×10^{-10}
256	1.50×10^{-10}	1.14×10^{-10}	2.35×10^{-10}	7.93×10^{-11}
512	9.90×10^{-11}	5.39×10^{-11}	1.37×10^{-10}	5.23×10^{-11}
640	7.81×10^{-11}	5.89×10^{-11}	7.39×10^{-11}	4.11×10^{-11}
1280	5.45×10^{-11}	3.93×10^{-11}	4.08×10^{-11}	1.85×10^{-11}
2560	3.40×10^{-11}	2.15×10^{-11}	1.92×10^{-11}	6.99×10^{-12}
5120	1.81×10^{-11}	1.17×10^{-11}	1.04×10^{-11}	3.32×10^{-12}
10240	1.26×10^{-11}	7.27×10^{-12}	5.20×10^{-12}	8.44×10^{-13}

4 CONCLUSIONS

There was no condition of important interference with the GPS standard signals, so we can obtain high-stability frequency and time standards. And we have gotten phase shifts measurements for several consecutive days, so we have determined the frequency stability for one day. But the nearest and frequently locked stations of LORAN-C system at CENAM, Queretaro, Qro. were Raymondville, Texas, and Gillette, Wyoming, both in GRI 96,100 microseconds. And we

obtain better performance when we lock the signal transmitted by Raymondville; usually this happens only at nights and seldom in the mornings. We think that distance (more than 1,500 km) was a critical factor to this situation. The results obtained are important because this is a preliminary work necessary for future research on simultaneous reception. We are planning to begin a coordinated comparison, common view by co-located receivers and by receivers separated by several thousand kilometers, like those at the primary labs NIST and NRC.

The results for the frequency stability of the GPS and LORAN-C systems obtained were those expected by theory. So this means that the Time and Frequency Division of CENAM has reliable high-stability signal reception and measurement systems. Accordingly, currently CENAM is a contributor to UTC. And we confirmed the usefulness of GPS due its great advantages with respect to the other radio dissemination techniques, because even with SA, the most important features of GPS include its high positional accuracy in three dimensions, global coverage, all-weather capability, continuous availability to an unlimited number of users, accurate timing capability, and ability to meet the needs of a broad spectrum of users.

5 REFERENCES

- [1] Special Issue on Time and Frequency 1972, *Proceedings of the IEEE*, **66**, pp. 473-648.
- [2] J.A. Klobuchar 1991, "*Ionospheric effects on GPS*," *GPS World*, April 1991.
- [3] A.S. Gupta, A.K. Hanjura, and B.S. Mathur 1991, "*Satellite broadcasting of time and frequency signals*," *Proceedings of the IEEE*, **79**, pp. 973-982.
- [4] D.W. Allan, D.D. Davis, M. Weiss, A.J. Clements, B. Guinot, M. Granveaud, K. Dorenwendt, B. Fisher, P. Hetzel, S. Akoi, M.K. Fujimoto, L. Charron, and N. Ashby 1985, "*Accuracy of International time and frequency comparison via GPS in common view*," *IEEE Transactions on Instrumentation and Measurement*, **IM-34**, 118-125.
- [5] A. Leick 1995, *GPS Satellite Surveying* (John Wiley & Sons, New York, New York, USA), 2nd ed.
- [6] D.W. Allan, M.A. Weiss, and J.L. Jespersen 1991, "*A frequency-domain view of time-domain characterization of clocks and time and frequency distribution systems*," *Proceedings of the 45th Annual Symposium on Frequency Control*, 29-31 May 1991, Los Angeles, California, USA (IEEE), pp. 667-678.
- [7] Model FS 700 LORAN-C Frequency Standard, Operating Manual and Programming Reference, 1993 (Stanford Research Systems, Inc.).
- [8] J. Vega, and R. Pelletier 1995, "*Diseño y construcción de un comparador de fase de alta resolución para patrones de frecuencia de alta estabilidad*," *Memorias del X Congreso Nacional de Instrumentación*, October 1995, Veracruz, Ver. México, pp. 90-94.
- [9] IEEE Standard No. 1139 "*Standard terminology for fundamental frequency and time metrology*," 1988.
- [10] "*Frequency domain stability measurements: a tutorial introduction*," NBS Technical Note 679, U.S. Department of Commerce/National Bureau of Standards.

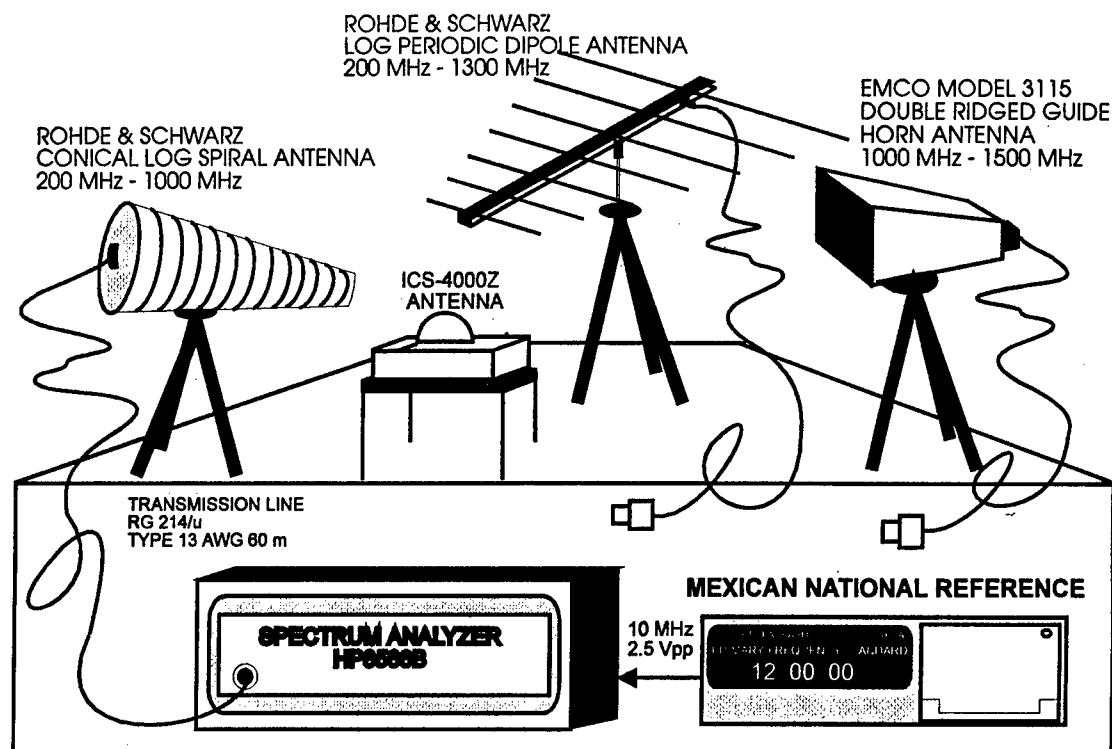


Figure 1. Implemented system to characterize the electromagnetic environment surrounding the GPS receiving antenna.

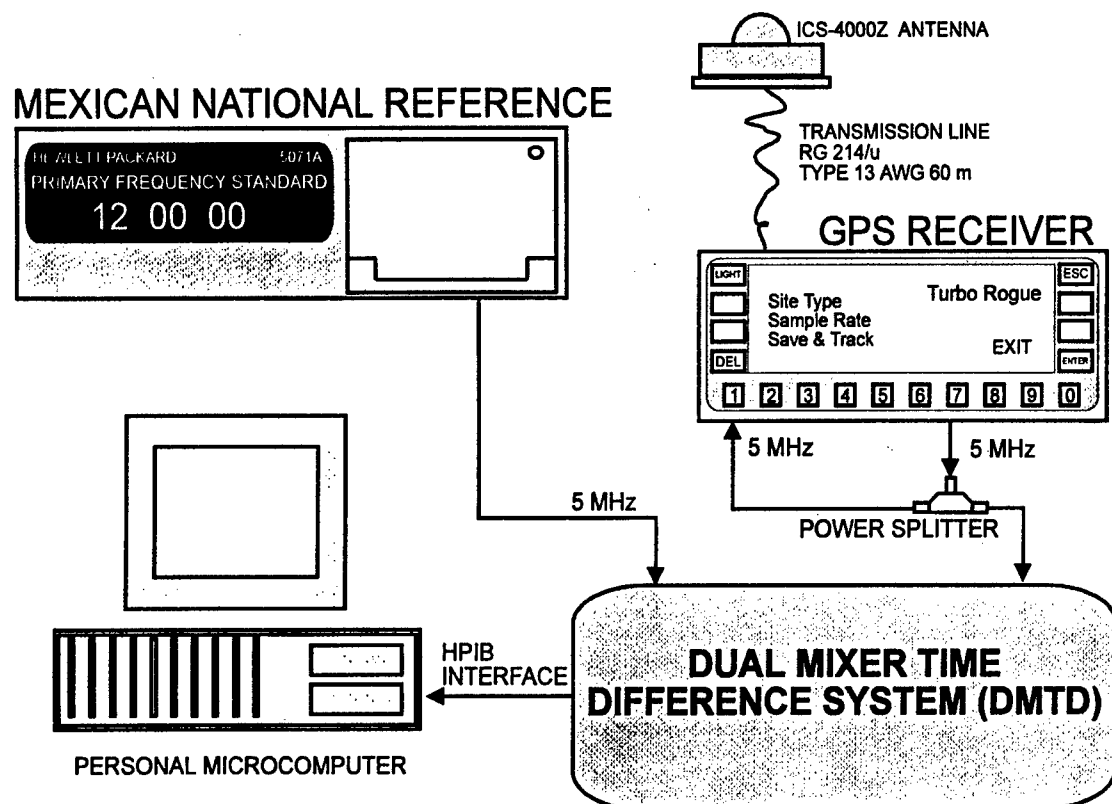


Figure 2. Implemented system to measure frequency stability for GPS and LORAN-C system.

PHASE SHIFT CESIUM vs GPS **MJD 49940**

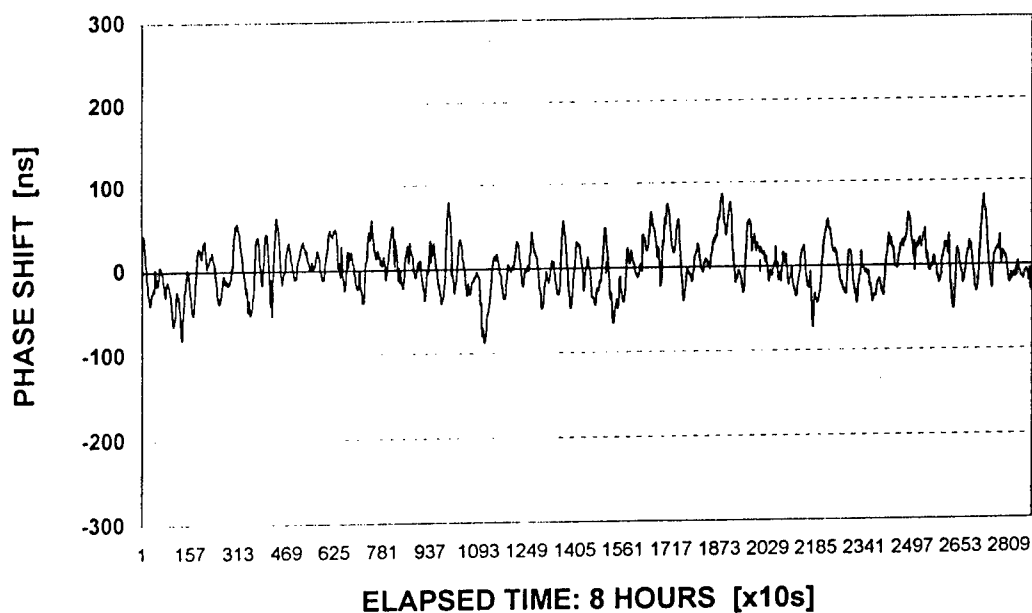


Figure 3. Typical standard frequency signal from GPS (elapsed time: 8 hours).

PHASE SHIFT CESIUM vs GPS **MJD 49940**

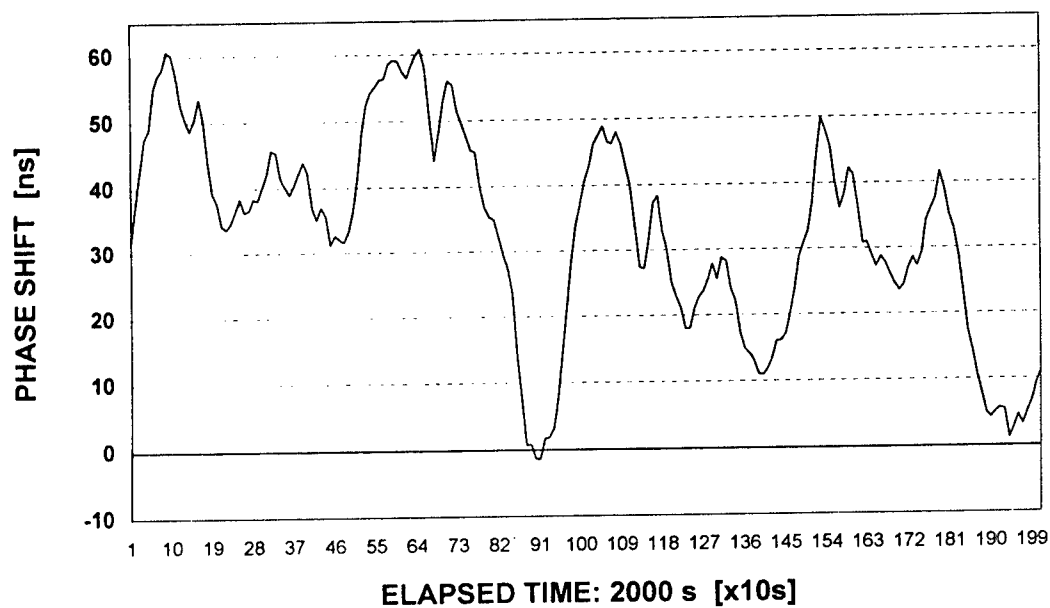


Figure 4. Typical standard frequency signal from GPS (elapsed time: 2,000 s).

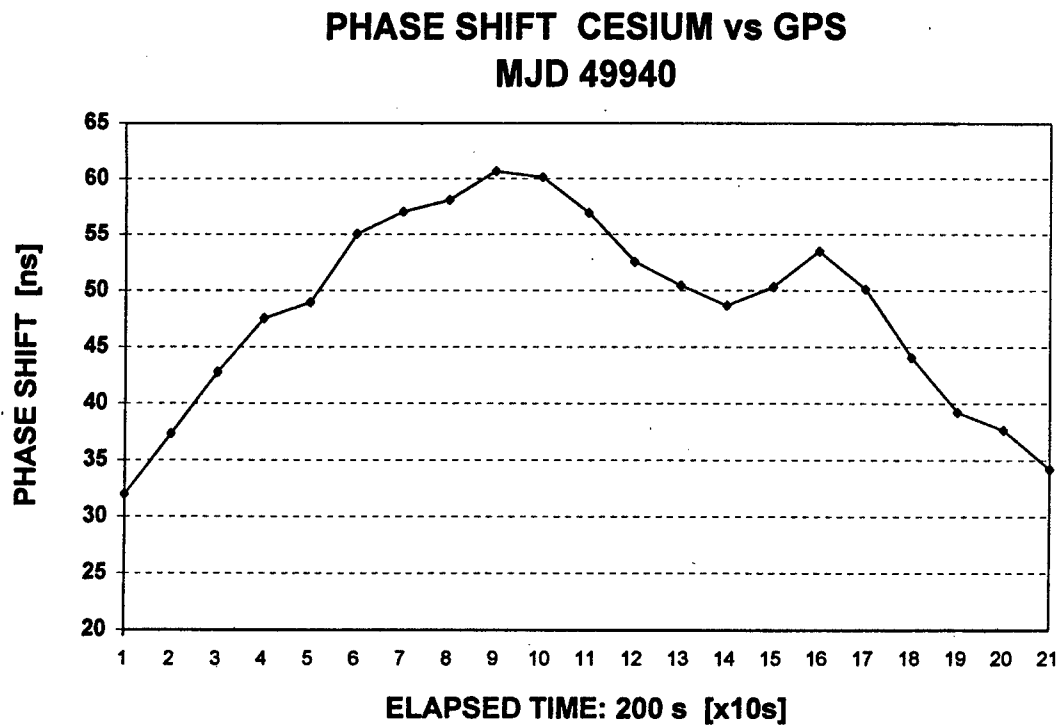


Figure 5. Typical standard frequency signal from GPS (elapsed time: 200 s).

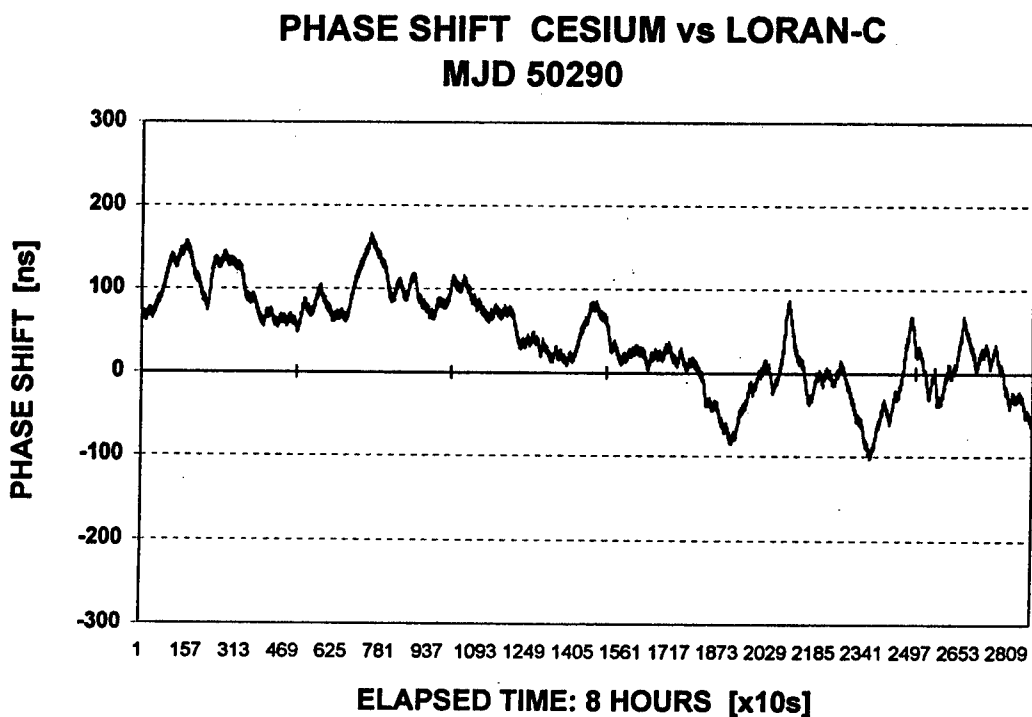


Figure 6. Typical standard frequency signal from LORAN-C (elapsed time: 8 hours).

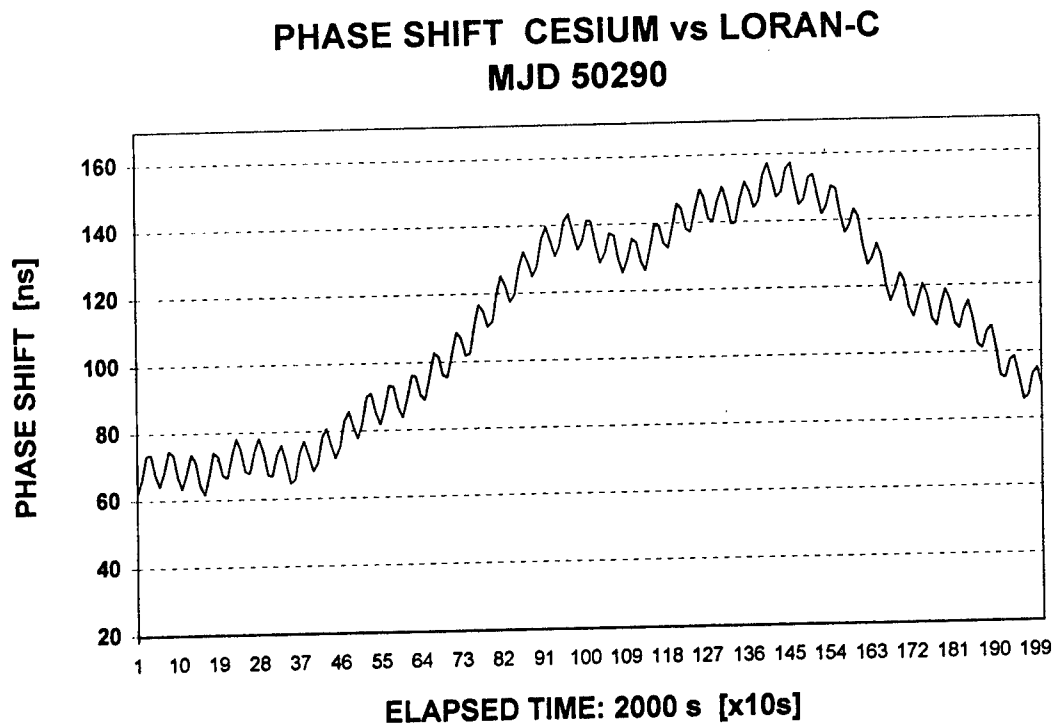


Figure 7. Typical standard frequency signal from LORAN-C (elapsed time: 2,000 s).

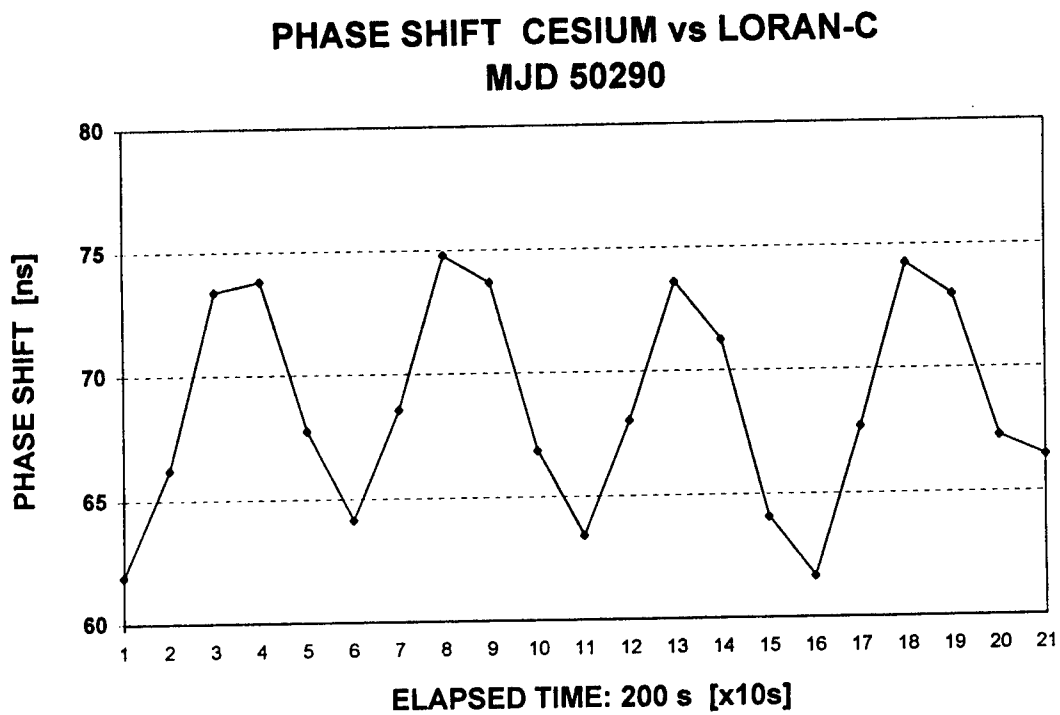


Figure 8. Typical standard frequency signal from LORAN-C (elapsed time: 200 s).

FREQUENCY STABILITY FOR GPS

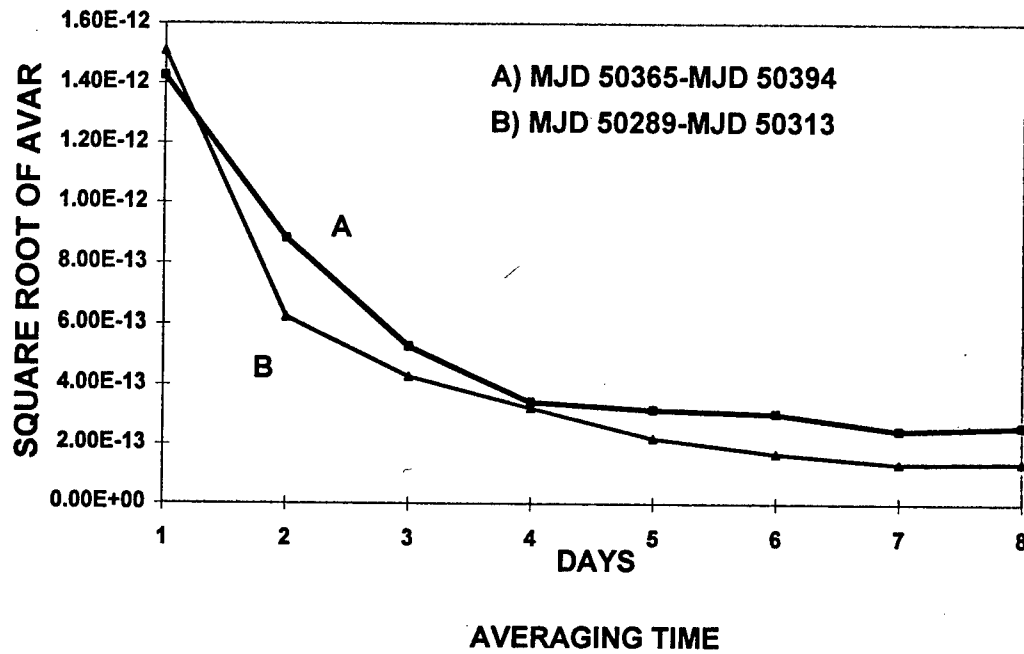


Figure 9. Frequency stability results for GPS for an averaging time of from 1 day to 8 days. (A) is from MJD 50365 to MJD 50394 and (B) is from MJD 50289 to MJD 50313.

STABILIZATION OF A FIBER-OPTIC LINK USING A TEMPERATURE-CONTROLLED FIBER SEGMENT

Richard L. Sydnor, Malcolm Calhoun, Jerry Lopez, and William Diener*
Jet Propulsion Laboratory, California Institute of Technology
4800 Oak Grove Drive, Pasadena, California 91109-8099, USA

Abstract

The Deep Space Network (DSN) of the National Aeronautics and Space Administration (NASA) is operated by the Jet Propulsion Laboratory (JPL), California Institute of Technology. The DSN uses fiber optics to distribute frequency and time to remote sites that may be as far as 32 kilometers from the Signal Processing Center (SPC) which contains the frequency standards and master clock. The fiber-optic cables are buried 1.5 meters underground. At this depth, the only apparent temperature variations are those due to the annual cycle, having a pseudo-sinusoidal behavior with a 1-year period and a diurnal cycle that is greatly reduced due to the insulation of the earth. Some variation is also caused by the air-conditioning cycling of the fiber-optic cable temperature in the plena of the buildings and the lengths of cable that are in the manhole vaults along the run. The resulting stability of the references at the remote site is well within the requirements of the DSN. However, the radio science requirements for the Cassini mission are much more stringent than the DSN requirements and the existing performance does not meet these requirements. The particular antenna (DSS-25) to be used for the 32 GHz portion of the Cassini radio science mission is 17 kilometers from the main control center and the apparent temperature variation (as measured by the delay variation) is 11°C peak to peak over the annual cycle. By inserting a temperature-controlled section of fiber-optic cable whose temperature is controlled in such a manner as to force the total delay to be constant, the annual variation (and small variations due to storm fronts passing through the area) can be reduced to a negligible amount. The length of this inserted fiber-optic section is > 3.74 kilometers and the temperature variation of this section over the year is 50°C. Details of the design and preliminary results are given.

INTRODUCTION

The Deep Space Network (DSN) of the National Aeronautics and Space Administration is operated by the Jet Propulsion Laboratory of the California Institute of Technology. It consists of three sites located at Goldstone, California; Robledo, Spain; and Tidbinbilla, Australia. Each of these sites has a Signal Processing Center (SPC) and a number of antennas ranging in size from 70 meters to 34 meters in diameter. The frequency and timing standards are located in the SPC and are connected to the various antennas by fiber-optic links. The links can be as

*The work described in this paper was carried out at the Jet Propulsion Laboratory, California Institute of Technology, under a contract with the National Aeronautics and Space Administration.

long as 32 kilometers to the antenna farthest from the SPC. The fiber-optic cables to these remote sites are buried 1.5 meters underground in order to reduce the temperature variations. At this depth, the diurnal component of the temperature variations is greatly reduced. Some effects due to storm fronts, with a period of 4 to 7 days, can be seen, and annual variations are still present.

The station involved in the Cassini radio science experiments at 32 GHz is DSS-25, shown on the map of Figure 1. This station is 17 kilometers from the SPC. The measured annual delay variations in this 17-kilometer cable are the result of a pseudo-sinusoidal annual temperature variation of 11°C peak to peak with a period of 1 year. The diurnal variation results in an Allan deviation of 2×10^{-15} at an averaging time, τ , of $\approx 1,000$ seconds. The fiber-optic cables are standard single-mode cables, with the exception of a few places where the cables are not buried, where the fibers are the "zero temperature fiber" made by Sumitomo. This installation meets the present DSN FTS requirements. This paper covers the effect of the diurnal and annual variations and the use of a thermally controlled section of the cable to stabilize the delay.

DELAY VARIATIONS

The phase variations at the end of the cable due to the temperature variations are:

$$\begin{aligned}\Delta\phi &= \frac{L}{c_e}(TC)\Delta T \sin(\omega_a t) \\ &= \frac{17 \times 10^3}{3 \times 10^8 0.7} 5.5 \sin(199 \times 10^{-9} t) \\ &= 627 \sin(199 \times 10^{-9}) \text{ radians.}\end{aligned}$$

The corresponding frequency variation is given by:

$$\begin{aligned}\Delta f &= \frac{d\Delta\phi}{dt} \\ &= 125 \times 10^{-6} \cos(199 \times 10^{-9}) \text{ radians/second} \\ &= 19.9 \times 10^{-6} \cos(199 \times 10^{-9}) \text{ hertz.}\end{aligned}$$

The resulting peak Allan deviation is: $\sigma_y(\tau) \approx 2 \times 10^{-15}$ at $\tau = 4$ months. Clearly, the Allan deviation is not large enough to degrade the performance of the reference frequency, but the phase variation of 627 radians can be troublesome for interferometric work.

Using the same equation for the diurnal variations, we find that the apparent mean temperature variation of 10 millidegrees gives a phase variation of 0.62 radians, a frequency variation of 4.5×10^{-5} hertz, and an Allan deviation of 2×10^{-15} for a τ of 1,000 seconds. This is worse than the required stability and is the main reason for the development of the thermal cable stabilizer.

For the Cassini mission we will use a cryogenic, sapphire-stabilized oscillator/flywheel with the JPL-developed Linear Ion Trap Standard (LITS). This combination will produce a much more stable reference than the hydrogen maser. Several changes in the distribution system are being made to retain this stability. The stabilized fiber-optic cable is just one of them.

The concept of the stabilizer involves inserting a section of fiber-optic cable in the distribution system with a length sufficient that, with a temperature variation of 50°C, it will compensate for the delay variations of the 17 km of buried fiber. Since the annual temperature variation of the buried fiber is 11°C, the length of the controlled section must be $(\frac{11}{50}) \times 17 = 3.74$ kilometers.

A diagram of the planned system is shown in Figure 2. In this figure, the reference signal (100 MHz) in SPC 10 is multiplied to 1 GHz in order to reduce the phase noise contributed by the link. The 1 GHz reference signal is then used to modulate a 1,310 nm laser. This laser has an internal isolator and another isolator is added to obtain the necessary isolation to produce low interaction between the laser and the reflections on the fiber. The optical signal then goes through the compensation fiber reel and then to the remote site.

At the remote site the signal is detected to reproduce the 1 GHz reference signal. A phase-locked loop is used to generate the necessary reference signal for the remote site (100 MHz). The 100 MHz is also used to modulate the 1 GHz signal. This produces the two sidebands with a suppressed carrier. The carrier is further reduced with a notch filter and the signal then modulates an 1,310 nm laser that also has additional isolation. The output of this laser is sent back to the original site over the same fiber that was used to send the original signal to the remote site. At the main site, the signal is down-converted to 100 MHz and then to base-band to produce an error signal. This error signal is filtered to remove the residual 100 MHz and to produce the correct dynamic and static stability for the loop. The output of the filter drives the temperature driver electronics to controls the temperature of the fiber-optic reel to vary the delay in such a manner to keep the error at zero, i.e., to maintain a constant delay in the system.

The temperature compensation fiber reel consists of 4 km of fiber wound on an aluminum reel 20 cm long and 20 cm in diameter. A Peltier cooler/heater is fastened to each end of the reel to minimize gradients and to decrease the response time. The normal operating temperature varies from 0°C to 50°C.

Preliminary tests in the laboratory show a reduction of delay variations by a factor of > 300 . This is enough to ensure that the contribution of phase variations due to the fiber-optic link will not degrade the frequency standards. The response time of the system is approximately 60 seconds. This is fast enough to reduce the variations due to air-conditioning cycle effects in the plena to acceptable levels.

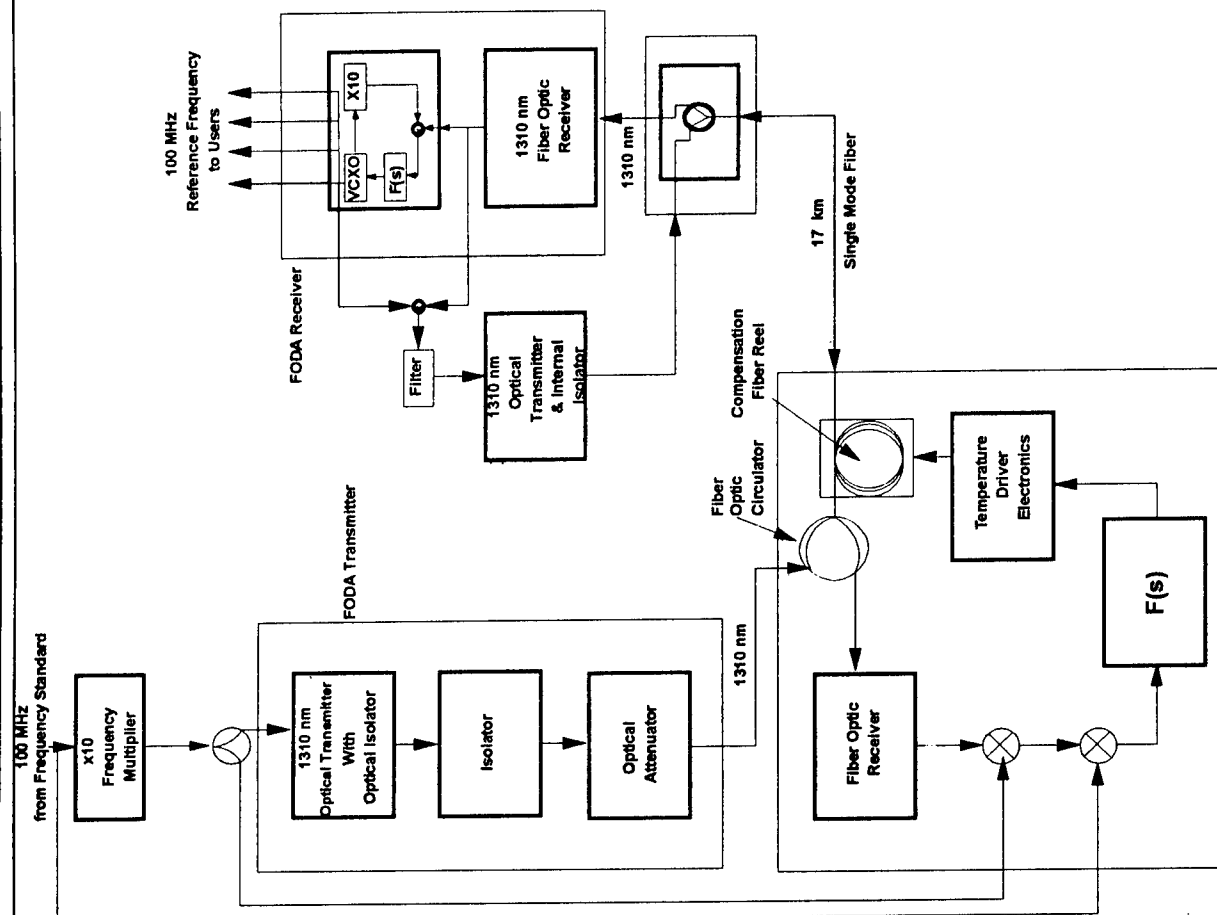


Figure 2 Phase Stabilized Fiber Optic Reference Frequency Distribution
Transmission Frequency 1 GHz, Pound System

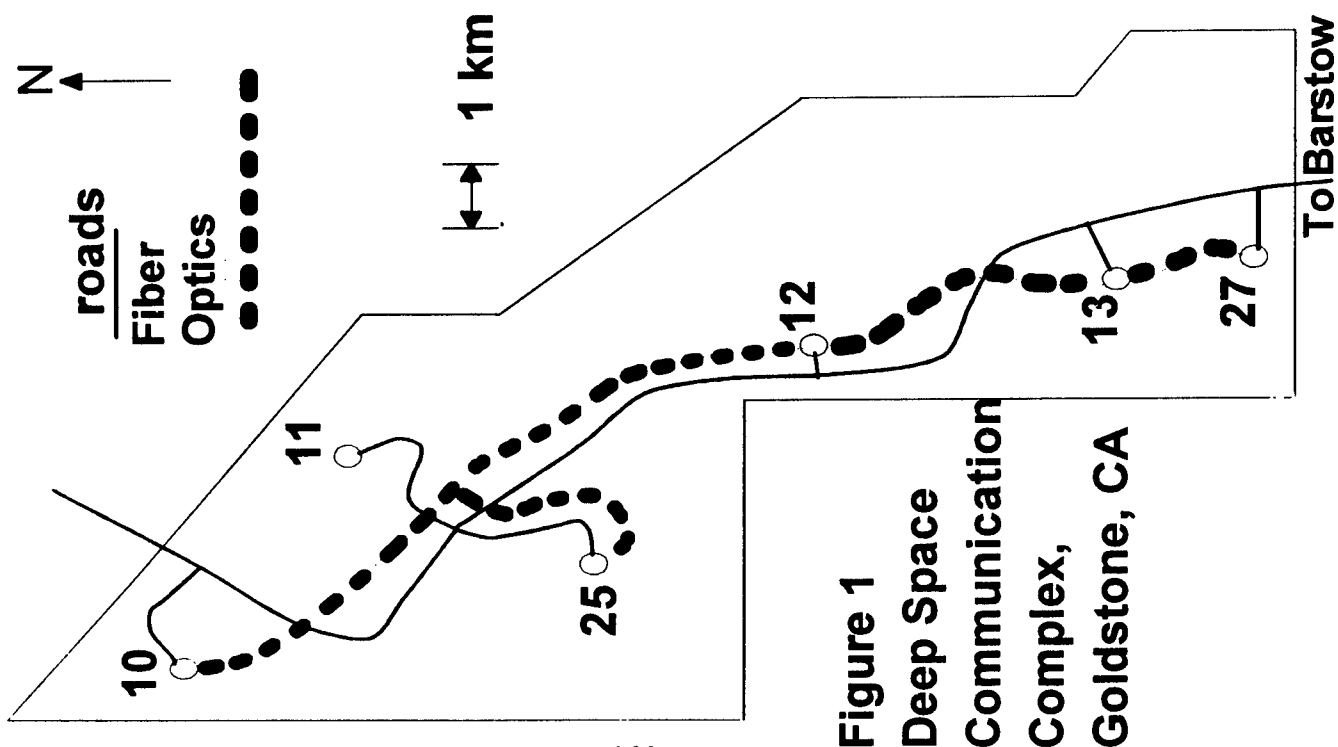


Figure 1
Deep Space
Communication
Complex,
Goldstone, CA

Questions and Answers

MARC WEISS (NIST): If you know the fluctuations, you've measured the change in the physical length of the cable, or actually the frequency offset, why not steer it with a microphasestepper instead of using all the hysteresis involved with the temperature?

RICHARD SYDNOR: Microphasesteppers put in little slopes and things which gives us degradation of the performance of the frequency standard. And besides, this system, since it's controlling the actual delay – not the phase delay, the actual time delay – now we can use that fiber for any other frequency we want to send through there, and they're all stabilized. It's a broadband system.

We've done what you've suggested at times in the past. But it's a single frequency device. You use up a fiber with one signal on it that's many gigahertz of bandwidth. And this is a much more practical thing, we think, than doing it that way.

MARC WEISS: Do you find any problem with hysteresis of the temperature cycle? You store heat in it and then you have to lose it.

RICHARD SYDNOR: Since it's a control loop, we haven't seen any problems with hysteresis.

BOYD MOORE (KAMAN SCIENCES CORP.): What kind of a response time are you seeing with this system?

RICHARD SYDNOR: We're trying to compensate for the diurnal variations primarily. And the response time that we're using now – I think we're running at 1-minute response time. The thermal time constant of the control spool is the main limiting thing. The roundtrip delay time is very small compared to the thermal response time of the spool, even though it's been made as fast as we could make it.

DEMONSTRATION OF SYNCHRONIZATION BETWEEN TWO GEOSYNCHRONOUS SATELLITES WITHOUT GROUND INTERVENTION

J. C. Camparo and R. P. Frueholz
Technology Operations

A. P. Dubin
Milsatcom Division

The Aerospace Corporation
P.O. Box 92957, Los Angeles, California 90009, USA

Abstract

In early 1996 Milstar became the first geosynchronous satellite system to employ crosslinks for synchronization and syntonization. At that time, the crystal oscillator onboard DFS-1, the first Milstar satellite, had its time and frequency tied (i.e., slaved) to the rubidium (Rb) atomic clock carried onboard DFS-2, the second Milstar satellite. The slaving of DFS-1 to DFS-2 was accomplished without ground intervention. All timing information required by the slaving algorithm was obtained through the DFS-1 to DFS-2 satellite crosslink. In this paper we discuss the drift and Allan variance of the two satellite clocks when operating independently, and show that both clocks are performing well. Additionally, we present ground station measurements of DFS-1 and DFS-2 time offsets that demonstrate satellite synchronization to better than 150 ns without ground intervention.

1 INTRODUCTION

Satellite navigation and communication often require fairly precise synchronization and syntonization among spacecraft clocks. In the traditional method for achieving synchronization, a ground station makes time-offset measurements to the various spacecraft clocks, and then updates the time and frequency of each satellite as needed. Though straightforward in its implementation, disadvantages to the traditional approach include the large workload placed on the ground station, the need to have several ground stations to view satellites in different orbital locations, and unaccounted-for delays in atmospheric propagation.

The Milstar communications system has chosen a different method for spacecraft synchronization and syntonization. Milstar's mission is to provide secure antijam communication capabilities for United States Department of Defense operations into the next century^[1], and in order to accomplish that task Milstar employs precise timekeeping on its satellites and at its ground control stations.^[2] A Milstar ground station makes time-offset measurements to an in-view

geosynchronous satellite, which for this illustrative discussion we will call the Master, and as a result of information passed along the satellite crosslinks, other satellites in the constellation (i.e., Slaves) autonomously synchronize and syntonize themselves to the Master. Since the ground station only needs to steer the time and frequency of a single satellite, its workload, and hence the timekeeping-related operational costs of the system, are held to a minimum. Moreover, since synchronization among the satellites is accomplished without transmission through the ionosphere, atmospheric propagation delays cannot perturb the synchronization among spacecraft clocks.

The first of six Milstar satellites, DFS-1, was launched on 7 February 1994, while DFS-2, the second Milstar satellite, was launched on 6 November 1995. Each satellite carries a set of precise clocks: DFS-1 carries crystal oscillators, while DFS-2 carries rubidium (Rb) atomic clocks.^[3] The ground stations maintain precise time with cesium (Cs) atomic clocks. Following the launch of the second Milstar satellite, crosslinks between DFS-2 and DFS-1 were activated and DFS-1's time and frequency was slaved to DFS-2. In the slaving procedure, DFS-1 uses satellite crosslink information to rapidly correct its time so as to stay synchronized to DFS-2, and to periodically correct its oscillator frequency. DFS-2 is synchronized to UTC by a ground station that periodically collects timing information from the satellite, and after a number of days commands time and frequency adjustments to the DFS-2 satellite clock.^[4] Timekeeping data can be collected by ground stations for both satellites, and is archived along with any commanded time and frequency corrections. Using the archived data we have been able to reconstruct "raw" time offsets for the DFS-1 and DFS-2 clocks, that is, the time offsets that would have been observed on the ground had the ground station made no time or frequency corrections to the satellite clocks. In the following we will show that an Allan variance analysis of these raw time offsets indicates that each clock is performing well, and that when crosslink synchronization is initiated DFS-1 achieves a 150 ns or better synchronization to DFS-2 without assistance from the ground.

2 DFS-1 AND DFS-2 CLOCK PERMORMANCE

Deterministic Timekeeping Variations

The reconstructed raw time-offset measurements of DFS-1 and DFS-2 are displayed by the thick lines in Figs. 1a and 1b respectively; thin lines show quadratic fits to the data. (In both figures, initial time and frequency offsets were subtracted from the data sets to better display the quadratic variation of time offset.) For DFS-1, the quadratic fit yields a $+9.8 \times 10^{-13}$ /day drift rate, which is quite good for a crystal oscillator clock.^[5] Moreover, DFS-1 has exhibited this same drift rate since October 1994. Analysis of the data presented in Figure 1b indicates that DFS-2 has a -1.5×10^{-12} /day drift rate. Though the magnitude of this drift rate is a bit larger than that of the crystal oscillator clock, it is nonetheless consistent with pre-launch expectations for the DFS-2 Rb atomic clock at this point in its operating life. With continued operation, the slowly varying frequency drift rate should drop well below the 10^{-12} /day level and should eventually become constant. The deviation of the raw time-offset data from the quadratic for the early part of DFS-2's time-offset history is a consequence of the atomic clock's warm-up behavior.^[6] The important point to note from Figure 1 for future discussion is that the aging rate of the DFS-1 clock is distinctly different from that of the DFS-2 clock.

Allan Variance

Taking the difference between the raw time-offset measurements and the quadratic fit, time-offset residuals may be computed. Computation of the Allan variance for the residuals requires

uniformly spaced measurements of oscillator frequency. Since the archived ground station measurements are not separated by a constant interval, interpolation of the data is necessary in order to generate a history of fractional frequency fluctuations amenable to Allan variance analysis. Vernotte et al.^[7] have shown that a Linear-Interpolation (LI) procedure is a viable strategy for interpolating unevenly spaced time error data, and we have employed their approach here.

Figure 2 shows the resulting Allan standard deviation, $\sigma_y(\tau)$, versus τ for the DFS-1 crystal oscillator and the DFS-2 Rb atomic clock. Dashed lines correspond to estimates of the Allan standard deviation based on a simple model: satellite to ground-station time-transfer noise dominates the Allan variance for τ less than 10,000 seconds, while random-walk frequency noise dominates $\sigma_y(\tau)$ for longer averaging times. (Satellite to ground-station time-transfer noise is associated with randomly varying delays at the transmitter and receiver.) For the crystal oscillator the long-term Allan standard deviation is well modeled by $\sigma_y(\tau) = 1.6 \times 10^{-14} \tau^{1/2}$, a value consistent with a high-performance crystal oscillator.^[8] For the Rb atomic clock the long-term Allan standard deviation is well modeled by $\sigma_y(\tau) = 2.2 \times 10^{-15} \tau^{1/2}$, again a value consistent with a well-functioning device.^[9]

3 AUTONOMOUS SYNCHRONIZATION

As noted in the Introduction, following the launch of DFS-2 the DFS-1 satellite became a slave to DFS-2, and therefore tied its crystal oscillator to the DFS-2 atomic clock using crosslink timing information. Given the archived data of DFS-1's time offset during the slaving period, along with ground station corrections to DFS-2 and DFS-1, it is possible to reconstruct the timekeeping behavior of DFS-1 while it was slaved to DFS-2. This is shown in Figure 3, where the black data points correspond to DFS-1 raw time-offset measurements, and the curve is a quadratic least squares fit to the data. (We note for future reference that DFS-1 slaving to DFS-2 was deactivated for several days during this period.) The fit yields a $-2.3 \times 10^{-12}/\text{day}$ fractional frequency drift rate. This is to be compared with the DFS-1 crystal oscillator's intrinsic drift rate of $+9.8 \times 10^{-13}/\text{day}$. The $-3 \times 10^{-12}/\text{day}$ change observed in DFS-1 drift is due to the fact that during this period DFS-1 maintained tight synchronization and syntonization to the DFS-2 Rb atomic clock, which had a negative drift rate. We further note that the discrepancy between DFS-1's (apparent) $-2.3 \times 10^{-12}/\text{day}$ drift rate and DFS-2's $-1.5 \times 10^{-12}/\text{day}$ drift rate is a consequence of the few days during this period when slaving was turned off. If an attempt is made to account for those few days, the DFS-1 and DFS-2 drift rates become nearly identical.

An estimate of the level of synchronization between DFS-1 and DFS-2 may be obtained from raw time-offset measurements made to both satellites by a single ground station. As illustrated in Figure 4 this occurred in early February 1996. On 8 February 1996 a ground station commanded a time and frequency correction to the DFS-2 atomic clock, and then began making time-offset measurements to DFS-1 (filled circles in the figure). Then, on 9 February 1996 the same ground station began making time-offset measurements to DFS-2 (open circles in the figure). The solid line is a quadratic fit to all the data, clearly indicating that the ground station synchronized DFS-2. DFS-1 was not corrected by any ground command, but rather by autonomous crosslink synchronization to DFS-2. Based on the deterministic and stochastic variations of the crystal oscillator's fractional frequency, and the fact that DFS-1 received its last correction from the ground on 4 February, DFS-1's time offset should have been appreciable on the scale of Figure 4 (i.e., at the $1\text{-}\sigma$ level somewhere within $\sim \pm 3 \mu\text{s}$). However, as a consequence of crosslink synchronization to DFS-2, DFS-1's time offset was near zero.

Computing the standard deviation of time-offset residuals from the quadratic regression line, we have $\sigma_{DFS-2} = 141$ ns and $\sigma_{DFS-1} = 207$ ns. These variations about the regression line are a consequence of: 1) satellite to ground-station time-transfer noise, 2) diurnal oscillations due to the satellite clocks' temperature sensitivities, and 3) crystal oscillator and atomic clock noise processes. Additionally, the DFS-1 variations must include the residuals associated with the slaving process. Consequently, we can obtain an upper bound on the slaving process's error in synchronizing DFS-1 to DFS-2 by combining these two standard deviation values:

$$\sigma_{slaving} \leq \sqrt{\sigma_{DFS-1}^2 - \sigma_{DFS-2}^2} = 152 \text{ ns} \quad (1)$$

Thus, the data demonstrate that the two spacecraft were synchronized to within ± 150 ns, independent of ground-station intervention.

4 CONCLUSIONS AND SUMMARY

As satellite navigation and communication applications increase, greater emphasis will be placed on synchronizing spacecraft clocks independent of ground intervention. In part, this situation will be motivated by a desire: 1) to reduce the workload at mission control ground stations and reduce system operating costs, 2) to control a geosynchronous constellation from a single location, and 3) to reduce unaccounted-for delays in atmospheric propagation. Milstar is the first satellite system to employ crosslink synchronization for geosynchronous spacecraft, and here we have demonstrated the efficacy of that method. Specifically, our results show that crosslink synchronization has allowed DFS-1 and DFS-2 to achieve a 150 ns (or better) level of synchronization without intervention from the ground.

8 REFERENCES

- [1] J. Fawcette 1983, "Milstar: hotline in the sky," **High Technology**, November 1983, pp. 62-67; M. Dornheim 1992, "Milstar 2 brings new program role," **Aviation Week & Space Technology**, 16 November 1992, pp. 63-64.
- [2] J.C. Camparo, and R.P. Frueholz 1995, "Monte Carlo simulations of precise time-keeping in the Milstar communications satellite system," Proceedings of the 26th Annual Precise Time and Time Interval (PTTI) Applications and Planning Meeting, 6-8 December 1994, Reston, Virginia, USA (NASA CP-3302) pp. 291-304.
- [3] J.C. Camparo, and R.P. Frueholz 1995, "Timekeeping performance of the Milstar DFS-1 satellite: October-December 1994," Aerospace Report No. TOR-95(5404)-4, 1 May 1995.
- [4] J.C. Camparo, and R.P. Frueholz 1994, "Precise timekeeping in Milstar: the Aerospace Corporation's Monte Carlo simulations," Aerospace Report No. TOR-94(4404)-5, 15 May 1994.
- [5] L.J. Rueger, J.R. Norton, and P.T. Lasewicz 1992, "Long-term performance of precision crystal oscillators in a near-earth orbital environment," Proceedings of the 1992 IEEE International Frequency Control Symposium, 27-29 May 1992, Hershey, Pennsylvania, USA, pp. 465-469.

- [6] C.H. Volk, and R.P. Frueholz 1985, "*The role of long-term lamp fluctuations in the random-walk of frequency behavior of the rubidium frequency standard: A case study,*" **Journal of Applied Physics**, 57, 980; H. Bethke, D. Ringer, and M. Van Melle 1985, "*Rubidium and cesium frequency standards status and performance of the GPS program,*" Proceedings of the 16th Annual Precise Time and Time Interval (PTTI) Applications and Planning Meeting, 27-29 November 1984, Greenbelt, Maryland, USA, pp. 127-141.
- [7] F. Vernotte, G. Zalamansky, and E. Lantz 1994, "*Noise and drift analysis of non-equally spaced timing data,*" Proceedings of the 25th Annual Precise Time and Time Interval (PTTI) Applications and Planning Meeting 29 November-2 December 1993 (NASA CP-3267), pp. 379-388.
- [8] M.B. Bloch, J.C. Ho, C.S. Stone, A. Syed, and F.L. Walls 1989, "*Stability of high quality quartz crystal oscillators: an update,*" Proceedings of the 43rd Annual Symposium on Frequency Control, 31 May-2 June 1989, Denver, Colorado, USA (IEEE), pp. 80-84.
- [9] H. Hellwig 1979, "*Microwave time and frequency standards,*" **Radio Science** 14, 561.

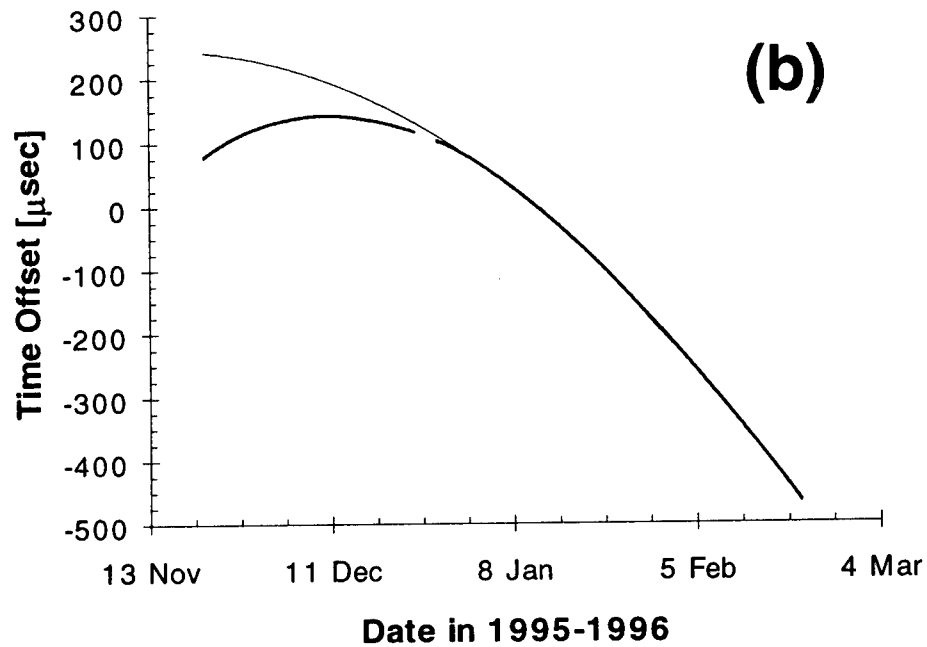
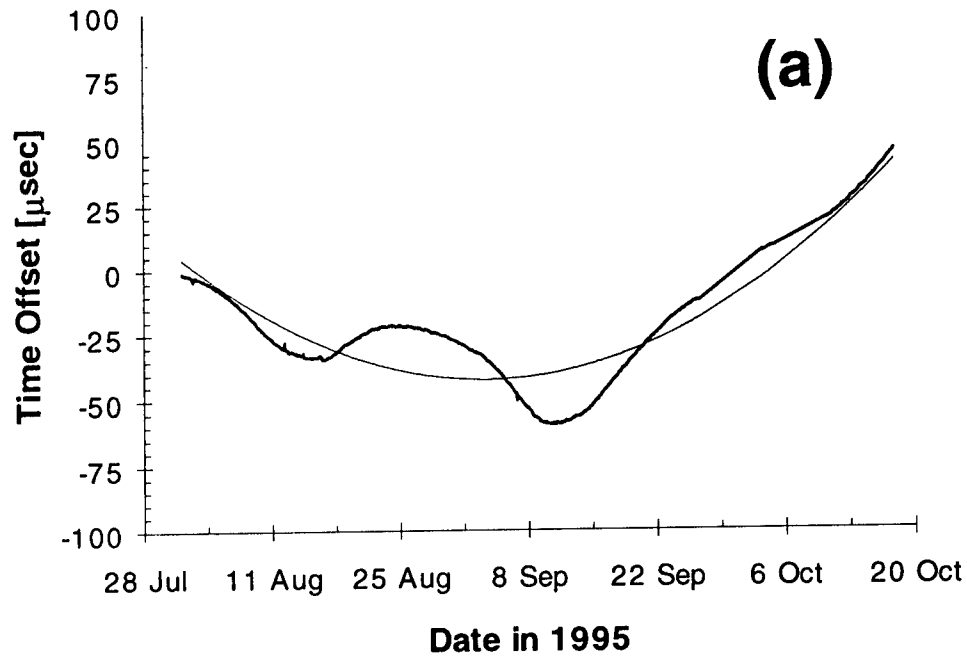


Figure 1: (a) Raw time-offset history of the crystal oscillator onboard DFS-1 (thick line). (b) Raw time-offset history of the Rb atomic clock onboard DFS-2 (thick line). Thin lines correspond to least squares quadratic fits to the data, and minor divisions of the abscissa correspond to seven day intervals.

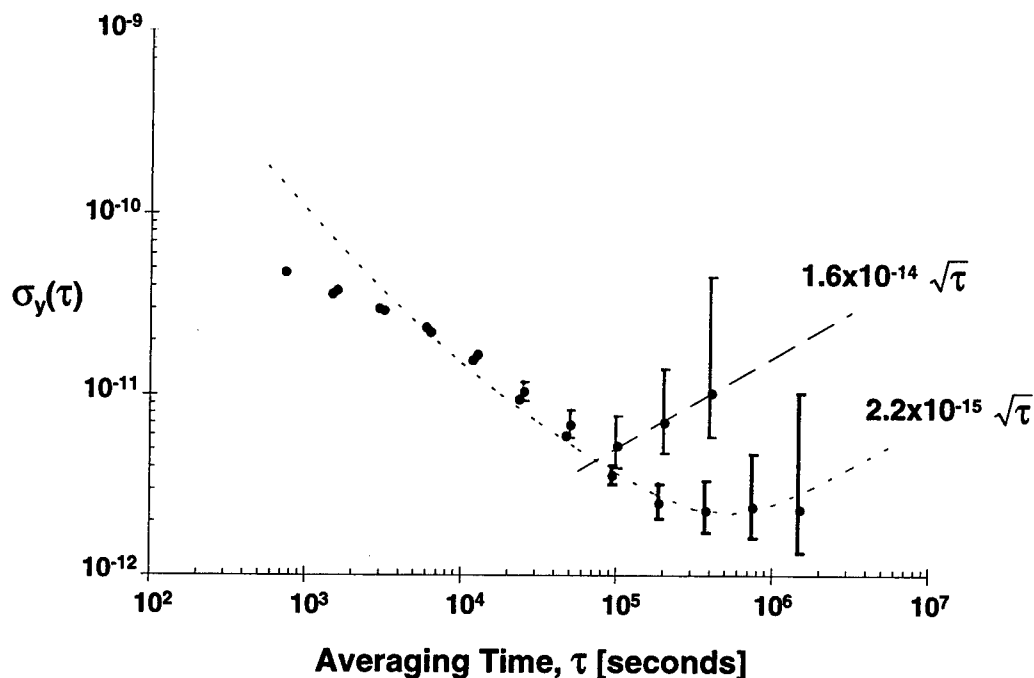


Figure 2: Allan standard deviation, $\sigma_y(\tau)$, versus averaging time, τ , for the DFS-1 crystal oscillator (gray) and the DFS-2 Rb atomic clock (black). The short dashed curve is the anticipated $\sigma_y(\tau)$ based on satellite to ground-station time-transfer noise and the Rb clock's random-walk of frequency noise. The long dashed line corresponds to the crystal oscillator's random-walk noise.

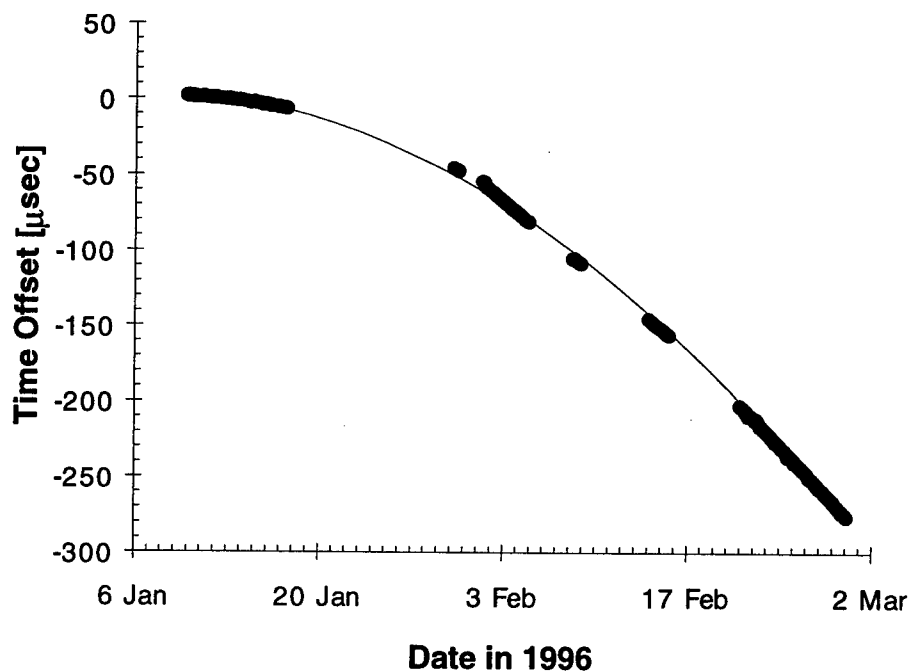


Figure 3: Raw time-offset of the DFS-1 crystal oscillator (black circles) while it was slaved to the DFS-2 Rb atomic clock. The thin curve is a least squares quadratic fit to the data.

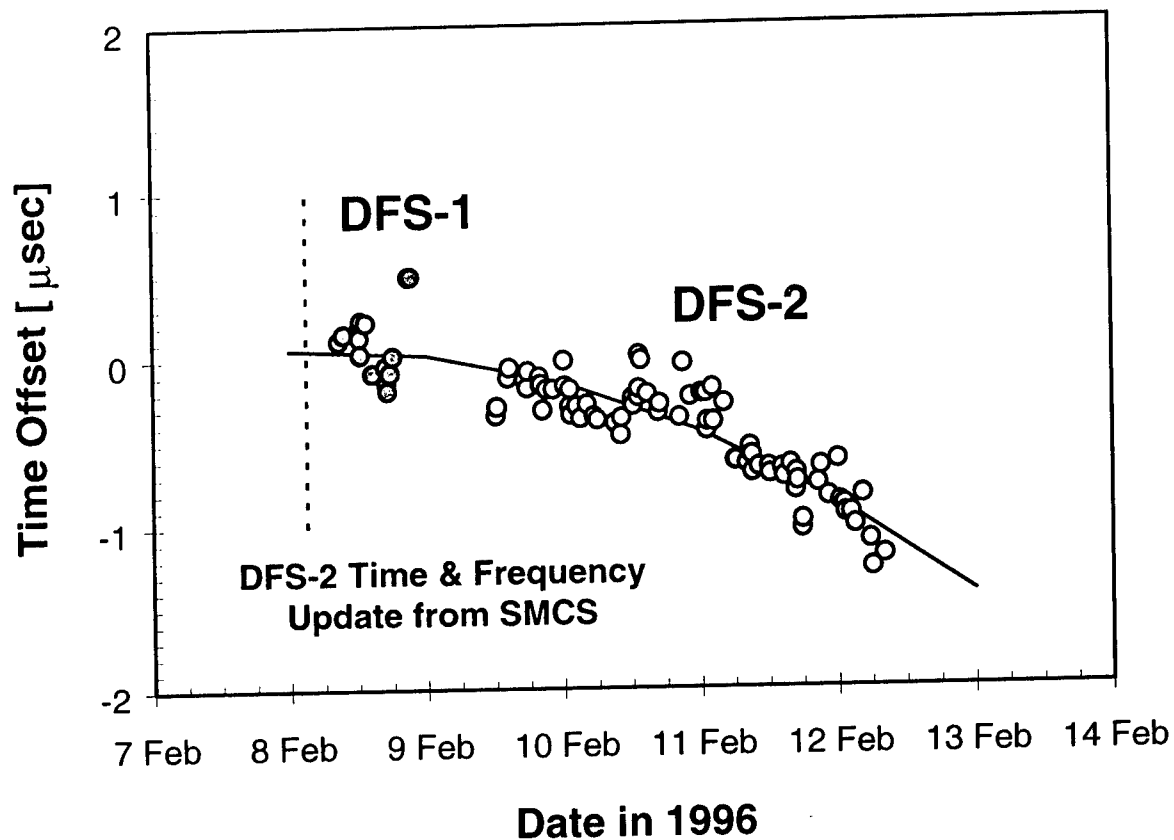


Figure 4: Raw time-offset measurements of the DFS-1 crystal (gray) and the DFS-2 Rb atomic clock (open) by the same ground-station. The dashed line indicates the date when the ground-station made a time and frequency correction to the DFS-2 Rb atomic clock, and the solid line is a quadratic fit to all the data. During this period, the last ground-station time and frequency correction to DFS-1 occurred on 4 February.

Questions and Answers

BOYD MOORE (KAMAN SCIENCES CORP.): How far apart were these satellites?

JAMES CAMPARO: They were both located over the Continental United States when these measurements were taken.

JAMES DeYOUNG (USNO): I don't remember the other two Milstar satellites; did they get a budget cut?

JAMES CAMPARO: No, no. The constellation is not complete.

MICHAEL GARVEY (FREQUENCY AND TIME SYSTEMS, INC.): Do you know what the nature of the locking algorithm is? Is this a frequency lock?

JAMES CAMPARO: One way that that can be accomplished is that the satellites can send out a message to each other. They agree on a time that they're going to send out a message. This clock sends out a message at 1:00, and it receives the message from the other satellite sometime later. And now it's got a differential time of arrival. It will then pass that differential time of arrival back sometime later, call it 1:10. And with that information, this satellite knows its own differential time of arrival at 1:00. It's gotten information on what the other satellite's differential time of arrival at 1:00; and it can use that information; it can take the difference between the two to estimate the time offset between the clocks without knowing the range, except for the Sagnac effect.

MICHAEL GARVEY: From your comments, it's a phase-lock loop essentially, since they're locking to time.

JAMES CAMPARO: Yes.

MARTIN BLOCH (FEI CORP.): Time lock!

PTTI: UTILIZATIONS AND EXPERIMENTATIONS AT HYDRO-QUÉBEC

Gilles Missout

Hydro-Québec Research Institute (IREQ)

1800 Montée Ste. Julie, Varennes J3X 151, Québec, Canada

Abstract

Hydro-Québec has a long history of PTTI applications. A brief review is presented on our phase angle measurement system and our special modified IRIG-B time code on microwave analog channels which are still in use. This is followed by a description of the use of GPS timing receivers for fault location on high-voltage lines and for synchronous measurement of the power grid. Then our recent experiments of time and frequency transmission on a 250-km overhead fiber optic ground wire is presented. This link uses one in-line optical amplifier. The absolute delay is characterized.

1 INTRODUCTION

Hydro-Québec has extensive experience with PTTI applications. Our first PTTI application consisted of time dissemination system using the Communications Technology Satellite^[1], after which we developed a voltage angle measurement system using LORAN-C.^[2] The use of power line carriers in the vicinity of LORAN-C signals prevented us from further developing this approach. For this reason and due to parallel developments elsewhere at Hydro-Québec, we built a modified IRIG-B time dissemination^[3,4,5] and are searching for other applications.^[6] This paper describes the former applications still in use and presents the latest PTTI developments at Hydro-Québec.

2 TIME DISSEMINATION ON ANALOG MICROWAVE CHANNELS

2.1 IRIG-B

IRIG-B was not successful with its standard configuration for two reasons: 1) the spectrum of the IRIG-B signal is not well adapted to the channel voice bandpass, and 2) the SSB modulation of the microwave link adds phase distortion. Use of a 2-kHz modulated carrier plus a pilot reference at 1 kHz provides a good way to disseminate time with an accuracy of about a few microseconds.

We have a master clock which is based on a triple system using a RbFS driving two time accumulators and a GPS clock. A majority decision system chose one clock to disseminate the timing signal in our network. Slave clocks placed at strategic points acted as protection against loss of the communication channel. Local Units are used in every substation to recover and distribute a standard IRIG-B code to users.

2.2 Chronological Recording of Events

The first requirement was to date every event in the power system to the nearest millisecond. Armed with these dates, someone could then possibly be able to retrace the event's history.

2.2 Power Frequency Control

Before the broad use of crystal clocks in every household, the electrical networks were the largest time dissemination systems in the world, which everyone depended on to keep their oven range clocks on time. To balance the load and the generation, we centrally controlled part of the generated power to maintain a 60-Hz clock on time compared to our IRIG-B time system. Figure 1 shows the Allan variance of the Hydro-Québec power system compared with the Eastern US system.

2.4 Voltage Angle Measurement System

The measurement of the voltage angle found between strategic points on the power system has the effect of applying a giant stethoscope on an electric grid, which reacts like Jell-O when shaken. Signature analysis provides major clues when searching through chronological reports of events, especially during major events (Fig. 2).

A voltage angle measuring system is still in operation. The IRIG-B system ensures the synchronization of remote units and, with the help of local rubidium clocks, has an accuracy rate of about 10 μ s.

2.5 GPS Applications

Portable Clock

We are equipped with a GPS-based portable clock used to calibrate the propagation delay of the IRIG-B signals.

Fault Locator

We have implemented an approach similar to the one developed by the Bonneville Power Administration, which also uses GPS as a synchronization system.

3 NEW DIGITAL COMMUNICATION SYSTEMS

Hydro-Québec is planning to replace its analog communication system with a SONET-type system using fiber-optic-equipped overhead ground wires. This kind of installation is special due to the fact that the fiber optics are exposed to outside elements (e.g. temperature, wind) to a greater extent than are telecommunications systems, which are usually buried. Also, the remote location limits the number of repeaters or line amplifiers which can be used. Typical hops could attain each 120-130 km.

Such a system requires adequate synchronization and the noise affecting the time and frequency propagation on the fiber optics is an important consideration. We were asked by Hydro-Québec's Telecommunications department to characterize the absolute propagation delay and its noise.

3.1 Measurement Setup

The optical link, which is 260 km long, is equipped with an optical line amplifier located about midway down the link. Figure 3 presents a diagram of the measurement setup. Cesium-beam clocks are used over the medium term and GPS clocks for the long term at each end. The 10-MHz output of the Chamouchouanne clock is modulated with a 1-pps marker and then used to externally modulate a laser (Fig. 4).

Halfway down, an optical line amplifier is used to boost the optical signal. At the receiving end, the optical signal is converted into an electrical signal. The 1-pps marker is retrieved to give the absolute delay, and the 10-MHz signal is analyzed in the frequency and time domains using the dual mixer time difference system with a 100-Hz beat frequency.

3.2 Measurement Results

Figure 5 shows the drift of the cesium at both points (note the three cesium clocks used at Chamouchouanne). Figure 6 gives the absolute delay over the course of 3 days. Figure 7 gives the TDEV of the received signal. The long-term portion is measured using the 1-pps information, the short-term portion using the 100-Hz beat. Figure 8 gives the frequency domain phase noise. On both curves we see a 0.5 to 1 Hz bump. Figure 9 clearly shows oscillation, related to span swings. The diurnal-nocturnal is included in TDEV.

4 CONCLUSION

Hydro-Québec is still active in PTTI applications. Our last measurements revealed a promising future for time and frequency dissemination on fiber-optic-equipped overhead ground wire. A hot topic will be at the convergence of synchronous measurement on power network and information technology.

5 ACKNOWLEDGMENTS

The author is grateful to many colleagues, specially to Carlos Cerda-Seitz and Yves Delisles, both from Hydro-Québec's Telecommunication department, which gave us the opportunity and ideas to conduct our fiber-optic experiments. Thanks also go to J. M. Houle, Gilles Provençal, Daniel Gagnon, and Louis Lamarche, whose work was crucial to the good results obtained.

6 REFERENCES

- [1] G. Missout, and P. Girard 1975, "*Study of a method of clock synchronization by satellite for future Hydro Quebec needs*," Proceedings of the IEEE Conference, 1975, Toronto, Canada, paper 75204, session 20.
- [2] G. Missout, and P. Girard 1980, "*Measurement of bus voltage angle between Montreal and Sept-Iles*," IEEE Transactions on P.A.S., 99, 536-539.
- [3] G. Missout, W. Lefrançois, and L. Laroche 1980, "*Time dissemination in the Hydro-Québec network*," Proceedings of the 11th Annual Precise Time and Time interval (PTTI) Applications and Planning Meeting, 27-29 November 1979, Greenbelt, Maryland, USA (NASA CP-2129), pp. 343-350.

- [4] G. Missout, J. Béland, and G. Bédard 1981, "*PTTI application at Hydro-Québec*," Proceedings of the 12th Annual Precise Time and Time interval (PTTI) Applications and Planning Meeting, 2-4 December 1980, Greenbelt, Maryland, USA (NASA CP-2175), pp. 377-385.
- [5] G. Missout, J. Béland, D. Lebel, G. Bédard, and P. Bussière 1982, "*Time transfer by IRIG-B time code via dedicated telephone link*," Proceedings of the 13th Precise Time and Time interval (PTTI) Applications and Planning Meeting, 1-3 December 1981, Washington, D.C., USA (NASA CP-2220), pp. 281-297.
- [6] G. Missout 1987, "*PTTI applications in power utilities*," Proceedings of the 18th Annual Precise Time and Time Interval (PTTI) Applications and Planning Meeting, 2-4 December 1986, Washington D.C., USA, pp. 491-502.

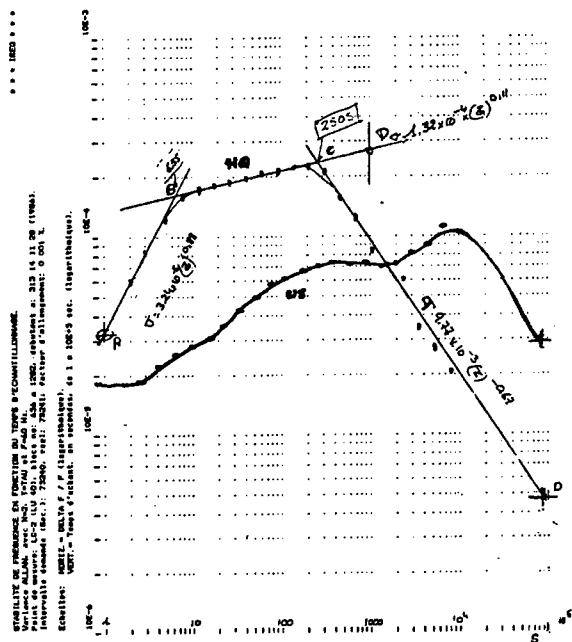


Figure 1. AVAR of HQ and Eastern US power Network

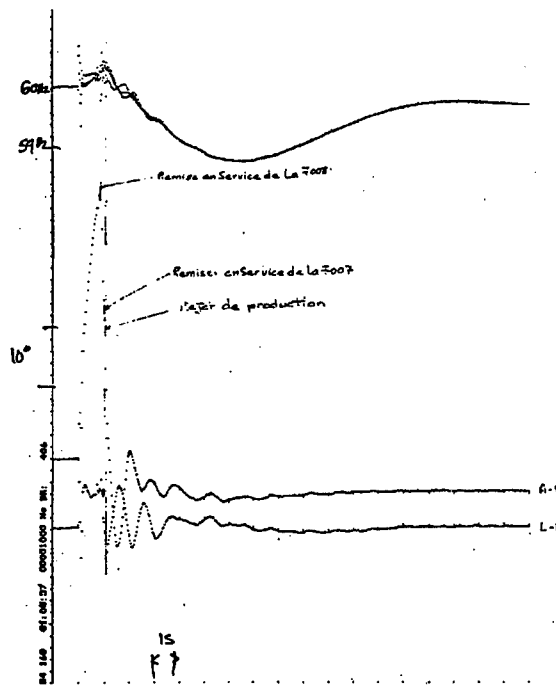


Figure 2. Double short - loss of generation

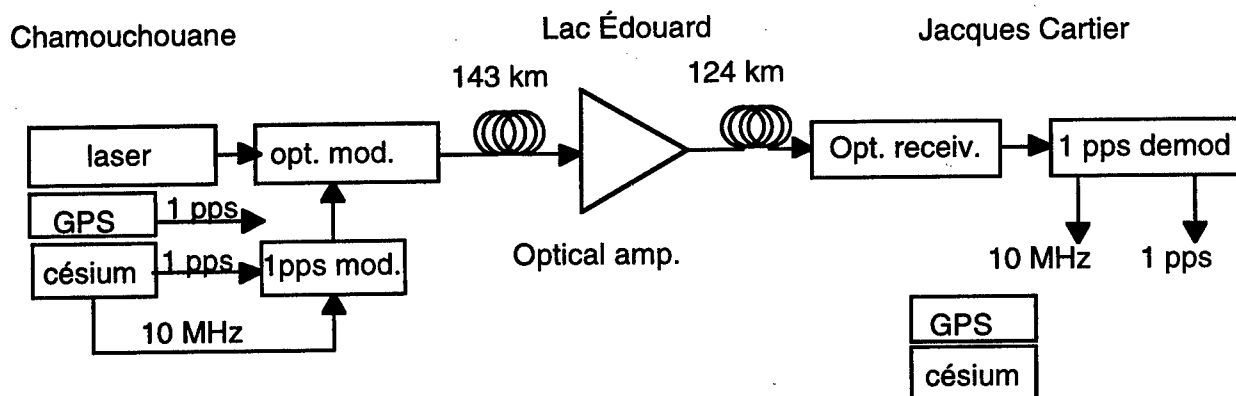


Figure 3. Measurement setup

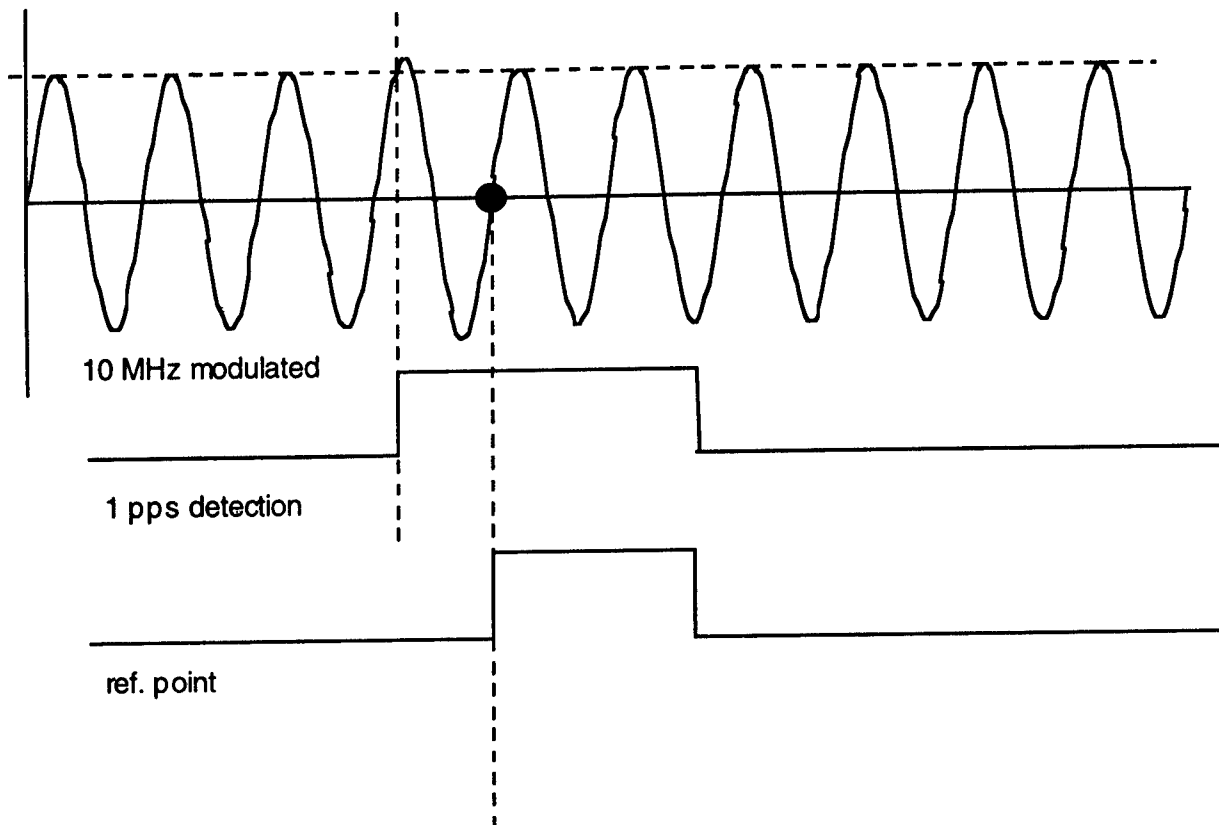


Figure 4. 1-pps frame information

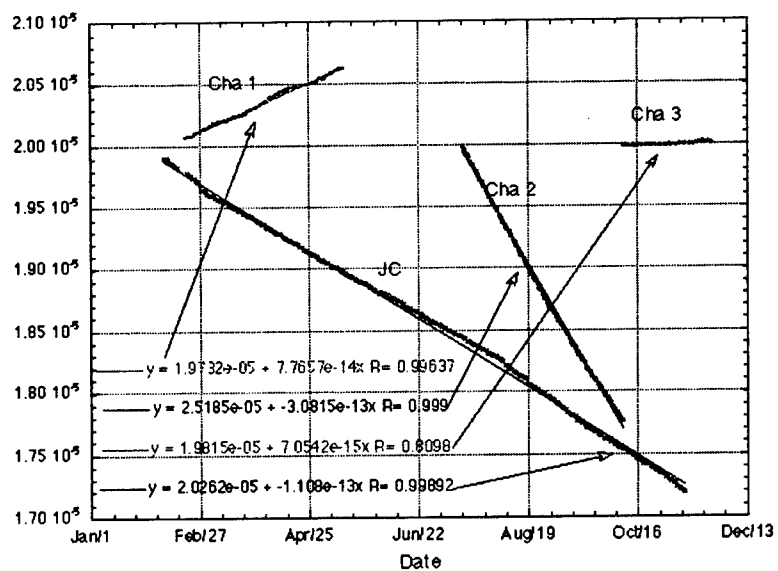


Figure 5. Cesium drift at both places

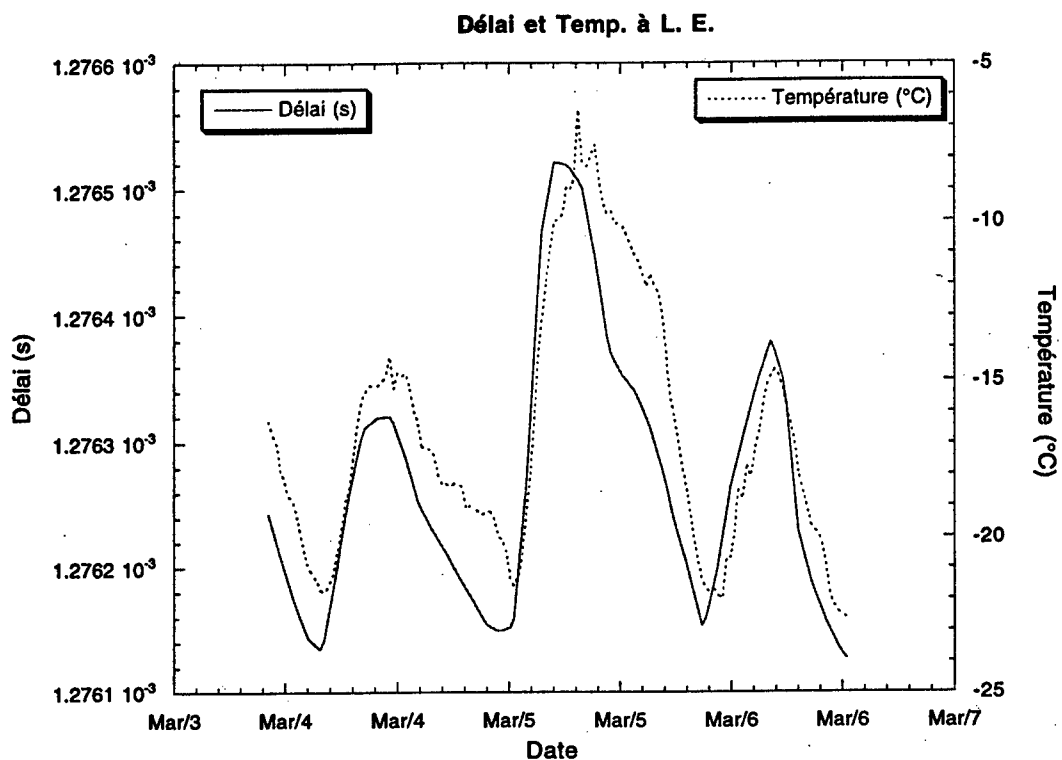


Figure 6. Delay and temperature on 3 days

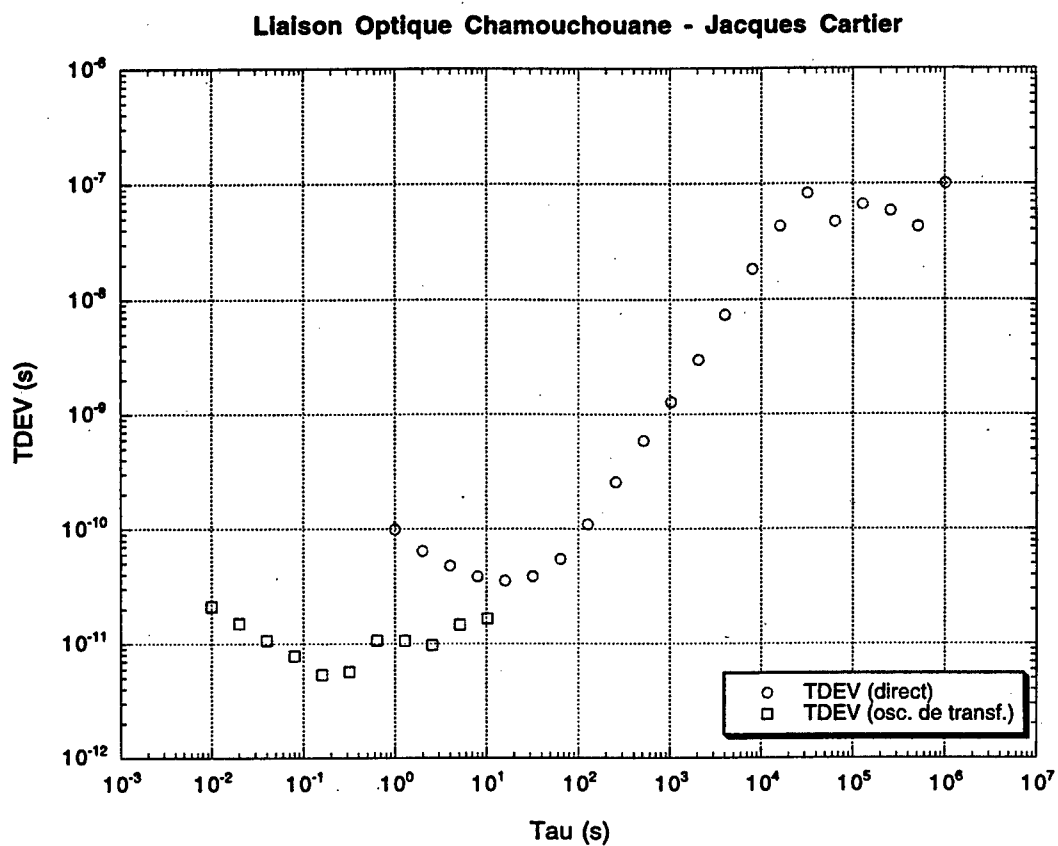
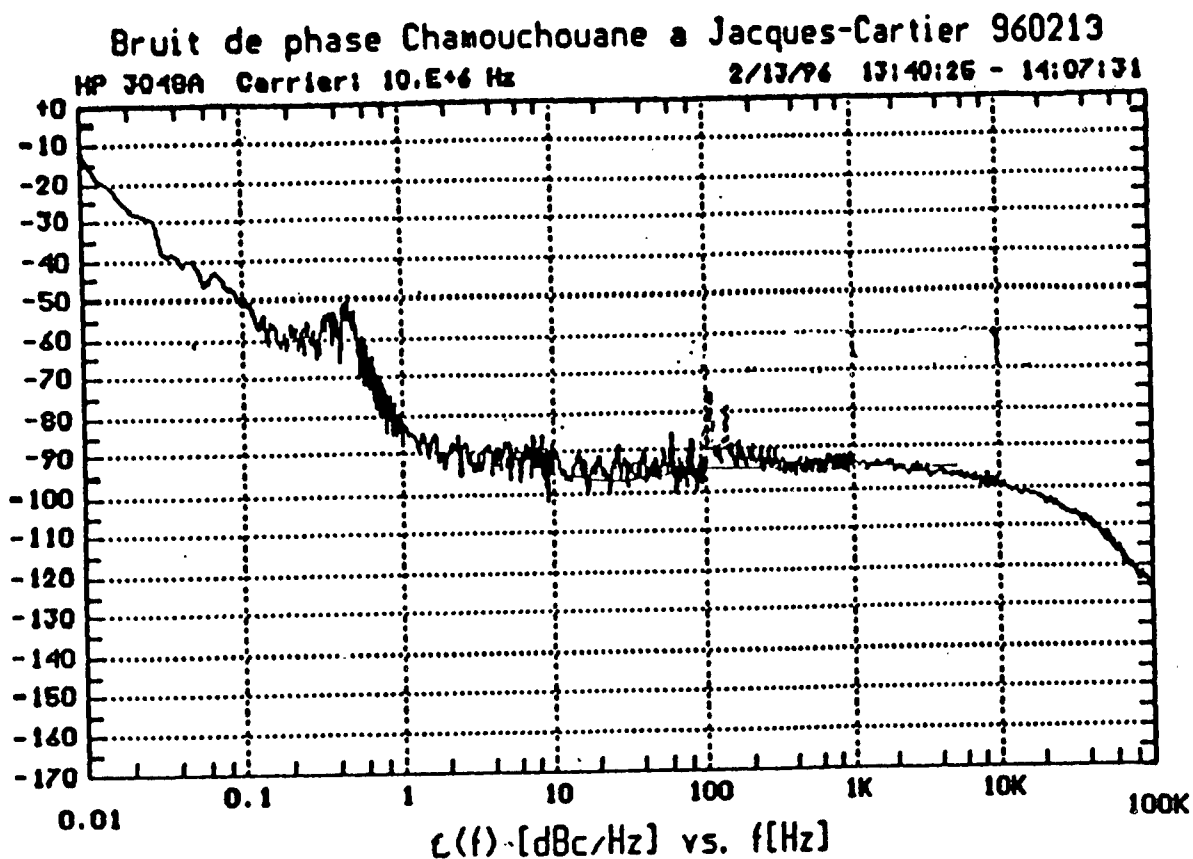


Figure 7. TDEV



Measurement Parameter Summary

Meas. Type : PHASE LOCK LOOP	K_VCO Method: MEASURED
Start Freq : 10.E-3 Hz	K_vco : 12.58 Hz/Volt
Stop Freq : 100.E+3 Hz	Loop Suppr. : VERIFIED
Min. Aves : 4	
Carrier Freq: 10.E+6 Hz	Closed PLL BW: 58.98 Hz
Det. In Freq: 10.E+6 Hz	Pk Tune Rnge: 104.900000 Hz
Entered Kvco: 10 Hz/Volt	Assumed Pole: 1.727E+3 Hz
Center Volts: 0 Volts	UUT : USER'S SRCE, MAN
Tune Range : 10 Volts	Ref. Srce : 10 MHz 'A', SYS, VCO
Ph. Detector: 5 TO 1600 MHz	Ext. Imbase : NOT IN USE
K_phi Method: MEASURED	On Converter: NOT IN USE
K_phi : 468.7E-3 V/Rad	HP11848A LNA: IN

Figure 8. Phase noise - frequency domain

Date et Heure			
16h51m34, 13/05/1996			
Cont			
Erre	Ecart type	Maximum	Minimum
3627E-3	8.04089E-6	2.70465E-3	2.66826E-3
ance	Root Allen Variance	RMS	Allen Variance
85592E-12	1.57981E-6	2.68628E-3	2.49581E-12

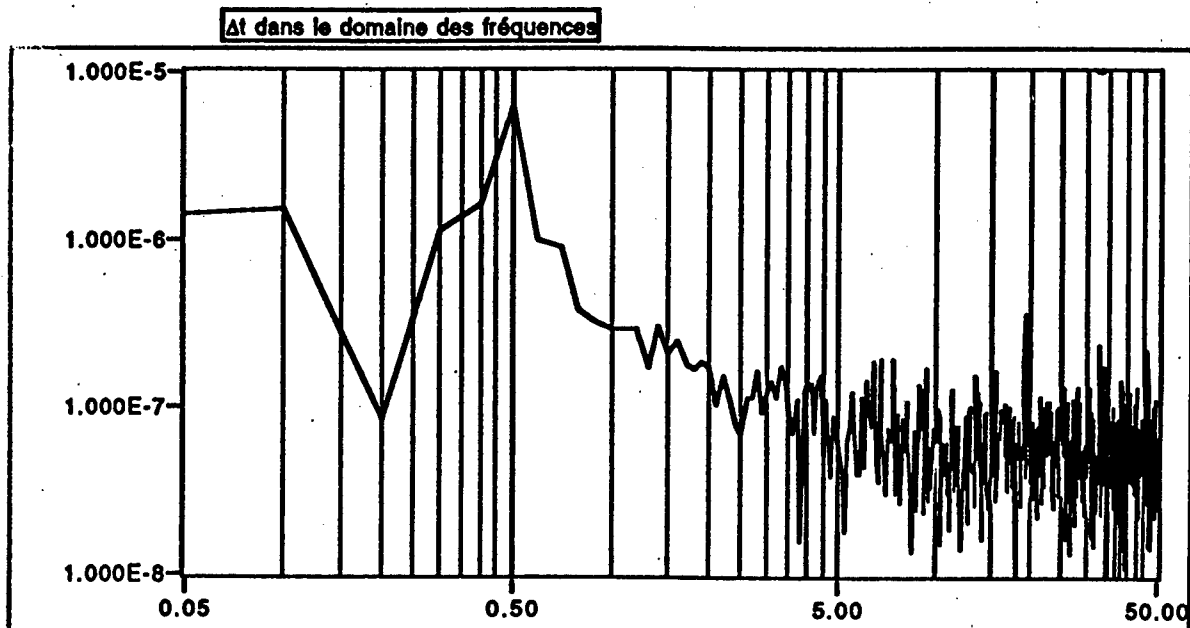
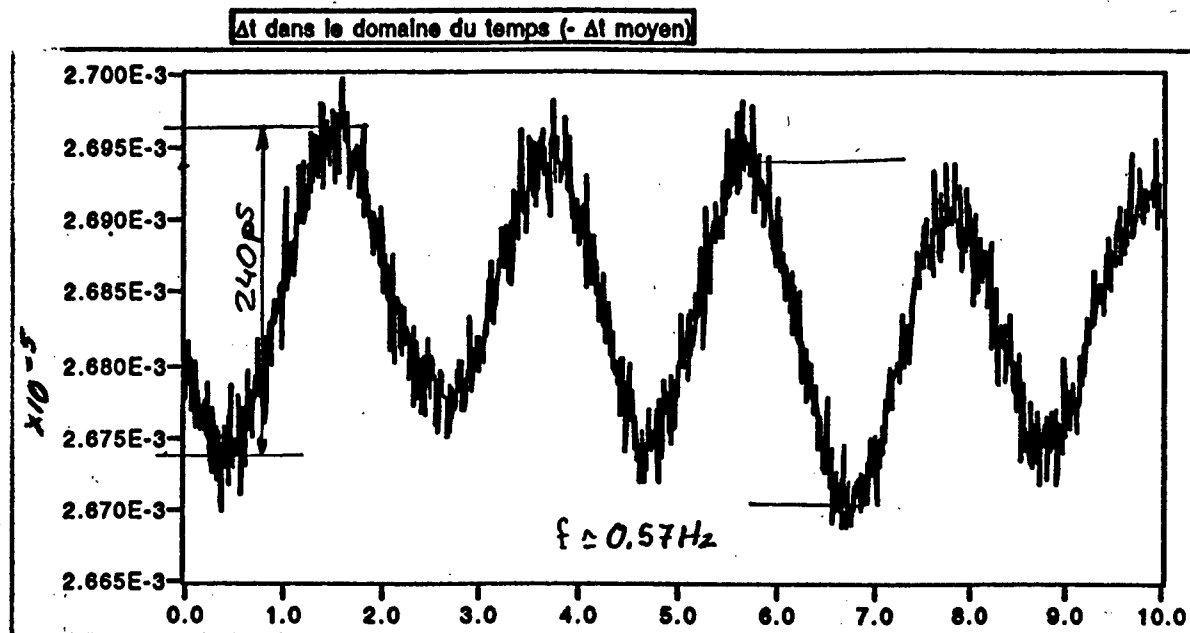


Figure 9. Phase oscillation

Questions and Answers

RICHARD KEATING (USNO): I understood you to say that the one-half hertz was linked to the slow oscillation of the microwave towers. Is that correct?

GILLES MISSOUT: No. The optical cable is suspended between power utility towers, not microwave towers. So you have towers at, I think, every 300 meters so the cable is suspended there and should calculate the period of oscillation; it's close to .5 hertz.

RICHARD KEATING: Is it driven by wind?

GILLES MISSOUT: Yes.

GPS AND RELATIVITY: AN ENGINEERING OVERVIEW

Henry F. Fliegel and Raymond S. DiEsposti
GPS Joint Program Office
The Aerospace Corporation
El Segundo, California 09245, USA

Abstract

We give and explain in detail the formulas for the relativistic corrections to be implemented in high-speed aircraft, or when using other satellites in connection with GPS, or when using GPS from another satellite. We explain how to use these formulas in various scenarios, give numerical examples, and itemize the pitfalls to be avoided by (for example) receiver manufacturers.

INTRODUCTION

The Operational Control System (OCS) of the Global Positioning System (GPS) does not include the rigorous transformations between coordinate systems that Einstein's general theory of relativity would seem to require – transformations to and from the individual space vehicles (SVs), the Monitor Stations (MSs), and the users on the surface of the rotating earth, and the geocentric Earth Centered Inertial System (ECI) in which the SV orbits are calculated. There is a very good reason for the omission: the effects of relativity, where they are different from the effects predicted by classical mechanics and electromagnetic theory, are too small to matter – less than one centimeter, for users on or near the earth. However, a new class of users, who employ satellites that obtain time and position in space from GPS, cannot be satisfied with the approximations in the current OCS. Furthermore, because those approximations have not been publicly analyzed and presented, there is much confusion in the GPS literature. Eminent scientists have been divided amongst themselves, wondering whether the OCS software does not need to be rewritten, especially since the Department of Defense is now requiring that the current specifications – 6 meters in User Range Error (URE) – are to be tightened under the Accuracy Improvement Initiative (AII). In this paper, we compare the predictions of relativity to those of intuitive, classical, Newtonian physics; we show how large or small the differences are, and how and for what applications those difference are large enough to make it necessary to correct the formulas of classical physics.

RELATIVITY: THE FORMULAS

If two observers determine what intuitively we call the same quantity – the distance between two points, or the time interval between two events – they will measure different lengths and times, if (1) they are moving with respect to each other, (2) one is higher or lower than another in a gravitational field, or (3) one is accelerating with respect to the other. Users of GPS

encounter all three effects, and should correct their measurements accordingly, by formulas which we now explain.

The Velocity Effect (Lorentz Contraction)

Case (1) is the province of special relativity. In classical physics, if a transmitter in a vacuum sends out a radio frequency F in its own frame of reference, and if a receiver is moving with velocity v at an angle A to the beam coming from the transmitter to the receiver, then the signal will be received at the Doppler shifted frequency f , where $f < F$ if A is less than 90° (receiver moving away from the transmitter). Now, if the transmitter and receiver are replaced by two units of hardware each of which both transmits and receives, each unit will measure the other's frequency as "too low." We accept intuitively the fact that there is no real paradox here. If the two units were colocated, then if one ran slower than the second, the second must run faster than the first; but if they are not colocated, what an observer measures depends not only on the hardware, but on the state of motion between them; and each observer perceives the motion the same way: "that other is receding from me at a rate $v \cos(A)$." If our problem is to measure f (which is what we observe), and to calculate F (which we must infer), then in classical physics

$$F = f \left(1 + \frac{v}{c} \cos(A) \right) \quad (1)$$

where c is the speed of light, or radio, in free space. If the receiver is moving at right angles to the line of sight, $\cos(A) = 0$, and $F = f$; there is no Doppler shift. But the relativistic equivalent of the same formula is

$$F = \gamma f \left(1 + \frac{v}{c} \cos(A) \right) \quad (2)$$

where γ is defined to be always equal or greater than one:

$$\gamma \equiv \frac{1}{\sqrt{1 - \frac{v^2}{c^2}}} \quad (3)$$

The γ formula looks like the formula for going from sine to secant in ordinary trigonometry, and for good reason. The effect of special relativity (see [1]) is a coordinate rotation through an angle, the arctangent of iv/c . There is a related angle, a real number P , such that $\sin(P) = v/c$, and $\gamma = \sec(P)$; this provides a convenient way of calculating γ . Like the secant, the γ factor (1) is very nearly equal to one for small angles (or v/c), because (2) it increases with the square of the angle v/c for small angles.

Notice that, even if $\cos A = 0$, the Doppler shift is no longer zero, but γ ; and so the frequency as received is lower than the frequency transmitted. Since we naively expect, from intuition and from classical physics, a Doppler shift of zero, the usual way to describe the relativistic result is to say that the moving transmitter's frequency standard or clock – moving in the receiver's frame of reference – appears to be running slow. Again, as in classical physics, each observer can consider himself at rest and the others to be moving; and it is no paradox that each measures the others as "too slow." The relativistic formulas defy our intuitions of time and space, but not the basic principles of logic; they can stand.

Now, the angle A should be corrected for aberration. From either a classical or a relativistic point of view, aberration is the change in the apparent direction from which a wavetrain appears to be coming because of the observer's velocity. In Eqs. (1) and (2) above, the cosine of the angle A should be calculated in the observer's frame of reference. If A' is the angle that is calculated in (for example, the so-called "Earth Centered Inertial" or ECI system of coordinates, then the relativistic equation to go from cosine of A' to the cosine of A is

$$\cos(A) = \frac{\cos(A') - \frac{v}{c}}{1 - \frac{v}{c} \cos(A')} \quad (4)$$

and this equation is exact. The reader may wonder why the omnipresent γ factor does not appear. It would, in the formulas for $\sin(A)$ and $\tan(A)$. However, we need $\cos(A)$, and the γ factor cancels out. (For the derivations of all the above equations, see [1].)

So then, to calculate the Doppler correction by which we correct the received frequency from a GPS satellite – for example, in crosslink ranging from one SV to another – we first calculate the relative speed of the transmitter to the receiver in the ECI frame, and the angle A' between relative velocity and the line of sight between transmitter and receiver, also in the ECI frame. We then apply Eq. (4) to obtain $\cos(A)$, and then Eqs. (2)-(3) to transform the observed frequency f to the true transmitted frequency F , in the transmitter's frame of reference.

Gravitational Effect

We now turn to Case (2) above, where the transmitter is higher or lower than the receiver, in a gravitational field. If a photon (whether of light or of radio) falls into a potential well, it is shifted to a higher frequency; climbing up, it loses frequency. The quantum acts like a material particle, gaining kinetic energy as it falls through the gravity field. In quantum mechanics, it is shown that the energy of the photon is $h f$, where h is Planck's constant and f is the frequency. If it were a material particle, then from special relativity its total energy would be $m c^2$, where the kinetic energy is included in the increase of the mass m from the rest mass m_0 . Since $h f$ is equivalent to $m c^2$, the mass m of the particle must correspond to $h f / c^2$ of the photon. Then, since the change in potential in going from one point to another is the change in energy of the particle per unit mass, that correspondence requires that

$$\Delta(hf) = m \Delta\phi = - \frac{hf}{c^2} \Delta\phi \quad (5)$$

or

$$\frac{\Delta f}{f} = - \frac{\Delta\phi}{c^2} \quad (6)$$

In the earth's gravitational field, if a radio signal passes from a satellite at distance R_{sv} from earth's center to a receiver (whether on another satellite or on the ground) at distance R_r , a good approximation for the frequency shift correction, to transform from the frequency measured on the ground to the frequency transmitted by the satellite, is

$$\frac{\Delta f}{f} = \frac{GM}{c^2} \left(\frac{1}{R_{sv}} - \frac{1}{R_r} \right) \quad (7)$$

So to the Doppler shift given by Eqs. (2), (3), and (4) we add the frequency shift from Eq. (7). If R_{rv} is greater than R_r , the correction is negative, and so by adding it to the received frequency f we obtain the frequency F of the transmitter in its own frame of reference.

Acceleration Effect

This is the correction to be made if an observer (= the receiver) is accelerating. In fact, the receiver, whether in an SV or on the ground, is certainly accelerated; it is either in free fall in orbit or subject to centripetal acceleration on the rotating earth. Acceleration effect can be absorbed in the gravity potential. The formal justification for doing so is the Principle of Equivalence in Einstein's general theory of relativity, which is best explained by an example. Suppose that a photon of light is radiated across a chamber through a distance r from wall A to wall B, along a line perpendicular to both walls. Suppose that the whole chamber is accelerating along this line, in the same direction as the photon is moving, by g meters/second squared. Define the initial velocity as zero at the instant that the photon is radiated; we are entitled to do this by the principles of special relativity. Now, by the time the photon arrives at the opposite wall, that wall is receding at a velocity $v = -gt$, where t is r/c , and as measured by a receiver on the receding wall the photon will be Doppler-downshifted by an amount (in classical approximation)

$$\frac{\Delta f}{f} = -\frac{v}{c} = -\frac{gt}{c} = -\frac{gr}{c^2} \quad (8)$$

But now consider a corresponding scenario in which the chamber is not accelerated, but in which a gravitational field produces a local acceleration due to gravity, g . As we have seen (Eqs. (5)-(7) above), the proportional frequency shift is the difference of gravitational potential divided by c squared. By the Principle of Equivalence, the product gr in Eq. (8) corresponds to this potential difference, and we can allow for the observer's acceleration by modifying the gravity term.

But we see that there is no need to do so, if we remember what this modification would be. The $-gt/c$ of Eq. (8) is simply the correction to the Doppler shift due to the change in the receiver velocity during the signal propagation time – in our example, the time it takes the photon to traverse (r). But if we compute the Doppler effect by Eq. (2), using the relative velocity between transmitter and receiver at the time of reception of the signal, we include the effect of Eq. (8) automatically. Only if we were to label signal events at the transmission time would we need to include Eq. (8) explicitly. Among GPS users, hardly anyone does so. If, for any reason, it is necessary so to do, rewrite Eq. (8) as

$$\frac{\Delta f}{f} = -\frac{\vec{a} \cdot \vec{r}}{c^2} \quad (9)$$

where \vec{a} is the user's vector acceleration in an inertial frame (e.g, the ECI), and \vec{r} is the vector from transmitter to receiver – at either transmission or reception time, in the “weak field approximation.” This is in the frequency domain; integrate, for timing receivers.

Summary of Corrections To Be Made

Here is the summary. In general, to correct the frequency measured by a receiver for all relativistic effects, to obtain the frequency at the transmitter, we perform the following steps.

(i) Obtain the velocity \vec{V} of the transmitting satellite, and the velocity \vec{v} of the receiver, in an ECI coordinate frame, for the times of reception. Calculate the angle between the receiver's velocity vector and the line from transmitter to the receiver, in the ECI frame. That is the angle A' of Eq. (4).

(ii) Apply Eq. (4) to obtain the corresponding angle A in the receiver's frame of reference.

(iii) Calculate the magnitude of the velocity of the GPS satellite with respect to the receiver, in the ECI frame. That is simply the magnitude of the vector difference $\vec{V} - \vec{v}$. Using Eq. (3), calculate γ .

(iv) Calculate the $\Delta f/f$ frequency shifts using Eqs. (2) and (7), and add them together. This is the total correction to be added to the received frequency to obtain the transmitted frequency.

To obtain the correction to add to the transmitted frequency in order to obtain the received frequency, perform the above steps and reverse the sign. To convert to the time domain, integrate, and assume any convenient zero of time. Without a timing receiver observing four satellites, one cannot synchronize to GPS time.

Since GPS receivers work in the time and not in the frequency domain, they handle the velocity, gravity, and acceleration shifts differently than described above. First, each GPS space vehicle (SV) clock is offset from its nominal rate by about -4.45×10^{-10} ($= -38$ microseconds per day) to allow for the relativistic offsets between the differences between the SV and the ground. Of this -38 microseconds per day, about -45 are due to the gravitational potential difference between the SV at its mean distance and the earth's surface, and $+7$ to the mean SV speed, which is about 3.87 km/sec. To this mean correction, each receiver must add a term due to the eccentricity of the GPS orbit. It can be shown that this effect produces a variation in the SV clock, as seen from the earth, of

$$\Delta T = -2 \frac{\vec{R} \cdot \vec{V}}{c^2} \quad (10)$$

where \vec{R} is the vector of position of the SV from the ECI, and \vec{V} the velocity vector. This is the equation given in ICD-GPS-200. It is appropriate for users on or near the earth's surface, but not users in space, who should apply the frequency correction equations given above, or their integrals to transform to the time domain.

STICKY WICKETS

We now turn to the misunderstandings that have arisen over the 15 years or so that GPS has been in operation. Most of the disagreements have semantics for a father. A few arose from the mathematics of relativity, in going from a rigorous treatment to the approximations that are found sufficient for the practical use of GPS.

The Newtonian World of the Operational Control System

The GPS Operational Control System (GPS) corrects the pseudoranges measured by its Monitor Stations for the sum of the gravitational and the velocity effects as discussed in the previous section, but computes the velocity effect only for the mean orbital speed of the satellite, which is about 3.87 km/sec. The question has been raised: why doesn't the operational software calculate the velocity effect using the speed of each satellite relative to each Monitor Station, which varies

sinusoidally as the Monitor Station is carried around the rotating earth? In principle, it should, but the effect is negligible for two reasons: (1) the nature of the pseudorange measurement; and (2) the size of the effect.

The pseudorange measurement can be regarded from two points of view. On the one hand, pseudorange is simply range, once the clock offsets are removed. As described in the previous section, the ranges measured by a moving observer are foreshortened by the γ factor. For an SV speed of 3.87 km/sec, $\gamma - 1$ is 8.33×10^{-11} . The range is typically about 30,000 km. The error incurred neglecting the γ factor is 30,000 km multiplied by 8.33×10^{-11} – that is, 2.5 millimeters. Close enough for government work.

On the other hand, the pseudorange measurement should be equivalent to accumulated Doppler, once the ionospheric delays are removed. If the MS accumulated Doppler measurements over a pass, then, since the OCS assumes Newtonian physics, it would use Eq. (1). In the more nearly correct world of special relativity, we should use Eq. (2), which differs from Eq. (1) by the γ factor. Not only the velocity term, but the observed frequency f , is multiplied by γ . And γ is not constant, because the rotation of the earth (up to 0.465 km/sec at the equator) vectorially adds to the 3.87 km/sec of the satellite when we compute the satellite speed relative to a Monitor Station. Corresponding to a possible v of 3.87 ± 0.465 km/sec, γ can vary from $8.33 \times 10^{-11} \pm 1.88 \times 10^{-11}$. The constant part is absorbed in the mean relativistic offset described above, but the variable part would alias into the accumulated Doppler range. For example, over one hour = 3,600 seconds, the error could be 1.88×10^{-11} times 3,600 seconds times $c = 20.3$ meters. Clearly, this would be a major source of error in the Operational Control System.

But this error would be incurred only if the station clocks were independent of the GPS satellite clocks, each MS keeping its own time. That's not the way the OCS works. Station time is estimated in the Kalman filter together with the SV clocks, and each MS clock is effectively being updated continuously by the satellites. The station clock is used only to bridge the gap in time between measurements; but since several satellites are always in view, these measurements are virtually instantaneous, except for the different signal propagation times from different satellites. These times are about 0.1 sec, and, multiplying by γ , once more we derive an error of about 2.5 millimeters.

However, this happy result depends entirely on the Kalman filter. At present, the filter is very "springy" – that is, it has a short time constant, because it is adjusted to absorb ephemeris errors which can change rapidly (for example, at the onset of eclipse). Station clocks, satellite clocks, and ephemeris parameters are all allowed to move together, and so Monitor Station time is controlled entirely by the satellite clocks. (If several satellites are in view, the Monitor Station clock is mathematically redundant, and in practice it drops out of the solution.) But if the filter were retuned to be very "stiff," with long time constant and reasonable weights assigned to the Monitor Station clocks, then the appropriate time over which the relativistic effects would act would no longer nearly equal the signal propagation time, but would be several hours or days; and then the error due to the neglected γ factor would approximate that incurred in the hypothetical accumulated doppler scenario – many meters.

In principle, the critics of GPS in the relativity debate have not been completely wrong. The neglected γ factor could hurt us. The OCS software should be reformulated. Nevertheless, in practice, neglect of relativity does not now contribute measurably to the GPS error budget, as the OCS software is currently configured.

The ECI Coordinate System

It has been said (e.g., [3] and [4]) that the Operational Control System (OCS) of GPS makes all calculations with respect to an ECI ("Earth Centered Inertial") frame of reference. This is a perfectly defensible statement, depending on how one chooses to describe the GPS time scale.

In actual practice, GPS operates in a mixed coordinate system: the spatial coordinates are ECI, but the time rate is appropriate to observers on the surface of the rotating earth, that is, in the ECEF. GPS time is steered as closely as possible to U.S. Naval Observatory time (UTC[USNO]), which in turn is steered closely to International Atomic Time (TAI = Temps International Atomique). By an important theorem of general relativity, ideal frequency standards on the rotating geoid run at the same rate, because the effect of the earth's rotation (by which clocks on the equator would run more slowly than clocks at the poles) is cancelled by the earth's gravitational potential (since clocks on the equator are farther from the earth's center, and so at higher potential, than clocks at the poles). So a frequency standard anywhere on the earth's surface runs at the same rate as one at either pole, and is offset by a constant rate from a (hypothetical) clock at the earth's center. By the definitions adopted by the International Astronomical Union (IAU), the ideal time that GPS, UTC, and TAI time scales realize as nearly as possible is called Terrestrial Time (TT), and the time interval unit of TT is the Standard International (SI) second on the geoid, also called the coordinate second. Then, in at least one sense, the time scale of GPS is defined in the ECEF coordinate frame. Also by Recommendation T1 of the Sub-Group on Time of the IAU Working Group on Reference Systems, "coordinate times in (a) non-rotating reference system having ... spatial origin at the geocenter ... (is) designated as Geocentric Coordinate Time (TCG)"; this definition was adopted by the IAU in its General Assembly in 1991. Therefore, if GPS were to operate in the ECI coordinate system in the strict sense, its time scale would be TCG, which is offset from TT, etc. by the potential difference between earth's center and its poles. This GPS does not do.

If a satellite user of GPS were naively to map all measurements "to an ECI frame," using Geocentric Coordinate Time (TCG), an error would be incurred of roughly 60 microseconds per day.

However, there is a sense in which the TAI time coordinate is related to the ECI. Although all ideal frequency standards run at the same rate on the geoid, clocks cannot be synchronized unless some sort of signals pass between them. Because of the earth's rotation, when clocks on different continents are compared by travelling frequency standards, satellite signals, or other means, corrections must be made for the relativistic Sagnac effect. To calculate these corrections, one must know the rate of the earth's rotation, that is, the angular rate of the ECEF frame relative to the ECI. Implicitly, then, in the process of forming TAI, to which GPS time is steered, reference is made to the ECI.

Missing Relativity Terms?

Oversimplifications such as in [4], which disseminated the mistaken notion that GPS time is calculated "in the ECI," ignoring the earth's rotation, misled Steven Deines, in his paper entitled, "Uncompensated relativity effects for a ground-based GPS receiver."¹⁵ Deines argued that

The current ...GPS relativity corrections were based on an Earth centered inertial reference frame. The derivation assumed [that] the receiver obtains inertial GPS coordinate

time from the satellites. However, the receiver has been treated tacitly as being stationary in the inertial frame... relativity effects for a ground-based receiver include gravity and Earth rotation. Airborne GPS receivers have larger effects, and spaceborne GPS receivers have the worst uncompensated relativity effects.

Deines used equations from Robert Nelson's work (see [6]) in an attempt to show that corrections depending on the earth's rotation should be added to those incorporated in existing GPS receivers according to ICD-GPS-200. A complete critique of Deines' derivations has been made by Neil Ashby.^[7] Deines overlooked cancellations among several of his terms, by which the Nelson expressions reduce to very nearly the formulation of ICD-GPS-200.

Nelson shows ([6], p. 21) that the transformation between a time increment dt' expressed in a rotating and/or linearly accelerated reference frame and a time increment dt in a nonaccelerating frame is given by

$$dt = \gamma \left[1 + \frac{\vec{W} \cdot \vec{\rho}}{c^2} + \frac{\vec{v} \cdot (\frac{d\vec{\rho}}{dt'} + \vec{\omega} \times \vec{\rho})}{c^2} \right] dt' \quad (11)$$

where \vec{W} is the acceleration, $\vec{\rho}$ the position vector of a GPS receiver, \vec{v} its velocity, and $\vec{\omega}$ the earth's angular rotation rate. If the ground station is motionless with respect to the earth's surface, then the acceleration vector \vec{W} is determined by $\vec{\omega}$ and by \vec{R} :

$$\vec{W} = \vec{\omega} \times (\vec{\omega} \times \vec{R}) \quad (12)$$

and also the velocity \vec{v} :

$$\vec{v} = \vec{\omega} \times \vec{R} \quad (13)$$

Then one may rewrite Eq. (11), letting the origin from which $\vec{\rho}$ is measured to be the GPS receiver, of which the position in ECI coordinates is the vector \vec{R} . Eq. (11) now becomes

$$dt = \gamma \left\{ 1 + \frac{[\vec{\omega} \times (\vec{\omega} \times \vec{R})] \cdot \vec{\rho}}{c^2} + \frac{(\vec{\omega} \times \vec{R}) \cdot (\frac{d\vec{\rho}}{dt'} + \vec{\omega} \times \vec{\rho})}{c^2} \right\} dt' \quad (14)$$

As Nelson says, terms cancel in Eq. (14) to give a very simple result. The cancellation is as follows. As is shown in vector algebra,

$$\vec{A} \cdot (\vec{B} \times \vec{C}) \equiv (\vec{A} \times \vec{B}) \cdot \vec{C} \quad (15)$$

Therefore, we can write

$$(\vec{\omega} \times \vec{R}) \cdot (\vec{\omega} \times \vec{\rho}) = [(\vec{\omega} \times \vec{R}) \times \vec{\omega}] \cdot \vec{\rho} = -\vec{\rho} \cdot [\vec{\omega} \times (\vec{\omega} \times \vec{R})] \quad (16)$$

and Eq. (14) becomes

$$dt = \gamma \left[dt' + \frac{1}{c^2} (\vec{\omega} \times \vec{R}) \cdot d\vec{p} \right] \quad (17)$$

Eq. (17) "is just what one would expect by a Lorentz transformation from the center of rotation to the instantaneous rest frame of the accelerated origin" ([6], p. 23). Except for the leading γ factor, it is the same as the formula derived in classical physics for the signal travel time from the GPS satellite to the ground station. As we have shown, introducing the γ factor makes a change of only 2 or 3 millimeters to the classical result. In short, there are no "missing relativity terms." They cancel out.

8 REFERENCES

- [1] L. Landau, and E. Lifshitz 1951, *The Classical Theory of Fields*, trans. M. Hamermesh (Addison-Wesley, Reading, Massachusetts, USA).
- [2] P.K. Seidelmann (ed.) 1992, *Explanatory Supplement to the Astronomical Almanac* (University Science Books, Mill Valley, California, USA).
- [3] N. Ashby, and J.J. Spilker, Jr. 1996, "Introduction to relativistic effects on the Global Positioning System," in *Global Positioning System: Theory and Applications*, Vol. I, ed. B. Parkinson and J.J. Spilker, Jr. (American Institute of Aeronautics and Astronautics, Inc., Washington, D.C., USA)
- [4] P.S. Jorgensen 1988-89, "Relativity and intersatellite tracking," *Journal of the Institute of Navigation*, **35**, 429ff.
- [5] S.D. Deines 1992, "Uncompensated relativity effects for a ground-based GPS receiver," 0-7803-0468, IEEE.
- [6] R.A. Nelson 1991, "An analysis of general relativity in the Global Positioning System time transfer algorithm," report prepared for Sachs/Freeman Associates Inc., Landover, Maryland, USA.
- [7] N. Ashby 1996, "Response to Steve Deines' Paper Entitled 'Missing Relativity Terms in GPS'," University of Colorado, Boulder, Colorado, USA (private communication).
- [8] "NAVSTAR GPS Space Segment/Navigation User Interfaces," ICD-GPS-200C, GPS JPO, 15 Dec 1994.
- [9] E. Kaplan (ed.) 1996, *Understanding GPS: Principles and Applications* (Artech House, Norwood, Massachusetts, USA).
- [10] MCS software listing obtained from John Berg of the Aerospace Corp., 8 July 1996.
- [11] "MAGR Computer Program Development Specification," XP-RCVR-MAGR, Part I, 23 Jan 1991.

Questions and Answers

STEVEN HUTSELL (USNO): You and I have been talking about this intermittently over the phone over the past couple months or so. Obviously, the question of trying to make the best utilization of the ephemeris and solar process noise values in the MCS Kalman filter is something to consider to try to best compensate for this. I have to plead ignorance on my behalf because I haven't done any studies really or any simulations. I'm wondering if you or anyone else at Aerospace has pursued this with different choices for simulation.

HENRY FLIEGEL: No, I told our sponsor that for the limited amount of money that he paid us, he gets about this much and no more. It would really take quite a bit of effort to simulate in detail what that Kalman filter is doing. And frankly, I don't think I have the expertise myself, but of course there are other people at Aerospace Corporation that do. But we would have to be turned on by the Air Force or by somebody that has a charge number.

GERNOT WINKLER (INNOVATIVE SOLUTIONS INT'L): I have two comments or questions to ask you for your reaction to that. Number one, you said that the Kalman filter has no place to put these residuals; or better, that they will not be able to show up in the ephemeris part because it does not agree with the observations.

But there's one parameter which is very sensitive, and that's the frequency offset in the clocks. You have any error in the frequency offset in the clocks, it will, of course, accumulate since the clock offset will be larger proportional to the time offset since the last upload. But that's the most sensitive part, and I'm not sure if your conclusion is correct in that regard.

Number two, for most time users who use GPS, they're exactly those which you have excluded from your consideration, because they do observe the satellites in 30-minute passes; and an apparent frequency offset of 10 to the minus 10th in 30 minutes produces an offset of more than 10 nanoseconds. And that's really the explanation for the bowing effect, isn't it?

HENRY FLIEGEL: I wonder if it is. Let me deal with your last point first. Of course, we are concerned that some users may in fact be affected by this. That's why we're putting out the report. And I don't know whether perhaps the bowing effect is at least part due to this, other parts, ionosphere and what have you.

To get back to your first point, remember, though, that we're continually reporting the measured offset of each clock in the system from GPS time. So we're absorbing and reporting the very thing that you're talking about.

GERNOT WINKLER: Excuse me, yes, of course, during the time when your Monitor Station sees the clock. But you're uploading predicted information. It is here that the residual error in the frequency offset will become important.

HENRY FLIEGEL: It may. But remember, the effect repeats – at least, in my calculations – day after day after day. So essentially, if you take a mean value for a given day, probably the predictions will not be too badly impacted.

My other point was I said only it would be very difficult to alias clock error into ephemeris to any large extent. But I'm not saying that the clock error has just disappeared.

CARROLL ALLEY (UNIVERSITY OF MARYLAND): I'm happy to hear Henry agree at the end that one should look very carefully at the details of the relativistic physics. And it has been my contention that if one does that, software changes alone in the current system might bring these UREs down below the 1-meter level, and get actual user performance down at the one to 2-meter level with the existing system. And it has been very difficult to get into the

system and to get the adequate support to do these studies. But I'm very happy that there seems to be an agreement that one should do this. It is not an expensive matter compared to the 10 or 12 billion that's being invested in the GPS.

I would like to make another point. When one looks at differential GPS, the correction that needs to be made primarily is the difference between the radial distance in the ephemeris and the time reading on the satellite. And I believe this comes in because of a mix-up, or aliasing if you will, between these two quantities in the iteration procedure that the Kalman filter is following. And that if one perhaps does the explicit recognition of the special relativistic effects – I mean, it took a long time to get general relativity down properly, but I think that is more or less correct now. But it's the absence of any explicit acknowledgment of special relativistic effects due to the speed of light being the same whenever measured by an observer, leading to the relativity of simultaneity and the associated Lorentz transformation physics – there's nothing of that at all modeled in the current system, and I think it should be. Thank you.

OPERATIONAL USE OF THE HADAMARD VARIANCE IN GPS

Steven T. Hutsell
USNO Alternate Master Clock
400 O'Malley Ave., Ste. 44
Falcon AFB, Colorado 80912-4044, USA

Wilson G. Reid
U. S. Naval Research Laboratory

1Lt Jeffrey D. Crum, USAF
2d Space Operations Squadron

1Lt H. Shawn Mobbs, USAF
2d Space Operations Squadron

James A. Buisson
Antoine Enterprises Inc.
Consultant to SFA, Inc.

Abstract

With upcoming GPS Block IIR launches scheduled, rubidium clock estimation will require more attention than ever before during the next decade of GPS operations. GPS Master Control Station (MCS) estimation architecture relies on a three-state polynomial clock model, which does not include a time-variant decay parameter for frequency drift. Since current GPS rubidium frequency standards exhibit significant time-dependent frequency drift changes, the MCS is compelled to make precise utilization of the random run FM process noise parameter, known as q_3 .

The work of various scientists over the past three decades has shown the Hadamard variance to converge for random run FM. At PTTI '95, the 2d Space Operations Squadron (2 SOPS) introduced an algorithm^[1] that presented a simple, convergent polynomial relationship between the Hadamard variance and the MCS's Kalman filter process noise parameters. Until recently, however, neither the Hadamard variance nor the Hadamard-Q equation had actually been put to use in GPS.

The Naval Research Laboratory (NRL) has now created analysis software designed to employ the Hadamard variance in their GPS clock analyses, to supplement their already existing software, which makes use of the Allan variance. This paper presents results of the NRL analysis using both the Allan and Hadamard variances for several operational GPS rubidium frequency standards, as well as results from the recent operational use of the Hadamard-Q equation, by 2 SOPS personnel, based on the NRL analysis data.

INTRODUCTION

The three-sample (Hadamard) variance equation has sporadically appeared in publications related to timing over the past three decades^[2]. In 1995, the 2d Space Operations Squadron (2 SOPS) reviewed the Hadamard variance for its potential use in GPS^[1]:

$${}_H\sigma_y^2(\tau) = \frac{1}{6(M-2)} \sum_{i=1}^{M-2} (\bar{y}_{i+2} - 2\bar{y}_{i+1} + \bar{y}_i)^2, \quad \bar{y}_i = \text{the time-averaged frequency over } \tau_i. \quad (1)$$

Since the Hadamard variance converges for two more noise types than the Allan variance, namely $\alpha = -3$ and $\alpha = -4$ (Figure 1), the Hadamard variance ideally corresponds to the noise types modeled by the GPS Master Control Station (MCS). 2 SOPS documented this relationship as follows^[1]:

$$H\sigma_y^2(\tau) = (10/3)q_0\tau^2 + q_1\tau^1 + (1/6)q_2\tau + (11/120)q_3\tau^3 \quad (2)$$

where q_1 , q_2 , and q_3 are the MCS's continuous time update clock process noise parameters, and q_0 is the parameter designed for representation error. The MCS Kalman filter employs process noise parameters to increase elements in the MCS Kalman filter's state covariance matrix during time update predictions. This compensation effectively models GPS frequency standards as having three individual random walk processes. The representation error parameter helps to compensate for white/flicker PM noise, some, but not all, of which is caused by the frequency standard itself. The relations between the noise types, spectral density exponents, and applicable Kalman filter parameters are tabulated in Figure 1^[1].

NRL HADAMARD VARIANCE SOFTWARE

Since the inception of GPS, the Naval Research Laboratory (NRL) has played an integral role in GPS frequency standard development and analysis^[3]. In recent years, NRL's on-orbit clock analysis has provided the valuable independent agency support to 2 SOPS necessary to ensure the integrity of GPS, upon which the navigation and timing communities have become dependent.

In the past two years, NRL has become a critical element in the optimization of GPS accuracy. Since October 1994, 2 SOPS has depended on NRL clock stability data as the means for fine-tuning GPS clock estimation in the MCS^[4]. The unique knowledge and experience levels of NRL personnel contribute to timely, understandable, and very presentable analysis updates, technical notes, and quarterly reports. By interfacing with personnel from 2 SOPS and the United States Naval Observatory (USNO), NRL is able to make intelligent judgments for refining, adjusting, and applying the appropriate corrections to raw data, resulting in analysis documents that are extremely useful and applicable to the GPS frequency standard community.

NRL's analysis capability utilizes data from timing receivers operated by both USNO and the National Imagery and Mapping Agency (NIMA). These data include measurements of GPS frequency standards referenced to the Department of Defense (DoD) Master Clock at USNO. In early 1996, NRL began studying the utility of the Hadamard variance, using both simulated data and real-world GPS frequency standard measurements^[5]. By modifying already existing software extensively refined for Allan variance analysis, in April 1996, NRL began including Hadamard deviation (the square root of the Hadamard variance) plots in many of their reports to 2 SOPS^[6]. Since then, NRL has produced Hadamard deviation analyses on all 12 rubidium frequency standards that have been activated on GPS Block II/IIA satellites^[7].

Many clock scientists have studied rubidium frequency standard stability using the Allan variance. These studies have usually demonstrated the dominating effect of frequency drift. For GPS Block II/IIA frequency standards, this effect is typically dominant even at $\tau = 1$ day. Figure 2 presents a composite of Allan deviation plots for several GPS rubidium frequency standards, showing the effect of this dominance.

As a result, many have applied linear frequency drift corrections to their clock data, prior to performing Allan deviation calculations against their data. This technique *can* work, assuming that the resulting data will still produce convergent results. This assumption holds when the *changes* in frequency drift are

insignificant. The smaller the time span of data used, the more likely this assumption can hold true. However, several papers in previous years have confirmed that, for Block II/IIA rubidium clocks, these changes are not trivial, and hence, such an assumption often will not hold. Figure 3 plots the step-corrected frequency offsets of nine Block II/IIA rubidium frequency standards, with respect to the DoD Master Clock, over the operational lifetimes of each respective clock. The frequency drift, detectable in the general slope, appears to change somewhat randomly, and differently between the respective clocks.

Figures 4 and 5 show an NRL comparison of linear-aging-corrected Allan deviation curves and the Hadamard deviation curves for nine Block II/IIA rubidium frequency standards, using the same spans of data for each clock's respective curve. The respective spans of data exclude initial warm-up time and end-of-life times during which several of the Block II/IIA rubidium clocks experienced frequency anomalies^[8]. This comparison produces three notable findings: 1) The Allan deviation plots, generally speaking, show higher values than those corresponding to the Hadamard deviation. 2) For equal τ values, the Allan deviation often tends to *insinuate* a higher order (lower α) noise type than what the Hadamard deviation will show. 3) The presence of random walk FM, commonly thought to be high in magnitude on GPS rubidium frequency standards, does not necessarily appear as dominant in the Hadamard deviation plots for several of the frequency standards.

These discoveries suggest that the relatively high Allan deviation values for τ values as little as 1 day and as large as 24 days appear to be significantly aliased by the non-trivial effects of changing frequency drifts. This conclusion strongly supports the use of Hadamard variance for long-term rubidium frequency standard analysis, simply because stochastic changes in frequency drift tend to show up on the Hadamard deviation as random run FM, and *not* as unwanted perturbations to stability calculations for smaller τ values. This minimization of aliasing, therefore, permits more precise determination of the magnitude of the lower order (higher α) noise types.

OPERATIONAL USE OF THE HADAMARD-Q EQUATION

Applying and fitting equation (2) to the data plotted in Figure 5 produces a wide variation of q values across the nine Block II/IIA rubidium frequency standards that have operated longer than four months. These variations are listed below and plotted in Figure 6.

SVN/FS#	Time Span	q_1 (s ² /s)	q_2 (s ² /s ³)	q_3 (s ² /s ⁵)
16/2	Aug 89-Jan 91	3.3 E-21	3.5 E-30	6.0 E-43
19/2	Dec 94-Present	1.8 E-22	1.3 E-31	4.4 E-44
20/2	Aug 94-Jan 96	1.5 E-22	1.5 E-33	3.0 E-46
24/1	Jan 94-Jul 95	2.3 E-22	4.5 E-33	3.8 E-45
24/2	Jul 95-Present	1.0 E-22	4.2 E-32	1.1 E-43
25/2	Mar 92-Dec 93	6.0 E-22	8.0 E-33	1.0 E-45
31/2	Jan 95-Present	1.0 E-22	6.0 E-32	9.0 E-44
32/2	May 95-Aug 96	8.0 E-22	1.0 E-31	4.0 E-45
36/2	Mar 94-May 95	2.3 E-22	1.5 E-32	4.5 E-44

Note that white/flicker PM does not usually show up on either the Allan or Hadamard deviation plots for τ values greater than or equal to 1 day. The MCS's parameter analogous to q_0 , known as the measurement noise increment value, is designed to account for general modeling errors, as well as white/flicker PM. The

MCS currently uses 0.74 m^2 for its measurement noise increment^[4]. Operators at 2 SOPS are currently focusing on fine tuning GPS satellite ephemeris and solar state estimation. A significant refinement in this area could reduce observed periodic effects of ephemeris cross-corruption into GPS clock state modeling, and thus could permit 2 SOPS to lower their q_0 values at a future date. Until such a time, personnel at 2 SOPS intend to keep this parameter fixed and equal for all satellites.

2 SOPS first used the Hadamard-Q equation operationally for the estimation of rubidium frequency standard #2 on SVN32. It's Hadamard deviation signature, based on a data span from May 1995 to May 1996, is replicated in Figure 7^[9]. The qs produced from this data, as compared to the old qs , are as follows:

SVN32	Time Span	$q_1 (\text{s}^2/\text{s})$	$q_2 (\text{s}^2/\text{s}^3)$	$q_3 (\text{s}^2/\text{s}^5)$
Old qs :	N/A	1.11 E-22	3.33 E-32	1.35 E-43
New qs :	May 95-May 96	6.66 E-22	1.35 E-31	1.66 E-43

Note that the new q_1 and q_2 values were both significantly larger than the older values. Prior to the NRL's Hadamard variance analysis, 2 SOPS had no integral operational means to validate the qs that the MCS had been using for rubidium clocks^[4]. The application of the Hadamard-Q equation using NRL's data has produced an unaliased, convergent result for operational use. 2 SOPS installed these new qs shortly after receipt of the report. Unfortunately, 2 SOPS had to deactivate SVN32's rubidium frequency standard #2 on 19 August 1996, shortly after the installation of these qs .

Currently, 2 SOPS makes use of q values produced by the Hadamard-Q equation for the clock state estimation of the three currently operational GPS rubidium frequency standards. SVN40's rubidium frequency standard #2, active from 1 August 1996 until 29 November 1996, did not operate long enough to produce a span of data sufficient for a Hadamard variance plot with acceptable confidence.

CONFIDENCE INTERVALS

To exploit Hadamard variance information for fine tuning MCS qs , the Hadamard deviation plots must have large enough τ values to show distinct signs of random run FM. As Figure 4 indicates, random run FM can *start* to appear for τ values ranging between 7-24 days. One *single* calculation of the third difference, for $\tau = 24$ days, requires 73 days of data. Furthermore, an adequate span of data is necessary to produce stability estimates with sufficiently small confidence intervals, for each respective τ value.

The Hadamard variance requires roughly 50 % more data to produce a single stability calculation, as compared to the Allan variance, given equal τ values. This requirement stems as a direct result of the Hadamard variance employing a third difference, as opposed to the Allan variance, which makes use of a second difference. In other words, given equal spans of data, using the Hadamard variance instead of the Allan variance reduces the degrees of freedom by one^[5]. The direct implication of this freedom reduction is that the Hadamard variance requires sufficiently larger spans of data in order to produce estimates with confidence limits comparable to those produced by the Allan variance.

Generally speaking, Hadamard variance analysis requires a minimum of about 8-10 independent calculations of the third difference to produce acceptable confidence in the stability value corresponding to a given τ . The need to calculate Hadamard deviations for τ values of about 24 days mandates the use of

about eight months of continuous data, to produce plots usable for Block II/IIA rubidium clock q derivation.

Intuitively, this requirement imposes a challenge, given the recent operational history of rubidium clocks. As documented during PTTI '95, Block II/IIA rubidium frequency standards have typically had unexpectedly short lifetimes. To date, *not one* of the 12 activated clocks has lasted as long as *two years*^[8]. By comparison, some Block II/IIA cesium clocks have outlasted the mean mission duration (six years) of the satellite. If this adverse trend continues, whenever NRL and 2 SOPS produce a set of q values suitable for use in the MCS, chances are that the rubidium clock in question may have already functioned for the *majority* of its operational lifetime. Hence, the Hadamard-Q equation can prove useful only if the frequency standard itself can operate for a sufficient duration *after* the derivation and implementation of the qs for that clock.

Note, however, that the windfall of the requirement for large spans of data is that the Hadamard variance produces confidence intervals that are *legitimate* in the presence of random run FM. Though Allan variance values may *appear* to show more confidence for GPS rubidium frequency standards, this "confidence" can prove to be misleading. The Allan variance, and for that matter, any stability metric, is valid *only* when it is convergent. Once that assumption is violated, as in the case of random run FM, the validity of the stability metric (in this case, the Allan variance) is in question.

TIME-VARIANT DECAY OF RUBIDIUM FREQUENCY DRIFT

Since the creation of rubidium frequency standards, many analysts have employed various techniques for applying *dynamic* corrections for frequency drift, as methods for removing systematic error from clock data, prior to analyzing the clock stability using the Allan variance. William J. Riley has intelligently employed such a technique for ground-test analysis of EG&G's space-rated production rubidium frequency standard, which will serve as the primary type of frequency standard for GPS Block IIR satellites. His technique models frequency as having a logarithmic decay^[10]. This type of model represents the decay of its derivative (frequency drift) as an inverse function of time, described by:

$$\text{Frequency Drift} = D_0 + AB/[B(T-T_0) + 1], \quad (3)$$

where D_0 is analogous to the currently existing MCS variable for frequency drift, which can be modeled as an estimable, random walk process; A and B are coefficients tunable to the magnitude and effective rate of the decay; T is the current Kalman filter time; and T_0 is the "reference time" against which the current Kalman filter time, T , is differenced, and to which the coefficients A and B are referenced.

Figure 8 shows an Allan deviation plot of several EG&G rubidium frequency standards, using data artificially corrected for the logarithmic decay modeling technique. The use of such techniques, along with the resurgence of the Hadamard variance, combined with the recently growing attention towards the Block IIR program, has initiated some very valuable discussion concerning the purpose of clock stability metrics.

The primary utility of a stability metric in GPS is its ability to quantify the *predictability* of a given frequency standard. One could think of a GPS atomic frequency standard's main purpose as its ability to physically predict time for spans ranging between 1.5 seconds and 210 days. Physical prediction is often augmented with clock modeling, as a prediction supplement. In such a scenario, as in the case of GPS, the predictability of an on-orbit clock is not only dependent on the performance of the frequency standard, but

is also limited by the sophistication of the *predictor*. Operationally speaking, the predictability of the system is only as good as the least sophisticated of the contributing elements, i.e., *a chain is only as strong as its weakest link*.

The current GPS estimation architecture relies on a three-state polynomial clock model, whose prediction during time updates uses the following polynomial expansion^[11]:

$$\begin{bmatrix} x(t+\tau) \\ y(t+\tau) \\ z(t+\tau) \end{bmatrix} = \begin{bmatrix} 1 & \tau & (1/2)\tau^2 \\ 0 & 1 & \tau \\ 0 & 0 & 1 \end{bmatrix} \begin{bmatrix} x(t) \\ y(t) \\ z(t) \end{bmatrix} + \begin{bmatrix} \Delta x \\ \Delta y \\ \Delta z \end{bmatrix} \quad (4)$$

where τ is the prediction span, and $x(t)$, $y(t)$, and $z(t)$ are the phase, frequency, and frequency drift values, respectively, of the clock in question. Note that $y(t)$ is the time derivative of $x(t)$, and $z(t)$ is the time derivative of $y(t)$. $\Delta(x)$, $\Delta(y)$, and $\Delta(z)$ are random error increments, independent of $x(t)$, $y(t)$, and $z(t)$, having a prediction covariance P represented by a function of the Kalman filter process noises (qs)^[41]:

$$P = E \left[\begin{bmatrix} \Delta x \\ \Delta y \\ \Delta z \end{bmatrix} \begin{bmatrix} \Delta x & \Delta y & \Delta z \end{bmatrix} \right] = \begin{bmatrix} q_1\tau + q_2\tau^3/3 + q_3\tau^5/20 & q_2\tau^2/2 + q_3\tau^4/8 & q_3\tau^3/6 \\ q_2\tau^2/2 + q_3\tau^4/8 & q_2\tau + q_3\tau^3/3 & q_3\tau^2/2 \\ q_3\tau^3/6 & q_3\tau^2/2 & q_3\tau \end{bmatrix} \quad (5)$$

Note that, currently, *no* parameters representing any type of time-variant decay of frequency drift exist within the GPS estimation architecture. EG&G has successfully demonstrated how a logarithmic model can well represent the major systematic component of a changing frequency drift^[11]. Additionally, another available decay modeling technique is the exponential model. Implementation of an exponential model would involve the inclusion of additional Kalman filter parameters, used as follows^[12]:

$$\text{Frequency Drift} = D_0 + D_1[e^{**}\{D_2(T-T_0)\}], \quad (6)$$

where D_0 is the currently existing MCS variable for frequency drift, which effectively models frequency drift as an estimable, random walk process; D_1 and D_2 are coefficients designed to represent the initial magnitude and effective rate of decay, respectively; T is the current Kalman filter time; and T_0 is the "initialization time" against which the current Kalman filter time, T , is differenced.

Nonetheless, until such a time that GPS can take advantage of logarithmic or exponential compensation for systematic changes in frequency drift, the Hadamard variance is the *sole* available metric that best represents the predictability of rubidium frequency standards in GPS. A recent Hadamard variance analysis of an EG&G space-rated rubidium frequency standard, shown in Figure 9, suggests that, even using MCS prediction, Block IIR rubidium frequency standards look *very* promising in terms of stability/predictability^[11].

CONCLUSIONS

1. The GPS program would benefit from retaining the availability of the three random walk degrees of freedom for satellite Kalman filter clock estimation.
2. The GPS program should earnestly consider the incorporation of time-variant decay parameters, as described earlier, as *additional* degrees of freedom in GPS clock estimation architecture.
3. GPS clock stability plots using data preliminarily corrected for systematic errors, such as the logarithmically corrected Allan deviation, are useful for identifying the possible benefit of future systematic models within GPS estimation architecture.
4. The use of a clock stability metric for identifying the predictability of a clock within a given system is most representative when the metric corresponds to the predictor/estimator involved. As such, the Hadamard variance best corresponds to current GPS rubidium clock estimation architecture.
5. Analysts who present stability plots at various symposia can greatly help their audience by identifying their purpose behind their respective choices of stability algorithms. Though a systematically compensated stability plot may be useful for identifying removable systematics, it may prove misleading when trying to present performance metrics with a reasonable degree of fairness.
6. Generally speaking, the need to obtain sufficient confidence in the magnitude of random run FM, present in GPS rubidium clocks, necessitates using at least eight months worth of data, after initial clock warm-up.
7. The importance of the Hadamard variance will continue to increase as more GPS satellites operate rubidium frequency standards. The operational start of Block IIR program will induce a sharp increase in the use of rubidium frequency standards. This increased usage will further the importance of optimized extended autonomous navigation and timing predictions. Inaccurate estimation of frequency drift could result in hundreds of meters of ranging error, and microseconds of time transfer error during autonomous operations^[13,14]. With the first Block IIR launch scheduled for 1997, the role of the Hadamard variance will increase dramatically.
8. If GPS chooses to implement time-variant frequency drift decay models at a future date, any residual existence of unmodeled random run FM will emphasize the need for continued use of q_3 , and, thus, the Hadamard variance.

ACKNOWLEDGMENTS

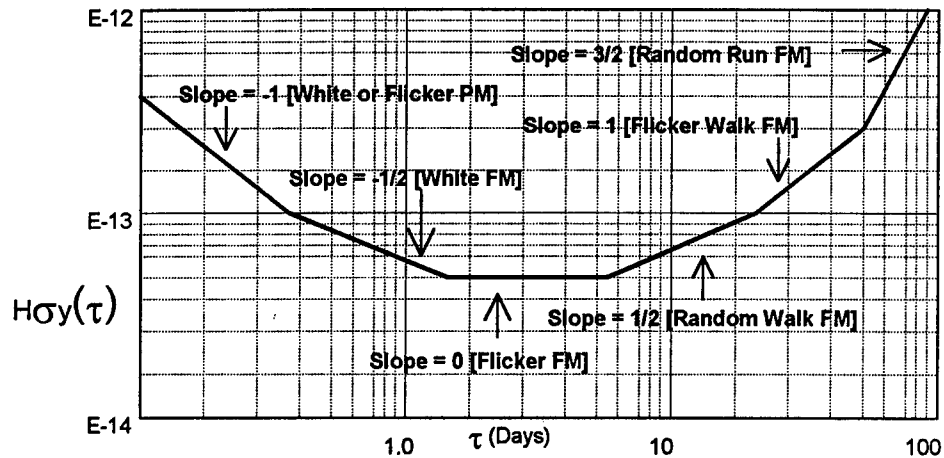
The authors wish to thank the following people and agencies for their generous assistance with both our timing improvements and this paper:

David W. Allan, Allan's TIME
Ronald L. Beard, NRL
Lee A. Breakiron, USNO
Thomas B. McCaskill, NRL
William J. Riley, EG&G

REFERENCES

- [1] S.T. Hutsell 1996, "*Relating the Hadamard variance to MCS Kalman filter clock estimation*," Proceedings of the 27th Annual Precise Time and Time Interval (PTTI) Applications and Planning Meeting, 29 November-1 December 1995, San Diego, California, USA (NASA CP-3334), pp. 291-302.
- [2] J. Rutman 1978, "*Characterization of phase and frequency instabilities in precision frequency sources: fifteen years of progress*," **Proceedings of the IEEE**, **66**, 1048-1075.
- [3] T.B. McCaskill, W.G. Reid, M.M. Largay, and J.A. Buisson 1985, "*On-orbit frequency stability analysis of the GPS NAVSTAR-1 quartz clock and the NAVSTARs-6 and -8 rubidium clocks*," Proceedings of the 16th Annual Precise Time and Time Interval (PTTI) Applications and Planning Meeting, 27-29 November 1984, Greenbelt, Maryland, USA, pp. 103-125.
- [4] S.T. Hutsell 1995, "*Fine tuning GPS clock estimation in the MCS*," Proceedings of the 26th Annual Precise Time and Time Interval (PTTI) Applications and Planning Meeting, 6-8 December 1994, Reston, Virginia, USA (NASA CP-3302), pp. 63-74.
- [5] T.B. McCaskill 1996, "*Analysis of NAVSTAR rubidium clocks using Allan and Hadamard variances*," NRL Technical Note No. 4, 16 April 1996.
- [6] W.G. Reid, and J.A. Buisson 1996, NRL Quarterly Report No. 96-2, 15 April 1996.
- [7] W.G. Reid, and J.A. Buisson 1996, "*Performance of Block II rubidium clocks*," NRL Technical Note No. 5, 8 October 1996.
- [8] G.L. Dieter, and G.E. Hatten 1996, "*Observations on the reliability of rubidium frequency standards on Block II/IIA GPS satellites*," Proceedings of the 27th Annual Precise Time and Time Interval (PTTI) Applications and Planning Meeting, 29 November-1 December 1995, San Diego, California, USA (NASA CP-3334), pp. 125-134.
- [9] W.G. Reid, and J.A. Buisson 1996, NRL Analysis Update No. 32-22, 9 May 1996.
- [10] W.J. Riley 1996, EG&G letter to the Aerospace Corporation, 12 September 1996.
- [11] F. Danzy, J.D. White, and R.L. Beard 1996, "*Long term testing of EG&G space rubidium clocks*," Performance Analysis Working Group, 21-22 August 1996, U.S. Naval Research Laboratory.
- [12] "*MCS Kalman filter*," USAF Second Space Wing Operations Mission Support Study Guide 3-01, 3rd edition, 8 March 1996.
- [13] D.W. Allan 1995, "*The impact of precise time in our lives: a historical and futuristic perspective surrounding GPS*," Proceedings of ION's 51st Annual Meeting, 5-7 June 1995, pp. 397-404.
- [14] K.R. Brown 1991, "*The theory of the GPS composite clock*," Proceedings of ION GPS-91, 11-13 September 1991, Albuquerque, New Mexico, USA, pp. 223-242.

NOISE TYPES IDENTIFIED BY THE HADAMARD DEVIATION



Noise Type	Power-Law Spectral Density Exponent	$H\sigma_y(\tau)$ Log-Log Slope	Process Noise Parameter
White PM	$\alpha = 2$	-1	q_0
Flicker PM	$\alpha = 1$	-1	q_0
White FM	$\alpha = 0$	-1/2	q_1
Flicker FM	$\alpha = -1$	0	
Random Walk FM	$\alpha = -2$	1/2	q_2
Flicker Walk FM	$\alpha = -3$	1	
Random Run FM	$\alpha = -4$	3/2	q_3

FIGURE 1

FREQUENCY STABILITY OF BLOCK II/IIA RUBIDIUM CLOCKS REFERENCE DOD MASTER CLOCK AGING UNCORRECTED

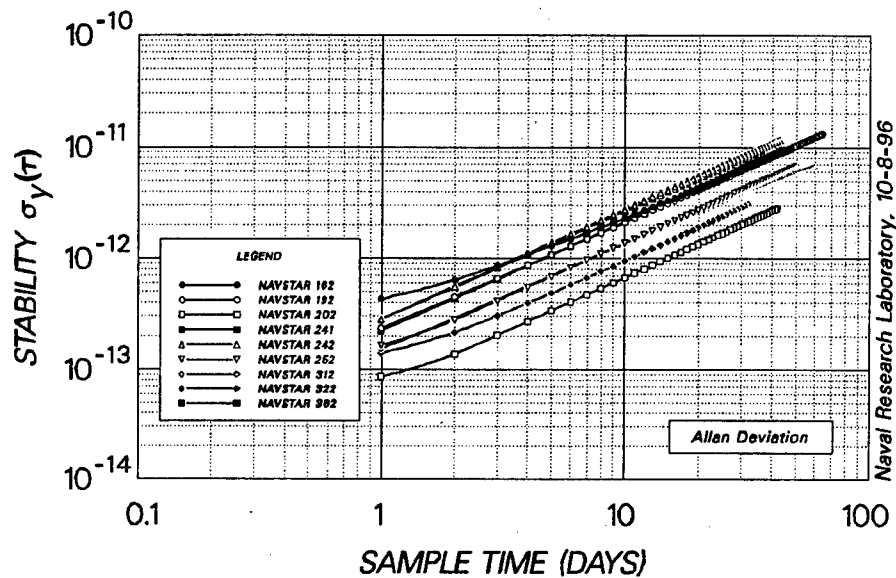


FIGURE 2

BLOCK II/IIA RUBIDIUM CLOCKS CORRECTED FREQUENCY OFFSET FROM DOD MASTER CLOCK

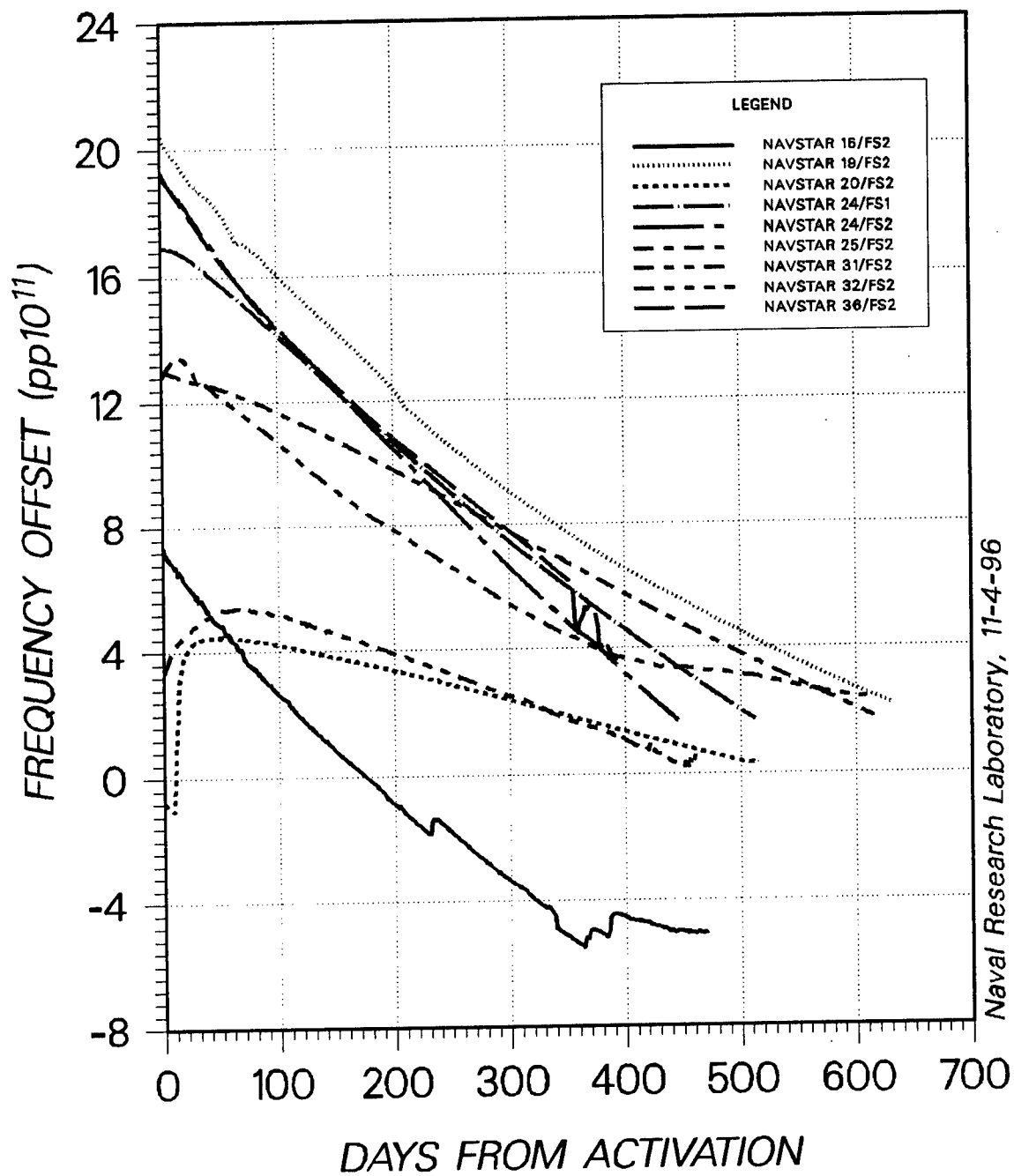


FIGURE 3

FREQUENCY STABILITY OF BLOCK II/IIA RUBIDIUM CLOCKS
REFERENCE DOD MASTER CLOCK
AGING CORRECTED

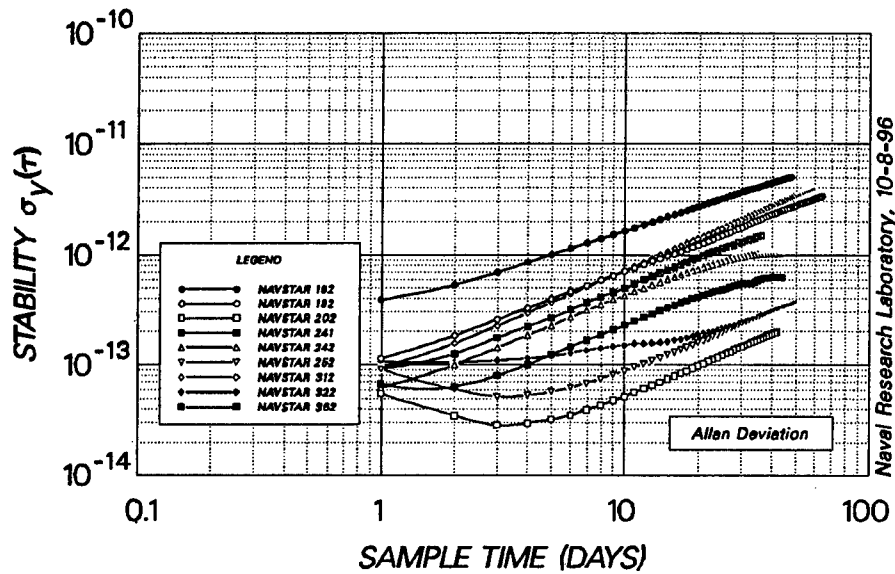


FIGURE 4

FREQUENCY STABILITY OF BLOCK II/IIA RUBIDIUM CLOCKS
REFERENCE DOD MASTER CLOCK

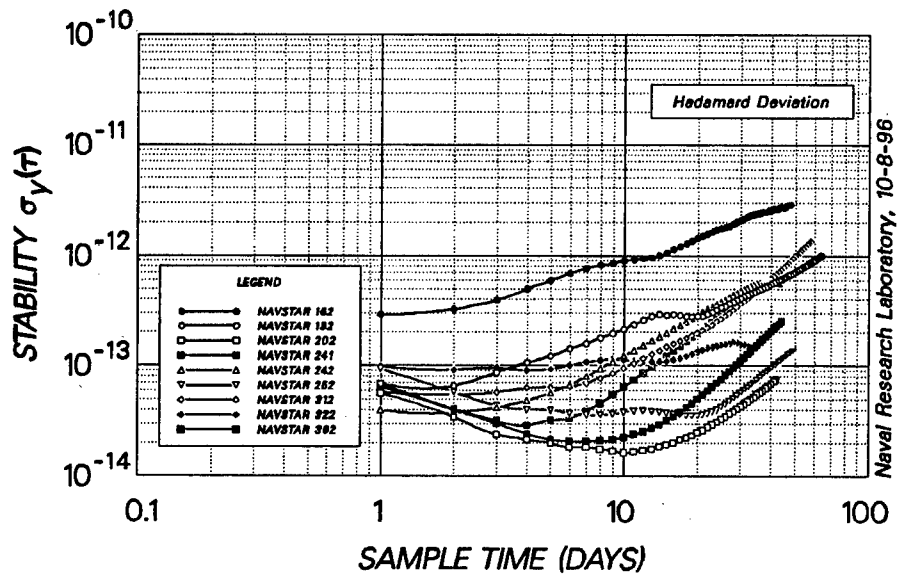


FIGURE 5

PROCESS NOISE COMPARISON

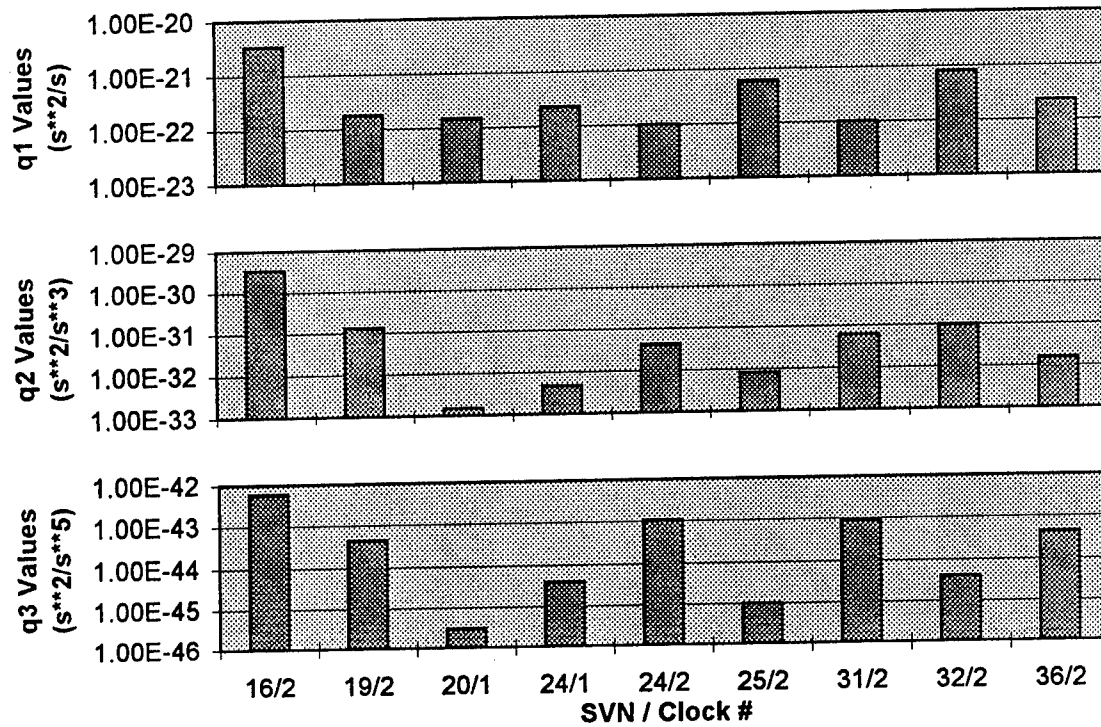


FIGURE 6

FREQUENCY STABILITY OF RUBIDIUM OSCILLATOR (NO.85)
 NAVSTAR 32 (Block II-16, Plane F-1)
 DoD Master Clock (PPS)
 13-MAY-95 to 4-MAY-96

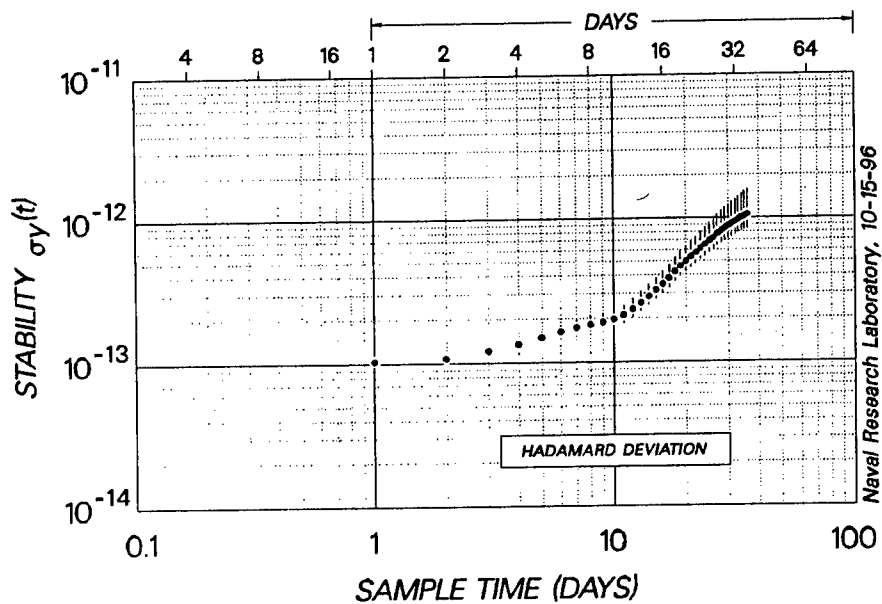


FIGURE 7

ALLAN DEVIATION: LOGARITHMIC FREQUENCY DECAY REMOVED

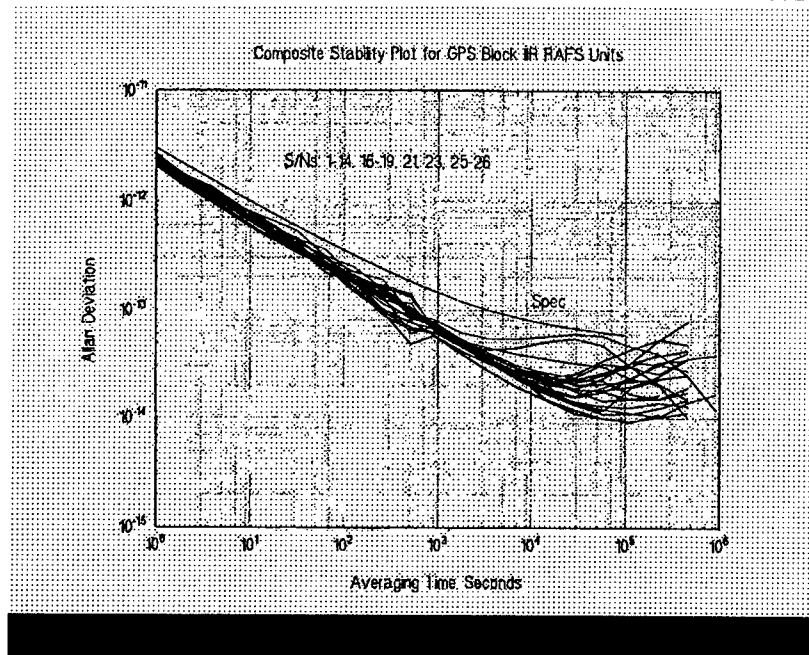


FIGURE 8

FREQUENCY STABILITY OF RUBIDIUM OSCILLATOR (NO.4)
 EG&G, INC.
 HYDROGEN MASER (NO.N1)
 25-OCT-95 to 11-APR-96

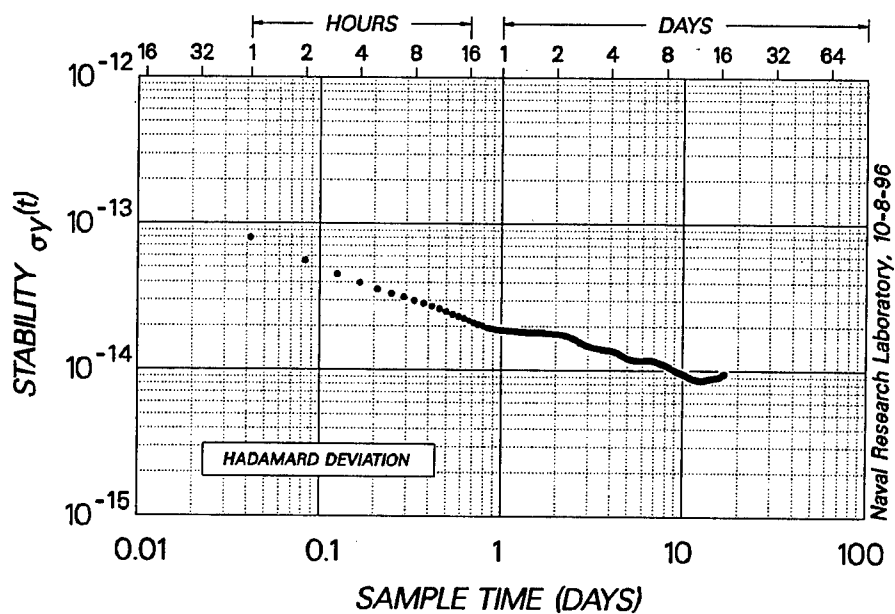


FIGURE 9

Questions and Answers

DAVID ALLAN (ALLAN'S TIME): I would like to commend you, Steve, for an outstanding paper and work. I think this is very commendable. I think with the change of the ability to characterize each individual clock in the constellation, we should see a significant improvement in the composite clock stability. And this should be very noticeable. We should see the long-term noise performance of the composite clock go down.

One question: Have you seen a logarithmic behavior on the orbit rubidiums? Have you tried to model those?

STEVEN HUTSELL: Let's put this plot up. It's hard to tell; I think in a couple of them, yes, you could probably very easily fit a logarithmic or exponential curve that will probably take out most of the rate of change. But on the others – you look at SVN 31, I believe it is – I don't know if that's something that would work best.

And the other challenge with that is we have to know what the coefficients of a logarithmic equation are ahead of time because we're doing real time or future prediction. It's a challenge. My general opinion about that is, I think the majority of systematic change on the IIR rubidiums is like what you said, a decay. But for II and IIAs, I think there's more noise occurring in it than systematic.

DAVID ALLAN: The other important point, I think, as we go into autonomous mode and long-term, if you even want to think about 180-day or 60-day autonomy, then your ability to predict behavior over much longer time is very important, having these long-term characterizations nailed down. So that should impact the autonomy as well.

The last point I'd like to make is the one you really made, but I'd like to hammer home with a big nail. That is that we ought not to model systematics with statistics. If we can get hold of a systematic, we should use our best estimator to deal with it because we'll do much better in prediction if we can model it using logarithmic or whatever best kind of modeling deals with the systematic and not do it statistically.

CARROLL ALLEY (UNIVERSITY OF MARYLAND): The short-term stability of rubidium standards, from the point of view of the user, needs to be emphasized, so that if you can go more to the rubidium standards with the modeling that you've suggested, it could have this other advantage as well.

STEVEN HUTSELL: Yes, our hope is that the reliability of the IIR rubidiums will surpass that of the II and IIA. There was a great paper presented last year by Capt. Greg Hatten and Lt. Gary Dieter discussing what was previously not really well known to the community; and that was the somewhat disappointing reliability of rubidium frequency standards in GPS.

But you're right. If you look at this – as a fair comparison, if you have white FM, given enough data to produce enough confidence, the Hadamard variance and the Allan variance will converge to the same number. That's only for white FM.

But as a comparison, you're seeing some frequency standards with stability on the order of 4 parts in 10 to the 14th, which is exceptional. And as you saw, the EG&G rubidium on the order of 2 parts in 10 to the 14th. Yes, I would agree.

A SIMPLE ALGORITHM FOR APPROXIMATING CONFIDENCE ON THE MODIFIED ALLAN VARIANCE AND THE TIME VARIANCE*

Marc A. Weiss
Time & Frequency Div., 847.5
National Institute of Standards and Technology
325 Broadway, Boulder, Colorado 80303, USA
(303) 497-3261

Charles A. Greenhall†
Jet Propulsion Laboratory
4800 Oak Grove Dr., 298-100, Pasadena, California 91109, USA
(818) 393-6944

Abstract

An approximating algorithm for computing equivalent degrees of freedom of the modified Allan variance and its square root, the modified Allan deviation (MVAR and MDEV), and the time variance and time deviation (TVAR and TDEV) is presented, along with an algorithm for approximating the inverse chi-squared distribution. These two algorithms allow relatively simple computations of confidence intervals on MDEV and TDEV, the latter currently used as a standard in the telecommunications industry. These algorithms enable users to present variance results with confidence intervals corresponding to any useful probability for most data lengths and noise types.

1 INTRODUCTION

We present here a simplified algorithm for calculating approximate confidence intervals on the modified Allan deviation, MDEV, and therefore also on the related time deviation TDEV. The algorithm has two parts: the first gives approximate equivalent degrees of freedom, edf, for the fully overlapped estimate of MVAR; the second gives approximate values of the inverse chi-squared distribution. An algorithm for estimating edf for the other measure commonly used in time and frequency metrology, the original Allan deviation, was published previously.^[1]

Confidence intervals are defined in terms of edf and the chi-squared distribution as follows. If s^2 denotes the usual sample variance of n independent and identically distributed Gaussian measurements (white noise) with actual variance σ^2 , then

*Contributions of the U.S. government are not subject to copyright.

†The work of this author was performed at the Jet Propulsion Laboratory, California Institute of Technology, under a contract with the National Aeronautics and Space Administration

$$U = \frac{s^2}{\sigma^2} \cdot \nu \quad (1)$$

has a chi-squared distribution with $\nu = n - 1$ degrees of freedom.^[2] In the classical situation, the number of degrees of freedom associated with σ^2 is an integer value depending only on the number of measurements, and exact confidence limits on the measurement variance are easily calculated using percentiles of the appropriate chi-squared distribution. For example, Figure 1 shows the chi-squared distribution with 10 degrees of freedom, and also depicts the percentiles a and b that are needed to calculate uncertainty bounds on σ^2 at the 0.95 confidence level from a particular s^2 based on 11 Gaussian measurements.

A 95% confidence interval is obtained as follows. First, we find values a and b such that the probability is 0.95 that U of Eq. (1) lies between a and b . This condition is equivalent to each of the following inequalities:

$$a < \frac{s^2}{\sigma^2} \cdot \nu < b;$$

$$\frac{\nu}{b} < \frac{\sigma^2}{s^2} < \frac{\nu}{a}; \quad (2)$$

$$\frac{\nu}{b} \cdot s^2 < \sigma^2 < \frac{\nu}{a} \cdot s^2.$$

The lower and upper bounds in the final inequality are confidence limits on the unknown variance σ^2 . Note that the confidence factors ν/b and ν/a needed in the calculations are independent of the actual data. They give the magnitude of the confidence interval as a function of the number of points used to compute the variance. Hence, we can compute these confidence factors for various data lengths. The factors $1 - \nu/b$ and $\nu/a - 1$ give the multipliers for the magnitude of the lower and upper confidence intervals on the variances, respectively. For deviations such as TDEV, the corresponding multipliers are $1 - \sqrt{\nu/b}$ and $\sqrt{\nu/a} - 1$.

Since the common time and frequency stability measures (AVAR, MVAR, TVAR) are calculated from data arising from non-white noise processes, the confidence limit procedure outlined above is an approximate method^[3] that is based on approximating the distribution of U in Eq. (1) with the chi-squared distribution with degrees of freedom

$$\nu = \frac{2(\sigma^2)^2}{Var(s^2)}, \quad (3)$$

where σ^2 represents the appropriate stability measure, TVAR, for example, s^2 represents its corresponding estimator, and $Var(s^2)$ is the variance of the s^2 estimator. The quantity ν , which now depends on the noise type, is called the equivalent degrees of freedom, edf, since it need not be integer-valued.

In this contribution we have combined a previously published edf approximation algorithm^[4] with an algorithm for approximating the inverse of the chi-squared distribution function. The latter algorithm is based on work of Barnes used in deriving tables in [5], but not published, and formulas from Abramowitz and Stegun (A&S).^[6] Previously, tables for confidence of TDEV and MDEV were published in [7]. These are exact computations for edf and the associated confidence intervals for various cases in computing TDEV and MDEV. We compare

values approximating the exact edf and confidence factors in tables in [7], finding a worst case disagreement of -9.7% for the edf and +10.8% for the confidence intervals. Most cases are much better than that. The confidence intervals are pessimistic if they are too large and optimistic if they are too small. In many cases here, pessimism is better than optimism, since the true value of the variance is more certain to lie in a larger range than a smaller. For the comparison with the published tables the confidence intervals are no smaller than -3.3%.

2 APPROXIMATION FOR EQUIVALENT DEGRESS OF FREEDOM

This version of the formula is restricted to the case of the usual fully overlapped estimator of MVAR or TVAR ([8], Eq. (12); [4], Eq. (6), $m_1 = 1$).

Let

N = number of time residuals,

m = averaging time / sample period,

$M = N - 3m + 1$, the number of terms summed in the estimate,

$q = M/m$.

Restrictions:

$N \geq 16$,

$m \leq N/5$.

The approximate edf is given by

$$edf = \frac{a_0 q}{1 - a_1/q}, \quad (4)$$

where a_0 and a_1 are given in Table I as functions of m and the noise type.

Table I. Coefficients for Approximate edf Calculation

Noise Type	$m = 1$		$m = 2$		$m > 2$	
	a_0	a_1	a_0	a_1	a_0	a_1
White PM	0.514	0	0.935	0	1.225	0.589
Flicker PM	0.576	0	0.973	0	1.003	0.602
White FM	0.667	0	1.010	0	0.968	0.571
Flicker FM	0.811	0	1.027	0	0.947	0.416
Random-Walk FM	1.000	0	0.866	0	0.768	0.411

Under the assumptions given above, a maximum error of 11.1% in this approximation has been observed. Usually, it is much less.

3 APPROXIMATION FOR INVERSE OF CHI-SQUARED DISTRIBUTION

Let U be a chi-squared random variable with ν degrees of freedom (ν can be nonintegral). Let $0 < p < 1$. Define $x = x(p, \nu)$ as the 100 p percentile of the distribution of U ; thus p is the probability that $U < x$. The algorithm given below computes an approximation to x .

Restrictions:

$$\nu \geq 1,$$

$$0.005 \leq p \leq 0.995.$$

Maximum observed error with these restrictions: 3%

if $p \leq \frac{1}{2}$ and $\nu \leq 10$ then

! Method: truncate power series in A&S [6] 26.4.6, invert by iteration

$$a = \nu/2$$

! Calculation of $G = \Gamma(1+a)$ (A&S 6.1.35)

$$\text{constants: } c_1 = -0.5748646, c_2 = 0.9512363, c_3 = -0.6998588, c_4 = 0.4245549, c_5 = -0.1010678$$

$n = \text{integer part of } a$

$$y = a - n$$

$$G = 1 + c_1 y + c_2 y^2 + c_3 y^3 + c_4 y^4 + c_5 y^5$$

for $k = 1$ to n ! Do nothing if $n = 0$

$$G = G(y + k)$$

next k

$$A = pG$$

$$u = 0$$

for $i = 1$ to 7

$$g = 1 + \frac{u}{a+1} \left(1 + \frac{u}{a+2} \left(1 + \frac{u}{a+3} \right) \right)$$

$$u = \left(\frac{Ae^u}{g} \right)^{1/a}$$

next i

$$x = 2u$$

else

! Method: A&S 26.4.17

$$p_1 = \min(p, 1-p)$$

! Calculation of $X = \text{inverse of normal distribution at } 1-p_1$ (A&S 26.2.22)

$$\text{constants: } a_0 = 2.30753, a_1 = 0.27601, b_1 = 0.99229, b_2 = 0.04481$$

$$t = \sqrt{-2 \ln p_1}$$

$$X = t - (a_0 + a_1 t) / (1 + b_1 t + b_2 t^2)$$

$$s = \text{signum}(p - \frac{1}{2}) \quad ! \quad \text{signum}(u) = 1 \text{ if } u > 0, -1 \text{ if } u < 0, 0 \text{ if } u = 0$$

$$b = 2 / (9\nu)$$

$$x = \nu \left(1 - b + sX\sqrt{b} \right)^3$$

4 A NUMERICAL EXAMPLE

Before giving tabular results, we show by example how they are used and how they are calculated by the algorithms given above. Assume the situation of the last line of Table II below: white PM noise, 1,025 time residuals, and averaging time = 128 sample periods. Suppose that an MDEV value s is computed by a fully overlapped estimate. The tabulated 95% lower and upper factors are 33.89% and 104.1%. Therefore, a 95% confidence interval for the true MDEV is 0.661 s to 2.041 s .

The tabulated edf and confidence factors are obtained as follows: $N = 1,025$, $m = 128$, $M = 1025 - 3 \times 128 + 1 = 642$ (the number of summands in the estimate), $q = M/m = 5.0156$, $a_0 = 1.225$, $a_1 = 0.589$ from Table I, edf = 6.9617 from Eq. (4). For 95% confidence we need to compute the 2.5% and 97.5% chi-squared levels. The inverse chi-squared algorithm, with $\nu = 6.9617$ and $p = 0.025$, gives $x = 1.6720$ as the 2.5% level, denoted by a in Eq. (2). Similarly, the 97.5% level is 15.928, denoted by b . The computed confidence factors are $1 - \sqrt{\nu/b} = 0.3389$, $\sqrt{\nu/a} - 1 = 1.0405$. (Note that the values in Table II were computed from values of a_0 and a_1 having more significant digits than the ones given in Table I.)

5 RESULTS

The data in the tables are the results for white PM with fully overlapped estimates. Table II gives the approximate edf and confidence factors. Table III gives the percentage errors from the exact values as found in [7]. The errors for white PM are the largest of the various noise types.

6 REFERENCES

- [1] C.A. Greenhall 1991, "Recipes for degrees of freedom of frequency stability estimators," *IEEE Transactions on Instrumentation and Measurement*, IM-40, 994-999.
- [2] P.G. Hoel 1971, *Introduction to Mathematical Statistics* (John Wiley & Sons, New York, New York, USA).
- [3] D.B. Sullivan, D.W. Allan, D.A. Howe, and F.L. Walls (eds.) 1990, *Characterization of Clocks and Oscillators*, National Institute of Standards and Technology Technical Note 1337.
- [4] C.A. Greenhall 1995, "Estimating the Modified Allan Variance," *Proceedings of the 1995 IEEE International Frequency Control Symposium*, 31 May-June 2 1995, San Francisco, California, USA, pp. 346-353.

- [5] D.A. Howe, D.W. Allan, and J. Barnes 1981, "*Properties of Signal Sources and Measurement Methods*," Proceedings of the 35th Annual Frequency Control Symposium, 27-29 May 1981, Philadelphia, Pennsylvania, USA, pp. 1-47 = NIST Technical Note 1337, TN14-TN60.
- [6] M. Abramowitz, and I. A. Stegun 1972, **Handbook of Mathematical Functions** (Dover, New York, New York, USA; republication, with corrections, of work originally published by the National Bureau of Standards, 1964).
- [7] M.A. Weiss, F.L. Walls, C.A. Greenhall, and T. Walter 1995, "*Confidence on the Modified Allan Variance and the Time Variance*," Proceedings of the 9th European Frequency and Time Forum (EFTF), March 1995, Besançon, France.
- [8] D.W. Allan, and J.A. Barnes 1981, "*A modified Allan variance with increased oscillator characterization ability*," Proceedings of the 35th Annual Frequency Control Symposium, 27-29 May 1981, Philadelphia, Pennsylvania, USA, pp. 470-474 = NIST Technical Note 1337, TN254-TN258.

Table II. Approximate edf and Confidence Factors

Noise Type: White PM

<i>N</i>	<i>m</i>	edf	lower 68%	upper 68%	lower 95%	upper 95%
17	1	7.714	17.74	39.14	32.79	94.61
17	2	5.610	19.67	50.41	36.24	128.7
33	1	15.94	13.65	23.38	25.52	52.42
33	2	13.09	14.71	26.67	27.40	60.97
33	4	7.543	17.87	39.82	33.03	96.58
65	1	32.40	10.29	14.96	19.46	31.99
65	2	28.05	10.91	16.33	20.60	35.19
65	4	17.29	13.23	22.17	24.78	49.37
65	8	7.241	18.12	41.10	33.47	100.3
129	1	65.31	7.622	9.916	14.58	20.63
129	2	57.97	8.030	10.62	15.33	22.17
129	4	36.86	9.746	13.84	18.48	29.42
129	8	16.98	13.33	22.43	24.94	50.03
129	16	7.091	18.24	41.78	33.69	102.3
257	1	131.1	5.579	6.715	10.76	13.74
257	2	117.8	5.857	7.123	11.28	14.60
257	4	76.04	7.128	9.095	13.66	18.84
257	8	36.55	9.780	13.91	18.54	29.58
257	16	16.83	13.37	22.56	25.02	50.36
257	32	7.016	18.31	42.13	33.80	103.3
513	1	262.8	4.045	4.610	7.856	9.332
513	2	237.5	4.241	4.867	8.229	9.864
513	4	154.4	5.177	6.141	10.00	12.53
513	8	75.73	7.141	9.116	13.68	18.89
513	16	36.40	9.798	13.95	18.57	29.66
513	32	16.75	13.40	22.63	25.07	50.53
513	64	6.978	18.34	42.30	33.86	103.8
1025	1	526.1	2.913	3.195	5.685	6.421
1025	2	476.9	3.052	3.363	5.954	6.766
1025	4	311.1	3.737	4.214	7.267	8.513
1025	8	154.1	5.182	6.148	10.01	12.54
1025	16	75.58	7.148	9.126	13.69	18.91
1025	32	36.32	9.806	13.97	18.59	29.70
1025	64	16.71	13.41	22.67	25.09	50.62
1025	128	6.959	18.36	42.39	33.89	104.1

Table III. Percentage Error: $100(\text{Approximate} - \text{Correct})/\text{Correct}$

Noise Type: White PM

<i>N</i>	<i>m</i>	edf	lower 68%	upper 68%	lower 95%	upper 95%
17	1	-3.4	0.2	2.2	1.0	3.2
17	2	-9.7	2.2	8.4	3.0	10.8
33	1	-1.6	-0.1	0.2	0.5	1.4
33	2	-4.2	0.8	2.0	1.4	3.7
33	4	3.4	-2.1	-2.9	-1.2	-3.1
65	1	-0.8	-0.3	-0.2	0.2	0.5
65	2	-2.0	0.1	0.5	0.6	1.3
65	4	3.9	-2.2	-3.3	-1.5	-2.6
65	8	-3.6	0.3	2.4	1.0	3.4
129	1	-0.4	-0.4	-0.4	0.0	0.1
129	2	-1.0	-0.2	-0.1	0.3	0.5
129	4	4.0	-2.3	-3.0	-1.7	-2.6
129	8	-2.9	0.4	1.1	1.0	2.3
129	16	-5.3	0.9	3.9	1.6	5.2
257	1	-0.2	-0.5	-0.5	-0.1	-0.1
257	2	-0.5	-0.4	-0.3	0.0	0.1
257	4	4.1	-2.4	-2.9	-1.9	-2.5
257	8	-2.7	0.5	1.0	1.0	1.7
257	16	-4.6	1.1	2.3	1.6	3.6
257	32	-5.8	1.0	4.3	1.8	5.7
513	1	-0.1	-0.5	-0.5	-0.1	-0.1
513	2	-0.2	-0.5	-0.5	0.0	0.0
513	4	4.1	-2.4	-2.8	-1.9	-2.4
513	8	-2.6	0.6	0.9	1.0	1.4
513	16	-4.4	1.2	2.0	1.7	2.8
513	32	-5.0	1.3	2.6	1.8	4.0
513	64	-5.9	1.0	4.4	1.8	5.8
1025	1	-0.1	-0.5	-0.5	-0.1	-0.1
1025	2	-0.1	-0.5	-0.5	-0.1	-0.1
1025	4	4.2	-2.5	-2.7	-2.0	-2.4
1025	8	-2.6	0.6	0.8	1.0	1.3
1025	16	-4.3	1.3	1.9	1.7	2.5
1025	32	-4.8	1.4	2.2	1.8	3.1
1025	64	-5.2	1.3	2.6	1.9	4.1
1025	128	-5.9	1.0	4.4	1.8	5.8

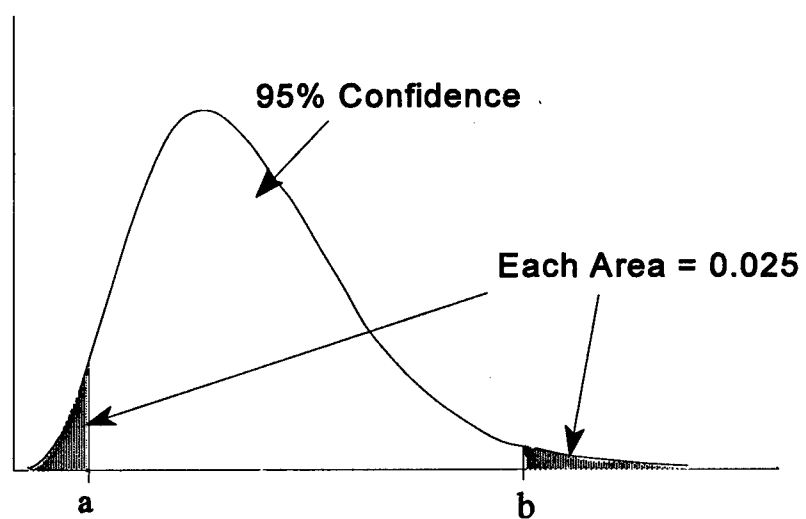


Figure 1 Finding the 95% confidence limits under the chi-squared distribution with 10 degrees of freedom.

Questions and Answers

JOHN DICK (JPL): Where does the number 68 percent come from? And what do you recommend as confidence limits in our use of error bars on Allan deviation plots?

MARC WEISS: Sixty-eight percent is a typical one sigma kind of number. When you take a standard deviation, it's typically a one sigma kind of number. Sixty-eight percent probability is one sigma on a normal distribution; that's where that came from. Ninety-five percent is two sigma. Three sigma is the 99 percent, I believe.

So that's where I chose those. Now which one to use depends on the application and how much you're willing to be wrong. If two times out of three is good enough, then one sigma's good enough. But if you want it to never fail, three sigma is not good enough.

I think that's a very important question. In our systems, we really need to think about what happens if they fail; and how much do we want to avoid that; and how much are we willing to pay for it. And when you write a spec, another big question is, "Should the confidence bars be included in the spec?" Should you write a spec that says, "The Allan variance shall not exceed this number with a 95 percent probability?" There are problems with that because if you do that, that's going to change how long you test the system in order to show it meets the spec.

ROBERT DOUGLAS (NRC, CANADA): In calculating the exact values, we presumably are using a Gaussian normal distribution so you can calculate the second moments. Is that right?

MARC WEISS: Do you want to answer that, Chuck?

CHARLES GREENHALL (JPL): Yes, we're assuming the second differences of phase are normal.

ROBERT DOUGLAS: Then my question is do you have any recommended procedures for checking that this is in fact true in our datasets?

CHARLES GREENHALL: No. There are tests for normal distribution.

PULSAR-APPROPRIATE CLOCK STATISTICS

Demetrios N. Matsakis and Frederick J. Josties
U.S. Naval Observatory
Washington, DC 20392, USA

Abstract

Because pulsar phase, spin rate, and spin-down rate cannot be determined a priori, a pulsar's possible contribution to a time scale is best measured using a statistic insensitive to these quantities. One such statistic is $\sigma_z(\tau)$ (Matsakis, Taylor, and Eubanks 1996, hereafter [1]), which is based upon the third-order polynomial variations of the clock phases and named in analogy to $\sigma_y(\tau)$. It is similar to measures based upon the variance of the third differences, but more robust in the presence of data gaps. About 6 years of data, from MJD 47752 to 50343 (18 Aug 89-17 Sep 96), were used to determine the $\sigma_z(\tau)$ of cesium and maser standards in a variety of imperfect but probably acceptable ways; directions for improved reductions are also indicated. Because of the considerably improved stability of cavity-tuned masers and Hewlett-Packard Model 5071 cesium standards, the best results use only the data taken since MJD 49400 (17 Feb 94), by which time most of the new standards had been acquired. An upper limit to the time variation of the fine structure constant is also given.

INTRODUCTION

The possibility of using the exceptional rotational stability of millisecond pulsars to generate a time scale has long been of interest.^[2-7] Although the phase, rate, and spin-down of their observed radio pulsations are physically meaningful (see [8]), they are not predictable on the basis of measurable quantities, so that their contribution to any state-of-the-art terrestrial time scale can only be to constrain derivatives of higher order than the frequency drift. While this precludes their use as absolute frequency standards, incorporating pulsar data in the time scale is still a highly worthy goal.

Clock data are commonly analyzed using a statistic called σ_y , the square root of the "Allan variance," which is proportional to the mean square of the second differences of a series of clock offset measurements. Second differences are used because they are insensitive to the clock phase offset and frequency bias, and because the frequency noise of these standards is often white over time scales of less than a few days or weeks. In the presence of arbitrary frequency drifts and the "redder" noise components which dominate these time series on longer time scales, it is a natural extension to consider statistics such as the Hadamard variance, which is based upon the third differences.^[9] Due to the irregular spacing of pulsar data, Taylor^[4] suggested use of a statistic analogous to the Modified Hadamard Variance, which he termed σ_z , which is related to a third-order fitted polynomial of the timing residuals; the definition of σ_z was slightly altered by Matsakis, Taylor, and Eubanks.^[1] This statistic describes the lowest-order deviations remaining in a pulsar time series after the phase, frequency, spin-down rate, and astrometric parameters have been determined by comparison with terrestrial time, and their effects removed.

Since σ_z is inherently insensitive to the pulsar properties which are observationally arbitrary, it is ideally suited for comparing pulsar stabilities with those of other time scales. Such comparisons are made in [1] and elsewhere; this paper presents an analysis of the σ_z characteristics of the individual frequency standards kept at the U.S. Naval Observatory (USNO).

THE USNO CLOCK DATA

The USNO clock data were taken using the Digital Acquisition System (DAS), and consist of hourly timing differences between the "zero crossings" of the 5 MHz signal output by individual frequency standards and the USNO Master Clock #2 (MC2), which is referred to as UTC(USNO) by the International Bureau of Weights and Measures (BIPM), and in this time period was the output of a maser steered daily toward the weighted mean of the USNO ensemble, which itself is steered toward TAI. Data from 70 Hewlett-Packard Model 5071 cesium standards and 12 cavity-tuned Sigma-Tau masers were used; data from older-style frequency standards were ignored. The data measurement precision was less than 35 picoseconds rms (Breakiron, private communication).

Individual clock differences with MC2 were converted to frequencies and edited for outliers. Four maser and five cesium clock time series with jumps were subdivided into two series each so as to avoid imposing large rate or drift jumps in the data. Data from one cesium clock were subdivided into three series. For four masers and ten cesium clocks, the need to break a time series up was not clear, and so both the original series and the "optional" subsets were retained. The number of standards plotted is, therefore, slightly larger than the number of physical clocks we had, and about double the number of standards currently used by the USNO to compute its time scales.

PAIRWISE COMPUTATION OF σ_z

Once the editing was complete, the σ_z statistic was generated for the difference series generated by subtracting each clock's frequency data from other clock data, from MC2, from the USNO mean, from the free-running USNO time scale A.1, from the spline-interpolated MC2-TAI, and from the spline-interpolated TT(96) time series, which is generated by the BIPM particularly for pulsar work (see [10]).

To compute (and define) σ_z using frequency data instead of timing residual data, the recipe given in [10] was adapted as follows:

1. For each clock, phase data pairs separated by 1 day were differenced to generate the frequencies $y(t_i)$.
2. The data were divided, according to time of measurement, into subsequences defined by continuous intervals of length τ .
3. By minimizing the weighted sum of squared differences, $[(y(t_i) - Y(t_i))]^2$, the data in each subsequence were modelled to the derivative of the cubic function used by [1]:

$$Y(t) = c_1 + 2 \times c_2(t_i - t_0) + 3 \times c_3(t_i - t_0)^2 \quad (1)$$

The weights were chosen to be unity. All overlapping subsequences were included if they contained four or more measurements and the interval between first and last measurement was

at least $\tau/\sqrt{2}$.

3. It follows that

$$\sigma_z(\tau) = \frac{\tau^2}{2\sqrt{5}} \langle c_3^2 \rangle^{1/2}, \quad (2)$$

where angle brackets denote averaging over the subsequences, weighted by the inverse squares of the formal errors in c_3 .

A comparison with analyses based upon the Hadamard variance, such as Hutsell^[11], Hutsell et al.^[12], and Walter^[13,14], can be made by noting that the "square root of the modified Hadamard variance" has a τ -dependence similar to that of σ_z , after allowance is made for the factor of $\sqrt{3/10}$ normalization difference and for the fact that the τ used here is three times larger than the τ used to define the Hadamard variance.

ESTIMATION OF INDIVIDUAL AND AVERAGE σ_z

If one is willing to make the questionable assumption, which is discussed in the next section, that the clock errors are independent and uncorrelated, then the σ_z^2 associated with each clock difference is equal to the sum of the "intrinsic" σ_z^2 variances of each clock. It then becomes mathematically possible to derive the individual variances from a least-squares fit to all pairs via an N-cornered-hat analysis, which is a weighted least-squares solution to find those values for individual clock σ_z^2 's which best fit the statistics of the clock pair-difference σ_z^2 's.

In the solutions individual clock pairs can be weighted in several ways. Solutions were generated by weighting each pair identically, by using the statistical weights derived from variances near τ of a month when compared to MC2, by downweighting or dewatering masers or cesiums, by excluding all but the best third of any type (as measured by their deviations from MC2 at intermediate periods), and by combinations of these. While there was not a large difference between the results of these weighting schemes for any given clock, the lowest individual variances usually were those inferred from the formal errors generated by assuming an identical "white" error dominating all measurements, so that the results depend only on the irregularities in data spacing.

Different solutions were found using subsets of the data. Lower variances were found if the data were restricted to be after MJD 49400, and still lower were found by excluding clocks which did not completely fill the interval from MJD 49400 to 50343.

In Figures 1 a-d the data for the individual cesium standards are plotted, using only data after MJD 49400 and weighting each clock pair by the formal error with MC2. Figure 2 is a similar plot for the masers. Note that individual standards can differ by an order of magnitude.

In Figures 3 and 4, various averages of the (non-imaginary) derived values of σ_z are plotted. Most of the curves are from estimates derived with different weighting schemes. Denoted with a "1" is the average when the standards are compared to MC2, while that with a "2" is the average comparing the standards to TAI. The curves are presented as an indicator of robustness. The limits to the technique are shown by the fact that the curves in Figure 3, which incorporate all the data, are higher than those in Figure 4, which are based on only data taken more recently than MJD 49400. The estimates in Figures 3 and 4 are not corrected for the bias due to the fact that the average measured value of σ_z^2 has a chi-squared distribution and for this distribution the median-centered logarithm of σ_z is lower than the average value

by $.017/n$, where n is the number of degrees of freedom.^[11] Applying this correction yields median-centered curves lower than the plotted figures. The difference, in logarithmic units, is .17 for the longest τ (7.9), and half as much for $\tau = 7.6$.

ROBUSTNESS OF THE SOLUTIONS

The N-cornered-hat method will not reveal any "external" error which is correlated with the ensemble average, and it is sensitive to the fact that the observed variances are themselves random variables (see [15]). It also can give highly erroneous results in the presence of large measurement noise, data gaps, nonstationarity, and nonzero correlations between clock outputs. Such problems often lead to the derivation of negative estimates for individual clock σ_i^2 s (which were discarded in this work). The derivation of negative variances increases with τ because the clock correlations fail to average to zero as the number of independent points decreases. Some benefit is gained from the stochastic character added to the covariance terms by data gaps and other irregularities.

In any event, the solution results do not appear to vary significantly when different weighting functions are used in the fit, and they are consistent with comparisons between each clock and TAI or the various USNO time series which are more accurate and stable than their components. Not surprisingly, the scatter between the different methods increases at the longest intervals, which is the regime where the approximations are most questionable.

It is possible to generate improved clock variances by making a definable and explorable set of assumptions about the characteristics of just one reference clock^[16-19] or through use of a reference time scale much more precise than the individual clocks. Using these variances, it is possible to estimate the characteristics of the noise. Although the presence of non-white noise is obvious in all the figures, we have not attempted to quantify its characteristics. This is best done by a multivariate approach^[13], which is based upon the use of complementary statistical measures, such as σ_y . We intend to address these problems in subsequent papers.

AN ASIDE ON COSMOLOGICAL IMPLICATIONS

It has been pointed out^[20] that variations in the fine structure constant, such as those predicted by recent grand unified theories and Dirac's Large Numbers Hypothesis, would lead to a differential drift in frequency standards which are based upon different atomic transitions. The frequency drifts of best-measured individual standards in this analysis range over 3×10^{-13} /year peak to peak, and we find no significant difference between the two types of standards to a 1-sigma upper limit of 2.5×10^{-14} /year. According to the formulas of [20], this corresponds to a limit of 3.2×10^{-14} /year in the fractional variation of the fine structure constant, and is similar to a limit they derive by comparing mercury- and hydrogen-based standards. It is possible that a large variation in the fine structure constant is being fortuitously masked in our data by some equally large (differential) instrumental effect common to one type of standard as maintained at the USNO. We consider this to be extremely unlikely because, if it were true, a different differential instrumental effect (of a specific magnitude) would also have to be present in the data analyzed by [20], which involved different atomic elements and different institutions—the mercury-based clocks were built by and maintained at the Jet Propulsion Laboratory and the primary cesium standards were built and maintained by the Physikalisch-Technische Bundesanstalt (PTB).^[21]

COMPARISONS WITH PULSAR DATA

The purpose of this paper is to present the observed clock statistics, but no discussion of those statistics would be complete without a comparison with pulsar data. In the last figure, data from Figures 3 and 4 of [1] are combined. The σ_x statistic of the timing difference between two pulsars and TAI are presented, as is the comparison between the free-running terrestrial time scales of the USNO (A.1) and the PTB, to which the BIPM steered TAI over the time range of the pulsar data. To generate these curves, data from MJD 44979 to 50079 were used (more recent data were not used because no high-quality pulsar data are available to us due to the Arecibo telescope upgrade work). Although one would infer from those curves that pulsar data can contribute meaningfully to time scales over periods exceeding a few years, the recent incorporation of HP 5071 cesiums and cavity-tuned masers into the terrestrial time scales results in none of the comparisons being stationary in a statistical sense. The lowest-lying curve shows the difference between the two terrestrial time scales when only the last 2 years of data are used, which corresponds to the introduction of the new standards. Since the pulsar data analysis necessarily depends upon comparison with the older time scales, an adequate pulsar database for comparison will not be available for several more years.

ACKNOWLEDGMENTS

We thank John Prestage, Marshall Eubanks, and Lee Breakiron for many helpful discussions.

REFERENCES

- [1] D.M. Matsakis, J.H. Taylor, and T.M. Eubanks 1997, submitted to *Astronomy and Astrophysics*.
- [2] D.C. Backer, S.R. Kulkarni, C. Heiles, M.M. Davis, and W.M. Goss 1982, "A millisecond pulsar," *Nature*, **300**, 615-618.
- [3] B. Guinot, and G. Petit 1991, "Atomic time and the rotation of pulsars," *Astronomy and Astrophysics*, **248**, 292-296.
- [4] J.H. Taylor 1991, "Millisecond pulsars, nature's most stable clocks," *Proceedings of the IEEE*, **79**, 1054.
- [5] V.M. Kaspi, J.H. Taylor, and M.F. Ryba 1994, "High-precision timing of millisecond pulsars. III. Long-term monitoring of PSRs B1885-109 and B1937+21," *Astrophysical Journal*, **428**, 713-728.
- [6] G. Petit 1996, "Limits to the stability of pulsar time," Proceedings of the 27th Annual Precise Time and Time Interval (PTTI) Applications and Planning Meeting, 29 November-1 December 1995, San Diego, California, USA (NASA CP-3334), pp. 387-396.
- [7] G. Petit, and P. Tavella 1996, "Pulsars and time scales," *Astronomy and Astrophysics*, **308**, 290-298.
- [8] D.N. Matsakis and R.S. Foster 1996, *Amazing Light*, ed. R. Chiao (Springer Press, New York, New York, USA), p. 445.
- [9] J.A. Barnes, and D.W. Allan 1967, "An approach to the prediction of Coordinated Universal Time," *Frequency*, **5**, 15.

- [10] B. Guinot 1995, "*Scales of time*," *Metrologia*, **31**, 431-440.
- [11] S.T. Hutsell 1996, "*Relating the Hadamard variance to MCS Kalman filter clock estimation*," Proceedings of the 27th Annual Precise Time and Time Interval (PTTI) Applications and Planning Meeting, 29 November-1 December 1995, San Diego, California, USA (NASA CP-3334), pp. 291-302.
- [12] S.T. Hutsell, W.G. Ried, J.D. Crum, H.S. Mobbs, and J.A. Buisson 1997, "*Operational use of the Hadamard variance in GPS*," these Proceedings.
- [13] T. Walter 1993, "*A multi-variance analysis in the time domain*," Proceedings of the 24th Annual Precise Time and Time Interval (PTTI) Applications and Planning Meeting, 1-3 December 1992, McLean, Virginia, USA (NASA CP-3218), pp. 413-426.
- [14] T. Walter 1994, "*Characterizing frequency stability: a continuous power-law model with discrete sampling*," *IEEE Transactions on Instrumentation and Measurement*, **IM-43**, 69-79.
- [15] P. Lesage, and C. Audoin 1973, "*Characterization of frequency stability: a continuous power law model with discrete sampling*," *IEEE Transactions on Instrumentation and Measurement*, **IM-22**, 157.
- [16] A. Premoli, and P. Tavella 1993, "*Estimating the instabilities of N clocks by means of comparison measurements*," Proceedings of the 24th Annual Precise Time and Time Interval (PTTI) Applications and Planning Meeting, 1-3 December 1992, McLean, Virginia, USA (NASA CP-3218), pp. 385-398.
- [17] A. Premoli, and P. Tavella 1993, "*A revised 3-cornered hat method for estimating frequency standard instability*," *IEEE Transactions on Instrumentation and Measurement*, **IM-42**, 7-13.
- [18] P. Tavella, and A. Premoli 1992, "*Characterization of frequency standard instability by estimating their covariance matrix*," Proceedings of the 23rd Annual Precise Time and Time Interval (PTTI) Applications and Planning Meeting, 3-5 December 1991, Pasadena, California, USA (NASA CP-3159), pp. 265-276.
- [19] P. Tavella, and A. Premoli 1994, "*Estimating the instabilities of N clocks by measuring differences of their readings*," *Metrologia*, **30**, 479-486.
- [20] J.D. Prestage, R.L. Tjoelker, and L. Maleki 1995, "*Atomic clocks and variations of the fine structure constant*," *Physical Review Letters*, **74**, 3511.
- [21] A. Bauch, K. Dorenwendt, B. Fischer, T. Heindorff, E.K. Müller, and R. Schröder 1987, "*CS2: The PTB's new primary clock*," *IEEE Transactions on Instrumentation and Measurement*, **IM-36**, 613-616.

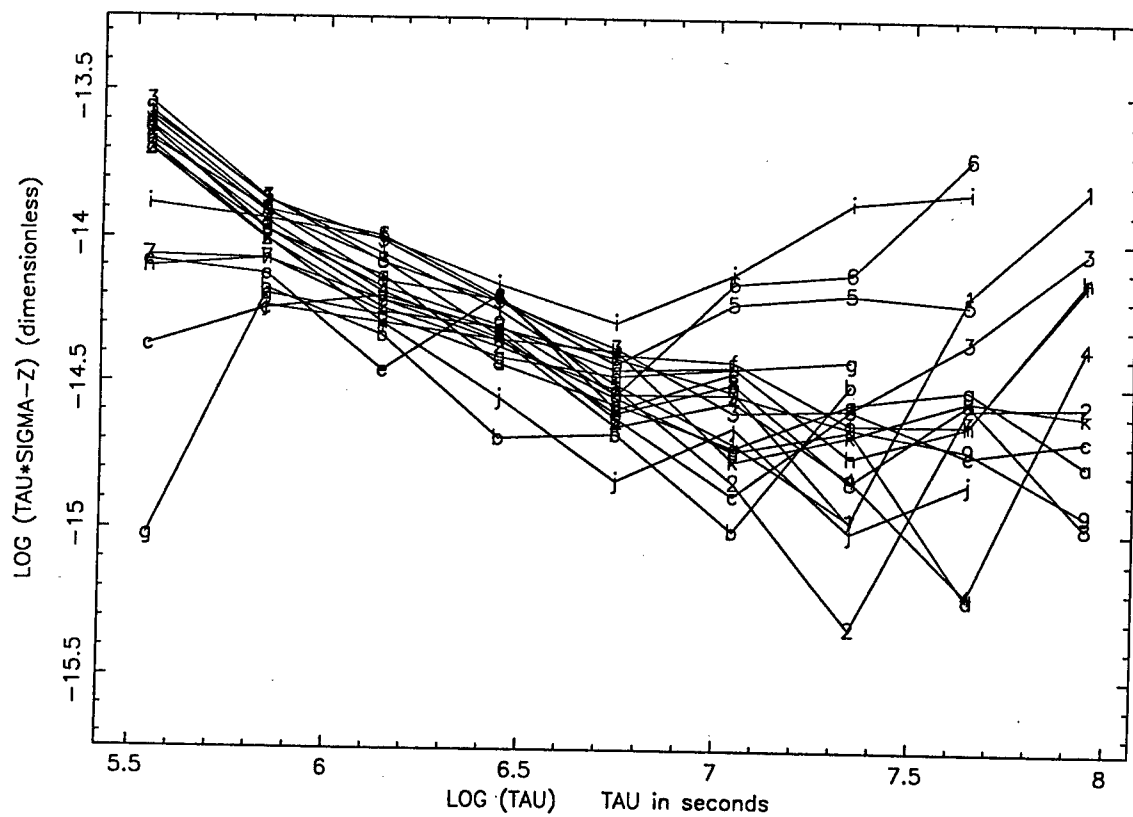


Figure 1 a. Twenty individual cesium 5071s, MJD 49400-50343

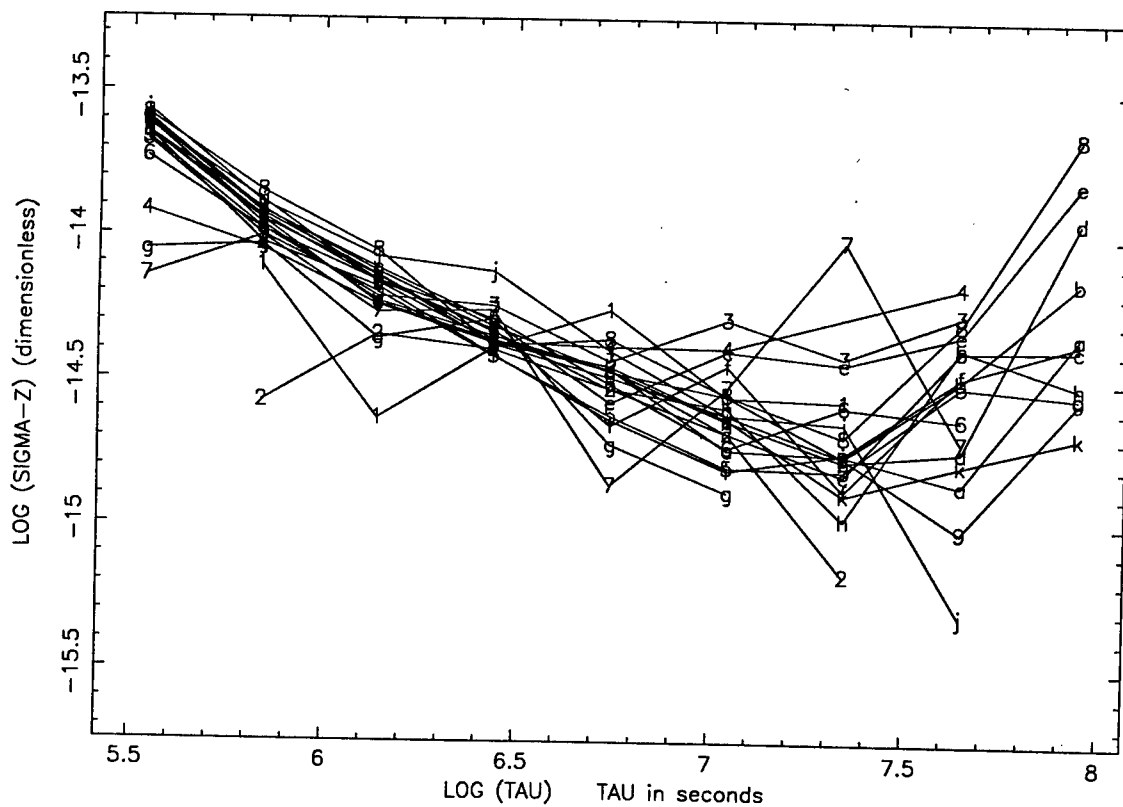


Figure 1 b. Twenty more individual cesium 5071s, MJD 49400-50343

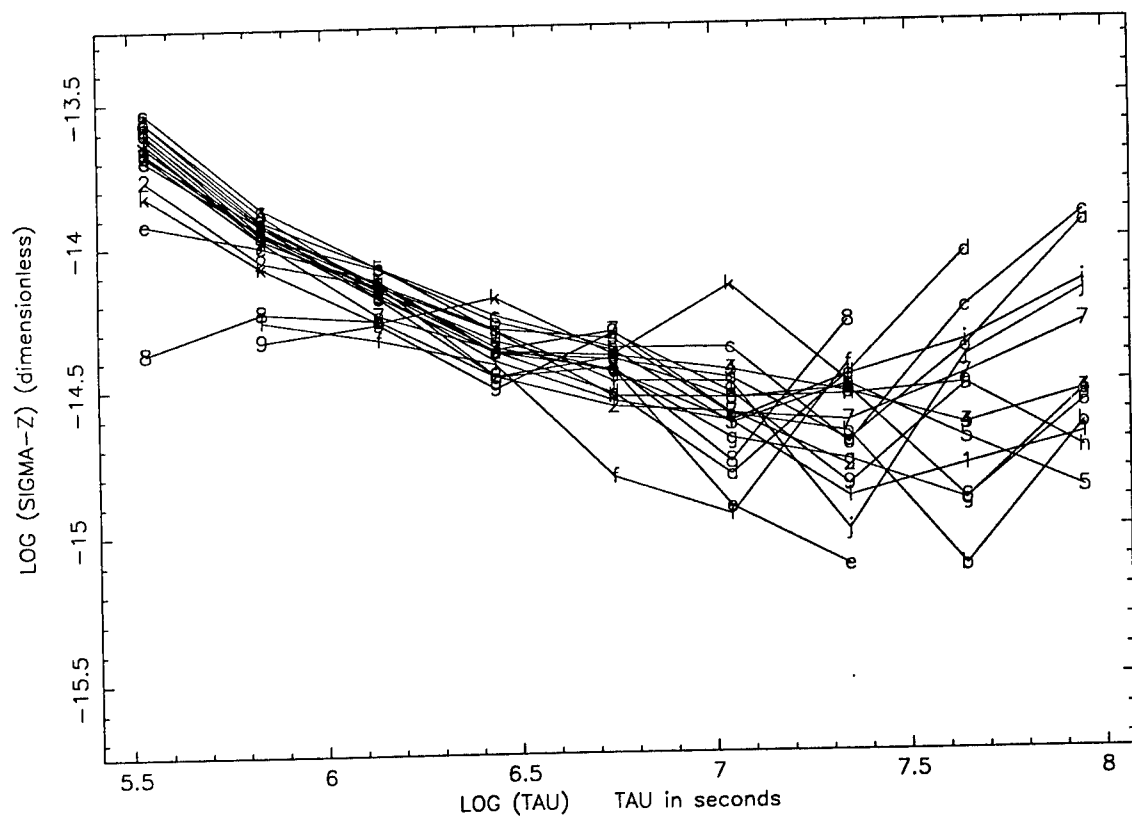


Figure 1 c. Another twenty individual cesium 5071s, MJD 49400-50343

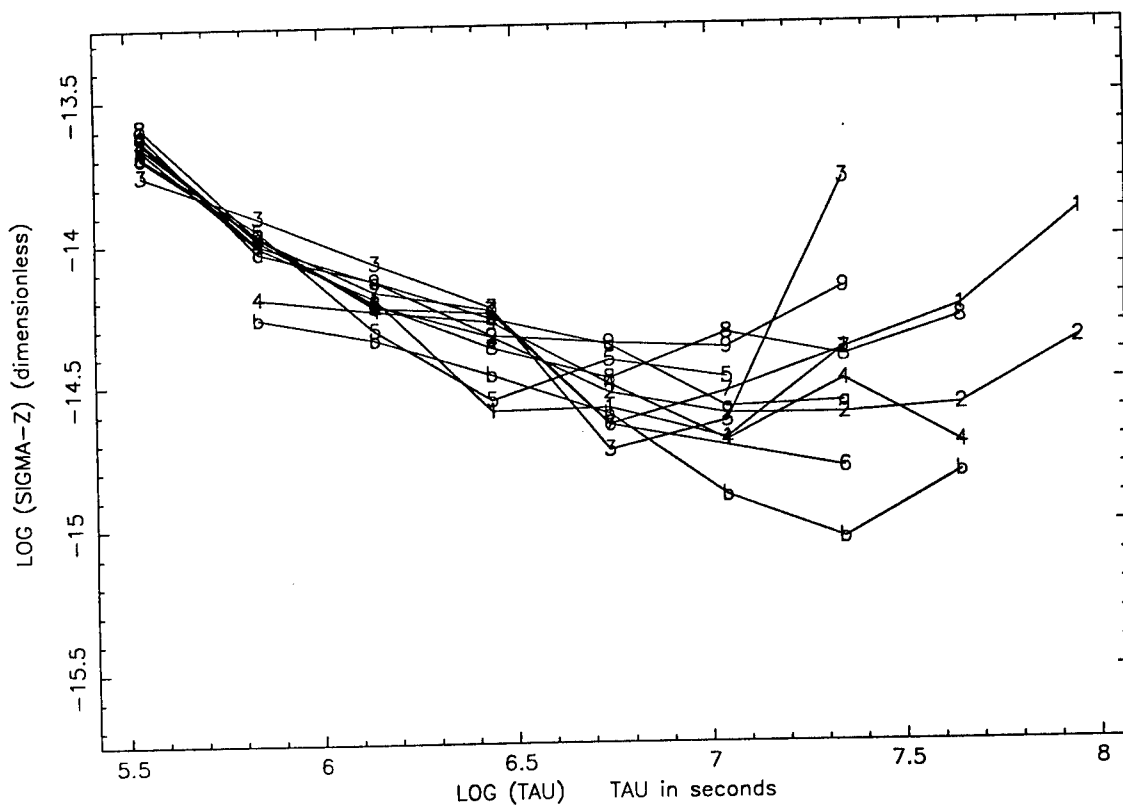


Figure 1 d. Ten individual cesium 5071s, MJD 49400-50343

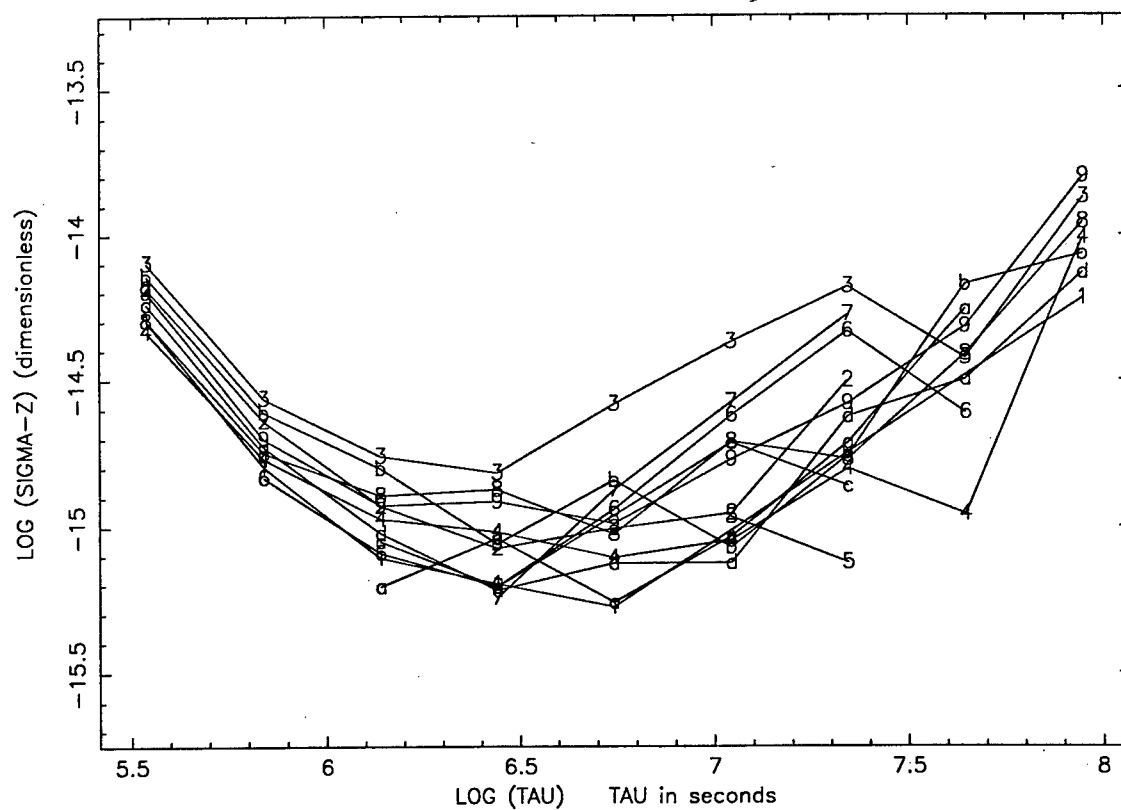


Figure 2. Individual Sigma-Tau hydrogen masers, MJD 49400-50343

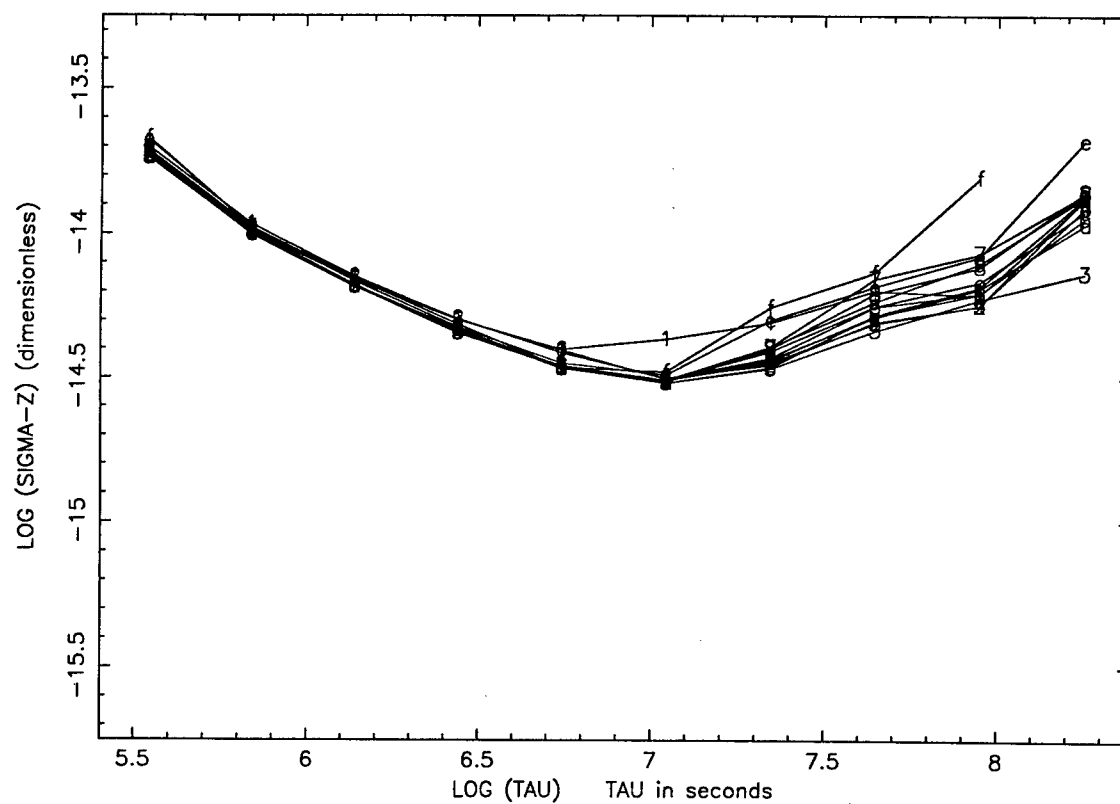


Figure 3 a. Averages of cesium 5071 standards, MJD 47752-50343

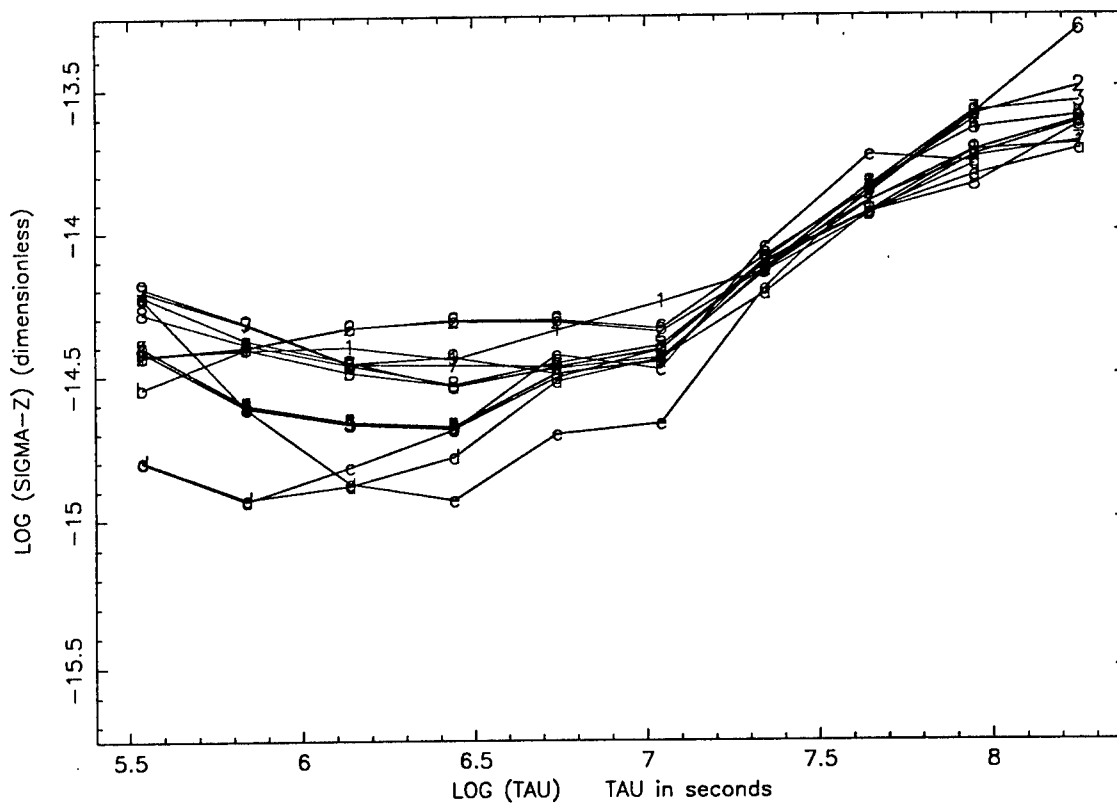


Figure 3 b. Averages of Sigma-Tau masers, MJD 47752-50343

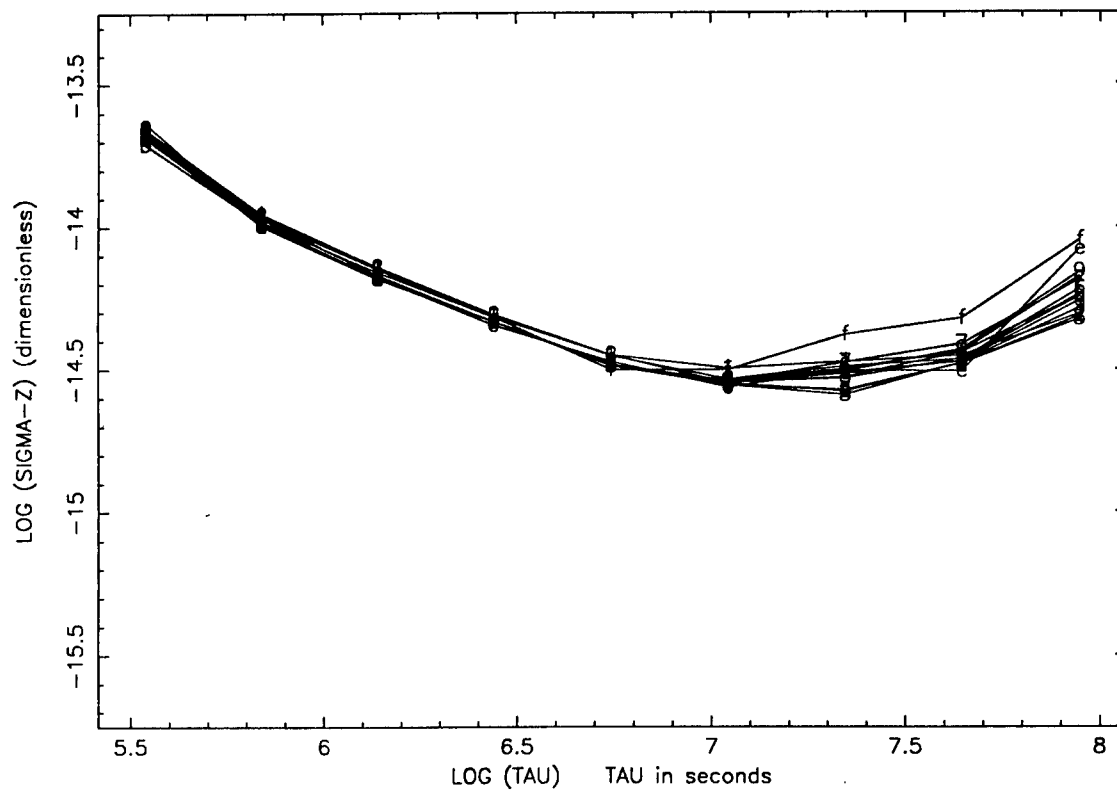


Figure 4 a. Averages of cesium 5071 standards, MJD 49400-50343

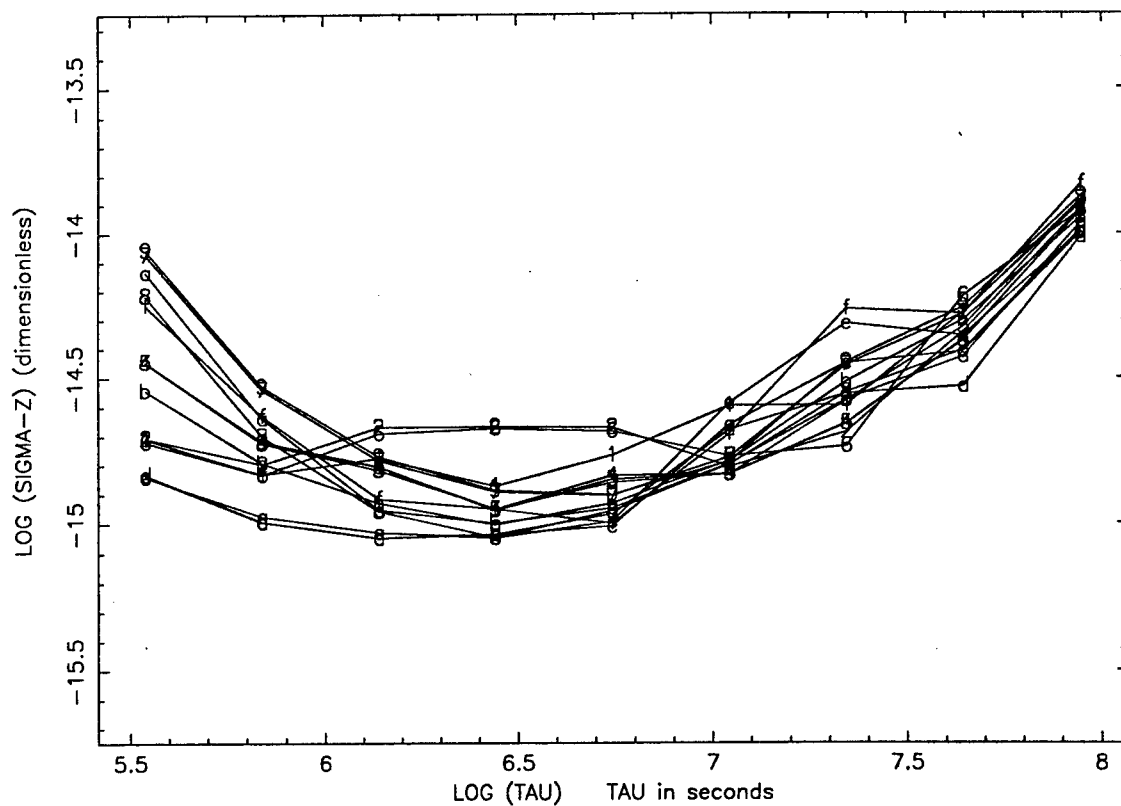


Figure 4 b. Averages of Sigma-Tau masers, MJD 49400-50343

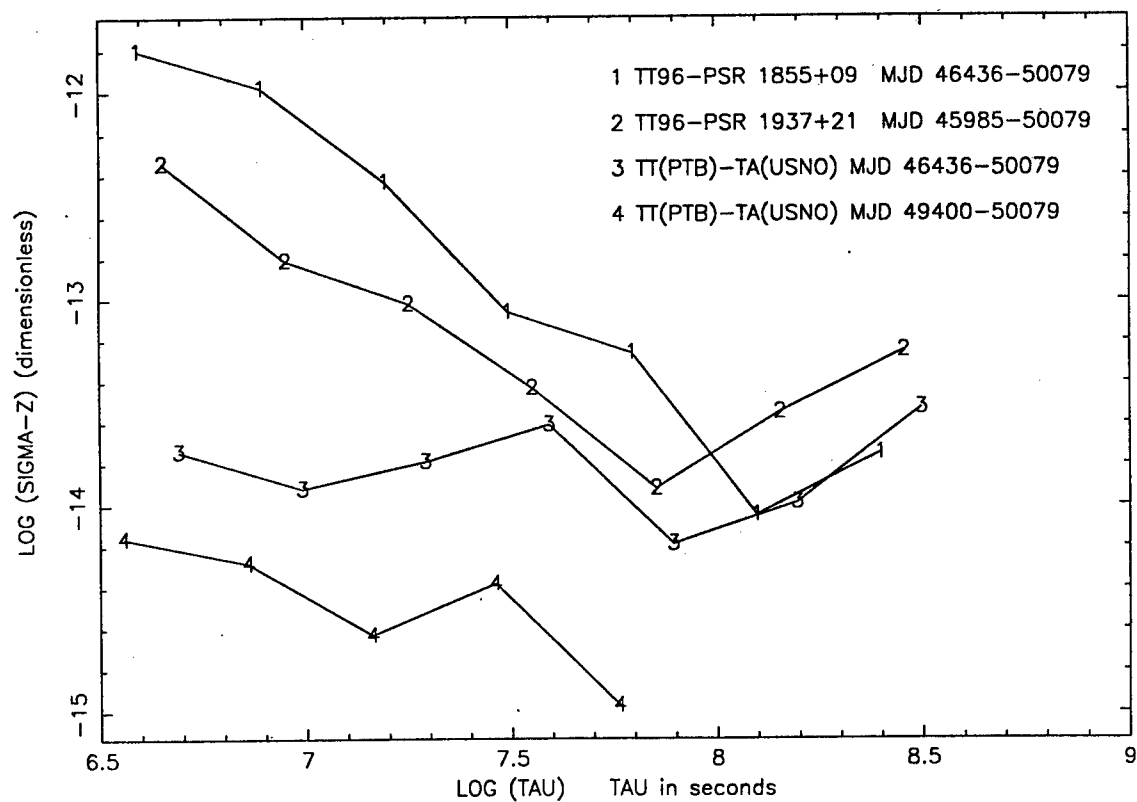


Figure 5. Pulsar and terrestrial time scale stabilities

PTB'S PRIMARY CLOCK CS1: FIRST RESULTS AFTER ITS RECONSTRUCTION

Andreas Bauch, Harald Brand, Thomas Heindorff,
Bernd Fischer, and Roland Schröder
Physikalisch-Technische Bundesanstalt, Time-Unit Laboratory,
Bundesallee 100, D-38116 Braunschweig, Germany

Abstract

The paper describes the reconstruction of PTB's primary clock CS1 and gives first results obtained. In view of the important role of the CS1 among the primary clocks within the international network of timing laboratories, a short look to its history is also given.

INTRODUCTION

According to its definition of 1967, the SI-unit second is realized with cesium atomic clocks. About 220 commercial devices are operated in the timing centers which are linked to a worldwide network under supervision and coordination of the International Bureau of Weights and Measures. In addition, a few laboratory standards have been developed for which a complete evaluation of all potential systematic frequency-shifting effects is sought. As their specific role in the network, they enable the scale unit of the International Atomic Time, TAI, to be as close as possible to the SI second, as realized on the rotating geoid. The PTB CS1 belonged to the group of so-called primary standards of frequency and time since 1969. It was intermittently operated until 1978 and used for the steering of PTB's atomic time scale. Between 1978 and 1995 the CS1 was operated continuously as a clock. Throughout all the years it contributed with maximum statistical weight to the formation of the free atomic time scale, EAL. Of course, more important was the fact that for many years the CS1, and since 1986 also the CS2 of PTB, were the only primary clocks with a significant contribution to the steering of TAI. The CS1 standard uncertainty had been specified to $3 \cdot 10^{-14}$ [1], and that of the CS2 to $1.5 \cdot 10^{-14}$ [2]. Only recently, with the NIST-7[3] and the FO-1[4], were frequency standards put into operation with a smaller standard uncertainty. The performance of the PTB clocks can at best be inferred from a comparison of their rates against TAI, as depicted in Fig. 1. The reader may note the former annual variations in the rate of TAI, as well as the systematic offset between the TAI and the two clocks around 1988-1990, when the TAI steering coefficient had been kept constant for some years.

Inevitably, many components of the CS1 were subject to aging. The vacuum system, in particular, had remained untouched since 1978, including the cesium charge of the oven. Last but not not least, having developed the CS2, the CS3[5], and the CSX[6,7], some new knowledge had been acquired in the laboratory. All that motivated a careful inspection and rejuvenation of the CS1 with the aim of improving the short-term and long-term frequency instability and eventually reducing its type B uncertainty. The clock was out of service from August 1995 until February 1996. On the 29th, to be well remembered, the atomic beam was again turned on.

THE CS1: WHAT IT WAS AND WHAT IT IS

The CS1 had served as the model for all later clock developments at PTB. The original design by G. Becker, G. Kramer, B. Fischer, and E. K. Müller^[8] already allowed the frequency-shifting effects of the atomic velocity, the cesium multilevel structure, and magnetic and electric fields to be evaluated with great accuracy. It incorporated therefore:

- a) an axially symmetric atomic beam system with a point beam source and a small detector on axis;
- b) an axial magnetic quantization field; and
- c) magnetic lenses for the state selection and velocity filtering.

After a modification of the atomic-beam-generating system around 1977^[9], the atoms contributing to the clock transition signal occurred in a narrow velocity interval of about 8 m/s with a mean velocity of about 92 m/s. Fig. 2 gives an impression of the mechanical design of the CS1 as it is now. The vacuum system has been refurbished, but the atomic-beam-generating system has been kept as it was. Differing from the previous situation, the microwave cavity is now installed in the new central vacuum chamber, which at the same time serves as the support of the quantization field solenoid. The cavity consists of the central waveguide, which is similar to the one used in the CS3^[5] and the two terminal parts that are of ring-shaped design, as was proposed by A. De Marchi.^[10] The electronic system has been gradually improved and has been for a few years of the same kind as the one described in some detail in [5,11].

FIRST EXPERIMENTAL RESULTS

The spectrum of the seven $(F=4,m) - (F=3,m)$ transitions recorded with the CS1 is depicted in Fig. 3, together with the clock transition signal in higher resolution. During the initial test period we operated a rather intense atomic beam and the frequency instability σ_y ($\tau = 1$ s) is predicted to be $4 \cdot 10^{-12}$, based on the 62.5 Hz linewidth and the signal-to-noise ratio of 900 in 1 Hz bandwidth, calculated from the shot noise of the beam and the thermal detector noise. The frequency instability observed in comparison with an active hydrogen maser agrees perfectly with the predicted value.

During the assembly of the new central vacuum chamber, we shaped the magnetic field along the atomic beam path by using a set of trimming coils on both ends of the main solenoid. The final result, obtained with a field probe moved along the beam axis, is shown in Fig. 4. Later, with the atomic beam available, the $(4,3) - (3,3)$ resonance was used to fine-tune the fields and to make the center of the central Ramsey fringe coincide with the center of the wide Rabi pedestal. Currently the difference is only 1.2 Hz, measured with a statistical uncertainty of 0.2 Hz.

One beam reversal was performed until now which yielded an end-to-end cavity phase difference of $\phi = 150 \mu\text{rad}$. As explained in [5], the type B uncertainty component associated with the end-to-end phase difference is independent of ϕ itself. It is only dependent on:

- a) the spatial distribution of the phase of the microwave field across the atomic beam diameter inside the irradiation sections of the cavity; and
- b) the degree of perfection with which the atomic beam retraces its path through the cavity.

During assembly, the beam retrace was simulated and, adding all mechanical tolerances found, a beam retrace could be systematically in error by 0.2 mm. Concerning a), the use of ring-shaped terminal parts should result in a distributed phase difference reduced by at least a factor of 10, in theory^[10], compared to the value in conventional cavities.^[2, 5, 6] Although in previous experiments only a factor of 4 was found^[12], it should nevertheless be possible to correct for the ϕ -dependent frequency shift with a type B uncertainty of well below 10^{-14} .

OUTLOOK

It is premature to make a final emphatic statement on the characteristics of the "new" CS1. By following the evaluation step by step as it was laid down in [5] and comparing with the experimental results obtained until now, there is good reason to expect the type B uncertainty of the CS1 to be 10^{-14} or slightly below. The pitfalls may lie in an insufficient shielding of microwave stray fields inside the beam tube, in Majorana transitions occurring along the beam path^[7], and possibly in an unexpectedly large sensitivity of the end-to-end phase difference of the cavity to temperature.^[13] These effects have to be carefully examined before the CS1 will be put into final operation as a clock again.

REFERENCES

- [1] K. Dorenwendt 1986, "Realization and dissemination of the second," *Metrologia*, **22**, 186-189.
- [2] A. Bauch, K. Dorenwendt, B. Fischer, T. Heindorff, E. K. Müller, and R. Schröder 1987, "CS2: the PTB's new primary clock," *IEEE Transactions on Instrumentation and Measurement*, **IM-36**, 613-616.
- [3] J.H. Shirley, W.D. Lee, and R. Drullinger 1996, "The evaluation of NIST-7: a new era," Proceedings of the 5th Symposium on Frequency Standards and Metrology, 15-19 October 1995, Woods Hole, Massachusetts, USA, ed. J.C. Bergquist (World Scientific, Singapore), pp. 380-384.
- [4] A. Clairon, S. Ghezali, G. Santarelli, P. Laurent, S.N. Lea, M. Bahoura, E. Simon, S. Weyers, and K. Szymaniek 1996, "Preliminary accuracy evaluation of a cesium fountain frequency standard," Proceedings of the 5th Symposium on Frequency Standards and Metrology, 15-19 October 1995, Woods Hole, Massachusetts, USA, ed. J.C. Bergquist (World Scientific, Singapore), pp. 49-59.
- [5] A. Bauch, T. Heindorff, R. Schröder, and B. Fischer 1996, "The PTB primary clock CS3: type B evaluation of its standard uncertainty," *Metrologia*, **33**, 249-259.
- [6] A. Bauch, T. Heindorff, and R. Schröder 1985, "Measurement of the frequency shift due to distributed cavity phase difference in an atomic clock," *IEEE Transactions on Instrumentation and Measurement*, **IM-34**, 136-138.
- [7] A. Bauch, and R. Schröder 1993, "Frequency shifts in a cesium atomic clock due to Majorana transitions," *Annalen der Physik*, **2**, 421-449.
- [8] G. Becker, B. Fischer, G. Kramer, and E.K. Müller 1969, "Neuentwicklung einer Cäsiumstrahlapparatur als primäres Zeit- und Frequenznormal an der PTB," *PTB-Mitteilungen*, **79**, 77-80.

- [9] G. Becker 1979, "*The performance of primary Cs beam clocks using quadrupole and hexapole deflection systems: consequences for time keeping,*" Proceedings of the 11th Annual Precise Time and Time Interval (PTTI) Applications and Planning Meeting, November 1979, Goddard Space Flight Center, Greenbelt, Maryland, USA, pp. 113-137.
- [10] A. De Marchi, J. Shirley, D.J. Glaze, and R. Drullinger 1988, "*A new cavity configuration for cesium beam primary frequency standards,*" **IEEE Transactions on Instrumentation and Measurement**, IM-37, 185-190.
- [11] R. Schröder 1991, "*Frequency synthesis in primary cesium clocks,*" Proceedings of the 5th European Frequency and Time Forum (EFTF), 12-14 March 1991, Besançon, France, pp. 194-200.
- [12] H. de Boer, B. Fischer, T. Heindorff, and R. Schröder 1990, "*Experimental data on a new Ramsey cavity for cesium atomic clocks,*" Proceedings of the 4th European Frequency and Time Forum (EFTF), 13-15 March 1990, Neuchâtel, Switzerland, pp. 523-526.
- [13] A. De Marchi, O. Francescangeli, and G.P. Bava 1993, "*Dimensional sensitivity of end-to-end phase difference in ring terminated Ramsey cavities,*" **IEEE Transactions on Instrumentation and Measurement**, IM-42, 448-452.

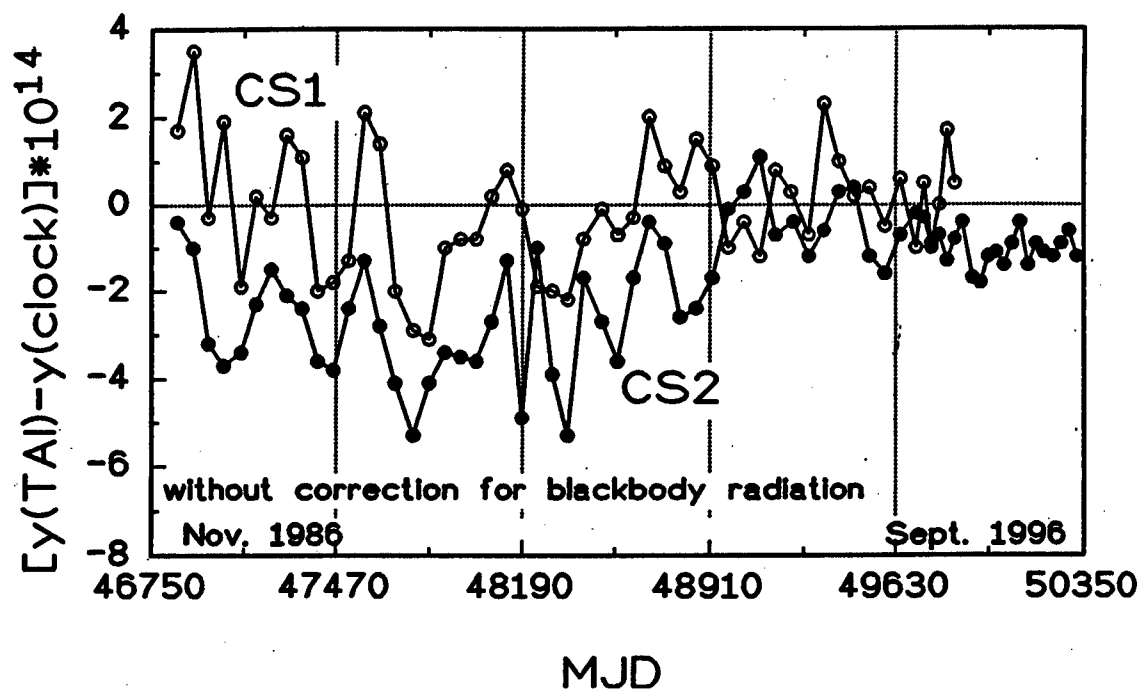


Figure 1. Ten years of frequency comparisons of the primary clocks CS1 and CS2 of the PTB with International Atomic Time, TAI. The data from BIPM Circular T are 60-day averages, the symbols are plotted at the end of each interval. MJD: Modified Julian Date.

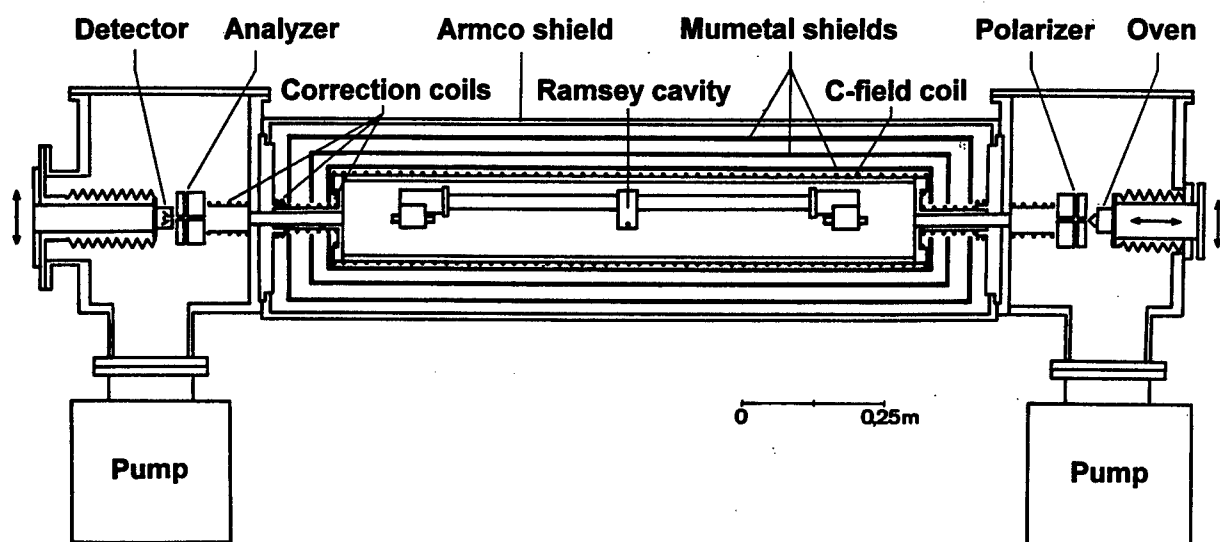


Figure 2. Vertical section through the reconstructed CS1 primary clock.

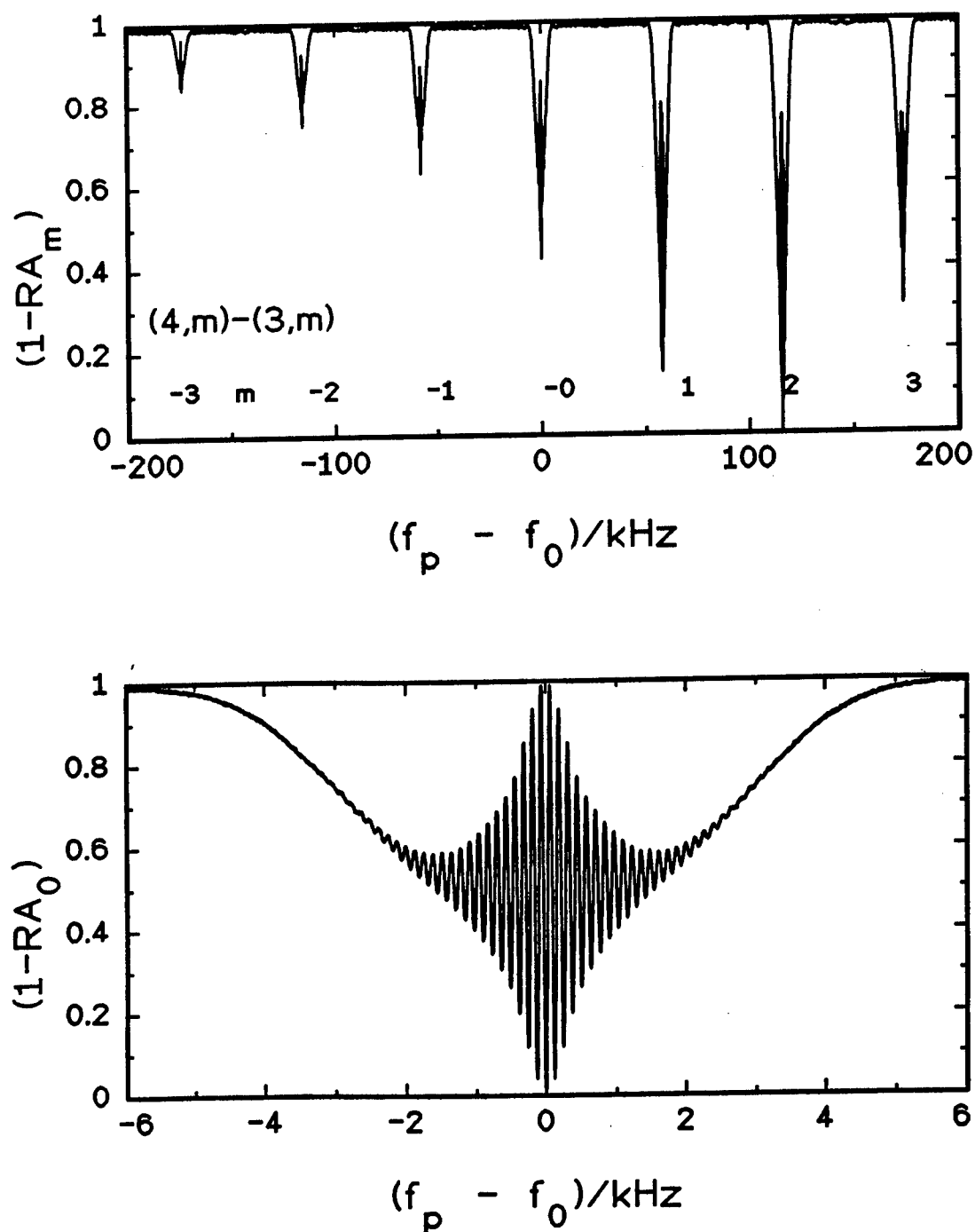


Figure 3. Microwave resonance signals recorded in the CS1. The CS1 beam optics result in an observation of the resonances in the flop-out mode; RA_m is the normalized resonance amplitude of the $(4,m)-(3,m)$ transition; $f_p - f_0$: frequency detuning of the microwave probing frequency from the $(4,0)-(3,0)$ resonance frequency f_0 . Upper graph: spectrum of the $(4,m)-(3,m)$ transitions; the maximum of RA_2 is set to 1. Lower graph: clock transition signal, whose maximum amplitude is set to 1.

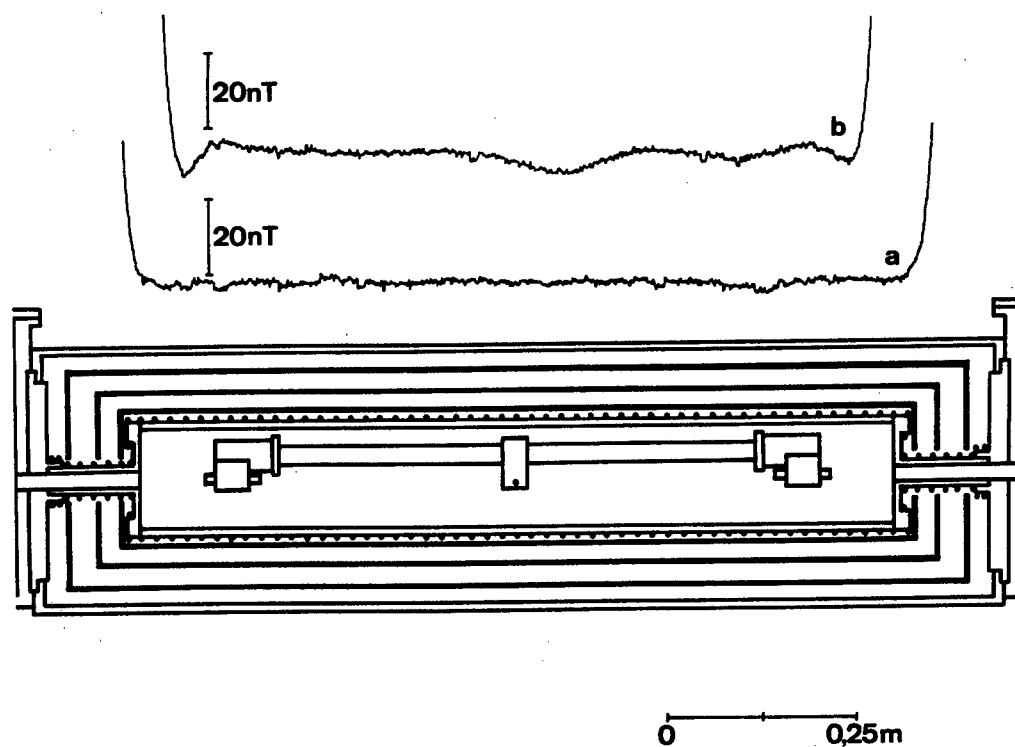


Figure 4. Plots of the axial magnetic field in the beam tube of the CS1. The position of the cavity, the magnetic shields, the solenoid and the trimming coils are shown for clarity; a) residual earth field; b) C-field after final adjustment of the current through the trimming coils, zero suppressed.

Questions and Answers

MARC WEISS (NIST): How often do you reverse the beam?

ANDREAS BAUCH: Historically, we did it every 6 weeks. Since we've operated the standard, we have done it once. So I have one measurement of the antenna phase difference, which the frequency difference in between the two directions is 5 parts in 10^{13} . But what we will do in the future, we have not yet decided. A couple of times per year, three or four times per year probably.

THE JPL Hg+ EXTENDED LINEAR ION TRAP FREQUENCY STANDARD: STATUS, STABILITY, AND ACCURACY PROSPECTS*

R. L. Tjoelker, J. D. Prestage, and L. Maleki
Jet Propulsion Laboratory, California Institute of Technology
4800 Oak Grove Drive, MS 298-100, Pasadena, California 91109, USA

Abstract

Microwave frequency standards based on room temperature $^{199}\text{Hg}^+$ ions in a Linear Ion Trap (LITS) presently achieve a signal-to-noise and line-Q-inferred short-term frequency stability of $\sigma_y(\tau) = 2 \times 10^{-14}/\tau^{1/2}$. Long-term stability has been measured for averaging intervals up to 5 months with apparent sensitivity to variations in ion number/temperature limiting the flicker floor to about 5×10^{-16} at 100,000 seconds. A two-segment version of the linear ion trap (LITE) has also recently demonstrated excellent frequency stability for measurement intervals up to one week. Nearly an order of magnitude improvement in long-term stability compared to the LITS is expected since this trap configuration operates with reduced linear ion density during the microwave interrogation period.

INTRODUCTION

Mercury Linear Ion Trap frequency Standards (LITS) have been developed at JPL to address the practical needs of the NASA Deep Space Network (DSN) with the goal of providing frequency stability substantially better than the hydrogen masers currently in use in each DSN station. The DSN requires high-frequency stability for communication and tracking of a variety of spacecraft throughout the solar system. The stability needs vary from less stringent requirements for navigation, to more demanding requirements for very long baseline interferometry, gravity wave searches, and radio science experiments. Most recent frequency and timing stability requirements for the upcoming Cassini mission to Saturn are near 10^{-15} stability from 1 to tens of thousands of seconds. Frequency standards in the DSN must provide very high stability and operate continuously at remote locations from JPL. This requires the standards to be reasonably transportable, operate autonomously, and be very reliable.

THE LINEAR ION TRAP STANDARD (LITS)

The ongoing development of the LITS^[1-5] based on the 40.5 GHz ground state hyperfine transition of ^{199}Hg ions^[6] has recently led to the development of an engineering model for

*The work described here was performed by the Jet Propulsion Laboratory, California Institute of Technology, under a contract with the National Aeronautics and Space Administration.

the DSN.^[7] Ions confined in a trap allow for long interrogation times and high atomic line Q. Continuous operation is made practical using a ^{202}Hg lamp to generate 194.2 nm radiation for atomic state selection and a helium buffer gas for ion cooling.^[8] The large 40.5 GHz $^2\text{S}_{1/2}(F=0, m_F=0)$ to $^2\text{S}_{1/2}(F=1, m_F=0)$ ground state hyperfine transition in mercury is less susceptible to magnetic and Doppler shifts than in transitions in lighter atoms, providing good long-term frequency stability with minimal environmental regulation. The linear ion trap provides a way to increase the detected fluorescence signal-to-noise ratio (S/N) without increasing the second order Doppler shift.^[1] The $^{199}\text{Hg}^+$ hyperfine transition is typically interrogated using Ramsey successive oscillatory fields with two 0.4-second microwave pulses separated by an interrogation time ranging from 1 to 30 seconds, depending on the local oscillator.

Presently achieved signal-to-noise and line Q with a LITS (Figure 1) imply a short-term frequency stability of $\sigma_y(\tau) = 2 \times 10^{-14}/\tau^{1/2}$.^[7] A major challenge to realizing the full stability has been the stability of the local oscillator. To date, only a quartz VCXO or some hydrogen masers have had sufficient reliability to serve as LO's for trapped ion frequency standards in the DSN. In both cases the achievable frequency stability is compromised due to local oscillator frequency noise at multiples of the interrogation cycle frequency.^[9] Liquid helium-cooled sapphire resonator technology provides stability that is sufficient to not degrade the LITS stability. Unfortunately the need to periodically fill a helium Dewar has limited the practicality of using cryogenic sapphire as a permanent local oscillator. A program at JPL has recently been initiated to develop a continuously operating Compensated Sapphire Oscillator (CSO) cooled with a closed cycle refrigerator to ≈ 10 K.^[10] The frequency stability goal of 3×10^{-15} for 1 to 100 seconds will provide an ideal local oscillator for the LITS. The CSO/LITS combination will meet all radio science and gravity wave search frequency-stability needs in the DSN for the upcoming Cassini mission to Saturn. Figure 2 shows schematically the LITS short-term stability when operated with a quartz VCO or a hydrogen maser as the LO. Also shown is the projected stability when operated with the CSO under development and the LITS operating at $\sigma_y(\tau) = 2 \times 10^{-14}/\tau^{1/2}$.

The long-term stability (and potential accuracy) is fundamentally related to the size of sensitivity to environmental perturbations and the ability to know and control (measure) them. The three largest frequency offsets in present LITS operation^[3] are: 1) the Second-Order Zeeman Shift (DC magnetic fields); 2) the Second-Order Doppler shift (due to thermal and driven ion motion); and 3) a pressure shift due to collisions with the helium buffer gas. In the LITS, the entire trap, UV optics systems, and Helmholtz coils are surrounded by five large nested magnetic shields. This magnetic shielding is sufficient to reduce external magnetic field fluctuations by 20,000, providing a fractional frequency sensitivity to external fluctuations of $\approx 2 \times 10^{-17}/\text{mG}$. The trap/optics/shield region requires thermal regulation to only 0.1°C to achieve a frequency stability of 10^{-15} . Long-term stability requires the ion number/temperature to be stable over the length of the averaging interval. The ion number depends on several operating parameters, trap well depth, ion load and loss rate, and the condition of the vacuum. The vacuum system has a base pressure of $\approx 1 \times 10^{-9}$ torr, a mercury background pressure of about $\approx 5 \times 10^{-10}$ torr and a helium buffer gas pressure of $\approx 10^{-5}$ torr. Mercury vapor is generated by heating a small sample of HgO to approximately 200°C, and helium is introduced through a heated quartz helium leak and stabilized to an ion gauge pressure measurement. Possible aging of the vacuum system, ion gauge, or changes in the Hg pressure as a function of HgO temperature over time are presently not controlled though the electron current used to ionize ^{199}Hg atoms and the temperature of the HgO source are regulated. The longest continuous stability measurement to date in this "open loop" operation is a 5-month comparison between an early research standard (LITS-2) and a cavity-tuned hydrogen maser.^[4,5] Over this 5-month interval the relative long-term drift was measured to be $2.1 (\pm 0.8) \times 10^{-16}/\text{day}$. Stability comparisons up to 1 month have been

performed between two LITS standards, with the flicker floor of the earliest LITS standards LITS-1 and LITS-2 measured at 5×10^{-16} at 100,000 seconds.^[5] The source of this limit, though not completely resolved, apparently arises from variations of the ion number/temperature as a function of vacuum parameters which change slightly under environmental perturbations.

RECENT RESULTS WITH THE EXTENDED LINEAR ION TRAP STANDARD (LITE)

An extended version of the current LITS standards (often referred to as "LITE" or "Shuttle trap") provides several advantages to the current LITS scheme.^[11,12] The LITE consists of two separate trap regions, a magnetically shielded region for microwave interrogation, and a separate region for ion loading and state preparation/detection using 194 nm light. Ions are "shuttled" back and forth between these two regions using only DC potentials. Practical advantages are that the LITE can be made much smaller (perhaps even for spaceflight^[13,14]), more maintainable (because of improved access to lamp and photon detectors), and should offer reduced sensitivity to environmental perturbations. Performance advantages, especially towards further improvements of long-term stability and accuracy should result by operating at reduced ion densities during microwave interrogation. Therefore, the sensitivity to the portion of the second-order Doppler shift most difficult to keep stable (i.e. ion number fluctuation in the trapping RF field) is significantly reduced without reducing signal-to-noise or line Q. This long-term performance gain comes without further improvements to environmental regulation or compromising continuous reliable operation.

Figure 3 shows the 40.507 GHz signal resulting from Ramsey interrogation of ions in the first LITE trap. The resonant frequency measured represents the magnetically shielded hyperfine transition, though fluorescence detection actually occurred when the ions were subject to the earth's ambient magnetic field. The inferred performance in Figure 3 is $\sigma_y(\tau) = 5.9 \times 10^{-14}/\tau^{1/2}$, accomplished with an 11.1-second interrogation time and only a single detection system. With a second collection system a $\sqrt{2}$ improvement would give a performance of $4 \times 10^{-14}/\tau^{1/2}$, already within a factor of 2 of the best ever measured in a LITS. Figure 4 shows a 5-day stability comparison using a hydrogen maser as the local oscillator and an SAO hydrogen maser^[15] as the reference. The performance shown indicates good intermediate-term stability between 20 and 20,000 seconds (the data shown for times less than 20 seconds are an artifact of the measurement technique). For comparison times longer than 20,000 seconds, the stability is most likely limited by drift in the maser. Longer-term comparisons to a LITS have yet to be done, though it is expected that the long-term stability of the LITE will be significantly better than the current LITS.

A new "shuttle" trap standard currently being developed in our laboratory solely for performance enhancements is shown in Figure 5. Significantly improved magnetic field homogeneity should allow operation at lower magnetic fields by a factor of nearly 8, reducing sensitivity to external and applied magnetic perturbations. The extended trap will have an interrogation region 7 times longer than in the present LITS, reducing sensitivity to all long-term systematics affected by ion number/temperature variations. In principle, this could reduce the flicker floor to $\approx 1 \times 10^{-16}$ with corresponding improvements to long-term stability without additional environmental regulation.

Though there is still much stability and accuracy to be gained operating at room temperature, stability performance significantly below 10^{-16} will most likely require cold ions (and a superb LO). Unfortunately most ion-based microwave standards require ultraviolet light for optical pumping and/or laser cooling. While single laser-cooled ions may in principal provide the

highest accuracies^[16], the need for stability and practical UV laser system currently makes the approach of direct laser-cooling and detection inappropriate for the DSN. An alternative approach, which may prove to be more practical, may be the possibility of using laser-cooled neutral atoms for state detection and cooling of trapped ions.^[14]

CONCLUSION

A mercury linear ion trap frequency standard has been developed for continuous operation and tested in the NASA Deep Space Network. Measured signal-to-noise and atomic line Q indicate that a short-term stability performance of $\sigma_y(\tau) = 2 \times 10^{-14}/\tau^{1/2}$ can be achieved when operated with an appropriate local oscillator. Recent developments in sapphire resonator fabrication has resulted in an effort at JPL to develop a continuous operating Compensated Sapphire Oscillator (CSO). This oscillator when steered with the LITS should provide frequency stability around 10^{-15} from times ranging from 1 second to months.

Initial measurements taken with the first LITE (shuttle) standard show a short-term stability similar to the LITS. A stability measurement for 5 days indicated that the flicker floor is at least equivalent to the LITS with significant improvements to long-term stability expected. In a second generation "shuttle" trap currently under development, the flicker floor resulting from current environmental sensitivity may be reduced by a factor of 7. When operated with the CSO as a local oscillator very low flicker floors, perhaps breaking into the 10^{-17} region, should be possible for averaging times less than 100,000 seconds. Longer-term stability (and potential accuracy determination) should also be improved by the achievable sensitivity reduction. This would be accomplished using the same electronics as the LITS and the same low degree of environmental regulation.

REFERENCES

- [1] J.D. Prestage, G.J. Dick, and L. Maleki 1989, "New ion trap for frequency standard applications," *Journal of Applied Physics*, **66**, 1013-1017.
- [2] J.D. Prestage, R.L. Tjoelker, G.J. Dick, and L. Maleki 1992, "Ultra-stable Hg+ trapped ion frequency standard," *Journal of Modern Optics*, **39**, 221-232.
- [3] R.L. Tjoelker, J.D. Prestage, G.J. Dick, L. and Maleki 1993, "Long term stability of Hg+ trapped ion frequency standards," *Proceedings of the 1993 IEEE International Frequency Control Symposium*, 2-4 June 1993, Salt Lake City, Utah, USA, pp. 132-138.
- [4] R.L. Tjoelker, J.D. Prestage, G.J. Dick, and L. Maleki 1994, "Recent stability comparisons with the JPL linear trapped ion frequency standards," *Proceedings of the 1994 IEEE International Frequency Control Symposium*, 1-3 June 1994, Boston, Massachusetts, USA, pp. 739-743.
- [5] R.L. Tjoelker, J.D. Prestage, and L. Maleki 1996, "Record frequency stability with mercury in a linear ion trap," *Proceedings of the 5th Symposium on Frequency Standards and Metrology*, 15-19 October 1995, Woods Hole, Massachusetts, USA, ed. J.C. Bergquist (World Scientific, Singapore), pp. 33-38.
- [6] F.G. Major, and G. Werth 1981, "Magnetic hyperfine spectrum of isolated $^{199}\text{Hg}^+$ ions," *Applied Physics*, **15**, 201-208.

- [7] R.L. Tjoelker, C. Bricker, W. Diener, R.L. Hammel, A. Kirk, P. Kuhnle, L. Maleki, J.D. Prestage, D. Santiago, D. Seidel, D.A. Stowers, R.L. Sydnor, and T. Tucker 1996, "*A mercury ion frequency standard engineering prototype for the NASA Deep Space Network*," Proceedings of the 1996 IEEE International Frequency Control Symposium, 5-7 June 1996, pp. 1073-1081.
- [8] L.S. Cutler, R.P. Giffard, and M.D. McGuire 1985, "*Thermalization of ^{199}Hg ion macromotion by a light background gas in an RF quadrupole trap*," *Applied Physics*, B36, 137-142.
- [9] G.J. Dick, J.D. Prestage, C.A. Greenhall, and L. Maleki 1991, "*Local oscillator induced degradation of medium-term stability in passive atomic frequency standards*," Proceedings of the 22nd Annual Precise Time and Time Interval (PTTI) Applications and Planning Meeting, 4-6 December 1990, Vienna, Virginia, USA (NASA CP-3116), 487-508.
- [10] R. Wang, and G.J. Dick 1997, "*10 Kelvin compensated sapphire resonator for Cassini mission*," Proceedings for the Scientific Applications of Clocks in Space Workshop, 7-8 November 1996, Pasadena, California, USA.
- [11] J.D. Prestage, R.L. Tjoelker, G.J. Dick, and L. Maleki 1993, "*Improved linear ion trap package*," Proceedings of the 1993 IEEE International Frequency Control Symposium, 2-4 June 1993, Salt Lake City, Utah, USA, pp. 148-154.
- [12] J.D. Prestage, R.L. Tjoelker, G.J. Dick, and L. Maleki 1995, "*Progress report on the improved linear ion trap physics package*," Proceedings of the 1995 IEEE International Frequency Control Symposium, 31 May-2 June, 1995, San Francisco, California, USA, pp. 82-85.
- [13] J.D. Prestage, and L. Maleki 1994, "*Space flyable Hg^+ frequency standards*," Proceedings of the 1994 IEEE International Frequency Control Symposium, 1-3 June 1994, Boston, Massachusetts, USA, pp. 747-754.
- [14] J.D. Prestage, R.L. Tjoelker, L. Maleki 1997, "*Trapped ion clock for space applications*," Proceedings for the Scientific Applications of Clocks in Space Workshop, 7-8 November 1996, Pasadena, California, USA.
- [15] Smithsonian Astrophysical Observatory, Cambridge, Massachusetts 02138, USA.
- [16] J.D. Miller, D.J. Berkeland, F.C. Cruz, J.C. Bergquist, W.M. Itano, and D.J. Wineland 1996, "*A laser-microwave double resonance frequency standard using $^{199}\text{Hg}^+$ ions in a cryogenic linear trap*," Proceedings of the 1996 IEEE International Frequency Control Symposium, 5-7 June 1996, Honolulu, Hawaii, USA, pp. 1086-1088.

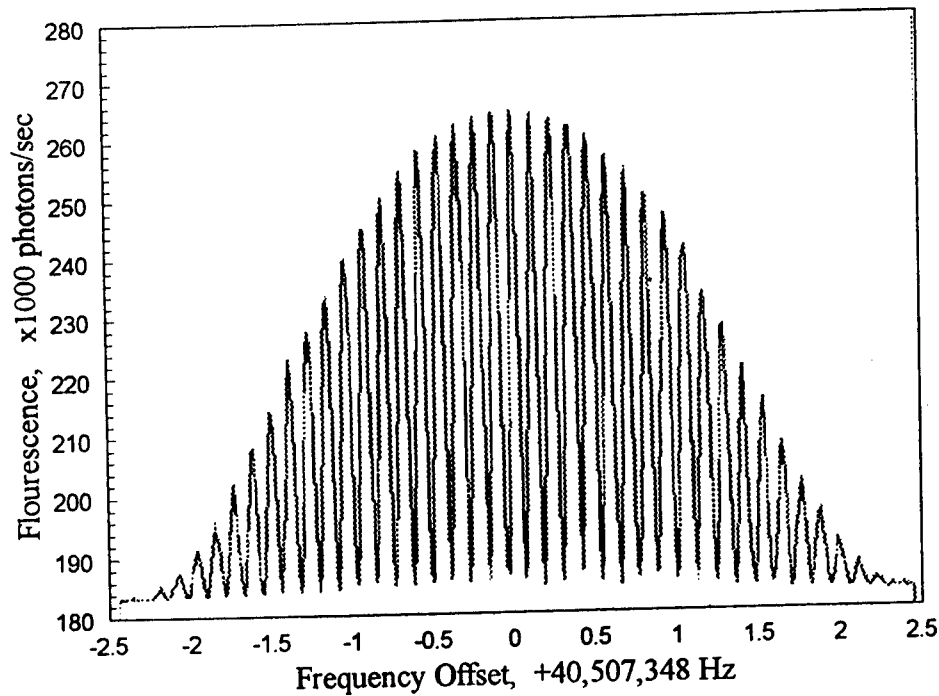


Figure 1: The 8 second Ramsey interrogation signal from the engineering prototype LITS-4 (cycle time 12 seconds). This signal to noise and line Q correspond to a stability of $2.0 \times 10^{-14}/\tau^{1/2}$

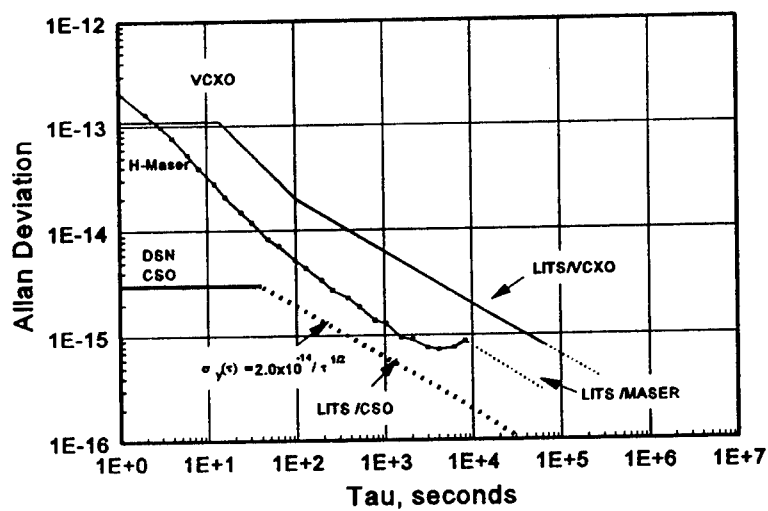


Figure 2: LITS performance shown using either a quartz VCO or a hydrogen maser as the local oscillator. Also shown is the expected performance with a continuously operating compensated sapphire oscillator under development and the LITS operating at $2.0 \times 10^{-14}/\tau^{1/2}$.

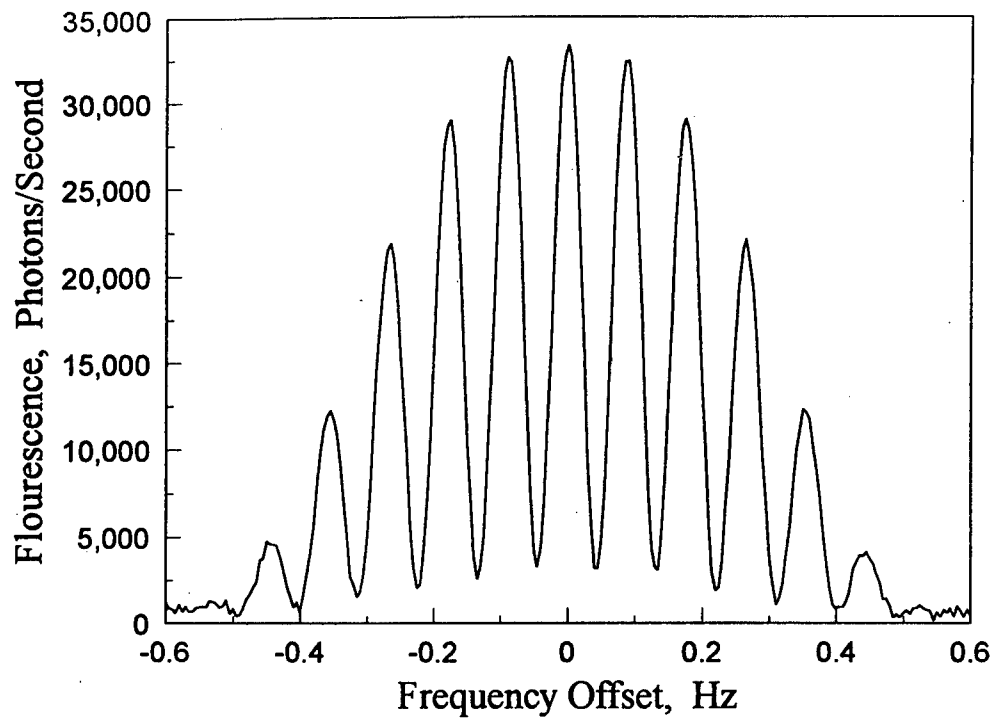


Figure 3: Ramsey interrogation fringes from 11.1 second interrogation cycle in the first LITE research standard.

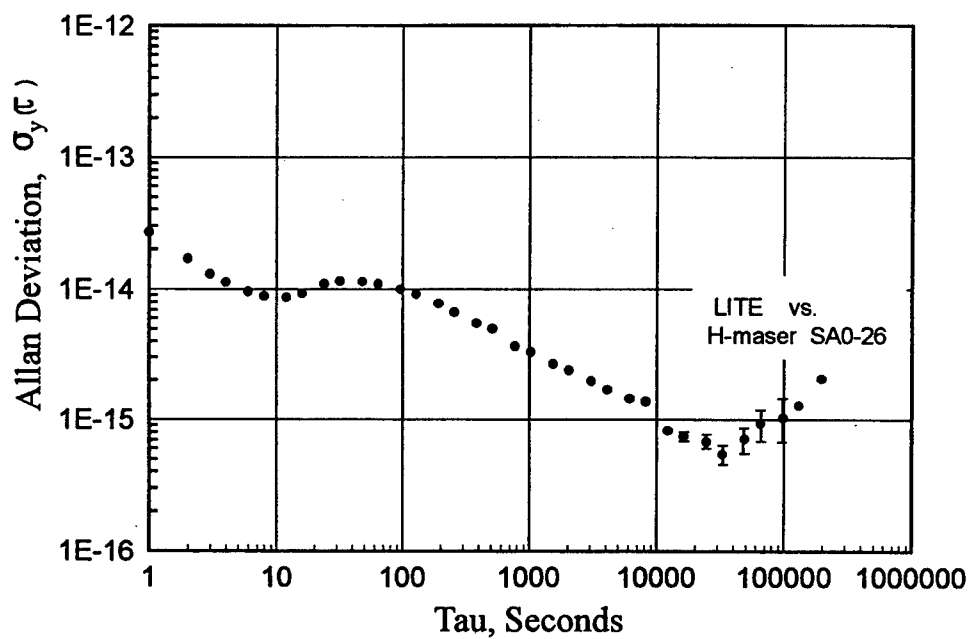


Figure 4: Five day frequency stability comparison of the first LITE research standard to the hydrogen maser SAO-26.

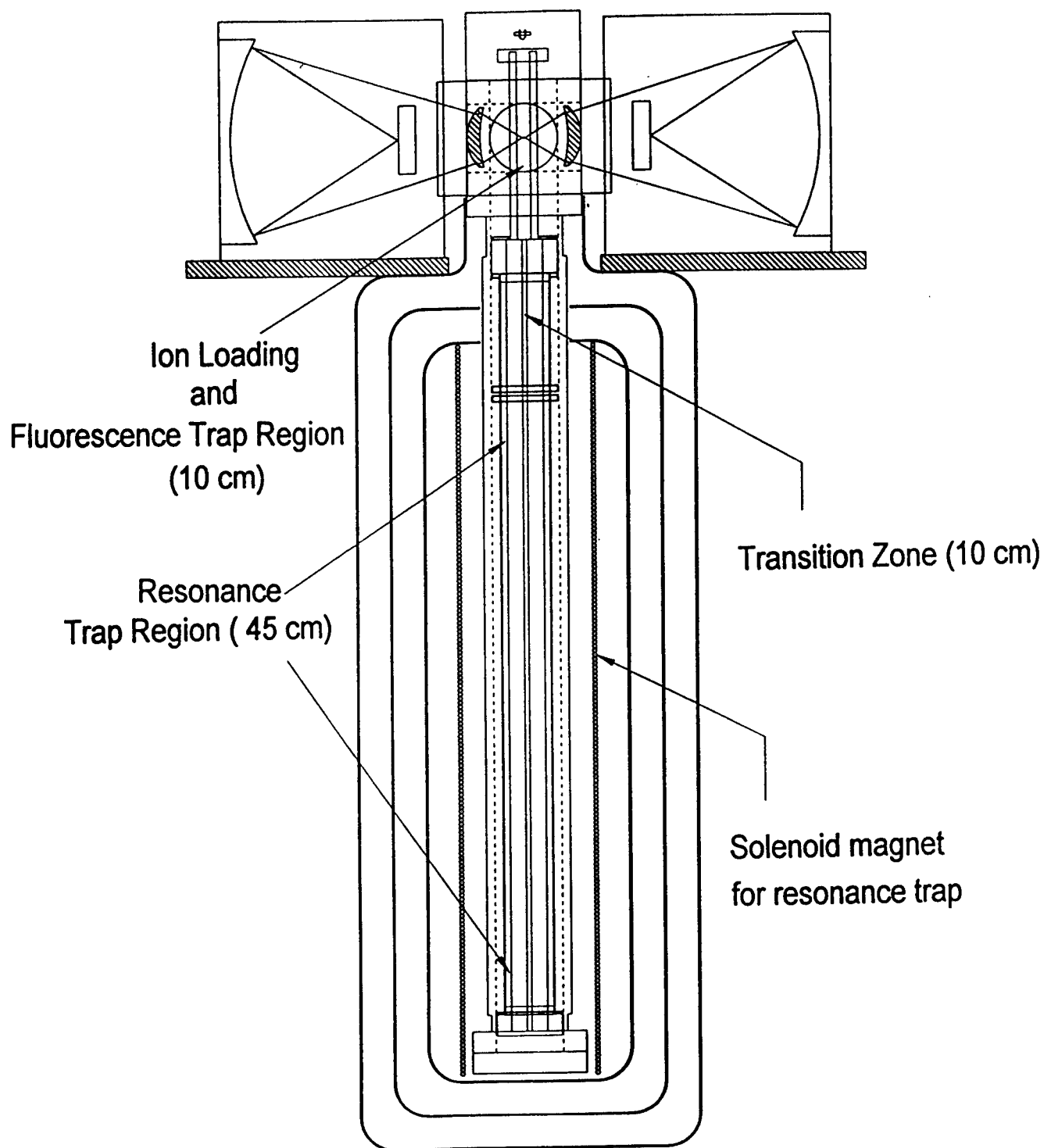


Figure 5: A scaled representation of the new "shuttle" trap incorporated into an existing LITS vacuum and optical system. The microwave resonance region is seven times longer than in the original LITS to reduce sensitivity to the Second-Order Doppler shift.

Questions and Answers

ANDREAS BAUCH (PTB, GERMANY): I understood that this local oscillator degradation comes about by the multiples of phase noise of the local oscillator, multiples of the modulation frequency.

ROBERT TJOELKER: That's correct.

ANDREAS BAUCH: If you do that at the multiples of your modulation frequency, the quartz in your maser will be the determining local oscillator, not the maser itself. Am I wrong? So I didn't understand why there can be such a large difference between locking it to the maser or to the quartz. What's your attack time in the maser?

ROBERT TJOELKER: The attack time in the maser is usually longer, first of all, because we take advantage of the high Q. So we run 8 to 16 seconds interrogation when we use a maser as a local oscillator; as opposed to the quartz, we must attack it much quicker, so we operate the quartz at about 3-second interrogation time.

ANDREAS BAUCH: Okay, there's a difference in the operation.

ROBERT TJOELKER: Yes, total performance difference isn't only the so-called Dick effect. There was also just a loop effect of getting the crystal down there as well.

ANDREAS BAUCH: You stated pressure dependence of the frequency is about 10 to the minus 13th per 10 to the minus 5th torr. If you have a 10 to the minus 13th frequency shift. How you can you stabilize this to one per mil?

ROBERT TJOELKER: That's the total offset; we operate at 10 to the minus 5th torr. An ion-gauged controller, that's the question on long-term stability, for example.

ANDREAS BAUCH: Yes, that's what I'm asking you.

ROBERT TJOELKER: Right. Certainly on the short term, they can do a part per thousand easily. For the very, very long term, there's, as far as I see it, two potential long-term aging mechanisms. I think a lot of the rest are going to be random systematics that are railed, for example; pressure and thermal sensitivities are railed, the way they would creep in. There would be aging of the ion-gauged control for the reference. Or there's the mercury pressure, which at the moment we run open loop. We just control the temperature on the mercury sample, which gives some baseline pressure. Over very, very long times, that could change.

There are ways of dealing with both, but at the moment we don't.

ANDREAS BAUCH: So you want to say the performance you have achieved is with commercial vacuum measurement equipment?

ROBERT TJOELKER: That's correct.

ANDREAS BAUCH: An active loop on the helium pressure?

ROBERT TJOELKER: That's right. It's a heated quartz leak that's servoed to an ion gauge controller.

NIST-7, THE U.S. PRIMARY FREQUENCY STANDARD: NEW EVALUATION TECHNIQUES*

R. E. Drullinger, J. H. Shirley, and W. D. Lee
National Institute of Standards and Technology
325 Broadway, Boulder, Colorado 80303, USA

Abstract

Primary frequency standards achieve their accuracy by direct reference to the definition of the second and evaluation of all known sources of systematic error that may perturb the measured resonance in the atom. NIST-7, the U.S. primary frequency standard, is a thermal, atomic-beam machine that uses optical pumping for atomic state preparation and detection, and digital frequency control. This technology enables the new evaluation techniques described here. All known systematic effects are determined by means of experiments not involving, or limited by, precision frequency measurements. This both speeds the evaluation and reduces the combined standard uncertainty. Its present value is $5 \cdot 10^{-15}$ for NIST-7.

INTRODUCTION

The second is defined to be "the duration of 9,192,631,770 periods of the radiation corresponding to the transition between the two hyperfine levels of the ground state of the cesium 133 atom."^[1] It is left entirely to the individual primary standards laboratories to build and operate devices that realize this definition. Since it is impossible to build an apparatus without biases (there are electric and magnetic fields, relativistic effects, instrumental effects, etc.), standards laboratories must devise techniques to deal with them. They have been doing so throughout 45 years of advancing technology. Increasingly sophisticated techniques have been developed to evaluate these inevitable perturbations.

Past technology has been reviewed in [2]. The present U.S. primary frequency standard, NIST-7, uses a transitional technology. Like its predecessors, it uses a beam of atoms moving with thermal velocities, with all of the attendant shifts and limits associated with that motion. However, it differs from the conventional thermal beam standard in that it uses optical pumping for the required initial atomic state preparation and subsequent detection. (See [3,4] for reviews of this technology and its implementation in NIST-7.) It also uses a digital servo system for frequency agile synthesis of the microwave radiation. These changes have allowed the development of powerful tools for the evaluation of the biases to the measured atomic resonance. These tools have led to a reduced uncertainty in the operating frequency of the standard. The rest of this paper outlines this new evaluation and the results we have achieved to date.

*Contribution of the U.S. Government, not subject to copyright.

TRADITIONAL EVALUATION

Every conceivable frequency-biasing effect in a primary standard must be evaluated to a level that is small compared to the desired overall accuracy. The long list of biases that must be evaluated contains effects that cause shifts ranging from parts in 10^{10} down to parts in 10^{15} and less. In traditional evaluations, the comparatively large frequency bias from the second-order Zeeman effect is evaluated in a highly leveraged way by measuring the first-order Zeeman splittings and then calculating the much smaller second-order shift. Similarly, the second-order Doppler effect is evaluated by measuring the atomic velocity and then modeling the very small relativistic shift. However, the accepted technique for evaluating numerous small frequency bias terms has been to observe the dependence of the standard's frequency on some operating parameter.^[5] Examples are the magnetic field inhomogeneity, line overlap shifts, and various imperfections in the electronics.

This process involves measuring the frequency of the standard against a stable reference, then varying an operating parameter such as microwave power or magnetic field followed by another long, precise frequency measurement. The measured frequency difference F is given by

$$F = \nu_{\text{cs}} - \nu_{\text{ref}} + \sum_i b_i \pm \sigma_F, \quad (1)$$

where ν_{cs} is the frequency of the unperturbed cesium hyperfine resonance, ν_{ref} is the frequency of the reference, and b_i are all known frequency biases. The type A uncertainty^[6] in the measurement is σ_F , imposed by the averaged measurement noise. ν_{ref} is assumed to be constant over the measurement period. This representation reveals the limits to an evaluation that is based upon measuring the parametric dependence of the standard's frequency. First, the bias of interest may not vary strongly with the operating parameter. Second, many biases may change with the same operating parameter obscuring the significance of the measurement. Finally, the uncertainties of the biases are limited by the measurement uncertainty σ_F . There are also concerns regarding how best to combine the individual uncertainties for the overall error budget due to significant correlations between biases.

NEW EVALUATION TOOLS

Traditionally, second-order Zeeman and Doppler biases have been evaluated by measuring a different parameter (first-order Zeeman shift and atomic velocity) which is much more sensitive to the fundamental biasing mechanism. These measurements are then used to calculate the impact on the standard's frequency through a physical model. Using NIST-7, with its optical pumping and digital servo system, we have been able to extend this philosophy to all of the known sources of frequency bias. Some of the techniques have already been published and are cited here. The details of others are being prepared for future publication. For space reasons, we mention only briefly some of the frequency shifts and the techniques we use to evaluate them.

Shifts resulting from the magnetic field inhomogeneity, cavity pulling, and overlap of neighboring Zeeman lines are evaluated by measuring the offset of each Ramsey fringe from its corresponding Rabi pedestal in the Zeeman spectrum. These shifts are relatively large and are easily measured. ($\Delta y \approx 10^{-9}$ to 10^{-10} , where y is fractional frequency.) With suitable models, these measured frequency offsets enable us to calculate shifts in the clock transition that are very small ($\Delta y \approx 10^{-15}$ to 10^{-17} ^[7]). Fluorescence light shift is quantitatively amplified by changing the optical pumping

transition and laser geometry. Similarly, distributed cavity phase shift is investigated by using movable beam masks placed in front of the cavity beam windows to measure both the atomic beam illumination of the cavity as well as the frequency shift as a function of beam alignment.

To ensure control over microwave phase shifts, the atoms must experience the microwave field only within the microwave cavity. Microwave radiation leaking into the drift regions between the state preparation and detection zones must be low enough that its contribution to the transition probability is small compared to the degree to which the atomic line will be split. Radiation leaking from microwave components is located using a heterodyne detector^[8], much as helium and a mass spectrometer are used to search for leaks in a vacuum system.

Spectral impurities in the microwave radiation used to interrogate the clock transition can lead to line asymmetry and pulling effects.^[9] We have investigated the spectral purity of our RF source by heterodyning it against a similar source. We have analyzed it for correlated AM and PM that would introduce unbalanced sidebands.^[10] We find that frequency errors due to spectral impurities in our source are much less than one part in 10^{16} .

Other nonideal behavior in the electronics can lead to shifts in the measured line position. Electromagnetic interference in the servo electronics can result in biases to the main servo integrator. Most of the error-causing signal paths do not appear on a block diagram of the system and are very difficult to anticipate in paper studies of the servo system. As an example of this type of error, we find a bias equivalent to two parts in 10^{15} from the synchronous operation of the CRT monitor of the main servo computer. Errors of this type are investigated by using the digital demodulator and a modified software integrator in the absence of the actual clock signal. The averaged output of the demodulator then reveals any biases. The advantage in this class of experiments comes when the experiment is configured so the noise relative to the signal being investigated is reduced compared to normal operation. Amplitude modulation on the laser or microwave source that is synchronous with the main frequency servo is measured using a power detector driving the servo demodulator and integrator. Synchronous FM on the laser is studied by measuring laser-induced fluorescence just in front of the oven. Here, the atomic beam is much more intense and has lower relative shot noise. Various signal cross-talk pathways within the servo electronics are identified by simply blocking the atomic signal from the clock.

In addition to this set of evaluation tools for the known sources of bias, we do a number of additional experiments to verify our results. Our evaluation tools are model-dependent. Experimental verifications of the models have been performed. In addition, independent techniques have been used to evaluate several biases. Parametric tests like those done in traditional evaluations have been performed as a broad test of our methods. Examples are the frequency of the standard as a function of microwave power or magnetic field. These experiments involve modeling the simultaneous change of several biases. While not useful as direct evaluation tools, they are powerful search techniques for overlooked effects. A more detailed discussion of these experiments will be published soon.

DATA REDUCTION

Using the techniques just outlined, we are able to determine the known biases except end-to-end phase shift with uncertainties that are small compared to the normal type A uncertainty of the frequency measurements. Subtracting all these biases from the measured frequency, we are left with a reduced difference frequency:

$$f = \nu_{\text{cs}} - \nu_{\text{ref}} + V\phi + \delta f. \quad (2)$$

Here, $V\phi$ is the frequency bias resulting from the effective, end-to-end phase difference ϕ and δf is the measurement error due to noise. The coefficient V equals $1/2\pi T$ for a single atomic velocity, where T is the transit time for an atom to cross the drift region between the two excitation regions. For a distribution of velocities, V is the ratio of two velocity integrals whose integrands depend on microwave power and modulation amplitude. The effective phase difference ϕ is constant if atomic trajectories are stable (constant distributed cavity phases) and microwave leakage is eliminated.

When the atomic beam is reversed and we again remove the known biases from our measured frequency, we obtain a reduced difference frequency:

$$f' = \nu_{\text{cs}} - \nu_{\text{ref}} - V'\phi + \delta f'. \quad (3)$$

The sign of the phase difference has reversed and the measurement error $\delta f'$ is uncorrelated with δf . V and V' differ slightly because different oven temperatures and beam alignments in the two directions lead to differing velocity distributions. From Eqs. 2 and 3 we can extract the phase shift ϕ with an uncertainty limited by that of the difference:

$$f - f' = (V + V')\phi + \delta f - \delta f'. \quad (4)$$

We obtain values of ϕ with each evaluation, so we can test its stability over long times. No significant change has been observed in the last 3 years.

If we combine Eqs. 2 and 3 in a weighted average, we eliminate the end-to-end phase shift bias:

$$\bar{f} \equiv (V'f + Vf')/(V + V') = \nu_{\text{cs}} - \nu_{\text{ref}} + (V'\delta f + V\delta f')/(V + V'). \quad (5)$$

The cancelling of the phase-shift bias depends only on the accuracy of V and V' , not on the uncertainties δf and $\delta f'$. Further, the type A uncertainty in \bar{f} is less than the uncertainty of either f or f' alone. We have subtracted the known biases and weighted the combination using the known differences in velocity distribution and microwave power for the frequency measurements in two beam directions. We are then able to combine the measurements as if they had been a single run twice as long. This process can be extended to combine reduced frequency differences from several beam reversals.

RESULTS

Figure 1 is a plot of the frequency difference between NIST-7 and the hydrogen maser (M2) we have been using as our reference. The error bars represent the combined standard uncertainty. Independent comparisons between this maser and other masers, UTC(NIST), and TAI show it to be remarkably stable and characterized by a linear frequency drift. In this plot, all of the known systematic frequency shifts to the cesium resonance have been removed. Thus, the data represent the frequency difference between the unperturbed cesium resonance and the maser. The data indicate that the maser exhibits a linear fractional frequency drift rate of

$+7 \cdot 10^{-17}$ /day. A residual scatter of $2 \cdot 10^{-15}$ about the linear fit is consistent with the type A uncertainty of the individual frequency measurements.

The results of an evaluation are summarized in Table 1. We can now evaluate every known bias term with a fractional frequency uncertainty no more than $\approx 2 \cdot 10^{-15}$ and often much less. However, biases for fluorescence light shift and distributed cavity phase shift have not yet been experimentally verified to this level.

CONCLUSION

We have developed a set of evaluation tools and techniques that allow all known systematic effects to be evaluated through experiments that are not limited by precise frequency measurements. This speeds the overall evaluation process and leads to improved independence of the various bias terms and a smaller uncertainty in their value. The present combined standard uncertainty for NIST-7 is $5 \cdot 10^{-15}$.

REFERENCES

- [1] Proceedings of the Sessions of the 13th General Conference of Weights and Measures, Paris, France, October 1968, p. 103.
- [2] A.G. Mungall 1986, "*Frequency and time – national standards*," **Proceedings of the IEEE**, 74, 132-136.
- [3] M. Arditi 1982, "*A caesium beam atomic clock with laser optical pumping, as a potential frequency standard*," **Metrologia**, 18, 59-66.
- [4] R.E. Drullinger 1990, "*Optically pumped primary frequency standards*," Proceedings of the 44th Annual Symposium on Frequency Control, 23-25 May, 1990, Baltimore, Maryland (IEEE), pp. 76-81.
- [5] See, for example, J. Vanier and C. Audoin 1989, **The Quantum Physics of Atomic Frequency Standards** (Adam Hilger, Ltd., Bristol, UK), p. 845.
- [6] "*Guide to the Expression of Uncertainty in Measurement*," International Organization for Standardization (Geneva, Switzerland, 1993).
- [7] J.H. Shirley, W.D. Lee, G.D. Rovera, and R.E. Drullinger 1995, "*Rabi pedestal shifts as a diagnostic tool in primary frequency standards*," **IEEE Transactions on Instrumentation and Measurement**, IM-44, 136-139.
- [8] W.D. Lee, J.P. Lowe, J.H. Shirley, and R.E. Drullinger 1994, "*Microwave leakage as a source of error and long-term instability in cesium atomic-beam frequency standards*," Proceedings of the 8th European Forum on Time and Frequency (EFTF), 9-11 March 1994, Weihenstephan, Germany, pp. 513-516.
- [9] W.D. Lee, J.H. Shirley, F.L. Walls, and R.E. Drullinger 1995, "*Systematic errors in cesium beam frequency standards introduced by digital control of the microwave excitation*," Proceedings of the 1995 IEEE International Frequency Control Symposium, 31 May-2 June 1995, San Francisco, California, USA, pp. 113-117.

- [10] J.F. Garcia Nava, F.L. Walls, J.H. Shirley, W.D. Lee, and M.C. Delgado Aramburo 1996, "*Environmental effects in frequency synthesizers for passive frequency standards*," Proceedings of the 1996 IEEE International Frequency Control Symposium, 5-7 June 1996, Honolulu, Hawaii, USA, pp. 973-979.

Table 1. Evaluation Results

Physical Effect	Bias ($\cdot 10^{-15}$)	Uncertainty ($\cdot 10^{-15}$)
Second-order Doppler	≈ -300	1
Second-order Zeeman	$+10^5$	0.1
Cavity pulling	-5	1
Rabi pulling	≤ 0.1	0.1
Cavity phase (end-to-end)	$\approx \pm 750$	0.7
Cavity phase (distributed)*	0	4
Fluorescence light*	-0.01	0.1
Blackbody	-20	1
Gravitation	+180	0.1
Electronics		
RF spectral purity	0	0.1
Integrator offsets, Signal feedthrough	0	1
Modulation induced AM on RF or laser	-2	2
Microwave leakage	0	0.1
Combined Standard Uncertainty		5

(* see text)

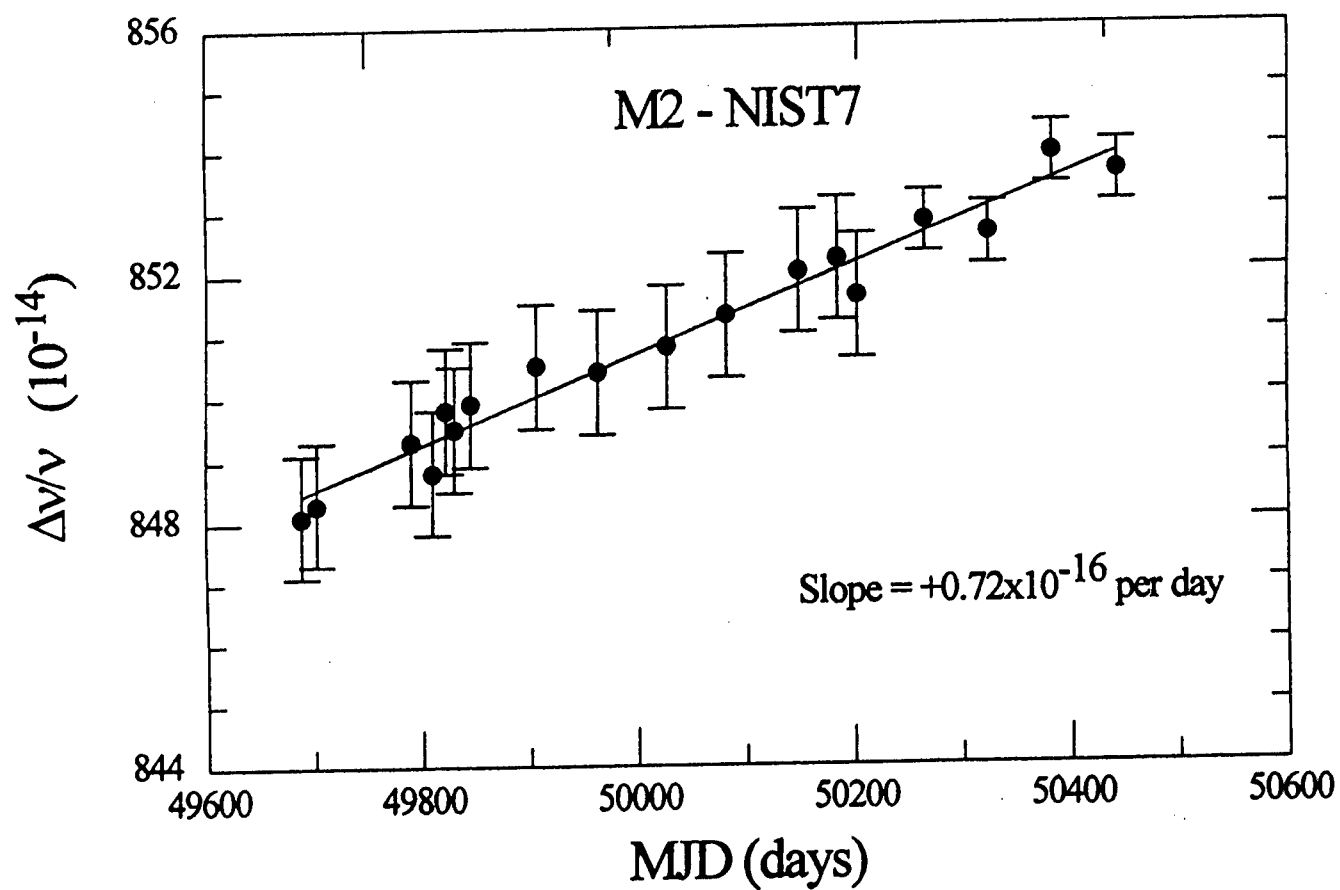


Figure 1. This plot shows the frequency difference between NIST-7 and our reference (M2) over a period of 2 years.

Questions and Answers

GERNOT WINKLER (INNOVATIVE SOLUTIONS INT'L): I have one question. You mentioned that, in your concept of the primary frequency standard, you have to switch not concepts but definitions when you come to the top. Wouldn't it be better to follow what I believe is the more generally adopted procedure or nomenclature to call a primary frequency standard a standard which can reproduce the undisturbed frequency of cesium within a given or specified tolerance? And the difference between yours and, for instance, Hewlett-Packard's is that you can do that to 5 parts in 10 to the 15th, compared to Hewlett-Packard's claim of 1 part in 10 to the 12th. I believe that's their latest number.

ROBERT DRULLINGER: I don't know how they would obtain the information of how close to the definition they approached without reference to some other standard. Whereas, this technology can do it internally without reference to a superior device.

GERNOT WINKLER: Well, for all standards, including yours, you have to allow that we have still some unknown effects. And the only way to get over that is compare independently constructed standards and have an internal measure of scatter which could serve as an estimate of your final obtainable accuracy.

ROBERT DRULLINGER: I'm sorry I didn't have time to go into all of the details. But in addition to this set of experiments that I do, I have a number of broad-brush things. For example, I revert to that old style of changing the microwave power. When I do, 15 parameters change; and the output frequency of the clock changes enormously. But I apply all of my known corrections and I look to see if they bring that back to normal. So that's a broad sweeping approach to look to see if I missed anything. And with half a dozen such cross-checks, I have found no exceptions yet.

So the appearance is, at the level we're claiming, we have a complete set.

DAVID ALLAN (ALLAN'S TIME): The root-sum-square assumes there's no correlation between any of the entries. Do you know that's the case?

ROBERT DRULLINGER: A valid question. The answer is in two parts. I reported this simply so that we're speaking apples and apples. All of the other primary standards have been using that as the way to report.

It happens that, with this evaluation technique, I believe I can prove a much greater degree of independence of the biases than with the typical one. And so I think I'm on solid ground to use the root-sum-square technique.

A DERIVATION OF THE DICK EFFECT FROM CONTROL-LOOP MODELS FOR PERIODICALLY INTERROGATED PASSIVE FREQUENCY STANDARDS*

Charles A. Greenhall
Jet Propulsion Laboratory
California Institute of Technology
4800 Oak Grove Dr., Pasadena, California 91109, USA

Abstract

The phase of a frequency standard that uses periodic interrogation and control of a local oscillator (LO) is degraded by a long-term random-walk component induced by downconversion of LO noise into the loop passband. The Dick formula for the noise level of this degradation can be derived from explicit solutions of two LO control-loop models. A summary of the derivations is given here.

INTRODUCTION

In 1987, following a suggestion of L. Cutler, G.J. Dick^[1] described a source of long-term instability for a class of passive frequency standards that includes ion traps and atomic fountains. In these standards, the frequency of a local oscillator (LO) is controlled by a feedback loop whose detection and control operations are periodic with some period T_c . For each cycle, the output of the detector is a weighted average of the LO frequency error over the cycle. The weighting function $g(t)$, derived from quantum-mechanical calculations, depends on the method by which the atoms are interrogated by the RF field generated by upconversion of the LO signal to the atomic transition frequency.^[1,2,3] In general, $g(t)$ can be zero over a considerable portion of the cycle. The LO control signal over each cycle is a function of the detector outputs from previous cycles.

The purpose of a frequency-control loop is to attenuate the frequency fluctuations of the LO inside the loop passband, while tolerating them outside the passband. As Dick saw, though, the periodic interrogation causes out-of-band LO noise power, near the cycle frequency $f_c = 1/T_c$ and its harmonics, to be downconverted into the loop passband, thus injecting random false information about the current average LO frequency into the control signal. This random false frequency correction causes a component of white FM, or random walk of phase, to persist in the output of the locked LO (LLO) over the long term. Dick gave a formula for the white-FM noise level contributed by this effect, namely:

*The work described here was performed by the Jet Propulsion Laboratory, California Institute of Technology, under a contract with the National Aeronautics and Space Administration.

$$S_y^{LLO}(0) = 2 \sum_{k=1}^{\infty} \frac{g_k^2}{g_0^2} S_y^{LO}(kf_c), \quad (1)$$

where $S_y^{LLO}(f)$ is the spectral density of the Dick-effect portion of the normalized frequency noise of the LLO, $S_y^{LO}(f)$ is the spectral density of the normalized frequency noise of the free-running LO, and g_k is the Fourier coefficient

$$g_k = \frac{1}{T_c} \int_0^{T_c} g(t) \cos(2\pi k f_c t) dt, \quad (2)$$

where $g(t)$ is assumed to be symmetric about $T_c/2$. This level of white FM near Fourier frequency zero contributes an asymptotic component of Allan variance given by:

$$\sigma_y^2(\tau) \sim \frac{S_y^{LLO}(0)}{2\tau} \quad (f_c \tau \rightarrow \infty). \quad (3)$$

My purpose here is to supplement previous derivations^[1,2,3,4] of the Dick formula (Eq. 1) by an approach that uses explicit time-domain solutions of simple LO control loop models with a general detection weighting function $g(t)$. Careful interpretation of these solutions yields formulas for the LLO spectral density, and conditions for the validity of the Dick formula. These models are not represented to be realistic models of actual frequency standards. By exhibiting the presence of the Dick effect in models of transparent simplicity, I intend to remove any remaining doubt of its existence and to isolate its essential nature, in the hope of aiding efforts to reduce it.

This paper gives only a summary of the solution method; details will be submitted elsewhere.

CONTROL-LOOP MODELS

Figure 1 shows two models for an LO control loop. Model 1 is intended to correspond to Dick's models.^[1,2] Model 2 extends the model of Lo Presti, Patanè, Rovera, and De Marchi^[4] to a general weighting function. A unified treatment of the two models is presented at the expense of a conflict of notation between this paper and [4]: because the model of Lo Presti et al. includes the effect of alternate interrogation of the two sides of a Ramsey fringe, the cycle period T_c used here corresponds to the sample period $T_s = 2T_c$ in [4], and the $g(t)$ used in Model 2 really consists of two periods of the $g(t)$ used in Model 1.

In Model 1, the box G_1 represents a linear time-invariant filter with impulse response $g(t)/(T_c g_0)$ for $0 < t < T_c$, and zero elsewhere. It is important to observe that G_1 has unity gain at DC. Its transfer function is

$$G_1(f) = \frac{1}{T_c g_0} \int_0^{T_c} g(t) e^{-i2\pi f t} dt. \quad (4)$$

The output of the box G_1 at time t is

$$G_{1yLLO}(t) = \frac{1}{T_c g_0} \int_0^{T_c} g(u) y_{LLO}(t-u) du,$$

which is fictitious unless t is a multiple of T_c . The output of the sampler at time nT_c is the normalized interrogation report

$$G_1 y_{LLO}(nT_c) = \frac{1}{T_c g_0} \int_0^{T_c} g(u) y_{LLO}(nT_c - u) du. \quad (5)$$

for the n th cycle. (Recall the symmetry of $g(t)$ about the midpoint of the cycle.) The detection noise term v_n can represent photon-count fluctuations in frequency standards with optical detection, for example. The cumulative sum of the error signals, multiplied by a gain factor λ between 0 and 1, is the frequency correction y_n that is applied to the LO during the next cycle. Except for initial conditions, Model 1 is specified completely by (Eq. 5) and the equations

$$y_n - y_{n-1} = \lambda (G_1 y_{LLO}(nT_c) + v_n), \quad (6)$$

$$y_{LLO}(t) = y_{LO}(t) - y_{n-1}, \quad (n-1)T_c < t \leq nT_c, \quad (7)$$

in which it is convenient to suppose that n runs through all integers.

In Model 2, the hold and integration operations emit a delayed linear interpolation of the cumulative sum of the input to the hold, modulo a constant of integration. Let y_n be λ times that cumulative sum. Then y_n again satisfies Eq. (6). In place of Eq. (7) we have

$$y_{LLO}(t) = y_{LO}(t) - \left(\frac{t}{T_c} - n + 1\right) y_{n-1} - \left(n - \frac{t}{T_c}\right) y_{n-2}, \quad (n-1)T_c < t \leq nT_c. \quad (8)$$

In Model 1, the frequency correction during a cycle is constant; here, it is a ramp.

SUMMARY OF SOLUTION METHOD

The derivation of the LLO frequency spectrum from these model equations is carried out by the following steps.

First, by isolating the digital aspects of the models, one can solve for y_n . In Model 1, substitution of Eq. (7) into Eq. (6) gives a first-order difference equation for y_n in terms of the quantity

$$w_n = G_1 y_{LO}(nT_c) + v_n. \quad (9)$$

The solution of this difference equation has the form $y_n = H_{d1} w_n$, where H_{d1} is a unity-gain lowpass digital single-pole filter with transfer function

$$H_{d1}(z) = \frac{\lambda}{1 - (1 - \lambda)z^{-1}}.$$

The time constant is approximately T_c/λ for $\lambda \ll 1$. The transient component of the solution is neglected. Model 2 gives a second-order difference equation that is solved by the two-pole filter

$$H_{d2}(z) = \frac{\lambda}{1 - \phi_1 z^{-1} - \phi_2 z^{-2}},$$

whose coefficients depend in a simple way on $g(t)$ and the gain factor λ . Under a reasonable assumption on $g(t)$, one can adjust the gain to make the filter overdamped, critically damped, or underdamped.

Second, with y_n known, it is evident from Eq. (7) or Eq. (8) that the LLO frequency is a known function of time on each cycle. Because of the piecewise nature of the solution, we need to use care in its interpretation to obtain a well-defined spectrum. Let us agree that the low-frequency spectral behavior of the LLO phase is adequately known if we can determine the discrete-time spectrum of the phase when sampled with period T_c . In turn, we know the sampled-phase spectrum if we know the discrete-time spectrum of the sequence of average LLO frequencies. Let $\bar{y}_{LLO}(nT_c)$ be the average value of LLO frequency over the cycle ending at nT_c . Knowing the LLO frequency as a function of time over this cycle, we can generate an explicit formula for the average frequency. This formula is shown as a block diagram in Fig. 2, which applies to both loop models. The block labeled "average" is the continuous-time moving-average filter for period T_c ; the following sampler gives the sequence of LO frequencies averaged over successive cycles. The only component that depends explicitly on the model is the block labeled H_e , a unity-gain lowpass digital filter with transfer function $z^{-1}H_{d1}(z)$ for Model 1, $\frac{1}{2}(z^{-1} + z^{-2})H_{d2}(z)$ for Model 2.

Third, the two-sided LLO frequency spectrum can be deduced from the block diagram of Fig. 2 by observing that the diagram is equivalent to a certain continuous-time operation followed by a single sampler. In terms of the two-sided LO frequency spectrum $S_y^{LO}(f)$ and detection-noise spectrum $S_v(f)$, the LLO spectrum can be written as follows:

$$S_y^{LLO}(f) = S_y^0(f) + S_y^1(f), \quad |f| \leq f_c/2,$$

where

$$S_y^0(f) = \left| \frac{1 - z^{-1}}{i2\pi f T_c} - H_e(z) G_1(f) \right|^2 S_y^{LO}(f) + |H_e(z)|^2 S_v(f), \quad (10)$$

the main spectrum, so to speak, and

$$S_y^1(f) = \sum_{k \neq 0} \left| \frac{1 - z^{-1}}{i2\pi (f T_c + k)} - H_e(z) G_1(f + k f_c) \right|^2 S_y^{LO}(f + k f_c), \quad (11)$$

the aliased spectrum. In these formulas, $z = e^{i2\pi f T_c}$. The sum includes both positive and negative k .

MAIN AND ALIASED SPECTRA

Consider the main part (Eq. 10) of the LLO frequency spectrum. The LO spectrum is multiplied by a factor that is $O(f^2)$ as $f \rightarrow 0$. This is the basic action of the first-order frequency control loop, which attenuates the excursions of the LO inside the loop bandwidth. For example, flicker FM in the LO is reduced to flicker PM in the LLO, and random walk FM is reduced to white FM. In addition, there is a lowpass-filtered white detection noise in the LLO frequency. We can regard $H_e(z)G_1(f)$ as the closed-loop transfer function from LO frequency noise to LO correction signal.

The Dick effect is supposed to come from a long-term white-FM component in the aliased spectrum. There is such a contribution if the aliased spectrum (Eq. 11) is continuous and positive at $f = 0$. Under reasonable conditions, this is so, and we may set $f = 0$ ($z = 1$) in Eq. (11). Because $H_e(1) = 1$, we have

$$S_y^1(0) = 2 \sum_{k=1}^{\infty} |G_1(kf_c)|^2 S_y^{LO}(kf_c), \quad (12)$$

where we have now used the symmetry of the summands about zero frequency. This formula holds for one-sided spectral densities also.

The numbers $|G_1(kf_c)|^2$ are invariant to cyclic translations of the function $g(t)$ in time. It follows that the result (Eq. 12) is invariant to shifts in the time origin, i.e., if the LLO phase is sampled on any time grid with spacing T_c , then the samples will include a white-FM component with spectral density (Eq. 12) at zero frequency. If $g(t)$ is symmetric about $T_c/2$ for our time origin, then

$$G_1(kf_c) = \frac{g_k}{g_0},$$

where g_k is given by Eq. (2). Thus, Eq. (12) extends the Dick formula (Eq. 1) to asymmetric weighting functions.

The Dick formula, which gives the limiting value of spectral density at zero Fourier frequency, is exact for both models, even though the LLO spectrum at nonzero frequencies is different for the two models. A simple approximation for the aliased spectrum (Eq. 11) holds if the gain constant λ is much less than 1. Then the loop bandwidth is much less than f_c (time constant much greater than T_c). Assume also that $G_1(kf_c + f)$ and $S_y^{LO}(kf_c + f)$ can be regarded as approximately constant for nonzero k and for f within the loop bandwidth. Then, for such f , the aliased spectrum has approximately the same shape as the frequency response of the digital filter H_e , with value at 0 given by the Dick formula. For both models, this shape is approximately Lorentzian. Thus, the Dick-effect Allan variance component takes the asymptotic white-FM form (Eq. 3) only for averaging times τ greater than roughly twice the loop time constant. In this approximation, the Dick-effect and detection noises appear inside the loop bandwidth, the non-aliased LO noise outside.

REMARKS

Although I have not considered any other models, the Dick effect appears to be an inherent property of periodic local-oscillator control loops. For the two models treated here, this was shown by a careful interpretation of explicit solutions for the output frequency as function of time.

I have now come full circle on this topic. My involvement began in 1987 when John Dick asked me to derive the spectrum of $G_{1y_{LO}}$ after sampling. I did not understand: in Fig. 1, G_1 is applied to y_{LLO} , not to y_{LO} . Nevertheless, I did the calculation, thereby contributing the factor 2 in Dick's formula. Now, from the block diagram in Fig. 2, we see how the sampled $G_{1y_{LO}}$ fits into the picture. Could the Dick effect be cancelled by replacing the averaging filter by a G_1 filter? Alas—this block diagram is merely a graphical representation of a mathematical formula; it has no physical existence.

REFERENCES

- [1] G.J. Dick 1988, "*Local oscillator induced instabilities in trapped ion frequency standards*", Proceedings of the 19th Precise Time and Time Interval (PTTI) Applications and Planning Meeting, 1-3 December 1987, Redondo Beach, California, USA, pp. 133-147.
- [2] G.J. Dick, J.D. Prestage, C.A. Greenhall, and L. Maleki 1991, "*Local oscillator induced degradation of medium-term stability in passive atomic frequency standards*", Proceedings of the 22nd Precise Time and Time Interval (PTTI) Applications and Planning Meeting, 4-6 December 1990, Vienna, Virginia, USA (NASA CP-3116), pp. 487-508.
- [3] G. Santarelli, Ph. Laurent, A. Clairon, G. J. Dick, C. A. Greenhall, and C. Audoin 1996, "*Theoretical description and experimental evaluation of the effect of the interrogation oscillator frequency noise on the stability of a pulsed atomic frequency standard*," Proceedings of the 10th European Frequency and Time Forum (EFTF), March 1996, Brighton, UK (IEEE Conference Publication 418).
- [4] L. Lo Presti, F. Patanè, D. Rovera, and A. De Marchi 1996, "*A simulation guided analytical approach to the theory of the Dick effect*," Proceedings of the 1996 IEEE International Frequency Control Symposium, 5-7 June 1996, Honolulu, Hawaii, USA, pp. 1106-1112.

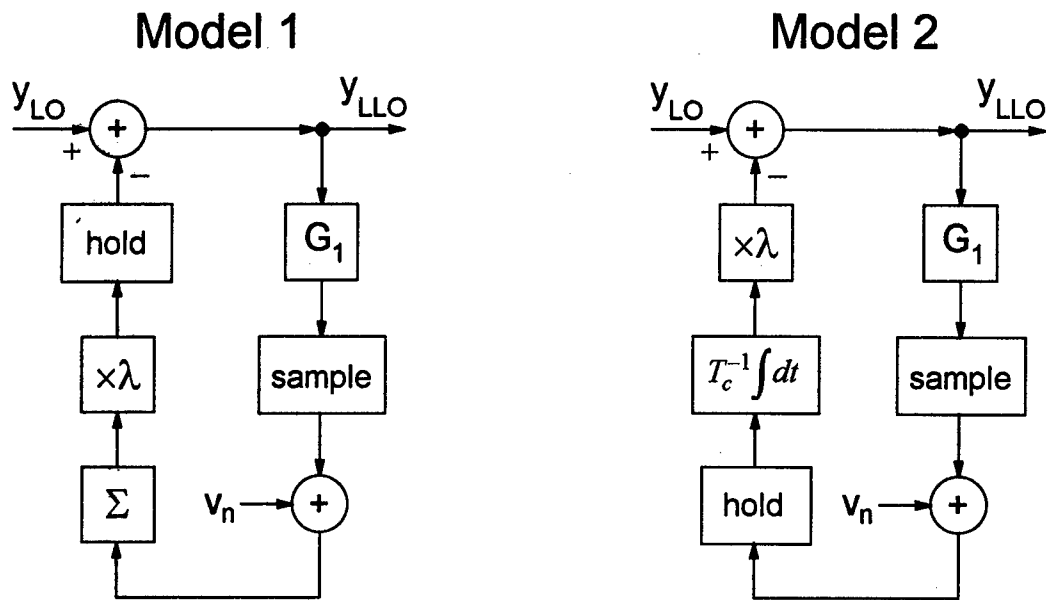
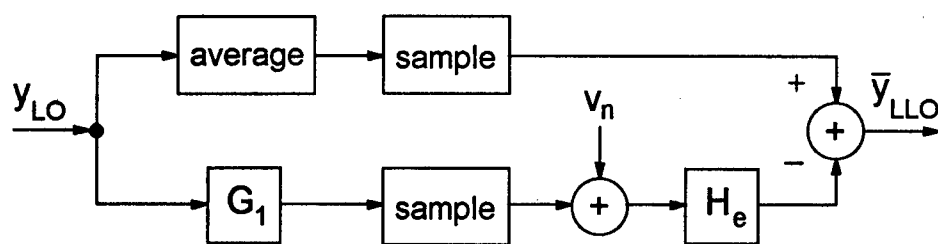


Fig. 1. Simplified models of local-oscillator control loops



$$\text{Model 1: } H_e(z) = \frac{\lambda z^{-1}}{1 - (1 - \lambda) z^{-1}}$$

$$\text{Model 2: } H_e(z) = \frac{\frac{\lambda}{2}(z^{-1} + z^{-2})}{1 - \phi_1 z^{-1} - \phi_2 z^{-2}}$$

Fig. 2. Solution of both models for LLO frequency averages

TEMPERATURE CONTROL FOR HYDROGEN MASER FREQUENCY STANDARDS

Yigen Fu, Zhongshi Zhou, and Xiaofan Liu
Beijing Institute of Radio Metrology and Measurement
P.O. Box 3930 Beijing, 100854 Peoples Republic of China

Abstract

Hydrogen masers with excellent long-term frequency stability are now used for frequency standards. In recent years, a lot of research and development of compact H-masers has been done at the Beijing Institute of Radio Metrology and Measurement. The long-term frequency stability and temperature coefficient of frequency are greatly affected by the temperature stability of the interior cavity. Therefore, one must pay attention to the interior cavity temperature control system in the development of compact H-masers. In this paper we will discuss and stress the following points:

(1) There are two representative methods in cavity frequency control. The first method is a combination of cavity temperature control and cavity frequency servo. The second method is the above, combined with total temperature compensation.

(2) The partial temperature compensation is used with cavity temperature control and cavity frequency servo in this method. The method of partial temperature compensation has a short time delay, and can reduce the effect of the temperature gradient. By using high-stability temperature sensors and multilayer, multipoint temperature controls, the temperature control accuracy can increase. In our H-masers, accurate decimal frequency synthesizers, high-velocity and high-isolation switches, low-noise up-frequency converters, and high-stability automatic frequency control systems have been developed. Hence, the achieved accuracy of the cavity frequency servo is better than 1 Hz.

(3) Since the above method was adopted, the performance of the compact H-masers has greatly improved in the laboratory.

1 INTRODUCTION

Hydrogen maser, with its excellent medium-term and long-term frequency stability, is now used as frequency standard. The hydrogen atomic frequency standard has now found a wide application in the fields of atomic time keeping, radio astronomy, aerospace, satellite navigation, etc., which has aroused great concern and brought about a lot of researches all over the world. In recent years, Beijing Institute of Radio Metrology and Measurement has made a lot of fruitful researches in the development of compact hydrogen maser. According to documents and our experience, the control on cavity resonant frequency is one of the key issues in the development of hydrogen maser.

The long-term frequency stability is mainly decided by the frequency tuning of resonant cavity and the cavity servo control system. Of these two factors, the former is related to temperature coefficient of the cavity, material property of the resonant cavity, aging change in storage bulb coating property, effect of magnetic field, etc., which sets a higher demand on the temperature control system of the frequency standard. This paper will discuss two representative schemes in the cavity frequency control, and an analysis and a comparison will be made on them. The paper will also present our scheme, i.e. to combine partial temperature compensation and cavity temperature control with cavity frequency servo. By adopting partial temperature compensation method, high-stability temperature sensor and multilayer and multipoint temperature control in our hydrogen maser, the interior cavity is possessed of a satisfactory temperature stability. And precision decimal frequency synthesizer, high-speed/high-isolation switch, low-noise up frequency converter and high-stability automatic frequency control system have been developed, which leads to an accuracy of cavity frequency servo better than 1Hz. Thanks to the above schemes, the performance of the compact hydrogen maser is greatly improved.

2 COMPARISON OF THE SCHEMES IN THE CAVITY FREQUENCY CONTROL

Two schemes in the cavity frequency control are involved at present.

The first one is to combine cavity temperature control with cavity frequency servo, which is a common scheme. The dimensions of the resonant cavity and storage bulb will influence the cavity frequency as the temperature varies, so the temperature stability is very important and it is necessary to keep temperature constant via a temperature control circuit. In order to reduce tractive effect, the automatic servo system of cavity frequency is employed besides precision constant temperature. The common electronic circuit tuning is easy, reliable and fast, which can improve the performance by several orders of magnitude. Therefore, the cavity temperature control and the cavity servo are two main necessary links for cavity frequency control.

The second one is to combine total temperature compensation and cavity temperature control with cavity frequency servo. The total temperature compensation method is stated below: Measure the frequency by cavity frequency sensor first, then feed the error signal of this frequency value into the control loop to drive the compensating heater which serves to regulate the cavity temperature control system, thus cavity frequency control can be realized. The relation between the master heater and the compensating heater can be adjusted by step-by-step method. When the ambient temperature changes slowly, the frequency-temperature coefficient can be adjusted to a very small value by compensation; when it changes dynamically, outer-layer temperature control and heat compensation can prevent and delay the dynamic interaction, however, the temperature compensation and the adjustment of time constant are comparatively troublesome.

For this reason, we adopt the scheme of combining partial temperature compensation and cavity temperature control with cavity frequency servo. In fact, the partial temperature compensation method is to adopt an additional sensitive element to measure the temperature change at a correlation point; through compensation by electronic circuit, a high-performance constant temperature can be obtained. As temperature measurement, balance and compensation are conducted in two different positions, the influence of the temperature gradient can be reduced; moreover, the partial temperature compensation method has the advantages of short time delay, convenient circuit regulation, etc.

3 CAVITY FREQUENCY SERVO CONTROL SYSTEM

The cavity servo control system is composed of two decimal frequency synthesizers, two IF up frequency conversion circuits, high-speed synchronous switch, microwave up frequency converter, error signal control loop, varactor diode fitted in the physical cavity, etc. Through these unit circuits, the feed-cavity signals f_1 and f_2 alternatively changing controlled by 10Hz symmetrical square wave. The frequency cavity functions as a high-Q frequency discriminator. f_1 and f_2 reference sources are very stable, $f_1=f_0+\Delta f$, $f_2=f_0-\Delta f$ (taking Δf as 15kHz) and $(f_1+f_2)/2=f_0$ (hydrogen atom transition frequency). If the resonant frequency of the physical cavity is equal to the hydrogen atom transition frequency, the error signal equals zero; if the cavity frequency is higher, an error signal is generated through frequency discrimination, and a voltage with negative polarity is delivered from the control loop and applied on the varactor diode, then the reverse bias of the diode drops, the junction capacitance increases and the raised cavity frequency is pulled back to f_0 ; otherwise, if the cavity frequency is lower, the dropped cavity frequency is pulled back to f_0 .

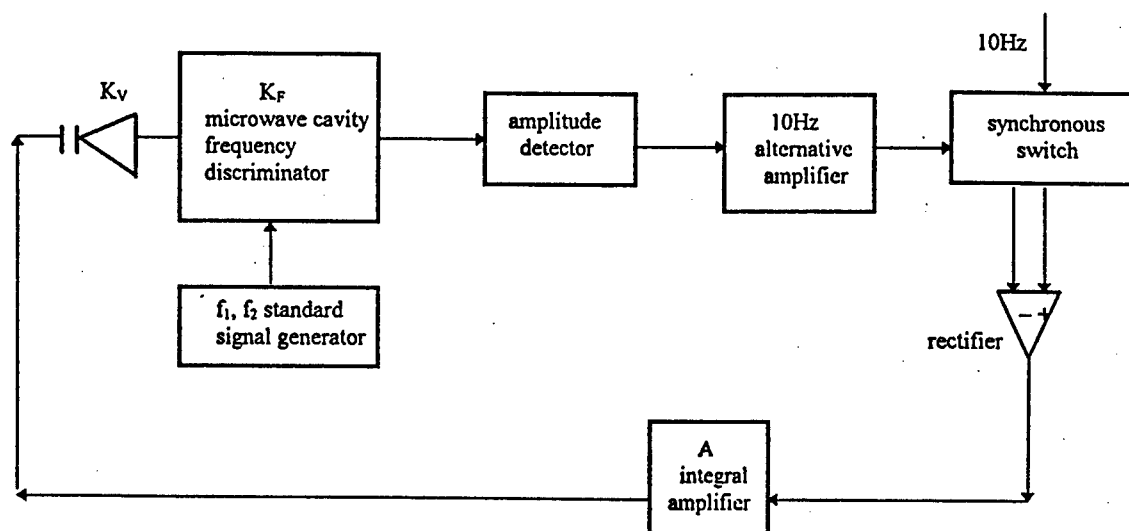


Fig.1 Block diagram of cavity frequency servo control system

Fig.1 is block diagram of cavity frequency servo control system, whose control equation can be written as:

$$\Delta f_N / \Delta f_0 = 1 / (1 + K_F \cdot |K_V| \cdot A)$$

where,

Δf_0 : frequency drift caused by various factors of the physical cavity

Δf_N : remainder frequency deviation caused by automatic servo of the cavity frequency

K_F : sensitivity of the frequency discriminator

K_V : voltage-control sensitivity of the varactor diode

A: total gain of the alternative amplifier, integral amplifier, etc.

It can be seen from above that K_F , K_V and A should be greater so as to decrease the remainder frequency deviation. However, the unstability of the system will be increased with the increase of the gain; therefore, a compromise scheme should be considered in design; and a varactor diode with small temperature coefficient, high-Q value and a certain linearity should be selected (Note: Its direction and height should be taken into consideration when it is fitted into the physical cavity.). In addition, it is also very important to reduce the phase noise at the sideband frequencies f_1 and f_2 of f_0 and the noise of all components in the control loop, to raise the spectral purity and the stability of the loop, to design an appropriate bandwidth, etc.

Through well-conceived design and delicate debugging, the technical problem has been solved and the control accuracy of the cavity frequency servo system is better than 1Hz.

4 PRECISION TEMPERATURE CONTROL CIRCUIT

The temperature stability of the temperature-control system is a function of the system structure and the circuit design.

4.1 Structure of the Temperature-Control System

As the key part of the hydrogen maser, the resonant cavity is required of a highest temperature stability; besides, the cover, neck and some microwave elements also need a constant temperature. In view of this, we have designed a constant-temperature system with a fair temperature-keeping effect and double-layer and multipoint control function.

4.2 Outer-Layer Temperature Control Circuit

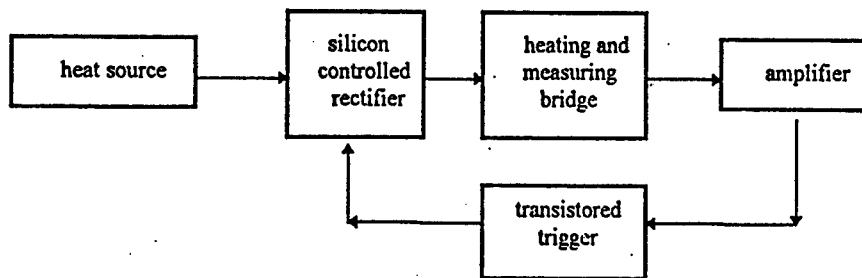


Fig.2 Block diagram of outer-layer temperature control circuit

As shown in Fig.2, heating and measuring are conducted in the same bridge which adopts double-wire non-inductive resistor and whose four arms are made of two materials, i.e. manganin wire and copper wire, actually acting as a temperature sensitive element. In the positive half-wave state of the circuit, the difference signal from the bridge, having been amplified and phase discriminated, forms a trigger pulse to trigger the controlled silicon element, then the heating voltage enters the heating bridge via the controlled silicon element. At first, the system stays in a cooling state and the difference signal is comparatively large, so the controlled silicon, with a great angle of flow, is in a fast heating state. When the constant-temperature zone approaches the set temperature, both the difference angle and the angle of flow of the controlled silicon become smaller. At last, the system stays in a balanced state when heat dissipation equals heating. It has been proven from our over-two-year tests that this circuit is characterized by stable and reliable operation, simple structure, easy adjustment and comparatively high temperature stability.

4.3 Interior-Layer Temperature Control Circuit

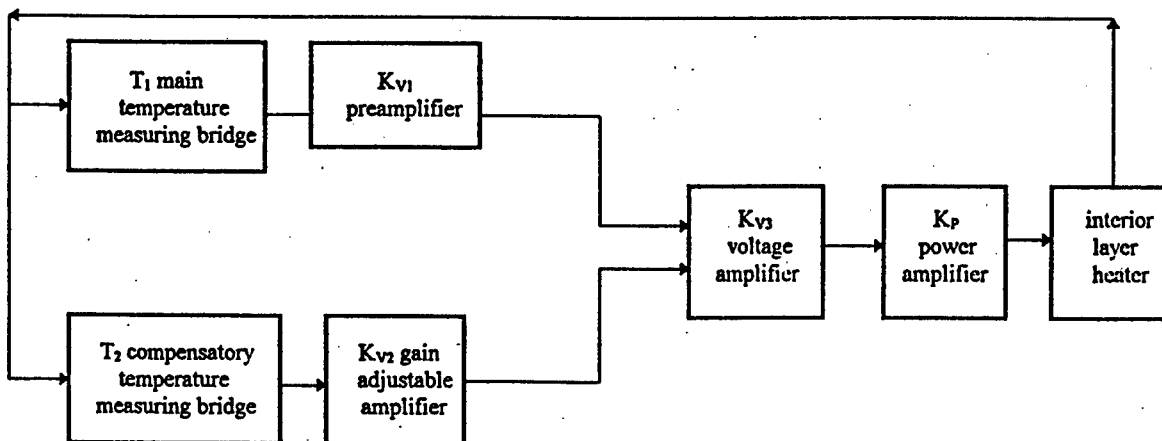


Fig.3 Block diagram of interior-layer temperature control circuit

The structure of the circuit is shown in Fig.3. The circuit features as follows. First, it adopts platinum-resistance thermometer with a fair long-term stability as its temperature-sensitive element so as to reduce its self-heating effect; secondly, by adopting partial compensation circuits T_2 and K_{V2} , selecting optimum correlation compensating point and adjusting gain G_{V2} , the temperature-control effect of improving the performance by 1~2 orders of magnitude can be got; thirdly, its preamplifier is characterized by a low noise, high sensitivity and reliable wiring. Moreover, the bridge and the preamplifier are in a temperature-control environment.

The delicate design and adjustment of double-layer and multipoint temperature control will lead to a satisfactory temperature stability of the interior cavity.

5 TEST AND TEST RESULTS

A series of tests are required in the development of hydrogen maser, such as tests of short-term, medium-term and long-term frequency stability and test of frequency accuracy; test of frequency-temperature coefficient having a closest relation with temperature, tests of interior-layer short-term and long-term temperature stability, test of interior-layer temperature sensitivity, etc.

The test method of the frequency-temperature coefficient is to place the hydrogen maser in a constant-temperature environment and to raise the ambient temperature by Δt . After the temperature gets stable, measure the variation of its output frequency; the test method of the interior-layer temperature sensitivity is to place the hydrogen maser in a constant-temperature environment and to raise the ambient temperature by Δt . After the temperature gets stable, measure the variation of its interior-layer temperature; the test method of the interior-layer short-term and long-term temperature stability is to adopt the standard platinum-resistance thermometer commonly used in the world, assisted by a stable and sensitive bridge or a high-performance digital ohmmeter.

All methods and devices involved have been certified by relevant metrical authority.

Up to now, repeated tests have been performed, and the test curves are respectively shown in Fig.4 and Fig.5.

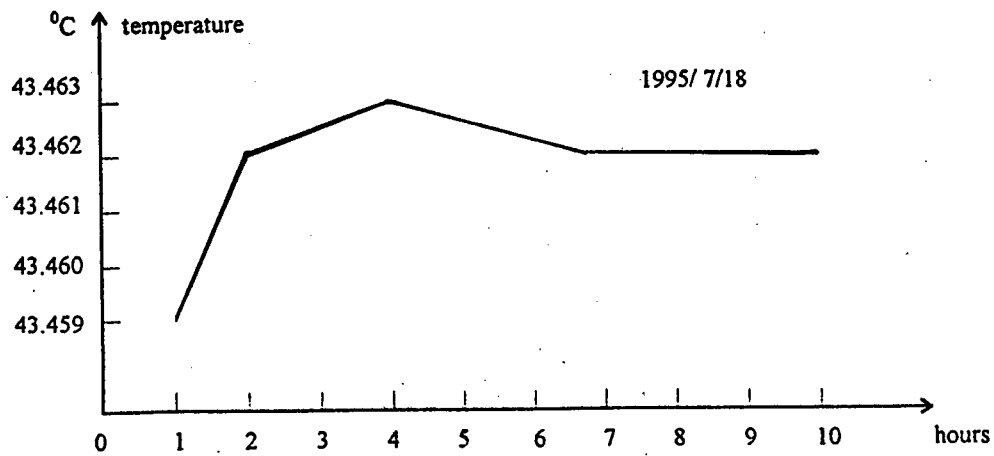


Fig.4

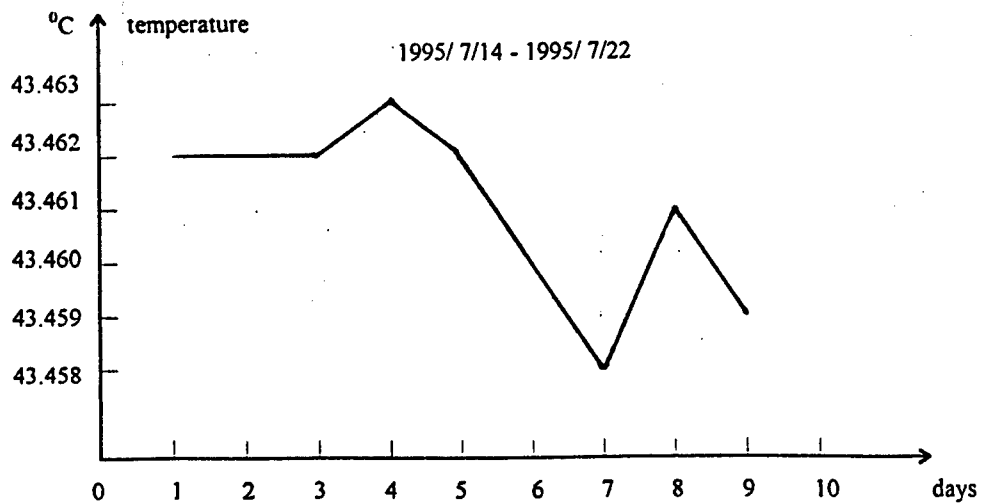


Fig.5

Interior layer 10 hours temperature stability ± 0.002 °C

Interior layer 9 days temperature stability ± 0.003 °C

When the ambient temperature changes by 1 °C, the interior-layer temperature change is 10^{-3} °C.

6 CONCLUSIONS

The cavity frequency control scheme of combining partial temperature compensation and cavity temperature control with cavity frequency servo is adopted. According to the test result of the interior-layer temperature stability of $\underline{0.002}$ °C and the control accuracy of the cavity frequency servo system better than 1 Hz, it can be ensured that both the frequency-temperature coefficient and the long-term frequency stability of the hydrogen maser are better than 1×10^{-14} .

We gratefully acknowledge Ms. Yanjun Zhang's energetic assistance in our undertakings in development and test.

7 REFERENCES

- [1] Y. Fu, "Temperature control system for compact hydrogen maser," Beijing Institute of Radio Metrology and Measurement (restricted).
- [2] Z. Zhou, "Electronic receiver system for hydrogen maser," Beijing Institute of Radio Metrology and Measurement (restricted).
- [3] H.T.M. Wang 1982, "Characteristics of oscillating compact hydrogen masers," Proceedings of the 36th Annual Symposium on Frequency Control, 2-4 June 1982, Philadelphia, Pennsylvania, USA (U.S. Army Electronics and Development Command), pp. 249-254.
- [4] F.L. Walls 1987, "Analysis of high performance compensated thermal enclosures," Proceedings of the 41st Annual Symposium on Frequency Control, 27-29 May 1987, Philadelphia, Pennsylvania, USA (IEEE), pp. 439-443.
- [5] Y.G. Gouzhva, A.G. Gevorkyan, A.L. Myasnikov, G.M. Kruyukov, V.Z. Gankin, O.N. Kornishov, and S.D. Teplova 1995, "Activities of the Russian Institute of Radio Navigation and Time in development of GLONASS on-board Q-enhanced oscillating compact H-maser," Proceedings of the 1995 IEEE International Frequency Control Symposium, 31 May-2 June 1995, San Francisco, California, USA, pp. 140-148.
- [6] N.A. Demidov, E.M. Zhov, B.A. Sakharov, and A.A. Vljanov, "The investigation of performances of compact active and passive H-masers," Institute of Electronic Measurements KVARZ, N. Novgorod, Russia Gagarin Prospect 176 Russia 603009 Nizhny Novgorod.

FIRST COMMERCIAL PROTOTYPE OF AN OPTICALLY PUMPED CESIUM-BEAM FREQUENCY STANDARD

Michel L. Baldy
Tekelec Telecom
29, Avenue de la Baltique
91953 Les Ulis Cedex, France

Abstract

Tekelec has developed the first commercial prototype of an Optically Pumped Cesium-Beam Frequency Standard with the scientific support of the Laboratoire de l'Horloge Atomique (LHA) and the financial support of the French Military Administration (DGA). This work is based on years of experience of the LHA on cesium atomic clocks, especially on short atomic clocks and on the experience of Tekelec in time and frequency for systems (timekeeping, time distribution, synchronization, etc.) and components (quartz oscillators, rubidium atomic clocks, etc.). The first prototype is under characterization and the first results are presented in this paper.

INTRODUCTION

The huge growth of synchronization and positioning requirements for military, civilian, or space applications will rapidly increase the need for ever more accurate and cheaper frequency standards. We believe that the optically pumped cesium-beam frequency standard is a good candidate for these applications.

The optical pumping technology has improved widely the performances of laboratory clocks and is used in the best National Primary Atomic Clocks (LPTF^[1], NIST^[2]) replacing the magnetic deflection technology.

The Laboratoire de l'Horloge Atomique (LHA) has demonstrated^[3,4] the ability of this technology to improve short system performance and, therefore, is of great interest for industrial applications.

Furthermore, the greater simplicity of this technology will lead to lower price.

PRINCIPLE OF OPERATION OF AN ATOMIC CLOCK

The scheme of Figure 1 represents the general operation diagram used in an atomic clock to stabilize the 10 MHz signal generated by a quartz crystal oscillator (OCXO) with the atomic resonator using a synchronous detection. The heart of such a clock is the cesium-beam resonator. The operation is based on the population difference between the two hyperfine

levels of the ground state of the cesium-133 atom on which the definition of the second is based (Figure 2). The operation principle of a resonator is based on three main parts described Figure 3:

- The atomic preparation realizes the population inversion. The two hyperfine levels populations are naturally equivalent; the preparation eliminates one population (in the case of magnetic field technology) or realizes an optical pumping of the atoms to one hyperfine level (optical pumping technology). After preparation all the beam atoms are located on one level ($F=4$).
- The microwave interaction is realized by a microwave cavity; basically if the frequency is exactly tuned to the transition between the two hyperfine levels, there is a stimulated recombination. So the second hyperfine level is populated again ($F=3$).
- The clock signal detection analyzes the population of this level by a hot wire detector (magnetic deflection) or by the fluorescence given by optical pumping.

DESCRIPTION OF THE TEKELEC RESONATOR

The Tekelec cesium-beam resonator is described Figure 4. In the high vacuum conditions maintained by an ion pump, a cesium oven generates a very low divergence thermal cesium beam. This beam is shaped by several graphite diaphragms. The atomic preparation and signal detection are obtained by optical pumping using the same laser diode. The fluorescence signal in the preparation area is used to slave the laser diode frequency to the 3-3 transition of the D2 line ($6^2S_{1/2} \rightarrow 6^2P_{3/2}$) of the cesium frequency diagram (Figure 2). A Ramsey microwave cavity excited at 9.192631 GHz by a coaxial antenna is used for RF interaction. It is magnetically shielded and a low and very uniform static C-field is applied. In the detection area, the fluorescence signal is used as the clock signal. A second magnetic shield protects the optical areas and the cavity.

MAIN ADVANTAGES OF THE TECHNOLOGIES USED

The main advantages of the optical pumping compared to using a magnetic field are:

- the atomic preparation is complete, increasing the signal-to-noise ratio,
- all the atoms participate in the clock signal (twice as much as with magnetic deflection), allowing a lower cesium consumption,
- there is no strong magnetic field near the microwave cavity,
- the Rabi-Ramsey spectrum is very symmetric, increasing the accuracy and allowing a lower C-field, which decreases the magnetic sensitivity of the clock,
- the cesium speed distribution is well known, increasing the accuracy,
- there is no hot wire detector, which is very fragile, and limits the lifetime of the resonator,
- the technology is much simpler (without deflection), which will lead to lower cost.

Furthermore, we use an electric coupling and a cavity geometry giving an odd number of longitudinal modes, and then a phase difference of 180° between the two oscillatory fields that the atoms experience in succession. The LHA^[5] has demonstrated that this configuration improves the frequency stability.

MAIN CHARACTERISTICS OF THE TEKELEC CLOCK

The aim of Tekelec is to produce a state-of-the-art cesium-beam frequency standard for an attractive price. The accuracy will be better than $1 \cdot 10^{-12}$. The stability in time and frequency domains are given Figures 5 and 6. The stability planned is given by $\sigma_y(\tau) = 6.3 \cdot 10^{-12} \tau^{-1/2}$ between 2 and 400,000 seconds, with a flicker floor at $1 \cdot 10^{-14}$. As far as we know, these characteristics are the best values published for a commercial standard.

FIRST RESULTS

A prototype has been realized and is under characterization. The full numerical electronics have been tested and their phase noise fulfills the planned frequency domain characteristics. The Rabi-Ramsey resonance fringes have been obtained and are represented in Figure 7. The difference between two fringes is 42 kHz, corresponding to a C-field of 6 μ T. These fringes present a minimum at the center (black fringe) which is characteristic of an electric coupling of the cavity (antenna). The spectrum is very symmetric, as expected. The central line, which is used as clock signal, is given in Figure 8. The linewidth (FWHM) of the central line is 600 Hz, which is the theoretical value for the cavity length and the atoms' speed. This value, combined with a signal-to-noise ratio of 10,000, will lead to a stability better than the planned stability. The LHA^[6], in a similar size resonator, has obtained $\sigma_y(\tau) = 2 \cdot 10^{-12} \tau^{-1/2}$, with a flicker floor of $2 \cdot 10^{-14}$, a line width of 660 Hz, and an old and nonoptimized analog electronic system. So we believe that, with our resonator and our modern fully automatic and optimized digital electronic system we will fulfill, and even improve, the expected performance of the clock.

CONCLUSION

Tekelec has developed a prototype of an optically pumped cesium beam frequency standard with the scientific support of the LHA. The first results show that the goal of the Tekelec clock, to be the state of the art of commercial frequency standards, is reachable. This belief is confirmed by the very good results obtained by the LHA in a equivalent lab prototype and with an old-fashioned electronic system. This prototype will be industrialized in two versions: one in the conventional 19", 3U size and one compact version for military applications.

REFERENCES

- [1] E. de Clerck, G.D. Rovera, and A. Clairon 1994, "*Progress on the LPTF optically pumped primary frequency standard*," Proceedings of the 8th European Frequency and Time Forum (EFTF), 9-11 March 1994, Weihenstephan, Germany, pp. 497-502.
- [2] R.E. Drullinger, J.P. Lowe, D.J. Glaze, and J. Shirley 1993, "*NIST-7, the new U.S. primary frequency standard*," Proceedings of the 7th European Frequency and Time Forum (EFTF), March 1993, Neuchâtel, Switzerland, pp. 549-551.

- [3] P. Petit, V. Giordano, N. Dimarcq, P. C  rez, C. Audoin, and G. Th  obald 1992, *Miniature optically pumped cesium beam resonator*, "Proceedings of the 6th European Frequency and Time Forum (EFTF), March 1992, Noordwijk, Netherlands, pp. 83-86.
- [4] P. Petit, V. Giordano, P. C  rez, B. Boussert, C. Audoin, and N. Dimarcq, *"Performance of a 2 dm³ optically pumped cesium beam tube: a progress report"*, Proceedings of the 8th European Frequency and Time Forum (EFTF), 9-11 March 1994, Weihenstephan, Germany, pp. 517-522.
- [5] C. Audoin, V. Giordano, N. Dimarcq, P. C  rez, P. Petit, and G. Th  obald 1993, *"Properties of an optically pumped cesium beam frequency standard with $\phi = \pi$ between the two oscillatory fields"*, Proceedings of the 7th European Frequency and Time Forum (EFTF), March 1993, Neuch  tel, Switzerland, pp. 537-540.
- [6] B. Boussert 1996, thesis, Universit   de Paris, XI Orsay.

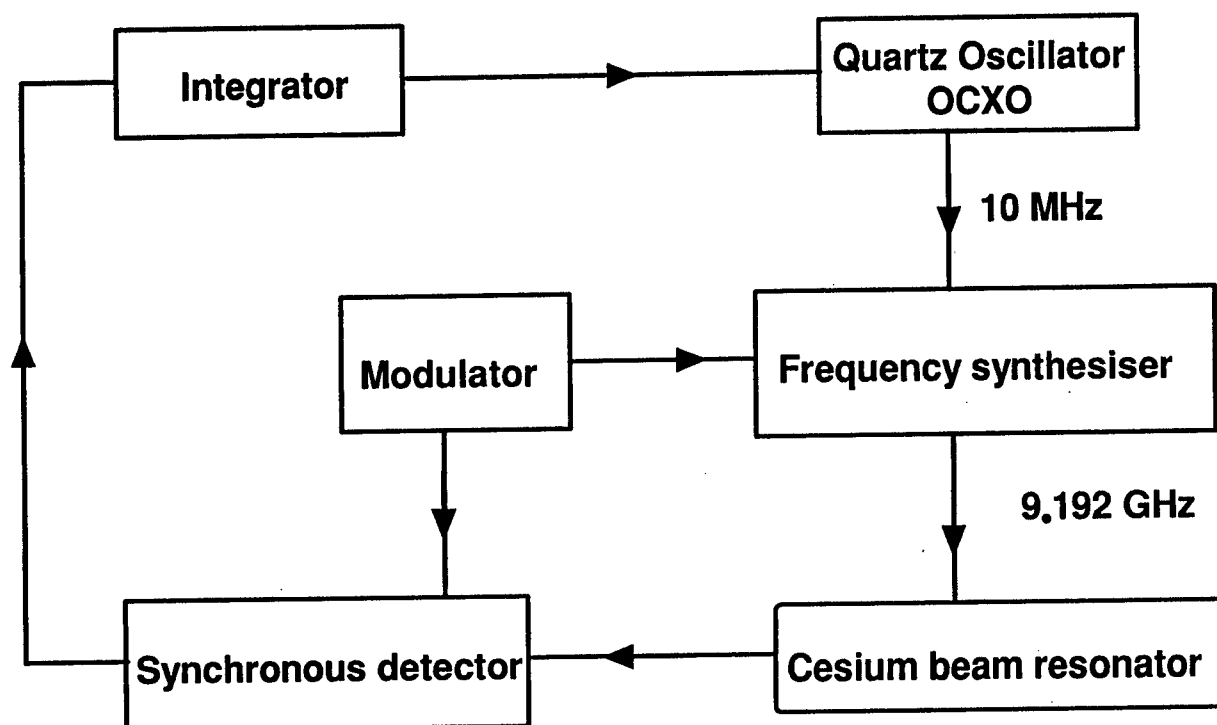


Figure 1 : Block diagram of the operation of an atomic clock

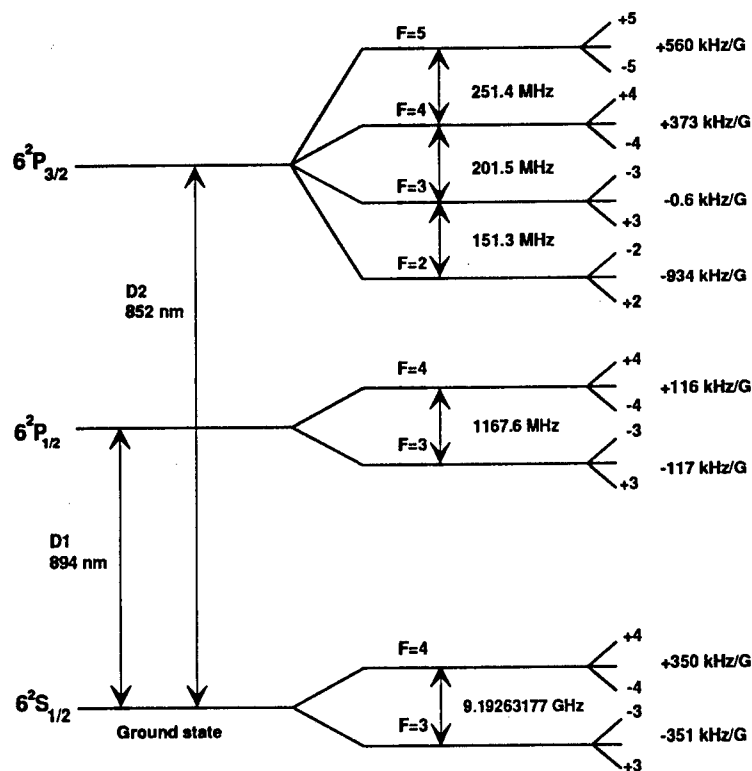


Figure 2 : Energy levels of the cesium 133 atom

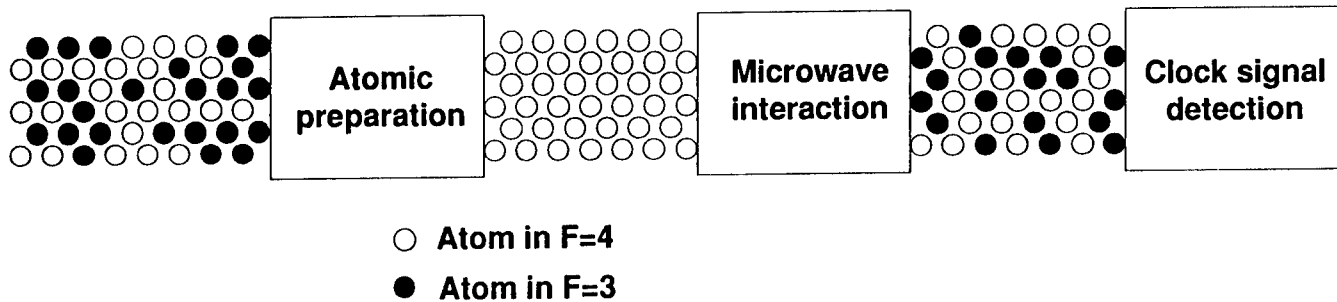


Figure 3 : Atomic resonator principle

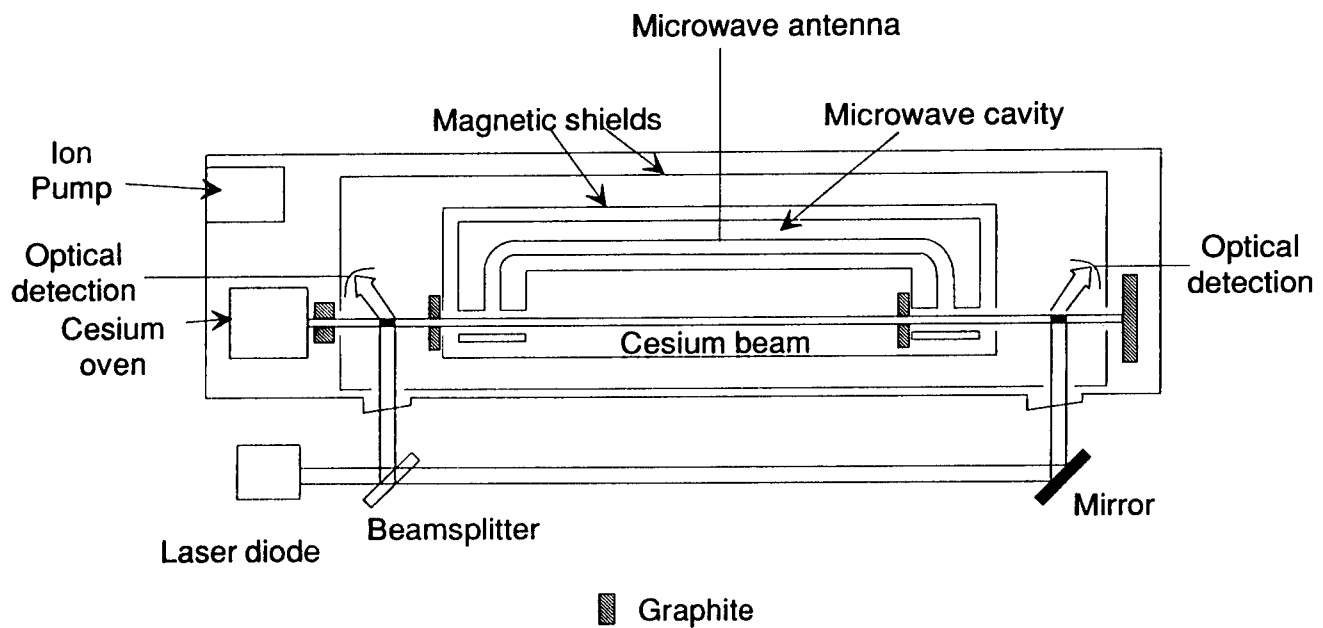


Figure 4 : Optically pumped cesium beam resonator

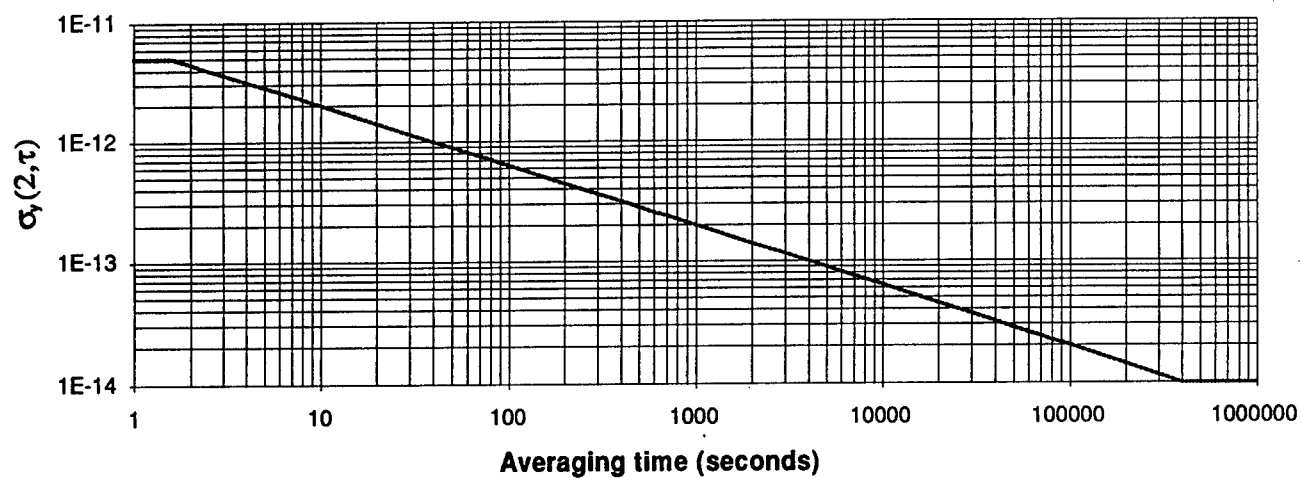


Figure 5 : Time domain stability (Allan deviation)

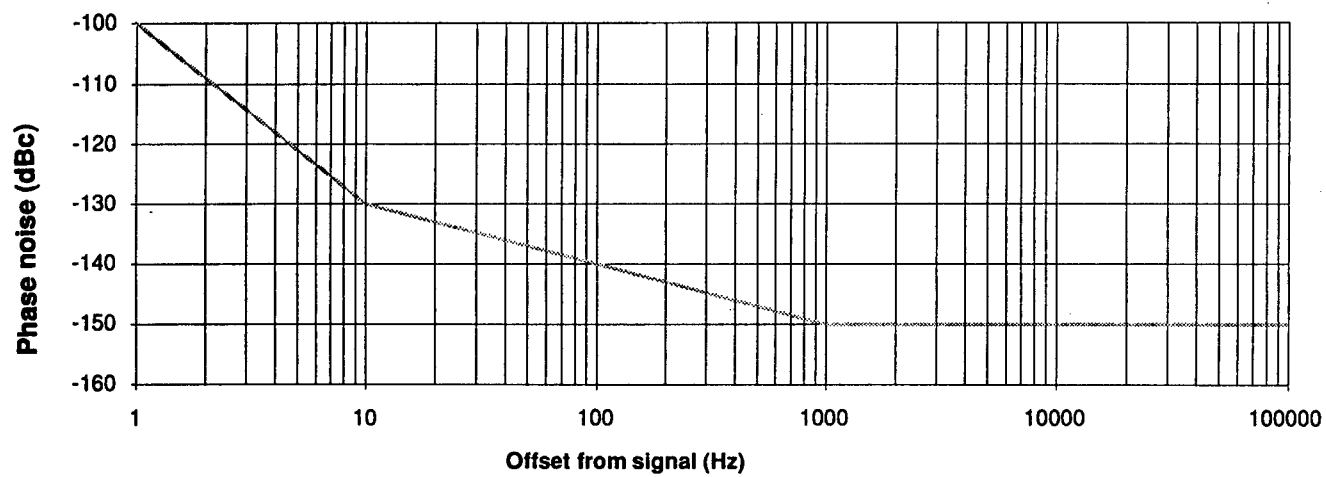


Figure 6 : Frequency domain stability

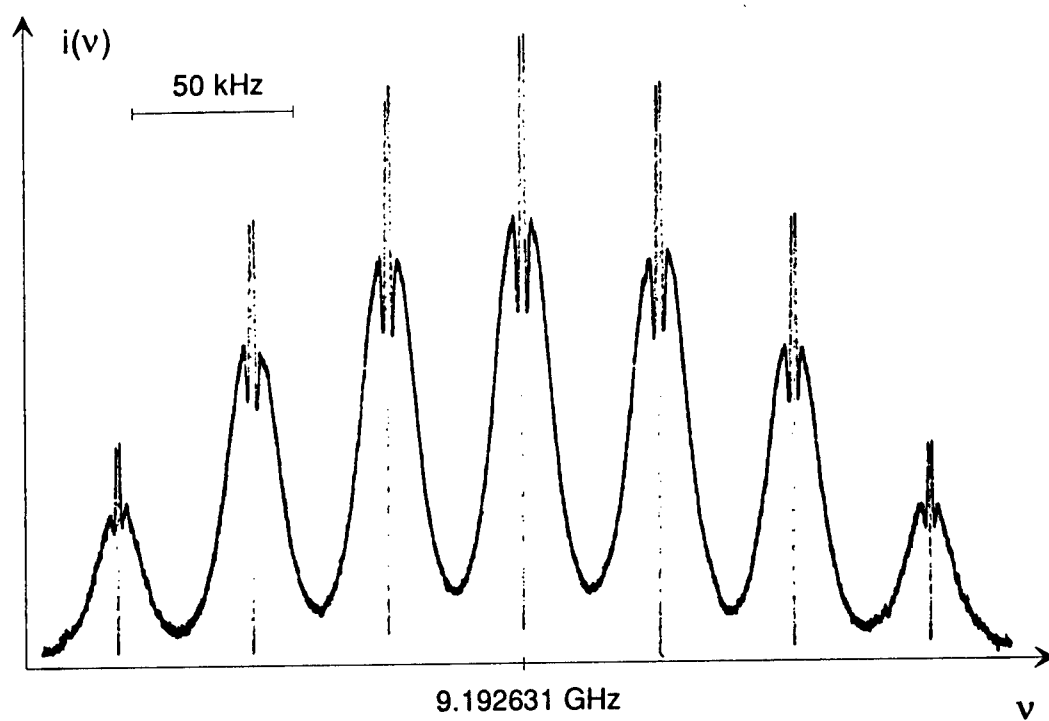


Figure 7 :Rabi-Ramsey fringes

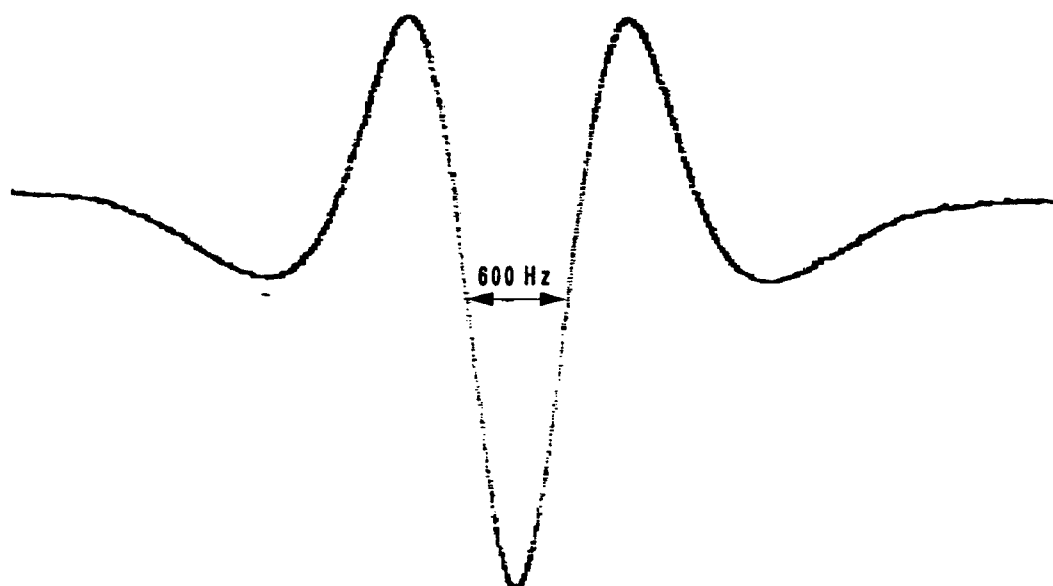


Figure 8 :Central line of the Rabi-Ramsey fringes

ULTRASENSITIVE HIGH RESOLUTION LASER SPECTROSCOPY AND ITS APPLICATION TO OPTICAL FREQUENCY STANDARDS

Jun Ye, Long-Sheng Ma*, and John L. Hall
JILA, University of Colorado, and
National Institute of Standards and Technology
Campus Box 440, University of Colorado, Boulder, Colorado 80309, USA

Abstract

Advanced laser stabilization techniques now permit one to lock laser frequencies onto line centers of natural atomic/molecular resonances with unprecedented precision and accuracy, leading to improved visible optical frequency standards. A novel approach of cavity-enhanced frequency modulation spectroscopy is demonstrated to enjoy a record high sensitivity (6×10^{-13} integrated absorption), working with a rich spectrum of weak molecular overtone transitions. The resultant high signal-to-noise ratio allows a Nd:YAG laser to be stabilized on the overtone transition at the level of 1×10^{-14} in 800 seconds. For the work of coherent optical frequency connection, we present our recent development of an optical frequency comb generator with a 3-terahertz span.

INTRODUCTION

Establishing frequency standards in the optical domain has been an extremely active field since the invention of the laser. Ultimate invariance tests of many fundamental physical postulates and constants can be approached only with the highest available optical spectral resolution, precision, and sensitivity offered by the frequency-based metrology. In addition, optical frequency references provide a direct link between the units of length and time, and they are invaluable in coherence optical communications. Owing to its higher operating frequency, it is natural to expect an optical resonance quality factor Q to be a few orders higher than those in the microwave domain. Therefore, optical frequency standards can potentially be more stable and precise. Of great long-term interest is the prospect of being able to bring into the microwave domain the superior stability and accuracy of suitable optical frequency sources.

To effectively use a laser as a stable and accurate optical local oscillator, active control of its frequency is needed due to the strong coupling between the laser frequency and its cavity. The laser's fast linewidth needs to be reduced to produce not only the desired short-term stability, but also a long coherence time appropriate for interrogation of narrow atomic or molecular transitions. Short-term stability is usually achieved by stabilizing the optical phase/frequency relative to a passive reference, such as a high-finesse stable Fabry-Perot cavity. As a fast

*Permanent address: Department of Physics, East China Normal University, Shanghai, People's Republic of China

frequency discriminator, the passive reference cavity is preferred over the preselected atomic or molecular resonance because of its linear response to the field and a high signal-to-noise ratio (S/N). Frequency stability at the 10^{-16} level has been measured with a cavity-stabilized laser.^[1] Tunability of such a cavity/laser system can be fulfilled by techniques such as the frequency-offset optical phase-locked-loop (PLL).^[2]

Long-term stability and reproducibility of the local oscillator (laser) can be obtained by locking to preselected natural resonances. Special optical techniques were invented to eliminate common sources of line broadening such as the Doppler effect. In the high resolution domain of laser spectroscopy, many research developments provide a number of sophisticated methods, such as saturated absorption spectroscopy, two-photon spectroscopy, optical Ramsey fringes, optical double resonance, quantum beat, and laser cooling and trapping.^[3] Usually one or several atomic or molecular transitions are located within the tuning range of the laser to be stabilized. Molecular ro-vibrational lines are used effectively for laser stabilization in the infrared, in systems such as the methane-stabilized HeNe at $3.39\ \mu\text{m}$, and osmium-tetroxide-stabilized CO_2 lasers at $10\ \mu\text{m}$. They now typically offer a precision of 10^{-12} .^[4] Until recently the molecular iodine transitions have been used exclusively as the frequency references in the visible spectrum and the precision has been limited to 10^{-11} . However, the rapid progress in the field of cooling and trapping of atoms and ions promises a major advance in high-resolution spectroscopy. Indeed, we have already witnessed a new visible standard based on an intercombination transition of cold Ca atoms.^[5] An optical transition linewidth as narrow as a few tens of Hz (Q of 10^{13}) has also been observed using a cooled and trapped single $^{199}\text{Hg}^+$ ion at $282\ \text{nm}$.^[6] Such narrow transitions provided by free atoms or ions could offer an ultimate optical frequency standard free from virtually all of the conventional shifts and broadenings to the part in 10^{16} level.

While systems involved with laser cooling and trapping are expected to offer the highest quality optical frequency sources, compact and low cost systems are competitive practical choices even though their performance may be a decade worse. Here we present such a system, which involves a solid-state laser (Nd:YAG) stabilized either on an I_2 transition at $532\ \text{nm}$ (after frequency doubling) or directly on an overtone transition of HCCD molecule at $1.064\ \mu\text{m}$. The stability of the system has already been demonstrated at the level of 10^{-14} at $800\ \text{s}$.

Stabilizing lasers on molecular overtone resonances is a particularly exciting prospect. These vibrational-overtone lines provide rich spectra of reference grids in the visible domain, while they maintain the same $\sim\text{kHz}$ linewidths as their fundamental counterparts, limited by molecular fluorescent decay at the vibration frequency. Molecular ro-vibrational lines are also less sensitive to external perturbations. However, owing to the extreme weakness of these otherwise attractive overtone transitions, they were not adopted as suitable frequency references in the visible until recently.^[7,8] (For example, in our stabilization work of Nd:YAG laser, the employed HCCD overtone transition strength is only about one millionth of the I_2 line.) In this paper we present our recent development of a new cavity-enhanced frequency modulation spectroscopy which has enabled us to achieve record high detection sensitivities. The resulting excellent S/N for these weak but narrow overtone lines has opened the door for realizing thousands of high quality frequency references in the visible and near infrared.

The realization of the stable frequency sources in the optical range has resulted in parallel development of absolute and precise frequency measurement in the visible and near-infrared spectral region. A few frequency synthesis chains have been developed to phase-coherently connect the frequency of optical references to the cesium primary standard. (For example, see references [9] and [10].) These synthesis chains are complex systems and can only cover some discrete frequency marks in the optical spectrum. Difference frequency of many terahertz could still remain between a targeted frequency and a known reference. Over the years,

several approaches have been proposed and tested in searching for reliable and simpler solutions to make coherent transfer over large optical frequency gaps. Some recent popular schemes include: frequency interval bisections^[11], optical-parametric oscillations (OPO)^[12], optical comb generations^[13,14], sum-and-difference in near infrared^[15], and four-wave mixing in laser diodes.^[16] All these techniques rely on the principle of difference-frequency synthesis, in contrast to the frequency harmonic generation method normally used in traditional frequency chains. To deal with relatively smaller frequency gaps on the order of a few terahertz, optical frequency comb generators certainly provide the most direct and simple approach. An electro-optic crystal is strongly excited by velocity-matched microwave fields to produce a significant phase modulation index for the light passing through the crystal. This electro-optic modulator is then placed inside a low-loss optical cavity, which resonates with the carrier frequency and all subsequently generated sidebands. This approach greatly enhances the modulation efficiency and the result is a rich spectrum of equally spaced lines spanning a few THz. In this article we will present the comb generator developed in our laboratory and discuss its use in our frequency measurement schemes.

NOISE-IMMUNE CAVITY-ENHANCED OPTICAL HETERODYNE MOLECULAR SPECTROSCOPY ("NICE-OHMS")

The P(5) line of the ($\nu_2 + 3\nu_3$) overtone band of the $^{12}\text{C}_2\text{HD}$ molecule lies within the tuning range of the Nd:YAG laser at $1.064\ \mu\text{m}$. Its transition dipole moment is 0.069 millidebye (1 debye = 3.33564×10^{-30} C·m, a typical atomic transition dipole moment) and the linear absorption is calculated to be $8.7 \times 10^{-7}/\text{cm}\cdot\text{torr}$. This weak transition strength makes it difficult to obtain the necessary level of nonlinear interaction between the light and the molecules to yield the sub-Doppler saturated absorption resonance. For metrology work, we usually use a low gas pressure (a few millitorr, 1 torr = 133 Pa) to avoid excessive pressure-related shifts and broadenings. When the pressure is sufficiently low, the average molecules will be in a free-flight regime, where they pass through the light field without suffering any collisions. Even in this case, the corresponding saturation power (the molecules see the light field as a π -pulse) is calculated to be 51 W. Under these circumstances, placing molecules inside a high-finesse cavity^[17] is beneficial in several aspects. The cavity extends the effective cell length by a factor of ($\text{Finesse} \cdot 2/\pi$) while it builds up sufficient internal power for saturation. This helps to limit both the source and detection power to reasonable levels. The geometrical self-cleaning and mode-matching of the two counter-propagating waves inside the cavity are important for obtaining narrow and unshifted resonance lines.^[18] In addition, the cavity itself provides a ready reference for short-term laser stabilization.

The use of the sharp cavity resonance, however, presents a challenge for a simple and yet effective modulation recovery scheme in signal detection. One direct method is to lock the laser on the cavity and dither the cavity resonance around the molecular resonance. Indeed, this technique is employed when we want to calibrate the size of the saturated absorption signal. However, the modulation frequency is by far too low to get away from the technical noise. Additionally, the narrow cavity resonance effectively converts any small laser frequency noise into amplitude noise, thus deteriorating the detection S/N. In our new modulation and detection scheme, we frequency modulate the input laser beam at exactly the splitting frequency of the cavity free-spectral-range (FSR). The cavity-transmitted light is subsequently detected and demodulated. The small frequency variations of the laser will still lead to some amplitude fluctuations and small optical phase shifts of the transmitted carrier, but they will also have exactly the same effects on the sidebands which are transmitted on adjacent or nearby cavity axial orders. Therefore, the transmitted light still accurately represents an FM spectral triplet,

with minimal AM conversion due to the relative laser/cavity frequency jitter. Thus, the detection noise level can approach the intrinsic AM noise of the laser at the modulation frequency. When an intracavity molecular resonance is present around one of the three cavity modes which accept the triplet light field, it will weaken and phase-shift the corresponding FM component to upset the FM balance and thereby create an RF heterodyne signal in the cavity transmission.

In short, the aforementioned modulation strategy allows the cavity to greatly enhance the molecular signal without any noise penalty. Therefore, the detection sensitivity is directly enhanced by the factor of $(\text{Finesse} \cdot 2/\pi)$, compared with the conventional FM spectroscopy.^[19] We refer to this modulation/detection scheme as noise-immune cavity-enhanced optical heterodyne molecular spectroscopy, i.e. "NICE-OHMS."

Fig. 1 shows the general experimental setup. Although the extreme accuracy of laser/cavity locking is no longer required for the detection of molecular signal, the laser linewidth relative to the cavity needs to be sufficiently narrowed so that its full power spectrum can be efficiently coupled into the cavity. Additionally, this laser/cavity locking loop serves as the short-term stabilizer for the laser frequency. The cavity discrimination signal is derived from the Pound-Drever-Hall RF sideband technique.^[20] The electro-optic modulator 2 (EOM2) produces the 4 MHz FM sidebands which are detected in cavity reflection. The frequency servo action is carried out by the laser's internal piezo-electric transducer (PZT) and an external stabilizer^[21], which uses just an acousto-optic modulator (AOM). The AOM provides sufficient servo bandwidth while the PZT corrects any slow deviations of the laser frequency. Fig. 2 illustrates the frequency noise spectral densities of the cavity error signal when the laser is unlocked, locked by the laser PZT only, and locked by the combined effort of the PZT and the AOM. The superior servo system with the PZT and AOM produces a frequency noise spectral density of only ~ -34 dB Hz/ $\sqrt{\text{Hz}}$ (20 mHz/ $\sqrt{\text{Hz}}$). This indicates the laser's linewidth relative to the cavity is a mere 1.3 mHz.^[22] This locking performance can be further improved as the shot-noise-limited frequency noise spectral density is shown to be only 0.2 mHz/ $\sqrt{\text{Hz}}$.

It is important to have a precision scanning capability for our spectrometer to perform high resolution studies of the signal lineshape, linewidth, and the line center. This is accomplished by the frequency-offset-locking loop shown in Fig. 1. The stable reference is provided by a second Nd:YAG laser which is frequency doubled and locked on an I_2 transition at 532 nm.^[23] The heterodyne beat signal between the two lasers is phase-locked to a synthesizer. To improve S/N and baseline stability, we modulate the cavity frequency around the molecular resonance by an FM dither on the synthesizer and use an audio lock-in for signal recovery. The same synthesizer is then frequency stepped by a computer to force the cavity/laser system to scan out the molecular resonance. Signal averaging over many scans (\sim one minute each) is available with the long-term stability of the laser/ I_2 frequency reference system in the sub-10-Hz domain.

Phase modulation of the laser beam at the FSR frequency is generated by the resonantly coupled EOM1 and detected in cavity transmission by an InGaAs p-i-n diode in a resonant RF tank circuit. The modulation signal is provided by a low-phase-noise crystal voltage-controlled-oscillator (VCO). The modulation index of ~ 0.5 is chosen so that the central carrier still effectively saturates the molecular absorption, while the sidebands are large enough to give a strong heterodyne cross-term. An isolation AOM directly after the cavity prevents optical feedback from the detector. Subsequent phase sensitive RF demodulation yields the molecular dispersion signal. During the cavity scan, its FSR will change slightly. To maintain the noise-immune property, we actively track the VCO frequency to the cavity FSR by applying a small frequency dither on the VCO, which is then also detected in cavity reflection. This control loop is also shown in Fig. 1.

Synthesized HCCD gas (81%/19% HCCD/HCCH by integration of the ^1H NMR spectrum, ~55% chemical purity by a residual gas analyzer) is placed inside a cavity with an FSR of 319.695 MHz and finesse of 31,900. One mirror is flat, the other has a 1 m radius of curvature. The intracavity beam waist is ~0.410 mm, dictating the room temperature transit time limit of 270 kHz FWHM.^[24] For our 10 mtorr sample gas, the linear absorption through our 46.9 cm long cavity (single pass) is 1.6×10^{-7} , leading to an absorption coefficient of 6.2×10^{-7} /torr-cm for pure HCCD, in good agreement with the available band strength data.^[25] The cavity has a resonant transmission efficiency of 41%, which decreases by 1.3×10^{-3} near the Doppler profile peak (a contrast of 0.32%). Tuning onto the saturation resonance increases the maximum transmission by 138×10^{-6} , corresponding to a saturation depth of 10.6%. From a 75 mW input light, the cavity has a power buildup to 300 W, giving a saturation parameter of ~0.46.

In our frequency stabilization experiment, we usually use the central carrier to interact with the molecules. This central component is intrinsically sensitive only to the dispersion part of the molecular resonance, independent of the detection phase of the RF local oscillator.^[19] The additional dither modulation on the cavity resonance itself requires an audio lock-in to further process the RF-demodulated signal, and the resultant signal lineshape shows a derivative form of dispersion. Fig. 3 shows a typical scan of the overtone resonance with 5.3 mtorr sample gas and a 640 kHz peak-to-peak cavity dither. The lineshape model is based on Wahlquist's modulation-broadening formalism for a dispersion signal.^[26] The diminutive fit residual, after a 10 times magnification, indicates a well-understood lineshape in our spectrometer. The transition linewidth of 705 kHz (after removal of the modulation broadening by the fit) is due to the power- and pressure-broadenings of the 270 kHz transit time linewidth. The power-broadening contribution to the linewidth can be removed by knowing the saturation level at the operating pressure. The pressure broadening (FWHM) rate is then determined to be 34.7 ± 0.8 MHz/torr. The zero-pressure, zero-intensity extrapolated linewidth is 290 ± 7 kHz, very near the value of 270 kHz set by the transit time. We can summarize these results by an expression for the saturation intensity: $I_{\text{sat}} = 6103 (\Gamma_T + 34.7 P)^2 \text{ W/mm}^2$, where Γ_T is the FWHM (in MHz) associated with the transit time, and P is the pressure in torr. The equivalent intracavity saturation power in the free-flight regime is 117 W, reduced to 29.3 mW input by the cavity enhancement of 4,000. We have also measured a pressure shift of the line center $\sim +250$ ($\pm 20\%$) Hz/mtorr with our current sample gas.

To obtain a proper discrimination lineshape of the molecular resonance for the laser to lock onto, we use the second harmonic detection on the audio lock-in to obtain a second derivative of dispersion. This is shown in Fig. 4 with 10 mtorr gas. With the saturated absorption in the 1.7×10^{-8} domain, we obtained a S/N of 8,700 at 1 s averaging, ~2 times above the calculated shot noise limit. This corresponds to a noise-equivalent detection sensitivity of 2×10^{-12} for integrated absorption at 1-s averaging. (Recently we have further improved this sensitivity to 6×10^{-13} by using an improved cavity.) This level of S/N sets the frequency rms noise when the laser is locked on the molecular line.

FREQUENCY STABILIZATION RESULTS

For testing the quality of this C_2HD overtone resonance as an optical frequency standard at $1.064 \mu\text{m}$, we lock the laser/cavity system onto the line and measure the heterodyne beat against the known Nd:YAG/I2 reference system.^[23] The molecular error signal is integrated and then fed onto the cavity PZT to maintain the proper cavity length. We find 10 mtorr is the optimum gas pressure for a maximum slope of the molecular locking error signal, by taking into account the combined parameters of linear absorption, saturated absorption hole

depth and the pressure-broadened linewidth. In Fig. 5 the counted beat frequency vs. time shows a drift ~ 20 Hz/h. The second Nd:YAG laser (after frequency doubling) is locked on I_2 : R(56) 32-0, component a_{10} .^[23] With the mean value of the beat frequency between the two lasers at 5252.2261 ± 0.0026 MHz, we determine the absolute frequency of the P(5) line in the $(\nu_2 + 3\nu_3)$ band of the $^{12}\text{C}_2\text{HD}$ to be $281,635,363.962 \text{ MHz} \pm 20.2 \text{ kHz}$. The 20 kHz uncertainty is mainly due to the limited knowledge of the absolute frequency of the Nd:YAG/ I_2 , a secondary standard. At 1-s averaging we obtain a frequency noise of ± 100 Hz, in direct agreement with the S/N available at $1.064 \mu\text{m}$. (The Nd:YAG/ I_2 reference system has a 20 Hz rms, 8×10^{-14} frequency noise at 1 second as tested with a second I_2 spectrometer.) The corresponding Allan variance of $\sigma_y = 3.4 \times 10^{-13}/\sqrt{\tau}$ improves to 1×10^{-14} at a longer integration time (> 800 s), a promising indicator for an ultrastable frequency reference. The visible noise bump around ~ 200 s on the Allan variance is associated with the lab room temperature cycling period.

Linewidth narrowing is offered by slow molecules since the natural lifetime of the overtone transition is about 300 times longer than our current transit time.^[27] The cavity input power is reduced 75 times from our maximum available power to 1 mW. A low power is necessary so that the low Rabi frequency leads to appreciable saturation only for the slowest molecules. In our < 2 mtorr sample gas, the mean-free-path of molecules is ~ 30 times longer than the transverse field dimension, thereby creating the so-called transit-time regime. The saturation now becomes inhomogeneous, with molecules from different transverse velocity groups contributing different intensities and widths. Slow molecules which spend their whole lifetime inside the field will have a constant and velocity-independent saturation parameter, controlled primarily by the collisional broadening. Considering their shorter interaction times, faster moving molecules will see a reduced saturation and will mostly contribute to the wings of the resonance. Fig. 6 shows a resonance with a linewidth of ~ 20 kHz, without correction for the modulation broadening by a 30 kHz peak-to-peak dither of the cavity. This is 13 times narrower than that set by the room temperature transit-time-limit, and is mainly limited by the relatively high pressure (1.8 mtorr). At present the limited S/N associated with the low power has prevented us from taking full advantage of this narrow linewidth. With an improved system this approach will enable us to access the information of free molecules with minimized second order Doppler shift ($\sim 2 \times 10^{-14}$), thereby creating an optical frequency standard of potentially high accuracy.

OPTICAL FREQUENCY COMB GENERATORS

An optical frequency comb (OFC) generator is a simple system employing only one laser. Yet it offers a unique property of supplying a comb of equally spaced spectral lines around the carrier. These lines are modulation sidebands generated by an electro-optic modulator (EOM). To enhance the optical-RF field interactions, the EOM is placed inside a low loss optical cavity in resonance with the carrier and all the sidebands. In other words, the RF modulation frequency equals an integer multiple of the cavity FSR. In principle, the span of the generated comb is limited only by the system dispersion, which can be carefully compensated following designs in ultra-fast laser systems. A 4-THz wide OFC has already been observed at $1.5 \mu\text{m}$ ^[28], showing the possibility of shifting 2% of the optical frequency in a single step. We note that an appropriately low-noise RF oscillator should be used to drive the EOM so that high-order sidebands do not quickly collapse due to the multiplied phase noise amplitude.

The power spectrum of the OFC is shown^[28] to be proportional to an exponential function. Denoting P_k as the power of the k th sideband, we have $P_k \propto \exp(-|k|\pi/\beta F)$ where β is the modulation index of the EOM and F is the finesse of the crystal-loaded cavity. To improve the efficiency of the comb generator and to have a single pure spectral line output for optical

frequency metrology, we replace the cavity output mirror with a short filter cavity to resonantly output an individual sideband from the comb. If the FSR of this filter cavity is larger than the comb width, then the filter will be resonance-free until one reaches the desired sideband. Therefore, the filter cavity will not alter the comb generation process until a good match occurs between its resonance and a sideband, beyond which the comb spectrum will be sharply cut off. The filtered single spectral line can be conveniently detected by heterodyne-mixing with a tunable laser source. Since we extract the full power of the chosen sideband out of the comb generator while keeping the carrier and all other sidebands trapped inside, we can expect an important improvement of the detection S/N. Using a filter cavity not only resonantly increases the signal size of the desired sideband output, but also reduces the detected noise level as the larger DC powers distributed among the carrier and lower order sidebands are not detected.

In this experiment we use a prototype EOM.^[29] It consists of a broadband antireflection coated Mg:LiNbO₃ crystal (2x1x35.4-mm) embedded in a resonant microwave cavity. The cavity design employs a waveguide geometry to force the match between the microwave phase velocity and the optical group velocity through the crystal. The microwave resonance at 10.5 GHz has a bandwidth of ~0.3 GHz and a Q factor of 230. A modulation index of ~0.8 is obtained with a microwave power of 0.6 W. This EOM is placed inside our three-mirror cavity, as shown in Fig. 7. All three mirrors are identical lens substrates with an effective focal length of 25 cm. The convex faces are antireflection coated at 633 nm, while the flat faces are coated to have high reflectivity, about 99.6%. With two such mirrors (M1 and M2) we build a cavity with a finesse of 680 and a transmission efficiency of 20%, implying a transmission coefficient (T) of 0.2% for each mirror. The cavity FSR is 1/16 of the EOM RF frequency. When loaded with the cold crystal, the finesse and efficiency drop to 200 and 2%, respectively, corresponding to a 1.1% one-way loss through the modulator. Turning on the RF power to the EOM further drops the cavity efficiency to 0.15% for the overall modulated output, due to the increased mismatch of input coupling when sideband generation enhances the carrier loss. The filter cavity formed by mirrors M2 and M3 has a finesse of 400, a FSR of ~2 THz, and an efficiency ~30%, and increases the output power of the selected sideband by a factor of 150. The PZT mounted on the filter cavity output mirror M3 is used to tune the filter bandpass frequency. Approximately 150 μ W power of a polarization-stabilized He-Ne laser is incident on the comb generator. Part of the output light from the OFC generator is monitored by a DC photo detector, while the other part is sent to an avalanche photodiode (APD) for heterodyne-mixing with an external-cavity tunable diode laser at 633 nm.

Fig. 8 shows the DC-monitored output spectrum of our OFC generator as we continuously tune the filter cavity resonance over part of the comb spectrum. A comb span wider than 1 THz is clearly visible from one side of the carrier frequency. The filter cavity has a FWHM of ~5 GHz. This gave enough resolution to resolve individual sidebands spaced 10.5 GHz apart. Based on the observation that high-order (~100th) sidebands still have a good S/N, we expect to see a wider comb with a filter cavity having a larger FSR. (It will also need a higher finesse to maintain its resolution.) The slope on this comb spectrum is roughly 16 dB/THz.

About 15 μ W power from an external cavity tunable 633 nm diode laser is used for the heterodyne detection of the OFC sideband. Fig. 9 shows the resulting beat spectrum. The filter cavity resonance is subsequently tuned onto the 48th (505 GHz), 96th (1.01 THz), and 144th (1.515 THz) sideband of the He-Ne laser. In a 100 kHz bandwidth we obtain S/N of 35 dB, 26 dB, and 20 dB, respectively. The noise floor is fixed by the shot noise of the detected light power, increased by the APD's excessive noise factor. These beat signals can be easily counted via a tracking-filter comprised of a voltage-controlled RF oscillator phase-locked onto the beat signal.

As the filter cavity selects out a particular sideband, it causes little effect on the lower order sidebands being generated inside the comb generator. However, once the energy in a sideband is coupled out, the comb generation beyond that is strongly reduced. This mechanism is confirmed in the following way. We park the filter cavity resonance on top of the 48th sideband, and then we position the diode laser frequency successively to be in line with the 47th, 48th, and 49th sideband. Heterodyne detection shows that a fraction of the 47th sideband power leaked out due to the finite width of the pass-filter (-17.7 dB below the 48th sideband). The magnitude of the 49th sideband is lower by 5.6 dB, -23.3 dB relative to the 48th sideband. This good spectral purity will improve further using a filter cavity of higher efficiency or better finesse.

CONCLUSIONS

The experimental demonstration of the noise-immune cavity-enhanced optical heterodyne molecular spectroscopy (NICE-OHMS) has firmly established itself among the most sensitive detection methods currently available. Its powerful utilities in the laser frequency stabilization and ultra-high resolution spectroscopy are also indispensable for realizing thousands of molecular overtone transitions in the visible and near-IR as high-quality optical frequency/wavelength references. The work of Nd:YAG laser frequency stabilization using the P(5) transition in the C₂HD ($\nu_2+3\nu_3$) overtone band at 1.064 μm has achieved similar results to that using iodine transitions with modulation transfer spectroscopy,^[23] despite the fact that the C₂HD transition is a million times weaker than that of iodine. Slow molecules optically selected should provide more accurate information about the resonance line center of free molecules. The relative stability of this system is already better than most visible frequency standards, including those recommended by CIPM/CCDM in 1992.^[4] Potential improvements on our system would be to use larger mode-size and higher finesse cavities to further enhance the resolution and sensitivity.

We have realized a wide span (> 3 THz) optical frequency comb generator. We improve the comb generator efficiency by replacing the output mirror with a short filter cavity to allow efficient escape of the selected comb component. With limited power available from a He-Ne laser, we are able to demonstrate a 1.5 terahertz heterodyne beat signal with a S/N of 20 dB at 100 kHz bandwidth. We intend to use this OFC generator to bridge gaps between stronger and spectrally narrower iodine molecule absorption lines around 633 nm and the R(127) transition where the He-Ne laser is traditionally stabilized. An interesting Neon transition (1S5 \rightarrow 2P8) at 633.6 nm can also be measured in its absolute frequency. We are also planning to improve our frequency chain for the green iodine transitions at 532 nm.^[23] We are in the process of establishing grids of molecular ro-vibrational lines as frequency references over the red part of the visible spectrum. As the spacing between adjacent rotational lines usually lies anywhere between a few hundred GHz to a few THz, this OFC generator covering THz frequency gaps becomes an essential part of our phase coherent frequency chains.

ACKNOWLEDGMENTS

The authors are grateful to Bruce Tiemann who synthesized the HCCD sample gas. We also thank Tim Day for providing the 10.5 GHz resonant EOM. This work was supported in part by the NIST and in part by the ONR, AFOSR, and NSF.

REFERENCES

- [1] C. Salomon, D. Hills, and J.L. Hall 1988, *Journal of the Optical Society of America*, B5, 1576.
- [2] R. Barger, and J.L. Hall 1969, *Physical Review Letters*, 22, 4.
- [3] J.L. Hall 1993, in *"Frequency-stabilized lasers and their applications," Proceedings of the SPIE*, 1837, 2.
- [4] T. Quinn 1994, *Metrologia*, 30, 523.
- [5] H. Schnatz, B. Lipphardt, J. Helmcke, F. Riehle, and G. Zinner 1996, *Physical Review Letters*, 76, 18.
- [6] J.C. Bergquist, W.M. Itano, and D.J. Wineland 1994, in *Frontiers in Laser Spectroscopy*, International School of Phys. <Enrico Fermi>, Course= CXX, ed., T.W. Hänsch and M. Inguscio, p. 359.
- [7] M. de Labachellerie, K. Nakagawa, and M. Ohtsu 1994, *Optical Letters*, 19, 840.
- [8] J. Ye, L-S. Ma, and J.L. Hall 1996, *Optical Letters*, 21, 1000.
- [9] D.A. Jennings, C.R. Pollock, F.R. Petersen, R.E. Drullinger, K. M. Evenson, J.S. Wells, J.L. Hall, and H.P. Layer 1983, *Optical Letters*, 8, 136.
- [10] C.O. Weiss, G. Kramer, B. Lipphardt, and E. Garcia 1988, *IEEE Journal of Quantum Electronics*, QE-24, 1979.
- [11] H.R. Telle, D. Meschede, and T.W. Hänsch 1990, *Optical Letters*, 15, 532.
- [12] N.C. Wong 1990, *Optical Letters*, 15, 1129.
- [13] M. Kourogi, K. Nakagawa, and M. Ohtsu 1993, *IEEE Journal of Quantum Electronics*, QE-29, 2693.
- [14] L.R. Brothers, D. Lee, and N.C. Wong 1994, *Optical Letters*, 19, 245.
- [15] D.A. Van Baak, and L. Hollberg 1994, *Optical Letters*, 19, 1586.
- [16] C. Koch and H.R. Telle 1996, *Journal of the Optical Society of America*, B13, 1666.
- [17] P. Cerez, A. Brillet, C. Man-Pichot, and R. Felder 1980, *IEEE Transactions on Instrumentation and Measurement*, IM-29, 352.
- [18] J.L. Hall, and C.J. Bordé 1976, *Applied Physics Letters*, 29, 788.
- [19] G.C. Bjorklund 1980, *Optical Letters*, 5, 15; J. L. Hall, L. Hollberg, T. Baer, and H.G. Robinson 1981, *Applied Physics Letters*, 39, 680.
- [20] R.W.P. Drever, J.L. Hall, F.V. Kowalski, J. Hough, G.M. Ford, A.J. Munley, and H. Ward 1983, *Applied Physics*, B31, 97.
- [21] J.L. Hall, and T.W. Hänsch 1984, *Optical Letters*, 9, 502.
- [22] D. Hils, and J.L. Hall 1989, in *Frequency Standards and Metrology*, ed. A. De Marchi (Springer-Verlag, Berlin, Germany).

- [23] P. Jungner, M. Eickhoff, S. Swartz, J. Ye, J.L. Hall, and S. Waltman 1995, **IEEE Transactions on Instrumentation and Measurement**, **44**, 151; M.L. Eickhoff and J.L. Hall 1995, *ibid.*, 155.
- [24] C.J. Bordé, J.L. Hall, C.V. Kunasz, and D.G. Hummer 1976, **Physical Review**, **A14**, 236.
- [25] M. Temsamani, J. Vander Auwera, and M. Herman 1993, **Molecular Physics**. **79**, 359.
- [26] R. L. Smith 1971, **Journal of the Optical Society of America**, **61**, 1015.
- [27] S.N. Bagayev, V.P. Chebotayev, A.K. Dmitriyev, A.E. Om, Y.V. Nekrasov, and B.N. Skvortsov 1994, **Applied Physics**, **B52**, 63; and C. Chardonnet, F. Guernet, G. Charton, and C.J. Bordé 1994, **Applied Physics**, **B59**, 333.
- [28] M. Kourogi, K. Nakagawa, and M. Ohtsu 1993, **IEEE Journal of Quantum Electronics**, **QE-29**, 2693.
- [29] Designed by T. Day and built at New Focus Corp.

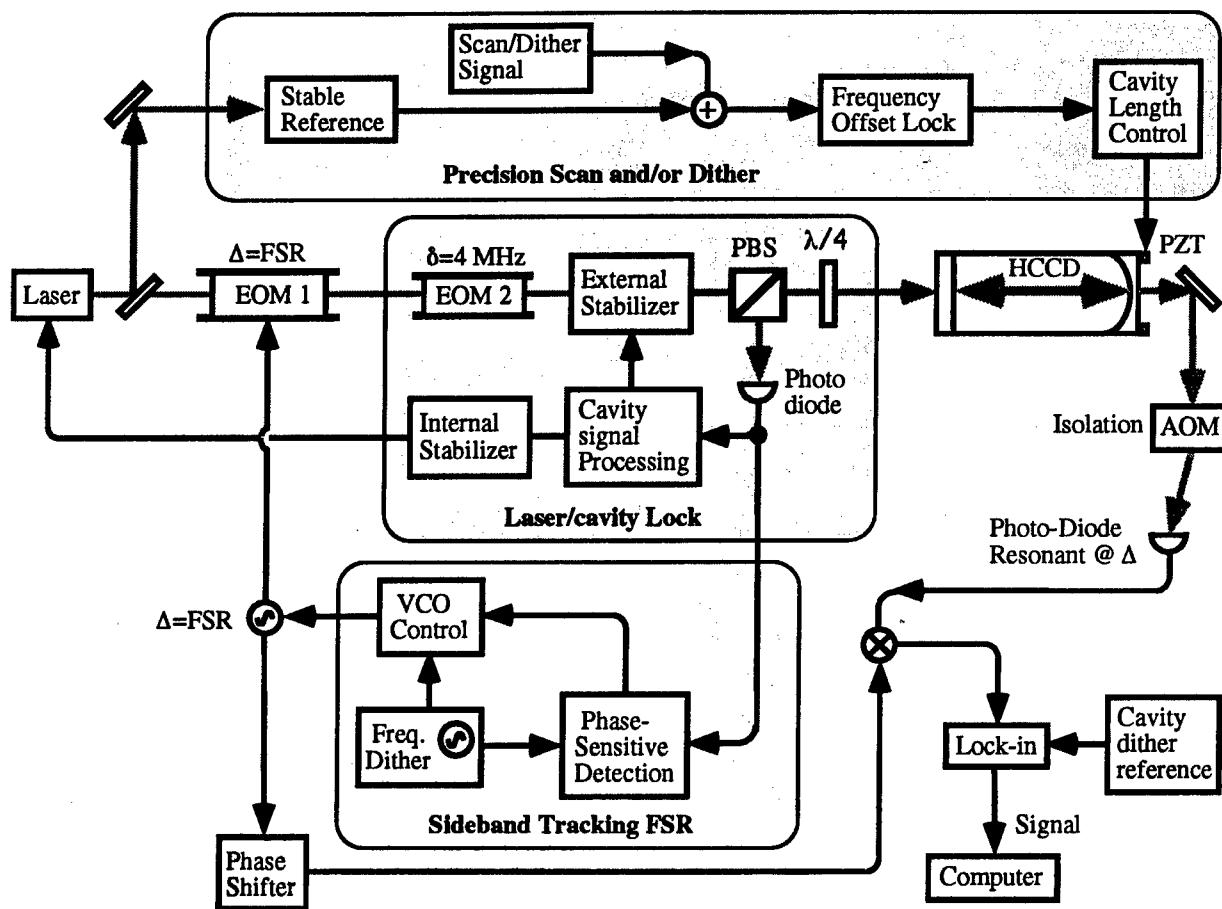


Figure 1 General experimental setup for the NICE-OHMS spectrometer.

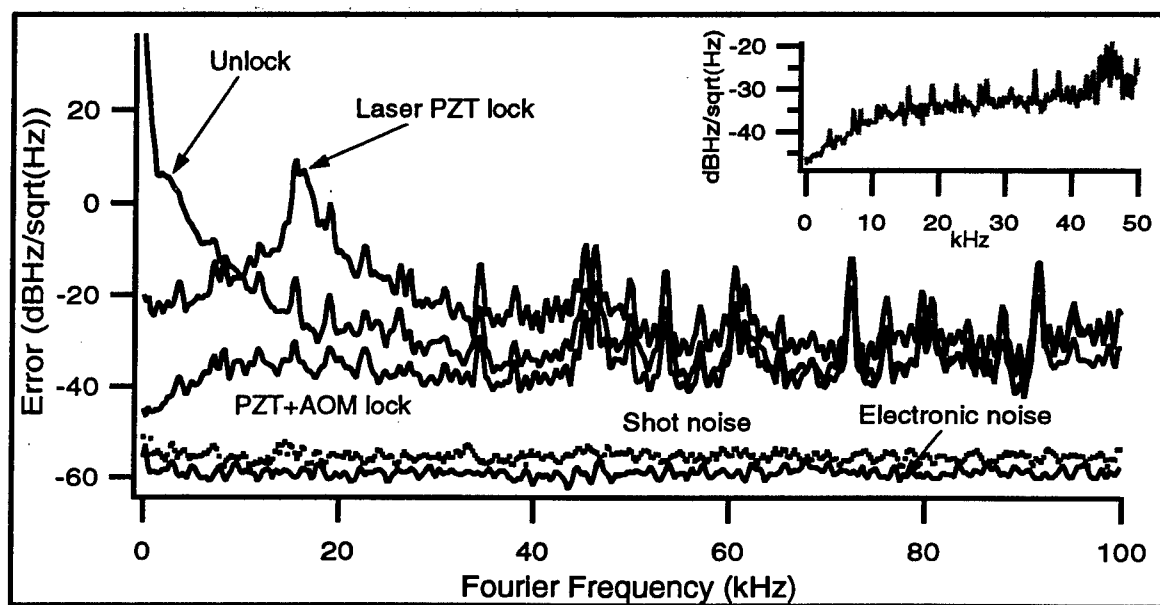


Figure 2 Laser/cavity locking frequency noise spectral density.

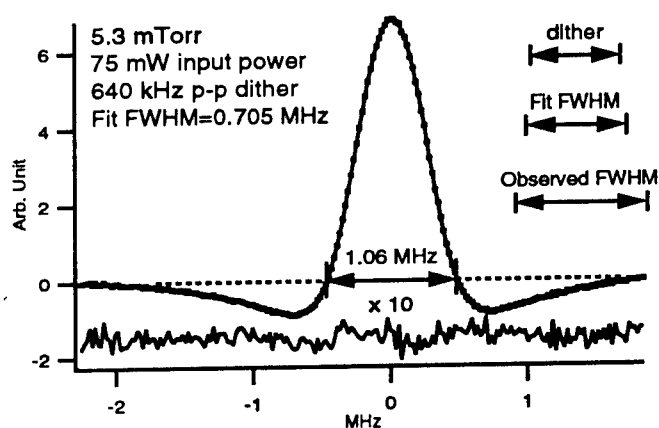


Figure 3 Frequency scan of the C_2HD ($v_2 + 3v_3$) P(5) line and overlaid theoretical fit, with fit residuals magnified by 10 times.

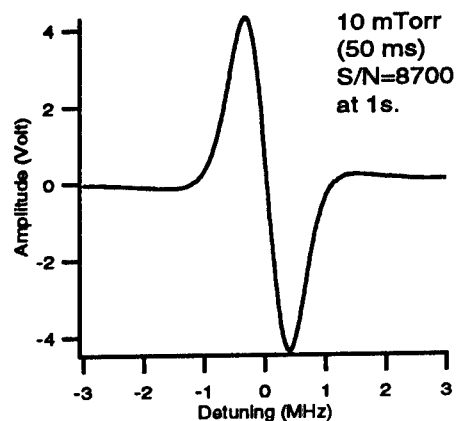


Figure 4 Molecular discrimination signal used for stabilizing Nd:YAG laser, obtained by the 2nd harmonic detection of the molecular dispersion.

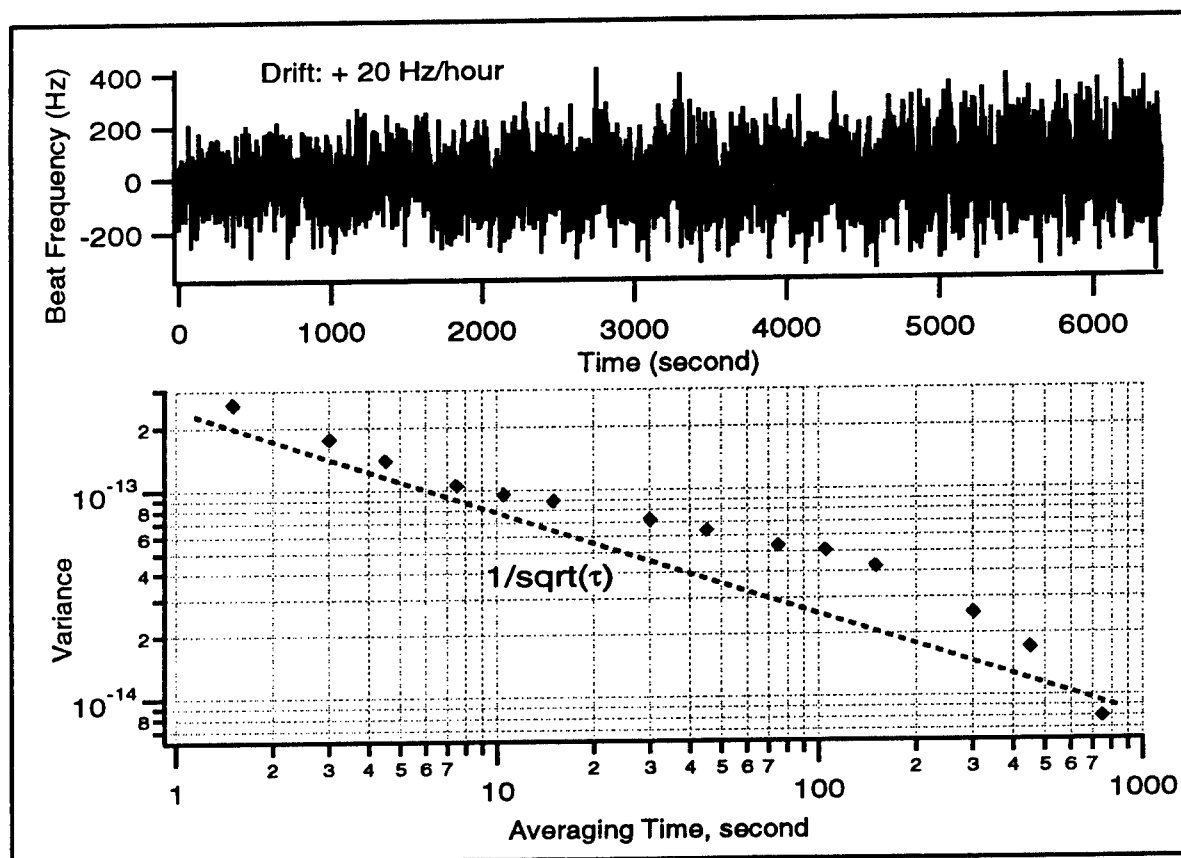


Figure 5 Time record of the beat frequency between two stabilized lasers and the Allan variance.

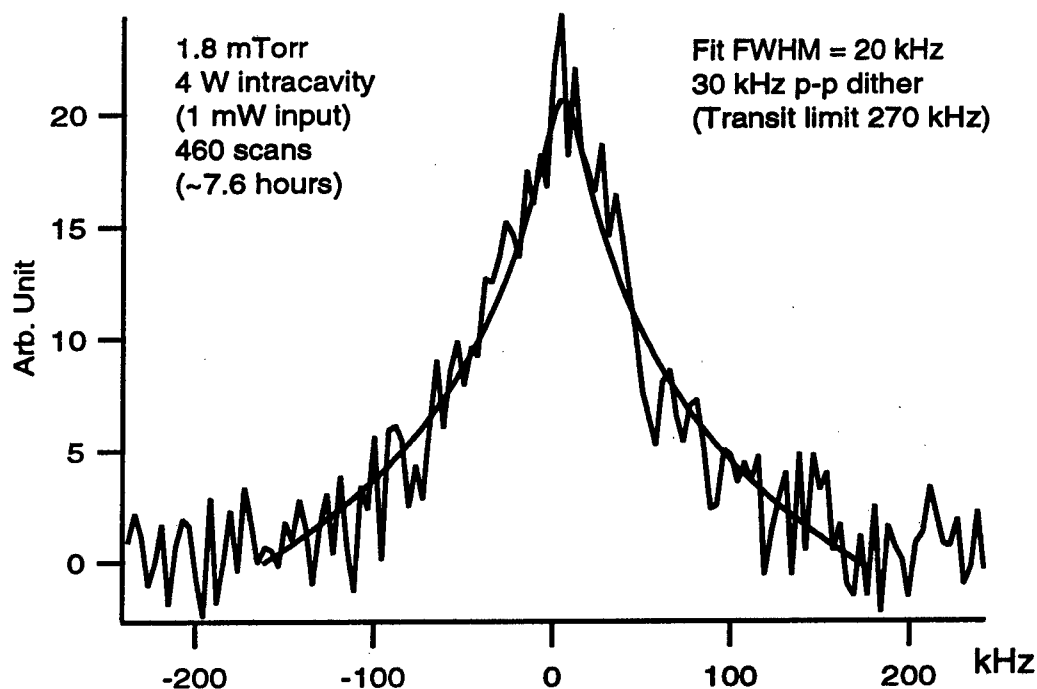


Figure 6 With low power and gas pressure, slow molecules give a linewidth 13 times below the transit limit.

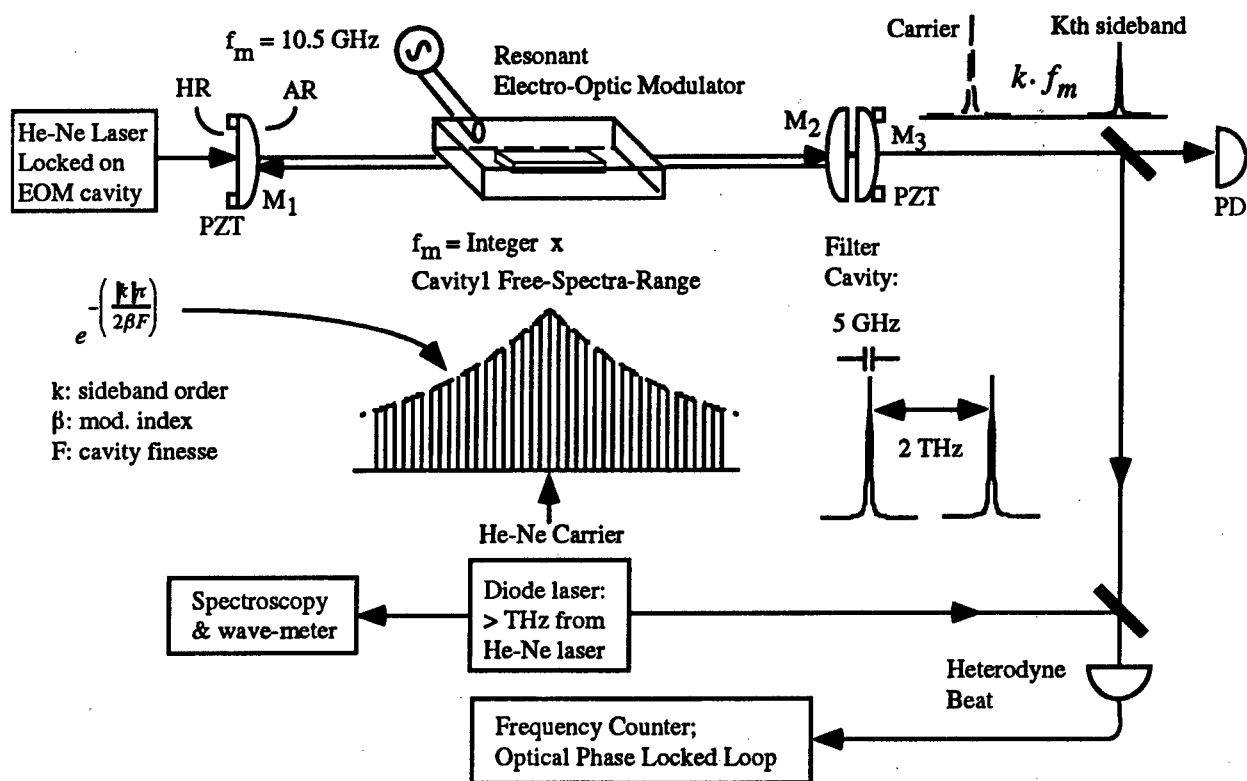


Figure 7 Schematics for optical frequency comb generator.

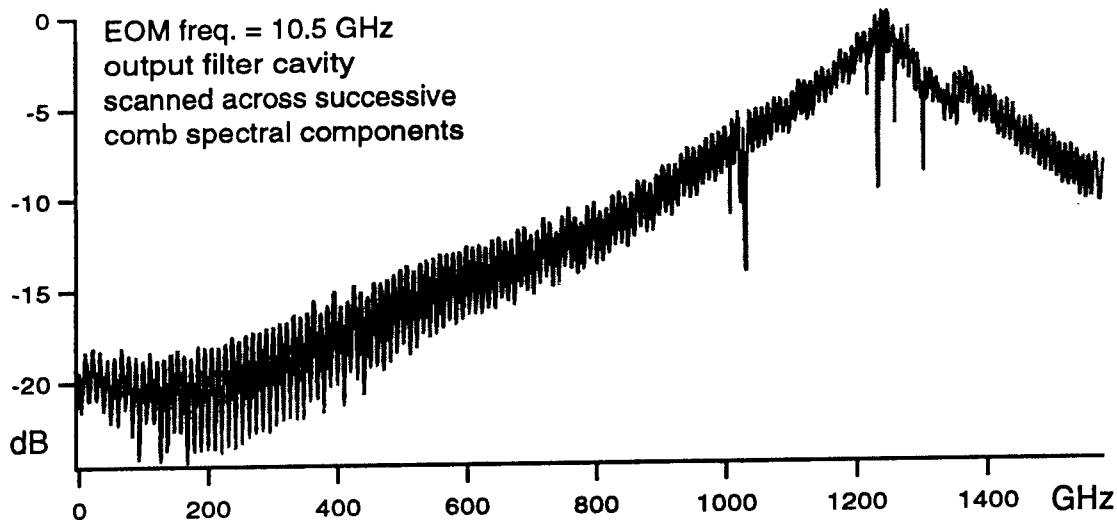


Figure 8 Optical comb generator output spectrum as the filter cavity resonance is scanned through the comb spectrum. Comb line spacing is 10.5 GHz.

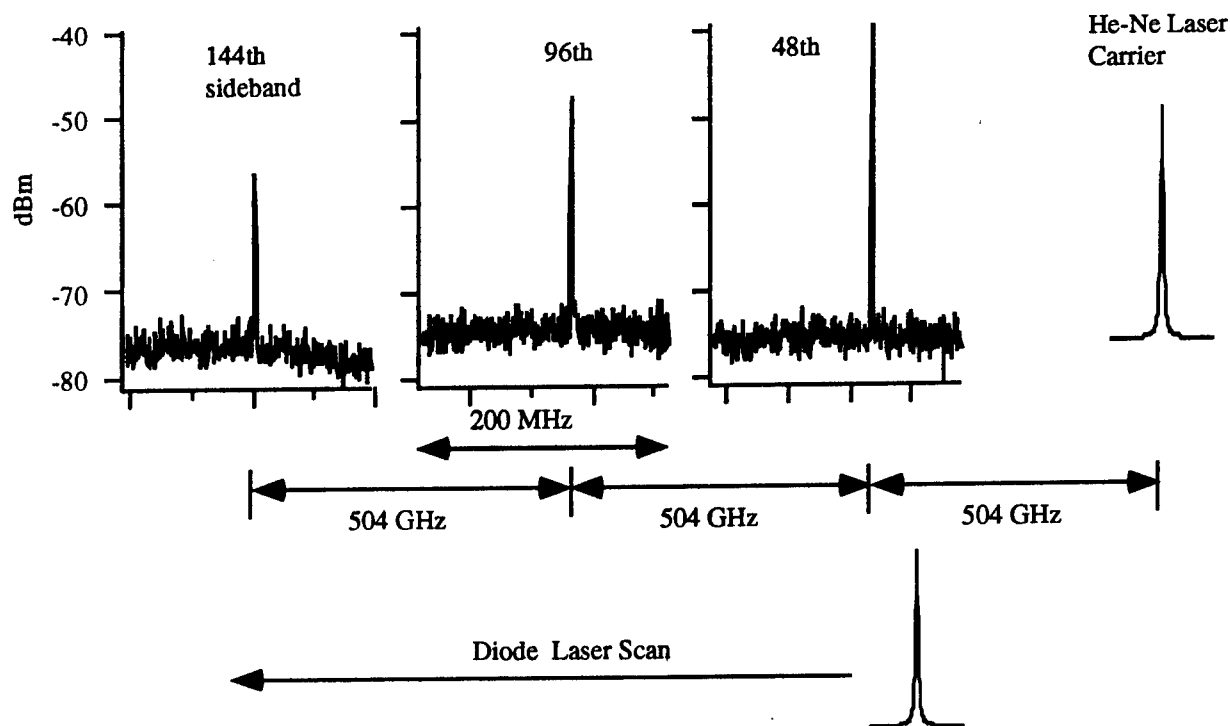


Figure 9 Beat between the diode laser and the 48th (505 GHz), 96th (1.01 THz), and 144th (1.515 THz) sidebands of the He-Ne laser. All with 100 kHz resolution bandwidth.

Questions and Answers

DEMETRIOS MATSAKIS (USNO): I notice some deviations on your Allan plot at about 100 seconds. Do you know what caused them?

JUN YE: Demetrios is talking about this little bump on the Allan variance. And if you really try to make a line, this line actually follows very nicely to 1 over the square root of τ . That means it's a white noise. However, there's a bump that shows up. That means you have a sinusoidal modulation on your beep frequency. And really if you use a digital low-pass filter (such as that by the decimation process) to process the time record of the beat frequency, the small sinusoidal modulation will emerge from the noise.

The problem with this 5-minute kind of modulation is due to the air temperature cycling our laboratory. When the temperature changes in the lab, it will affect the optical path lengths of some residual interferometers within our spectrometer. For example, the thickness of a glass window could change. The change of these residual fringes could shift the stabilized optical frequency. And that shows up as a modulation in our beat frequency record.

REPORT FROM THE ITU-R WORKING PARTY 7A ON TIME SIGNALS AND FREQUENCY STANDARD EMISSIONS

**Gerrit de Jong
NMI Van Swinden Laboratorium
P.O. Box 654, 2600 AR Delft, the Netherlands**

Abstract

The Working Party 7A (WP-7A) on "Time Signals and Frequency Standard Missions" is one of the four Working Parties of Study Group 7 "Science Services" (SG 7) of the Radiocommunication Sector of the International Telecommunication Union (ITU-R). The subjects which are addressed in the WP-7A meetings on the basis of input documents as answers to Questions are: (worldwide) Standard frequency and time (T&F) dissemination from terrestrial transmitters and from satellites, including GPS, GLONASS, and Two-Way Satellite T&F transfer, time codes, requirements for high precision time, performance of T&F standards, time scale stability characterization, signal delays in antennas and other circuits, time delay measurements, compensation methods in SDH/SONET systems, etc. The results of the discussions during the meetings are presented, preferably in the form of ITU-R Recommendations to the ITU member states.

Also, for the purpose of communication of the best use and selection of T&F systems to a wide group of users, the writing of handbooks in WP-7A has been started with contributions from internationally recognized specialists. The manuscript of the first handbook has been finished under Dr. R. Sydnor as main editor and D.W. Allan as co-editor. The English version has been prepared for press and is also being translated into French and Spanish.

Several ITU-R Study Group and Working Party meetings were held in Geneva in October 1996. The results of the last WP-7A meeting, held 8 to 16 October 1996, are presented.

ITU-R Working Party 7A Schedule

1996

**Publication of accepted Recommendations:
1995 TF Series Fascicle**

Oct 8-16 Meeting WP 7A in Geneva

Oct 17-18 Meeting of Study Group 7 in Geneva

Publication TF Handbook Selection & Use Precise T/F Systems

1997

June 2-6 Meeting WP 7A

June Meeting SG 7

Oct Meeting Radiocommunication Assembly

**1998 Publication accepted Recommendations:
1997 TF Series Volume**

Draft revision of Question ITU-R 111/7

Signal Delays in Antennas and other Circuits and their Calibration for High-Accuracy Time Transfer

- * What methods can be recommended and standardized to calibrate delay introduced by antennas and associated circuits for accurate time transfer (down to below one nanosecond)**
- * What parameters influence the delay**
- * What environmental effects affect delay**
- * What level of agreement exists between calibrated Two-Way and GPS/GLONASS Time Transfers**
- * what standard reference systems would be useful for calibration purposes**

Frequency Comparisons of Remotely Located Standards at the 10^{-15} Level of Uncertainty

The ITU Radiocommunication Assembly,

Considering

- that the stability of primary and some commercial frequency standards at the 10^{-14} level at one day and expected to improve to the 10^{-16} level;
- that present time transfer are at best stable to about one nano second and need an integration time of many days to reach a frequency transfer at 10^{-15} level;
- that;

decides that the following Questions should be studied

- *How can frequency be transferred at the 10^{-15} level within a day?
- *What means of self calibration and self monitoring are needed for these highly reproducible and accurate transfers?

Standard Frequencies and Time Signals

(Question ITU-R 106/7)

Additions and revisions to the Annex, tables 1 and 2

DCF 77, WWVB, Loran-C, etc.

EXAMPLES

The examples contain actual and fictitious data (especially for calibration).

```
* TWUSNO49.933
* FORMAT 01
* LAB USNO
* REV DATE 1995-07-10
* ES USNO01 LA: N 38 55 00.000 LO: W 77 04 00.000 HT: 51.30 m
* REF-FRAME WGS84
* LINK 04 SAT: IS706 NLO: W 53 00 00.000 XPNDR: 99999.999 ns
* SAT-NTX: 11922.3750 MHz SAT-NRX: 14221.6275 MHz
* CAL 002 TYPE: GPS MJD: 49639 EST. UNCERT.: 5.000 ns
* CAL 003 TYPE: GPS MJD: 49649 EST. UNCERT.: 5.000 ns
* LOC-MON NO
* MODEM MITREX 2500A
*
* EARTH-STAT LI MJD STTIME NTL TW DRMS SMP ATL REFDELAY RSIG CI S CALR ESDV
* LOC REM hhmss s s ns s s s ns ns ns ns
USNO01 TUG01 04 49933 140200 299 0.263265762933 1.529 300 299 0.000001334100 9.999 002 1 296.350 99999.
USNO01 NPL01 04 49933 141000 299 0.260419315503 0.613 300 299 0.000001334200 9.999 999 0 99999.999 99999.
USNO01 VSL01 04 49933 141800 299 0.261451406897 0.387 300 299 0.000001334200 9.999 999 0 99999.999 99999.
USNO01 PTB01 04 49933 143400 299 0.262748501558 1.822 233 232 0.000001334240 9.999 003 1 449.500 99999.
```

Draft New Opinion

Operational Use of Geostationary Direct TV Satellites for Time transfer

(Question ITU-R 103-1/7)

Considerings:

- availability of direct TV satellites
- positioning tolerance +/- 0.1 degree
- common view accuracy 10 ns when satellite position is known good enough

Opinion:

* TV satellite operators should make available the satellite coordinates with a resolution for example up to 100 m each 60 minutes. This could be done on an Internet site or incorporated in the TV signal

Draft New Opinion

Future Use of the Global Navigation Satellite System (GNSS) for High-Precision Time Transfer

(Questions ITU-R 103-1/7 and 152-1/7)

Considerings:

- satellite navigation signals have been simultaneously used for distribution of time and frequency
- a new enhanced system (GNSS) will be introduced in 1998 to 1999
- time oriented navigation receivers showed uncertainties below 10 ns

Opinion:

- * new time-oriented receivers should be studied and developed
- * suitable delay calibration methods should be developed to enable uncertainties less than 1 ns

Liaison Statement to ITU-T Study Group 13, Working Party

Cooperation in the study and developement of Time Transfer and/or Distribution using overhead capacity in SONET/SDH Networks

Contact Points for WP 7A:

- * D.W. Hanson, NIST, Boulder, CO., USA

and:

- * T.R. Bartholomew, TASC, Anapolis Junction, MD., USA.

Progress of the TF Series of Handbooks

Handbook on the Use of Satellite Time and Frequency Dissemination

editor: J.McA. Steele (UK)

* manuscript planned to circulate December 1996.

Handbook on the Selection and Use of Precise Frequency and Time Systems

main editor: R. Sydnor (USA)

* accepted and in press at the ITU, Geneva.

THE SELECTION AND USE OF PRECISE FREQUENCY AND TIME SYSTEMS

Richard L. Sydnor*

Jet Propulsion Laboratory, California Institute of Technology
4800 Oak Grove Drive, Pasadena, California 91109-8099, USA

Abstract

The ITU-R has authorized the creation of a handbook, "The Selection and Use of Precise Frequency and Time Systems." This handbook is designed for use by the beginner in the field and for undeveloped countries that wish to establish a national laboratory or calibration laboratory. The lack of such a handbook is serious, so the ITU has decided to generate one. The editor, Richard L. Sydnor, and the assistant editor, David Allan, have selected authors for the various chapters from experts in the field and have correlated the work and generated the various drafts for the final version.

The chapters and their authors are:

Preface and Forward	H. G. Kimball, ITU
Glossary	CCIR and ISO
Chapter 1 Introduction and Basic Concepts	Claude Audoin, Laboratoire de l'Horloge Atomique, France
Chapter 2A Local Frequency and Time Sources	Andreas Bauch, Physikalische-Technische Bundesanstalt, Germany
Chapter 2B Steering References	Roger Beehler, NIST
Chapter 3 Characterization: Frequency Domain, Time Domain, Environment	Laurent-Guy Bernier, Observatoire de Neuchâtel, Switzerland
Chapter 4 Measurement Techniques (Metrology)	Fred Walls, NIST
Chapter 5 Characteristics of Various Frequency Standards	Richard Sydnor, Jet Propulsion Laboratory
Chapter 6 Time Scales	Claudine Thomas, BIPM, France
Chapter 7 Uses of Frequency Sources	Patrizia Tavella ¹
	Sigfrido Leschiutta ^{1,2}
	Franco Cordara ¹
	¹ Istituto Elettronico Nazionale, Italy
	² Polytechnico di Torino, Italy
Chapter 8 Operational Experience, Problems, Pitfalls	Richard Sydnor, Jet Propulsion Laboratory
Chapter 9 Future Prospects	Michel Granveaud, Observatoire de Paris, France
Chapter 10 Conclusions	Richard Sydnor, Jet Propulsion Laboratory
	Leonard Cutler, Hewlett-Packard
	Donald Sullivan, NIST

*The work described in this paper was, in part, performed by the Jet Propulsion Laboratory, California Institute of Technology, under a contract with the National Aeronautics and Space Administration, and, in part, by the organizations listed with the various authors of the chapters.

INTRODUCTION

The International Telecommunications Union — Radio (ITU-R) has decided that, in view of the fact that no handbook or general reference book covering the field of precise frequency standards exists, and that the need for such a book is critical for the developing countries and for students of the field, one should be generated. The authors were selected by the editors and have graciously donated their time and expertise to the completion of the book. Without their efforts and cooperation this work could not have been completed. Each chapter includes a list of references for those wishing to explore the topics of the chapter in detail. The book is now in the hands of the ITU-R for translation into several languages and will soon be available.

PREFACE, FORWARD, AND GLOSSARY

Mr. H.G. Kimball, the past chairman of the ITU-R, wrote the preface explaining the reason for publishing the book. The editors have written the forward giving a general description of the book and its contents, and where to find different topics. The glossary of terms used in the time and frequency field is based on the glossary that was originally generated by the CCIR (now the ITU-R) with additional definitions from ISO where there are differences or omissions.

CHAPTER DESCRIPTIONS

Chapter 1: Introduction and Basic Concepts

A historical background of the development of atomic frequency standards is given. The physics underlying commercially available atomic frequency standards are described and the means of applying them to frequency standards are outlined. The criteria which determine the performance of the various standards are discussed. In addition, quartz crystal oscillators are described because of their use in all the frequency standards. Every atomic frequency standard includes a quartz crystal oscillator and a certain amount of the performance of the frequency standard is due to the performance of the quartz crystal oscillator. Since this book is not designed to teach people how to design new frequency standards, but rather in how to use them, only commercially available precise frequency standards are covered, i.e., cesium beams, rubidium gas cells, hydrogen masers, and, of course, quartz oscillators.

Chapter 2A: Local Frequency and Time Sources

The actual implementation block diagrams and critical design parameters of the frequency standards based on the physics concepts of Chapter 1 are described and the use of the quartz crystal oscillator in each is outlined. Cesium, rubidium, hydrogen masers, and quartz crystal oscillators are covered in detail. Passive and active standards are covered.

Chapter 2B: Steering References

A complete listing of all the possible references that are available for syntonizing local frequency standards and for synchronizing local time standards to UTC coordinating with the SI second are given. Advantages and disadvantages of each are given, as well as the relative cost and complexity of operation of each of them.

Chapter 3: Characterization: Frequency Domain, Time Domain, Environment

Complete descriptions of the various measures of frequency and time stability, as used in the frequency and time field as well as those used in the communications field, written from a communications point of view, are presented. Cross-references are given to relate the communications point of view with the conventional frequency and time point of view. High-noise oscillators and low-noise oscillators are covered, as are the effects of frequency multiplication, and multiplicative and additive noise. This chapter covers true variance, $\sigma_y(\tau)$, $\text{Mod}\sigma_y(\tau)$, $S_\phi(f)$, $L(f)$, $S_x(f)$, TIE, structure functions, the Hadamard variance, and the high-pass variance.

Chapter 4: Measurement Technology (Metrology)

Measurement techniques for determining the characteristics of the frequency source are discussed in detail. Actual hardware examples of each technique are given, as well as things to be careful about. This is an updated and condensed version of some of the tutorials that have been given in the past.

Chapter 5: Characteristics of Various Frequency Sources

The actual performance in the time domain and frequency domain of available frequency sources are given. Systematic effects are included, giving the sensitivity of the different sources to environmental conditions and aging.

Chapter 6: Time Scales

The different time scales are defined and discussed, including TAI (International Atomic Time), UTC (Coordinated Universal Time), ET (Ephemeris Time), and UT# (the different Universal Times). A discussion of the means of generating time scales and examples of each are given, including the algorithms used by NIST and BIPM. The availability of documents for coordinating a local time scale with the BIPM are given, with examples of each.

Chapter 7: Uses of Frequency Sources

The many uses for frequency sources are described with specific examples described in detail.

Chapter 8: Operational Experience, Problems, Pitfalls

The real world operation of frequency sources with *caveats* about things that may degrade their performance. Reliability of the different sources is discussed and data are given for some standards.

Chapter 9: Future Prospects

Likely changes to expected in the future with the continual improvement of frequency sources and new technology are discussed.

Chapter 10: Conclusions

A wrap-up of the contents of the handbook and its use.

SUMMARY

The final draft was submitted to the ITU-R and is due to be published at the end of 1996.

APPENDIX: TABLE OF CONTENTS

Preface

Foreward

Glossary

Chapter 1 Introduction and Basic Concepts

1.1 Historical Sketch

1.2 Basic Principles of Frequency Standards

1.2.1 Quartz Crystal Frequency Standards

1.2.2 Atomic Frequency Standards

1.2.2.1 Spectroscopic Properties of Interest

1.2.2.2 Passive and Active Atomic Frequency Standards

1.3 Basic Metrology Concepts

1.3.1 Frequency Stability

1.3.1.1 Definition

1.3.1.2 Quartz Crystal Oscillators

1.3.1.2.1 Random Frequency Fluctuations

1.3.1.2.2 Systematic Effects

1.3.1.3 Atomic Frequency Standards

1.3.1.3.1 Short Term Frequency Stability

1.3.1.3.2 Medium Term Frequency Stability

1.3.1.3.2.1 Medium Term Frequency Stability in Passive Frequency Standards

1.3.1.3.2.2 Medium Term Frequency Stability in Active Frequency Standards

1.3.1.3.2.3 Long Term Frequency Stability

1.3.2 Accuracy

1.3.2.1 Residual Frequency Offsets

1.3.2.2 Definition

1.3.2.3 Primary and Secondary Frequency Standards

1.3.3 Reproducibility, Resettability

1.3.4 References

Chapter 2A Local Frequency and Time Sources

2A.1 Introduction Chapter 2 Available Frequency and Time Sources

2A.2 Quartz Crystal Frequency Standards

2A.2.1 Basic Principles

2A.2.2 The Resonator

2A.3 The Rubidium Gas Cell Frequency Standard

2A.4 The Hydrogen Maser

2A.5 The Caesium Beam Frequency Standard

2A.6 References

Chapter 2B Steering References

2B.1 Introduction

2B.2 Factors to be Considered in the Selection and Use of Alternative Time-and-Frequency
Dissemination Services and Techniques

2B.3 Comparisons of Alternative Sources and Dissemination Techniques for Precise
Time-and-Frequency References

2B.4 Additional Techniques Relating to the Use of the Various Alternative Services,
Systems, and Techniques

2B.5 Bibliography Related to Time-and-Frequency Steering Techniques

Table 2B.1 Characteristics of Some Potential Sources and Dissemination Techniques
for Precise Time-and-Frequency Reference Information

Table 2B.2 Additional Information Relating to the Practical Use of Various Alternative
Sources of Time-and Frequency Signals

Chapter 3 Characterisation: Frequency Domain, Time Domain, Environment

3.1 Introduction

3.2 Model of the Oscillator

3.2.1 The Phasor Model and the Analytic Signal

3.2.2 The Low Noise Oscillator

3.2.3 Spectrum of the Low-Noise Oscillator

3.2.4 The High Noise Oscillator

3.2.5 Spectrum of the High Noise Oscillator

3.2.6 Effect of Frequency Multiplication

3.2.7 Demodulation of the Noise Processes

3.2.8 Standard Definition of Noise Processes

3.2.8.1 Amplitude and Phase Noise Processes

3.2.8.2 Time Error Process

3.2.8.3 Instantaneous Frequency Process

3.2.9. Multiplicative and Additive Noise

3.2.9.1 Multiplicative Noise

3.2.9.2 Additive Noise

3.2.10 Polynomial Model

3.3 Characterisation: Definitions Methods

3.3.1 Spectral Domain

3.3.1.1 Basic Definitions

3.3.1.2 Spectral Purity Concepts

3.3.2 Time Domain

3.3.2.1 Introduction

3.3.2.2 Basic Concepts

3.3.2.2.1 Model of the Frequency Counter

3.3.2.2.2 Moving Average Operator

3.3.2.2.3 Increment Operator

3.3.2.3 Basic Time Domain Measurements

3.3.2.3.1 The True Variance

3.3.2.3.2 The Classical Allan Variance

3.3.2.3.3 The Modified Allan Variance

3.3.2.3.4 The Time Interval Error

3.3.2.3.5 The Time Variance

3.3.2.3.6 Other Time Domain Measurements

3.3.2.3.7 The Multi-variance Analysis

3.3.2.4 Pitfalls

3.3.2.4.1 Effect of Zero-Crossing Detection

3.3.2.4.2 Effect of Dead-Time

3.3.2.4.3 Effect of System Bandwidth

3.3.2.4.4 Truncation Effects

3.3.2.5 Algorithms

3.3.2.5.1 Frequency Averaging by Phase Sampling

3.3.2.5.2 Computation of Classical Allan Variance

3.3.2.5.3 Computation of Modified Allan Variance

3.3.2.5.4 Summary

3.3.2.6 Applications

3.3.2.7 Conversion between Time & Frequency Domains

3.3.3. Environmental

3.3.3.1 Definitions

3.3.3.2	Pitfalls
3.4	A Bridge to Next Chapter
3.5	Appendix: Random Processes
3.5.1	Introduction
3.5.2	Definition of a Random Process
3.5.3	Stationary Random Processes
3.5.4	Non-Stationary Random Processes
3.5.5	Auto-Correlation Function
3.5.6	Power Spectral Density
3.5.7	Linear Filtering of Random Processes
3.6.	References
Chapter 4	Measurement Techniques (Metrology)
4.0	Introduction
4.1	Direct Measurements of Time (Phase) and Frequency
4.1.1	Direct Measurements of Time (phase)
4.1.2	Direct Measurements of Frequency
4.2	Heterodyne Measurements of Frequency and Phase (Time)
4.2.1	Heterodyne Measurements of Phase (Time)
4.2.2	Heterodyne Measurements of Frequency
4.2.3	Heterodyne Measurements of PM Noise
4.2.4	Dual Mixer Time Measurements Systems
4.2.5	Picket Fence Based Measurement Systems
4.2.6	Digital Techniques for Frequency and PM measurements
4.2.7	Three-Cornered Hat Measurements
4.2.8	Cross-Correlation Measurement Systems
4.3	Single-Oscillator Measurements of Frequency and PM Noise
4.3.1	Delay-Line Measurements of Frequency and PM Noise
4.4	Measurements of AM Noise
4.5	References
Chapter 5	Characteristics of Various Frequency Standards
5.1	Definitions and Discussion: Measures and Implications
5.1.1	The Characterisation of Random Processes
5.1.1.1	$L(f)$, $S_{\phi}(\tau)$
5.1.1.2	$\sigma_y(\tau)$, $\text{mod}\sigma_y(\tau)$, $\sigma_z(\tau)$
5.1.2	Systematic Effects
5.1.2.1	Environmental Effects
5.1.2.1.1	Temperature
5.1.2.1.2	Humidity
5.1.2.1.3	Barometric Pressure
5.1.2.1.4	Magnetic Field
5.1.2.1.5	Power Line Voltage, Noise, and Interruptions
5.1.2.1.6	Acceleration, Vibration, and Shock
5.1.2.1.7	Ageing
5.1.2.1.8	Drift
5.2	Characteristics of Various Frequency Standards
5.3	References
Chapter 6	Time Scales
6.1.	Introduction
6.1.1.	Universal Time
6.1.2.	Ephemeris Time
6.1.3.	International Atomic Time
6.1.4.	Coordinated Universal Time

- 6.2. Time scales in general relativity
 - 6.2.1. Coordinate systems in general relativity
 - 6.2.2. The 1991 IAU Resolution A4
 - 6.2.2.1. Recommendation I
 - 6.2.2.2. Recommendation II
 - 6.2.2.3. Recommendation III
 - 6.2.2.4. Recommendation IV
 - 6.2.3. International Atomic Time
 - 6.2.4. Other coordinate time scales
- 6.3. Generation of time scales
 - 6.3.1. Expected qualities
 - 6.3.1.1. Reliability
 - 6.3.1.2. Stability
 - 6.3.1.3. Accuracy
 - 6.3.1.4. Delay of access
 - 6.3.2. Timing data
 - 6.3.2.1. General form of timing data
 - 6.3.2.2. Comparison of clocks located on the same site
 - 6.3.2.3. Comparison of clocks located on remote sites
 - 6.3.2.4. Smoothing of data measurement noise
 - 6.3.3. Stability algorithm
 - 6.3.3.1. Definition of an average time scale
 - 6.3.3.2. Length of the basic interval of computation
 - 6.3.3.2.1. Update of TA every interval of duration T
 - 6.3.3.2.2. Update of TA when the interval of duration nT is ended
 - 6.3.3.3. Weighting procedure
 - 6.3.3.3.1. General ideas
 - 6.3.3.3.2. Weighting procedure in AT1(NIST)
 - 6.3.3.3.3. Weighting procedure in ALGOS(BIPM)
 - 6.3.3.4. Frequency prediction
 - 6.3.3.4.1. General ideas
 - 6.3.3.4.2. Frequency prediction in AT1(NIST)
 - 6.3.3.4.3. Frequency prediction in AOSLG(BIPM)
 - 6.3.4. Accuracy of the scale interval of a time scale
 - 6.3.5. Examples
 - 6.3.5.1. Stability of some independent time scales
 - 6.3.5.2. Steering of some local representations of UTC
- 6.4. Dissemination of time scales
- 6.5. Conclusions
- 6.6 References

Chapter 7 Uses of Frequency Sources

- 7.1 Uses of Frequency Sources in Science and Technology
- 7.2 Metrology
 - 7.2.1 Accuracy Comparison between the Standard of Time and Those of the Other Basic Quantities
 - 7.2.2 Relations between the Unit of Time and Other Units
- 7.3 Fundamental and Applied Physics
 - 7.3.1 g, Acceleration Due to Gravity
 - 7.3.2 GM, Gravitational Constant Times Earth Mass
 - 7.3.3 The Gravitational Field of the Earth
 - 7.3.4 Very Large Baseline Interferometry (VLBI) and Quasi-VLBI
- 7.4 Positioning and Navigation
 - 7.4.1 Conical Navigation
 - 7.4.2 Circular or Spherical Navigation
 - 7.4.3 Hyperbolic Navigation

- 7.4.4 Hyperbola, Hyperboloid and their Properties
- 7.4.5 Accuracy Requirements for the Frequency Standards used in Navigation Systems
- 7.5 Telecommunications
 - 7.5.1 Analogue Systems
 - 7.5.2 Digital Systems
- 7.6 Other Applications
 - 7.6.1 Automotive Applications
 - 7.6.2 Electrical Power Systems and Compressed Gas Dispatching
 - 7.6.3 Instrumentation
 - 7.6.4 Doppler Radar
- 7.7 References

Chapter 8 Operational Experience, Problems, Pitfalls

- 8.0 Overview
- 8.1 Frequency and Time Tools
 - 8.1.1 Choice of a Reference
 - 8.1.1.1 Assessing What is Needed
 - 8.1.1.2 Steered versus Free-running Clock
 - 8.1.2 Tools for Operational Use
 - 8.1.2.1 F/T System Stability
 - 8.1.2.1.1 Measurement Noise
 - 8.1.2.1.2 Measuring Clock Performance
 - 8.1.2.2 System Reliability
 - 8.1.2.2.1 Failure Rates
 - 8.1.2.2.2 Problems in Dealing with Errors
 - 8.1.2.3 System Accuracy
 - 8.1.2.4 Practical Hardware Problems
- 8.2 Data and Examples from Operational Experience
 - 8.2.1 Frequency and Time Standards
 - 8.2.2 Examples of Problems
 - 8.2.3 Frequency and Time Comparisons
 - 8.2.3.1 Is Linear Regression Best?
 - 8.2.3.2 Problem with Cycle Ambiguity
 - 8.2.4 Other Data, System Set-up, and Processing Ideas and Problems
 - 8.2.4.1 Models versus Reality
 - 8.2.4.2 Data Formats
 - 8.2.4.3 Retrieving and Storing Data
 - 8.2.4.4 Installation Concerns
 - 8.2.4.5 Care and Replacement
- 8.3 Conclusion
- 8.4 References

Chapter 9 Future Prospects

- 9.1 Introduction
- 9.2 General Overview
- 9.3 Gas Cell Devices
- 9.4 Caesium Beam Standards
- 9.5 Hydrogen Masers
- 9.6 Trapped Ion Standards
- 9.7 Caesium Fountain
- 9.8 Quartz Oscillators
- 9.9 Oscillator Stabilised to GPS
- 9.10 Oscillator Stabilised with Cooled Sapphire Resonator
- 9.11 Optical Frequency Standards
- 9.12 Summary

Chapter 10 Conclusions

10.1 General Observations

10.2 Clocks and Oscillators

10.3 Measurement Methods and Characterisation

10.4 Time Scales, Coordination, and Dissemination

10.5 Realities

Questions and Answers

JAMES CAMPARO (AEROSPACE CORP.): How are you people going to get copies of this to us?

RICHARD SYDNOR: Okay, I have a few copies here for people who are really interested. They are draft copies, there might be a few typos here and there and that sort of thing. If anyone wants to leave their name with me, I will contact you as soon as it's published and give you addresses and actual prices so that you can order copies.

JAMES CAMPARO: Would that be for both handbooks?

RICHARD SYDNOR: It's the same location for both handbooks, but I will give you information on this one. And then if you write to the address, they'll send you a catalog.

GERRIT de JONG (NMI VAN SWINDEN LAB, NETHERLANDS): The other handbook is not yet ready, so it's only this handbook.

JAMES CAMPARO: So you were referring to the one coming out in December?

GERRIT de JONG: No, only the manuscripts will be finished. So it will take maybe half a year or longer.

JOHN VIG (ARL): It sounds like there's a lot of good reference information in this book. Is there any chance that we could get at least some of it on the Web? Both Frequency Control and the PTTI now have a Web site.

RICHARD SYDNOR: Well, we have a copyright problem. It belongs to ITU. It would be a good idea. I can make a couple inquiries to find out. The price is quite reasonable, \$30 or so for a technical book that's 200 and some odd pages full of information; and a lot of references if you wanted to delve deeper there into any of the topics.

JOHN VIG: I know that at least the contributions by government authors are not copyrighted.

RICHARD SYDNOR: Yes, but there are a lot of foreign authors, you know, some of the primary authors are from Europe. It's an international book, it's not a US book.

THE IEEE FREQUENCY CONTROL SYMPOSIUM

John R. Vig
U.S. Army Research Laboratory, AMSRL-SE-RE
Ft. Monmouth, New Jersey 07703-5601, USA
E-mail: j.vig@ieee.org

Abstract

A brief overview of the IEEE International Frequency Control Symposium is presented. The presentation includes:

- *A brief history of the Symposium*
- *Technical fields covered by the Symposium*
- *The Symposium awards, and recent winners*
- *A summary of the 1996 meeting, the 50th anniversary celebration, in Hawaii*
- *Dates and places of upcoming Symposia*
- *Information about the sponsoring organization, the IEEE Ultrasonics, Ferroelectrics, and Frequency Control Society.*

History of the FCS

- Started as a gathering of government researchers and (DoD) contractors
- First symposium was held in a conference room at Ft. Monmouth, NJ; next three at the Officers' Club; 5th to 13th at a hotel in Asbury Park; the next 20 yrs in Atlantic City, NJ, then in Philadelphia 1980-87.
- Proceedings published since the 10th.
- Sponsored by the U.S. Army till 1982; cosponsored by Army & IEEE 1983-90; and by the IEEE since 1991.
- Attendees 100% U.S. at start; <50% U.S. in recent yrs

FCS Topics

Group 1

- A. Fundamental Properties of Materials
- B. Theory and Design of Resonators and Filters
- C. Sensors and Transducers

Group 2

- A. Oscillators - BAW and SAW
- B. Oscillators - Microwave to Optical
- C. Synthesizers and Other Circuitry
- D. Noise Phenomena and Aging

Group 3

- A. Atomic and Molecular Frequency Standards
- B. Frequency and Time Coordination
- C. Measurements and Specifications
- D. Applications of Frequency Control

FCS Awards

- The **Cady Award** is to recognize outstanding contributions related to **piezoelectric** frequency control and sensor devices.
- The **Rabi Award** is to recognize outstanding contributions related to the fields of **atomic and molecular** frequency standards, and **time transfer** and dissemination.
- The **Sawyer Award** is to recognize outstanding contributions in the development, production or characterization of **piezoelectric materials**, or to recognize **entrepreneurship** or **leadership**.

FCS Dates and Places

- Held in late-May or early June
- 50th was held in Hawaii in June 1996
- 1997: Disney World, Orlando, FL
(submission deadline is Jan 6)
- 1998: Pasadena, CA
- 1999: Besancon, France (joint with EFTF)

UFFC-Soc & FCS Web Site

- <http://bul.eecs.umich.edu/~uffc/>
or <http://www.ieee.org/society/uffc>
- Searchable data base of all FCS paper abstracts
- Call-for-Papers
- Dates and places of future symposia
- Description of awards and list of past winners
- List of past FCS officials

THE CCDS WORKING GROUPS

Claudine Thomas
Bureau International des Poids et Mesures
Pavillon de Breteuil, 92312 Sèvres Cedex, France

Abstract

The Comité Consultatif pour la Définition de la Seconde (CCDS) deals with the definition and realization of the second, and the establishment and diffusion of the International Atomic Time (TAI) and the Coordinated Universal Time (UTC). As other consultative committees, it has created a number of Working Groups in order to advise on specified problems. At present, there exists three CCDS Working Groups:

- *the CCDS Working Group on TAI, which includes a Sub-Group on GPS and GLONASS Time Transfer Standards,*
- *the CCDS Working Group on Two-Way Satellite Time Transfer, and*
- *the CCDS Working Group on Application of General Relativity to Metrology.*

This paper gives reports of the work done within the these groups, together with their future actions.

CCDS: COMITE CONSULTATIF POUR LA DEFINITION DE LA SECONDE
Consultative Committee for the Definition of the Second

President: Prof J. Kovalevsky

Membership: Institutions or laboratories

+

Invited guests (experts invited for one particular session of the CCDS)

+

Prof B. Guinot, member by appointment

+

The Director of the BIPM and the Physicists of the BIPM Time Section

RECOMMENDATIONS → CIPM → CGPM

REPORT for each session

Last session (13th): 12-13 March 1996 (≈ 3 years)

CCDS WORKING GROUPS

Working Group on TAI

Chairman: Dr P. Pâquet, ORB

Rapporteur of the last session: Dr G. Petit, BIPM

Sub-Group on GPS and GLONASS Time Transfer Standards (CGGTTS)

Chairman: Dr D.W. Allan, Allan's TIME

Secretary: Dr C. Thomas, BIPM

Working Group on Two-Way Satellite Time Transfer

Chairman: Dr W.J. Klepczynski, ISI

Secretary: Dr W. Lewandowski, BIPM

Working Group on Application of General Relativity to Metrology

Chairman: Prof B. Guinot

Secretary: Dr C. Thomas, BIPM

Working Group on the Expression of Uncertainties in Primary Frequency Standards

Chairman: Dr R. Douglas, NRC

Working Group on TAI

Charter

1. To examine the remarks and requirements expressed by the users of the service of TAI
2. To prepare directives for the improvement of the service of TAI to be submitted for approval by the CCDS and then by the CIPM

Membership

Representatives of the four unions IAU, IUGG, URSI and ITU, and of the CIPM

The Director of the BIPM, the person in charge of TAI at the BIPM

Meetings of representatives of the timing laboratories before CCDS meetings

Actions

Last meeting: black-body radiation shift

Change of the upper limit of weight in TAI computation

TAI updates every 5 days

Publication of $[UTC - UTC(k)]$ within ± 1 ns

Requirement for data before the 5th of the month

Future

Watch upon TAI

Sub-Group on GPS and GLONASS Time Transfer Standards

Charter

Standardization of commercial GPS and GLONASS receiver software and hardware
→ improvement of the accuracy of GPS and GLONASS time transfer

Membership

Experts of time laboratories + representatives of receiver manufacturers
(formal meetings + open forums)

Actions

Standardization of one-channel one-frequency C/A GPS time receiver software:
TECHNICAL DIRECTIVES
Adaptation to GLONASS time receiver software

Future

Standardization of GPS and GLONASS time receiver hardware:
sensitivity to outside temperature
Problems of calibration
Multichannel GPS and GLONASS receivers: CCDS formal request

Working Group on Two-Way Satellite Time Transfer

Charter

CCDS 11th meeting (1989): BIPM *ad-hoc* Working Group

Its task is to define conditions of the operational system:

- * satellites and frequency bands,
- * specifications of the earth stations,
- * station calibration,
- * measuring procedures and schedules,
- * data processing.

CCDS 12th meeting (1993): CCDS Working Group with the task of:

- * assisting the establishment of regular two-way experiments and their evaluation,
- * preparing a standard format for data exchange.

Membership

Experts of time laboratories + representatives of modem manufacturers
Annual formal meetings + meetings of station operators

Actions

Field-trial experiment in 1994-95 with 6 stations in Europe & 2 in USA
Demonstration of the permanent operation of a network of stations
Development of a standard data format
Potential for high accurate frequency and time transfer

Future

Re-start of operational links
Improvement of earth station operation
Newly developed modems
Problems of calibration
Two-way frequency transfer between primary frequency standards

Working Group on Application of General Relativity to Metrology

Charter

1. Preparation of a report on the interpretation and use of SI units in the framework of the Theory of General Relativity
2. Studies on the consequences of the increasing accuracy of the realizations of the SI units

Membership

Experts in General Relativity+ members of timing laboratories

Actions

Publication of a *Metrologia* International Report on point 1
'Application of General Relativity to Metrology'
by B. Guinot, March 1997

Future

Point 2

CONFERENCE AND WORKING GROUP UPDATES: THE EUROPEAN FREQUENCY AND TIME FORUM

Sigfrido Leschiutta

Politecnico di Torino
Dipartimento di Elettronica
Corso Duca degli Abruzzi 24
10129 Torino, Italy

Istituto Elettrotecnico Nazionale
G. Ferraris
Strada delle Cacce 91
10135 Torino, Italy

Michele Serafino (guest researcher)
Politecnico di Torino
Torino, Italy

Abstract

The European Frequency and Time Forum (EFTF) is an international conference and exhibition, providing information on recent advances and trends of scientific research and industrial developments in the fields of Frequency and Time. EFTF was inaugurated in 1987, by the action of French and Swiss researchers, as a meeting and discussion point for the European PTTI community, but the Forum soon attracted participants from all over the world. The average number of participants is between 250 and 300, with researchers coming from 20-25 countries: The number of papers (invited, presented, posters) rounds to 100-130. The wide spectrum of contributions compels the use of two sessions in parallel; the duration is of three days, usually in March. The venue is alternatively in France (Besançon) and Switzerland (Neuchâtel), but in recent years some events were held alternately in other European countries.

1 INTRODUCTION

EFTF Forum started ten years ago by the initiative of French and Swiss researchers, active in the Frequency and Time field, in two nearby regions of the two countries. Indeed, going back in time to the past centuries, clockmaking activities were widespread in a French region, west of Jura mountains, the Franche-Comptée, and in a Swiss region, around Neufchâtel, in the east side of the same chain. Among the promoters were Prof. R. Besson, the designer of the BVA crystal resonator, and Dr. P. Kartaschoff, of the Swiss PTT administration, and designer, in the early sixties, of the largest cesium tube frequency standard ever made, with an interaction length of over 4 m.

In the next section some details are given about the organization and the venues. News concerning the number of participants, the distribution of papers, and the running of the sessions will be covered in the third section, while in the last an attempt is made to find out the guidelines of development in PTTI matters that can be obtained merely by inspection of the papers submitted in the past ten years at the European Forum on Frequency and Time.

2 THE FORUM

The Forum is organized by an Executive Committee, formed by well known French and Swiss experts in the field: A. Audoin, R. Besson, M. Ecabert, J.J. Gagnepain, P. Kartashoff, and B. Schlueter.

The Executive Committee is assisted by an international Scientific Committee, formed by a large number of experts coming from all over the world. The Scientific Committee meets twice per year, during the Forum and in the fall of the year in order select the papers and to appoint some invited speakers. Papers are solicited by a standard call for papers, sent usually in May.

Each venue of the Forum is supported, from a financial point of view, from local and scientific organizations of the guest country.

The venue were held in the towns listed in Table I.

Table I - EFTF Venues

1st	1987	Besançon	France
2nd	1988	Neuchâtel	Switzerland
3rd	1989	Besançon	France
4th	1990	Neuchâtel	Switzerland
5th	1991	Besançon	France
6th	1992	Noordwijk	The Netherlands-ESA
7th	1993	Neuchâtel	Switzerland
8th	1994	Weißenstephan	Germany
9th	1995	Besançon	France
10th	1996	Brighton	UK
11th	1997	Neuchâtel	Switzerland

3 CONTRIBUTIONS PRESENTED AT THE FORUM

On the average at the annual venue are presented about from 80 to 100 papers, with a maximum observed in 1993 of 121; in that year the attendees were 334, coming from 24 countries. An average of 250-300 people attended the meetings in the last few years.

Usually the invited papers are 5 to 8, the oral presentations around 70, and the posters about 30-40, as can be deduced from Table II.

Table II - Papers Presented to EFTF

	atomic	resonators	posters	total
1987	22	40	-	66
1988	42	32	-	74
1989	29	38	-	67
1990	46	31	32	77
1991	27	27	16	64
1992	39	24	25	88
1993	37	39	45	121
1994	33	25	33	91
1995	33	21	47	103
1996	27	42	38	107

Table II commands some remarks. Under the heading *atomic* are considered papers dealing with atomic frequency standards, metrological matters, time scale formation, synchronization, and dissemination or space uses requiring the utmost accuracy.

Under the heading *resonators* are considered also the materials, measurement techniques on quartz, new materials for oscillators, sensors, and SAW devices. The posters are roughly divided in equal parts between the two headings with the same rule for the oral presentations; over the period 1987-1996, 333 papers can be classified as *atomic* and 339 as *resonators*.

It is worth to note that in Europe, and mostly in France, there is active a strong community of researchers working on piezoelectric materials and devices.

The strong diversification of the interest of the attendees between the two aforesaid "headings" and their parity in number compels the adoption of parallel sessions for a large part of the Meeting.

4 TRENDS OF THE PTTI RESEARCH

The study of some 900 papers over a span of 10 years offers the unique possibility to delineate some trends in the PTTI research. This study is presented in another paper at this PTTI Meeting^[1], but nevertheless some features can be pointed out considering the papers presented at the Forum. A couple of disclaimers are in order: since the field of interest of the authors concentrated under the heading *atomic*, no attempt will be made to trace trends in the *resonators* area, which anyway seems stable. The second is based on the careful control by part of the Scientific Committee of the quality and balance of the program offered; the trends are indeed originated by the "offer" of the papers, but these trends are possibly filtered in order to give a balanced view with a good appeal for the audience.

Confirmed is the traditional interest in the European labs on cesium devices; on the average 10 papers per year are dealing with this kind of standard, in its three approaches: the classic one with magnetic state selection (on the average 6 papers/year), with optical selection (from 1990), and with the cooled fountain (more recently). The first paper on the latter very interesting approach was presented by Clairon et al., in 1991.^[2] As regards the other standard frequency sources, hydrogen masers are under study; meanwhile the rubidium-cell peak of interest was in the first nineties, and it is now declining, but optically pumped Rb masers were proposed, mainly by China. The interest in lasers, as frequency and length standard seems to increase in

the very last years. Regarding comparison methods, Omega, VLF, and Loran-C disappeared after 1990 and the interest on GPS was particularly strong in 1990-1993; the system being now a well known standard, only special applications are reported. The two-way method, after an upsurge in 1990, now is extensively studied, with 20 some papers in 5 years. Considering other topics belonging to precise Time and Frequency activities, three are worth mentioning:

- studies on time scale formation and algorithms, with 5-6 contributions per year since 1991,
- research on frequency synthesis and on the electronic circuits (multipliers, distribution amplifiers, dividers, etc.) to be designed if we really are interested to the path leading to a stability of 10^{-18} ,
- applications requiring utmost accuracies,
- digital telecommunication as time and frequency dissemination systems,
- clock noise modelization/statistics, and
- traceability issues.

5 FUTURE EFTF VENUES

In 1995 an agreement was reached for joint meetings between EFTF and the IEEE International Frequency Control Symposium (FCS). The first of these joint meetings is planned for April 1999, in Besançon, France; the second will take place in 2003 somewhere on or near the East Coast of the United States. The intention of the EFTF and the IEEE/FCS is that these two venues be a test of the concept of joint conferences.

Torino, November 1996

6 REFERENCES

- [1] F. Cordara, A. De Marchi, M. Serafino, and S. Leschiutta 1997, these Proceedings.
- [2] A. Clairon, *et al.* 1991, "A laser cooled cesium atomic fountain: towards a high performance clock," Proceedings of the 5th European Frequency and Time Forum (EFTF), March 1991, Besançon, France, pp. 228-236.

STATUS REPORT ON RADIONAVIGATION SYSTEMS AND THE INSTITUTE OF NAVIGATION

Laura G. Charron
U.S. Naval Observatory
Washington, DC 20392, USA

Abstract

Due to emerging technology, primarily the Global Positioning System (GPS), the systems used for navigation, as well as for the transfer of PTTI, are undergoing rapid change. The latest status for the continued deployment of systems such as TRANSIT (NNSS), LORAN-C, and OMEGA are reported. A synopsis of the Institute of Navigation GPS Conference, particularly as it relates to timing applications, is presented.

FEDERAL RADIONAVIGATION PLAN

Purpose

Statement to set forth policy and plans for Federally provided radionavigation systems

Individual System Plans

GPS: Operated by DoD and managed by the Interagency GPS Executive Board

Standard Positioning Service (SPS) will be available to all users on a continuous, worldwide basis, for the foreseeable future free of any direct user charge

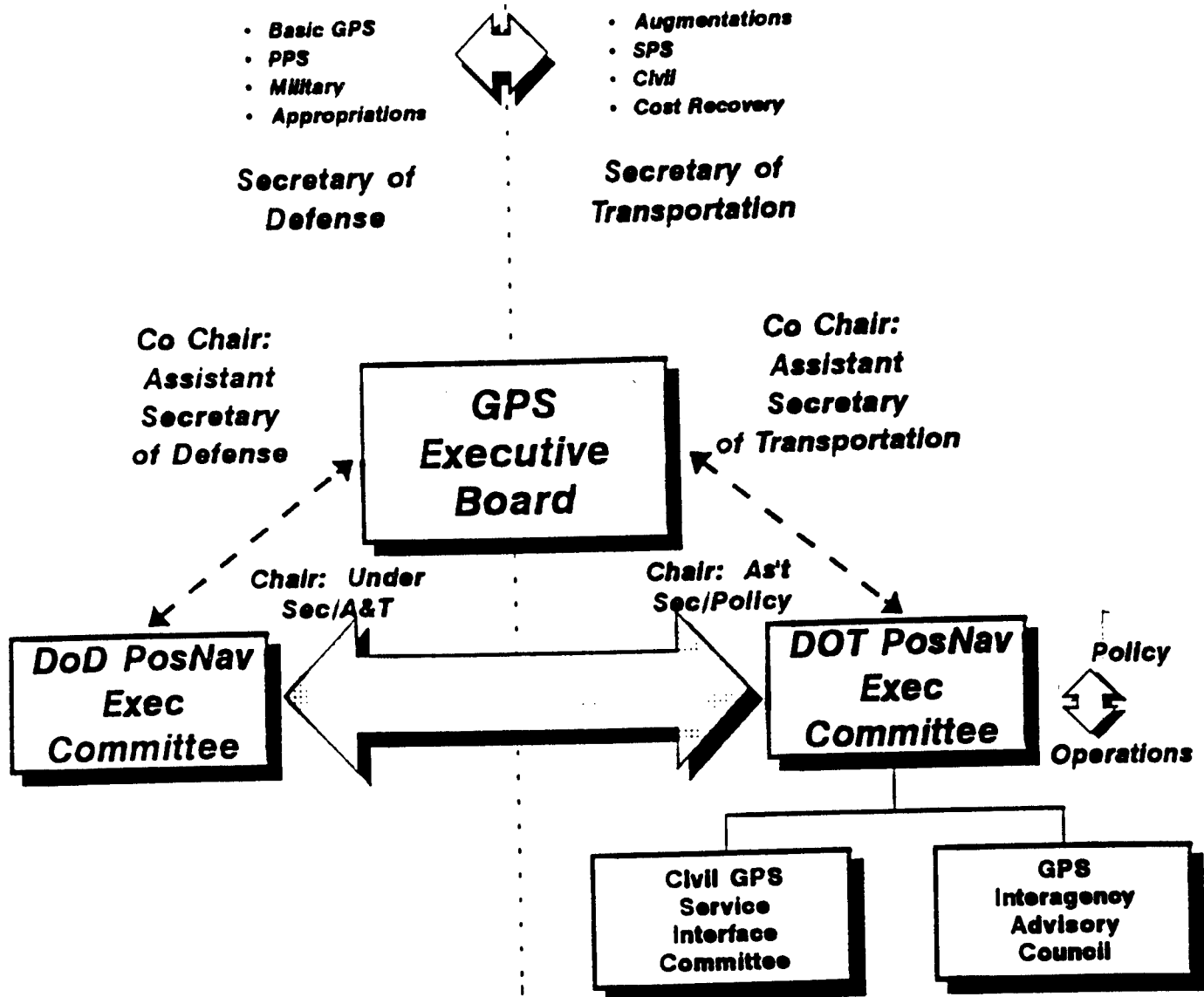
Precise Positioning Service (PPS), the most accurate service directly available from GPS without augmentations, is available to US and allied military and US Federal Government users

Augmentations to GPS: The US Government will not constrain the peaceful use of SPS-based differential GPS services as long as applicable US statutes and international agreements are adhered to.

Loran-C: The US plans to terminate Loran-C operations on December 31, 2000. DOT will prepare a report on Loran-C requirements in consultation with users and the Secretary of Commerce as required by USCG Authorization Act 1996

Omega: The US plans to terminate Omega operations on 30 September 1997

Transit: Ceases operation as a positioning and timing system on 31 December 1996



Joint DOD/DOT POS/NAV Management Structure

FEDERAL RADIONAVIGATION PLAN 1996 (available after 1 January 1997)

Sources

Volpe National Transportation Systems Center
Kendall Square, Cambridge, MA 02142-1093, USA

ATTN: Elizabeth Carpenter FAX 617-494-2628

USCG Navigation Information Service World Wide Website

<http://www.navcen.uscg.mil/>

National Technical Information Service
Springfield, VA 22161, USA

Phone (703) 487-4650 or (703) 487-4660

INSTITUTE OF NAVIGATION

Purpose

The Institute of Navigation is a non-profit professional society dedicated to the advancement of the art and science of navigation. It serves a diverse community including those interested in air, space, marine, and land navigation, and position determination. Although basically a national organization, its membership is worldwide, and it is affiliated with the International Association of the Institutes of Navigation.

Information

The Institute of Navigation
1800 Diagonal Road, Suite 480
Alexandria, VA 22314, USA

Phone (703) 683-7101; fax (703) 683-7177

Website: <http://www.ion.org>

UPCOMING MEETINGS—1997

January 14-16:

“Navigation and Positioning in the Information Age,”
Loews Santa Monica Beach Hotel, Santa Monica, California, USA

June 30 - July 2:

The 53rd Annual Meeting
Grand Hyatt, Albuquerque, New Mexico, USA

September 16-19:

ION GPS-97
Kansas City Convention Center, Kansas City, Missouri, USA

ION GPS-96

September 1996, Kansas City, Missouri, USA

Sessions:

- | | |
|--------------------------------------------------|--------------------------------------------------|
| A1: Precision Approach | B1: Aircraft Applications |
| A2: New Product Descriptions | B2: Land Applications |
| A3: GPS & GLONASS Performance | B3: Atmospheric Effects |
| A4: Marine Application | B4: Multipath |
| C1: Wide Area Augmentation Systems (WAAS) | D1: GNSS & WAAS Architectures |
| C2: Kinematic Positioning & Ambiguity Resolution | D2: Surveying & Geodesy |
| C3: Integrated Systems | D3: Space Applications |
| C4: Attitude Determination | D4: Student Session |
| E1: GPS & GLONASS Application | F1: Precise Positioning Using Reference Networks |
| E2: Military Applications | F2: Specialized Military Equipment Technology |
| E3: Integrity | |

Working Group: GLONASS/GPS Interoperability

PRECISION TIME AND FREQUENCY TRANSFER UTILIZING SONET OC-3

Malcolm Calhoun, Paul Kuhnle, and Richard Sydnor
Jet Propulsion Laboratory, California Institute of Technology
4800 Oak Grove Drive, Pasadena, California 91109, USA

Sam Stein
Timing Solutions Corporation
Boulder, Colorado 80304, USA

Al Gifford
U.S. Naval Observatory
Washington, DC 20392, USA

Abstract

An innovative method of distributing precise time and reference frequency to users located several kilometers from a frequency standard and master clock has been developed by the Timing Solutions Corporation of Boulder, CO. The Optical Two-Way Time Transfer System (OTWTTS) utilizes a commercial SONET OC-3 facility interface to physically connect a master unit to multiple slave units at remote locations (in this particular implementation, five slave units are supported). Optical fiber is a viable alternative to standard copper cable and microwave transmission. Coaxial cable is lossy with relatively poor temperature stability. Microwave transmission is expensive and may introduce unwanted noise and jitter into the reference signals. Optical fibers are the preferred medium of distribution because of low loss, immunity to EMI/RFI, and temperature stability. At the OTWTTS remote end, a slave local oscillator is locked to the master reference signal by a clock recovery PLL. Data signals are exchanged in both directions in order to calibrate the propagation delay over long distances and to set the slave time precisely to the master on-time 1 pps. The OTWTTS is capable of maintaining, without degradation, the HP 5071 cesium standard stability and spectral purity at distances up to 10 km from the frequency standards central location.

This paper discusses measurements of frequency and timing stability over the OTWTTS. Two reels of optical fiber, each 10.6 km in length, were subjected to sinusoidal temperature variations from -20°C to $+50^{\circ}\text{C}$ over a 24-hour period. The master and slave units were independently subjected to $+15^{\circ}\text{C}$ to $+25^{\circ}\text{C}$ temperature variations (hardware specification). Measurements were made of frequency stability, 1 pps jitter, phase noise, accuracy, and temperature coefficient. Preliminary results indicate that the OTWTTS performs as specified and does not degrade the quality of the cesium reference signal. Worst case environmental tests of the OTWTTS indicate the Allan deviation to be on the order of parts in 10^{14} at averaging times of 1,000 and 10,000 seconds; thus, the link stability degradation due to environmental conditions still maintains HP 5071 cesium standard performance at the user locations.

The OTWTTS described in this paper was designed and built by Timing Solutions Corporation of Boulder, CO. Environmental testing of the hardware and associated optical fibers was performed at Jet Propulsion Laboratory, Pasadena, CA, under contract with the U.S. Navy Fleet Industrial Supply Center, Bremerton, WA.

INTRODUCTION

The Optical Two-Way Time Transfer System (OTWTTS) utilizes a commercial SONET OC-3 facility interface to physically connect a master unit to multiple slave units at remote locations (in this particular implementation, five slave units may be supported).^[1] Optical fiber is a viable alternative to standard copper cable and microwave transmission. Coaxial cable is lossy with relatively poor temperature stability. Microwave transmission is expensive and may introduce unwanted noise and jitter into the reference signals. Optical fibers are the preferred medium of distribution because of low loss, immunity to EMI/RFI, and temperature stability.^[2] At the OTWTTS remote end, a slave local oscillator is locked to the master reference signal by a clock recovery PLL. Data signals are exchanged in both directions in order to calibrate the propagation delay over long distances and to set the slave time precisely to the master on-time 1 pps. The OTWTTS is capable of maintaining, without degradation, the HP 5071 cesium standard stability and spectral purity at distances up to 10 km from a centrally located frequency standard. In addition to the 5 MHz reference frequency and the on-time 1 pps, IRIG-B time code is transported from the master to the slave units. The OTWTTS performance is reported later in this paper.

OTWTTS OVERVIEW

The OTWTTS functions as a phase-lock loop that controls the time and frequency of a slave clock to agree with a master timing source. The slave may be separated from the master unit by a distance as large as 10 km. The OTWTTS exchanges data and time signals in both directions to set the slave time and to calibrate the delay over the optical fibers. A top-level block diagram of the OTWTTS is shown in Figure 1. The specified operating temperature range for both the slave and master units is +15°C to +25°C. The temperature range for the optical fiber cable is -20°C to +50°C. It is expected that the master and slave units will be located in a controlled environment and will not experience large temperature variations, whereas the optical cable may have long runs that are exposed to the elements. The physical link between the OTWTTS master and the slave is via single-mode optical fibers. The interface between the master/slave electronics and the physical link is a SONET OC-3 assembly. The 155.52 Mb/s clock of the master OC-3 interface is locked to the 5 MHz from the master station frequency standard. The on-time 1 pps from the frequency standard, as well as IRIG-B time code, are inputs to the OTWTTS master unit. A block diagram of the OTWTTS master unit is shown in Figure 2.

The remote slave unit recovers the frequency information from the SONET OC-3 data. The transmitted clock frequency is regenerated by a clock recovery circuit in the slave unit. The clock recovery loop is a digital loop which tracks the phase of the master signal as received at the slave unit including variations in line length between master and slave due to temperature variations. A wideband phase-lock loop is used to filter the SONET data transitions. Time signals are returned to the master unit from the slave in order to set the time of the slave and to stabilize the recovered clock frequency. The OTWTTS is constructed such that the forward delay and the reverse delay are exactly equal, making it possible to calculate the one-way time delay, as well as the master-slave clock difference. The slave unit block diagram is shown in Figure 3.

The SONET OC-3 line interface module directly terminates a single-mode optical fiber.^[2] The OC-3 carries the standard ST-3 telecommunications payload and operates at a bit rate of 155.52 Mb/s. The SONET 155.52 Mb/s clock is locked to the 5 MHz of the master frequency standard.

The generated high precision timing markers take advantage of timing which is inherent to the SONET equipment.

TEST CONFIGURATION

For OTWTTS testing, the hardware along with the supporting optical fibers was configured as shown in Figure 4. A hydrogen maser frequency standard was used as the source. The 1 pps was generated by feeding the reference 5 MHz into a time code generator. The master unit, slave unit, and the optical fibers were moved individually into an environmental test chamber as required for the testing. The test chamber used was a Tenney Environmental Systems, Model T20RC-3, which easily accommodates the temperature ranges specified for the OTWTTS. Baseline noise floor and stability tests were conducted on the test system alone, without the OTWTTS, to verify that the test equipment would not contaminate the test data. Next, the Allan deviation was taken with the OTWTTS operating at normal room temperature, which was assumed to be near actual operating conditions for the system hardware. The result of this test is shown in Figure 5.

The on-time 1 pps delay variations were made using a HP 5370B Time Interval Counter. The 1 pps into the master unit was compared with the 1 pps out of the slave unit for delay variations and for pulse jitter. The 1 pps jitter measured at the slave unit is 30 ps for 1,000 averages. For testing, two reels of Corning SMF 28 single mode fibers were used as the physical connections between the master and slave units. This particular optical fiber has a thermal coefficient of delay of approximately 7 ppm/°C. Each reel of fiber was measured precisely to a length of 10.56 km. The fibers used in the testing had no cable jacketing, ensuring relatively fast response to thermal variations.

TEST RESULTS

Figure 6 shows the Allan deviation of the OTWTTS with the two 10.56 km reels of fiber in the environmental test chamber with temperature variations from -20°C to +50°C. The temperature variation is sinusoidal with a period of 24 hours in this particular test. Note that there is a diurnal degradation of the 5 MHz stability from parts in 10^{15} to approximately 6×10^{14} . Also observe that the peak-to-peak phase delay variation in the reference frequency is 2.5 ns; thus, the temperature sensitivity of the system to the fiber is 3.3×10^{-12} s/°C/km. The 1 pps delay variations were recorded utilizing this same test configuration. Figure 7 is a plot of the 1 pps delay variations, approximately 2 ns peak to peak. The solid sinusoidal line on the graph represents the controlled temperature variations.

Figures 8 and 9 show the phase noise density as measured at the output of the 5 MHz distribution at the slave unit, 0 to 10 Hz and 0 to 10 KHz, respectively. The noise floor of the OTWTTS is below the HP 5071 specification with some margin. There is a low frequency spur that is related to the digital synthesizer at the slave unit. The spur magnitude was measured to be -80 dBc while the spur specification for the OTWTTS is -75 dBc. Observe the multiple low-frequency spurious responses which are by-products of the SONET digital data transfer. These spurs are multiples of approximately 1/3 Hz. The spur magnitude measured in the SONET OC-3 without the OTWTTS control loop is approximately -70 dBc, whereas the spurs at the output of the OTWTTS have been reduced to -100 dBc or less. Table 1 summarizes some of the test results of the OTWTTS.

Table 1. OTWTTS Performance Measurement

UNIT UNDER TEST	ΔT ($^{\circ}\text{C}$)	$\Delta 1$ pps	5 MHz $\Delta t/t$
OPTICAL CABLE	-20 to +50	2 ns p-p	2.5 ns p-p
OTWTTS MASTER	+15 to +25	800 ps p-p	800 ps p-p
OTWTTS SLAVE	+15 to +25	900 ps p-p	300 ps p-p

SUMMARY

The measured performance of the OTWTTS meets the stated specifications of a controlled slave clock such that its time and frequency agree with the master unit. The slave unit maintains high performance cesium quality stability and signal characteristics at the remote slave location under worst case environmental variations. The two-way master/slave 1 pps jitter is less than 100 ps. The commercial SONET OC-3 interface performs as a vehicle for precise time and frequency transfers.

ACKNOWLEDGMENT

The research described in this paper was partially carried out by the Jet Propulsion Laboratory, California Institute of Technology, under a contract with the National Aeronautics and Space Administration.

REFERENCES

- [1] "Optical two-way time transfer system" (product description), TS96.0097, Timing Solutions Corporation, Boulder, Colorado 80304, USA.
- [2] M. Calhoun, P. Kuhnle, and J. Law 1993, "Environmental effects on the stability of optical fibers used for reference frequency distribution," Proceedings of the 39th Annual Meeting of the Institute of Environmental Sciences, May 1983, Las Vegas, Nevada, USA.
- [3] OC-3 ATM LIMO, preliminary publication, Odetics, Inc., Anaheim, California 92808, USA.

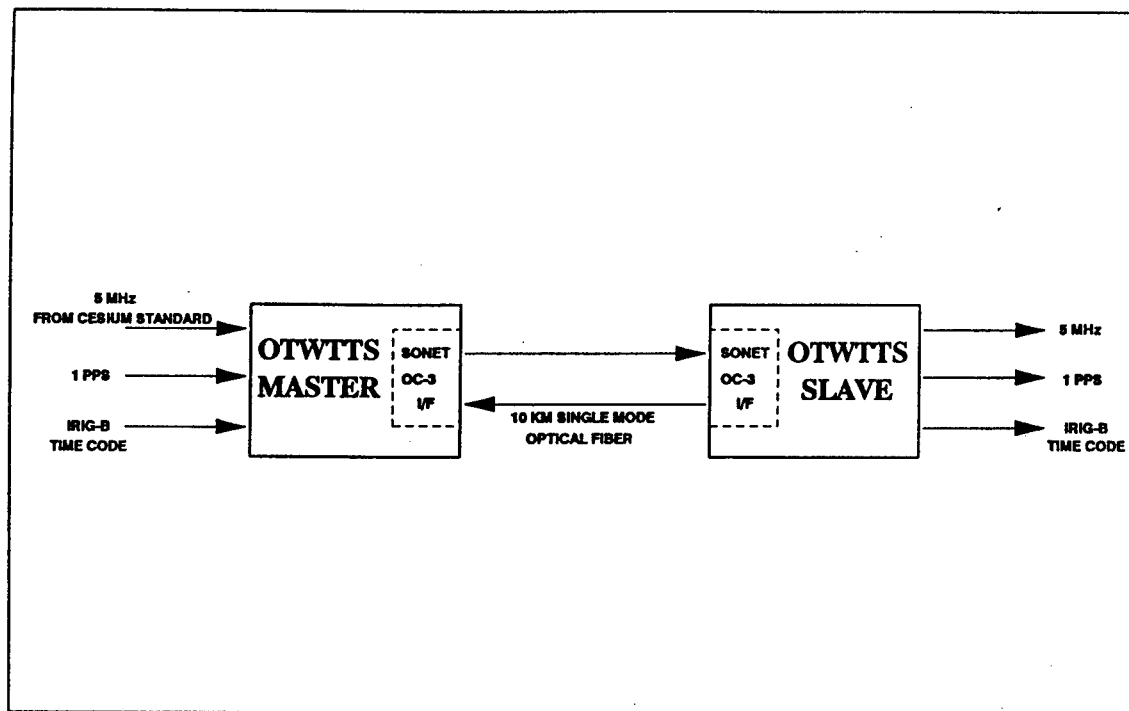


Figure 1. Block Diagram of the Optical Two-Way Time Transfer System

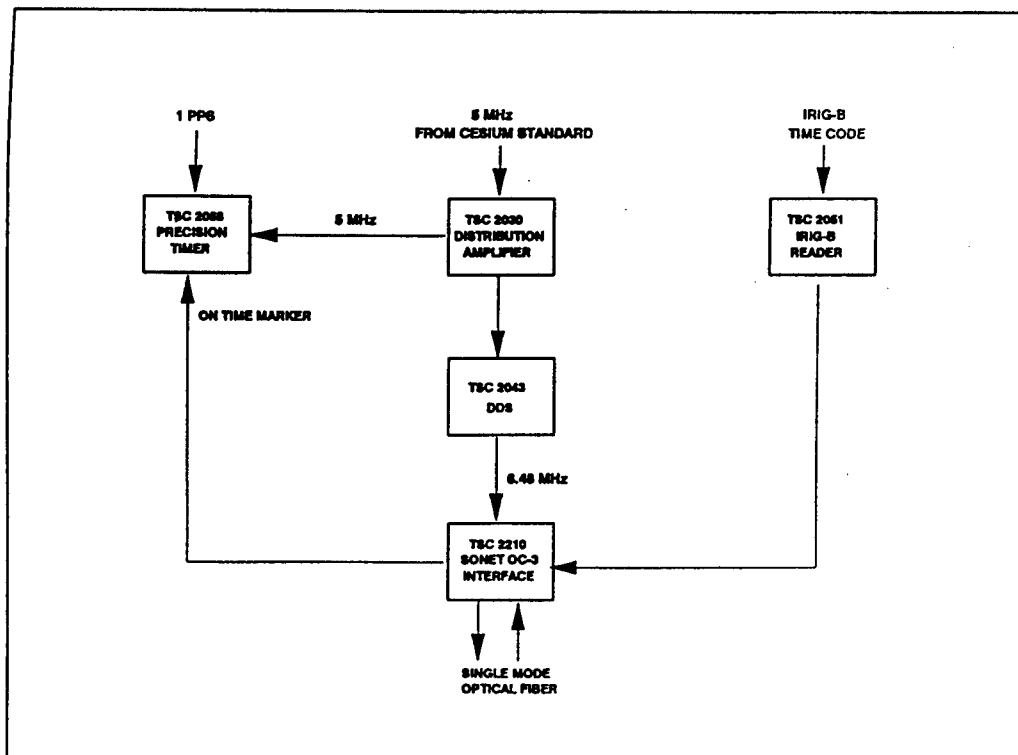


Figure 2. OTWTTS Master Unit Block Diagram

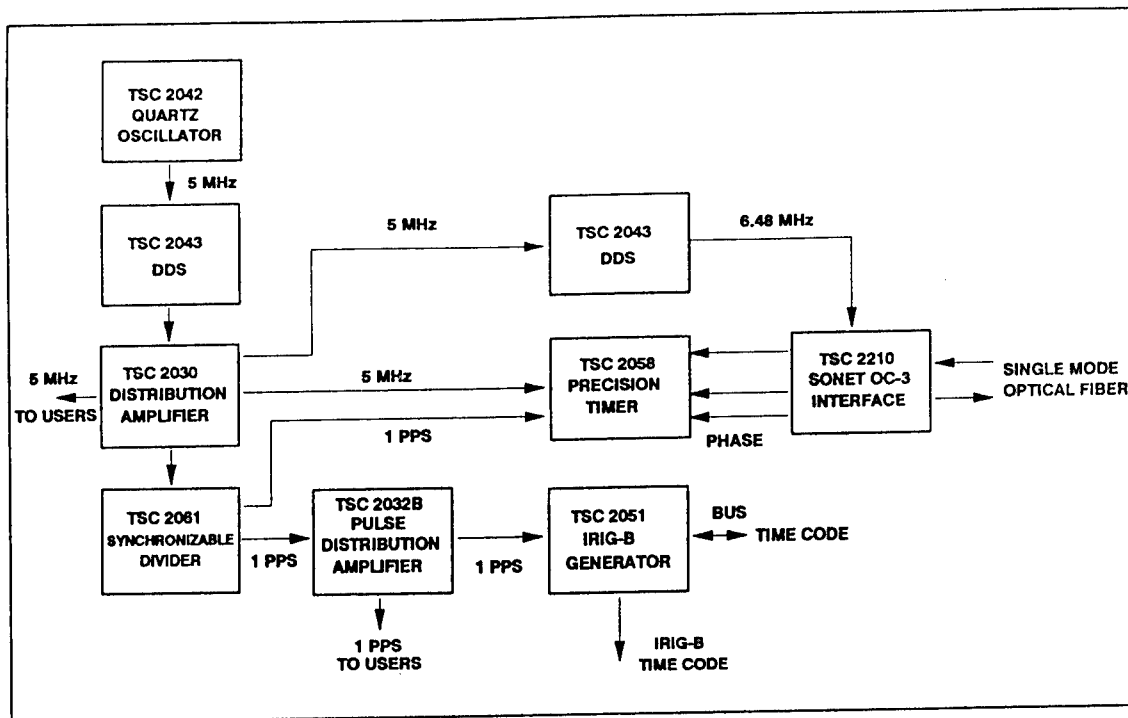


Figure 3. OTWTTTS Slave Unit Block Diagram

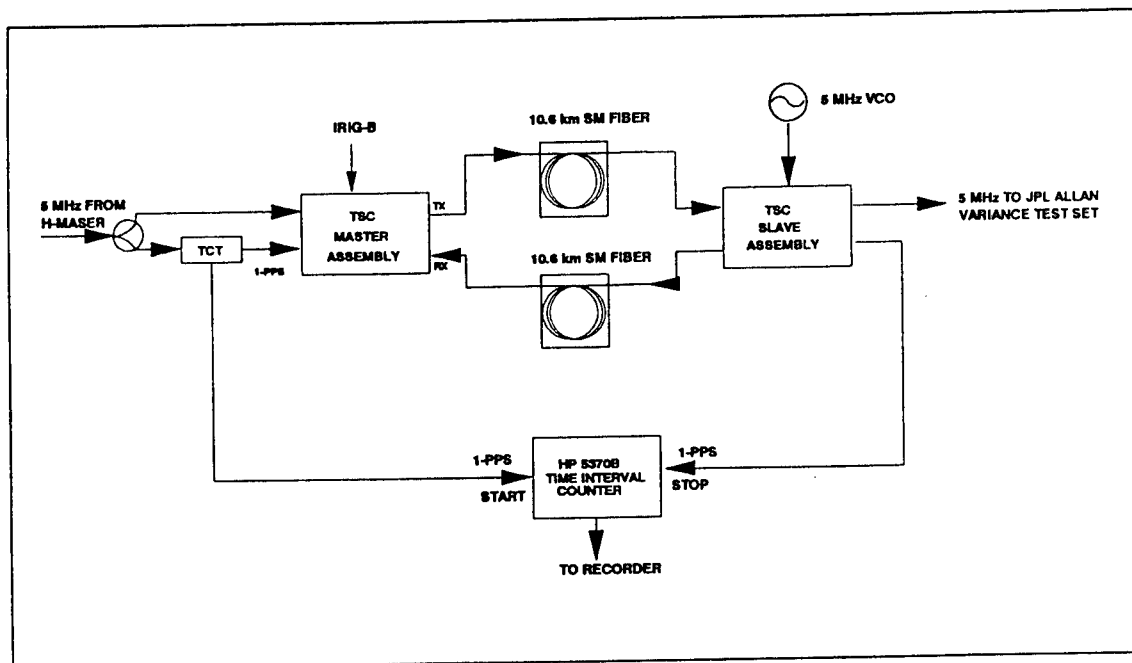


Figure 4. Test Configuration for the TSC Master-Slave Time Transfer System

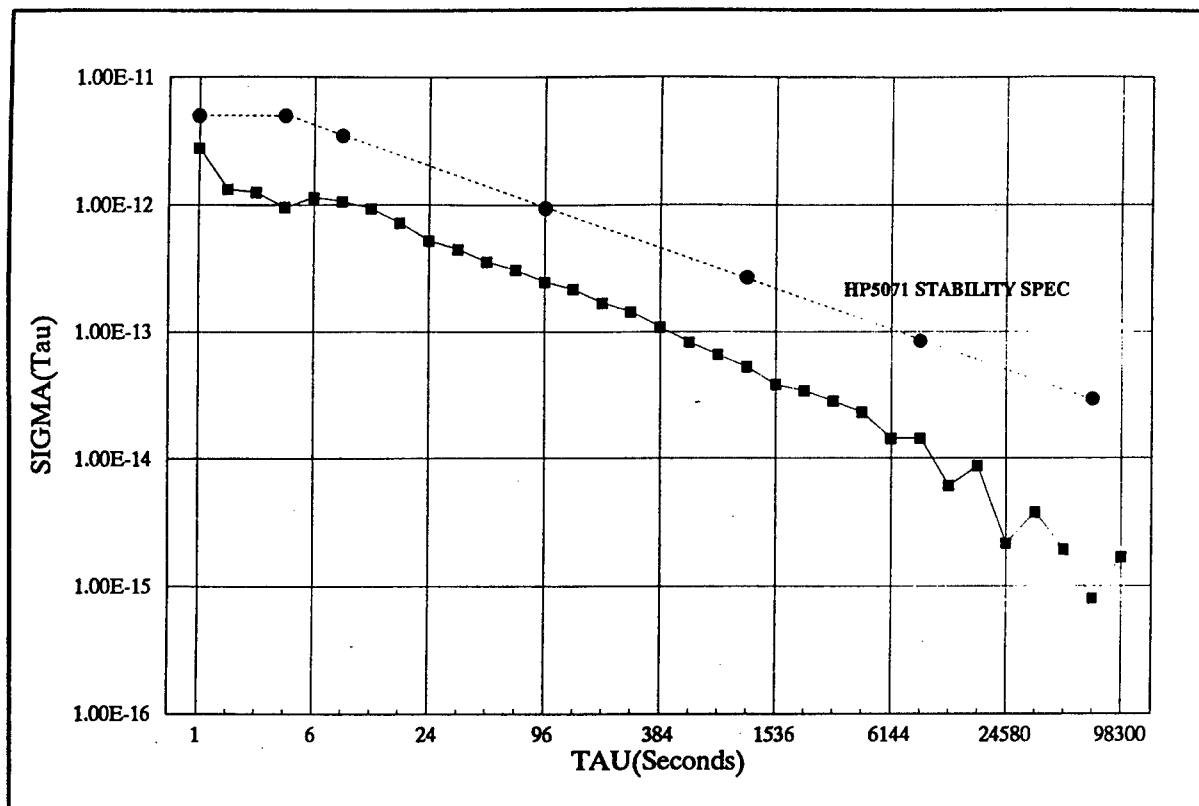


Figure 5. Allan Deviation, OTWTTS 5 MHz Distribution

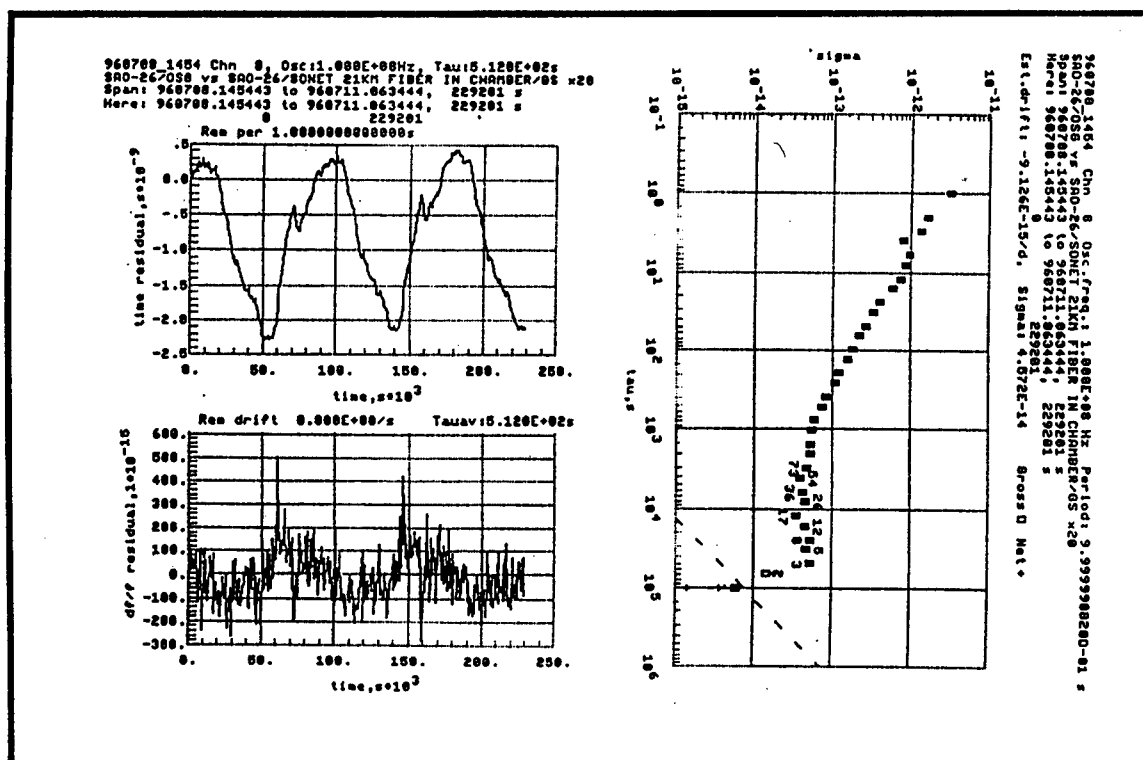


Figure 6. Allan Deviation, OTWTTS with 10.56 km Fiber Temperature Cycled

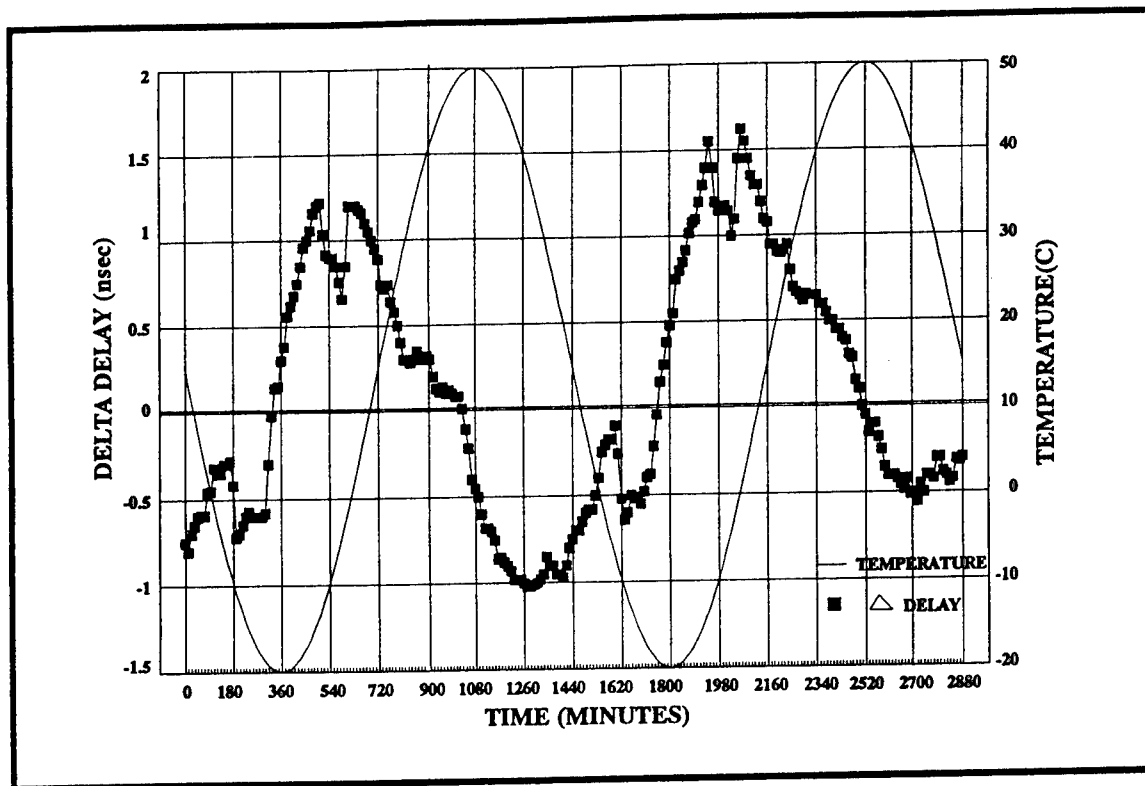


Figure 7. OTWTTS Slave 1 PPS Delay Variations with Temperature Cycling

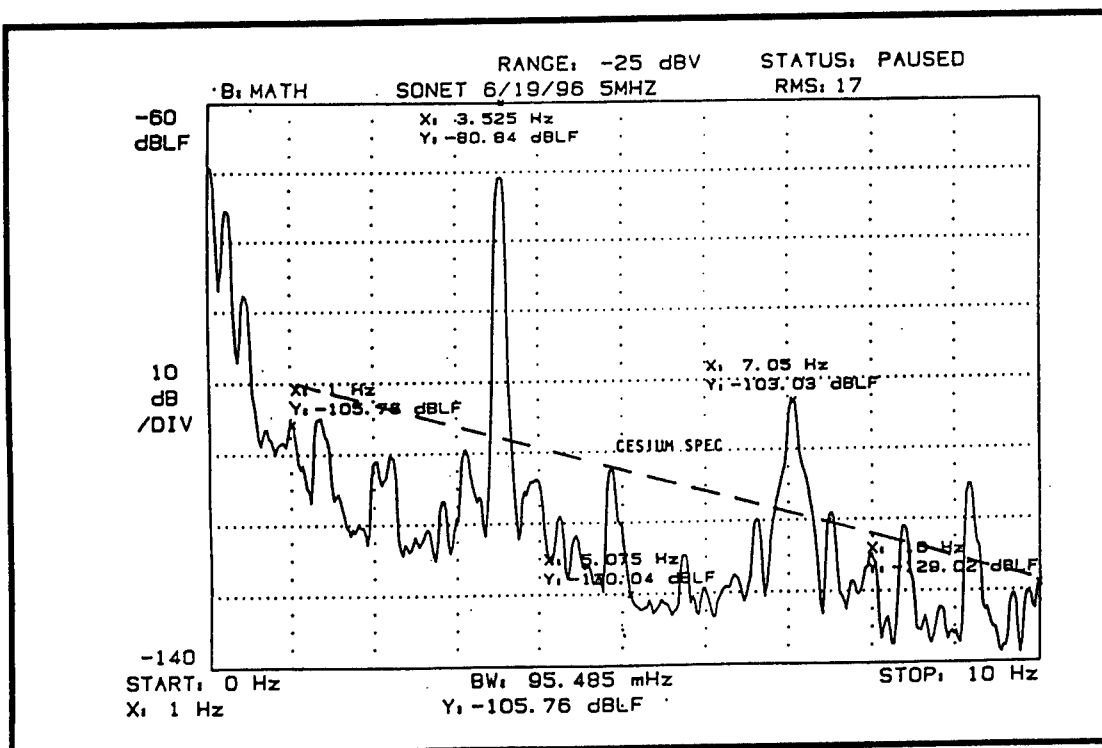


Figure 8. OTWTTS Slave Phase Noise Density, 0 to 10 Hz

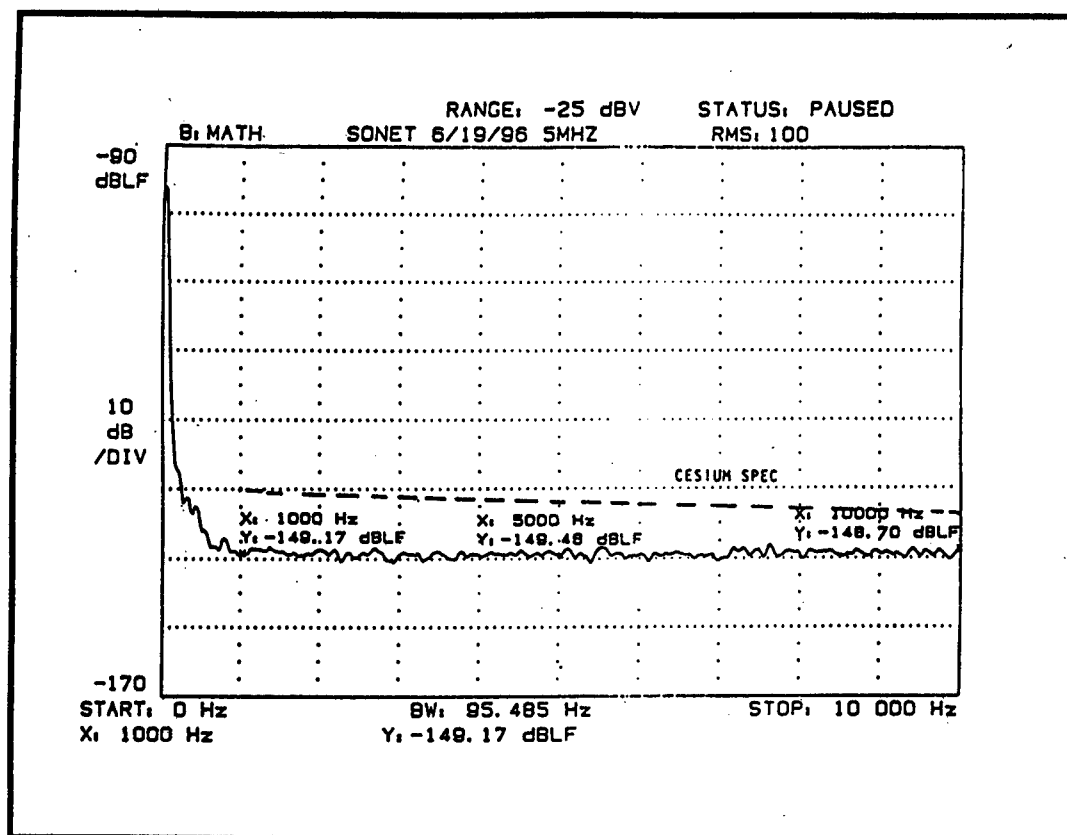


Figure 9. OTWTTTS Slave Phase Noise Density, 0 to 10 KHz

Questions and Answers

MICHAEL GARVEY (FREQUENCY AND TIME SYSTEMS, INC.): Malcolm, you showed a plot of Allan deviation, I believe. And I wasn't quite sure what the measurement configuration there was, but it looked like the link shows white frequency noise.

MALCOLM CALHOUN: Yes.

MICHAEL GARVEY: Naively, I would have expected some form of phase noise.

MALCOLM CALHOUN: Actually it's the same data except for the longer averaging times. There are some noise contributions from the SONENT which I'm not sure we ever totally characterized. We made some measurements on just the raw SONENT devices themselves before Sam's phase-lock loop and cleanup, and there were some horrendous spurs at roughly one-third of second time intervals. Some of them were as high as minus 70 dBc. So I think there's some contributions back there close in that are due to the SONENT data that didn't totally get filtered out. I'm not sure, Sam might want to address that question.

SAM STEIN (TIMING SOLUTIONS CORP.): I'm not exactly sure, Mike, of the interpretation of this plot, but the link noise is white phase noise. So that if you measure Allan deviation between the master and the slave with them sitting next to each other, the noise averages out as $1/\tau$.

MARC WEISS (NIST): The delay changes by 2 nanoseconds with temperature. And if it's simply due to the change in fiber length, I would have thought, with the two-way mode, that that would still cancel below the 2-nanosecond level. I'm wondering if you had some idea what the cause of the 2-nanosecond change was.

MALCOLM CALHOUN: It should cancel below the 2-nanosecond level. There is a possibility that there was an error in the measurement of the links of our two fibers. There could have been as much as a 4-meter difference in the links of the two cables; that would be roughly 4 nanoseconds.

Now, we did reverse the position of the two cables, and we still measured the 2 nanoseconds delay variation. We're going to do some more testing.

Yes, I agree with you. It should have been smaller than 2 nanoseconds.

A COMPARISON OF THE HIGHEST PRECISION COMMONLY AVAILABLE TIME TRANSFER METHODS: TWSTT AND GPS CV

James A. DeYoung, Francine Vannicola, and Angela D. McKinley
U.S. Naval Observatory, Time Service Department
3450 Massachusetts Avenue NW, Washington, DC 20392, USA
dey@herschel.usno.navy.mil, fmv@cassini.usno.navy.mil, amd@tycho.usno.navy.mil

Abstract

The U.S. Naval Observatory (USNO) in Washington, D.C., is now operating its Alternate Master Clock (AMC), located at Falcon Air Force Base, Colorado. UTC(USNO)-UTC(AMC) is determined independently by the Global Positioning System (GPS) common view (CV) and the Two-Way Satellite Time Transfer (TWSTT) method. The GPS CV time transfer data are formed from strict 13-minute common-view tracks. The TWSTT data are single 5-minute runs taken once every hour. In this study, the performances of the GPS CV time transfers from Standard Positioning Service (SPS) C/A code single-channel receivers using the modeled ionosphere, Precise Positioning Service (PPS) dual-frequency receivers using the measured ionosphere, and TWSTT are compared.

ACKNOWLEDGMENTS

We thank the USNO Time Service Department, Washington, D.C., employees involved in TWSTT and GPS; Dr. G.M.R. Winkler and Dr. W.J. Klepczynski, formerly of USNO, for making the investment in TWSTT hardware at USNO over the years, and Bill Bollwerk and Steven Hutsell of the USNO AMC at Falcon AFB, Colorado.

Introduction to the Topic...

GPS Common-View (GPS CV) and Two-Way Satellite Time Transfer (TWSTT) are being performed between USNO, Washington, DC and the USNO Alternate Master Clock (AMC), Falcon AFB, CO.

This paper will show the results of a comparison of the two time transfer methods for UTC(USNO(MC2))-UTC(USNO AMC (MC1)).

GPS Hardware

- Stanford Telecom (STel) Time Transfer System (TTS) Model 5401C
- Single-channel receiver, dual-frequency, P-code/Y-code (i.e. authorized, correcting for selective availability and anti-spoof)
- Ionosphere measured
- Antenna coordinates good to < 1 meter

GPS receiver tracking schedules are optimized to...

- maximize the number of usable common-view passes
- have balanced use of all satellites
- have a track at the beginning, middle, and end of a pass
- have none tracked below 20 degree elevation

45 degree limit used for this paper resulted in a usable CV about every hour which is comparable to the TWSTT sampling rate.

TWSTT Hardware

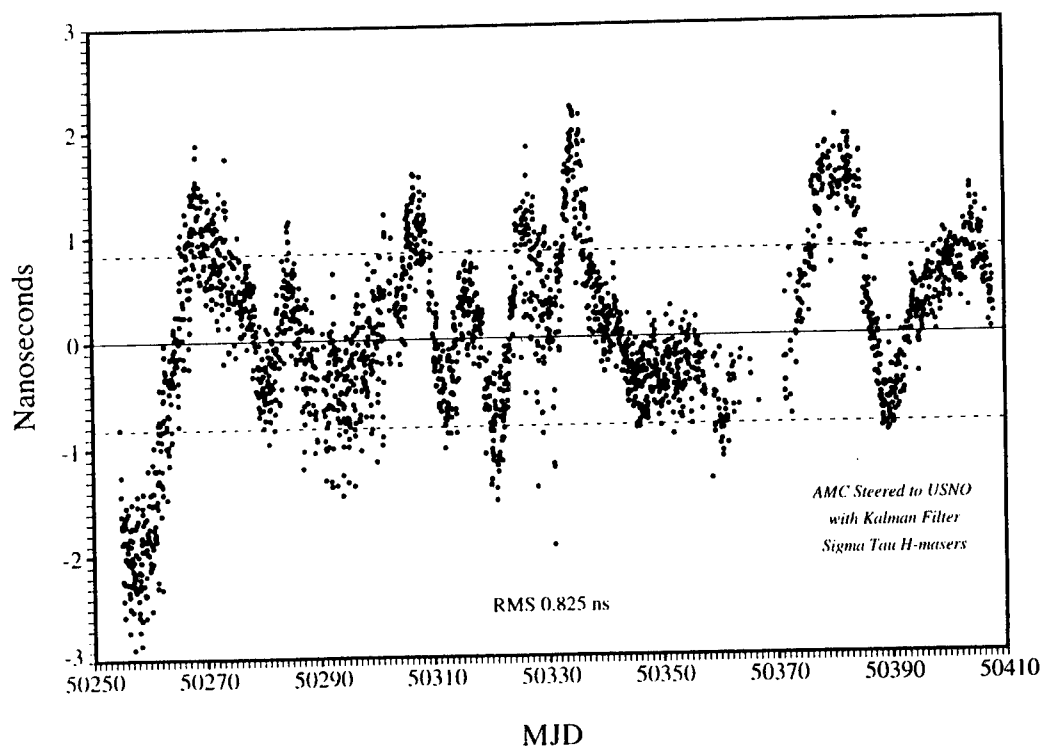
- Allen Osborne Associates, Inc. TWT-100 "Atlantis" Modem
- PRN-coded (2.5 MHz), Spread-Spectrum, bi-phase-modulated, 70 MHz IF, Ku-band RF transmissions
- All known delays accounted for, Total delays measured by portable VSAT and confirmed with portable clock comparison
- Baseline distance is 1475 miles (2374 km)
- Commercial geostationary Ku-band satellites at 103.1 degrees West, GSTAR-1 and follow-on GE-1 were used

IMPORTANT TWSTT DETAILS

- Sampling rate is @1 hour (a 5 minute long (300 second) set of 1pps comparisons then an average taken)
- Prototype software package (C and Linux-bugs still exist) is used to allow automation of
 - ◆ modem control
 - ◆ data collection and scheduling
 - ◆ error handling and resolution
 - ◆ data preparation and transfer
- Final data used by Kalman filter for subsequent steering of the USNO AMC Hydrogen maser synthesizer at USNO AMC

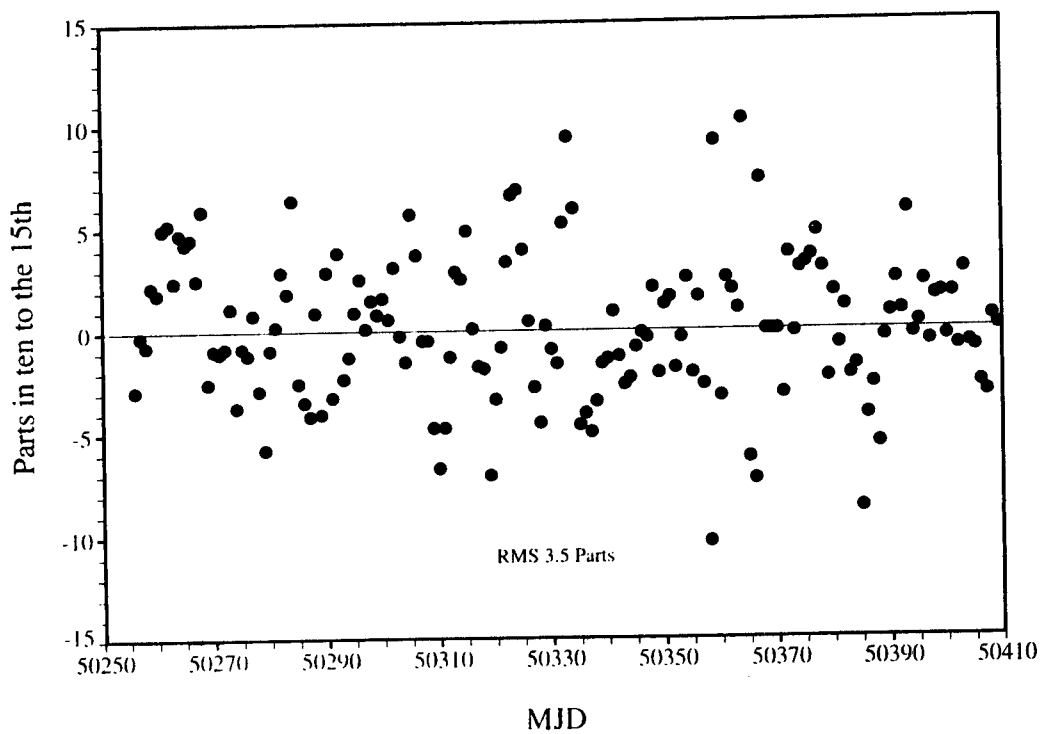
UTC(USNO(MC2)) - UTC(USNO AMC(MC1))

via TWSTT



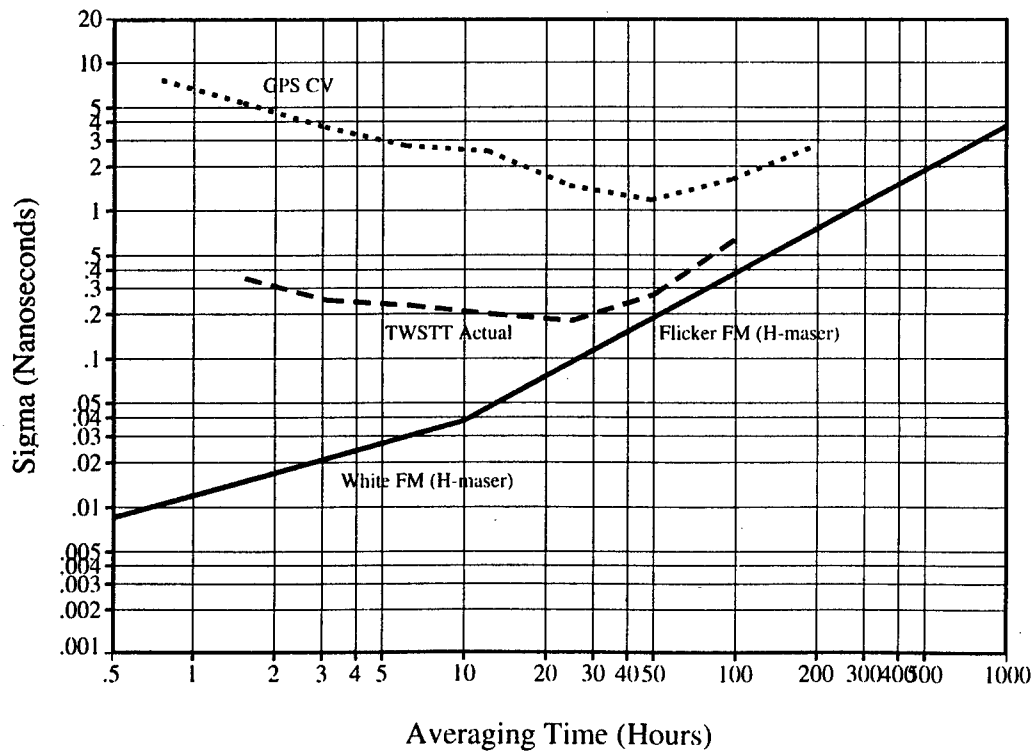
UTC(USNO(MC2)) - UTC(USNO AMC(MC1))

Daily Frequency Offsets



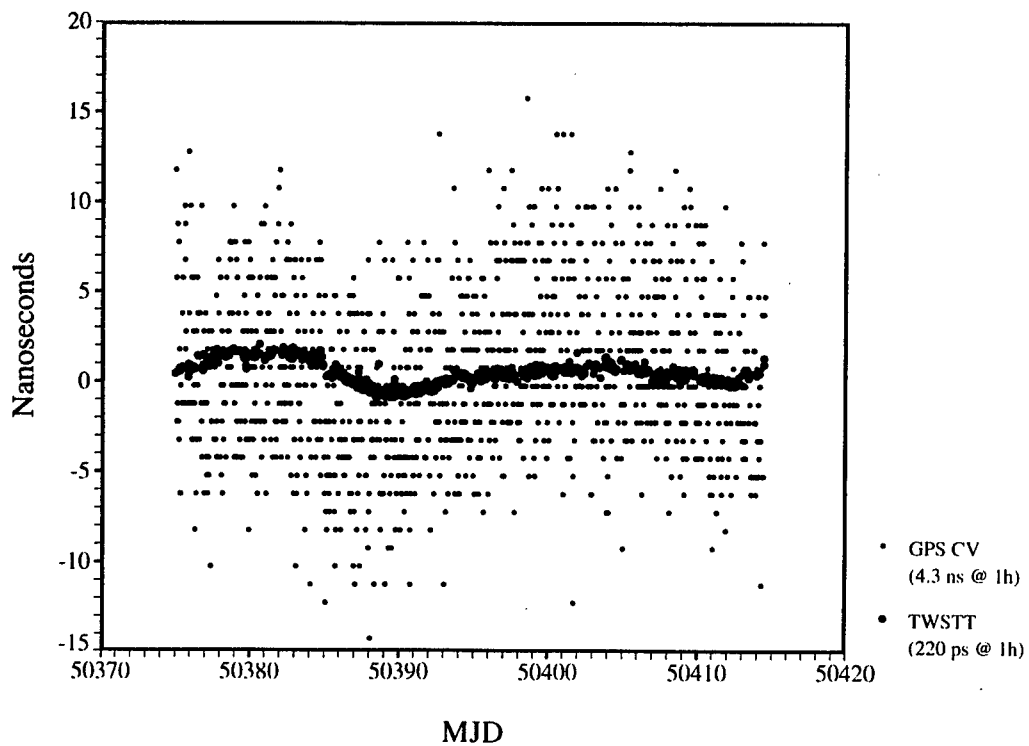
Time Transfer and Clock Instabilities (TDEV)

MJD 50372 to 50404 (32d)

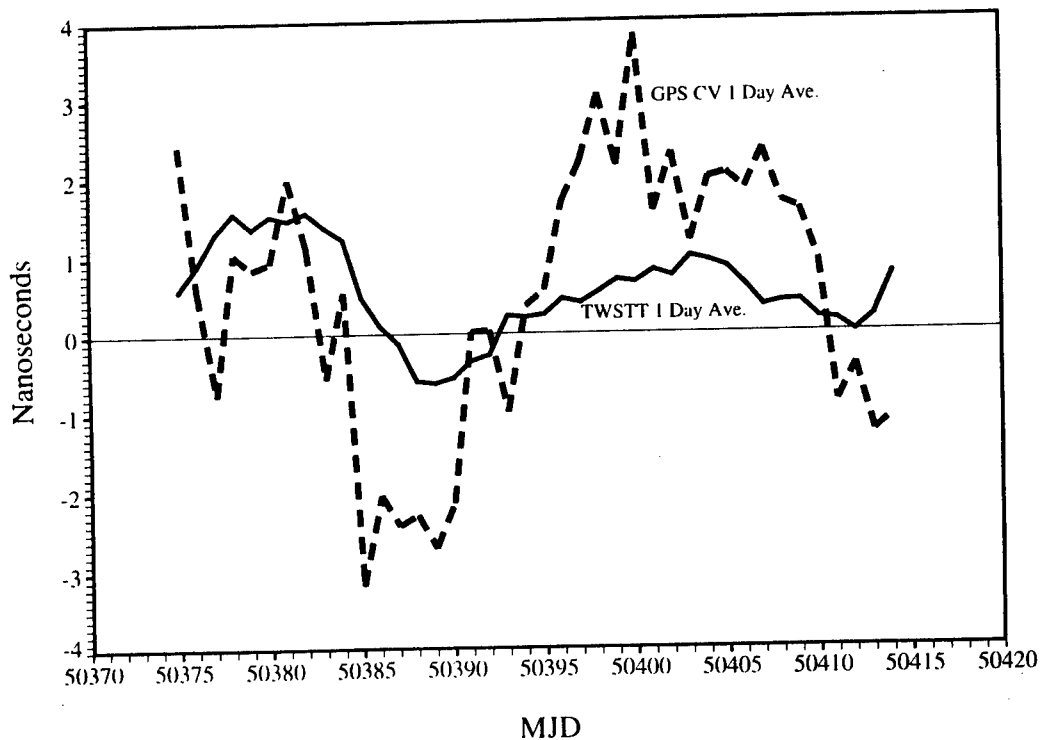


UTC(USNO(MC2)) - UTC(USNO AMC(MC1))

via GPS CV and TWSTT (Sampling Rate @ ~1h)



UTC(USNO(MC2)) - UTC(USNO AMC(MC1))
via GPS CV and TWSTT (1d simple Means)



IMPORTANT RESULTS FROM THIS WORK

- Near-optimal sampling rates achieved in TWSTT and shows clearly TWSTT is useful for comparing and/or steering the best clocks over long distances.
- Realized Time-Domain performance (RMS) of 800 picoseconds over 160 days
- Realized Frequency-Domain performance (RMS) of 3.8 parts in ten to the 15th over 160 days
- One-day simple averages formed from GPS CVs show systematics at the 3 to 4 nanosecond level with respect to TWSTT!
- "Learning experiences"

Questions and Answers

DAVID STOWERS (JPL): I have kind of a tangential question asking why would you have selected LINUX as the control software operating system?

JAMES DeYOUNG: From my point of view, I'm a UNIX person. Ultimately, I think the decision was that the prototype software that we're using is under development by NRL, and the path of least resistance ultimately was to use their software. You have to remember that the Alternate Master Clock came up very quickly. The hardware was installed in an extremely short amount of time, so very little software work had been done in preparation because all of this stuff happened within the space of basically a year. So we had to get something together very, very quickly.

Ultimately, I think, LINUX, the UNIX script language with which I'm most familiar, made it very easy to do all of the error control, talk to the interface and see which is a socket server and all of these things. And it's a beautiful way to actually control hardware and those sorts of things. I mean, ultimately I think it's the way to go. To do this in DOS or some other method would be extremely difficult, if not impossible.

DAVID STOWERS: I guess the question I should have asked was versus a commercial UNIX operating system.

JAMES DeYOUNG: Well, seeing that we have had some firmware problems, at least at that level, LINUX may not be the way to go, and that's going to be investigated down the road, because we do have to improve the reliability of the time transfers. Anywhere from 70 to 90 percent are done per day in two-way automatically and we need to get that basically to a hundred.

FIRST RESULTS FROM GLONASS COMMON-VIEW TIME COMPARISONS REALIZED ACCORDING TO THE BIPM INTERNATIONAL SCHEDULE

**W. Lewandowski, J. Azoubib
Bureau International des Poids et Mesures
Pavillon de Breteuil, 92312 Sèvres Cedex, France**

**A.G. Gevorkyan, P.P. Bogdanov
Russian Institute of Radionavigation and Time**

**J. Danaher
3S Navigation**

**G. de Jong
NMI Van Swinden Laboratorium**

**J. Hahn
Deutsche Forschungsanstalt fuer Luft und Raumfahrt**

Abstract

Currently the most popular method of comparing remote clocks is to use the GPS and GLONASS satellite navigation systems. The comparisons via GLONASS signals were suspended for many years because full deployment of the system was delayed and there were no commercial time receivers. This paper presents the first results from GLONASS common-view time comparisons, obtained using a GLONASS receiver of type ASN-16 from Russian Institute of Radionavigation and Time (RIRT) and an R-100 type of 3S Navigation while following a BIPM tracking schedule.

INTRODUCTION

The use of GLONASS signals which, for time synchronization, have characteristics similar to those of GPS was restricted for a long time because there were no commercial time receivers. In late 1993, the Russian Institute of Radionavigation and Time (RIRT) completed the development of a GLONASS time receiver, satisfying BIPM requirements and based on its own airborne ASN-16 receiver. To obtain and process GLONASS time measurements automatically, an interface between the ASN-16 and a personal computer was built. In the near future these receivers will be put into operation at the Russian State Time/Frequency

Reference in VNIIFTRI, Mendeleev, and in other Russian Time Service laboratories. In mid-1995, 3S Navigation commercialized the GLONASS R-100 receiver in accordance with BIPM requirements. These receivers were installed at the BIPM, USNO, VSL, NIST, DLR, and other laboratories. After the appearance of these special timing receivers, the BIPM published the first tracking schedule for international time and frequency comparisons by GLONASS common views. Regular measurements and data exchange between laboratories began 4 January 1996.

This paper provides a tentative estimation of the uncertainty of time comparisons by GLONASS common views, describes the main characteristics of the ASN-16 and R-100 receivers, and gives the first results of time comparisons between several laboratories in Europe and North America according to the BIPM international GLONASS schedule.

METHODS OF CLOCK SYNCHRONIZATION VIA GLONASS SIGNALS

The common-view method presupposes that multiple clock sites simultaneously measure a satellite's signals and exchange their results.^[1] The mutual difference of clock times ΔT_{A-B} between two locations A and B is determined from the relationship:

$$\Delta T_{A-B} = \Delta T_A - \Delta T_B, \quad (1)$$

where ΔT_A and ΔT_B represent the offsets of the clocks from GLONASS time. The time difference between the user clock and the GLONASS time is given by the relationship:

$$\Delta T = S - \tau_{rel} - \tau_{ion} - \tau_{trop} - \tau_{rec} - D/c + \Delta T_{sat}, \quad (2)$$

where S is the measured pseudorange between the satellite and the user (that is, the difference in two identical codes: one received by the receiver, the other generated by the receiver; each synchronized by its own clock); τ_{rel} is a relativistic term; τ_{ion} is the propagation delay due to the ionosphere; τ_{trop} is the propagation delay due to the troposphere; τ_{rec} is the receiver delay; D is the distance from the satellite to the user; c is the speed of light; and ΔT_{sat} is the difference between satellite clock and GLONASS time.

The distance from the satellite to the user is computed on the basis of broadcast ephemerides x_i, y_i, z_i and the known coordinates of the receiver antenna x_A, y_A, z_A . The difference between the satellite clock and GLONASS time is determined on the basis of time and frequency corrections τ_i and γ_i , where τ_i is the time scale shift t_i of the i th satellite relative to the GLONASS time, and γ_i is the relative difference between the calculated carrier-frequency value of the radiated navigation radio-frequency signal of the i th satellite and its nominal value.

Because the GLONASS navigation message does not include model parameters, the user computes the ionospheric delays either using models based on fixed parameters stored autonomously in the single frequency receiver or using a two-frequency technique. In both cases a model is used to compute the tropospheric delays. The receiver delay is determined by calibration.

From Eq. (2), it follows that accuracy of measurements is defined by: the uncertainty in measurements of the pseudorange; the instability of the receiver delay; inaccuracy in accounting for the relativistic term; inaccuracy in modelling the ionospheric and tropospheric delays; the uncertainty in the antenna coordinates; the uncertainty of the satellite ephemerides; and the

error of the satellite clock. As several components are common to A and B, the accuracy of the difference is significantly better than that of the individual values.

Table 1 gives tentative uncertainty budgets for GLONASS time comparisons in common-view mode, at distance d , for C/A-code receivers, for one 13-minute track and for the average of 30 tracks over one day. In making these calculations it is assumed that: the noise of the laboratory clocks and the rise time of the reference pulses are negligible; ground antenna coordinate uncertainties are of the order of 10 m; ephemerides uncertainties are of the order of 25 m; and a model with fixed parameters is used to determine the ionospheric delay.

BRIEF DESCRIPTION OF GLONASS TIME RECEIVERS

Table 2 lists laboratories which observe GLONASS according to the tracking schedule for international time and frequency comparisons by GLONASS common views and laboratories which have expressed interest in using GLONASS common views. The ASN-16, designed by RIRT, is a one-channel, one-frequency unit designed for airborne navigation.^[2] When used for time determination, it provides, via one chosen satellite, an output of 1 Hz synchronized to GLONASS time. That is why, for time comparisons via GLONASS signals using the ASN-16 receiver, an additional time intervalometer is necessary. To eliminate the need for this instrument the ASN-16 receiver was redesigned to provide a time difference with an external signal of 1 Hz. In this form, the ASN-16 receiver is designated ASN-16-02 and it provides fully automated measurements through an interfacing to a PC. The uncertainty of time determination between the user clock and satellite clock by this receiver is not worse than 60 ns (rms). Tests of two ASN-16-02 receivers at the RIRT show, that uncertainty of GLONASS common-view time comparisons is not worse than 10 ns (rms) for averages including not less than 15 tracks per day.

Receivers of the type R-100 are manufactured by 3S Navigation. The R-100/10 receiver is also one-channel, one-frequency, C/A-code unit. It provides time differences between the user clock and the satellite clock with an uncertainty not worse than 60 ns (rms) and common-view time comparisons with an accuracy of a few nanoseconds (rms) when calibrated relatively. The R-100/30 receiver is a two-channel, two-frequency, two-system GPS/GLONASS, instrument which uses P-code for GLONASS and C/A-code for GPS. It provides independent measurements for each channel and for GLONASS accounts for ionospheric delays by the two-frequency technique. The uncertainty of time determination between the user clock and satellite clock is not worse than 60 ns (rms) and the accuracy of common-view time comparisons is a few nanoseconds (rms) for differentially calibrated receivers.

Both receivers are controlled by a PC and use a standard format developed for GPS common-view technique by the CCDS Group on GPS Time Transfer standards.^[3] The R-100 receivers use also the standard formulae and parameters adopted for GPS. The ASN-16-02 receiver does not follow these standards.

ESTIMATION OF GLONASS COMMON-VIEW TIME TRANSFER UNCERTAINTY

In this paper we consider ten time links on baselines ranging from zero to 9,000 km. We show that the baseline length affects the precision and accuracy of satellite common-view time transfer. The greater the distance, the larger the effect of uncertainties in the satellite

ephemerides and ionospheric delay on time transfer. However, uncertainties of the antenna coordinates (see Table 1) may add a major contribution to the uncertainty of the common-view link even over a short baseline.

Table 3 shows the results of uncertainty estimations of GLONASS common-view time comparisons between clocks in some laboratories noted above, for intervals of one month. We have chosen to express the uncertainties of GLONASS time links in terms of the root-mean-square (rms) of the differences between raw and smoothed values. The data analysis covers the nine-month period in which the first and second international GLONASS schedules were implemented. From 7 to 62 GLONASS common views were available daily. Vondrak smoothing^[4], which acts as a low-pass filter with cutoff periods ranging from about 1 day for a 0-km baseline to about 10 days for a 9,000-km baseline, was performed on the raw GLONASS common-view values. This cutoff period was chosen as representing, approximately, the limit between short time intervals, for which measurement noise is dominant, and longer intervals, for which clock noise prevails. The number of common views per link and cutoff periods are given in Table 4. The results are illustrated by Figure 1. At the RIRT the method of least-squares interpolation was employed, together with a linear model for time differences with one-day averaging. The link RIRT - VSL is also reported with the RIRT approach (marked * in Table 3). The uncertainties derived from two methods are similar.

At the BIPM a procedure to remove constant biases between observations in different directions of the sky is used operationally for the treatment of GPS data. It has been shown for GPS common views that for the short baselines, up to 1,000 km, these constant biases are mostly due to errors in the differential coordinates of the laboratories involved.^[5] We have chosen the link DLR - VSL to illustrate the use of this procedure for GLONASS common views. Figure 1 shows the common views before removal of biases, and Figure 2 shows the same views after removal of biases. The rms is reduced from 7.9 ns to 2.4 ns. This is a strong indication that differential coordinates between these two laboratories have an error of several meters. In fact we already know (see Table 1) that the GLONASS antenna coordinates at the DLR and VSL have errors of several meters in the ITRF. The reasons of expressing GLONASS antenna coordinates in the ITRF reference frame are explained in detail in [6] elsewhere in these Proceedings.

To evaluate the performance of the GLONASS common-view method, we also computed the [UTC(DLR) - UTC(VSL)] by the GPS common-view method. The results are given in Table 5 and in Figures 3 and 4. There is a constant shift of 324 ns between the two methods, partly due to the use of uncalibrated GLONASS and GPS receivers and partly to the less accurate geodetic coordinates available for GLONASS. When a constant shift is removed from the difference between GPS and GLONASS results, values obtained are strikingly low, generally 1 ns. Figures 3 and 4 illustrate the removal of biases from GPS observations. The slight improvement, from 2.5 ns to 1.7 ns rms, is due to an error of about 0.5 m in differential coordinates between these two laboratories.

CONCLUSION

- 1) The appearance of special timing receivers of types ASN-16-02 from the RIRT (Russia) and R-100 from 3S Navigation (USA) has made it possible to begin regular international time comparisons of clocks using GLONASS common views according to the BIPM tracking schedule.
- 2) The first results show that the uncertainty of GLONASS common-view time comparisons is

of the order of a few nanoseconds (rms) for distances of up to 1,000 km, and of the order of 10 nanoseconds for intercontinental distances. This is comparable with the performance of GPS measurements.

3) The overall accuracy of GLONASS time links is inferior to that of GPS. Improvements will be made possible by: determination of accurate ground-antenna coordinates in the ITRF,

- differential calibration of GLONASS receivers,
- adoption of standardized software,
- double-frequency measurement of ionospheric delay,
- use of postprocessed precise ephemerides,
- keeping the antennas in constant temperature.^[7]

ACKNOWLEDGMENTS

The authors are pleased to express their gratitude to their colleagues in the BIPM, RIRT, 3S Navigation, VSL, and DLR for their participation in the execution of measurements and the processing and analysis of data.

REFERENCES

- [1] D.W. Allan, and M.A. Weiss 1980, "*Accurate time and frequency transfer during common-view of a GPS satellite*," Proceedings of the 34th Annual Symposium on Frequency Control, 28-30 May 1980, Philadelphia, Pennsylvania, USA (U.S. Army Electronics Research and Development Command), pp. 334-346.
- [2] Y. Gouzhva, A. Gevorkyan, P. Bogdanov, and V. Ovchinnikov 1994, "*Full automated system for receiving and processing GLONASS data*," Proceedings of the ION GPS-94 7th International Technical Meeting, 20-23 September 1994, Salt Lake City, Utah, USA, pp. 313-316.
- [3] D.W. Allan, and C. Thomas 1994, "*Technical directives for standardization of GPS time receiver software*," *Metrologia*, **31**, 67-79.
- [4] J. Vondrák 1969, "*A contribution to the problem of smoothing observational data*," *Bulletin of the Astronomical Institute of Czechoslovakia*, **20**, 349-355.
- [5] B. Guinot, and W. Lewandowski 1989, "*Improvement of the GPS time comparisons by simultaneous relative positioning of the receiver antennas*," *Bulletin Géodésique*, **63**, 371-386.
- [6] W. Lewandowski, P. Moussay, A.G. Gevorkyan, P.P. Bogdanov, W.J. Klepczynski, M. Miranian, and J. Danaher 1997, "*A contribution to the standardization of GPS and GLONASS time transfers*," these Proceedings.
- [7] W. Lewandowski, J. Azoubib, P. Guerin, F. Meyer, and M. Vincent 1997, "*Testing Motorola Oncore GPS receiver and temperature protected antennas for time metrology*," these Proceedings.

Table 1. Tentative uncertainty budgets for GLONASS common-view time comparisons.

Component	For a single track, /ns		For 30 tracks, /ns	
	$d=1000$ km	$d=9000$ km	$d=1000$ km	$d=9000$ km
Satellite clock error (cancel in CV mode)	0	0	0	0
antenna coordinates	60	60	11	11
Satellite ephemerides	4	40	1	7
Ionosphere (day time, normal solar activity, elevation > 20 deg.)	2	30	1	5
Troposphere (elevation > 20 deg.)	2	2	2	2
Instrumental delay (relative)	2	2	2	2
Receiver software	2	2	2	2
Multipath propagation	5	5	1	1
Receiver noise (13-min average)	3	3	1	1
Total	61	78	12	14

Table 2. Laboratories observing GLONASS and showing interest.

Laboratory	Equipment	Estimated uncertainty of GLONASS antenna coordinates in the ITRF /m
1. Laboratories observing GLONASS:		
BIPM (Sevres, France)	R-100/10 R-100/30 with GPS option	0,3
USNO (Washington D.C., USA)	R-100/10	0,1
NIST (Boulder, Colorado, USA)	R-100/30 with GPS option	
3S (California, USA)	R-100/10 R-100/30 with GPS option	10,0
RIRT (St.Petersburg, Russia)	ASN-16-01	10,0
VSL (Delft, Netherlands)	R-100/30 with GPS option	4,0
DLR (Oberpfaffenhofen, Germany)	R-100/30 with GPS option	3,0
BIRM (Beijing, China)	ASN-16-02	
2. Laboratories in preparation or showing interest:		
VNIIFTRI (Mendeleev, Russia)	ASN-16-02	
TL (Chung-Li, Taiwan)	R-100/30	
NPLI (New Delhi, India)	R-100/10	
IFAG (Wetzell, Germany)	R-100	
CSIR (Pretoria, South Africa)	R-100/30	

Table 3. Estimated uncertainties of GLONASS common-view links.

Common-view links	Distance /km	Estimated uncertainty / ns								
		Date 1996								
		Jan	Feb	Mar	Apr	May	Jun	Jul	Aug	Sep
BIPM(100/30)- BIPM(100/10)	0	4	4	4	4	4	4	4	4	4
BIPM(100/30) - VSL	400	-	-	-	-	10	10	10	10	10
VSL - DLR	400	-	-	-	-	8	7	9	8	8
BIPM(100/10) - DLR	500	-	-	-	-	9	9	8	9	8
BIPM(100/30) - DLR	500	-	-	-	-	9	9	7	8	8
RIRT - VSL	2100	-	-	-	14	13	13	16	15	15
RIRT-VSL*	2100	-	-	-	-	-	16	15	17	17
BIPM(100/30) - RIRT	2200	14	6	8	7	5	5	7	7	6
BIPM(100/30) - 3S	8400	16	18	13	11	-	-	-	-	-
RIRT - 3S	11000	23	17	15	-	-	11	-	18	16

* Computed by RIRT

Table 4. Number of common views per link and cut-off periods.

Common-view links	Distance /km	Number of common views per day	Cut-off period /day
BIPM(100/30)-BIPM(100/10)	0	41	1
BIPM(100/30) - VSL	400	27	1 to 2
VSL - DLR	400	41	1
BIPM(100/10) - DLR	500	38	1 to 2
BIPM(100/30) - DLR	500	62	1 to 2
RIRT - VSL	2100	16	5 to 6
RIRT-VSL*	2100	14	
BIPM(100/30) - RIRT	2200	18	1
BIPM(100/30) - 3S	8400	12	4 to 5
RIRT - 3S	11000	7	8 to 10

Table 5. Comparison of GPS and GLONASS common-view time transfer for August and September 1996 at five-day interval.

UTC(DLR)-UTC(VSL)				
MJD	by GPS /ns	by GLONASS /ns	GPS - GLONASS /ns	GPS - GLONASS - 324 /ns
50299.0	1862	1539	323	-1
50304.0	1860	1535	325	1
50309.0	1874	1549	325	1
50314.0	1887	1564	323	-1
50319.0	1892	1568	324	0
50324.0	1897	1572	325	1
50329.0	1905	1580	325	1
50334.0	1908	1581	327	2
50339.0	1912	1587	325	1
50344.0	1911	1587	324	-1
50349.0	1917	1591	326	1
50354.0	1906	1581	325	1

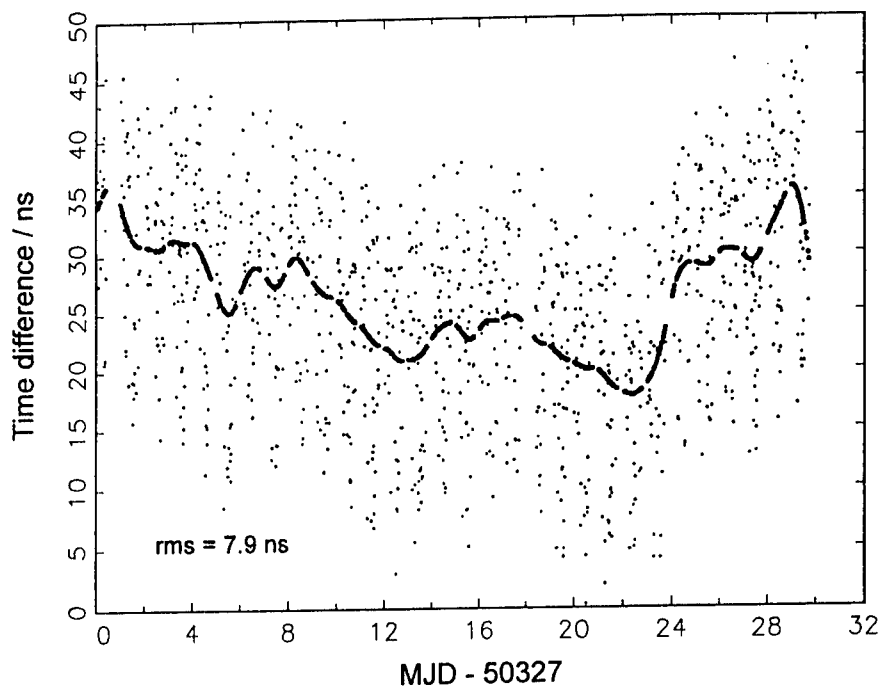


Figure 1. $[UTC(VSL) - UTC(DLR)]$ plus a constant, by GLONASS common views.

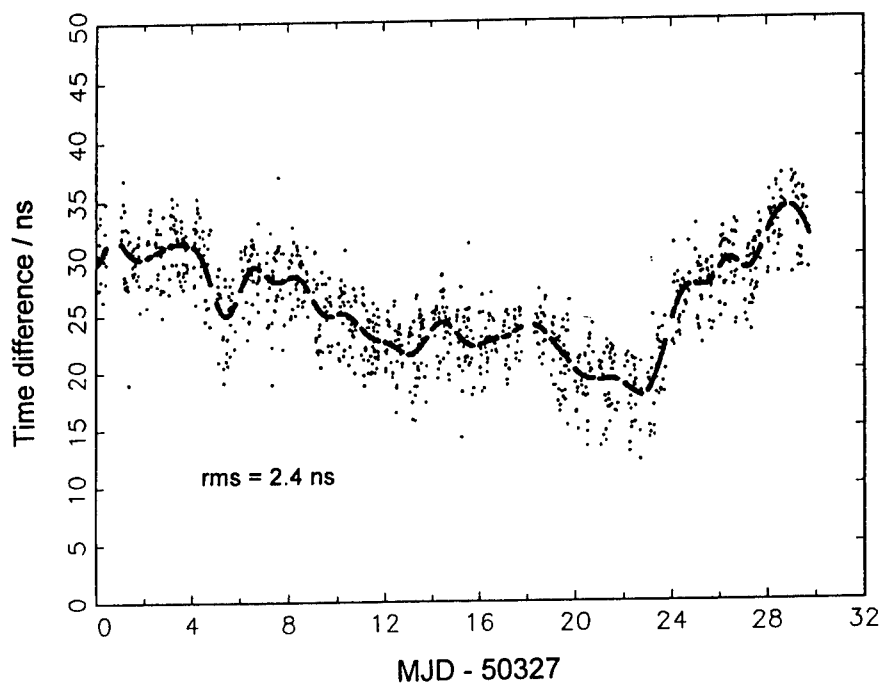


Figure 2. $[UTC(VSL) - UTC(DLR)]$ plus a constant, by GLONASS common views after removal of the biases.

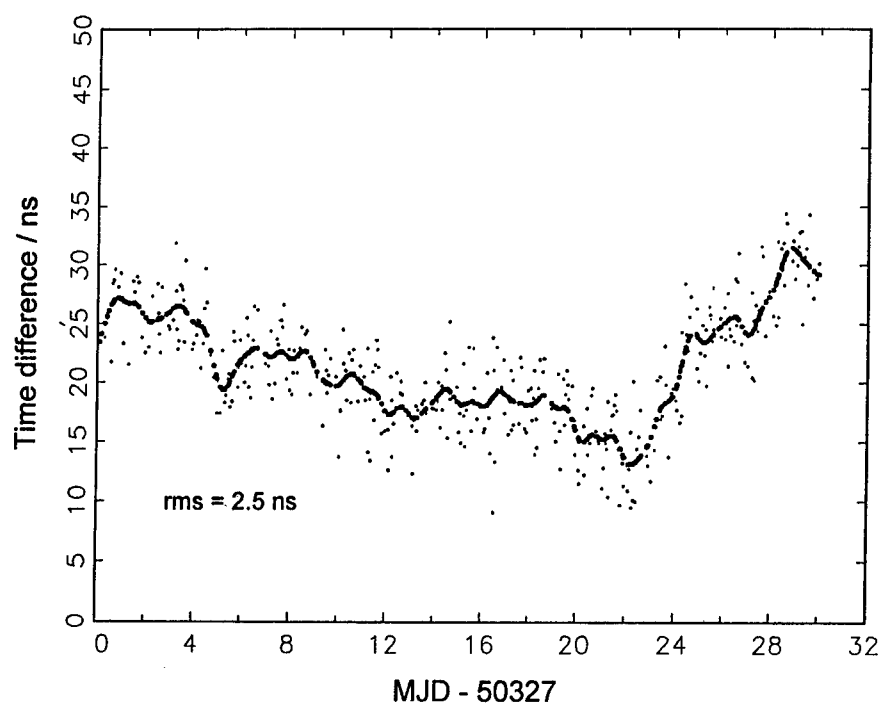


Figure 3. $[UTC(VSL) - UTC(DLR)]$ plus a constant, by GPS common views.

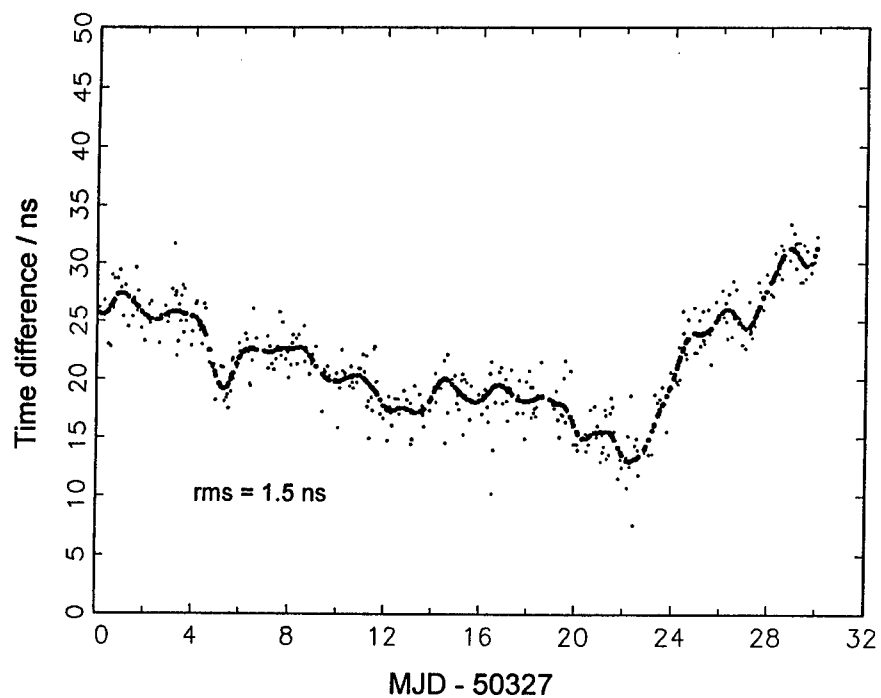


Figure 4. $[UTC(VSL) - UTC(DLR)]$ plus a constant, by GPS common views after removal of the biases.

A CONTRIBUTION TO THE STANDARDIZATION OF GPS AND GLONASS TIME TRANSFERS

**W. Lewandowski, J. Azoubib
Bureau International des Poids et Mesures
Pavillon de Breteuil, 92312 Sèvres Cedex, France**

**A.G. Gevorkyan, P.P. Bogdanov
Russian Institute of Radionavigation and Time**

**W.J. Klepczynski*
ISI Corporation**

**M. Miranian
United States Naval Observatory**

**J. Danaher
3S Navigation**

**N.B. Koshelyaevsky
Russian National Time and Frequency Service**

**D.W. Allan
Allan's TIME**

Abstract

The international time metrology community has already succeeded in the implementation, in the almost all type of GPS time receivers, of uniform software for the treatment of raw data. For the GLONASS and GPS/GLONASS time receivers now arriving on the market, it was decided to adapt, roughly and for temporary use, standards devised for GPS. In this paper specific problems for these two new type receivers are identified and solutions for standards and format update are suggested. The paper also reports briefly on international decisions recognizing advantages of using of both systems.

So far, no standards address the difficulties experienced with time receiver hardware. The best-known hardware problem is sensitivity to external temperature. This paper suggests that the temperature of antennas be held constant by enclosing them in temperature-stabilized ovens.

*Formerly with the United States Naval Observatory.

INTRODUCTION

Over a period of about 15 years the uncertainties quoted for GPS international time comparisons have improved, falling from a few tens of nanoseconds to a few nanoseconds. Recent progress has included the successful implementation of standards for software and data format.^[1] The use of GLONASS for international time transfer was delayed until last year by the lack of commercial time receivers. Their recent appearance, plus knowledge accumulated during a decade of GPS practice, allowed rapid progress in the use of GLONASS for time transfer.^[2] To speed up implementation of the GLONASS common-view technique, some standards devised for GPS by the CCGTTS^[2] were adapted for temporary GLONASS use. This comes close to fulfilling immediate needs, but must be considered as a provisional solution because it does not address specific GLONASS issues such as the use of ionospheric and tropospheric corrections, relativistic corrections, satellites ephemerides, antenna coordinates, etc. A new family of dual-system GPS/GLONASS time receivers now available will create new opportunities, but will also call for technical directives to describe the use of two systems in a single receiver. Considering the above, the 13th meeting of the Comité International pour la Définition de la Seconde (CCDS) transformed the CCDS Group on GPS Time Transfer Standards (CGGTTS) into the CCDS sub-Group on GPS and GLONASS Time Transfer Standards (CGGTTS). Also, a CCDS recommendation and declaration addressed the issue of common use of GPS and GLONASS satellites and stressed the need for both systems to respect international standards for time reference and reference frames.

This paper identifies specific software problems to be standardized for GLONASS and GPS/GLONASS time transfers and suggest an adapted data output format. Until now no standards have been issued to address difficulties related to time receiver hardware. The best-known hardware problem is sensitivity to external temperature and this paper suggests that the use of temperature stabilized ovens be standardized for GPS and GLONASS antennas in use for high precision time-transfer applications.

BRINGING GPS AND GLONASS TOGETHER

The arrival of GLONASS underlines the need for Global Navigation Satellite Systems to adopt common system of reference. In fact, GPS and GLONASS use different systems for both positioning and timing. This does not preclude the interchangeable use of the 48 satellites composing the two constellations, but does complicate it. GPS already follows international standards, and its closeness to them is constantly improved. This is not the case for GLONASS, but a far-reaching and important recommendation, S 4 (1996), issued this year by two international committees, the Comité International des Poids et Mesures and its Consultative Committee CCDS^[3], specifies a basis for harmonizing GPS, GLONASS, and other upcoming global navigation satellite systems. This recommends:

- the synchronization as close as possible to UTC the reference times of satellite navigation systems with global coverage (including GPS, GLONASS, INMARSAT, GNSS1, and GNSS2),
- the transformation of reference frames of these systems to be in conformity with the terrestrial reference frame (ITRF) maintained by the International Earth Rotation Service,
- the use of both GPS and GLONASS receivers at timing centers.

The recommendation does not make GLONASS depend on GPS or GPS on GLONASS, but requests that both systems follow internationally recognized standards for time and space. Given the increasing importance of civil applications, the Russian authorities are likely to consider more strict application of international standards to GLONASS.^[4]

Also, the Executive Board of the United States Civil GPS Service Interface Committee (CGSIC), which is a forum for the exchange of GPS information between military and civilian elements, has recognized that the common use of GPS and GLONASS for civil applications is a very positive development. The CGSIC Executive Board is, however, well aware that the two systems use different references for timing and positioning, and fully supports the above named recommendation. The similar questions civil GLONASS users would like to bring to the attention of GLONASS authorities. However, the absence in Russia of a body similar to CGSIC nowadays limits interaction between civil users and military holders of GLONASS. Some Russian experts consider that Information Center of Russian Space Forces, so called CSIC (Coordination Scientific Information Center), should play such a role.

The same CCDS meeting issued a declaration^[3] which asks the CGGTTS:

- to contact manufacturers of receivers and request them to adapt their systems, both in hardware and software, to the time and frequency laboratory requirements so that these receivers can, for example, record signals of GPS and GLONASS satellites in the dual frequency mode, in multichannels, in a data format defined by the group, have internal calibration, and be as far as possible insensitive to environmental conditions,
- to maintain these contacts and keep time and frequency laboratories informed of their actions and of the specific and operational advantages of unifying these receivers.

REFERENCE FRAMES

It is now general practice for laboratories engaged in accurate GPS time transfer to express ground-antenna coordinates with decimetric uncertainties in the ITRF, the internationally recognized ultra-accurate terrestrial reference frame. Postprocessed GPS precise ephemerides are also expressed in the ITRF. Although actual GPS broadcast ephemerides are expressed in the WGS 84, the newest realization of this reference frame agrees to within one decimeter with the ITRF. Also, because standards established by the CGGTTS have now been implemented, it is possible to introduce antenna coordinates expressed in the x,y,z Cartesian form into GPS time receivers. This avoids the transformation of geodetic coordinates into Cartesian form, a transformation which was necessary in previous types of GPS time receiver and created a possible source of errors. To sum up: the use of coordinate reference frames for GPS time transfer is well defined, well practiced, and fulfills all recommendations and standards.

The situation is somewhat different for GLONASS. Its geodetic reference frame PZ-90 can differ by up to 20 m from ITRF on the surface of earth and no accurate relationship between PZ-90 and ITRF is yet known.^[5,6] The simplest way to determine GLONASS antenna coordinates is to average a series of navigation solutions. But the uncertainties of such coordinates are no better than several meters and can have an impact on the accuracy of the common-view link of a few tens of nanoseconds. First users of GLONASS time receivers decided *ad hoc* to determine the GLONASS ground-antenna coordinates in the ITRF wherever this was possible. This has the obvious advantage of immediately providing the best possible consistency of antenna coordinates between various sites. At present the ITRF antenna coordinates introduced into R-100-type

receivers are transformed to the PZ-90 reference frame to make them consistent with broadcast ephemerides. All R-100-type receivers now in operation use the same transformation formulae and parameters. If this practice is retained, a set of standard parameters should be adopted and recorded in the file header; detailed changes are noted in Annex I.

In order to harmonize GLONASS with GPS and avoid operations on ultra-precise ITRF coordinates, another approach would be to keep the ITRF coordinates unchanged in the receiver and transform broadcast ephemerides from PZ-90 into ITRF according to a standardized set of formulae and parameters. These parameters would be recorded in the file header; detailed changes are noted in Annex I.

We should also expect that future GLONASS postprocessed precise ephemerides will be expressed in ITRF coordinates.

TIME REFERENCES

For time reference, GPS relies for its 'GPS time' on UTC(USNO), Coordinated Universal Time (UTC) as realized by the USNO. GLONASS relies for its 'GLONASS time' on UTC(SU), UTC as realized by the Russian Federation. UTC is produced by the BIPM and is the internationally recognized time reference for the whole earth. The deviation of UTC(USNO) from the UTC generally remains within 20 ns. This closeness of approach is attributed to the 50 or so cesium atomic-beam clocks and 15 or so active-cavity hydrogen masers that form the USNO ensemble. In the Russian Federation, however, UTC(SU), which is derived from an ensemble of active-cavity hydrogen masers, is drifting from UTC. The deviation, $[UTC - UTC(SU)]$ was approaching -8,000 ns in October 1996 (Fig. 1). Following the recommendation described above, however, the Russian authorities have, with effect 27 November 1996, brought the UTC(SU) into close alignment with UTC by applying a time step of 9,000 ns. The GLONASS Control System Center, which carries out the GLONASS operation, has been notified of this change, and it seems likely that GLONASS time will not be corrected.

The GPS operators keep GPS time within 100 ns (modulo 1 s) of UTC(USNO), and the actual value is generally much better than this. There have been a few exceptions, as in a period of about two weeks in December 1994 when, due to a malfunction, GPS time made an excursion from UTC(USNO) of about 270 ns (Fig. 2). But GPS broadcast a time correction allowing users to access UTC(USNO) with an uncertainty of 100 ns. This shows that the use of broadcast UTC(USNO) might be safer for some applications, as GPS time can always be subject to some anomaly.

For GLONASS, the difference between GLONASS Time and UTC in October 1996 was around 30,000 ns, and it is steadily drifting (Fig. 1). According to GLONASS ICD, the offset between GLONASS time and UTC(SU) should not exceed 1 millisecond. GLONASS does broadcast a time correction allowing users to access UTC(SU) with an uncertainty of 1,000 ns.

The differences between GPS time, GLONASS time, and UTC(SU) pointed above do not affect common-view time transfer, as readings of satellite clock vanish in the difference. This has only an effect during a common navigation solution from GPS and GLONASS. A single system navigation solution requires four satellites to determine four unknowns: position, x, y, z , and the user's clock bias. Present differences between GPS time and GLONASS time mean that a dual-system GPS/GLONASS navigation solution requires five satellites to determine position, x, y, z , the user's clock bias, and the clock offset between the two system times.

Reported in Fig. 1 are values of $[UTC - GLONASS\ time]$ which were published in BIPM

Circular T according to observations performed at University of Leeds with a GPS/GLONASS receiver designed and built in-house. The same differences, derived from GLONASS observation at the BIPM with a R-100/10 receiver, differ by a constant of about 1,250 ns. See the table below.

Date 1995	UTC - GLONASS time		
	by Circ. T (ns)	by "R-100/10" (ns)	Circ. T - "R-100/10" (ns)
Aug 10	-19812	-21055	1243
Aug 20	-20188	-21421	1233
Aug 30	-20549	-21813	1264

We know that R-100 receivers are not calibrated absolutely. Similar differences were observed using other R-100 receivers at the VSL and the DLR.^[7,8] We prefer to trust the Leeds values, because there the primary observations are [*GPS time* - *GLONASS time*]. The hardware delay is probably the same for GPS and GLONASS signals and should cancel in the difference.

Data from similar comparison with GLONASS data recorded with the Russian ASN-16-02 GLONASS receiver at the National Time and Frequency Service VNIIFTRI near Moscow are reported below.

Date 1996	UTC - GLONASS time		
	by Circ. T (ns)	by "ASN-16-02" (ns)	Cir. T - "ASN-16-02" (ns)
July 30	-30591	-30808	217
Aug 04	-30744	-30923	179
Aug 09	-30868	-31071	203
Aug 14	-31002	-31200	198
Aug 19	-31135	-31323	188
Aug 24	-31258	-31459	201

Here, we observe better agreement with the results from Leeds University published in Circular T, but it must be remembered that Russian receivers are also not absolutely calibrated and so do not provide an independent check.

Summing up, we note that, because GLONASS receivers are not calibrated absolutely, we know [*UTC* - *GLONASS time*] with an accuracy no better than 1 microsecond. GPS receivers are absolutely calibrated and [*UTC* - *GPS time*] is known with an accuracy of a few tens of nanoseconds. GLONASS provides worldwide real-time dissemination of UTC, as produced by the BIPM, to an average user with uncertainty of about 2 microseconds after recent improvement of the synchronization between UTC(SU) and UTC. GPS does the same with uncertainty of about 100 ns.

RECEIVER SOFTWARE

During a series of meetings at the beginning of 1990, the CCDS Group on GPS Time Transfer Standards developed a document called *Technical Directives for Standardization of GPS Time Receiver Software*.^[1] This document lists nine explicit directives for the standardization of software for single-frequency C/A-Code GPS time receivers, possibly operating in tandem with an ionospheric measurement system. These directives have since been implemented in most GPS time receivers. This has had immediate consequences through improvement of the accuracy and precision of GPS time links.

Since that time, some major developments in timing equipment have taken place. These are mainly the arrival in 1994 and 1995 of one-channel GLONASS C/A-Code^[9] and P-Code time receivers, and double-system multichannel GPS(C/A-Code)/GLONASS(P-Code)^[2] time receivers. To allow rapid development of these receivers it was decided to adapt, roughly and for temporary use, some standards devised for GPS by the CGGTTS. There is a consequent need to extend more rigorously and formally the technical directives to the needs of these new devices which is reflected in the decisions of the most recent CCDS meeting.

Below we describe suggested updates. GPS Technical Directives 1 to 4 and 6 to 9, and Annex I can be applied strictly to GLONASS data. Directive 5, Annex II, and Annex III, should be updated for GLONASS.

Comments on the adoption of GPS Technical Directive 5 for GLONASS:

GPS Technical Directive 5 requires that all modelled procedures, parameters, and constants needed in short-term data processing are deduced from the information given in the Interface Control Document (ICD) of the U.S. Department of Defense or in the NATO Standardization Agreement (STANAG). These are updated at each new issue. The GLONASS ICD does not include algorithms for the calculation of tropospheric and ionospheric corrections, nor does GLONASS broadcast ionospheric parameters. It is suggested, therefore, that in order to simplify common use of GPS and GLONASS for time transfer, that for GLONASS the same formulae for modelled tropospheric and ionospheric corrections be adopted as are used for GPS. However, the ionospheric correction for GLONASS should take into account the different GLONASS frequencies. In the case of dual-system GPS/GLONASS receivers, GPS broadcast ionospheric parameters should be applied to GLONASS ionospheric correction. For single-system GLONASS receivers, a set of adapted fixed parameters must be standardized. It has been verified experimentally that the use of fixed ionospheric parameters does not normally cause a deterioration of GLONASS data. This, however, cannot be true during strong solar activity.

Comments on the adoption of Annex II for GLONASS:

In GLONASS, as in GPS, the constant part of the relativistic correction to the frequency, consisting of the gravitational red shift and the second-order Doppler effect, is applied before launch to the satellite oscillators as a frequency offset (4.36×10^{-10} for GLONASS). Periodic relativistic corrections to take account of the eccentricity of the GLONASS satellite's orbit are applied when generating time and frequency corrections to the offset between satellite time and GLONASS time. These are uploaded to the satellite and transmitted in the navigation message. This implies that point (iii-5) of Annex II should not be applied to GLONASS data.

Most of the solutions suggested above are already applied to 3S Navigation-type receivers. On one point these receivers do not follow Technical Directive 9. This Directive requires that, for multichannel receivers, one data file should be created for each channel. 3S receivers put data from all channels and from two systems into one file. In practice, this way of handling data has proved to be very convenient and it is suggested that Directive 9 be changed to standardize the use of one file.

Suggested update of Annex III *GGTTS GPS Data Format Version 01* of Technical Directives is described in Annex I of this paper.

TEMPERATURE SENSITIVITY

It is now well documented and generally admitted that GPS time equipment is sensitive to external temperature. This sensitivity ranges from about 0.2 ns/°C to 2 ns/°C. Even for the lower value, the delay change can be the dominant contribution to the noise of time transfer by common view for periods of several days over short baselines of several hundred kilometers. The larger value makes it the dominant contributor to the noise of common-view time transfer even for intercontinental baselines. We illustrate this phenomenon for GPS equipment with the latest results recorded during calibration of a GPS reference receiver at the USNO covering a period of 11 months (Fig. 3). For GLONASS we report the first ever comparison of two GLONASS time receivers recorded at the BIPM during a period of 10 months (Fig. 5).

It can be seen that the GPS and GLONASS receivers have similar behavior both over periods of several days and for the full period of comparison. Short periods are characterized by the correlation with external temperature (Fig. 4 and Fig. 6). A rough estimate of the correlation coefficient is 0.2 ns/°C for both GPS and GLONASS. No seasonal effect is evident.

The modified Allan deviation shows white phase noise for periods of several months. This makes possible to average differences between two pairs of receivers for the whole duration of comparison. Corresponding standard deviation is 2.5 ns for GPS and 4.0 ns for GLONASS. The larger value for GLONASS is attributed to the somewhat noisier results obtained from the R-100/10 receiver, which were estimated by common-view comparisons with other laboratories.^[2] We omit here the constant differences between the receivers, which are not of interest for this presentation.

The sensitivity to external temperature suggests an effect linked to the parts of time equipment located in the open air, that is to the antenna and its cable. The receiver itself is usually located in an air-conditioned room. For several years different hypotheses were considered to explain the temperature dependence of timing equipment. All linked the problem to the electronics of the antenna, but none were verified and proved. Experiments showed that the changes were not due to the changes in antenna cable^[10], however length and material of the cables are important and must be considered.

As no practical way was found to resolve the problem electronically, another approach was suggested: the antenna should be protected by an oven with stabilized temperature.^[11] The temperature of the oven used at the BIPM was set at 38°C. Initial observations show that temperature stabilization of the antenna assembly appears to reduce or even eliminate diurnal delay variation. It is thought that this is due to stabilization of the temperature of the filters and amplifiers rather than the antenna element itself. Thus, it is possible to make the preliminary recommendation that GPS, GLONASS, and GPS/GLONASS antenna electronics and outdoor in-line amplifiers be temperature stabilized when they are used for precision time applications. Further studies will be performed to further confirm this recommendation.

However, the development of a built-in calibration system for time receivers is a challenge for timing community. This solution is the most adapted to resolve present difficulties with delay stability of GPS and GLONASS time equipment.

NEW DEVELOPMENTS

The accuracy of the GPS and GLONASS common-view time transfer could be improved by changing common practice in making common view observations. This section describes some of the suggestions that are likely to ultimately result in a considerable improvement in the

accuracy of common-view time observations. Typical practice in making common-view time observations is for all receivers in an area to track a single satellite for 780 seconds according to the schedule published by the BIPM. The time difference between the local reference clock and the GPS or GLONASS constellation time is computed by an agreed real-time algorithm and these data are output to a text-editable file. There is then a delay of 180 seconds until the start of the next tracking period.

The method of single satellite observation over a 780-second integration period results largely from the receiver tracking channel, memory size, and data communication bandwidth limitations that existed at the time this technique was developed. The real-time algorithm fits a straight line to short-term effects, such as multipath and atmospheric path delay variations, that would probably be amenable to more sophisticated processing algorithms if a more complete data set were available. Observations based on simultaneous observation of several satellites may yield an improvement of time-transfer accuracy in rough proportion to the square root of the number of satellites tracked.

For this reason it is suggested that common-view observations be made continuously and more often, and that all satellites in view (e.g. all-in-view) be observed. This can be done with multichannel receivers. The laboratories already equipped with such receivers could start experimentally to record all-in-view observations according to three possible schemes:

- with classical 780-second integration periods,
- with 15-second integration periods,
- at a rate of 1 per second; some laboratories already use this approach, known as Advanced Common View (ACS), on experimental basis.^[12]

Existing time-transfer receivers typically discard carrier phase and pseudo-range data after the time-transfer algorithm is executed. If these data are retained, it is likely that postprocessing with more complete orbital data and more sophisticated algorithms will lead to a more accurate time-transfer result. Already several trials have shown the advantages of using carrier phase measurements for frequency comparisons.^[13,14] The Receiver Independent Exchange Format (RINEX)^[15] provides a convenient format for recording GPS and GLONASS carrier phase and pseudo-range data. If the receiver has the capability, it is suggested that a RINEX format carrier phase and pseudo-range data file be generated at 15-second intervals for all satellites in view. This data file can then be used for postprocessing of precision time and frequency data.

CONCLUSIONS

- 1) The use of a common format, standard formulae, and parameters would simplify worldwide time dissemination and time transfer by GPS and GLONASS.
- 2) Because there are no official formulae for several of the corrections required for GLONASS time transfer, it is suggested that the formulae adopted for GPS be used wherever this is possible.
- 3) It is suggested that a single output file be used for multichannel GPS and GLONASS time observations.
- 4) It is suggested that, if the receiver has the capability, it should record in RINEX format, in a separate file, carrier phase and pseudo-range data generated at 15-second intervals for

all satellites in view. It is recommended that the 15-second carrier phase and pseudo-range data be computed using the 15-second pseudo-range quadratic fit method given in Annex I and Annex II of the *Technical Directives for Standardization of GPS Time Receiver Software*.^[1]

5) It is suggested that the ground antenna coordinates of GLONASS time receivers be expressed in the ITRF in Cartesian x, y, z form, and then transformed into PZ-90 using standard formulae and parameters adopted by all manufacturers.

Another suggested approach is to keep the ITRF coordinates unchanged in the receiver, and transform broadcast ephemerides from PZ-90 into ITRF according to a standardized set of formulae and parameters.

6) The time difference [*UTC - GLONASS time*] is known with an accuracy of about 1 microsecond, a poor value which results from the absence of absolutely calibrated GLONASS receivers. Such calibration is becoming urgent.

7) It is suggested that antennas electronic assemblies and any outdoor in-line amplifiers be temperature-stabilized. The use of temperature-stabilized enclosures should improve not only common-view time transfer and time dissemination, but also frequency comparisons by phase measurements.

8) The development of a built-in time calibration system for time receivers is a challenge for the timing community. This solution is the most adapted to resolve present difficulties with delay stability of GPS and GLONASS time equipment.

9) Appearance of multichannel time receivers raise the question of replacing the present mode of scheduled common-view observations by "all satellites-in-view" common-view observations.

8 REFERENCES

- [1] D.W. Allan, and C. Thomas 1994, "*Technical directives for standardization of GPS time receiver software*," *Metrologia*, **31**, 67-79.
- [2] W. Lewandowski, J. Azoubib, A.G. Gevorkyan, P.P. Bogdanov, J. Danaher, G. de Jong, and J. Hahn 1997, "*The first results of GLONASS common-view time comparisons realized according to the BIPM international schedule*," these Proceedings.
- [3] Report of the 13th Meeting of the CCDS (BIPM, Sèvres, France, 1996).
- [4] "*On activity for application of the Global Navigation Satellite System GLONASS for Civil Users*," Decree No. 237 of the Government of the Russian Federation, 7 Mar 1995.
- [5] U. Rossbach, H. Habrich, and N. Zarraoa 1996, "*Transformation parameters between PZ-90 and WGS 84*," Proceedings of the ION GPS-96 9th International Technical Meeting, 17-20 September 1996, Kansas City, Missouri, USA, pp. 279-285.
- [6] P.N. Misra, R.I. Abbot, and E.M. Gaposchkin 1996, "*Transformation between WGS 84 and PZ-90*," Proceedings of the ION GPS-96 9th International Technical Meeting, 17-20 September 1996, Kansas City, Missouri, USA, pp. 307-314.
- [7] G. de Jong G. 1996, personal communication.
- [8] J. Hahn 1996, personal communication.

- [9] Y.G. Gouzhva, A.G. Gevorkyan, P.P. Bogdanov, and V.V. Ovchinnikov 1994, "*Full autonomous system for receiving and processing GLONASS data*," Proceedings of the ION GPS-4 7th International Technical Meeting, 20-23 September 1994, Salt Lake City, Utah, USA, pp. 313-316.
- [10] G. Freon 1990, personal communication.
- [11] W. Lewandowski, P. Moussay, P. Guérin, F. Meyer, and M. Vincent 1997, "*Testing the Motorola Oncore GPS receiver and temperature-stabilized antennas for time metrology*," these Proceedings.
- [12] R.P. Giffard, L.S. Cutler, J.A. Kusters, M. Miranian, and D.W. Allan 1996, "*Continuous, multi-channel, common-view, L1-GPS time-comparison over a 4,000 km baseline*," Proceedings of the 1996 IEEE International Frequency Control Symposium, 5-7 June 1996, Honolulu, Hawaii, USA, pp. 1198-1205.
- [13] P. Baeriswyl, T. Schildknecht, J. Utzinger, and G. Beutler 1995, "*Frequency and time transfer with geodetic GPS receivers: first results*," Proceedings of the 9th European Frequency and Time Forum (EFTF), March 1995, Besançon, France, pp. 46-51.
- [14] G. Petit, P. Moussay, and C. Thomas 1996, "*GPS time transfer using carrier-phase and P-code measurements*," Proceedings of the 10th European Frequency and Time Forum (EFTF), March 1996, Brighton, UK (IEEE Conference Publication 418), pp. 46-51.
- [15] W. Gurtner 1994, "*RINEX: the Receiver Independent Exchange format version 2*," American Institute, University of Berne, Berne, Switzerland.

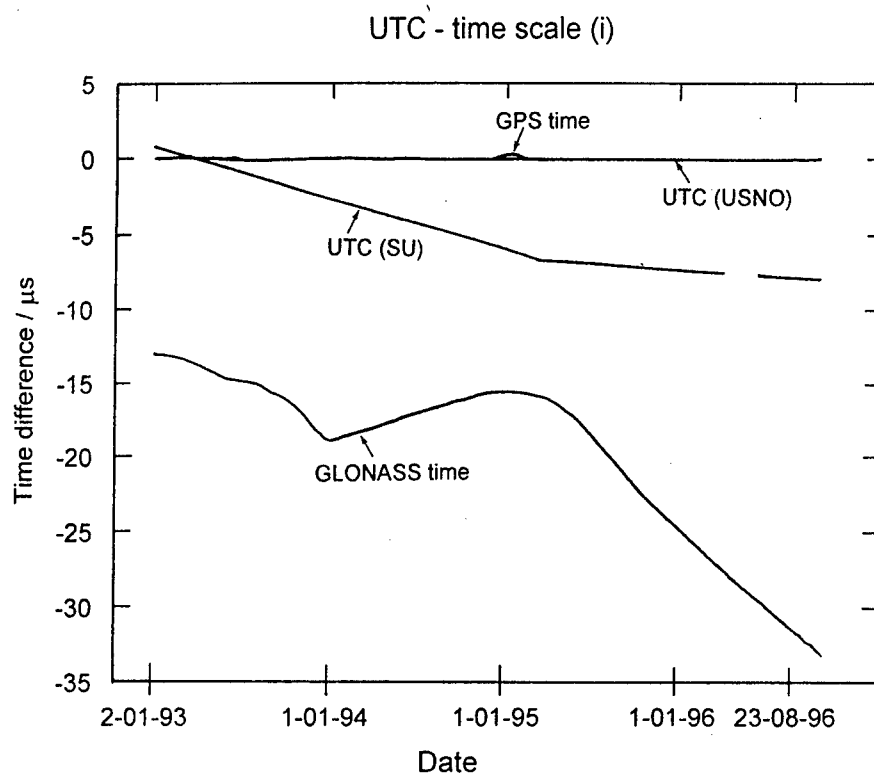


Figure 1: Deviation of UTC(USNO), UTC(SU), GPS time (modulo 1 s) and GLONASS time from UTC from 2 January 1993 to 28 October 1996.

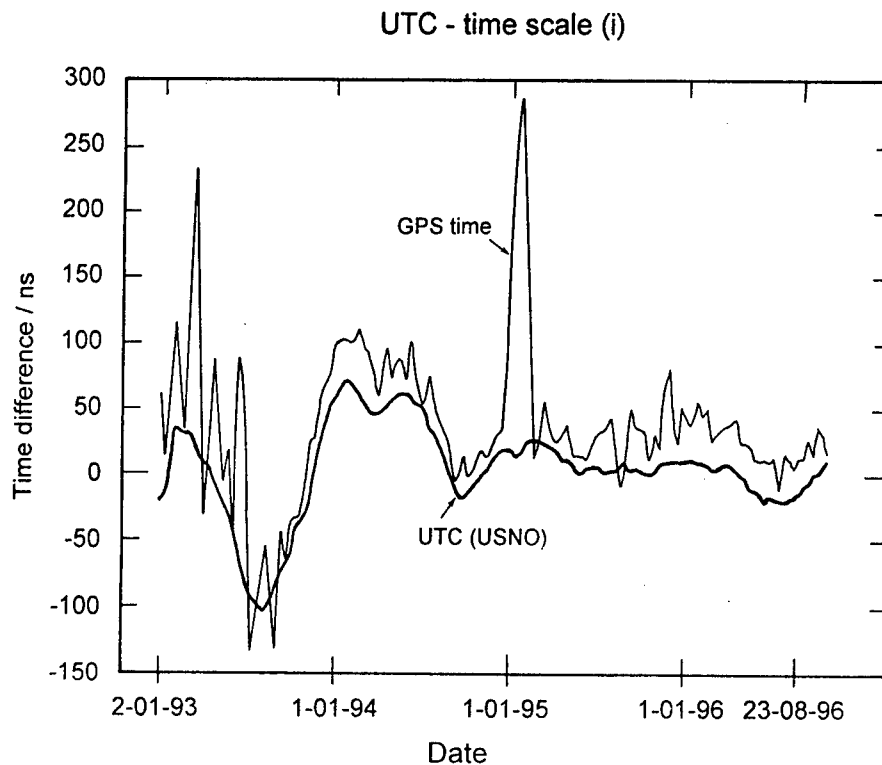


Figure 2: Expansion of Figure 5 highlighting the 270 nanosecond excursion of GPS time from UTC (modulo 1 s) at the end of 1994. 377

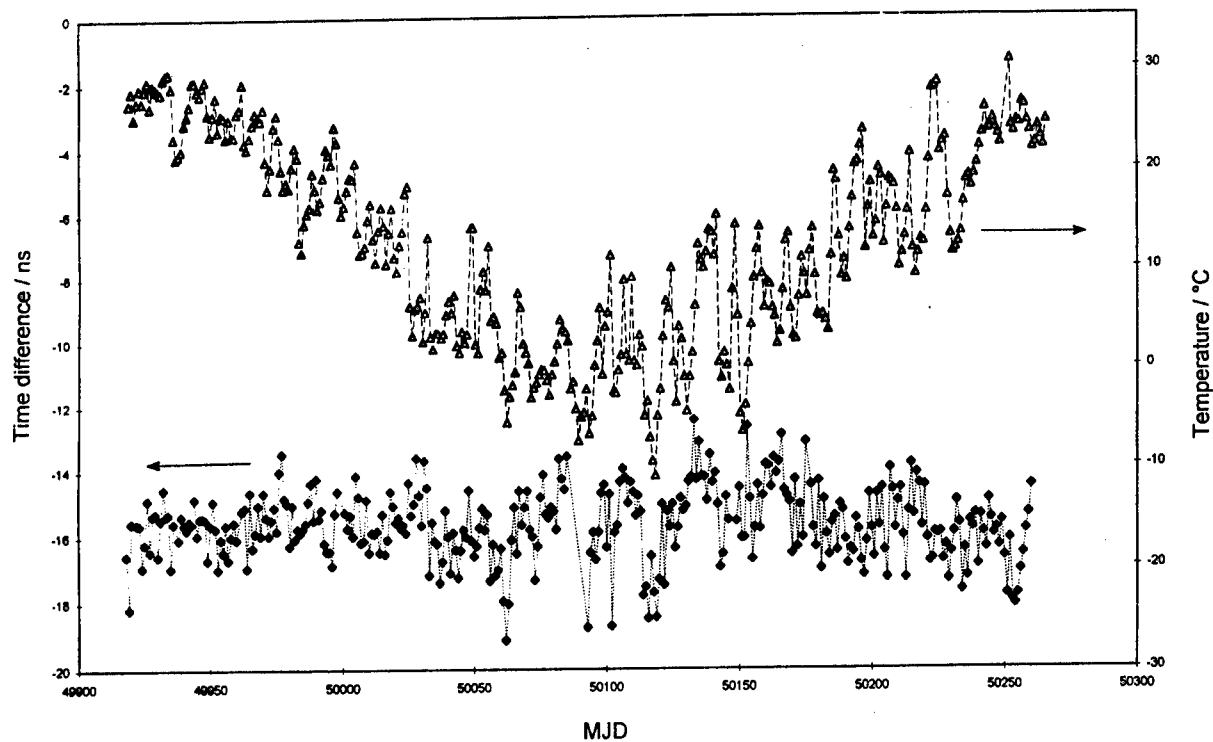


Figure 3. Daily averages of $[UTC(USNO) - GPS \text{ time}]$ by TTR6 - $[UTC(USNO) - GPS \text{ time}]$ by Stel502, and daily average temperature at USNO for a period of 11 months.

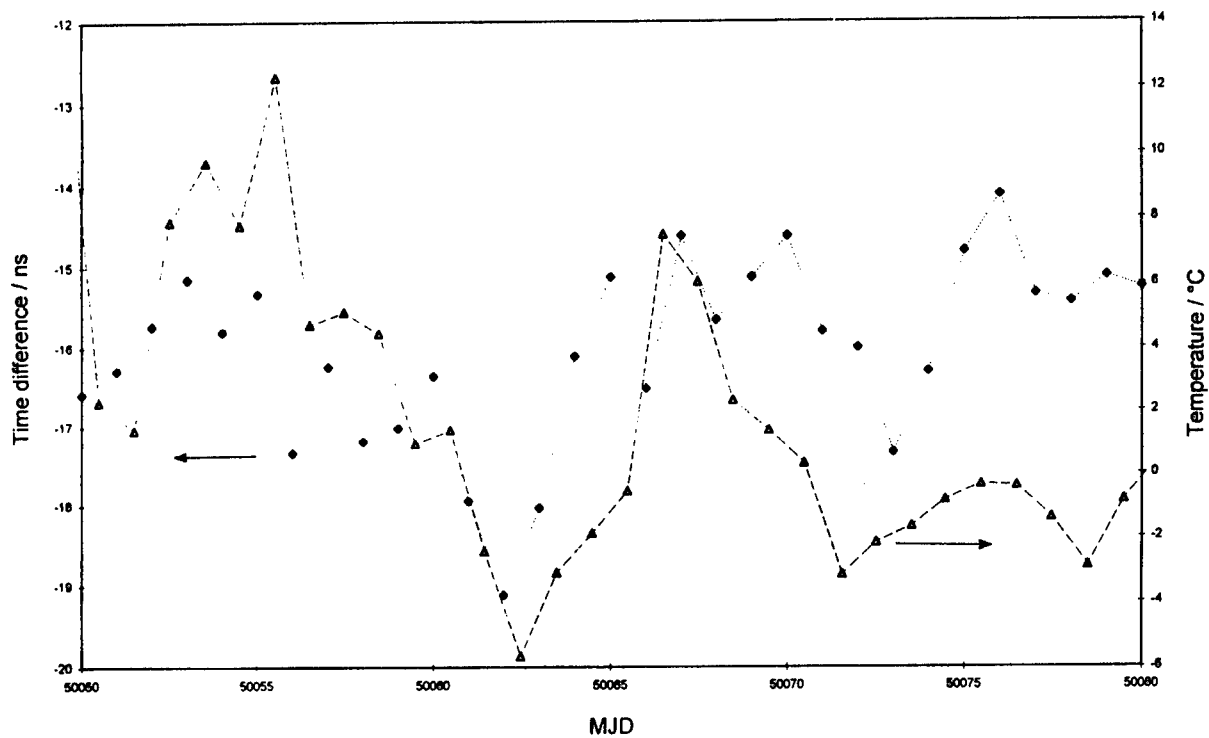


Figure 4. Daily averages of $[UTC(USNO) - GPS \text{ time}]$ by TTR6 - $[UTC(USNO) - GPS \text{ time}]$ by Stel502, and daily average temperature at USNO for a period of about 1 month.

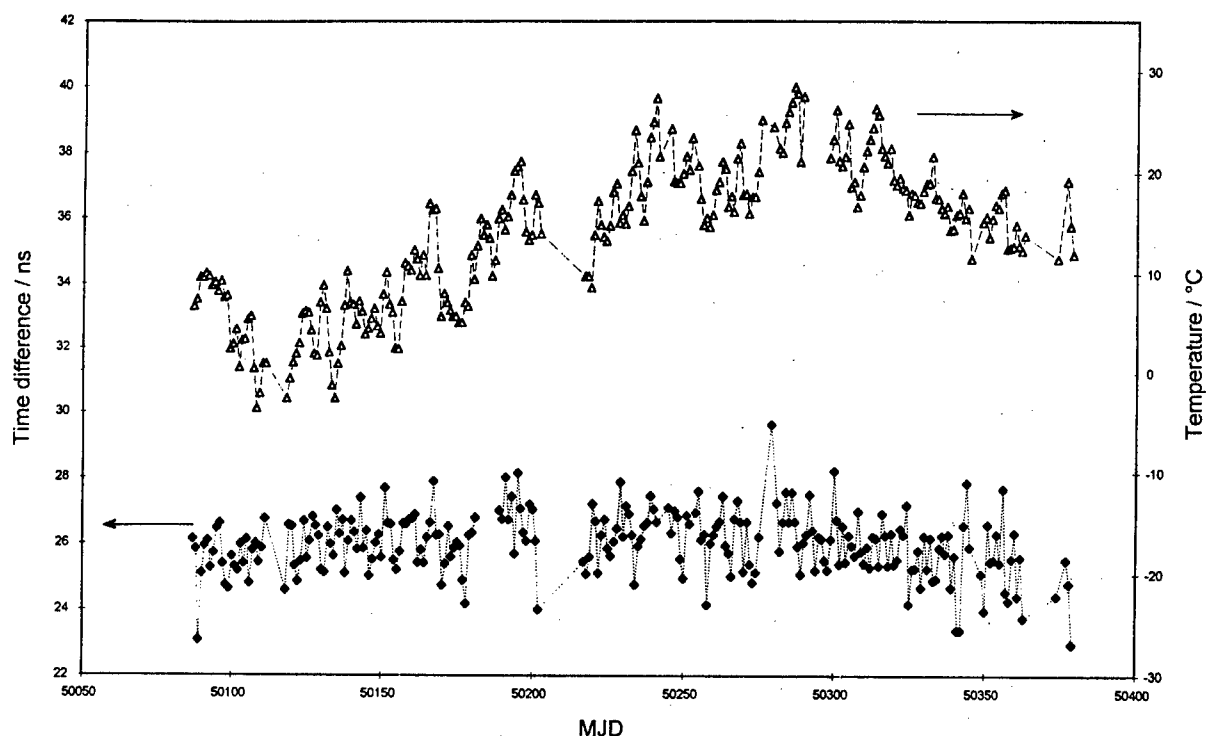


Figure 5. Daily averages of $[BIPM \text{ clock} - GLONASS \text{ time}]$ by R-100/10 - $[BIPM \text{ clock} - GLONASS \text{ time}]$ by R-100/30, and daily average temperature at BIPM for a period of 10 months.

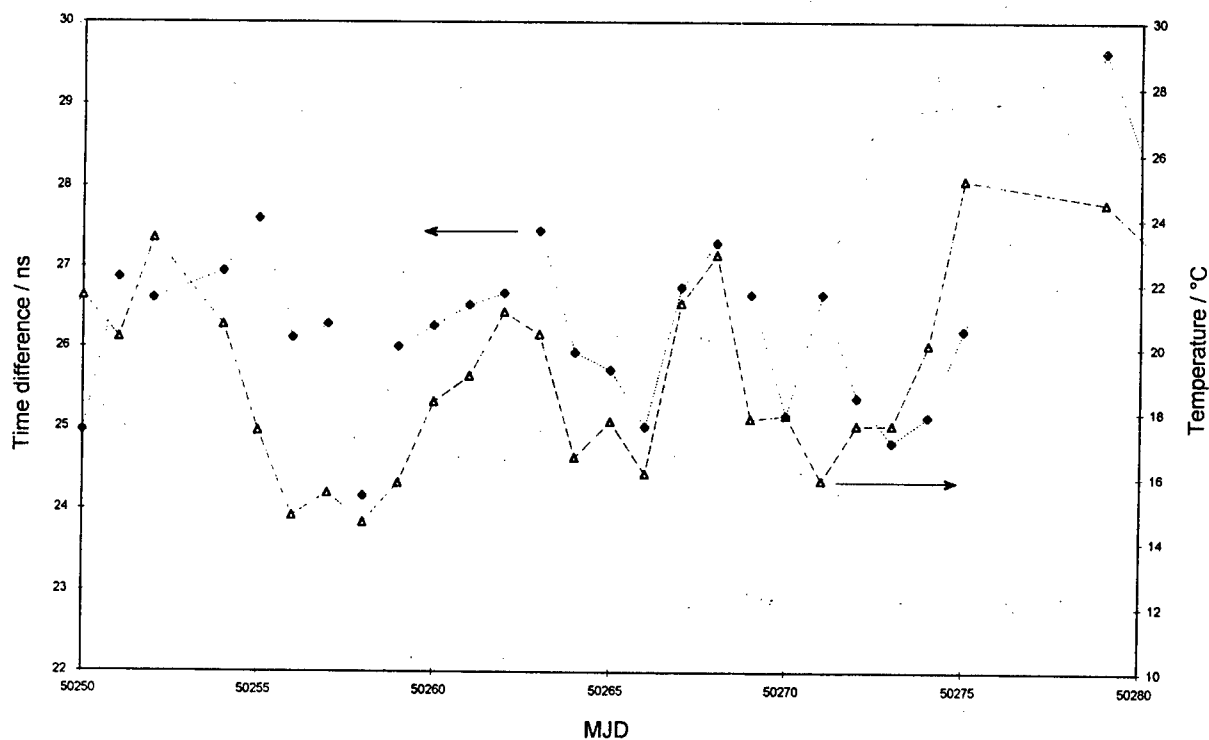


Figure 6. Daily averages of $[BIPM \text{ clock} - GLONASS \text{ time}]$ by R-100/10 - $[BIPM \text{ clock} - GLONASS \text{ time}]$ by R-100/30, and daily average temperature at BIPM for a period of about 1 month.

ANNEX I

A Suggested GPS Format Update for GPS/GLONASS

This is a suggested update of the CGGTTS GPS Data Format Version 01 as published in [1], for GPS/GLONASS, with suggested name CGGTTS GPS/GLONASS Data Format Version 02. Adopted notations are the same as for Version 01.

1. File header

Line 1-3: same as Version 01.

Line 4: "CH* = *" NUMBER OF CHANNELS
Number of receiver channels separately for GPS and GLONASS.
As many columns as necessary.

Line 5-6: same as Version 01.

Line 7-9: same as Version 01, but "GPS antenna" should be replaced by "GPS/GLONASS antenna"

Line 10: Designation of the reference frames, and if necessary transformation parameters between GLONASS and GPS frames.
As many columns as necessary.

Line 11: same as Version 01.

Line 12: "INT*DLY* = *" INTERNAL DELAY "*ns*(GPS)," INTERNAL DELAY
"*ns*(GLO)"
Internal delays entered in the receiver separately for GPS and GLONASS, in ns and given with 1 decimal.
As many columns as necessary.

Line 13: "CAB*DLY* = *" CABLE DELAY "*ns*(GPS)," CABLE DELAY "*ns*(GLO)"
Delays from the antenna to the main unit including delays in the antenna element, filters, electronics and cable length, entered in the receiver separately for GPS and GLONASS, in ns and given with 1 decimal.
As many columns as necessary.

Line 14-17: same as Version 01.

2. Line header

2.1 No measured ionospheric delays available

For no ionospheric measurements available line header update is as follows:

Line 18.1: "SAT*CL**MJD**STTIME*TRKL*ELV*AZTH***REFSV*****SRSV*****
REFSYS*****SRSYS**DSG*IOE*MDTR*SMDT*MDIO*SMDI*FR*HC*FRC*CK"
The acronyms are explained in Section 4 below. 113 columns.

2.2 Measured ionospheric delays available

With ionospheric measurements available line header update is as follows:

Line 18.2: "SAT*CL**MJD**STTIME*TRKL*ELV*AZTH***REFSV*****SRSV*****
REFSYS*****SRSYS**DSG*IOE*MDTR*SMDT*MDIO*SMDI*MSIO*SMSI*ISG*
FR*HC*FRC*CK"

The acronyms are explained in Section 4 below. 127 columns.

3. Unit header

Same as Version 01.

4. Data line

Line 20, columns 1-3: "123" SAT GPS or GLONASS satellite identification number.

- a. GPS satellite PRN number, 1 to 38. No unit.
- b. GLONASS almanac slot number plus 100, 101 to 124. No unit.

Line 20, columns 4-53: same as Version 01.

Line 20, columns 54-64: "+1234567890" REFSYS

Title changed from "REFGPS" to indicate reference to either constellation.
Data content same as Version 01.

Line 20, column 65: same as Version 01.

Line 20, columns 66-71: "+12345" SRSYS

Title changed from "SRGPS" to indicate slope for either constellation.
Data content same as Version 01.

Line 20, columns 72-101: same as Version 01.

4.1 No measured ionospheric delays available.

Line 20, columns 102-103: "12" FR

GLONASS transmission frequency channel number. 1 to 24. For GPS set to 0. No unit.

Line 20, column 104: space, ASCII value 20 (hexadecimal).

Line 20, columns 105-106: "12" HC

Receiver hardware channel number. 0 to 99. No unit.

Line 20, column 107: space, ASCII value 20 (hexadecimal).

Line 20, columns 108-110: "123" FRC

Frequency and Code type used for pseudo-range measurement, where:

- L1C - L1 C/A code,
- L1P - L1 P code,
- L2C - L2 C/A code (GLONASS future capability),
- L2P - L2 P code.

Line 20, column 111: space, ASCII value 20 (hexadecimal).

Line 20, columns 112-113: "12" CK

Data line check-sum for columns 1 to 111. Check-sum algorithm as defined for Version 01.

Line 20, columns 114-140: "123456789012345678901234567"

Optional comments on the data line, constituted of characters which are not included in the line check-sum CK.

4.2 Measured ionospheric delays available

Line 20, columns 102-115: same as Version 01.

- Line 20, columns 116-117: "12" FR
GLONASS transmission frequency channel number. 1 to 24. For GPS set to 0. No unit.
- Line 20, column 118: space, ASCII value 20 (hexadecimal).
- Line 20, columns 119-120: "12" HC
Receiver hardware channel number. 0 to 99. No unit.
- Line 20, column 121: space, ASCII value 20 (hexadecimal).
- Line 20, columns 122-124: "123" FRC
Frequency and Code type used for pseudo-range measurement, where:
L1C - L1 C/A code,
L1P - L1 P code,
L2C - L2 C/A code (GLONASS future capability),
L2P - L2 P code.
- Line 20, column 125: space, ASCII value 20 (hexadecimal).
- Line 20, columns 126-127: "12" CK
Data line check-sum for columns 1 to 125. Check-sum algorithm as defined for Version 01.
- Line 20, columns 128-140: "1234567890123"
Optional comments on the data line, constituted of characters which are not included in the line check-sum CK.

5. Example of Proposed Standard Format (fictitious data)

5.1 No measured ionospheric delays available, separate reference frames for GPS and GLONASS

CGGTTIS GPS/GLONASS DATA FORMAT VERSION = 02
 REV DATE = 1996-10-20
 RCVR = 3S Navigation, R-100/10 L1 GLONASS 2 CH, S/N 00102 Rev 002 1996-10-20
 CH = 1 (GPS), 1 (GLONASS)
 IMS = 99999
 LAB = 3S
 X = -2473157.78 m (GPS), -2473171.90 m (GLONASS)
 Y = -4706094.09 m (GPS), -4706086.67 m (GLONASS)
 Z = +3512042.48 m (GPS), +3512038.48 m (GLONASS)
 FRAME = ITRF for GPS, PZ-90 for GLONASS
 COMMENTS = NO COMMENTS
 INT DLY = 1366.0 ns (GPS), 1312.0 ns (GLONASS)
 CAB DLY = 100.0 ns (GPS), 105.0 ns (GLONASS)
 REF DLY = 30.0 ns
 REF = 3S
 CKSUM = FE

SAT	CL	MJD	STTIME	TRKL	ELV	AZTH	REFSV	SRSV	REFSYS	SRSYS	DSG	IOE	MDTR	SMDT	MDIO	SMDI	FR	EC	FRC	CK
107	34	50367	231000	780	273	3287	.1ns	.1ps/s	.1ns	.1ps/s	.1ns	.1ns	.1ps/s	.1ns	.1ps/s	.1ns	.1ps/s	.1ns	.1ps/s	.1ns
107	34	50367	232300	180	273	3287	+903734	+114	+1906	+69	41	9	177	-46	218	-34	21	1	L1C	C1
9	18	50367	232600	780	428	2719	+903764	+105	+1936	+60	42	9	156	-33	201	-30	21	1	L1C	B9
107	18	50367	232600	780	348	3257	+491057	-63	+2120	-72	29	9	119	-8	174	-16	0	0	L1C	4A
107	18	50367	232600	780	348	3257	+903854	+87	+1926	+41	42	9	142	-27	188	-28	21	1	L1C	BF

5.2 Measured ionospheric delays available, GLONASS satellite position transformed

CGGTTIS GPS/GLONASS DATA FORMAT VERSION = 02
 REV DATE = 1996-10-20
 RCVR = 3S Navigation, R-100/30, L1 GPS 12 CH, L1/L2 GLONASS 2 CH, S/N 00020 Rev 004 1996-10-01
 CH = 7 (GPS), 7 (GLONASS)
 IMS = R-100/30
 LAB = 3S
 X = -2473157.78 m (GPS, GLONASS)
 Y = -4706094.09 m (GPS, GLONASS)
 Z = +3512042.48 m (GPS, GLONASS)
 FRAME = ITRF, PZ-90->ITRF DX = 0.0 m, DY = 0.0 m, DZ = 4.0 m, ds = 0.0, Rx = 0.0, Ry = 0.0, Rz = -0.000003
 COMMENTS = NO COMMENTS
 INT DLY = 1366.0 ns (GPS), 1312.0 ns (GLONASS)
 CAB DLY = 100.0 ns (GPS), 105.0 ns (GLONASS)
 REF DLY = 0.0 ns
 REF = 3S
 CKSUM = 86

SAT	CL	MJD	STTIME	TRKL	ELV	AZTH	REFSV	SRSV	REFSYS	SRSYS	DSG	IOE	MDTR	SMDT	MDIO	SMDI	MSIO	SMSI	ISG	FR	EC	FRC	CK	
107	34	50367	231000	780	273	3287	.1ns	.1ps/s	.1ns	.1ps/s	.1ns	.1ns	.1ps/s	.1ns	.1ps/s	.1ns	.1ps/s	.1ns	.1ps/s	.1ns	.1ps/s	.1ns	.1ps/s	
107	34	50367	232300	180	273	3287	+903734	+114	+1906	+69	41	9	177	-46	218	-34	225	-10	09	21	1	L1C	C1	
9	18	50367	232600	780	428	2719	+903764	+105	+1936	+60	42	9	156	-33	201	-30	189	-40	20	21	1	L1C	B9	
107	18	50367	232600	780	348	3257	+491057	-63	+2120	-72	29	9	119	-8	174	-16	9999	9999	9999	9999	0	0	L1C	4A
107	18	50367	232600	780	348	3257	+903854	+87	+1926	+41	42	9	142	-27	188	-28	202	-30	17	21	1	L1C	BF	

ANNEX I

A Suggested GPS Format Update for GPS/GLONASS

This is a suggested update of the CGGTTS GPS Data Format Version 01 as published in [1], for GPS/GLONASS, with suggested name CGGTTS GPS/GLONASS Data Format Version 02. Adopted notations are the same as for Version 01.

1. File header

Line 1-3: same as Version 01.

Line 4: "CH* = *" NUMBER OF CHANNELS
Number of receiver channels separately for GPS and GLONASS.
As many columns as necessary.

Line 5-6: same as Version 01.

Line 7-9: same as Version 01, but "GPS antenna" should be replaced by "GPS/GLONASS antenna"

Line 10: Designation of the reference frames, and if necessary transformation parameters between GLONASS and GPS frames.
As many columns as necessary.

Line 11: same as Version 01.

Line 12: "INT*DLY* = *" INTERNAL DELAY "*ns*(GPS)," INTERNAL DELAY
"*ns*(GLO)"
Internal delays entered in the receiver separately for GPS and GLONASS, in ns and given with 1 decimal.
As many columns as necessary.

Line 13: "CAB*DLY* = *" CABLE DELAY "*ns*(GPS)," CABLE DELAY "*ns*(GLO)"
Delays from the antenna to the main unit including delays in the antenna element, filters, electronics and cable length, entered in the receiver separately for GPS and GLONASS, in ns and given with 1 decimal.
As many columns as necessary.

Line 14-17: same as Version 01.

2. Line header

2.1 No measured ionospheric delays available

For no ionospheric measurements available line header update is as follows:

Line 18.1: "SAT*CL**MJD**STTIME*TRKL*ELV*AZTH***REFSV*****SRSV*****
REFSYS****SRSYS**DSG*IOE*MDTR*SMDT*MDIO*SMDI*FR*HC*FRC*CK"
The acronyms are explained in Section 4 below. 113 columns.

2.2 Measured ionospheric delays available

With ionospheric measurements available line header update is as follows:

Line 18.2: "SAT*CL**MJD**STTIME*TRKL*ELV*AZTH***REFSV*****SRSV*****
REFSYS****SRSYS**DSG*IOE*MDTR*SMDT*MDIO*SMDI*MSIO*SMSI*ISG*
FR*HC*FRC*CK"

The acronyms are explained in Section 4 below. 127 columns.

3. Unit header

Same as Version 01.

4. Data line

Line 20, columns 1-3: "123" SAT GPS or GLONASS satellite identification number.

a. GPS satellite PRN number, 1 to 38. No unit.

b. GLONASS almanac slot number plus 100, 101 to 124. No unit.

Line 20, columns 4-53: same as Version 01.

Line 20, columns 54-64: "+1234567890" REFSYS

Title changed from "REFGPS" to indicate reference to either constellation.

Data content same as Version 01.

Line 20, column 65: same as Version 01.

Line 20, columns 66-71: "+12345" SRSYS

Title changed from "SRGPS" to indicate slope for either constellation.

Data content same as Version 01.

Line 20, columns 72-101: same as Version 01.

4.1 *No measured ionospheric delays available.*

Line 20, columns 102-103: "12" FR

GLONASS transmission frequency channel number. 1 to 24. For GPS set to 0. No unit.

Line 20, column 104: space, ASCII value 20 (hexadecimal).

Line 20, columns 105-106: "12" HC

Receiver hardware channel number. 0 to 99. No unit.

Line 20, column 107: space, ASCII value 20 (hexadecimal).

Line 20, columns 108-110: "123" FRC

Frequency and Code type used for pseudo-range measurement, where:

L1C - L1 C/A code,

L1P - L1 P code,

L2C - L2 C/A code (GLONASS future capability),

L2P - L2 P code.

Line 20, column 111: space, ASCII value 20 (hexadecimal).

Line 20, columns 112-113: "12" CK

Data line check-sum for columns 1 to 111. Check-sum algorithm as defined for Version 01.

Line 20, columns 114-140: "123456789012345678901234567"

Optional comments on the data line, constituted of characters which are not included in the line check-sum CK.

4.2 *Measured ionospheric delays available*

Line 20, columns 102-115: same as Version 01.

- Line 20, columns 116-117: "12" FR
GLONASS transmission frequency channel number. 1 to 24. For GPS set to 0. No unit.
- Line 20, column 118: space, ASCII value 20 (hexadecimal).
- Line 20, columns 119-120: "12" HC
Receiver hardware channel number. 0 to 99. No unit.
- Line 20, column 121: space, ASCII value 20 (hexadecimal).
- Line 20, columns 122-124: "123" FRC
Frequency and Code type used for pseudo-range measurement, where:
L1C - L1 C/A code,
L1P - L1 P code,
L2C - L2 C/A code (GLONASS future capability),
L2P - L2 P code.
- Line 20, column 125: space, ASCII value 20 (hexadecimal).
- Line 20, columns 126-127: "12" CK
Data line check-sum for columns 1 to 125. Check-sum algorithm as defined for Version 01.
- Line 20, columns 128-140: "1234567890123"
Optional comments on the data line, constituted of characters which are not included in the line check-sum CK.

TESTING MOTOROLA ONCORE GPS RECEIVER AND TEMPERATURE-STABILIZED ANTENNAS FOR TIME METROLOGY

W. Lewandowski, P. Moussay
Bureau International des Poids et Mesures
Pavillon de Breteuil, 92312 Sèvres, France

P. Guerin, F. Meyer, and M. Vincent
Observatoire de Besançon, Besançon, France

Abstract

With GPS now fully operational, the market for GPS navigation receivers is booming and one can purchase a multichannel GPS pocket-sized receiver for only a few hundred dollars. One of them, the Motorola Oncore eight-channel one-frequency receiver, is of special interest for timing because it provides a 1 pps output. Preliminary results of tests with the BIPM international GPS common-view schedule are given in this paper.

One identified source of instability in GPS time receiver hardware is a dependence on external temperature. This is typically of about $0.2 \text{ ns/}^\circ\text{C}$ and can approach $2 \text{ ns/}^\circ\text{C}$ for some types of receivers. In this paper it is shown that this problem can be resolved by enclosing antennas in temperature-stabilized ovens. Results are reported for Motorola and TTR6 Allen Osborne antennas.

INTRODUCTION

This paper treats two distinct topics. The first is a test of the low-cost Motorola Oncore GPS receiver for the use in time metrology. The second is a test of temperature-controlled antennas. However, the two tests were conducted together, as for a period the classic GPS time receiver, which served to test the Motorola, had its antenna covered by an oven with stabilized temperature, and for another period the Motorola antenna was covered by an oven. For this reason the paper, initially scheduled to report only on the use of the Motorola receiver, was extended to the second topic.

MOTOROLA RECEIVER

In the time-metrology community the GPS time receivers most commonly used are C/A code, one-channel, one-frequency devices. They were developed in the early 1980s and their high price, about twenty thousand dollars, has not changed. But with GPS now fully operational, the market for GPS navigation receivers is booming and one can purchase a multichannel GPS pocket-sized receiver for a few hundred dollars. One such receiver, the Motorola Oncore

eight-channel one-frequency receiver, is of special interest for timing because it provides a 1 pps output.

At the Observatoire de Besançon (OB) and the Bureau International des Poids et Mesures (BIPM) tests were made with Motorola Oncore receivers connected to local HP5071A cesium clocks with an external time intervalometer and a microcomputer. The setups at the two laboratories are shown in Figures 1 and 2.

At Observatoire de Besançon the first series of tests were carried out using two co-located XT Oncore receivers. The objective of the tests was to verify that a low-cost device of this kind could be used for the synchronization of the Auger Observatory, a cosmic ray project designed to observe ultrahigh energy particles. The time offset between the 1 pps signal from the receiver and the corresponding signal from a HP5071A cesium clock was measured. Data were acquired every second (the Auger application requires this) for each receiver. No schedule was used for this series of tests. Sessions were performed using the highest satellite in view. Scanning of the constellation was repeated every 10 minutes. Figure 3 shows the differences between two receivers at 1-second intervals over 1 hour. The data show a standard deviation of about 7 ns. This plot is typical of what was observed during sessions of up to 4 days.

At the BIPM the test of a VP Oncore receiver was carried out under conditions as close as possible to those which obtain during GPS common-view clock comparisons for the generation of International Atomic Time (TAI). The 1-second observations of the VP Oncore receiver were statistically treated following a standard procedure^[1] using tracks which have a duration of 13 minutes. However, all corrections added to the pseudorange measurements were provided by the VP Oncore receiver software. It is not yet known if this software uses standard formulae and constants. This will be checked in coming tests and, most probably, software which includes standards for time metrology will be developed. All one-channel "classical" time receivers, AOA TTR5, AOA TTR6, and Sercel, participating in this test, and one of the eight channels of the VP Oncore receiver was programmed with BIPM international GPS common-view schedule No. 27. Differential antenna coordinates of those receivers are known with an uncertainty of a few centimeters.

Having 13-minute tracks in standard format for the VP Oncore receiver allowed on-site comparison in common view (0 km baseline) with "classical" GPS time-transfer receivers. Differences between the VP Oncore and the TTR5 and the standard deviation of individual "common view" are shown on Figure 4. For reference, a comparison of two "classical" GPS time receivers, TTR5 and Sercel, is reported on Figure 5. The performance of the VP Oncore receiver is not quite so good, the difference, perhaps, being due to the use of nonstandard software. The noise exhibited by the time series of Figures 4 and 5 was analyzed by the use of a modified Allan variance. Both exhibit white phase noise up to an averaging interval of about 12 days (Figures 6 and 7).

To examine the possibility of a correlation with external temperature, daily averages of the differences between the receivers were computed. On Figure 8 we report results on the comparison of the VP Oncore receiver with the TTR5 and a comparison of the TTR5 and the TTR6. No significant difference between two pairs of comparisons can be observed except during the first period, when the antenna of the TTR6 was protected by a temperature-stabilized oven. This is explained in more detail below. No improvement of the VP Oncore results was observed when its antenna was enclosed in an oven.

TEMPERATURE-STABILIZED ANTENNAS

During last decade the performance of GPS common-view time transfer has improved by one order of magnitude through the use of high-accuracy ground-antenna coordinates, postprocessed precise ephemerides, and double-frequency ionospheric measurements. In good cases the uncertainty of this time transfer can approach 2 ns, but further progress is limited by the performance of the receiver hardware. One identified source of instability is a dependence on external temperature.^[2] This is typically about 0.2 ns/°C and can approach 2 ns/°C for some types of receivers. This maximum value results in a diurnal effect of about 20 ns and a seasonal effect of several tens of nanoseconds.

The sensitivity to external temperature suggests an effect linked to the parts of time equipment located in the open air, that is, to the antenna and its cable. The receiver itself is usually located in an air-conditioned room. For several years different hypotheses were considered to explain the temperature dependence of timing equipment. All linked the problem to the electronics of the antenna, but none were verified by experiment.

As no practical way was found to resolve the problem electronically, another approach was suggested: the antenna should be protected by an oven with a stabilized temperature. Such ovens are easy and cheap to construct, and are within the capabilities of any time laboratory. Detailed descriptions of the ovens built at the BIPM are shown in Figures 9 and 10. The temperature of the oven used at the BIPM was set at 38°C. This is the highest temperature recorded at Sèvres, which implies that only heating is required: cooling systems are much more complicated. Initial observations show that temperature stabilization of the antenna assembly reduces or even eliminates the diurnal delay variation. It is thought that the observed stabilization results from control of the temperature of the filters and amplifiers rather than of the antenna element itself. The results are reported on Figures 8, 11, and 12.

Although at the time of completion of this study a second oven had been constructed, only the first was used for the results covered here. Comparisons of two receivers with two protected antennas will be reported in a future study.

CONCLUSIONS

- 1) Tests of the GPS Motorola Oncore receiver reported in this paper demonstrate the metrological quality of this device and confirm the results of earlier work.^[3] Further effort is necessary to improve the operation of this receiver, mainly the application of standard procedures.
- 2) Preliminary results show that the use of temperature-stabilized enclosures for GPS time receiver antenna electronics reduce daily hardware delay variations. Further investigations are necessary.

REFERENCES

- [1] D.W. Allan, and C. Thomas 1994, "Technical directives for standardization of GPS time receiver software," *Metrologia*, **31**, pp. 67-79.
- [2] W. Lewandowski, and R. Tourde 1991, "Sensitivity to the external temperature of some GPS time receivers," Proceedings of the 22nd Annual Precise Time and Time Interval (PTTI) Meeting, 4-6 December 1990, Vienna, Virginia, USA (NASA CP-3116), pp. 307-316.

- [3] R.P. Giffard, L.S. Cutler, J.A. Kusters, M. Miranian, and D.W. Allan 1996, "*Continuous, multi-channel, common-view, L1-GPS time-comparison over a 4,000 km baseline,*" Proceedings of the 1996 IEEE International Frequency Control Symposium, 5-7 June 1996, Honolulu, Hawaii, USA, pp. 1198-1205.

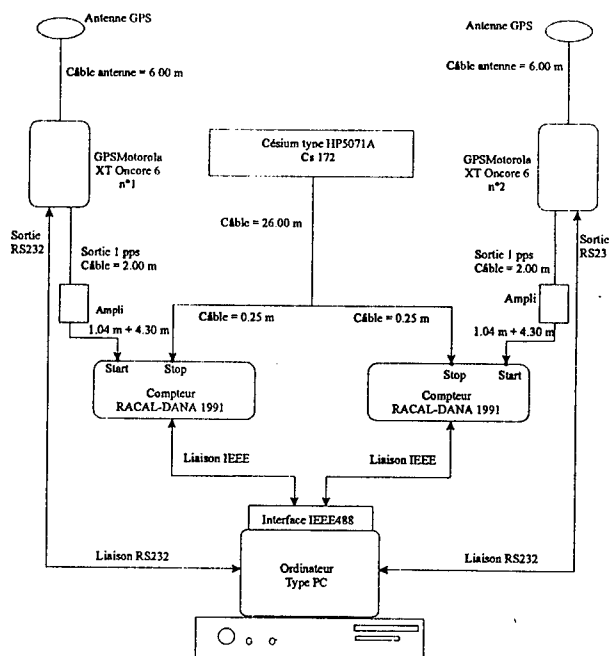


Figure 1. Experimental set-up at the Observatoire de Besançon.

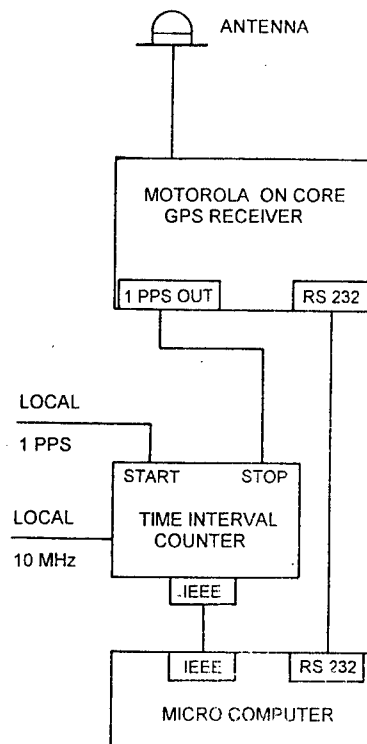


Figure 2. Experimental set-up at the BIPM.

Satellite switch (29->18) at t=09:50

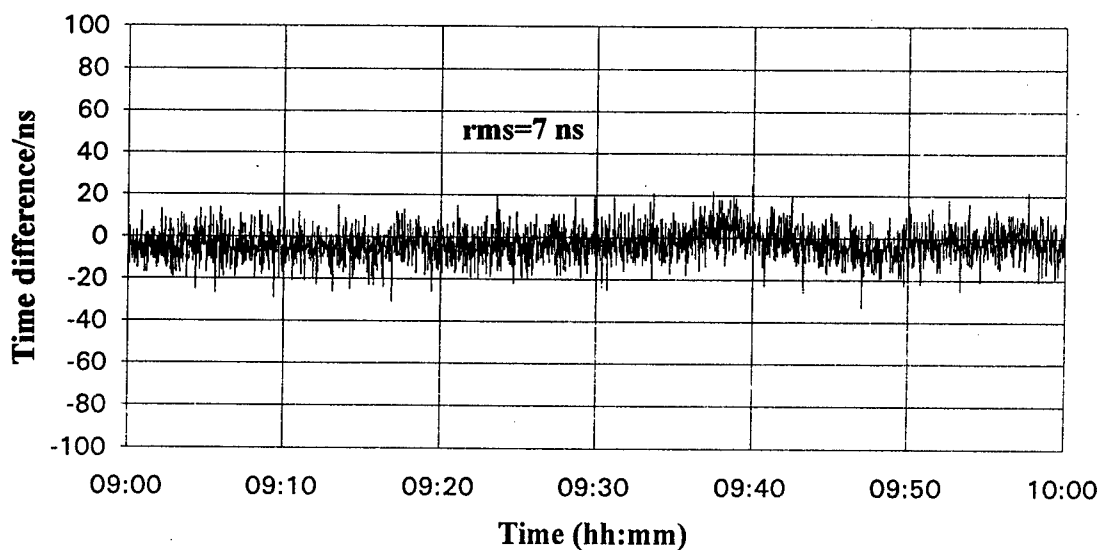


Figure 3. $[OB \text{ HP5071A} - \text{GPS time}]_{\text{XT ONCORE No 1}} - [OB \text{ HP5071A} - \text{GPS time}]_{\text{XT ONCORE No 2}}$ every second over 1 hour.

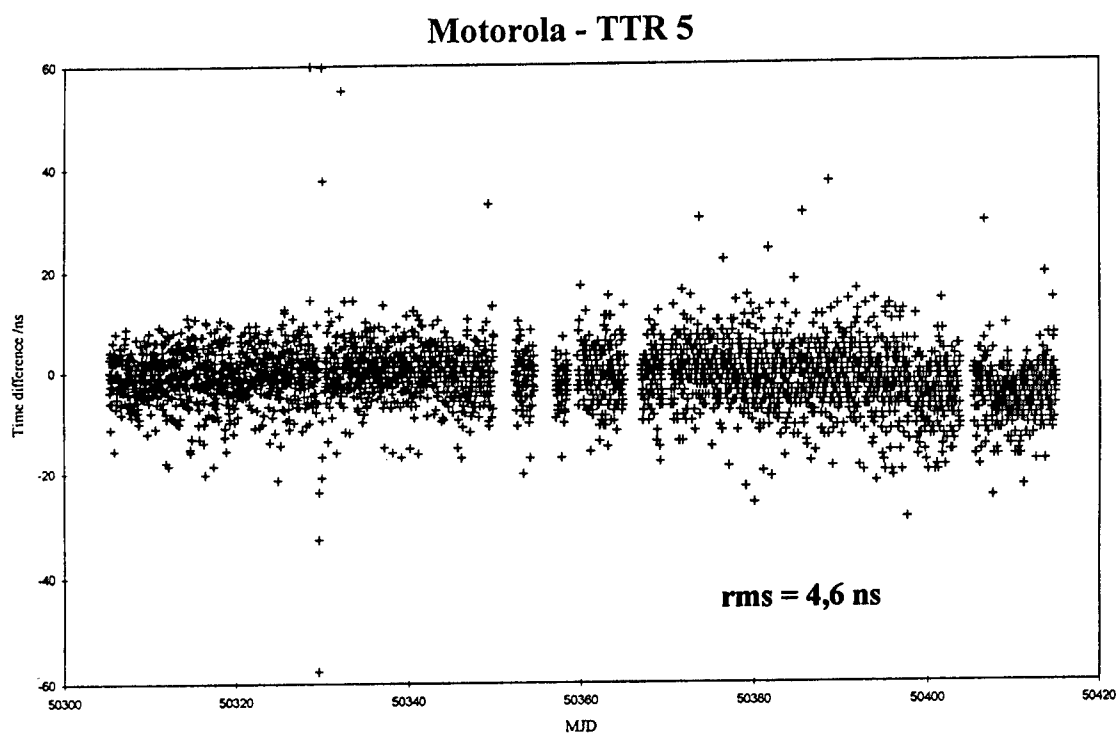


Figure 4. $[BIPM\ HP5071A - GPS\ time]_{VP\ ONCORE} - [BIPM\ HP5071A - GPS\ time]_{TTR5}$ for individual 13-minute tracks and corresponding standard deviation.

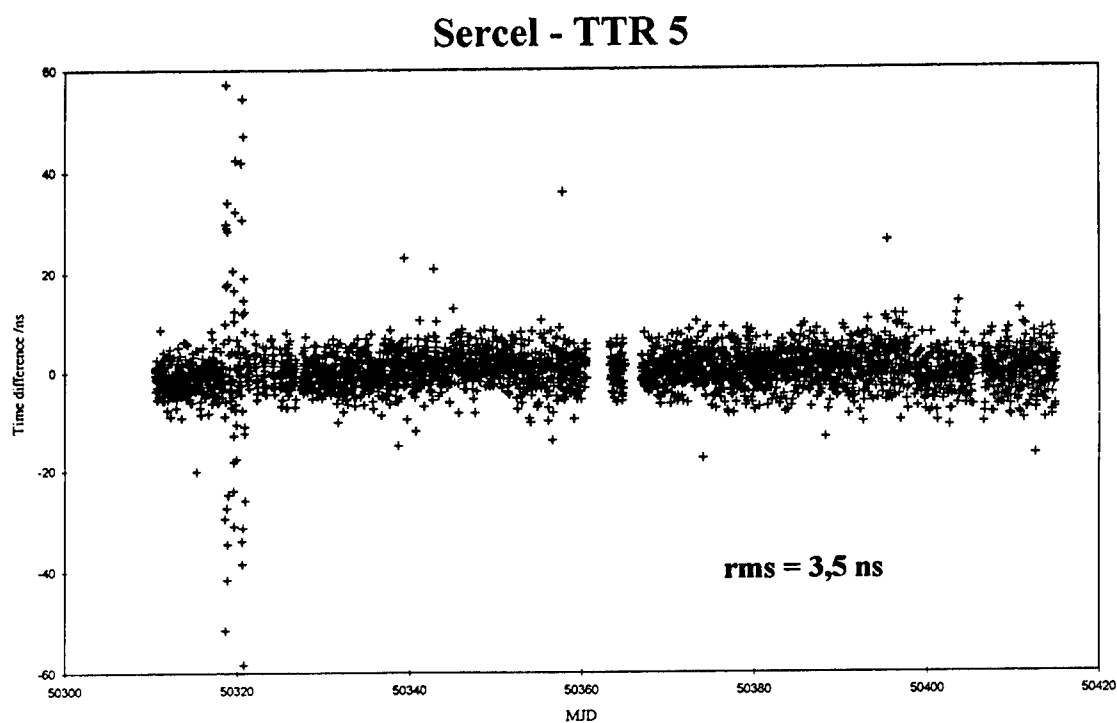


Figure 5. $[BIPM\ HP5071A - GPS\ time]_{SERCEL} - [BIPM\ HP5071A - GPS\ time]_{TTR5}$ for individual 13-minute tracks and corresponding standard deviation.

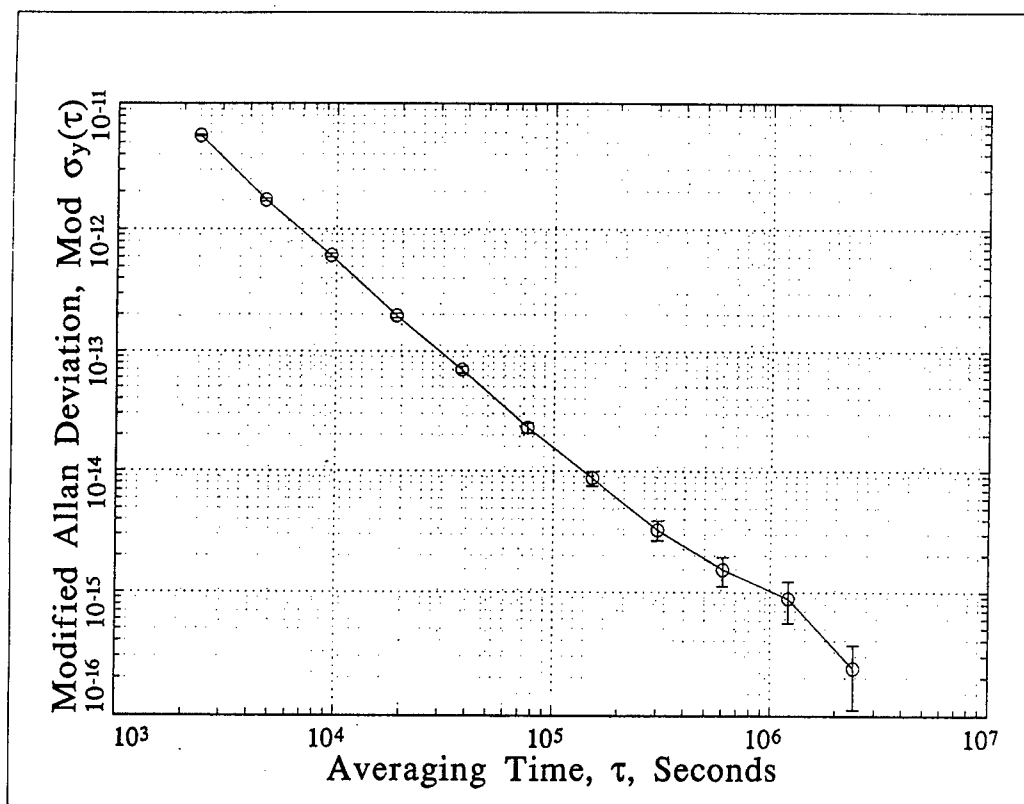


Figure 6. Square root of the modified Allan variance of the time series $[BIPM\ HP5071A-GPS\ time]_{VP\ ONCORE} - [BIPM\ HP5071A - GPS\ time]_{TTR5}$ reported on Figure 4.

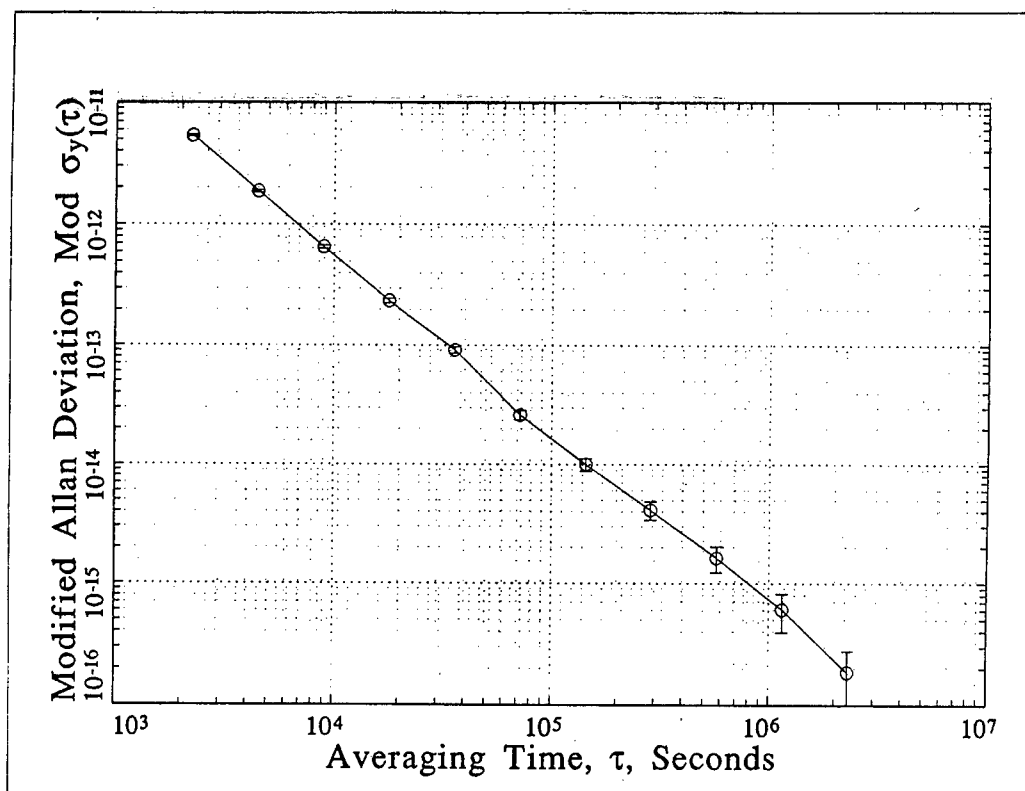


Figure 7. Square root of the modified Allan variance of the time series $[BIPM\ HP5071A - GPS\ time]_{SERCEL} - [BIPM\ HP5071A - GPS\ time]_{TTR5}$ reported on Figure 5.

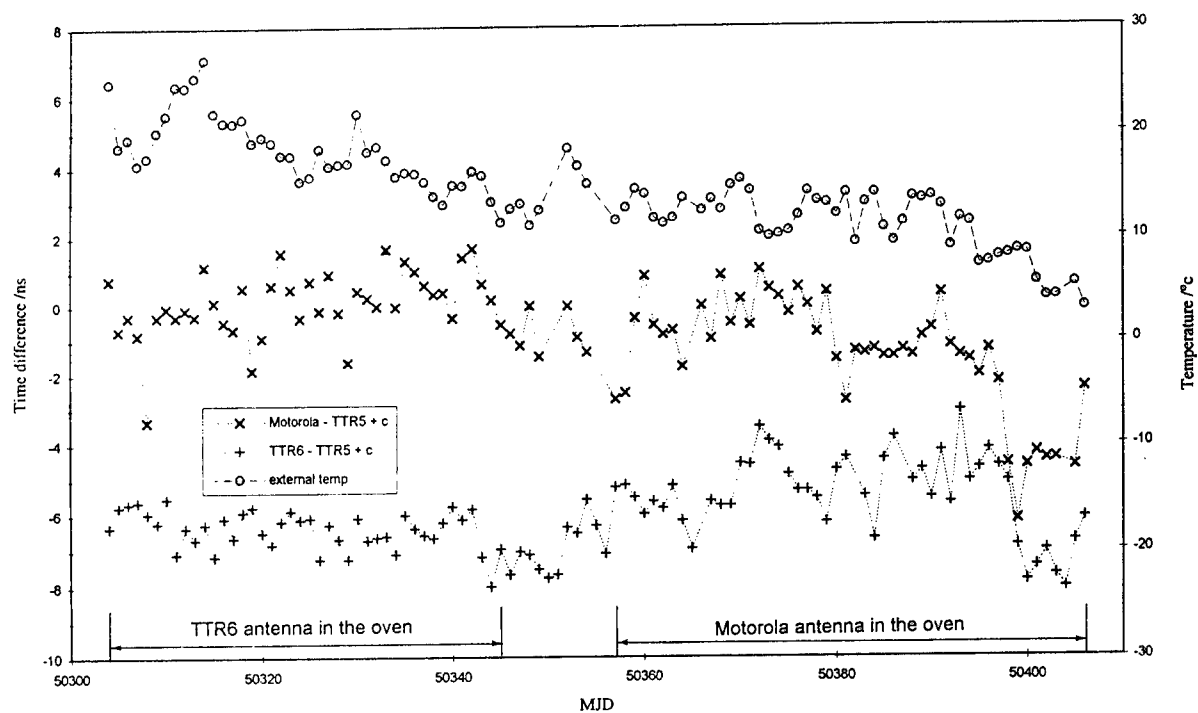


Figure 8. Daily averages of external temperature and daily averages of $[BIPM\ HP5071A-GPS\ time]_{VP\ ONCORE} - [BIPM\ HP5071A-GPS\ time]_{TTR5}$ and $[BIPM\ HP5071A-GPS\ time]_{TTR6} - [BIPM\ HP5071A-GPS\ time]_{TTR5}$.



Figure 9. GPS and GLONASS antennas at the BIPM. Two GPS antennas are covered by ovens.

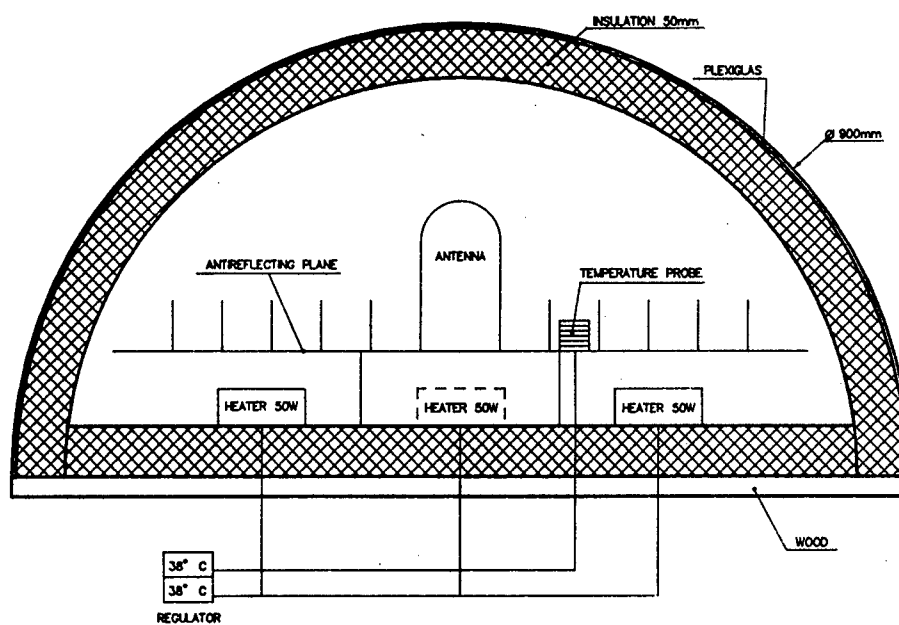
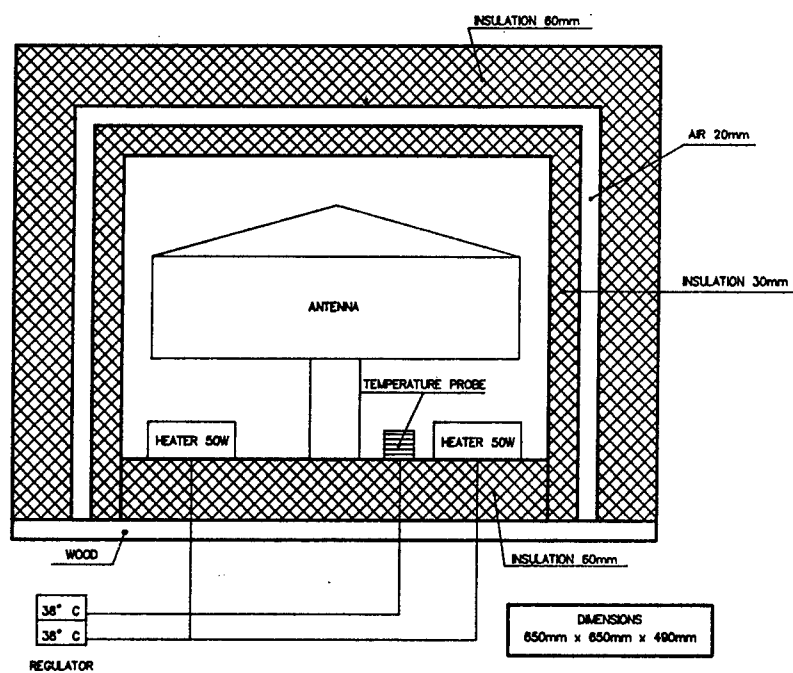


Figure 10. Two ovens built at the BIPM.

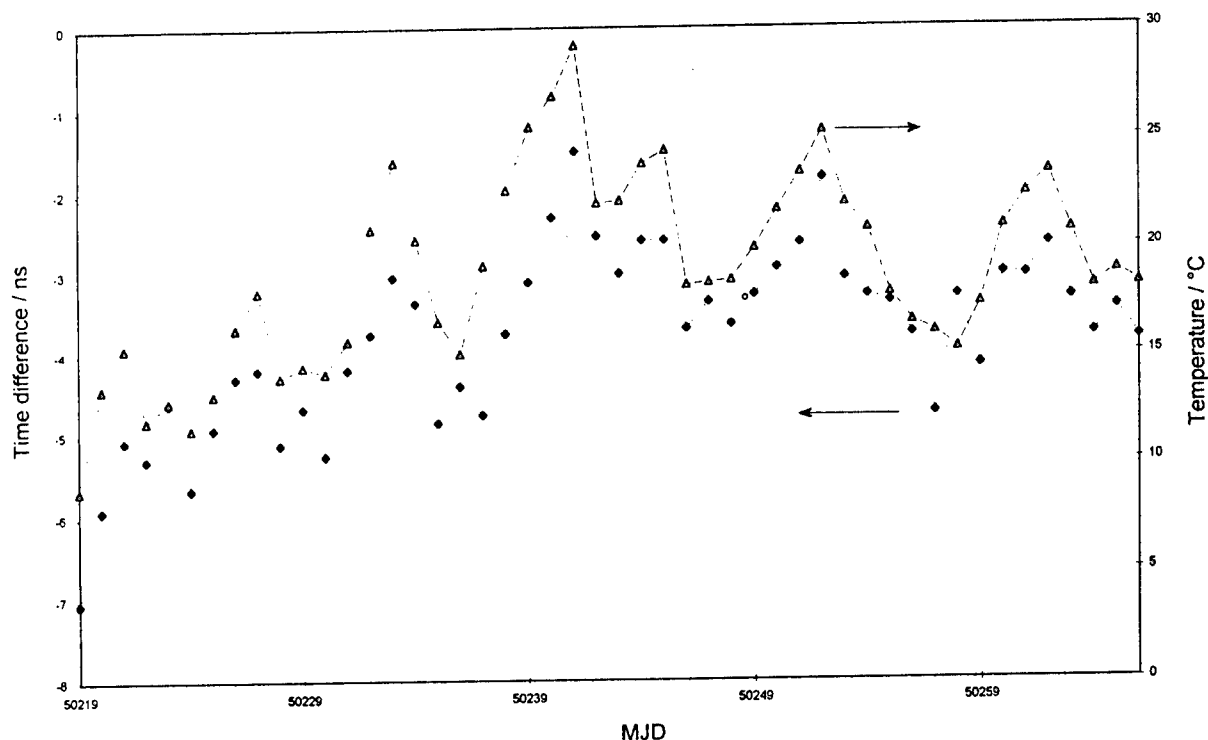


Figure 11. Daily averages of $[BIPM\ HP5071A - GPS\ time]_{TTR5} - [BIPM\ HP5071A - GPS\ time]_{TTR6}$, with TTR5 and TTR6 antenna no-protected by the oven, and daily average temperature at BIPM.

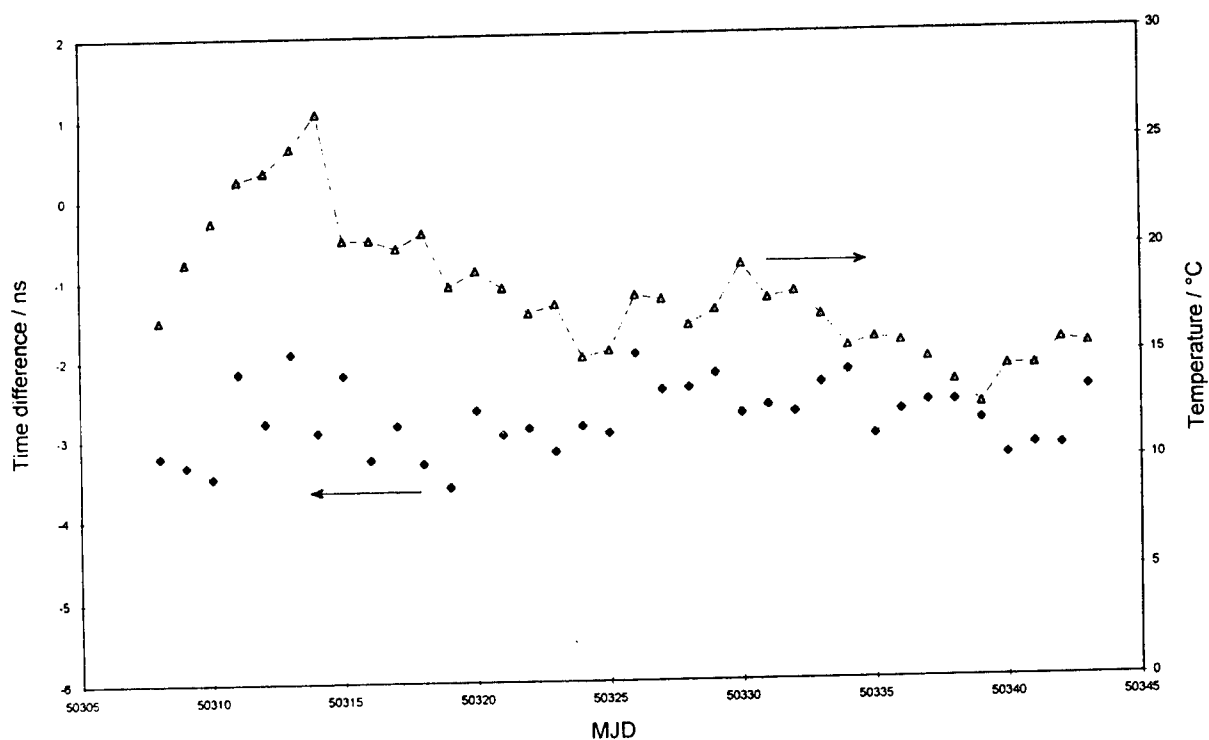


Figure 12. Daily averages of $[BIPM\ HP5071A - GPS\ time]_{TTR5} - [BIPM\ HP5071A - GPS\ time]_{TTR6}$, with TTR6 antenna protected by the oven, and daily average temperature at BIPM.

CONTINUOUS OBSERVATION OF NAVSTAR CLOCK OFFSET FROM THE DOD MASTER CLOCK USING LINKED COMMON-VIEW TIME TRANSFER

Wilson G. Reid
U.S. Naval Research Laboratory
4555 Overlook Ave., S.W., Code 8153
Washington, D.C. 20375-5354, USA

Abstract

Analysis of the on-orbit Navstar clocks and of the Global Positioning System (GPS) and National Imaging and Mapping Agency (NIMA) monitor station reference clocks is performed by the Naval Research Laboratory (NRL) using both broadcast and postprocessed precise ephemerides. The precise ephemerides are produced by NIMA for each of the GPS space vehicles from pseudorange measurements collected at the five GPS and seven NIMA monitor stations spaced around the world. That the time reference for the NIMA Washington, D.C., monitor station is the DoD Master Clock has enabled synchronized time transfer every 15 minutes via Linked Common-View Time Transfer from the DoD Master Clock to the other eleven monitor stations. Summing the offset of a space vehicle clock from a monitor station time reference with the offset of the monitor station time reference from the DoD Master Clock yields the offset of the space vehicle clock from the DoD Master Clock for the period during which the space vehicle was in view of the monitor station. Repeating this procedure for each of the monitor stations produces continuous overlapping observations of the offset of the Navstar clock from the DoD Master Clock. Following this procedure for the Navstar 29 cesium clock for 118 days during which there were no anomalies in either the space vehicle clock or the Washington, D.C., monitor station time reference yielded a measurement noise with a standard deviation of 1.1 nanoseconds. This was reduced to an estimated measurement precision of 641 picoseconds by averaging overlapping measurements from multiple monitor stations at each observation time. Analysis of the low-noise clock offset from the DoD Master Clock yields not only the bias in the time of the space vehicle clock, but focuses attention on structure in the behavior of the space vehicle clock not previously observable. Furthermore, the uniformly sampled database of 15-minute measurements makes possible for the first time the exhaustive computation of the frequency stability of the space vehicle clocks.

INTRODUCTION

Historically, the data available to NRL for analyzing the behavior of the GPS clocks—both space vehicle and monitor station—have been of two types. The first type consisted of measurements of the offset of the space vehicle clocks from the DoD Master Clock obtained by the U.S. Naval Observatory (USNO) from a linear least-squares fit to 13 minutes of 6-second measurements. These measurements were nominally timed according to a schedule issued by the Bureau International des Poids et Mesures (BIPM) for establishment of International

Atomic Time (TAI). Although this schedule was adequate for the purpose intended, the number of measurements was sparse compared to those taken by the GPS and NIMA monitor stations. Moreover, the 13-minute measurements utilized the broadcast ephemeris, and the receiver operated for some period of time at a single frequency requiring use of the ionospheric model transmitted in the navigation message. The second type of data—measurements made by the GPS and NIMA monitor stations—were synchronized to GPS system time and were scheduled on the hour and every 15 minutes thereafter during the time that the space vehicle was in view of the monitor station. The receivers, which operated at two L-band frequencies, measured the ionospheric delay. The phase offset was obtained using the post-fit precise ephemerides supplied by NIMA.

The first step in the analysis of any clock is to identify in the data all discontinuities—either spontaneous or those caused deliberately by the action of the Master Control Station—and to remove them. This was a time consuming task, since any correction attributed to a space vehicle clock had to be consistent with observations of that clock from the 13 monitor stations represented in the database. Similarly, any correction attributed to a monitor station clock had to be consistent with the data from the 24 space vehicle clocks that were observed by that monitor station. Correction of the discontinuities in the data for the 13 monitor stations and for the 24 active space vehicle clocks required the examination of no fewer than 312 files. After all corrections were made, the choice of a file for analysis was often predicated on which showed the lowest noise or which contained observations during the occurrence of an anomaly that was under investigation.

The next logical step in the time transfer work reported previously^[1] was to obtain a uniformly sampled database of 15-minute measurements of the offset of the space vehicle clocks from the DoD Master Clock using Linked Common-View Time Transfer from the DoD Master Clock to each of the remaining monitor stations. This has been accomplished by combining the files containing measurements of the phase offset of a space vehicle clock from each of the monitor stations and the files obtained from Linked Common-View Time Transfer, which contain a uniformly sampled database of 15-minute measurements of the offset of the monitor station clocks from the DoD Master Clock.

METHODOLOGY

If the uniformly sampled 15-minute measurements of the offset of a monitor station clock from the DoD Master Clock—obtained by Linked Common-View Time Transfer—are added to the 15-minute measurements of the offset of a space vehicle clock from the clock at that monitor station, the monitor station clock cancels out, leaving the 15-minute measurements of the offset of the space vehicle clock from the DoD Master Clock for the period of time that the space vehicle was in view of that particular monitor station. If the process is then repeated for each of the remaining monitor stations and the measurements of the offset of the space vehicle clock from the DoD Master Clock for the period of observation from each of the monitor stations are summed, then continuous coverage results. This process is described schematically in Table 1 for the Navstar 29 clock.

In Table 1 the three-byte numeric code 294 refers to the cesium clock in position #4 on the Navstar 29 space vehicle. The three-byte alphabetic codes refer to the monitor stations and are defined in Table 2. The entries in column #1 of Table 1 refer to the measurements of the offset of the space vehicle clock from the reference clock at the indicated monitor station. The entries in column #2, shown being added to the entries in column #1, refer to the uniformly sampled 15-minute measurements of the offset of the monitor station reference clock from the

DoD Master Clock obtained by Linked Common-View Time Transfer. Adding the entries in columns #1 and #2 yields the offset of the space vehicle clock from the DoD Master Clock for the period of observation of the space vehicle by the indicated monitor station. Accumulating the entries in column #3 yields continuous overlapping observations of the space vehicle clock from the DoD Master Clock.

Table 1

**PROCESSING TO OBTAIN CONTINUOUS PHASE OFFSET
OF THE NAVSTAR 29 SPACE VEHICLE CLOCK
FROM THE DOD MASTER CLOCK**

(294-ASC)	+	(ASC-WAS)	=	(294-WAS)	(ASC Observations)
(294-ARG)	+	(ARG-WAS)	=	(294-WAS)	(ARG Observations)
(294-BAH)	+	(BAH-WAS)	=	(294-WAS)	(BAH Observations)
(294-BEI)	+	(BEI-WAS)	=	(294-WAS)	(BEI Observations)
(294-CSP)	+	(CSP-WAS)	=	(294-WAS)	(CSP Observations)
(294-DGI)	+	(DGI-WAS)	=	(294-WAS)	(DGI Observations)
(294-ENG)	+	(ENG-WAS)	=	(294-WAS)	(ENG Observations)
(294-HAW)	+	(HAW-WAS)	=	(294-WAS)	(HAW Observations)
(294-KWJ)	+	(KWJ-WAS)	=	(294-WAS)	(KWJ Observations)
(294-QUI)	+	(QUI-WAS)	=	(294-WAS)	(QUI Observations)
(294-SMF)	+	(SMF-WAS)	=	(294-WAS)	(SMF Observations)
(294-WAS)				(294-WAS)	(WAS Observations)
<hr/>					
(294-WAS)					(All Observations)

The overlapping measurements from multiple monitor stations at each observation time are then averaged to get a single estimate of the offset of the space vehicle clock from the DoD Master Clock at each of the observation times. Because the averaging of multiple measurements, the measurement noise is correspondingly reduced.

Table 2

MONITOR STATION CODES

ASC	Ascension Island
ARG	Argentina
BAH	Bahrain
BEI	Beijing, China
CSP	Colorado Springs
DGI	Diego Garcia Island
ENG	England
HAW	Hawaii
KWJ	Kwajalein Island
QUI	Quito, Ecuador
SMF	Smithfield, Australia
WAS	Washington, D.C.

FEASIBILITY TEST

An algorithm was derived to manipulate the data as shown in Table 1 to test the feasibility of the process. Figure 1 is the offset of the Navstar 29 clock from the Washington, D.C. time reference and shows that, during the 118 days from 10 October 1995 to 5 February 1996, there were no anomalies in either the Navstar 29 clock or in the Washington, D.C., time reference¹. Superimposed in the figure is a plot of the residuals of a linear fit to the phase offset on an expanded scale which enables examination of the fine structure. Hence, in each line of Table 1, except for the measurement times which will differ, the data resulting from the sum should lie along the curve shown in Figure 1.

The offset of the Navstar 29 clock from the Colorado Springs time reference shown in Figure 2 reveals a number of discontinuities all of which occurred in the monitor station time reference. Figure 3, which is a plot of the offset of the Colorado Springs time reference from the Washington, D.C. time reference obtained through common-view time transfer, shows the same discontinuities in the Colorado Springs time reference, but with opposite sign since the Colorado Springs time reference is now the remote clock. Figure 4 is the result of adding the data in Figures 2 and 3 and corresponds to line 5 of Table 1. It can be seen that the behavior of the Colorado Springs time reference with all of its discontinuities drops out of the sum and that the resulting data does, indeed, lie along the same curve as the data in Figure 1.

This process was repeated for the other ten monitor stations, and each yielded data that were without discontinuities and that lay along the same curve as in Figure 1. Adding the measurements of the offset of the Navstar 29 clock from the Washington, D.C., time reference corresponding to the observations from each of the monitor stations (column #3 of Table 1) resulted in the data in Figure 5 which—except for short gaps in the data due to communications outages, power outages, receiver malfunctions, clock switches, etc.—filled in the measurement times completely with overlapping measurements, confirming the feasibility of the process. The raw overlapping measurements at each measurement time were then averaged to yield the smoothed 15-minute continuous observations of the Navstar 29 cesium clock from the Washington, D.C., time reference. In Figure 6 is plotted the residuals of a linear fit to the smoothed data, showing in detail the behavior of the phase every 15 minutes except, as noted, for the few areas where data were missing for the causes mentioned. This provides, then, the most definitive estimate of the behavior of the space vehicle clock.

MEASUREMENT STATISTICS

If the smoothed measurements are subtracted from the raw measurements the measurement noise shown in Figure 7 results. The histogram in Figure 8 shows the empirical probability distribution of the measurement noise to be decidedly normal, which is a consequence of the numerous additions inherent in the processing, implying multiple convolutions of individual density functions. By the Central Limit Theorem^[2] these convolutions tend to normality. In Figure 9 the normalized integrated periodogram of the measurement noise lies well within the 75% Kolmogoroff-Smirnov confidence interval, supporting the hypothesis that the noise is white, or uncorrelated. That the noise measurements are normally distributed and uncorrelated implies that they are also independent.

To estimate the precision of the smoothed measurement requires computation of the standard

¹ Although the time reference for the NIMA Washington, D.C., monitor station is nominally the DoD Master Clock, which is free of anomalies, whenever the receiver loses power the phase registration with the DoD Master Clock is lost, resulting in a discontinuity in the phase of the time reference.

deviation of the distribution of the sample mean—the sample being the overlapping measurements from multiple monitor stations made during the same 15-minute interval. Since the measurements in the sample are independent and identically distributed random variables, the standard deviation of the sample mean will be the standard deviation of the population from which the sample was taken reduced by $1/\sqrt{n}$, where n is the number of measurements in the sample. The number of noise measurements (n_{noise}) in Figure 7 was 28,653. The number of estimates (n_{mean}) of the offset obtained by taking the mean of each sample of raw measurements at the measurement times was 9,735. Dividing the two yields $n_{sample} = 2.94$ for the average size of the samples for which the mean was found. With the standard deviation of the measurement noise $\sigma_{noise} = 1.10$ nanoseconds from Figure 7, the standard deviation of the sample mean is

$$\sigma_{mean} = \frac{\sigma_{noise}}{\sqrt{n_{sample}}} = 641 \text{ ps}$$

FREQUENCY OFFSET

The one-day average frequency offset determined from the 15-minute data in Figure 6 is shown in Figure 10. Figure 11 is a plot of the same data seen through a 6-hour moving average filter used to reduce the white frequency noise which was determined from the frequency-stability profile in Figure 12 to be dominant at that sample time. Superimposed on the continuous coverage is the 1-day average frequency offset determined by direct measurement once per day between the space vehicle clock and the DoD Master Clock at the Naval Observatory. The direct measurements were the type of data routinely analyzed prior to institution of Linked Common-View Time Transfer. That the measurements made once per day by the Naval Observatory fall atop the smooth curve corresponding to continuous coverage suggests that what might have been interpreted as white frequency noise in the 1-day data is, in fact, undersampling of a process with possibly meaningful structure. Hence, the uniformly sampled database of 15-minute measurements can be seen to provide much higher resolution for analysis of the behavior of the space vehicle clocks.

FREQUENCY STABILITY

The uniformly sampled database of 15-minute measurements of the offset of the space vehicle clocks from the DoD Master Clock resulting from continuous coverage makes possible for the first time the direct and exhaustive computation of the frequency stability of the space vehicle clocks. Figure 12 is a plot of the frequency-stability profile for the Navstar 29 cesium clock for sample times of 15 minutes to 30 days. By exhaustive calculation is meant that the frequency stability is calculated for every multiple of the basic sample interval of 15 minutes up to the maximum sample time.

The stability for a sample time of one day was estimated from the continuous coverage to be 7.3 parts in 10^{14} , whereas the values estimated from the 15-minute data for each of the 12 monitor stations separately, i.e. the data represented by the entries in the first column of Table 1, ranged from 6.6 parts in 10^{14} for Bahrain to 1.18 parts in 10^{13} for Diego Garcia Island, which has been noisy for some time. That the estimate obtained from the uniformly sampled database falls within the range of values estimated from the observations made by the individual monitor stations is not surprising, since the uniformly sampled database was derived from observations made by all of the monitor stations. Where certain monitor stations are

known to be noisy, these might be omitted from the computation of the continuous coverage to preclude their degrading the estimate of the stability of the space vehicle clock.

The stability for a sample time of one day of 7.3 parts in 10^{14} is well within the GPS system specification of 2.0 parts in 10^{13} for cesium clocks. A flicker floor of 2 parts in 10^{14} appears to have been temporarily reached at about 8 days, but after about 12 days the profile turns sharply downward again. It appears that no confidence limits have been placed on the stability estimates, but the limits were, in fact, very small because of the very large number of phase triplets that entered into the calculation of the stability at each sample time.

CONCLUSIONS

Institution of the continuous coverage method, which makes use of Linked Common-View Time Transfer from the DoD Master Clock to the remaining monitor stations represented in the database, produces for each of the Navstar space vehicle clocks a uniformly sampled database of 15-minute measurements having low-noise, e.g. a 641-picosecond measurement precision for the Navstar 29 cesium clock. The new database makes the following contributions: (1) It provides much higher resolution for analysis of the behavior of the space vehicle clocks. (2) It makes possible for the first time the exhaustive computation of the frequency stability of the space vehicle clocks. And (3) the manual labor involved in the break correction process is substantially reduced by the analysis of $N + M = 37$ files in lieu of $N \times M = 312$ files, where $N = 24$ is the number of Navstar space vehicles currently active and $M = 13$ is the number of monitor stations represented in the database.

REFERENCES

- [1] W.G. Reid, T.B. McCaskill, O.J. Oaks, Laboratory, J.A. Buisson, and H.E. Warren 1996, "Common-view time transfer using worldwide GPS and DMA monitor stations," Proceedings of the 27th Annual Precise Time and Time Interval (PTTI) Applications and Planning Meeting, 29 November-1 December 1995, San Diego, California, USA (NASA CP-3334), pp. 145-158.
- [2] A. Papoulis 1965, *Probability, Random Variables, and Stochastic Processes*, McGraw-Hill Book Company, New York, New York, USA, p. 266ff.

**PHASE OFFSET OF NAVSTAR 29 CESIUM CLOCK FROM
Washington, D.C. Time Reference**

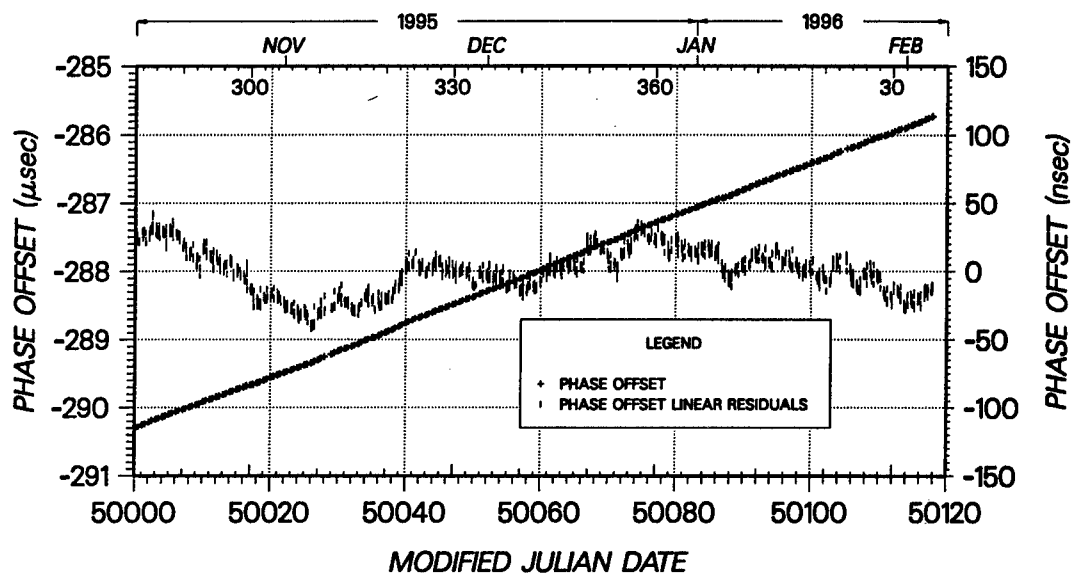


Figure 1

**PHASE OFFSET OF NAVSTAR 29 CESIUM CLOCK FROM
Colorado Springs Time Reference**

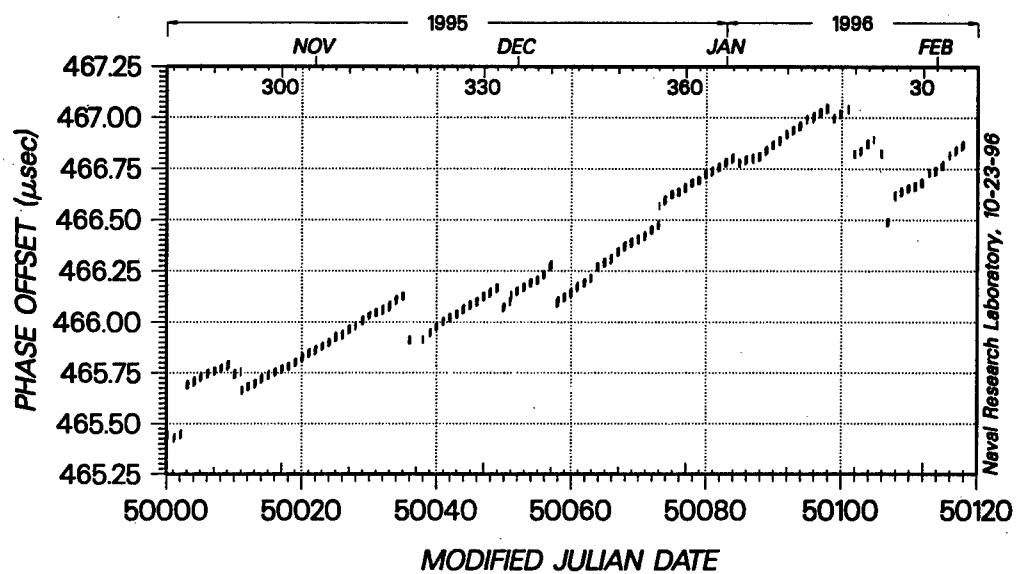


Figure 2

**PHASE OFFSET OF COLORADO SPRINGS TIME REFERENCE FROM
Washington, D.C. Time Reference Using
Common-View Time Transfer**

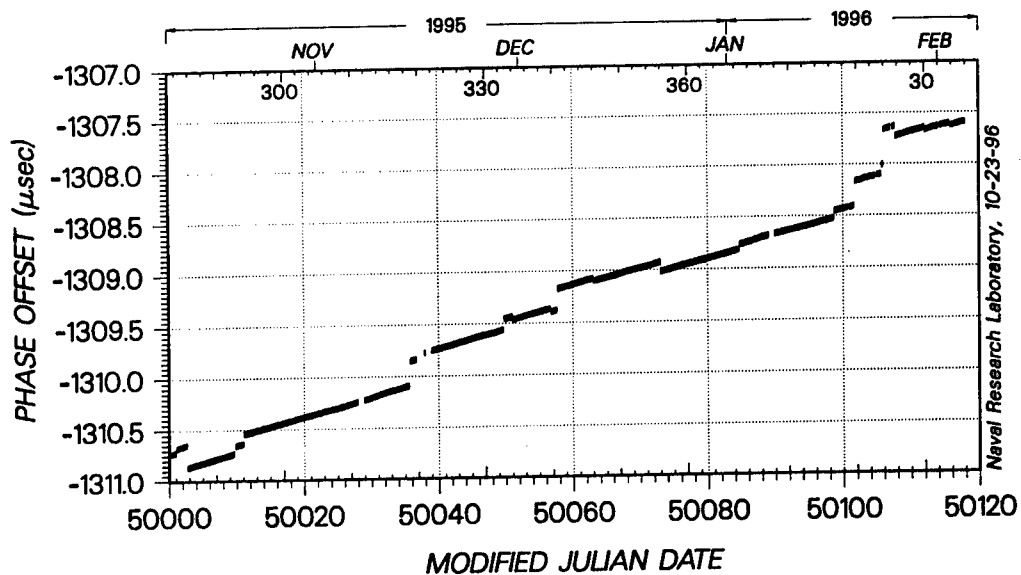


Figure 3

**PHASE OFFSET OF NAVSTAR 29 CESIUM CLOCK FROM
Washington, D.C. Time Reference Using
Colorado Springs Observations**

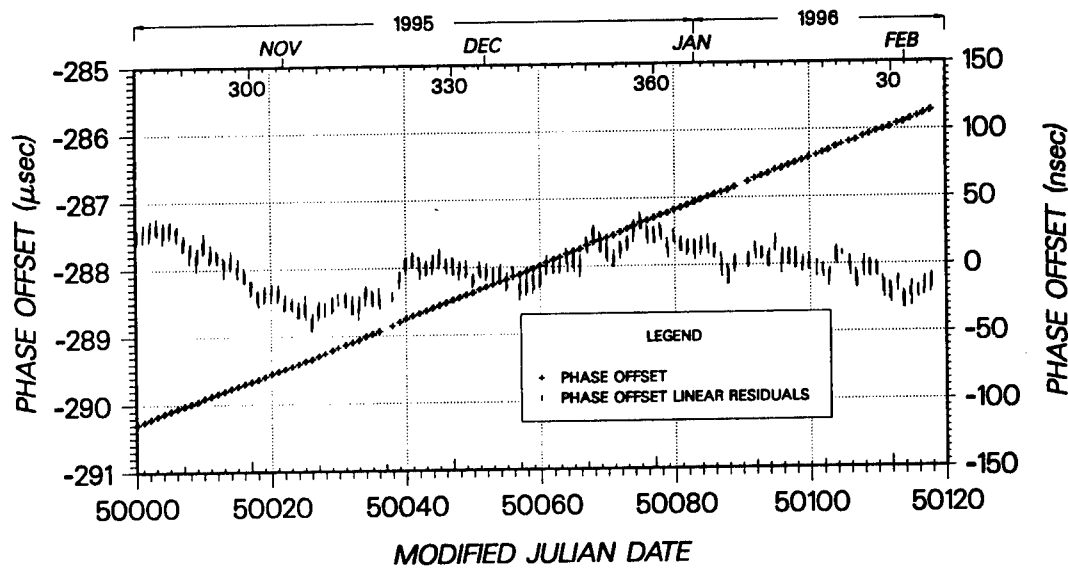


Figure 4

PHASE OFFSET OF NAVSTAR 29 CESIUM CLOCK FROM
Washington, D.C. Time Reference Using
Twelve Monitor Stations Observations
Raw Measurements

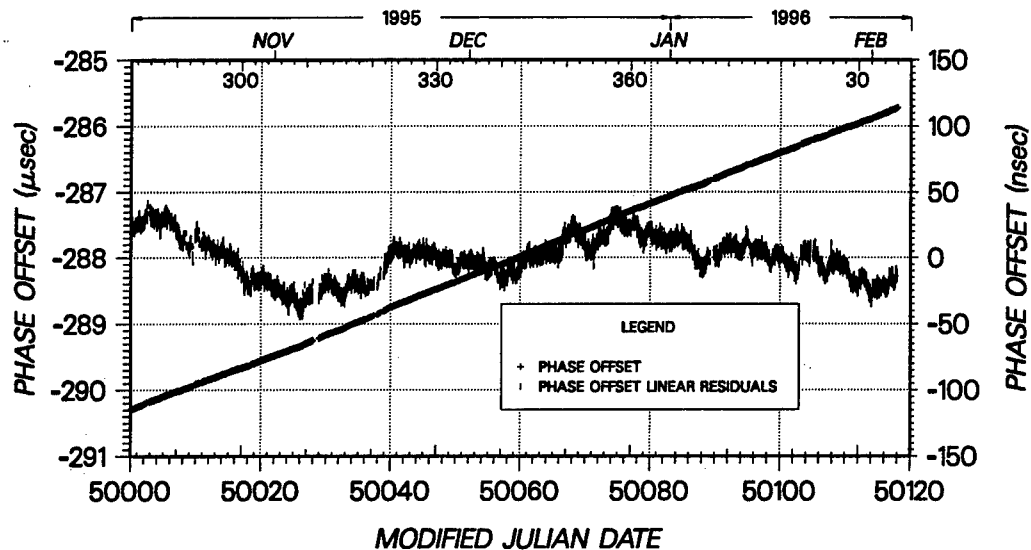


Figure 5

PHASE OFFSET OF NAVSTAR 29 CESIUM CLOCK FROM
Washington, D.C. Time Reference Using
Twelve Monitor Stations Observations
Smoothed Measurements

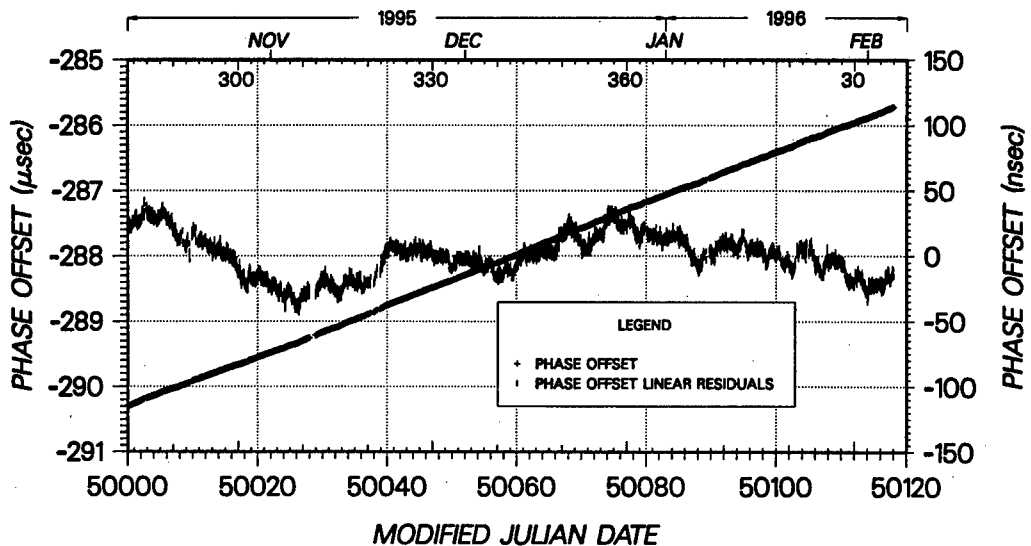


Figure 6

MEASUREMENT NOISE OF NAVSTAR 29 PHASE OFFSET FROM
Washington, D.C. Time Reference Using
Twelve Monitor Stations Observations

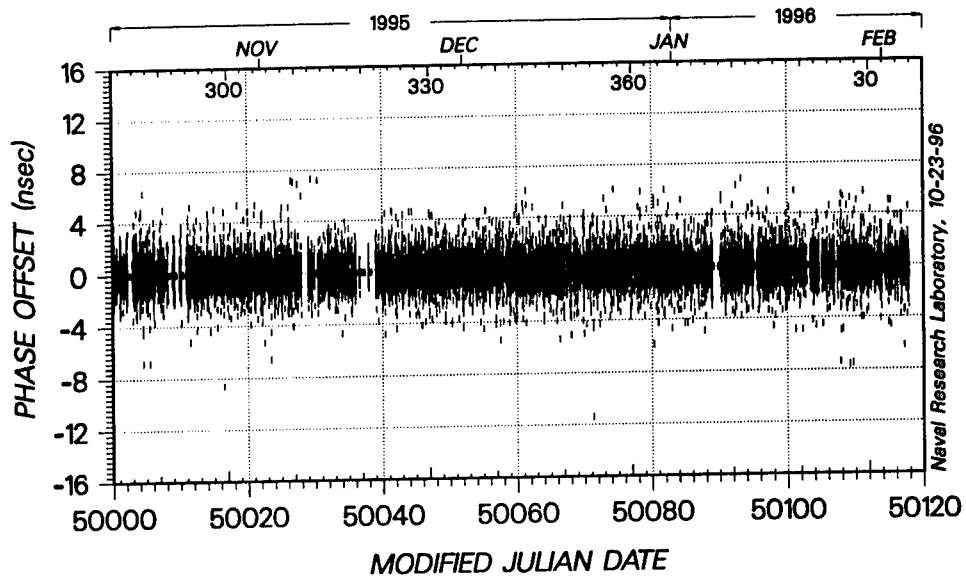


Figure 7

EMPIRICAL PROBABILITY DENSITY FUNCTION OF
MEASUREMENT NOISE OF NAVSTAR 29 CLOCK OFFSET FROM
Washington, D.C. Time Reference

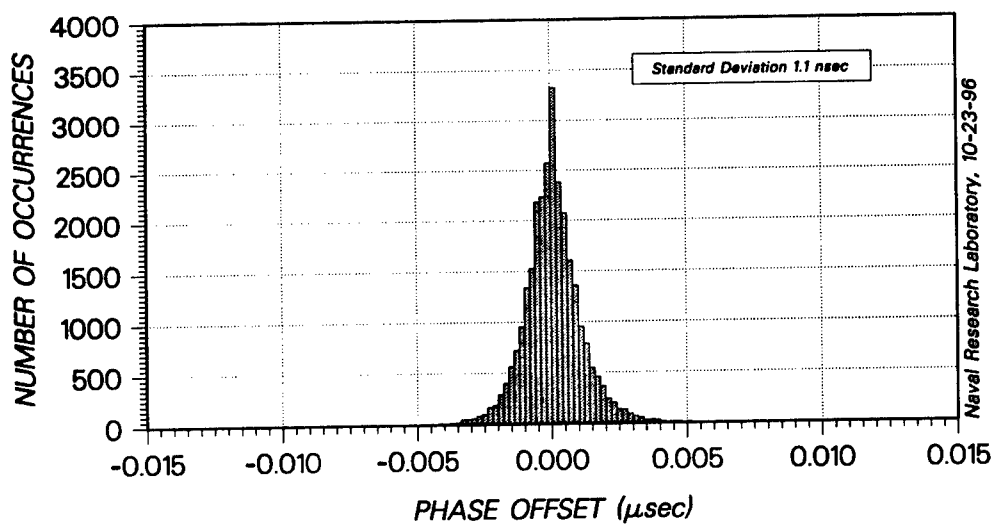


Figure 8

**NORMALIZED INTEGRATED PERIODOGRAM OF
NAVSTAR 29 CONTINUOUS COVERAGE MEASUREMENT NOISE**

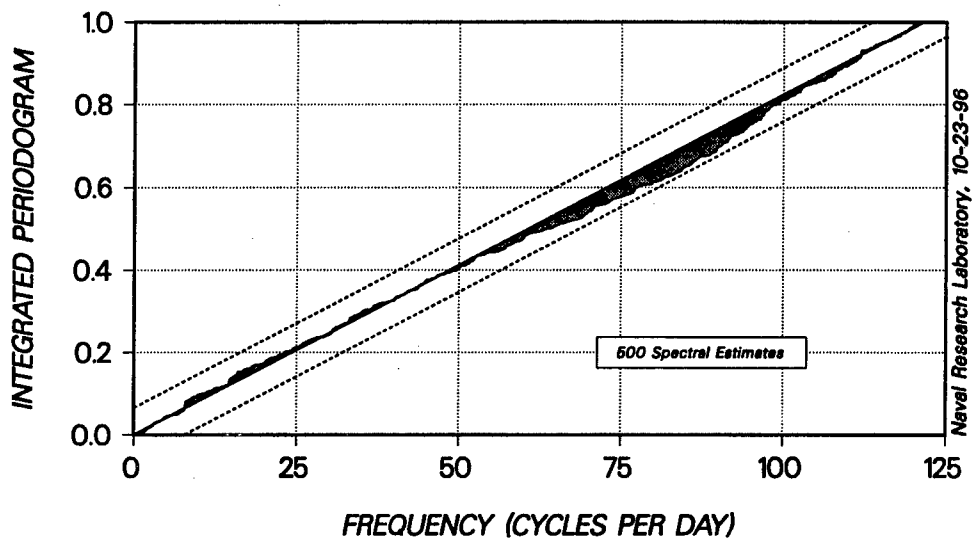


Figure 9

**FREQUENCY OFFSET OF NAVSTAR 29 CESIUM CLOCK FROM
Washington, D.C. Time Reference Using
Twelve Monitor Stations Observations**

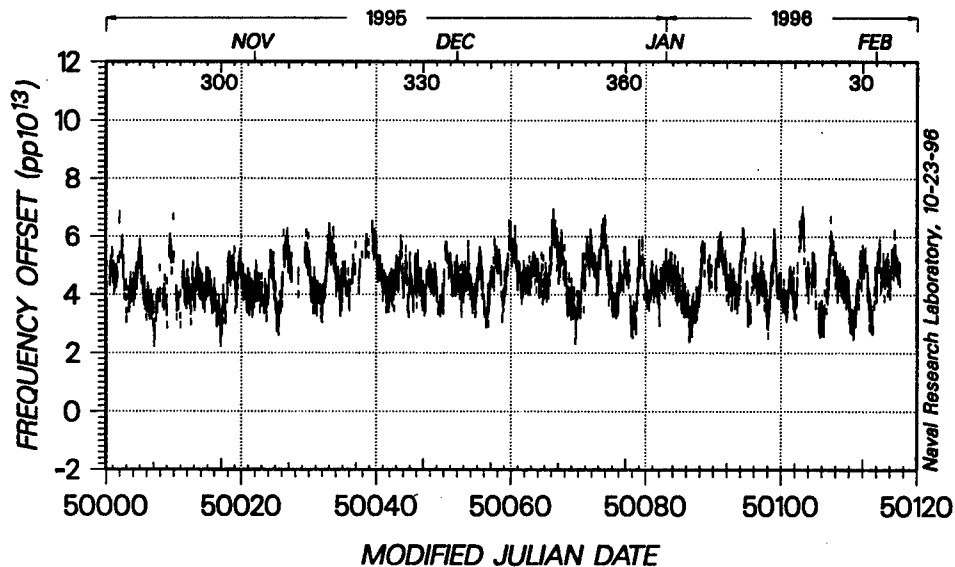


Figure 10

FREQUENCY OFFSET OF NAVSTAR 29 CESIUM CLOCK
*Comparison of Continuous Coverage and
 Direct Measurements*

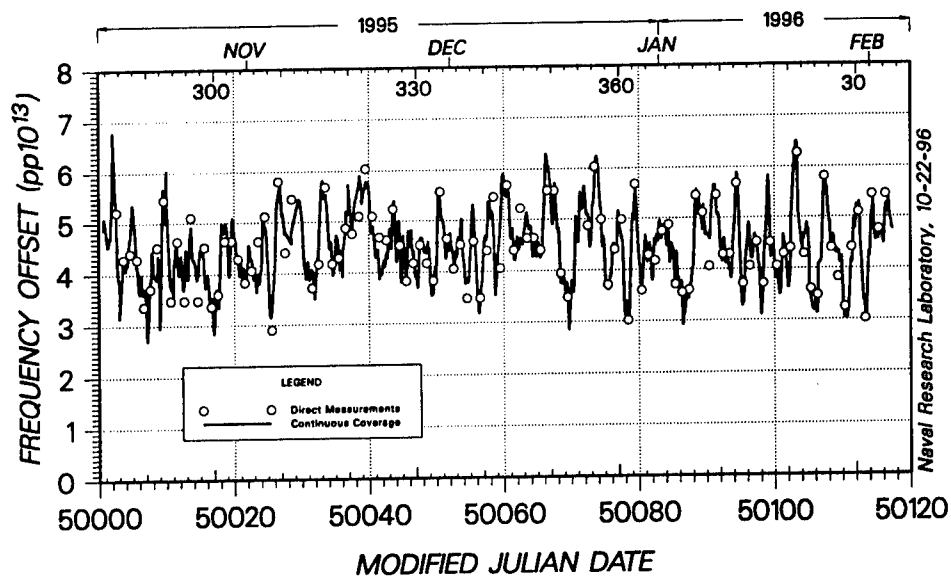


Figure 11

**FREQUENCY STABILITY OF NAVSTAR 29 CLOCK OFFSET FROM
 Washington, D.C. Time Reference Using
 Continuous Coverage
 10-OCT-95 to 5-FEB-96**

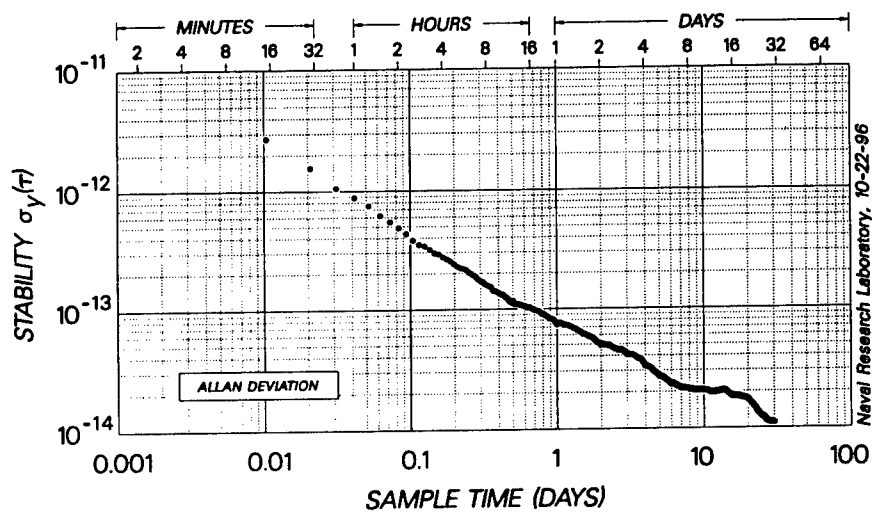


Figure 12

1996 GPS TIME TRANSFER PERFORMANCE

1Lt Jeffrey D. Crum, USAF
2d Space Operations Squadron
300 O'Malley Avenue, Ste. 41
Falcon AFB, Colorado 80912-3041, USA

Abstract

The requirements for GPS time transfer accuracy are more demanding than ever before. The Operational Control Segment has responded, providing a consistently accurate signal to the user community. This paper presents a summary of GPS Time Transfer performance for 1996 and offers several theories for the continued improved performance. Refined techniques in the areas of MCS satellite clock estimation and monitor station clock performance assessment are two areas with significant impact to GPS time. As historical perspective, 1995 time transfer performance is compared to the current year's data.

INTRODUCTION

Time transfer performance is a description of how accurately users can obtain Coordinated Universal Time (UTC) by tracking GPS satellites and using the timing information found in subframe 4, page 18 of the navigation message.^[1] This timing information includes:

- the accumulated leap seconds between GPS and UTC
- the effective date of a planned change in leap second count
- the GPS-UTC bias and drift estimates.

In accordance with a recent revision of ICD-GPS-202, the time transfer error of UTC(GPS) must be less than 28 nanoseconds (1σ).^[2] In other words, any authorized (PPS) user of the GPS navigation message must be able to correct to UTC to within 28 nanoseconds. Furthermore, the GPS time scale must be maintained to within 1 microsecond of UTC time, once the correction for leap seconds has been made.^[1] The data presented below will illustrate that GPS time transfer in 1996 performed well within these limits.

THE YEAR IN REVIEW

The United States Naval Observatory (USNO) provides daily timing information to the 2d Space Operations Squadron (2 SOPS), located at Falcon AFB, CO. Included in this information is the previous day's time transfer performance. This performance is represented by several values. First is the GPS-UTC AVGERR, a daily average of the UTC(GPS) - UTC(USNO) time difference for the GPS constellation. This value is obtained from up to 84 thirteen-minute,

single-satellite tracks by the operational USNO STel receiver. Associated with this value is the standard deviation from the AVGERR of the measurements used to determine the average. This value is labeled SIGMA. The RSS of the AVGERR and SIGMA produces the time transfer RMS for the previous day. This value is essentially an RMS of all of the UTC(GPS) - UTC(USNO) time difference errors for the previous day, and is the most reliable available indication of whether or not GPS is meeting the ICD-GPS-202 specification of 28 ns time transfer error.

Figure 1 shows a plot of the daily time transfer RMS and the associated AVGERR. The performance for 1996 marks a new milestone in the GPS program. For the first time ever, the GPS time transfer RMS for the year is below 10 ns. From 1 January 1996 - 1 November 1996, the time transfer RMS was an impressive 9.58 ns. At no point did errors exceed 20 ns, a testament to the dedication of, and the coordination between, the 2 SOPS operations crews and USNO Time Service personnel. The reader will note that Figure 1 includes four highlighted points of interest that will be explained below.

The year's highest daily time transfer RMS, 19.65 ns, occurred on 15 January 1996 (96015). On that date, SVN20/PRN 20 experienced a failure of its operational frequency standard. This failure was preceded by an abrupt change in phase and frequency which resulted in erratic ranging errors and degraded time transfer. The USNO receiver happened to track SVN 20/PRN 20 during this anomaly, and as a result the time transfer values for that day were unusually large.

There are three other points of interest in the Figure shown, labeled with the dates of occurrence. On 18 May 1996 (96139) the time transfer RMS was 12.21 ns. Under most circumstances, a time transfer value of this magnitude causes little concern. At the time of occurrence, however, the RMS had remained consistently below 10 ns for more than 20 days, and had reached as low as 7 ns on three separate occasions. Further investigation revealed that problems with an environmental chamber had caused a 2 to 3 ns/day runoff in UTC(USNO). Once detected and corrected, time transfer again returned to its sub-10-ns performance.

The spikes labeled on 4 August 1996 (96217) and 28 August 1996 (96241) were each due to single satellite anomalies concurrent with USNO receiver set tracking times. In the first instance, SVN 16/PRN 16 experienced platform stability problems. In the case of SVN 40/PRN 10, the newly activated rubidium frequency standard exhibited instability characteristic of a new rubidium clock.^[3] The instability on SVN 40 eventually required 2 SOPS analysts to set the navigation signal unhealthy for almost 3 days.

Despite the four instances outlined above, time transfer for 1996 set a new standard. For historical perspective, the same performance statistics are plotted for 1995 in Figure 2. The time transfer RMS for the time period 1 January 1995-1 November 1995 was 10.60 ns.

Figure 3 also illustrates the improved performance of time transfer from 1995 to 1996. This composite plot of the GPS-UTC values from 1 January 1995-1 November 1996 shows that 2 SOPS has remained well within the one microsecond requirement mandated by ICD-GPS-200.^[1] The large offset at the beginning of 1995 was due to a timing anomaly with the Colorado Springs Monitor Station (COSPM). This event was explained in detail in Capt. Steven T. Hutsell's 1995 PTTI paper, *"Ideas for future GPS timing improvements."*^[4]

THEORIES FOR IMPROVED PERFORMANCE

The operation of the GPS constellation is a very dynamic process. The operators and analysts of the 2 SOPS and outside agencies are constantly trying to improve upon the accuracy of the system. Their efforts include not only improving upon existing processes, but also establishing new operating principles based on lessons learned from anomalous conditions. This section will present examples of both refined techniques and new processes that have contributed to the improvement of GPS time transfer.

One of the most significant areas of recent improvement is the tuning of satellite clock estimation in the MCS Kalman filter. This process was presented to the community in December 1994 by Capt. Steven T. Hutsell in his paper, *"Fine tuning GPS clock estimation in the MCS."*^[5] The process of reviewing and updating process noise values for each of the operational on-orbit frequency standards continues on a quarterly basis. The result has been a significant improvement on the stability of GPS time. Figure 4 shows the Allan deviation plot for GPS time in 1995 and 1996. The efforts of the Naval Research Laboratory and the 2 SOPS deserve much of the credit for this improvement in stability.

In addition to the efforts to optimize satellite clock performance, analysts have taken measures to ensure that Monitor Station clock performance is also optimized. A series of hardware problems at the remote sites forced analysts to explore methods to minimize the impact of adverse conditions on the GPS time scale. The challenges presented themselves in the form of failed air conditioning units, which caused rapid fluctuations in both temperature and humidity. The effects of these changes have been shown to severely destabilize the HP 5061 cesium frequency standard.^[6] All four remote Air Force Monitor Stations use the HP 5061 cesium frequency standard. Since each Monitor Station clock is weighted roughly 10% (long-term) in the GPS composite clock, the effects of such conditions must be mitigated to protect the integrity of the GPS time scale. Analysts now have developed a knowledge base of how to detect and react to such conditions in such a way as to minimize the effect of substandard environmental conditions. The result has been a more robust and dynamic time scale, and improved time transfer performance.

One of the most recent timing improvements was the addition of the USNO Alternate Master Clock (AMC). The AMC is co-located with the MCS at Falcon AFB. This facility utilizes up to 12 HP 5071A Cesium frequency standards and up to three Sigma Tau hydrogen masers, and two "master clocks," AMC #1 and AMC #2, respectively. AMC #1, the operational reference, is steered to the DoD Master Clock at USNO via two-way time transfer. More importantly to the 2 SOPS, however, AMC #1 also provides the 5 MHz timing signal to the Colorado Springs Monitor Station (COSPM). COSPM now has an even more stable and more accurate signal than any of the other four Air Force Monitor Stations. Consequently, COSPM receives approximately 20% long-term weighting in the GPS composite clock. The connection of the AMC to COSPM was completed on 12 September 1996, so only preliminary data are available as of this writing.

Another improvement is the active pursuit of an optimum partitioning strategy. The disposal of the last Block I satellite and the successful launches of three new Block IIA satellites have required a constant review of the Kalman filter's estimating partitions. Following guidelines established in July 1993 by 2 SOPS analysts Capt. Dave Malinowski and 1Lt Bill Witwicki, system experts have ensured partitions are optimized for stability and monitor station visibility.^[7] This process will continue as GPS enters a new era with the first of several Block IIR satellite launches, scheduled to begin in January 1997.

Thanks to the efforts of both 2 SOPS and USNO personnel, the download of daily timing

data is a much more reliable process. Prior to 20 Oct 95, 2 SOPS operators would obtain the daily GPS-UTC offset and the previous day's time transfer performance via a Zenith Z-248 PC connected to a modem and a Guardsman encryption/decryption device. This setup was often unreliable, and the download was often delayed several hours.^[4] Since that time, however, the download hardware has been upgraded to a 486 Zenith PC connected to a keyed Secure Telephone Unit (STU-III). A PROCOMM PLUS[®] script automates the dialing and file transfer, greatly improving the reliability of the download. The result is a more consistent daily input of the GPS-UTC data.

CONTINUED IMPROVEMENTS

For the past several years, the focus of most efforts to improve GPS accuracy has been related to timing. As methods such as the ones outlined above have been implemented, errors that were once in the noise level have begun to emerge. Several presentations at the Performance Analysis Working Group (PAWG) in August 1996 highlighted periodic errors affecting GPS performance.^[8,9,10,11] Since ephemeris and clock state estimation are intrinsically linked within the MCS Kalman filter process, the removal of these periodics should further improve time transfer. An effort is currently underway to identify possible error sources and remove them in a safe and efficient manner.

The Block IIR program will introduce the latest technology in GPS timing. Ground testing of the EG&G rubidium frequency standard, the primary timing source for all Block IIR satellites, has produced some impressive results. The Naval Research Lab has provided Hadamard deviation plots for the EG&G Block IIR Engineering Design Model rubidium oscillator Serial No. 4 which show that the stability for a sample time of one day was $2 \cdot 10^{-14}$.^[12] Such performance is encouraging and could signal the breakthrough to the next level of GPS time transfer performance.

CONCLUSION

GPS time transfer for 1996 has established a new standard in performance. The analysts of the 2 SOPS and the outside agencies that support the mission will continue to strive for a more stable and accurate signal. The improvements summarized above will spawn new ideas for ways to safely contribute to the most stable and accurate GPS timing signal ever.

ACKNOWLEDGMENTS

The author would like to thank the following people and agencies for their generous assistance with both our timing improvements and this paper:

Steven T. Hutsell, USNO/AMC
Francine Vannicola, USNO
Jim Buisson, Antoine Enterprises, Inc.
Bill Bollwerk, USNO/AMC
Paul Wheeler, USNO
Paul Koppang, USNO
The men and women of the 2 SOPS.

REFERENCES

- [1] ICD-GPS-200, Revision C, 10 October 1993.
- [2] ICD-GPS-202, Revision A (draft), 23 September 1996.
- [3] G.L. Dieter, and G.E. Hatten 1996, "*Observations on the reliability of rubidium frequency standards on Block II/IIA GPS satellites*," Proceedings of the 27th Annual Precise Time and Time Interval (PTTI) Applications and Planning Meeting, 29 November-1 December 1995, San Diego, California, USA (NASA CP-3334), pp. 125-134.
- [4] S.T. Hutsell 1996, "*Ideas for future GPS timing improvements*," Proceedings of the 27th Annual Precise Time and Time Interval (PTTI) Applications and Planning Meeting, 29 November-1 December 1995, San Diego, California, USA (NASA CP-3334), pp. 63-74.
- [5] S.T. Hutsell 1995, "*Fine tuning GPS clock estimation in the MCS*," Proceedings of the 26th Annual Precise Time and Time Interval (PTTI) Applications and Planning Meeting, 6-8 December 1994, Reston, Virginia, USA (NASA CP-3302), pp. 63-74.
- [6] R.L. Sydnor, T.K. Tucker, C.A. Greenhall, W.A. Diener, and L. Maleki 1990, "*Environmental tests of cesium beam frequency standards at the Frequency Standards Laboratory of the Jet Propulsion Laboratory*," Proceedings of the 21st Precise Time and Time Interval (PTTI) Applications and Planning Meeting, 28-30 November 1989, Redondo Beach, California, USA, pp. 409-420.
- [7] S.T. Hutsell 1994, "*Recent MCS improvements to GPS timing*," Proceedings of ION GPS-94, 20-23 September 1994, Salt Lake City, Utah, USA, pp. 261-273.
- [8] W. Feess, Menn, and Zeitzew 1996, "*OCS performance analysis*," Proceedings of PAWG-96, 21-22 August 1996, Peterson AFB, Colorado, USA.
- [9] W. Feess 1996, "*Observations of GPS time at USNO*," Proceedings of PAWG-96, 21-22 August 1996, Peterson AFB, Colorado, USA.
- [10] C. Chuck, S. McReynolds, T. Metzger, and J. Moore 1996, "*GPS MCS Kalman filter performance*," Proceedings of PAWG-96, 21-22 August 1996, Peterson AFB, Colorado, USA.
- [11] S. Malys 1996, "*Comparison of URE characterization methods*," Proceedings of PAWG-96, 21-22 August 1996, Peterson AFB, Colorado, USA.
- [12] W.G. Reid, and J.A. Buisson 1996, "*Performance of Block II rubidium clocks*," NRL Technical Note No. 5, 8 October 1996.

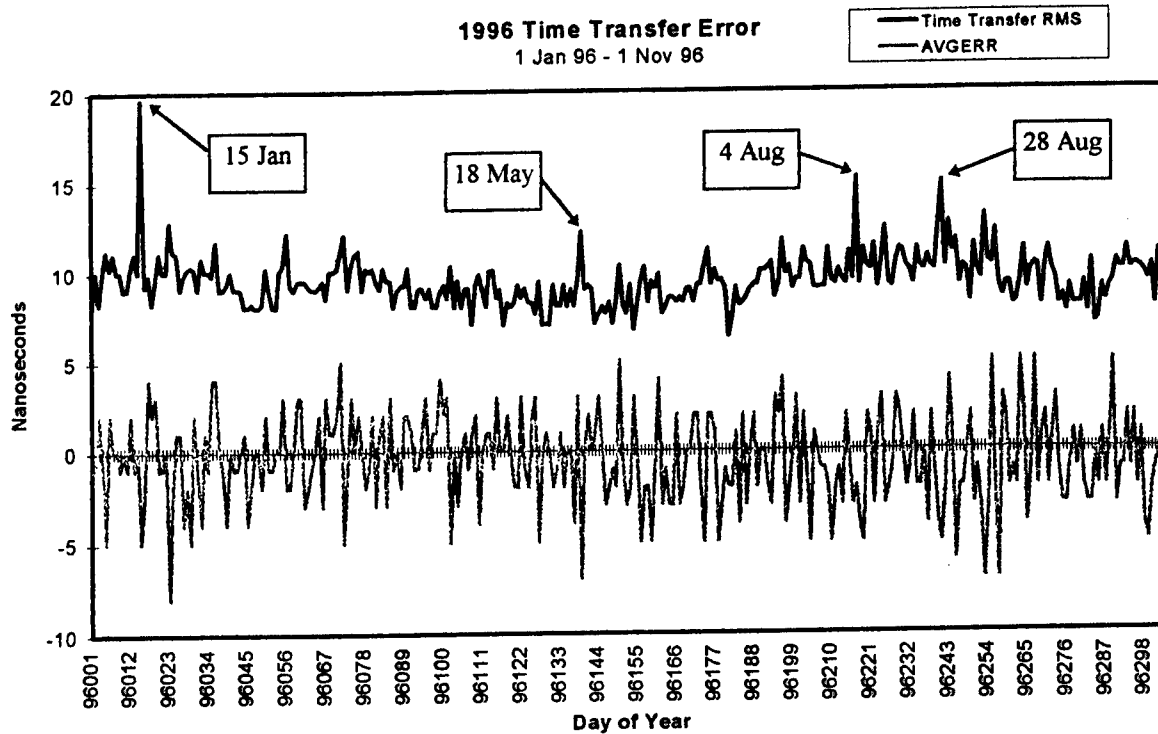


Figure 1: GPS Time Transfer: 1 Jan 96 - 1 Nov 96

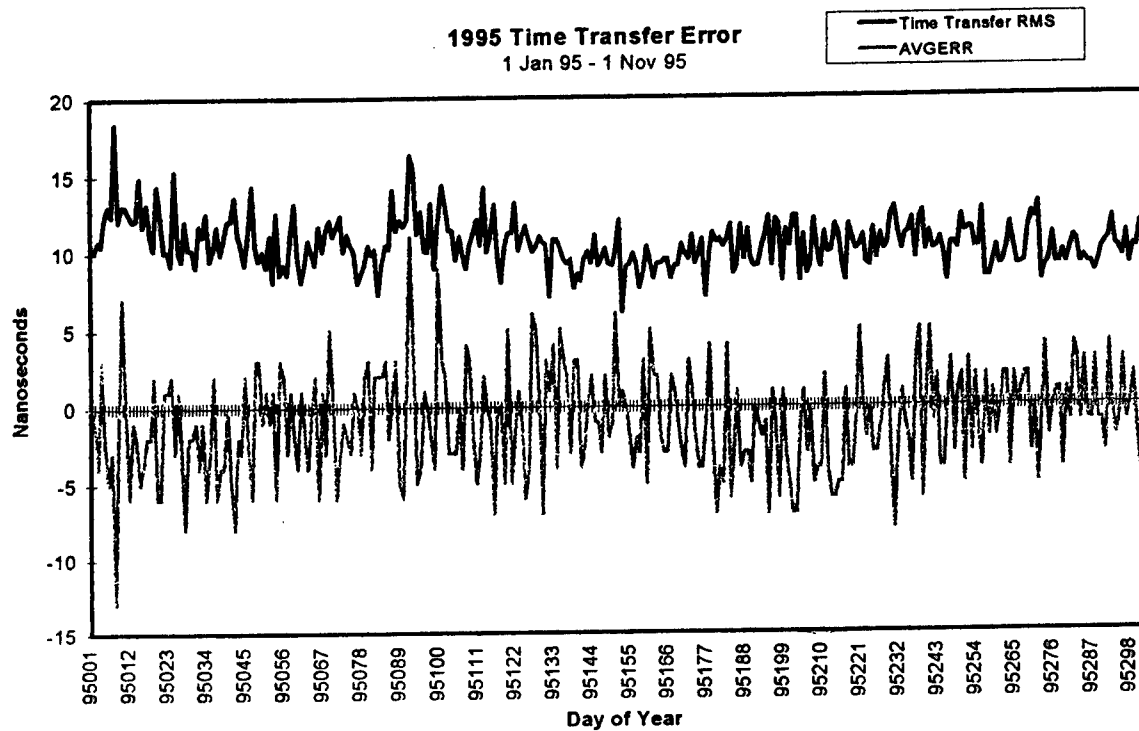


Figure 2: GPS Time Transfer: 1 Jan 95 - 1 Nov 95

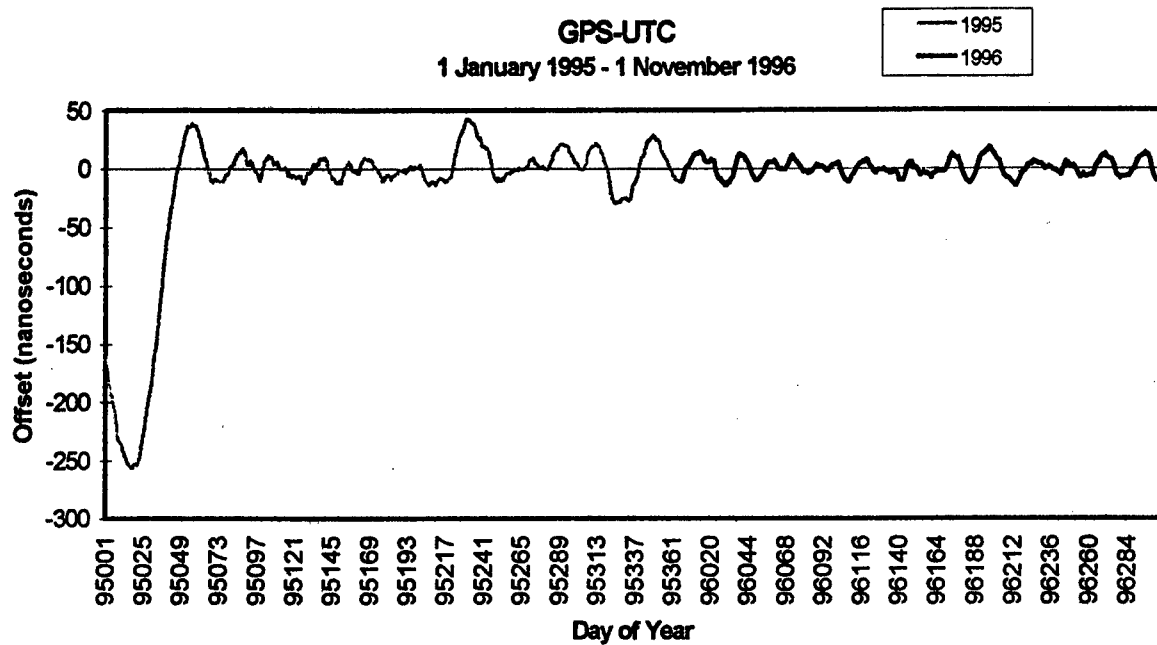


Figure 3: GPS-UTC, 1 Jan 95 - 1 Nov 96

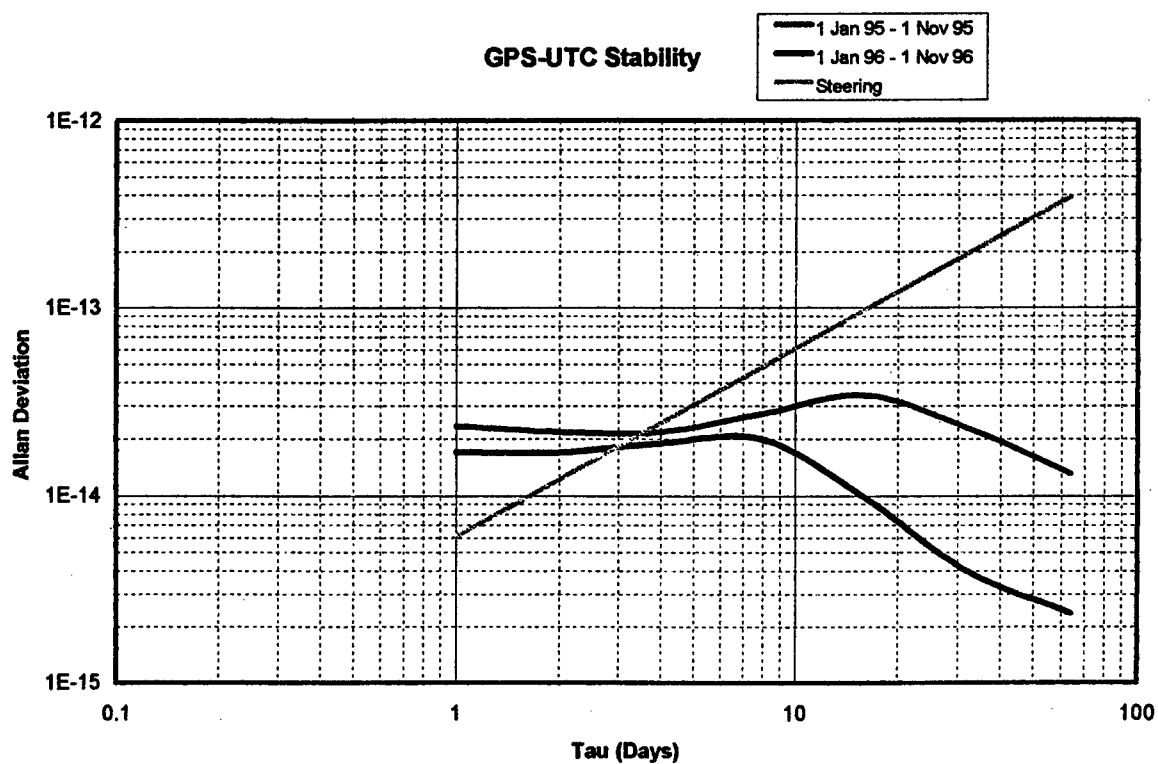


Figure 4: GPS Time Stability

Questions and Answers

RICHARD GRIFFIN (TEXAS INSTRUMENTS): You had mentioned the working group had had some errors. Not having an opportunity to attend that, could you just give a quick summary of what the top three or four major error sources are?

JEFFREY CRUM: Well, actually, that's one of the challenges facing us right now. We had probably at least five independent studies that were presented at the POG that identified kind of a periodic error affecting GPS performance. And yet at the same time, we didn't really have too many suggestions as to where that error was coming from or how we can help remove it.

So certainly if people have suggestions for places that we can start looking, we have an effort underway with some possible suggestions primarily dealing the ephemeris queuing on trying to mitigate the impact of that periodic. But we're certainly open to suggestions, and I think this is probably the right forum to ask for help.

DAVID ALLAN (ALLAN'S TIME): The 28-nanosecond sigma for UTC accuracy, is that a two-sigma accuracy number?

JEFFREY CRUM: That's just one sigma.

PERFORMANCE ANALYSIS OF THE GPS MONITOR STATION TIMING SUBSYSTEM ENHANCEMENT PROGRAM AT THE NAVAL RESEARCH LABORATORY

Ivan J. Galysh, Dwin M. Craig, and Wilson G. Reid
U.S. Naval Research Laboratory, Code 8152
4555 Overlook Ave. SW, Washington, DC 20375, USA

James A. Buisson
Antoine Enterprises, Inc.
Consultant to SFA, Inc.

Abstract

The U.S. Naval Research Laboratory designed, developed, and installed hardware and software for the GPS Monitor Station Timing Subsystem Enhancement (MSTSE) at the GPS Monitor Station (MS) located at the Kaena Point Satellite Tracking Station, Hawaii. From December 1995 to the present as part of the evaluation of the system, the U.S. Naval Observatory (USNO) has been performing time transfers through the Two Way Satellite Time Transfer portion of the MSTSE. It will be shown that the new cesium-beam frequency standard (CFS) HP5071 has been disciplined to the DoD Master Clock by the MSTSE during this period to within $\pm 3 \text{ pp } 10^{14}$. The phase measurement subsystem, of the MSTSE has, for the first time, allowed independent measurement of the two operational GPS Monitor Station HP5061 CFSs.

During June 1996 a modification was made to the MSTSE to reflect improvements in the system architecture developed during the initial evaluation period. This modification has increased system performance, improved reliability, and facilitated easy integration with future GPS Monitor Station improvements. This paper describes the equipment configuration and the test data collected after the installation of the MSTSE. Results are presented from data collected from June 1996 through October 1996.

INTRODUCTION

The GPS Monitor Station Timing Subsystem Enhancement project provides an improved timing subsystem to the existing GPS Monitor Station in Hawaii. In December 1995 the MSTSE was successfully installed at the Kaena Point Satellite Tracking Station located at Point Waiannae, Hawaii. Independent measurements of the two cesium-beam frequency standards (CFS) already at the Monitor Station have been taking place over the last 10 months. The HP5071 CFS in the MSTSE is the reference clock used for phase measurements of the two HP5061 CFSs. This HP5071 is also interfaced with the Two-Way Satellite Time Transfer (TWSTT) modem to enable remote syntonization of this CFS to the DoD Master Clock. In June of this year upgrades to

both hardware and software were made at the Hawaii site. The upgrade reflects improvements achieved subsequent to the initial deployment. The MSTSE now has better communication between the phase measurement system and the TWSTT modem. Network capability has been added that will facilitate easy integration of future GPS Monitor Station upgrades. The Hawaii MSTSE has demonstrated its ability to operate autonomously without operator intervention.

PURPOSE

The purpose of the MSTSE is to provide a very stable frequency source that is syntonized with the frequency of the DoD Master Clock. The MSTSE will provide a consistent frequency source independent of the quality of the cesium frequency standard being used. The stability of the standards varies and the MSTSE eliminates the need to selectively choose a standard.

SYSTEM CONFIGURATION

Figure 1 shows a block diagram of the hardware configuration. The MSTSE receives two 5 MHz signals from the Frequency Standard Element (FSE) rack through a fiber-optic interface. Figure 2 shows the photographs of the FSE rack and the MSTSE rack. The 5 MHz signals from the FSE rack are sent through distribution amplifier modules to the auto switch and to the dual mixer. The primary frequency standard is the HP5071. The 5 MHz signal is sent through a distribution amplifier module to the auto switch, to the dual mixer, and to the TWSTT modem. A 10 MHz signal from the HP5071 is used as a reference for the dual mixer.

The MSTSE configuration was designed to provide an open systems architecture. The system was designed based on the client/server model. Figure 3 shows the software architecture. All communications between client tasks and server tasks are through network sockets. Network capability was added to the system to allow client and server tasks to communicate with each other independently of the computer on which they reside. This is a distributed computing environment.

Server tasks are programs that provide one interface between the hardware it controls and the client tasks. The server tasks have command sets for controlling the hardware and retrieving data. Since each server interfaces with a unique piece of hardware, most of the commands are unique for each server. Each server is assigned a unique network socket port. The servers wait for commands from client tasks by monitoring its network socket port for a command. Three servers currently exist in the MSTSE. They are the auto switch server, the cesium server, and the TWSTT server.

The client tasks are programs that communicate with the servers. The client tasks send and receive information using standard UNIX read and write commands. Establishing a communications interface with the servers is simply a matter of opening a socket port that the server monitors. The clients need only to know the socket port and on which computer the server resides. A configuration file on each computer in the MSTSE contains a list of the servers, where they reside, and their network socket port.

The auto switch is an electronic switch that can redirect any of its three inputs using computer control. An internal oscillator allows smooth transitions when switching from one input source to another. It also filters out any other phase discontinuities that may be generated. A 5 MHz signal from each of the cesium frequency standards is connected to the inputs of the auto switch. The hardware interface between the auto switch and the measurement computer

is through the industry standard architecture bus. The auto switch is controlled by the auto switch server. The server has a command set that allows client tasks to switch any of the three inputs to the output. An external control signal from the watchdog timer can do the same thing and override the auto switch server commands. The auto switch itself has the capability to detect signal failures and switch out the failed signal. At this time, the system is designed to cut off the output completely when the primary frequency standard exhibits any type of failure. The auto switch server has other commands to initialize the input channels and to retrieve the auto switch status.

The TWSTT modem has been upgraded from a 386-based computer running DOS to a 486-based computer running a UNIX operating system. A network interface module was added to interface with the measurement computer. The TWSTT modem uses the 5 MHz and 1 pps from the HP5071 for synchronization. It performs time transfers initiated by USNO once a day and passes the results to the measurement computer. The TWSTT is controlled by the TWSTT server. The command set has commands to control the operating modes of the TWSTT modem. Commands are available to retrieve the operating status of the TWSTT modem and all data generated.

The TWSTT modem and the dual mixer use the HP5071 as a frequency reference source. The HP5071 is controlled by the cesium server. The cesium server interfaces with the HP5071 through a serial communications interface. A command set is provided to control the HP5071 and to retrieve data from it.

The dual mixer is made up of three modules. The frequency offset module is a crystal oscillator with its frequency offset 10 Hz from 5 MHz. The crystal signal is mixed with the three 5 MHz signals from the cesium frequency standards in the zero-crossing detector module. A beat frequency of about 10 Hz is generated with each 5 MHz signal and is passed to the event counter module. The event counter counts the number of zero crossings and tags the time the zero crossings occur for each 5 MHz signal. The measurement computer collects the counts and time tags and calculates the phase differences between the MSTSE reference clock and the two HP5061 frequency standards used by the GPS monitor station. The phase differences are collected once an hour.

The computer module is a 486 computer with 16 Mbytes of RAM and a 500 Mbyte hard disk. It has two serial ports, a parallel port, and a built-in video controller. One serial port is used to communicate with the HP5071. The parallel port is used to control the watchdog timer.

The watchdog chassis has a timer circuit that will trip the alarm circuitry if the measurement computer does not send a pulse over the parallel port. The measurement computer under normal conditions sends a pulse once a minute. Another signal from the measurement computer parallel port is used to trip the alarm immediately if an error is detected. When the alarm is tripped, a signal is sent to the auto switch external control port to shutdown the output. The "GO/NOGO" status signal to the Monitor Station is asserted to indicate an error condition in the MSTSE.

VERIFICATION, VALIDATION, AND TESTING

For the MSTSE Project there are two objectives: (1) discipline the frequency of the Monitor Station reference clock to stay within specified limits and (2) determine the quality of performance of the two Monitor Station HP5061 option 004 clocks and the MSTSE HP5071. Two-Way Time Transfer measurements between Hawaii and the DoD Master Clock began on a regular basis on 5 June 1996.

The clock configuration at the Hawaii Monitor Station consisted of the three cesium clocks connected to four channels of the measurement system: the HP5071 frequency standard (NRL S/N 449) in Channel A, an HP5061 frequency standard (AF S/N 281) in Channel B, an HP5061 frequency standard (AF S/N 194) in Channel C, and the same HP5071 frequency standard (NRL S/N 449) in Channel D. Data were observed once per hour. A dual-mixer system was used to measure the phase differences between each cesium clock.

This section compares the behavior of the disciplined HP5071 from two perspectives: (1) from the Two-Way Time Transfer between it and the DoD Master Clock, and (2) from the Linked Common-View Time Transfer between it and the DoD Master Clock. The offset in the latter case was obtained by summing the two data sets: (1) the linked Common-View Time Transfer from the DoD Master Clock to the Hawaii time reference, i.e., the HP5061 connected to Channel B of the clock quality measurement portion of the MSTSE, and (2) the offset between the HP5061 (Channel B) and the HP5071 (Channel A). The period covered by the report is from 5 June to 30 August 1996.

Figure 4 is the offset of the disciplined clock (HP5071 Channel A) from the Hawaii time reference (HP5061 Channel B) with a mean of -4.5 microseconds removed. The residuals of a linear fit to these data are presented in Figure 5, which shows the detailed structure of the data. Figure 6 is the offset of the Hawaii time reference (HP5061 Channel B) from the DoD Master Clock determined by Linked Common-View Time Transfer with a mean of 190 microseconds removed. The time reference at the Defense Imagery and Mapping Agency Monitor Station in Washington D.C. (whose measurements were used in the Linked Common-View Time Transfer) has accumulated a phase bias with respect to the DoD Master Clock as the result of arbitrary steps in the phase due to local station power outages. The detailed structure of these data can be seen in Figure 7, which are the residuals of a linear fit to the data in Figure 6. In summing the two data sets, i.e., the data in Figures 4 and 6, the Hawaii time reference drops out, leaving the offset of the disciplined clock from the DoD Master Clock except, as noted, for an arbitrary bias in the phase.

In Figure 8 is shown the mean residuals of the offset between the disciplined clock and the DoD Master Clock determined by both the Two-Way and the Linked Common-View Time Transfer. A discontinuity of -17 nanoseconds can be seen to have occurred on 15 July 1996 in the data from the Two-Way Time Transfer. USNO replaced a VSAT drawer on that date in the master TWSTT modem which coincides with the 17 nanosecond correction. Using the corrected Two-Way Time Transfer data, the offset of the disciplined clock from the DoD Master Clock obtained from both the Two-Way and the Linked Common-View Time Transfer can be seen in Figure 9 to be very closely correlated except for the second member of a pair of improperly spaced measurements on day 50285.

The four-day average frequency corresponding to the one-hour samples of phase offset obtained from the Linked Common-View Time Transfer is shown in Figure 10. Superimposed on these measurements are estimates of the frequency determined by the MSTSE from fitting a straight line to four successive measurements of the phase offset obtained by Two-Way Time Transfer at nominal 1-day intervals. The correlation between the Two-Way and the Linked Common-View Time Transfer is excellent.

The size and time of occurrence of the frequency tunes made to discipline the HP5071 clock are plotted in Figure 11. The first tune of $2.19 \text{ pp } 10^{13}$ was a jam syntonization triggered by initialization of the MSTSE. The tunes clustered in mid-July resulted from the phase discontinuity introduced by the Naval Observatory on 15 July. Twenty-two days can be seen to have elapsed in August during which time no tunes were required.

The estimates of the frequency of the disciplined clock determined by the MSTSE are reproduced in Figure 12 with the tuning goal of $\pm 3 \text{ pp } 10^{14}$ superimposed. Again, the initial frequency is offset by $-2.19 \text{ pp } 10^{13}$ because of the initialization of the MSTSE. The jam syntonization quickly brings the frequency of the clock to within the tuning goal. For the entire 128 days the frequency remained at or within the tuning goal except for one day in mid-July following the induced phase discontinuity.

Such close agreement between the Two-Way Time Transfer with subnanosecond accuracy and the Linked Common-View Time Transfer with subnanosecond precision provides strong validation of both methods. Furthermore, the precision of the Linked Common-View Time Transfer enabled identification of an anomaly in the Two-Way Time Transfer.

CONCLUSIONS

The first field installation of the MSTSE successfully established feasibility of the concept. The ability to independently measure the currently deployed cesium clocks has provided verifiable data as to the operational health of the existing timing system. The deployed MSTSE is operating without the need for operator intervention. Automated data collection and cesium clock syntonization with the DoD Master Clock have been continuously performed. The MSTSE has provided a disciplined frequency to within $\pm 3 \text{ pp } 10^{14}$ which relates to $\pm 3 \text{ ns}$ in phase. Upgrades in the hardware, software, and network configuration have made the MSTSE ready for any additional Monitor Station implementations.

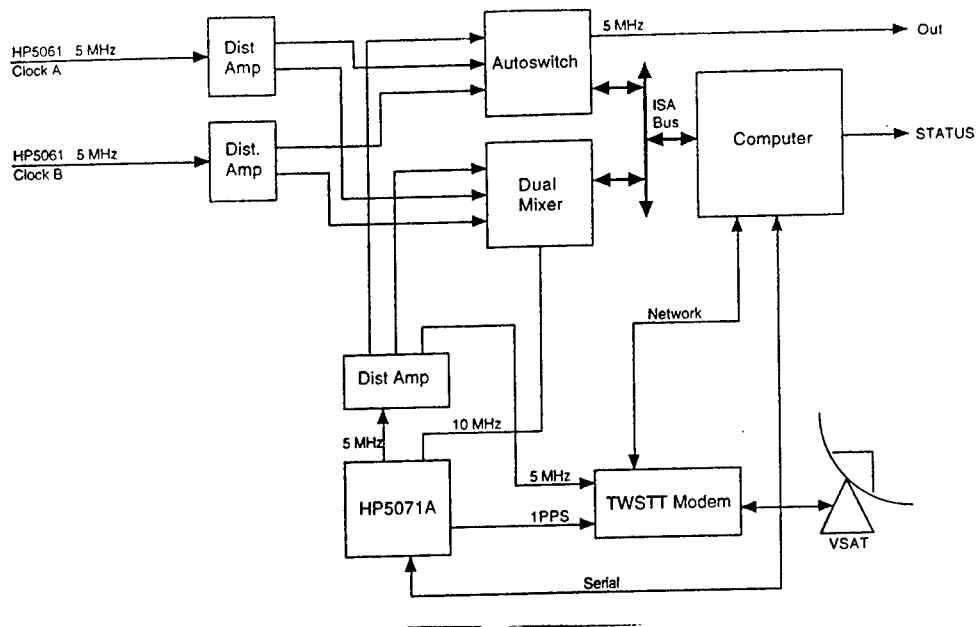


Figure 1. MSTSE hardware block diagram

Existing Frequency Standard Element (A6 Rack) and MSTSE (A12 Rack)
at the Hawaii GPS Monitor Station

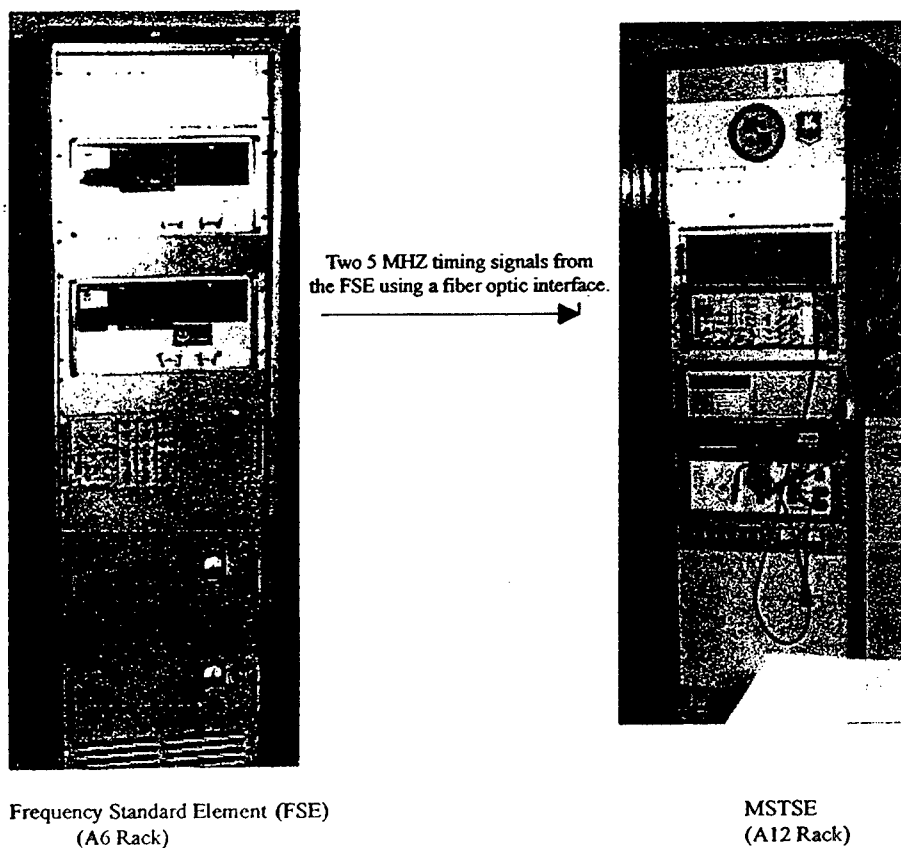


Figure 2. MSTSE rack and frequency standard element

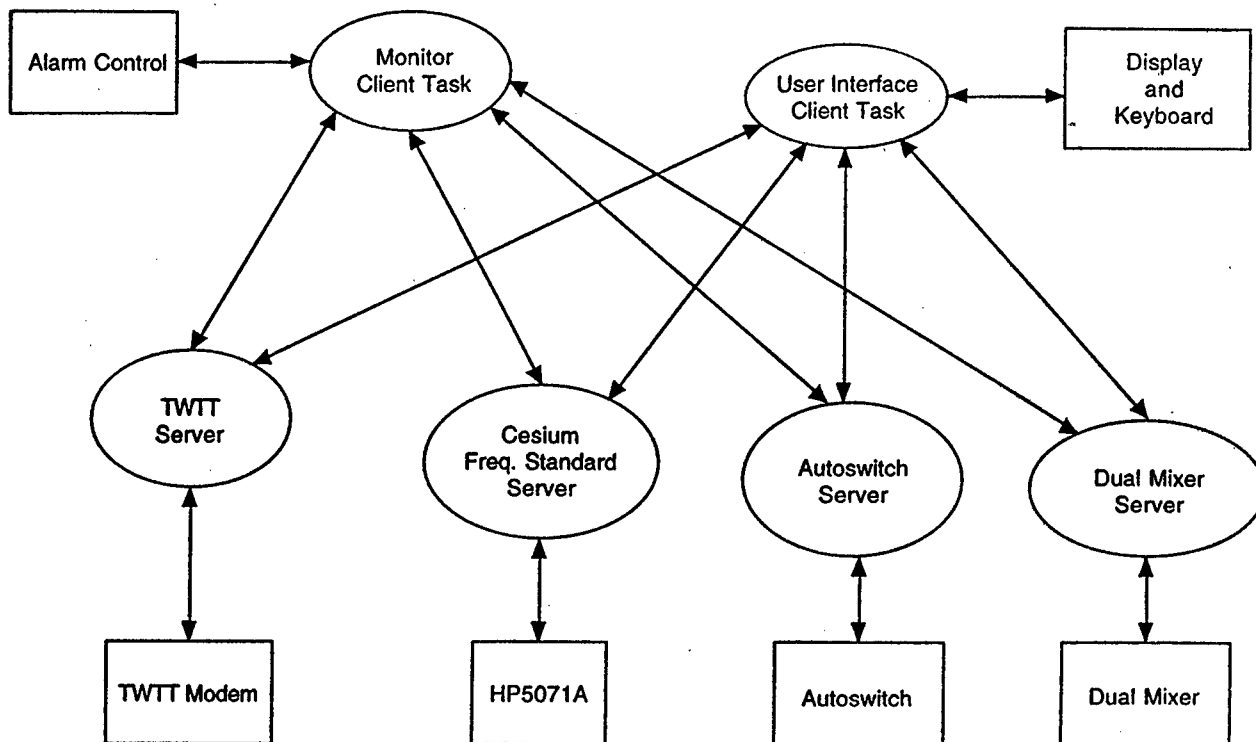


Figure 3. MSTSE software architecture

OFFSET OF THE HAWAII TIME REFERENCE FROM THE
DISCIPLINED HAWAII MSTSE CLOCK
CHANNEL A - CHANNEL B

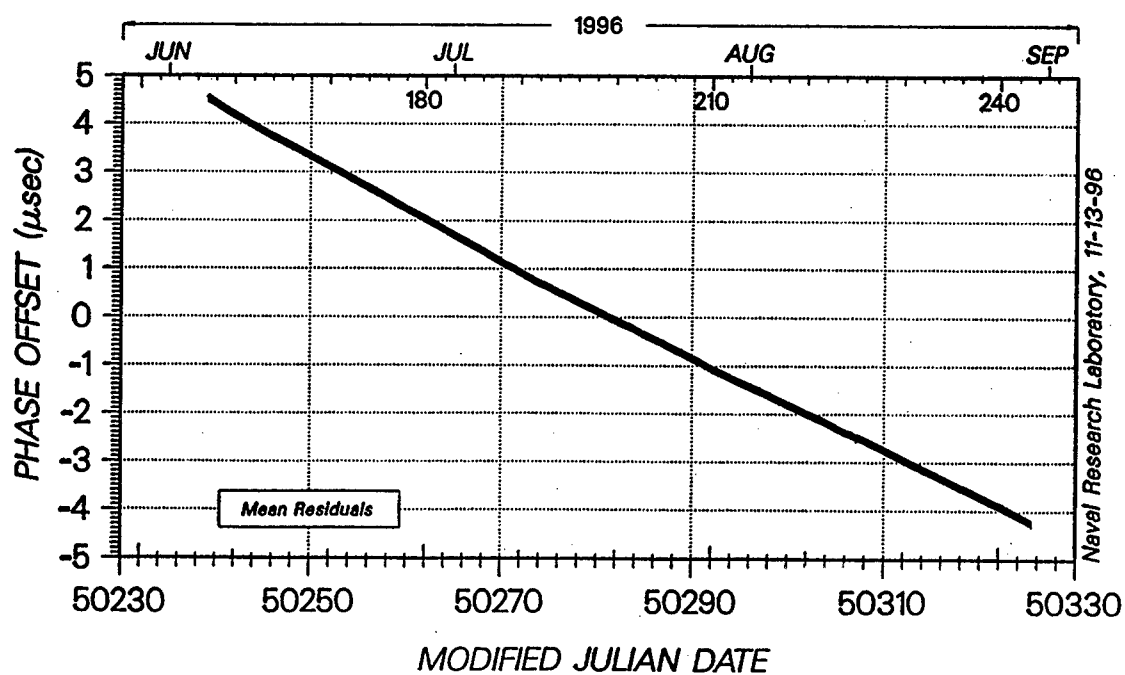


Figure 4

OFFSET OF THE HAWAII TIME REFERENCE FROM THE
DISCIPLINED HAWAII MSTSE CLOCK
CHANNEL A - CHANNEL B

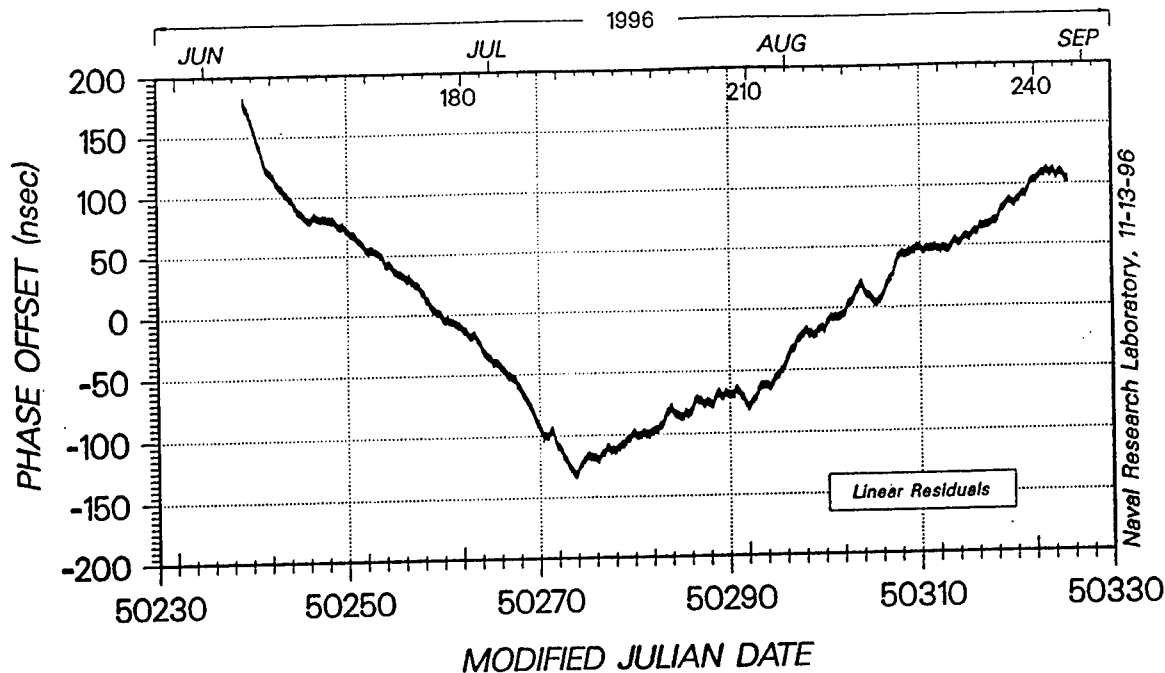


Figure 5

OFFSET OF THE HAWAII TIME REFERENCE FROM THE
DOD MASTER CLOCK USING
LINKED COMMON-VIEW TIME TRANSFER

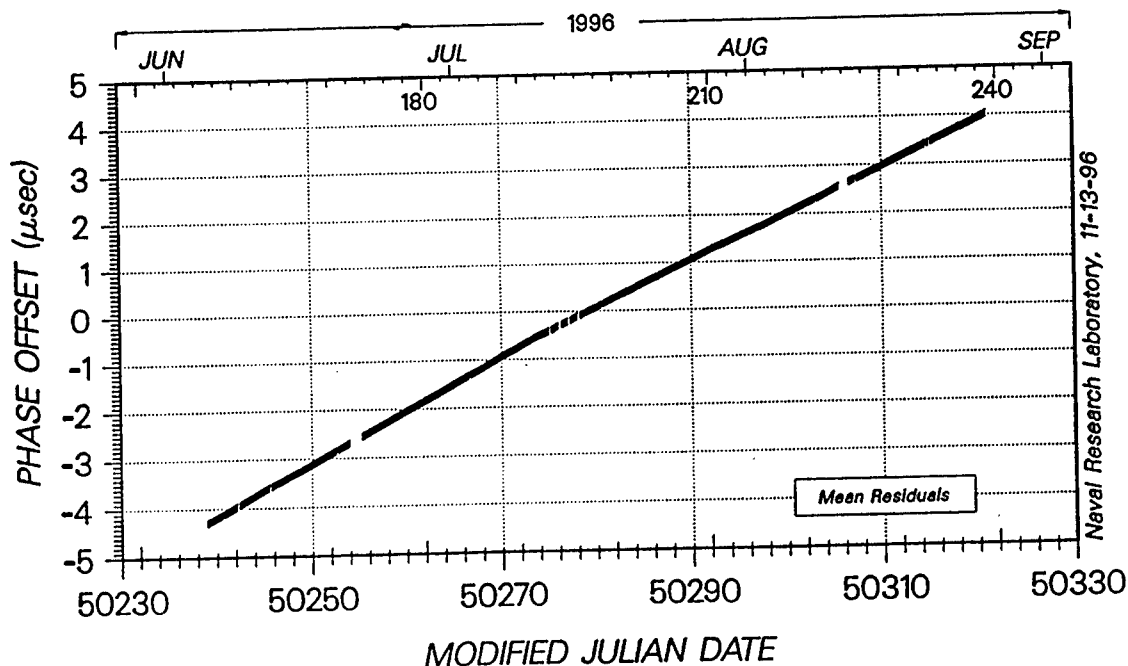


Figure 6

OFFSET OF THE HAWAII TIME REFERENCE FROM THE
DOD MASTER CLOCK USING
LINKED COMMON-VIEW TIME TRANSFER

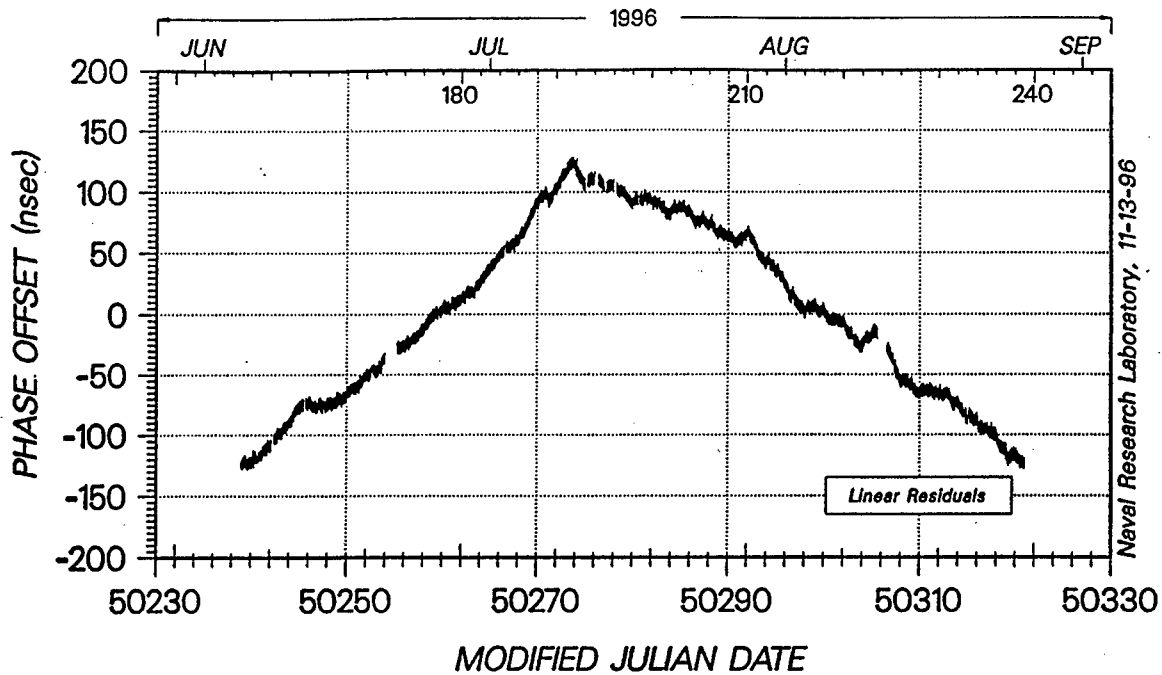


Figure 7

PHASE OFFSET MEAN RESIDUALS OF DISCIPLINED CLOCK FROM
DOD MASTER CLOCK USING
TWO-WAY TIME TRANSFER AND
LINKED COMMON-VIEW TIME TRANSFER

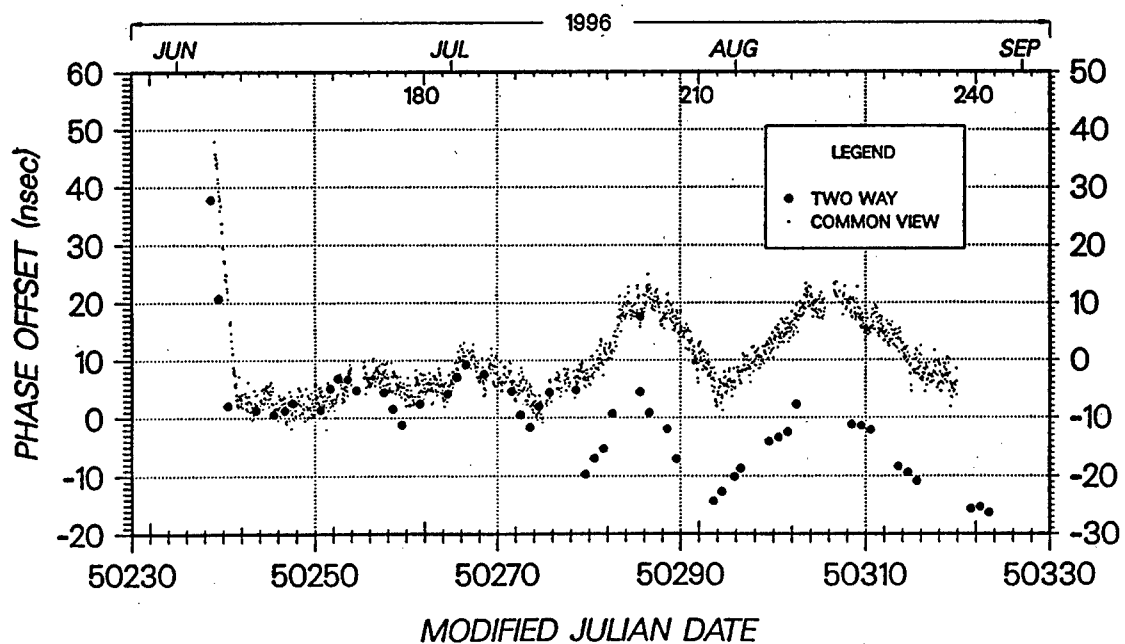


Figure 8

PHASE OFFSET MEAN RESIDUALS OF DISCIPLINED CLOCK FROM
THE DOD MASTER CLOCK USING
CORRECTED TWO-WAY TIME TRANSFER AND
LINKED COMMON-VIEW TIME TRANSFER

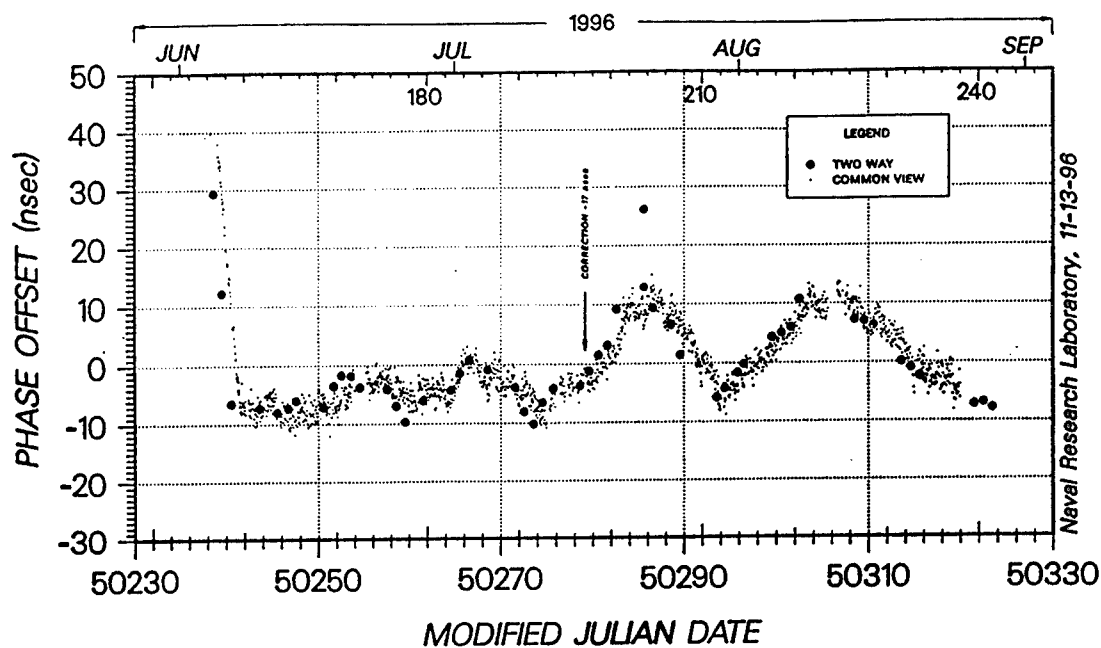


Figure 9

FREQUENCY OFFSET MEAN RESIDUALS OF DISCIPLINED CLOCK FROM
THE DOD MASTER CLOCK USING
TWO-WAY TIME TRANSFER AND
LINKED COMMON-VIEW TIME TRANSFER

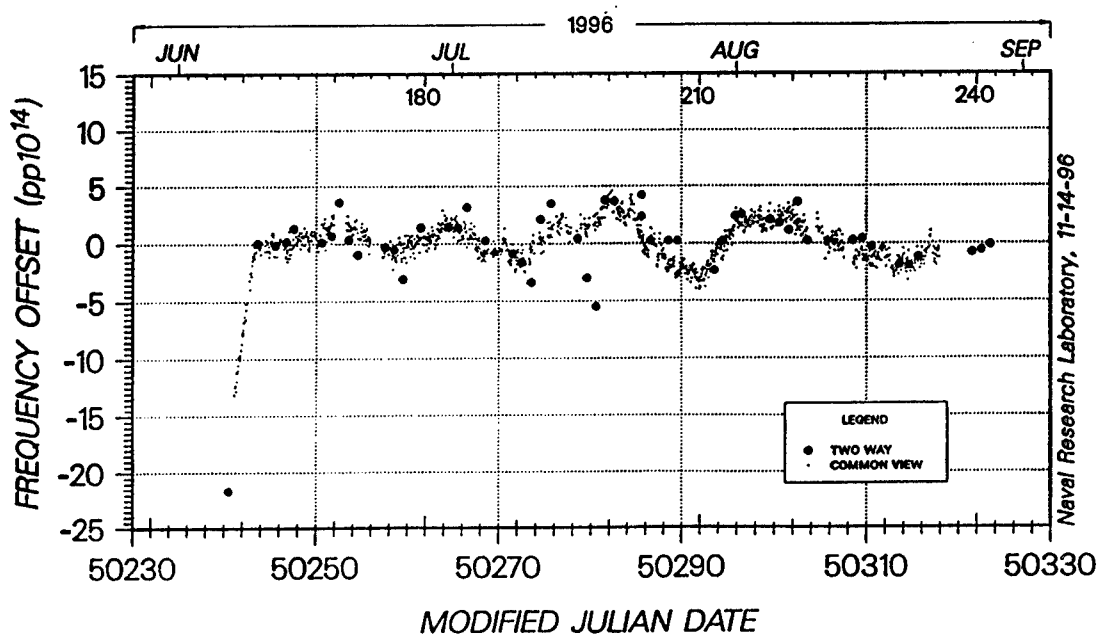


Figure 10
426

**FREQUENCY TUNES MADE TO THE DISCIPLINED HP5071 (S/N 449)
DETERMINED FROM TWO-WAY TIME TRANSFER BETWEEN
HAWAII AND THE DOD MASTER CLOCK**

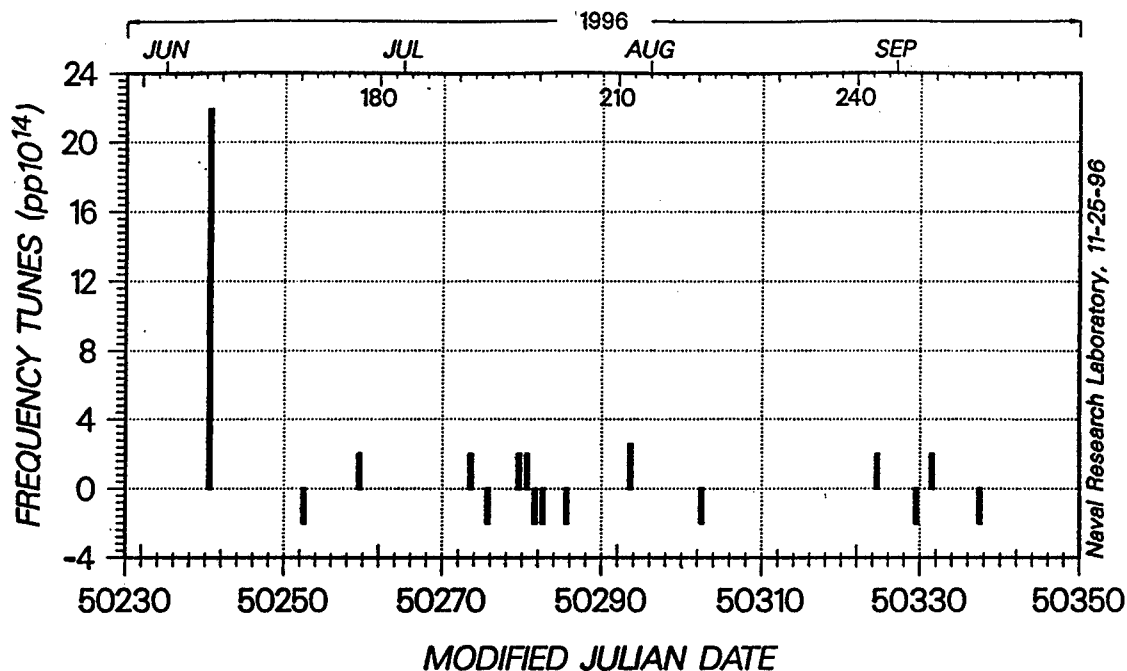


Figure 11

**FREQUENCY OFFSET OF THE DISCIPLINED HP5071 (S/N 449) FROM
THE DOD MASTER CLOCK DETERMINED BY
TWO-WAY TIME TRANSFER**

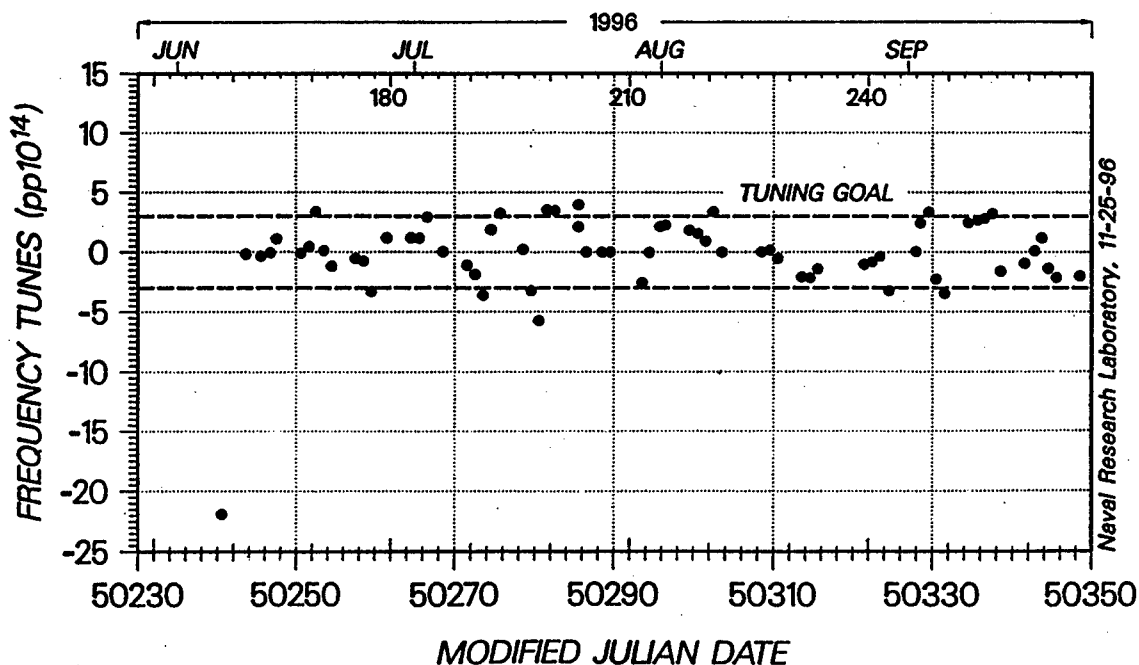


Figure 12

Questions and Answers

PAUL WHEELER (USNO): On your tuning chart, it looks like for every positive tune, the next tune was a negative tune. Was I interpreting that right and do you have an explanation for that?

DWIN CRAIG: No, that was just the way the system ended up. The software at the site, given the criteria that we gave it, generated the tunes. It's a coincidence.

THE END OF AN ERA: SVN 10 END-OF-LIFE FREQUENCY STANDARD TESTING

1Lt Gary L. Dieter
2d Space Operations Squadron
300 O'Malley Ave., Ste. 41
Falcon AFB, Colorado 80912-3041, USA

M.J. Van Melle
GPS Navstar Operations
Rockwell Space Operations Company
Falcon AFB, Colorado 80912-3041, USA

Abstract

When SVN 10 was boosted into its disposal orbit on June 20, 1996, it marked the end of the first phase of the Global Positioning System (GPS) program. SVN 10 was the last of the operational Block I GPS satellites. On 18 November 1995, it was set unhealthy to users for the final time after being operational for over 11 years. Due to its solar array capacity degradation, SVN 10's electrical power subsystem was no longer able to support its navigation payload after more than double its design life of 5 years. Personnel at the Master Control Station (MCS) were able, however, to maintain a navigation signal long enough to perform several end-of-life tests on the four onboard frequency standards. These tests on the one cesium and three rubidium standards varied in length and complexity. Several of the tests continued research begun during SVN 9's end-of-life testing. Areas of interest included temperature coefficient determination, voltage-controlled crystal oscillator (VCXO) open-loop operations, new clock initialization, C-field and VCXO tune range determination, Ramsey pattern generation, frequency standard failure analysis, and clock reinitialization performance characteristics analysis.

The results of these tests proved to be encouraging. After over 11 years in the space environment, there appeared to be no significant degradation to the navigation payload. Many of the test results supported conclusions made during SVN 9's end-of-life testing. It is hoped that these test results will prove to be useful to the GPS community by shedding more light on the performance characteristics of space-based frequency standards.

1 INTRODUCTION

On 20 June 1996, GPS SVN 10 (PRN 12) was boosted into its disposal orbit (the orbit perigee was increased by 178 nautical miles). This occasion marked the end of an era, as SVN 10 was the last of the operating GPS Block I satellites. Because of SVN 10's solar array capacity degradation and electrical power subsystem limitations, its navigation payload was set unhealthy to users on 18 November 1995 with a disposal in June 1996. The 2d Space Operations Squadron, responsible for operating and maintaining the GPS constellation through the GPS Master Control Station (MCS), performed end-of-life testing on several subsystems, including

the navigation payload. SVN 10's frequency standard end-of-life testing was accomplished from 25 January 1996 to 20 March 1996.

SVN 10 was launched on 8 September 1984 and its navigation payload was set healthy to users on 3 October 1984. It provided over 11 years of timing and navigation service to the GPS community, well beyond its intended design life of 5 years. SVN 10 was equipped with four frequency standards: three rubidium and one cesium. Three of its clocks were turned on for operational use. Cesium Frequency Standard (CFS) #4 was in operation from 23 September 1984 to 6 February 1992. Activation of Rubidium Frequency Standard (RFS) #2 was attempted on 6 February 1992. Due to problems discussed later in this paper, RFS #2 was never successfully activated. RFS #1 was used in operation from 6 February 1992 until SVN 10's last healthy day, 18 November 1995.

Seven tests were performed to evaluate how 11 years in the space environment affected SVN 10's navigation payload, specifically, its onboard frequency standards. Areas of interest included temperature coefficient change determination, voltage-controlled crystal oscillator (VCXO) open-loop operations, RFS #3 (unused during operational lifetime) initialization, C-field and VCXO tune range determination, Ramsey pattern generation, RFS #2 failure analysis, and RFS #1 reinitialization performance characteristics analysis. Many of these tests were also accomplished on SVN 9 during its end-of-life test period.^[1] This report will analyze any trends or changes with respect to those data. To maintain consistency, many of the procedures used for testing SVN 9 were repeated on SVN 10.^[1] SVN 10's frequency standard end-of-life testing was accomplished from 25 January 1996 to 20 March 1996.

2 TEMPERATURE COEFFICIENT DETERMINATION

The effects of temperature changes play a large role in determining the final frequency stability of GPS clocks. Rubidium frequency standards are more temperature-dependent than cesiums, and this is reflected in the GPS Block I program specifications for temperature coefficient. According to these specifications, Block I cesium standards must have a temperature coefficient of less than ± 2 parts in 10^{-13} per degree Celsius averaged over any 20 degrees in the 20–45 °C range.^[2] Rubidium standard specifications require a coefficient of less than ± 20 parts in 10^{-13} per degree Celsius averaged over the 25 - 37°C range.^[3] Because of this difference in the temperature coefficient, SVN 10's rubidium standards were equipped with Active Baseplate Temperature Control Units (ABTCUs).^[4] These heaters were designed to maintain clock temperature within $\pm 0.1^\circ\text{C}$ of one of four commandable settings.^[4] These settings are ($\pm 1.5^\circ\text{C}$): "A" = 26.5°C, "B" = 29.7°C, "C" = 33.5°C, "D" = 36.5°C.^[4]

The temperature coefficient of RFS #1 was measured by recording the MCS Kalman filter's estimate of A_1 ($\Delta f/f$), in the units of s/s, at ABTCU setting "D," along with the clock's exact temperature at that point. The ABTCU was then commanded to "C." Once the clock's temperature stabilized at the lower value, the Kalman filter's estimate of A_1 was again recorded (approximately 24 hours later), along with clock temperature. This process would be repeated for every lower ABTCU setting that could provide a stable temperature above the cyclic operating temperature of the rest of the payload. The standard's temperature coefficient was obtained by calculating the ratio of frequency change to temperature change. This coefficient was then compared to that obtained from ground testing in December 1981. This method of testing was also accomplished on SVN 9, with SVN 10's results serving as a good follow-up to those data.^[1] Tables 1 and 2 detail these observations when testing RFS #1.

Figure 1 shows how the Kalman's estimate of A_1 changed with each new ABTCU setting.

One can see a third change in A_1 , which is an attempt to set the ABTCU to setting "B." However, the payload operating temperature was above 29.7°C, and the ABTCU was unable to properly regulate the clock temperature at this lower setting. The results of testing settings "D" and "C" indicate that the temperature coefficient of RFS #1 degraded by a factor of 3.95 from December 1981 to January 1996. Therefore, it appears that 11 years of exposure to the space environment and a period of over 3 years spent on the ground has had an effect on the temperature coefficient of RFS #1. SVN 9's end-of-life testing produced similar results, showing that RFS #2's temperature coefficient degraded by a factor of three over a period of 10 years in space.^[1] The extent of this effect on the navigation mission is directly related to the ability of the ABTCU to regulate temperature to within its designed range of $\pm 0.1^\circ\text{C}$. Obviously, any degradation of the ability of the ABTCU to regulate temperature is more severe with a larger temperature coefficient.

3 VCXO OPEN-LOOP OPERATION

Nominally, GPS onboard frequency standards are operated in the VCXO closed-loop configuration. This configuration essentially combines the short-term stability benefits of a crystal oscillator with the long-term stability benefits of a physics package (rubidium or cesium). It is feasible that an operational scenario would occur in which all four physics packages aboard a satellite would prove to be unreliable, thereby necessitating the operation of one of the frequency standards in the VCXO open-loop configuration. This open-loop configuration allows the satellite time to be generated strictly off of the VCXO, without connection to the physics package. The purpose of this test is to observe standards in the open-loop configuration in order to give operators insight into how such a scenario might affect GPS operations.

The effects of operating in the open-loop configuration were tested by commanding the atomic loop open and tuning the VCXO. Also, the Kalman filter process noise values for the clock states were increased to better model the VCXO instabilities. The process noise value for A_0 (phase) was increased from $1.11 \cdot 10^{-22}$ to $2.22 \cdot 10^{-21} \text{ s}^2/\text{s}$. The process noise value for A_1 (frequency) increased from $44.4 \cdot 10^{-33}$ to $8.88 \cdot 10^{-28} \text{ s}^2/\text{s}^3$, and A_2 's (frequency drift) noise value increased from $9.00 \cdot 10^{-42}$ to $9.00 \cdot 10^{-41} \text{ s}^2/\text{s}^5$. At this point, the satellite's ranging signal was observed and analyzed. Navigation uploads were transmitted to the satellite when possible. This test was performed on two of SVN 10's clocks, RFS #1 and RFS #3. RFS #1 was operated in the open-loop configuration for approximately 27 hours, starting on 30 January 1996. RFS #3 was operated in the open-loop configuration for approximately 24 hours, starting on 5 March 1996. Based on SVN 9 end-of-life test results, it was expected that the open-loop configuration would not prove to be acceptable for operations.^[1] It was expected to see very large clock state terms and fairly frequent and large ranging errors.^[1] Table 3 details RFS #1 and RFS #3 open-loop characteristics.

All results were consistent with those obtained during SVN 9 testing.^[1] Although the process noise values allowed the MCS, through the Kalman filter process, to properly model the VCXOs, the characteristics of the VCXOs did not make maintaining the payload operationally realistic. This is due to the increased number of satellite contacts needed to keep ranging errors within operational specifications. As was the case with SVN 9, the clock states obtained for SVN 10's VCXOs were several orders of magnitude away from what we would expect of a normal RFS.^[1] Were SVN 10 set "healthy" during its open-loop tests, MCS operations crews would be performing navigation uploads at least once an hour to maintain its signal within specifications. Although operating a satellite in open-loop mode is feasible, it is most impractical considering MCS limitations.

4 RFS #3 INITIALIZATION

RFS #3 was a frequency standard which had eluded turn-on during the operational lifetime of SVN 10. CFS #4 and RFS #1 combined to last more than twice the design life of the vehicle, until the electrical power subsystem failed to meet demands. It was deemed useful to activate this clock during end-of-life testing to determine the effects, if any, of over 11 years of cold storage (8°C) in orbit. This was accomplished by activating the standard on 2 February 1996, initializing the payload, and allowing the MCS Kalman filter to model its clock states. Naval Research Laboratory (NRL) observed the clock's stability. This performance characteristic test of RFS #3 began on 8 February 1996 and lasted for approximately 4 weeks. The clock characteristics recorded by the MCS and NRL are described in Table 4.

FS #3 behaved nominally for a newly initialized Block I Rubidium standard. In the realm of stability, FS #3 met the 1-day stability program specification of $1.0 \cdot 10^{-12}$ and was easily acceptable for operational use.^[5] Estimated Range Deviations (ERDs) were also acceptable, even though SVN 10 was only uploaded with a fresh navigation message on a daily basis. Contingency uploads would be necessary as long as the clock maintained a changing drift rate. It is typical for rubidium frequency standards to eventually assume a negative, more predictable drift rate. Because it usually takes about 3 months to get to this point, we were unable to see FS #3 assume a negative, more consistent, drift rate (due to the time constraints of the testing). As one can see from the maximum drift movement, the clock was beginning to settle down with expectations that it would eventually assume a constant, negative drift rate. These test results are consistent with those of SVN 9 and support all SVN 9 new clock initialization conclusions.^[1]

5 C-FIELD AND VCXO TUNE RANGE DETERMINATION

All Block I frequency standards are equipped with the capability to retune the output frequency of the VCXO and the resonant frequency of the physics package via commands from the ground.^[6] As was the case with SVN 9, it was deemed beneficial to test how prolonged exposure to the space environment affected the tune ranges of the C-field and VCXO.^[1] This testing was accomplished by commanding the atomic loop open and tuning the VCXO to a maximum value. Once the Kalman filter had an estimate of A_1 , the command was sent to tune the VCXO to a minimum value, and A_1 was re-estimated. This process was repeated with the atomic loop closed to test the C-field. Once tune ranges were established, they were compared to tune ranges measured during ground testing in August 1981 and December 1981. Tables 5 through 7 show the C-field and VCXO tuning values along with the Kalman filter's estimates of A_1 . Tune ranges are listed, as well as comparisons with ground test data.

In five of the six test scenarios, the VCXO and C-Field tuning ranges of the frequency standards measured decreased during the 11-year on-orbit time of SVN 10. The only exception to this was the VCXO tuning range of RFS #3, which increased. The ranges of the C-fields shifted in the positive direction, while the ranges of the VCXOs shifted in the negative direction. Exposure to the space environment could have created these changes. The exact causes of these increases and decreases, however, are largely unknown. It is important to note that the changes and shifts in the tuning ranges are not significant (all less than 7% changes) when considering their operational applications. All test results supported the conclusions of SVN 9's end-of-life testing, with the exception of RFS #3's VCXO range data.^[1] SVN 9's VCXO ranges decreased over time, while SVN 10's RFS #3 VCXO range increased.^[1]

6 RAMSEY PATTERN DETERMINATION

The Ramsey pattern of a GPS cesium frequency standard can show certain conditions of the beam tube, such as where the center and side-lobe frequencies of that standard are located with respect to the clock's VCXO tuning range. It can also provide insight into the gain of the tube and the symmetry of the RF inserted into the tube. This test was devised to determine the characteristics of CFS #4's Ramsey pattern.

An operational frequency standard normally operates with the atomic loop closed and the center frequency located somewhere near the VCXO's 50% tune value. It is possible to plot the Ramsey pattern of a GPS cesium frequency standard by opening the atomic loop and commanding the VCXO to incremental tune values. In this case, increments of 10% were used. At each tuning value the beam current, indicative of the gain of the system, was recorded and plotted versus the tune percentage. The resulting plot of a Ramsey pattern shows peaks and valleys, with the peaks being either the center or side-lobe frequencies. Once the beam current is plotted versus the VCXO tune percentage, one can see where the center frequency may lie, depending on how much the VCXO has aged.

The measured Ramsey pattern for SVN 10's CFS #4 can be seen in Figure 2. According to our data, it seems as if the center frequency is located somewhere around the 70% VCXO tune. This would agree with the CFS #4 VCXO tune range test, which showed us that the VCXO tuning range shifted in the negative direction. The Ramsey pattern, however, does not clearly define the side lobes. This may be due to the fact that the gain of this standard has degraded so much that the side frequencies occur in the noise level. Also, it is possible that we needed a more granular (less than 10% tune intervals) search for those frequencies. Because there are no pre-launch Ramsey patterns to compare our results with, it is unclear exactly how much CFS #4's Ramsey pattern has changed over time.

7 RFS #2 FAILURE ANALYSIS

On 6 February 1992, SVN 10's RFS #2 was turned on due to performance degradation of the 7.5-year-old CFS #4. According to the Block I Orbital Operations Handbook (OOH), the nominal warm-up time for a Block I RFS is one hour.^[6] Two hours after the clock had been turned on, the atomic loop was commanded closed. The 10.23 MHz control voltage to the VCXO read 0.45 volts. The nominal reading for this clock would have been approximately 5.4 volts. The other two clock parameters were slightly low, but were close to their nominal readings. Personnel at the MCS tried to test the clock by opening the atomic loop and exercising the VCXO's tuning capability. When the loop was open, the VCXO loop control voltage responded as commanded. However, when the loop was closed, the loop control voltage returned to 0.45 volts. After the clock was on for a total of 2 hours 31 minutes, it was deemed unusable and was turned off. At the time, because of the necessity to set SVN 10 healthy, it was impossible for MCS personnel to thoroughly test RFS #2 in order to determine the cause of its failure. Therefore, RFS #1 was turned on and eventually set operational.

This end-of-life test was devised to attempt to bring RFS #2 on line, 4 years after its initial failure and perform a re-test. If this attempt was not successful, it was hoped the cause of RFS #2's failure mode could be narrowed down, if not identified. Since RFS #2 was originally given only 2 hours and 31 minutes to warm up due to operational considerations in 1992, the clock this time was given approximately 24 hours to warm up during this testing. The VCXO's tuning capability was again exercised, and power to the frequency standard itself was cycled. The commands which open and close the atomic loop were also sent to SVN 10, which cycled

the loop's closure mechanism.

As in 1992, MCS personnel were unsuccessful in getting the atomic loop of RFS #2 to close properly. The warm-up period of 24 hours did not allow the clock to operate properly. When the command was sent to open the loop, and VCXO tune words were sent to the clock, the loop control voltage again acted normally. However, there was no change when we attempted to close the loop. Cycling clock power as well as cycling the mechanism which is supposed to close the atomic loop proved to be unsuccessful. Once it was obvious the loop was not working properly, it was attempted to initialize the navigation payload and turn on L-band with RFS #2 in the open-loop configuration. After several attempts, it was impossible for MCS monitor stations to lock up on the L-band carrier.

After testing RFS #2, it is obvious there is a problem which prevents the atomic loop from being closed, similar to that encountered in 1992. However, from this testing, we learned it was not a matter of giving the clock enough warm-up time. Also, because we were unable to lock up on the L-band signal of SVN 10 when operating in the open-loop configuration at any VCXO tune value, it is assumed the problem with the standard lies with the VCXO and not necessarily with any other part of the clock (the physics package, in particular). This may indicate the VCXO had changed frequency so much that the loop could not capture the VCXO frequency.

8 RFS #1 REINITIALIZATION

RFS #1 had been operating for almost 4 years (6 February 1992–1 February 1996) when it was disabled to begin end-of-life testing on other onboard clocks. Upon deactivation on 1 February 1996, the operational characteristics of this clock were well within program specifications. Tables 8 and 9 detail values of 1-day stability and clock drift rate for RFS #1 before it was deactivated for end-of-life testing.^[7,8] The 1-day stability data were obtained from NRL's Navstar Analysis Update No. 10-6 and Quarterly Report No. 96-1.^[7,8] The clock drift rate data were obtained from the MCS Kalman filter's estimates of clock states.

RFS #1 was reactivated on 11 March 1996 and test data were received for 11 days, the final day being 27 March 1996. This test was designed to compare the performance characteristics of RFS #1 after being on for 4 years to the performance characteristics of RFS #1 after being off for 41 days and then powered on for 2 weeks. Also, it was intended to determine how quickly RFS #1 would achieve its previous characteristics (especially its stability and drift rate). Our expectation was RFS #1 would eventually assume the same performance characteristics it had when we turned it off in early February 1996. Certain questions remained. Exactly how long would it take to assume those characteristics, and would the clock reach those values within the short length of our testing?

RFS #1 was powered back up on 11 March 1996. Operators at the MCS were unable to get L-band data for SVN 10 until 15 March 1996. Data were received from 15 March 1996–27 March 1996. Table 10 describes RFS #1's performance characteristics during that time.^[9] The 1-day stability data were obtained from NRL's Navstar Analysis Update No. 10-7.^[9] The clock drift rate data were obtained from the MCS Kalman filter's estimates of clock states.

Before any of these data are analyzed, it is important to point out that MCS operators did not get a very long period of time to examine RFS #1's characteristics in March 1996. Because the clock was only on for approximately 2 weeks, and L-band data were only collected for approximately 11 days, it is hard to derive definite conclusions from this test. Both aspects which were analyzed (clock 1-day stability and drift rate) require a much longer period of time

than was operationally possible to obtain numbers that can be considered with high confidence levels. (During acceptance tests at the factory, however, clocks are normally given a 14-day warm-up period followed by a 10-day stability test period. A drift rate value is calculated from the last 5 days.) At only 11 days, the error bars for both 1-day stability and drift rate are rather large in magnitude.

We can, however, say some trends were definitely noticed. It certainly appears the March 1996 1-day stability figure obtained from NRL is consistent with 1-day stability figures obtained when RFS #1 was operational.^[7,8,9] It is assumed if we had more time to look at RFS #1 in March 1996, we would have seen its stability value of $0.77 \cdot 10^{-13}$ (recorded over an 11-day period) approach $0.36 \cdot 10^{-13}$, which was recorded over a 4-month period in 1995.^[7,8,9] Even after only 2 weeks of activation time, RFS #1 was well within the Block I 1-day stability specification of $1 \cdot 10^{-12}$.^[5,9]

Drift rate figures obtained in March 1996 indicated RFS #1 initially assumed a positive drift rate. After approximately 9 days of activation, the drift rate started to turn in the negative direction. Normally, rubidium standards require 2 to 3 months of warm-up time to assume a negative drift rate. Table 9 gives examples of RFS #1's drift rate in 1995, and Table 11 shows its drift rate during end-of-life testing. The negative drift rate it assumed after 11 days ($-8.04 \cdot 10^{-19}$ s/s²) was very comparable to that recorded in 1995 ($-8.97 \cdot 10^{-19}$ s/s²). It is possible that because this clock had been previously in operation for approximately 4 years, it required a much shorter warm-up period to assume a negative, more predictable drift rate. As previously mentioned, the drift rate comparisons are hard to accurately determine due to the amount of uncertainty in the measurements. It is fair to say, however, that a trend is noticeable. This trend indicates the frequency standard, in terms of drift rate, does not start from ground zero, but retains much of its "memory" from when it was turned off.

9 CONCLUSION

Based on the results of SVN 10 end-of-life frequency standard testing, one can state that over 11 years, the harsh space environment did not significantly impact the operational capability of the onboard clocks. All characteristics testing of temperature coefficient, new clock initialization, C-field and VCXO tuning, and clock reinitialization showed RFS #1 and RFS #3 were still capable of meeting operational specifications. Data have been obtained which indicate that although operating a satellite in VCXO open-loop mode is feasible, it is not operationally practical. Additional insight has been gained as to why RFS #2 failed to initialize in February 1992; a problem with the VCXO may very well have been the cause. It has been observed that the time it takes an RFS to assume a predictable, negative aging rate after turn-on is dependent on the amount of time it has been "burned in" (in our case, this "burn-in" time was 4 years). All conclusions from this set of clock testing seem to reinforce many conclusions ascertained from SVN 9's end-of-life testing.^[1] It is hoped the results of SVN 10's end-of-life navigation payload testing can serve as an additional data point in what will someday be a much larger pool of space-based frequency standard knowledge.

10 ACKNOWLEDGMENTS

The authors gratefully thank the following individuals and their agencies for assistance and encouragement:

SrA Shawn E. Feeney, 2d Space Operations Squadron
Mr. Gregory E. Hatten, University of Colorado, Boulder
Mr. Steven Hutsell, United States Naval Observatory
Mr. Wilson G. Reid, United States Naval Research Laboratory

11 REFERENCES

- [1] G.E. Hatten 1995, "*SVN 9 end-of-life testing*," Proceedings of the 26th Annual Precise Time and Time Interval (PTTI) Applications and Planning Meeting, 6-8 December 1994, Reston, Virginia, USA (NASA CP-3302), pp. 405-414.
- [2] "*Cesium standard procurement specification*," MC 474-0031, 15 July 1981 (Rockwell International, Inc.).
- [3] "*Rubidium standard procurement specification*," MC 474-0030, Revision F, Sequence 05, 5 May 1988 (Rockwell International, Inc.)
- [4] "*Block I GPS orbital operations handbook*," Vol. I, Sec. 2.6, "*Thermal control subsystem description*."
- [5] "*Rubidium standard procurement specification*," MC 474-0030, Revision F, Sequence 05, Fig. 5, 5 May 1988 (Rockwell International, Inc.)
- [6] "*Block I GPS orbital operations handbook*," Vol. I, Sec. 2.5, "*Navigation subsystem description*."
- [7] W.G. Reid, and J.A. Buisson, NRL Analysis Update No. 10-6, 28 February 1996.
- [8] W.G. Reid, and J.A. Buisson, NRL Quarterly Report No. 96-1, 1 March 1996.
- [9] W.G. Reid, G. Wilson, and J.A. Buisson, NRL Analysis Update No. 10-7, 22 April 1996.

Table 1. Results of ABTCU Setting Change

ABTCU Setting	Clock Temperature (°C)	A1 Kalman Estimate (s/s)
"D"	37.0	-5.76 e-11
"C"	34.0	-6.30 e-11

Table 2. Ground Test Data vs. End-Of-Life Data

Date of Testing	Temperature Coefficient ($\Delta f/f$ per °C)
December 1981 (Lab Testing)	4.5 10e-13
January 1996 (On-Orbit Testing)	17.6 10e-13

Table 3. RFS #1 & RFS #3 Open-Loop Data

VCXO Clock State	VCXO RFS#1	VCXO RFS#3
VCXO Clock Bias (A_0)	-4.03 e-4 (s)	+1.93 e-4 (s)
VCXO Clock Drift (A_1)	-3.30 e-9 (s/s)	-2.60 e-9 (s/s)
VCXO Clock Drift Rate (A_2)	-1.40 e-15 (s/s ²)	+1.31 e-15 (s/s ²)
Maximum Drift Movement	1.22 e-10 (parts/day)	6.9 e-11 (parts/day)

Table 4. RFS #3 Initialization Data

Clock State	RFS #3
Clock Bias (A_0)	1.44 e ⁻⁴ (s)
Clock Drift (A_1)	6.60 e ⁻¹² (s/s)
Clock Drift Rate (A_2)	3.10 e ⁻¹⁸ (s/s ²)
Stability (τ = one day) (Allan deviation data from NRL)	2.5 e-13 (aging correction = +4.79E-13 per day)
Avg. Max. Drift Movement (days 1-14)	7.44 e ⁻¹³ (parts/day)
Avg. Max. Drift Movement (days 15-25)	1.57 e ⁻¹³ (parts/day)

Table 5. RFS #1 VCXO & C-field Tune Range Data

C-field tune	On-orbit $\Delta f/f$	Lab Test $\Delta f/f$ (12/81)
0.0 %	-2.376 e-9 (s/s)	-2.770 e-9 (s/s)
100.0 %	+2.451 e-9 (s/s)	+2.141 e-9 (s/s)

VCXO tune	On-orbit $\Delta f/f$	Lab Test $\Delta f/f$ (12/81)
0.0 %	-2.549 e-7 (s/s)	-2.411 e-7 (s/s)
100.0 %	+2.311 e-7 (s/s)	+2.524 e-7 (s/s)

	On-orbit range $\Delta f/f$	Lab Test range $\Delta f/f$ (12/81)	change (%)
C-field	4.827 e-9 (s/s)	4.911 e-9 (s/s)	-1.7
VCXO	4.860 e-7 (s/s)	4.935 e-7 (s/s)	-1.5

Table 6. RFS #3 VCXO & C-field Tune Range Data

C-field tune	On-orbit $\Delta f/f$	Lab Test $\Delta f/f$ (8/81)
0.0 %	-2.280 e-9 (s/s)	-2.913 e-9 (s/s)
50.0 %	+2.30 e-10 (s/s)	-4.008 e-10 (s/s)
100.0 %	+3.163 e-9 (s/s)	+2.551 e-9 (s/s)

VCXO tune	On-orbit $\Delta f/f$	Lab Test $\Delta f/f$ (8/81)
0.0 %	-2.571 e-7 (s/s)	-2.185 e-7 (s/s)
100.0 %	+2.402 e-7 (s/s)	+2.470 e-7 (s/s)

	On-orbit range $\Delta f/f$	Lab Test range $\Delta f/f$	change (%)
C-field	5.443 e-9 (s/s)	5.464 e-9 (s/s)	-0.4
VCXO	4.973 e-7 (s/s)	4.655 e-7 (s/s)	+6.8

Table 7. CFS #4 VCXO & C-field Tune Range Data

VCXO tune	On-orbit $\Delta f/f$	Lab Test $\Delta f/f$ (7/82)
30.0 %	-2.046 e-7 (s/s)	-1.25 e-7 (s/s)
100.0 %	+1.435 e-7 (s/s)	+2.35 e-7 (s/s)

	On-orbit range $\Delta f/f$	Lab Test range $\Delta f/f$	change (%)
VCXO	3.481 e-7 (s/s)	3.60 e-7 (s/s)	-3.3

Table 8. RFS#1 One-Day Stability as Recorded By NRL^[7,8]

Time Period	One-Day Stability
2/13/92 - 11/19/95	1.34 e-13 (aging correction = -1.12 e-13 pp/day or $1/2 A_2 = -1.30 \text{ e-18 s/s}^2$)
9/1/95 - 1/1/96	0.36 e-13 (aging correction = -0.8 e-13 pp/day or $1/2 A_2 = -0.93 \text{ e-18 s/s}^2$)

Table 9. RFS#1 MCS Kalman Filter Clock Drift Rate Estimates

Time Period	Clock Drift Rate (A_2)
9/11/95 - 9/28/95	-9.15 e-19 (s/s ²)
9/29/95 - 10/13/95	-9.27 e-19 (s/s ²)
10/25/95 - 11/13/95	-8.48 e-19 (s/s ²)
Average of 3 time periods	-8.97 e-19 (s/s ²)

Table 10. RFS#1 One-Day Stability as Recorded By NRL^[9]

Time Period	One-Day Stability
3/15/96 - 3/27/96	0.77 e-13 (aging correction = +0.267 e-13 pp/day or $1/2 A_2 = +3.09 \text{ e-19 s/s}^2$)

Table 11. RFS#1 MCS Kalman Filter Clock Drift Rate Estimates

Time Period	Clock Drift Rate (A_2)
3/15/96 - 3/27/96	$+1.46 \text{ e-}19 \text{ (s/s}^2\text{)}$
3/15/96 - 3/20/96	$+1.81 \text{ e-}18 \text{ (s/s}^2\text{)}$
3/20/96 - 3/27/96	$-8.04 \text{ e-}19 \text{ (s/s}^2\text{)}$

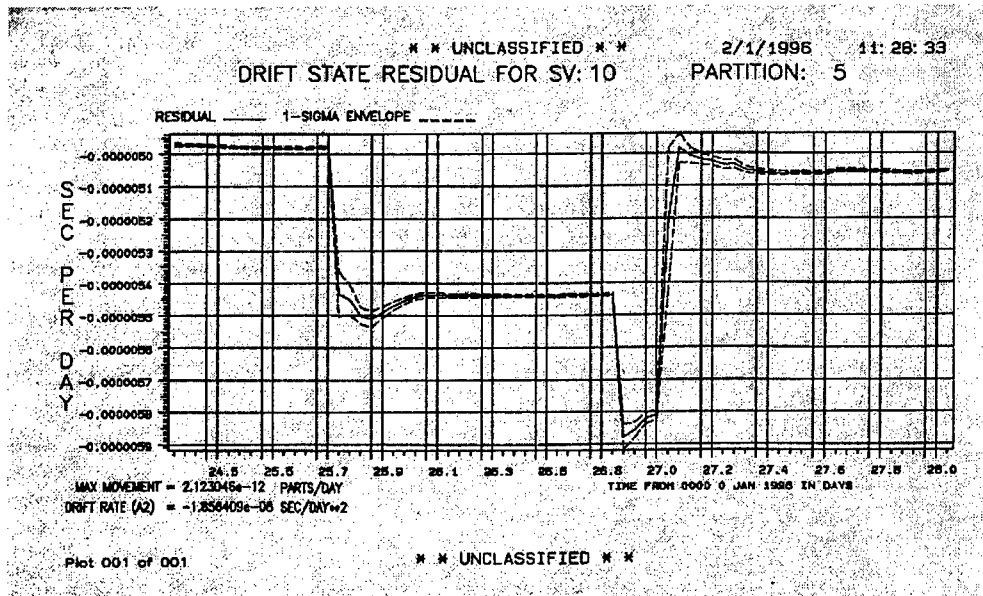


Figure 1. RFS #1 Drift Residuals During Temperature Variations

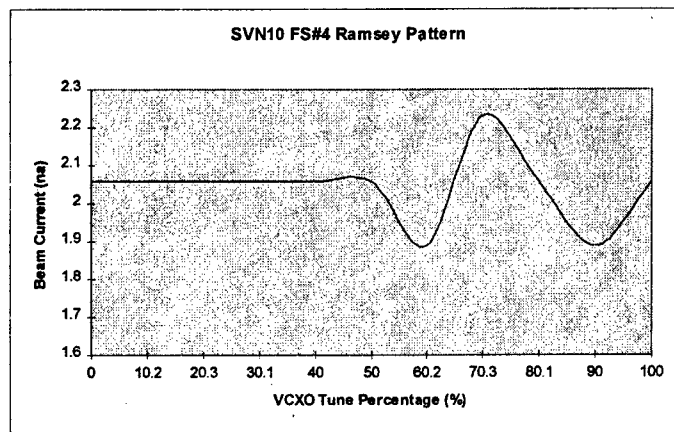


Figure 2. CFS#4 Ramsey Pattern

Questions and Answers

JAMES CAMPARO (AEROSPACE CORP.): The fact that you saw a faster return to the long-term drift rate could very well be as you're saying; it's known that it may take 30 to 60 days for the lamp's light shift to settle down and not be seen in the long-term stability. So if the liquid pool of rubidium in the lamp hadn't been moved, that could explain why it reached that normal drift coefficient so quickly.

GARY DIETER: Makes sense.

DAVID ALLAN (ALLAN'S TIME): The dynamic and steady state temperature coefficients are often quite different. Did you try to differentiate between these two at all?

GARY DIETER: No, we kind of understood that a temperature coefficient taken on the ground may be different because of natural orbital temperature variations in space. But all that we did was what we said, we just simply left it and took the measurements.

RICHARD KEATING (USNO): From time to time, there's been discussion of what sort of oscillator or clock to put on a satellite. From your presentation, it appears that you basically have ruled out crystal oscillators. Is that really true? Could it just be the type of oscillator you had?

GARY DIETER: I think what we ruled out is operating our current clocks that we have in space on their VCXs only. And when I say "ruled out," I'll say that it's, like we said before, operationally impractical.

PERFORMANCE EVALUATION OF THE GPS BLOCK IIR TIME KEEPING SYSTEM

Andy Wu

The Aerospace Corporation

4452 Canoga Drive, Woodland Hills, California 91364, USA

(310) 336-0437 (telephone), (310) 336-5076 (fax)

Wu@courier3.aero.org

Abstract

The Time Keeping System (TKS) is essential to the GPS Block IIR total navigation payload and must provide an accurate time base for each GPS space vehicle. Performance analysis of the TKS has been reported previously for the case in which a rubidium (Rb) atomic frequency standard is used as a reference. In this paper the system error model of the TKS is developed and the performance of the TKS output using either a cesium (Cs) or a rubidium (Rb) atomic frequency standards as a reference is evaluated. The contributions to the TKS output Allan deviation was examined from each of the three noise sources: atomic frequency standard (either Cs or Rb), voltage control crystal oscillator (VCXO), and phase meter (PM). In addition, since the TKS does not have a baseplate temperature controller and the VCXO of the TKS is temperature-sensitive, a TKS error is induced when the VCXO is subject to the orbital temperature variations or the space vehicle umbra during solar eclipse. These two temperature-induced TKS output errors are also examined. Sensitivities of the Allan variance at the TKS output for each of its independent input noises are provided and they are valuable for design trade-off and troubleshooting. The results of this paper compare favorably with those obtained by the TKS system testing. The paper will show that when the TKS components meet or exceed their specifications, the RAFS TKS and the CAFS TKS should meet their specifications.

1 INTRODUCTION

The GPS Block IIR Time Keeping System (TKS) is used to generate a system output frequency of 10.23 MHz from an Atomic Frequency Standard (AFS) as an input reference. The output frequency of either the Cs AFS (CAFS) or the Rb AFS (RAFS) is approximately 13.4 MHz. Dither frequency for the Selective Availability (SA), if enabled, is added to the TKS output. The block diagram of the TKS system model is shown in Figure 1. Both CAFS and RAFS as frequency references to the TKS are considered in this paper and are referred as the CAFS TKS and the RAFS TKS respectively. A reference epoch is generated every 1.5 s based on the AFS frequency and another 1.5 s interval system epoch is generated by the 10.23 MHz system clock of the VCXO. Both epochs are input to the Phase Meter (PM), and the PM computes the timing error between the two epochs in terms of number of cycles of an asynchronous 600 MHz clock. Considering the timing error value, the loop adjusts the phase of the epoch from the VCXO so that the VCXO is phase-locked to the reference AFS.

In this paper the system error model of the TKS is developed and the performance of the TKS frequency output is evaluated from each of the three noise sources: atomic frequency

standard (either Cs or Rb), voltage control crystal oscillator (VCXO), and phase meter (PM). In addition, since the VCXO is temperature-sensitive and the TKS does not have a baseplate temperature controller, the TKS error induced by the VCXO is also computed when the VCXO is subject to the orbital temperature variations or the space vehicle umbra during solar eclipse. The other intent of this paper is to provide as much relevant technical information as possible to the users of the GPS Block IIR Time Keeping System.

2 GPS TKS STABILITY REQUIREMENTS

The TKS stability requirements for the GPS Block II/IIA, Block IIR, and Block IIF using either a Rb AFS or a Cs AFS as an input reference is shown in Figure 2. It is interesting to note that the Allan deviation requirement of the Block II/IIA CFS TKS has a slope of $\tau^{-0.4247}$ instead of the theoretical value of $\tau^{-0.5}$. Also, the Block IIF TKS requirement is better than that of the Block IIR CAFS TKS and is not as good as that of the Block IIR RAFS TKS.

3 TKS BASIC NOISE MODELS

3.1 Phase Meter Phase Noise

The TKS phase meter noise was derived in [1] and it is shown to be a white phase noise. The power spectral density and the Allan variance are

$$S_p(f) = T_c^2/6 \quad (1)$$

$$\sigma_p^2(\tau) = T_c^2/(6\tau^2)$$

where T_c is a cycle period of the 600 MHz clock.

3.2 VCXO Frequency Noise

The VCXO frequency noise is characterized by the following Allan variance^[2]:

$$\sigma_v^2(\tau) = 10^{-24} + 10^{-27}\tau. \quad (2)$$

Assuming that the two terms of Eq. (2) are independent of each other, the power spectral density of the VCXO intrinsic frequency noise can be expressed as^[3]:

$$S_v(f) = 7.2134 \times 10^{-25}/f + 1.519 \times 10^{-28}/f^2 \quad (3)$$

3.3 AFS Frequency Noise

The Allan variances for both the CAFS and the RAFS are specified in [2,4].

$$\sigma_{AC}^2(\tau) = 9.0 \times 10^{-22}/\tau + 1.0 \times 10^{-26}, \text{ for the CAFS noise} \quad (4)$$

$$\sigma_{AR}^2(\tau) = 1.0 \times 10^{-23}/\tau + 2.5 \times 10^{-27}, \text{ for the RAFS noise}$$

The associated noise power spectral densities can be computed using well-known techniques^[3]:

$$\sigma_{AC}^2(f) = 1.8 \times 10^{-21} + 7.213 \times 10^{-27}/f, \text{ for the CAFS noise} \quad (5)$$

$$\sigma_{AR}^2(f) = 2.0 \times 10^{-23} + 1.803 \times 10^{-27}/f, \text{ for the RAFS noise}$$

The Allan deviations of the PM phase noise, the VCXO frequency noise, the CAFS frequency noise, and the RAFS frequency noise are shown in Figure 3. Note that the PM phase noise is governing for low τ and the VCXO frequency noise is dominant for the $\tau > 60$ s.

4 TKS TRANSFER FUNCTIONS

The system model of the TKS as shown in Figure 1 results in the equivalent system error model indicated in Figure 4, obtained using the Z-transform formation. T_s is the sample period of the TKS, and is 1.5 s. Also, two delays of one epoch each are introduced in Figure 4 to account for the fact that the effects of the computed VCXO frequency modification in the current epoch will not show on the Phase Meter until two epochs later. SA (dither frequency) is excluded, and the VCXO gain is assumed to be local linear. This model is applicable to both the CAFS TKS and the RAFS TKS. The transfer functions relating the TKS output frequency error (T) to the input noises of the AFS (A) frequency, the VCXO (V) frequency, and the Phase Meter (P) phase are:

$$TKS/PhaseMeter = H_{TP}(Z) = [a(K_1 + K_2)Z^{-1} - a(K_1 + 2K_2)Z^{-2} + aK_2Z^{-3}]/\Delta \quad (6)$$

$$TKS/AFS = H_{TA}(Z) = [aT(K_1 + K_2)Z^{-1} - aTK_2Z^{-2}]/\Delta \quad (7)$$

$$TKS/VCXO = H_{TV}(Z) = [1 - (3 - a)Z^{-1} - (3 - 2a)Z^{-2} - (1 - a)Z^{-3}]/\Delta \quad (8)$$

where

$$\Delta = 1 - (3 - a)Z^{-1} + [(3 - 2a) + aT(K_1 + K_2)]Z^{-2} - (1 - a + aTK_2)Z^{-3} \quad (9)$$

The Bode plots (frequency responses) for these transfer functions with a TKS loop time constant of 150 s ($a = 0.1199$, $K_1 = 8.2573 \times 10^{-5}$, and $K_2 = 0.17341$) are shown in Figure 5. A time constant of 150 seconds is chosen because it provides the best overall performance in terms of the TKS Allan deviation and transient response.^[2] It is seen that $H_{TA}(Z)$ is a lowpass filter, $H_{TV}(Z)$ is a highpass filter, and $H_{TP}(Z)$ is a low-gain bandpass filter to suppress the PM phase noise.

5 ALLAN DEVIATIONS OF THE TKS OUTPUT FREQUENCY

Since the TKS error model is a linear system, the power spectral density at the TKS output can be computed with the TKS transfer functions as provided in Section 4 and the power spectral densities from the three noise sources: CAFS or RAFS, VCXO, and PM as provided in Section 3. The resulting power spectral density can then be used to compute the Allan variance at the TKS output. The details of how to compute the TKS output Allan deviation using the frequency domain techniques and to achieve the desired computation accuracy can be found in [5]. The frequency domain technique was used because it provides another independent evaluation of the TKS performance and because the flicker noise contained in the VCXO and AFS noises can be evaluated precisely without approximation.^[6]

These Allan deviations at the TKS output are shown in Figure 6 and they can be considered as the sensitivities of the TKS output for each of the independent input noises. This technique can be used very effectively during the design, development, and testing phase of the program to determine the loop time constant, to define noise specifications, and to provide data for troubleshooting. It will be used later to identify the causes of some out of specification conditions. It is apparent from Figure 6 that for short average times the TKS performance is dominated by the VCXO and PM, while for long average times the TKS performance is governed by either the CAFS or the RAFS. The crossover average time is around 20 s for the CAFS TKS and around 1,700 s for the RAFS TKS.

Since the TKS noises are independent, the Allan deviation of the TKS can be obtained by root-sum-square of these independent TKS noises. The Allan deviations of the RAFS TKS output ($\sigma_{TR}(\tau)$), the RAFS TKS specification, and the RAFS input specification are shown in Figure 7. The figure shows that the RAFS TKS output is not as good as that of the RAFS input because of erosion from both the VCXO and the phase meter noises, as can be seen from the TKS sensitivity responses provided in Figure 6. The Allan deviations of the CAFS TKS output ($\sigma_{TC}(\tau)$) and the CAFS TKS specification are plotted in Figures 8. It shows that: the Allan deviation of the CAFS TKS output barely exceeds its specification for the average time from 170 s to 3,000 s. By examining the TKS sensitivity responses as provided in Figure 6, it is found that the out-of-specification condition is caused by the CAFS input noise. Since the Allan deviation test results of the GPS Block IIR CAFSs currently indicate that they are better than their specification, this should not present a problem. A sample of the measured Allan deviations of a CAFS and a RAFS are plotted in Figures 9 and 10, which are better than their specifications.

6 COMPARISON WITH THE TKS TESTING RESULTS

The Allan deviations of the GPS Block IIR TKS test results with a RAFS and a CAFS as an input are shown in Figures 7 and 8. The contribution from the house reference frequency standard (HP 5071A) has been removed from the test results. With the exception of the last test point of the CAFS TKS Allan deviation, the differences between the simulation results and the testing results are in good agreement and are less than 1 dB.

7 VCXO TEMPERATURE-INDUCED FREQUENCY NOISES

The VCXO is sensitive to temperature variations. Since the TKS does not have a baseplate temperature controller, a TKS error is induced when the VCXO of the TKS is subject to

the orbital temperature variations or the space vehicle umbra during solar eclipse. These two temperature-induced TKS output errors are examined below.

7.1 TKS Error Due to the Orbital Temperature Variations

When the VCXO is subject to an orbital temperature variation estimated to be ± 2.5 degrees maximum with a period of 12 hours, the VCXO temperature-induced frequency noise with a temperature coefficient specification of 4×10^{-11} (df/f)/°C can be described as:

$$V_O(t) = 4 \times 10^{-11} \times 2.5 \times \sin(2\pi f_o t + \Phi) \quad (10)$$

$$= 1 \times 10^{-10} \times \sin(2\pi f_o t + \Phi),$$

where $f_o = 1/(12 \times 3,600)$ is the orbital frequency with a period of 12 hours and Φ is an arbitrary starting phase angle. This TKS input frequency error with $\Phi = 90$ degrees is plotted in Figure 11. The TKS output frequency error due to this VCXO input frequency noise can be computed using the transfer function of $H_T V(Z)$ and the result is provided in Figure 12. It is 180 degrees out of phase from the input frequency noise, as confirmed by the VCXO phase angle plot of the Bode diagram of Figure 5. The resulting TKS output timing error can be obtained by integrating the output frequency error and is shown in Figure 13. The Allan deviation of this timing error is computed using the overlapping samples technique and is shown in Figure 14. As can be seen, it is below the RAFS TKS specification line.

The TKS Allan deviation induced by orbital VCXO effect can also be determined analytically. The TKS loop gain from the VCXO to the TKS output at the orbital period of 12 hours can be obtained from its Bode plot, as shown in Figure 5 or can be determined by

$$Gain = |H_{TV}(e^{j2\pi f T_s})|_{f=1/12 \times 3,600} \quad (11)$$

$$= 3.84 \times 10^{-4}.$$

Since the TKS error model is a linear system, the frequency error at the TKS output can be obtained as

$$V_{TO}(t) = 3.84 \times 10^{-4} \times 1 \times 10^{-10} \times \sin(2\pi f_o t + \Phi) \quad (12)$$

$$= 3.84 \times 10^{-14} \times \sin(2\pi f_o t + \Phi).$$

This is in perfect agreement with that shown in Figure 12 with $\Phi = 90$ degrees. The TKS output Allan variance from this sine frequency can be determined to be

$$\sigma_{TVT}^2(\tau) = 3.84^2 \times 10^{-28} \times \sin^4(\pi f_o \tau) / (\pi f_o \tau)^2. \quad (14)$$

The square root of this Allan variance is shown in Figure 14 and clearly agrees with that obtained early by simulation.

7.2 TKS Error Due to the Space Vehicle Umbra During Solar Eclipse

The temperature profile due to the space vehicle umbra can be modeled as a 2 degrees/hour shift for a 1/2 hour and then a settling at a constant temperature for 1/2 hour before sloping back to its original temperature.^[7] The resulting VCXO frequency error at the TKS input with a temperature coefficient of 4×10^{-11} (df/f)/°C is shown in Figure 11. The TKS output frequency error due to this VCXO input frequency noise can be computed using the transfer function of $H_{TV}(Z)$ and the result is provided in Figure 12. The resulting TKS output timing error is provided in Figure 13. The Allan deviation of this umbra error can be computed from this timing error and the result is shown in Figure 14. Again, this umbra-induced TKS error is below the RAFS specification line.

7.3 TKS Error Due to VCXO Out-of-Specification Temperature Coefficient

In the early delivery of the VCXOs, some of them have a temperature coefficient of 14×10^{-11} (df/f)/°C, that is, about 3.5 times of the specification. The TKS Allan deviations due to this out of specification for both the orbital and umbra effects are recomputed and are shown in Figure (15); as expected, they are much closer to the RAFS specification line. The Allan deviation of the RAFS TKS with the out-of-specification VCXO is also shown in Figure 15, and it meets the RAFS TKS specification.

8 CONCLUSIONS

The contributions to the TKS output Allan deviation from the three basic TKS noises as well as the VCXO orbital and umbra temperature-induced noises were computed. These formed the sensitivities of the Allan deviation at the TKS output for each of its input noises and they are valuable for design trade-off and troubleshooting. The results of this paper compare favorably with those obtained from the TKS system testing. When the TKS components meet their specifications, the RAFS TKS should meet its specification. The CAFS TKS should have no problem of meeting its specification, since the CAFS normally would exceed its specification.

9 REFERENCES

- [1] J. Han 1993, "Performance analysis of clock stability for GPS Block IIR satellites," ATM-93(3470-01)-5, The Aerospace Corporation, Woodland Hills, California, USA, 27 September 1993.
- [2] H. Rawicz, M. Epstein, and J. Rajan 1993, "The Time Keeping System for GPS Block IIR," Proceedings of the 24th Annual Precise Time and Time Interval (PTTI)

Applications and Planning Meeting, 1-3 December 1992, McLean, Virginia, USA (NASA CP-3218), pp. 5-16.

- [3] J. Barnes, *et al.* 1971, "*Characterization of frequency stability*," **IEEE Transactions on Instrumentation and Measurement**, IM-20, pp. 105-120.
- [4] A. Baker 1991, "*GPS Block IIR time standard assembly architecture*," Proceedings of the 22nd Annual Precise Time and Time Interval (PTTI) Applications and Planning Meeting, 4-6 December 1990, Vienna, Virginia, USA (NASA CP-3116), pp. 317-324.
- [5] A. Wu 1995, "*Allan deviation computation of a linear frequency synthesizer system using frequency domain techniques*," Proceedings of the 26th Annual Precise Time and Time Interval (PTTI) Applications and Planning Meeting, 6-8 December 1994, Reston, Virginia, USA (NASA CP-3302), pp. 393-404.
- [6] J.A. Barnes, and S. Jarvia, Jr. 1971, "*Efficient numerical and analog modeling of flicker noise process*," National Bureau of Standards Technical Note 604.
- [7] H. O'Donnel 1995, "*Effect of VCXO temperature-induced errors*," Lockheed Martin Astro-Space Interoffice Memorandum to A. Das, 24 August 1995.

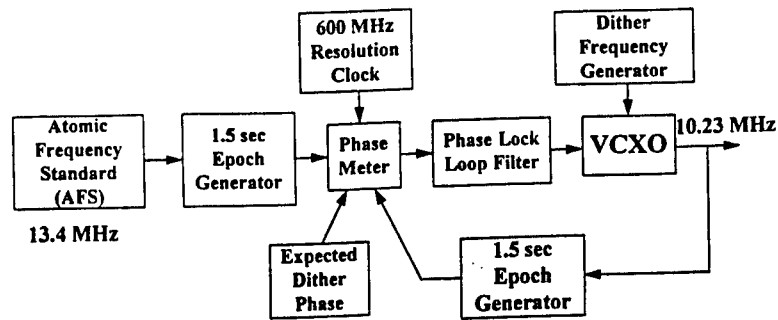
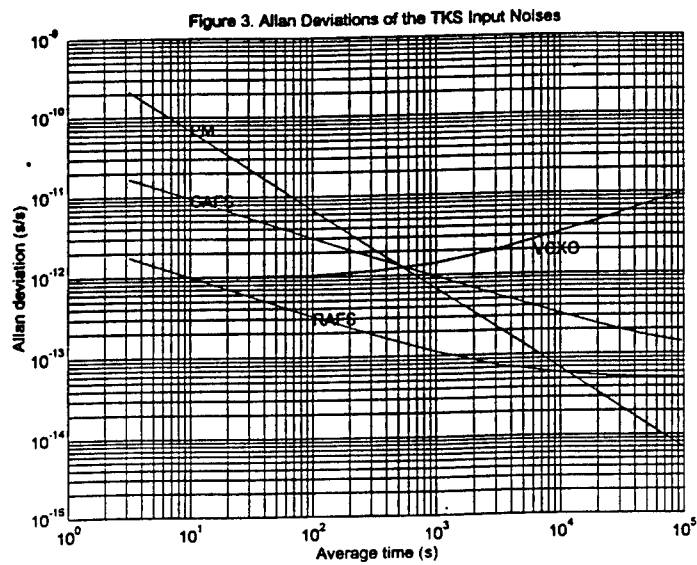
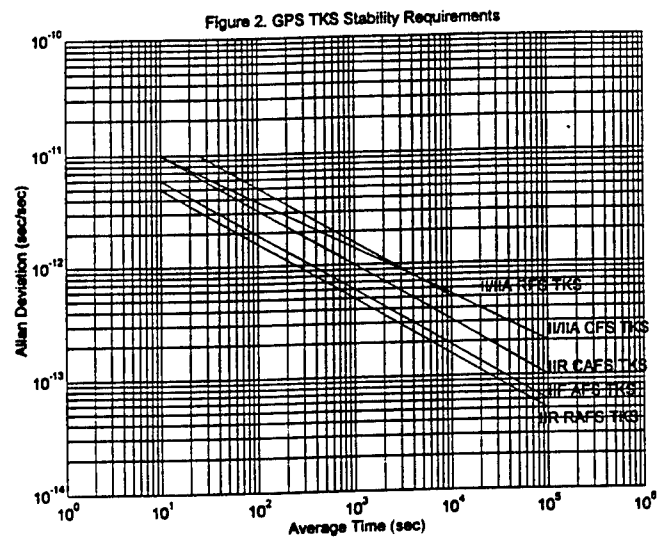


Figure 1. GPS Block IIR TKS System Model



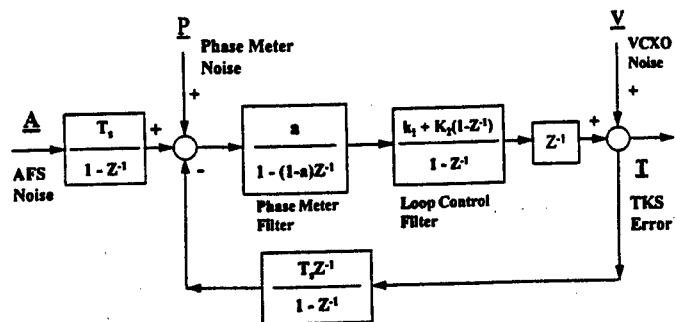


Figure 4. TKS Error Model

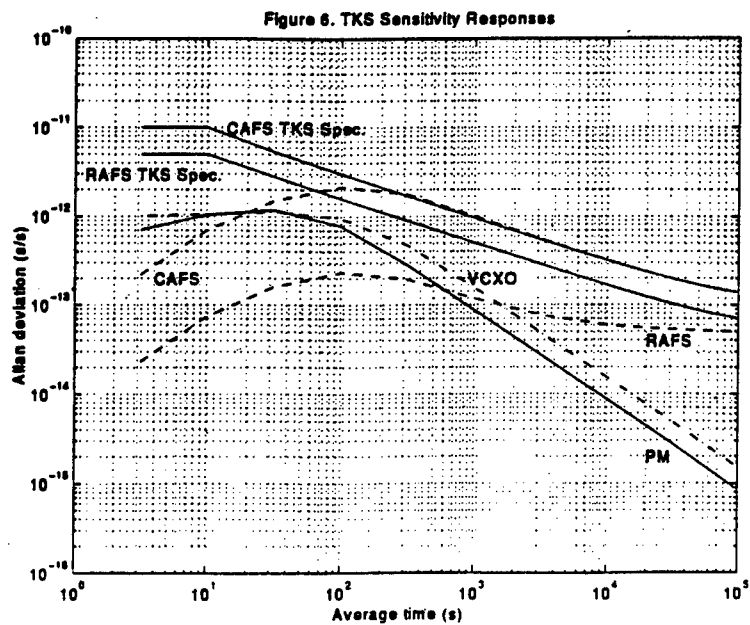
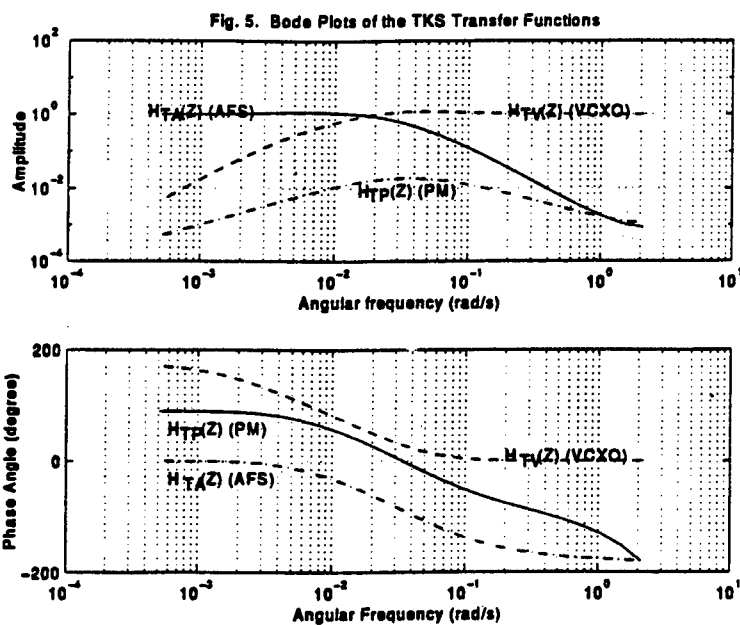


Figure 7. RAFS TKS Allan Deviations

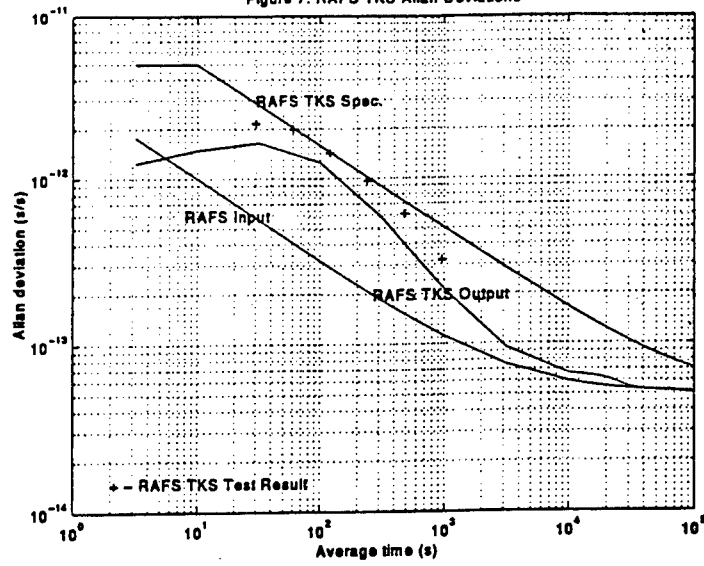


Figure 8. CAFS TKS Allan Deviations

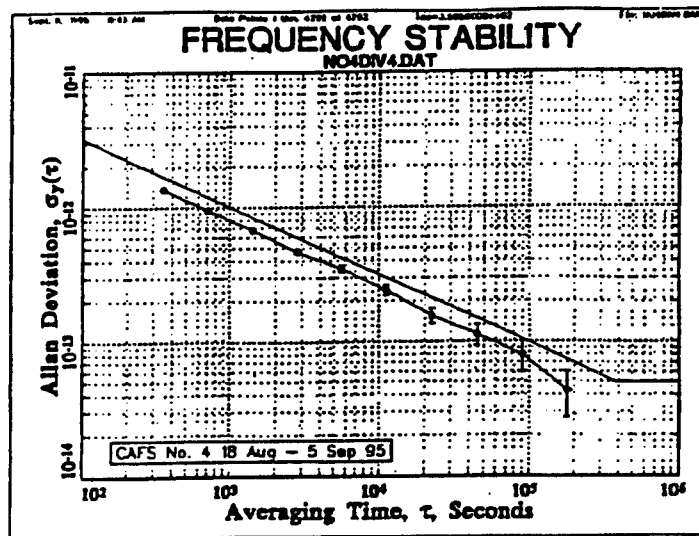
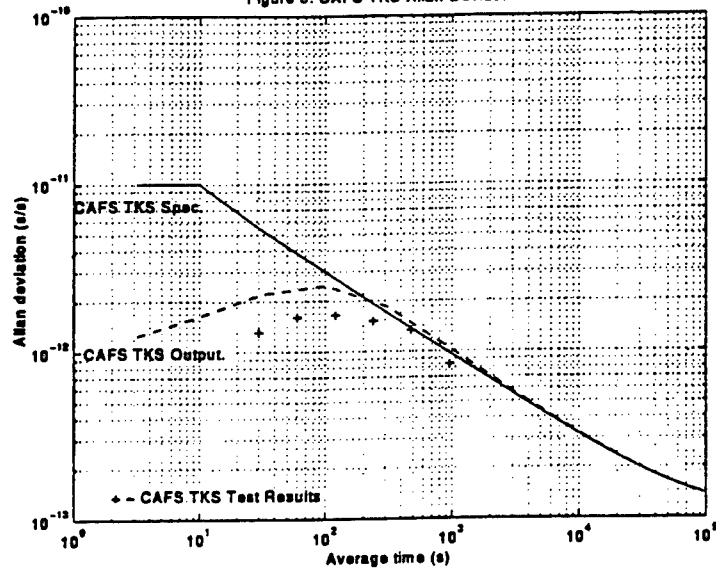


Figure 9. CAFS Test Result

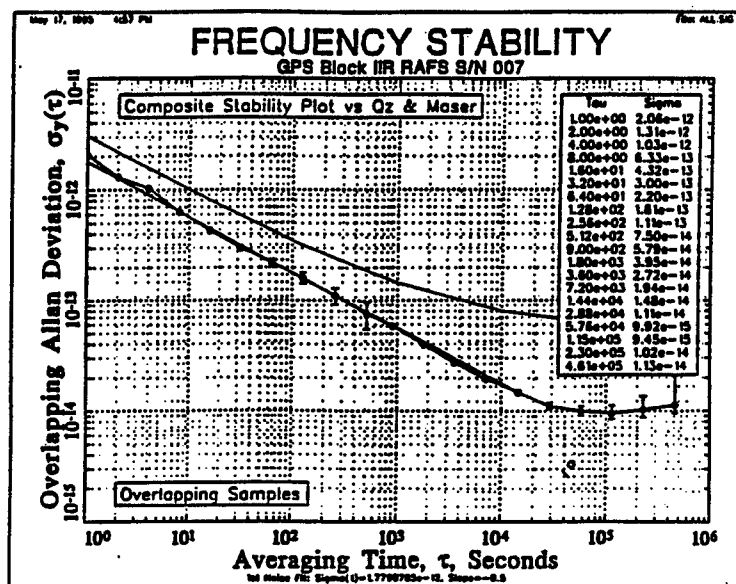


Figure 10. RAFS Test Result

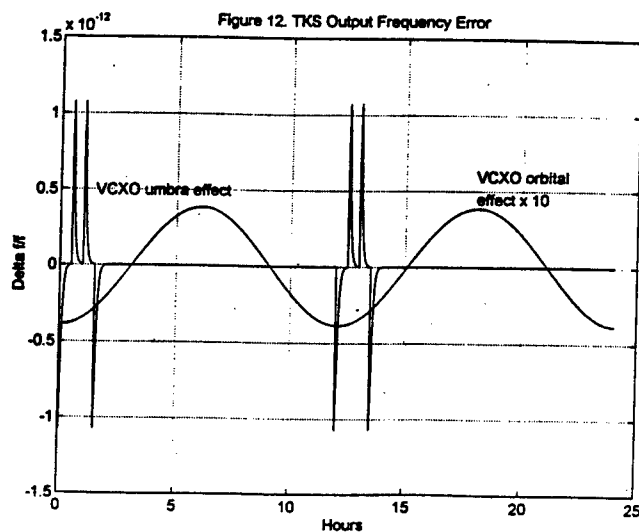
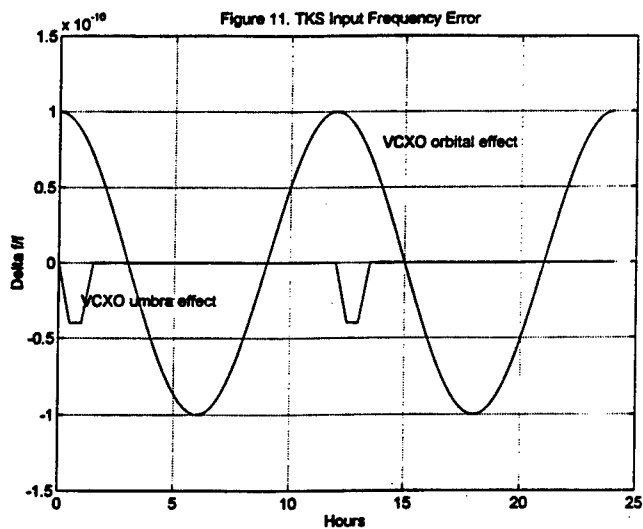


Figure 13. TKS Output Timing Error

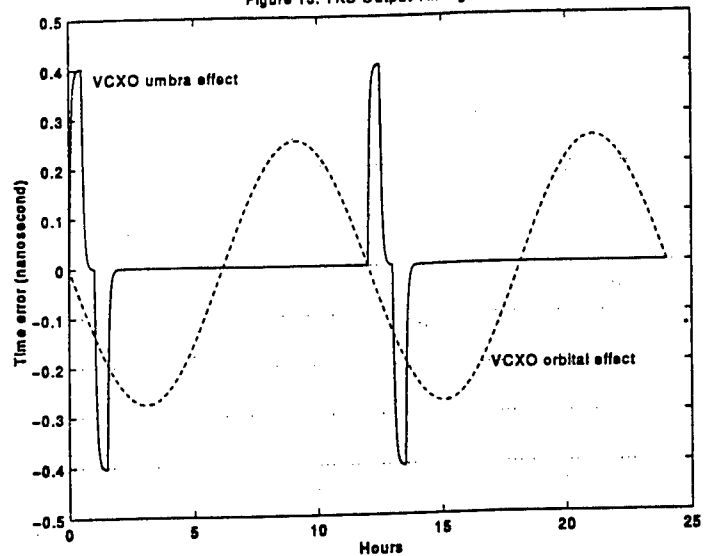


Figure 14. TKS Output Allan Deviations

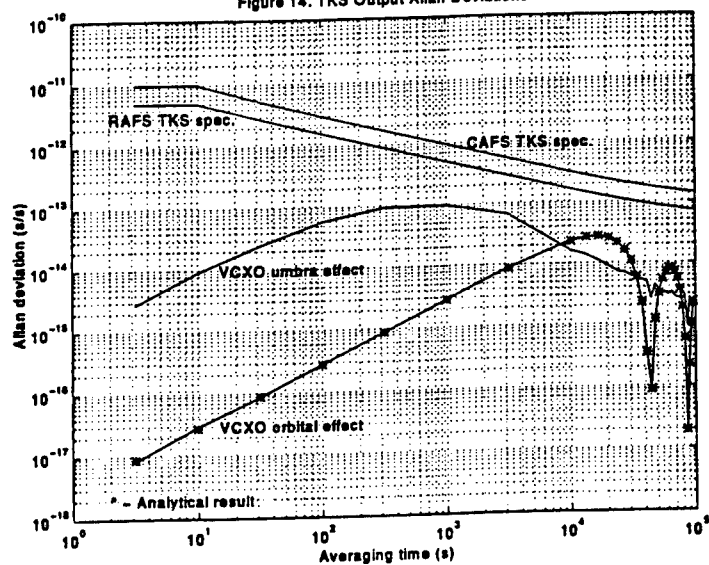
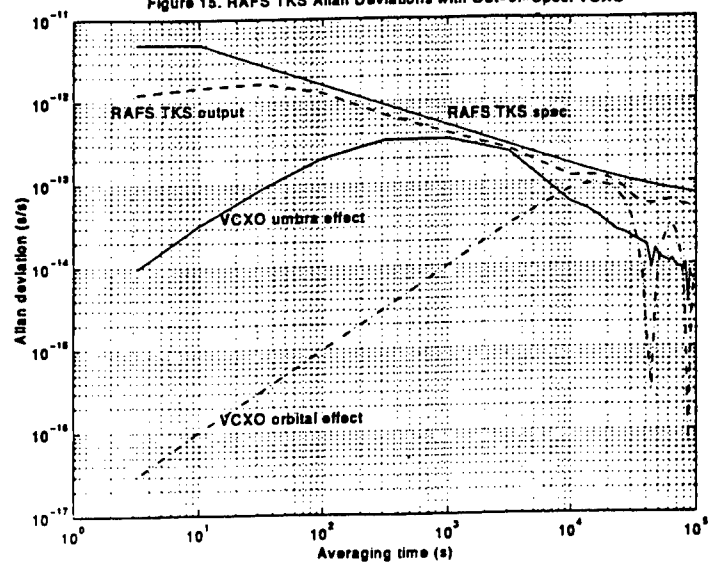


Figure 15. RAFS TKS Allan Deviations with Out-of-Spec. VCXO



Questions and Answers

STEVEN HUTSELL (USNO): There's an earlier plot that at least seems to indicate – and I'd like your opinion – that possibly with some manipulation of the gains, the servo could take better advantage of the physics package stability. I'd like your comment on that.

ANDY WU: The reason that 150 seconds was chosen was because the phase meter is so poor, having a resolution of 1.67 nanoseconds. So you need a long time constant to smooth it out. I did try one – let's say 12 or 15 seconds. And you're going to see the phase meter is going to pop over out here and you're going to have a problem.

GLONASS ONBOARD TIME/FREQUENCY STANDARDS: TEN YEARS OF OPERATION

Arkady B. Bassevich, Pyotr P. Bogdanov
Arvid G. Gevorkyan, and Arkady E. Tyulyakov
Russian Institute of Radionavigation and Time (RIRT)
2 Rastrelli Square, St. Petersburg 193124, Russia

Abstract

The GLONASS onboard time/frequency standards are one of the main elements determining the accuracy of phase synchronization of navigation signals emitted by the satellites and, consequently, the accuracy of navigation and timing determination by the users. In this connection, the maintenance of their accuracy and reliability parameters during operation is very important. The present paper submits the results of analysis of GLONASS onboard time/frequency standards operation as of 18 January 1996, when the space segment was completed by all 24 satellites.

INTRODUCTION

With the launching on 14 December 1995 of the last three satellites, the construction of the space segment of Russian Global Navigation Satellite System GLONASS was completed.

Three cesium-beam frequency standards, with a daily instability not more than 5×10^{-13} and a lifetime of 1 year each, are installed onboard the satellites. The monitoring and control of standards operation are executed on the basis of telemetric parameters and estimates of accuracy characteristics. Accuracy characteristics are estimated by means of processing the measured differences between satellite time scales generated by the standards' pulses and the common system time scale generated by the Main Synchronizer.

While being one of the main units of the GLONASS, the onboard time/frequency standards determine the normal satellite operation and the system's accuracy parameters as a whole. In this connection the maintenance of necessary accuracy and reliability parameters of onboard standards during its operation is a very important task. This paper presents the main characteristics of the GLONASS onboard standards, the technique of their accuracy parameter estimation, and the results of an analysis of the standards' operation as of 18 January 1996.

GLONASS ONBOARD STANDARDS CHARACTERISTICS

Since the second GLONASS stage of development, which began in May 1985, cesium-beam frequency standards have been used on all satellites as space-based frequency and time standards. The main specifications of these standards are given in Table 1.

The given characteristics of the frequency standards provide the mutual synchronization of satellite navigation signal phases with an accuracy of no more than 20 ns (σ) for a 12-hour interval.^[1]

Three frequency standards are used on each satellite: one is in operation and two others are in "cold" reserve. The checking and control of standard operation are executed on the basis of telemetric information and estimates of accuracy characteristics. Switch-on of the reserve standard is executed by a command from the ground station in case of malfunction of the standard's operation or deterioration of its accuracy characteristics.^[2]

ESTIMATION TECHNIQUE OF STANDARD ACCURACY CHARACTERISTICS

The estimation of the accuracy characteristics of GLONASS onboard frequency standards is based on processing the measured offset between satellite time scales, generated by the standard's signals, and System Common Time (SCT), generated by the Main Synchronizer (MS) of the system. The determination of the satellite time shift relative to SCT is executed on the basis of simultaneous one-way and two-way measurements of the range to the satellite, carried out by the phase monitor unit (PMU), located together with the MS.^[1]

The daily measured offset between satellite time scales and SCT (3 to 5 results) are processed by means of least-squares approximation using a linear model for time scale differences, and the individual values of fractional frequency uncertainty of the onboard standards are determined. Calculated then in terms of these values for each 10-day observation period are the following parameters:

the fractional frequency uncertainty of the standard

$$\left(\frac{\Delta f}{f}\right)^* = \frac{1}{N} \sum_{k=1}^N \left(\frac{\Delta f}{f}\right)_k,$$

the instability for averaging time 1 day (square root of the N-sample variance)

$$\delta^* = \sqrt{\frac{1}{N-1} \sum_{k=1}^N \left[\left(\frac{\Delta f}{f}\right)_k - \left(\frac{\Delta f}{f}\right)^* \right]^2},$$

where $\left(\frac{\Delta f}{f}\right)_k$ is the individual value of fractional frequency uncertainty of the onboard standard, and $N = 10$ – the number of individual values for a 10-day observation period.

With due account of the error of a measured offset between the satellite time scale and SCT by means of a PMU not exceeding 5 ns (σ) and an instability for an averaging time of 1 day for the MS not exceeding 5×10^{-14} , the error of individual values of the fractional frequency uncertainty of the onboard standard does not exceed 7.3×10^{-14} .^[3] Thus, at the 0.95 confidence level, true values of fractional frequency uncertainty of standard are within $\pm 2.8 \times 10^{-14} \times \left(\frac{\Delta f}{f}\right)^*$ and the instability for an averaging time of 1 day is within $(0.7 - 1.55) \times \delta^*$. Therefore, the adopted estimation technique of GLONASS onboard standard accuracy parameters is considered valid.

GLONASS ONBOARD STANDARD PARAMETERS AT OPERATION

For the GLONASS space segment as of 18 January 1996, the numbers of operating frequency standards and their accuracy characteristics are given in Table 2.

A diagram of operating time of frequency standards installed on the active satellites is shown in Figure 1. All cases of standard switch-off are caused by deterioration of the daily instability over of a given value of 5×10^{-13} . The histogram of distribution of the frequency standard's operating time is shown in Figure 2. The average value is 16.3 months and the spread is from 2 to 47 months.

The estimation results of GLONASS frequency standard accuracy characteristics show that, for most of standards during intervals of normal satellite operation, the fractional frequency uncertainty $\left(\frac{\Delta f}{f}\right)$ is within $\pm 5 \times 10^{-12}$, the instability for an averaging time of 1 day (δ) does not exceed 3×10^{-13} , and a systematic frequency drift is not observed or does not exceed a few parts in 10^{13} per month. Histograms of the distribution of the fractional frequency uncertainty and the instability for an averaging time of 1 day for all standards during 1995 are shown in Figures 3 and 4.

The adduced data show that the problem of maintenance of given characteristics for GLONASS onboard standards during their whole operating life still exists. The increase of accuracy and reliability characteristics of onboard standards is provided in the framework of the creation of the new GLONASS-M satellite. The newly developed cesium-beam frequency standard should have a daily frequency instability no more than 1×10^{-13} and an operating life of 3 years.^[1] However, delays with manufacturing of the new satellite have not allowed us to begin the checking of these new standards in real conditions.

CONCLUSION

Full deployment of the GLONASS space segment, consisting of 24 satellites, was completed on 18 January 1996. This fact permits one to speak about a 10-year period of operation of the onboard cesium-beam frequency standards, with a daily instability of no more than 5×10^{-13} and an operating life of 1 year each.

The results of estimation of frequency standard accuracy and reliability parameters show that, for most of them during intervals of normal satellite operation, the fractional frequency uncertainty is within $\pm 5 \times 10^{-12}$ and an instability for an averaging time of 1 day does not exceed 3×10^{-13} . The average value of a frequency standard's operating time is 16.3 months.

REFERENCES

- [1] Y.G. Gouzhva, A.G. Gevorkyan, A.B. Bassevich, and P.P. Bogdanov 1992, "High-precision time and frequency dissemination with GLONASS," *GPS World*, July 1992, pp. 40-49.
- [2] Y.G. Gouzhva, A.G. Gevorkyan, A.B. Bassevich, P.P. Bogdanov, and A.E. Tyulyakov 1994, "GLONASS on-board time/frequency standard - architecture and operation," *Proceedings of the 1994 IEEE International Frequency Control Symposium*, 1-3 June 1994, Boston, Massachusetts, pp. 776-781.

- [3] Y.G. Gouzhva, A.G. Gevorkyan, and P.P. Bogdanov 1992, "*Accuracy estimation of GLONASS satellite oscillators*," Proceedings of the 1992 IEEE International Frequency Control Symposium, 27-29 May 1992, Hershey, Pennsylvania, USA, pp. 306-309.

Table 1. Specifications for GLONASS cesium beam frequency standard

Parameter	Value
Output	5 MHz
Relative frequency accuracy	$\pm 1 \times 10^{-11}$
Stability, averaging time:	
- 1 s	5×10^{-11}
- 100 s	1×10^{-11}
- 1 hour	2.5×10^{-12}
- 1 day	5×10^{-13}
Temperature change of frequency (1/° C)	5×10^{-13}
Temperatures range (° C)	0 - 40
Power supply (DC)	27 V
Power consumption	80 W
Dimensions (mm)	370×450×500
Weigh (kg)	39.6
Operating life (hours)	17,500

Table 2. GLONASS space segment at the state of January 18, 1996

SN	Date of start	Operating standard	Date of switch on	$\left(\frac{\Delta f}{f}\right) \times 10^{-12}$	$\delta \times 10^{-13}$	Drift $\times 10^{-13}$
1	30.01.92	2	19.11.93	1.3	1.4	0.3
2	17.02.93	1	18.07.95	-7.5	4.9	-5.1
3	20.11.94	3	24.08.95	2.3	3.1	-1.2
4	20.11.94	1	16.12.94	1.0	2.3	0.0
5 ¹⁾	08.12.90	1	15.10.95	-0.3	3.1	-0.1
6	20.12.94	2	30.10.95	0.5	2.4	0.0
7	17.02.93	2	11.05.93	-0.6	1.6	0.4
8	30.01.92	1	20.02.92	0.5	1.4	-0.5
9 ²⁾	14.12.95	1	07.01.96	—	—	—
10	24.07.95	1	21.08.95	-0.5	1.0	-0.2
11	24.07.95	1	21.08.95	-0.5	1.6	0.6
12	11.08.94	1	07.09.94	-2.0	2.4	0.3
13	14.12.95	1	07.01.96	—	—	—
14	11.08.94	1	07.09.94	-3.8	1.3	0.3
15	24.07.95	1	26.08.95	-2.5	1.8	1.4
16	11.08.95	1	04.09.95	-0.6	1.5	-0.8
17	11.04.94	1	18.05.94	3.0	1.7	-0.2
18	11.04.94	1	16.05.94	2.5	1.4	0.7
19	07.03.95	2	30.07.95	0.5	2.0	0.5
20	07.03.95	1	30.03.95	-0.6	1.6	-1.5
21	30.07.92	3	26.05.95	-0.4	1.4	3.2
22	07.03.95	1	05.04.95	-2.1	2.3	-0.6
23	11.04.94	2	07.10.94	2.3	2.2	-0.7
24 ¹⁾	30.07.92	2	15.07.95	-11.2	4.5	1.8

Note: 1. At present SN 5 and SN 24 put not of action.
2. Reserve satellite No 778 is also set in point 9.

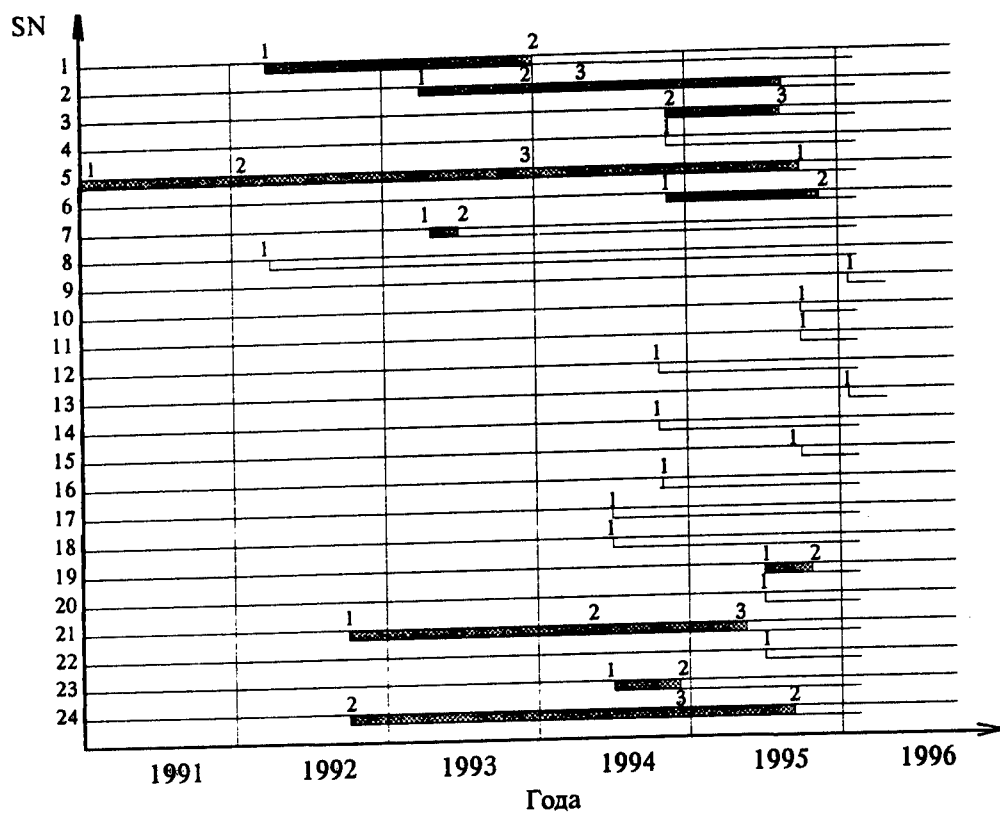


Figure 1. Diagram of operating time for GLONASS on-board standards

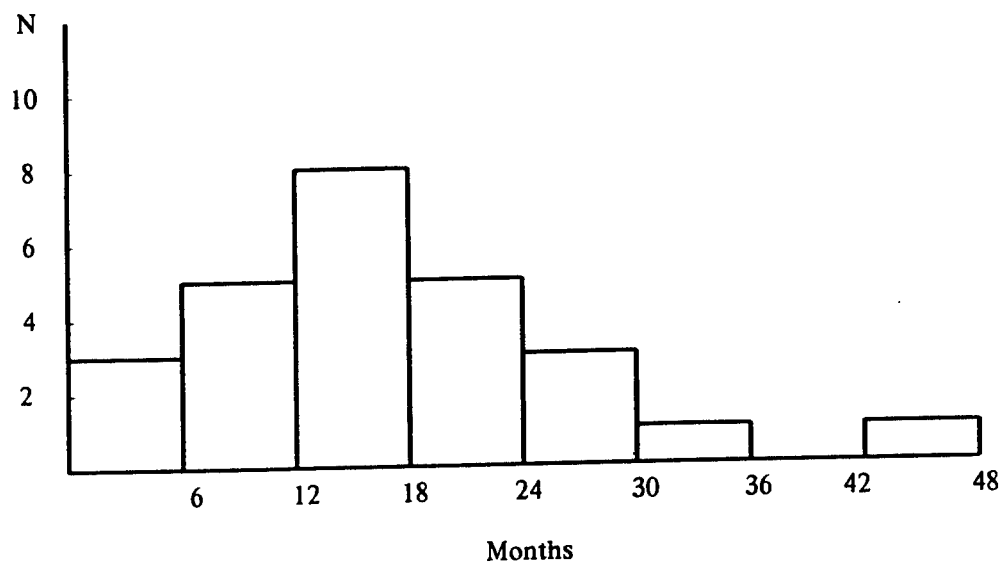


Figure 2. Distribution of operating time for GLONASS on-board standards

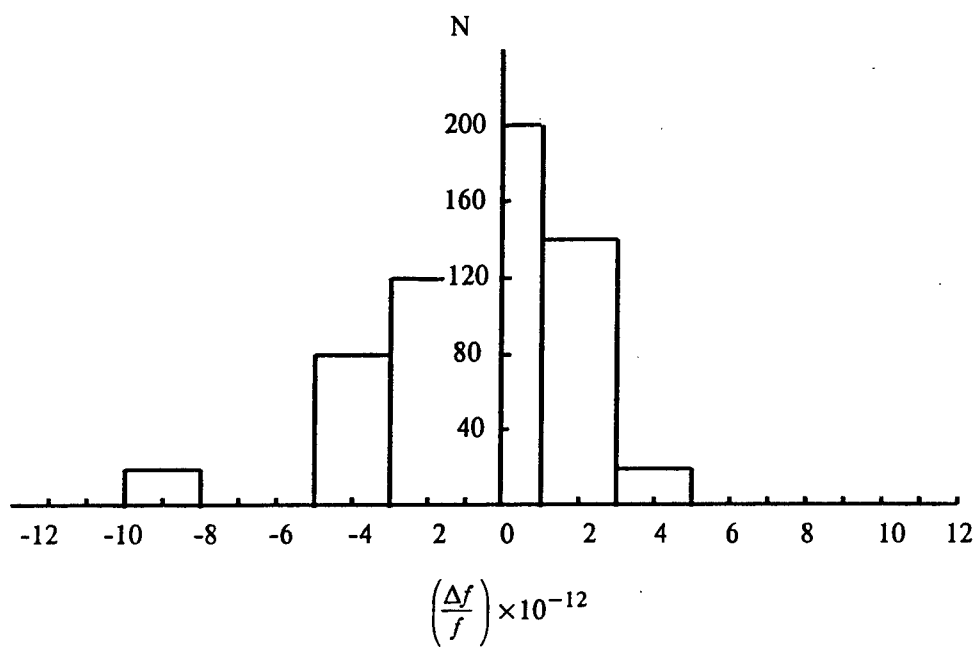


Figure 3. Distribution of the fractional frequency uncertainty for GLONASS on-board standards

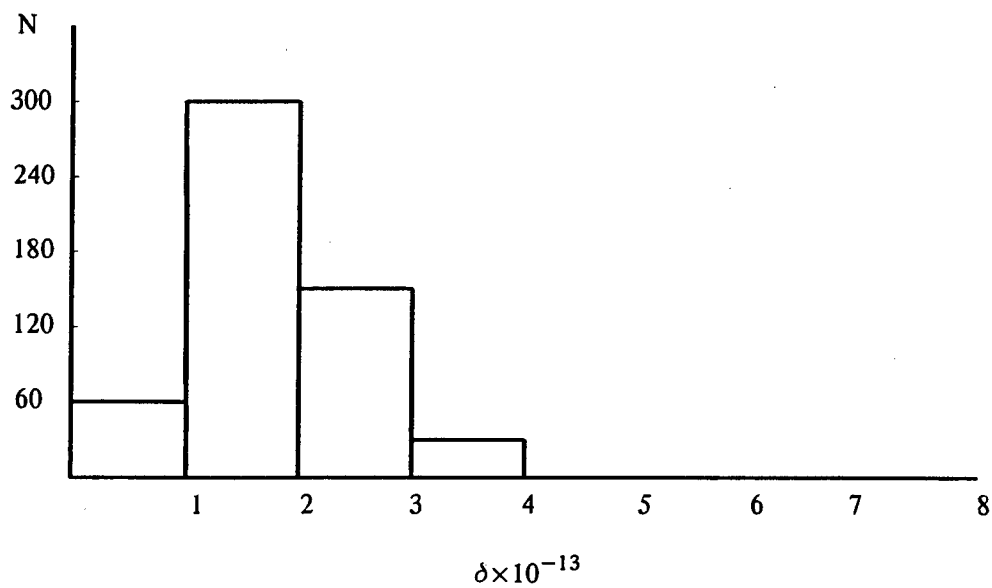


Figure 4. Distribution of instability for averaging time 1 day for GLONASS on-board standards

DESIGN OF A HYDROGEN MASER FOR SPACE

E.M. Mattison and R.F.C. Vessot
Smithsonian Astrophysical Observatory
Cambridge, Massachusetts 02130, USA

Abstract

An active atomic hydrogen maser for long-term use in space has been designed and built as part of the Smithsonian Astrophysical Observatory's Hydrogen Maser Clock (HMC) project. We describe features of the maser's mechanical, magnetic, and thermal design that are important to its performance in space. The flight hardware has been tested in a laboratory vacuum chamber. We report measurements of the performance of the maser's control systems.

CLOCKS IN SPACE: THE HYDROGEN MASER CLOCK PROGRAM

Frequency references – high stability clocks – increasingly find applications in space missions. Atomic clocks of ever increasing stability have present and potential uses as frequency references for the GLONASS and Global Positioning System navigation systems, local oscillators for space-based Very Long Baseline Interferometry, “proper” clocks for tests of general relativity, frequency references for detection of gravitational radiation, and “traveling clocks” for worldwide time transfer.

Clocks for use in space must satisfy several restrictions and requirements, many of which are also requirements or desirable features of earth-based clocks. These requirements include:

- Limitations on mass, size and power
- Requirements for reliable long-term unattended operation
- Ability to withstand vibrational loads during launch
- Ability to tolerate varying magnetic fields
- Ability to cope with a varying thermal environment.

An active atomic hydrogen maser for long-term use in space has been designed and built as part of the Smithsonian Astrophysical Observatory's Hydrogen Maser Clock (HMC) project. HMC is a NASA-sponsored program with the goal of producing and demonstrating a space-qualified hydrogen maser with drift-removed fractional frequency stability of 10^{-15} or better in one day. The HMC maser is an evolutionary outgrowth of a two-decade long SAO program of research and development of hydrogen masers for earth and space use.^[1,2,3] The maser and its control electronics have been designed as an integrated system to cope with the requirements of space flight. We discuss below characteristics of its mechanical, magnetic, and thermal design that are particularly relevant to use in space.

The HMC maser is designed for use with a variety of spacecraft, requiring only an appropriate mechanical connection and electrical interface. It was originally to be tested aboard the European Space Agency's Eureka spacecraft, and then, following cancellation of the planned Eureka reflight, on the Russian Mir space station.^[4] At present, the flight portion of the HMC program has been terminated, and the flight model maser and its electronics are undergoing laboratory testing at SAO.

MECHANICAL AND STRUCTURAL CHARACTERISTICS

The HMC maser's physics unit, shown in in cross-section in Figures 1 and 2, takes the general form of a cylinder 84 cm long and 43 cm in diameter. The maser's main components are its quartz storage bulb and low-expansion resonant cavity; the titanium vacuum tank that contains the cavity; a stainless steel vacuum manifold that includes two sorption pumps for scavenging hydrogen and two small ion pumps for removing other gases; a LiAlH_4 hydrogen source and a glass dissociator chamber for producing a beam of hydrogen atoms; electrical heaters, insulation, and thermistors for temperature control; and magnetic shields and solenoids for magnetic field control. In addition, the physics unit contains electronic components that amplify the 1,420 MHz maser signal from the cavity and electrically isolate the cavity from external perturbations. Separate units contain analog and digital control and monitoring electronics, the RF receiver that phase-locks a 100 MHz crystal oscillator to the maser signal, and a microprocessor that controls the maser's electronics and acts as an interface with the spacecraft's data and telecommand system. The masses of the major instrument elements are given in Table 1. Additional elements, whose masses depend upon the specific spacecraft used, are the bracket that mounts the maser to the spacecraft, and any additional spacecraft-specific electronics.

Table 1. HMC Instrument Mass Summary

Element	Mass (kg)
Maser physics unit	70.7
Control and RF electronics	27.9

Structurally, the maser is supported from a circular aluminum midplane plate, which supports the maser's resonant cavity and vacuum tank on one side, and its vacuum manifold and hydrogen source on the other. The midplane plate is the main structure for mounting the maser to the spacecraft. A titanium "aft neck" tube connects one end of the vacuum tank to the midplane plate and the vacuum manifold, while a similar "forward neck" connects the other end of the vacuum tank to the maser's cylindrical outer aluminum housing. The housing, in turn, transfers the forward neck's load to the midplane plate. By means of an ANSYS finite element model with approximately 2,800 nodes, the HMC maser has been designed to cope with the vibrational and accelerational loads of a Space Shuttle launch. It can withstand at least 15 g's rms, in all axes acting simultaneously, in a spectrum from 20 Hz to 2 kHz. The maser's lowest mechanical resonant frequency is 46 Hz. The flight cavity and vacuum tank, which are the most critical components, have been tested to flight input vibrational levels.

MAGNETIC FIELD CONTROL

A spacecraft in low earth orbit experiences the earth's magnetic field, with a magnitude of about 0.5 gauss and a variation over an orbit of up to ± 0.5 gauss, depending upon the spacecraft's attitude in orbit. In addition, some spacecraft create variable magnetic fields themselves, for example by magnetic torquers used for attitude control. The magnetic field within the maser's

storage bulb must be maintained at a level on the order of 0.3 milligauss. To achieve frequency stability of better than $\Delta f/f < 1 \times 10^{-15}$, the temporal variation of the internal magnetic field must be less than $\Delta H < 0.8 \times 10^{-6}$ gauss. To achieve these conditions, the HMC maser utilizes passive magnetic shields, internal solenoids, and an active magnetic compensation system.

As shown in Figure 1, the maser's resonant cavity and titanium vacuum tank are surrounded by a three-section, two-layer cylindrical printed circuit solenoid that creates the internal magnetic field of approximately 0.3 milligauss, and by four layers of concentric magnetic shields that attenuate external fields. The outermost shield extends to enclose the vacuum pump manifold and atomic hydrogen dissociator, reducing external fields that could perturb the state-selected atomic hydrogen beam. The measured shielding factor of these Hypernom shields is

$$S_{\text{passive}} = \frac{\Delta H_{\text{ext}}}{\Delta H_{\text{int}}} \approx 3.4 \times 10^5$$

The passive shields are augmented by an active magnetic compensation system. A single-axis fluxgate magnetometer sensor is mounted inside the outer shield to sense the axial field near the end of the maser. A compensation coil is wound on the outside cylindrical surface of the next shield, and a feedback circuit drives the coil to keep the field sensed by the magnetometer constant. The shielding factor for the total magnetic control system, determined by measuring the transverse ("Zeeman") resonance frequency in the oscillating maser's storage bulb, is

$$S_{\text{total}} \approx 2.8 \times 10^6$$

With this shielding factor, the expected maximum fractional frequency variation due to movement through the earth's field is on the order of $\Delta f/f \sim 2 \times 10^{-16}$.

THERMAL CONTROL SYSTEM DESIGN FEATURES

Temperature changes of the maser's resonant cavity and storage bulb affect the maser's output frequency. To keep frequency variations below the level of 1 part in 10^{15} , the cavity temperature must be maintained constant to approximately 10^{-4} °C. The HMC maser employs several strategies to achieve this level of temperature control. To control heat flow from the vacuum tank, the maser's structure is divided into three concentric isothermal control regions. Thermal gradients are controlled by subdividing each isothermal region into multiple independently controlled zones, by mounting controlled guard heaters on heat leakage paths, by separating heaters from the primary controlled structure (the vacuum tank), and by carefully calibrating and matching thermistors and setpoint resistors to ensure that all zones of an isothermal region control at the same temperature. Radiative heat flow is reduced by means of multilayer insulation in the spaces between the regions, which are evacuated by being open to the space environment, while conductive heat flow is controlled by design of the segmented nylon rings that support the magnetic shields.

As shown in Figure 2, the innermost isothermal region, which is the titanium vacuum tank that surrounds the resonant cavity, is maintained at 50°C. The resolution of the tank control system is 1×10^{-4} degrees. To reduce thermal gradients in the tank, the three tank heaters are separate from the tank itself, one being located on the outside surface of the inner magnetic shield that is directly outside the tank and the others on the titanium neck tubes where they connect to either end of the tank.

The tank, in turn, is surrounded by an aluminum oven that is located directly over the third magnetic shield and whose temperature is maintained at 41°C. The oven region acts as a guard to control heat that flows from the tank region both radiatively from the tank surface and conductively along the magnetic shield supports and the titanium support necks. The oven region consists of three control zones located on the cylinder and end surfaces of the oven, and two zones mounted on the outer ends of the support necks.

The third isothermal region consists of the midplane plate and an outer aluminum support shell that directly surrounds the fourth magnetic shield. This zone is maintained at approximately 27°C by a control thermistor and a set of heaters mounted on the midplane plate.

In addition to the thermal control zones that are integral with the maser, the system includes a controlled temperature guard station on the structure that mounts the maser to the spacecraft, to act as a first stage of isolation from the conductive environment. The entire instrument is surrounded with multilayer insulation to isolate it from the radiative environment.

The thermal control system incorporates several electronic and hardware features to achieve the high degree of thermal stability required. The digital electronic control system is based upon four 68HC11 microcontrollers, each of which can control up to five thermal zones. Each 68HC11 includes a microprocessor, an 8-bit analog-to-digital converter with an eight-channel multiplexer, and timer registers that are used as pulse-width modulators (PWM) for high-efficiency switched heater power control. The vacuum tank heaters, which are closest to the maser's resonant cavity, are powered by high-frequency (~8 kHz) PWMs to avoid perturbation of the maser oscillation; the other heaters are switched at a 30 Hz rate. The thermal control program incorporates a three-mode PID (proportional, integral, and differential) algorithm to eliminate proportional offset. (Differential control is included in the algorithm, but has not been found to be useful in this application.)

Components of the thermal control system have been chosen for thermal stability and low magnetic field production. Thermistors are glass-encapsulated, high-stability units that have been burned in. Monitor and control thermistors for each zone are chosen to be matched. Temperature setpoint resistors are chosen to have low temperature coefficients, and are physically mounted on a temperature-controlled zone within the maser for minimum temperature perturbation. Heaters are flexible printed circuits with Kapton film insulation. For each heater, identical etched foil elements are overlaid with opposite current flow, to minimize magnetic field production.

The ability of the thermal control system to stabilize the tank zone temperatures in the face of external temperature changes is shown by the data of Table 2. For these measurements, which were made on the engineering model of the maser, the temperatures of the maser support structure and the forward neck guard zone were separately lowered by 2°C.

Table 2. Response of Tank Control Zones to External Temperature Change

	ΔT (Support) = -2°C	ΔT (Fwd neck) = -2°C
ΔT (Tank forward):	$-0.1 \times 10^{-4} ^{\circ}\text{C}$	$+0.2 \times 10^{-4} ^{\circ}\text{C}$
ΔT (Tank cylinder):	$+1 \times 10^{-4} ^{\circ}\text{C}$	$-1 \times 10^{-4} ^{\circ}\text{C}$
ΔT (Tank aft):	$+3 \times 10^{-4} ^{\circ}\text{C}$	$-2 \times 10^{-4} ^{\circ}\text{C}$

REFERENCES

- [1] M.W. Levine, R.F.C. Vessot, E.M. Mattison, E. Blomberg, T.E. Hoffman, G. Nystrom, D.F. Graveline, R.L. Nicoll, C. Dovidio, and W. Brymer 1977, "*A hydrogen maser design for ground applications*," Proceedings of the 8th Annual Precise Time and Time Interval (PTTI) Applications and Planning Meeting, 30 November-2 December 1976, Washington, D.C., USA, pp. 249-276.
M.W. Levine, R.F.C. Vessot, E.M. Mattison, G. Nystrom, T.E. Hoffman, and E. Blomberg 1977, "*A new generation of SAO hydrogen masers*," Proceedings of the 31st Annual Symposium on Frequency Control, 1-3 June 1977, Atlantic City, New Jersey, USA (U.S. Army Electronics Command), pp. 525-534.
- [2] R.F.C. Vessot, M.W. Levine, E.M. Mattison, E.L. Blomberg, T.E. Hoffman, G.U. Nystrom, B.F. Farrell, R. Decher, P.B. Eby, C.R. Baugher, J.W. Watts, D.L. Teubr, and F.D. Wills 1980, "*Test of relativistic gravitation with a space-borne hydrogen maser*," *Physical Review Letters*, **45**, 2081.
- [3] E. M. Mattison 1989, "*Ultra-stable clocks for use in space*," *Advances in Space Research*, **9**, (9)13-(9)19.
- [4] E.M. Mattison, and R.F.C. Vessot 1996, "*High precision time transfer to test a hydrogen maser on Mir*," Proceedings of the 27th Annual Precise Time and Time Interval (PTTI) Applications and Planning Meeting, 29 November-1 December 1995, San Diego, California, USA (NASA CP-3334), pp. 181-192.

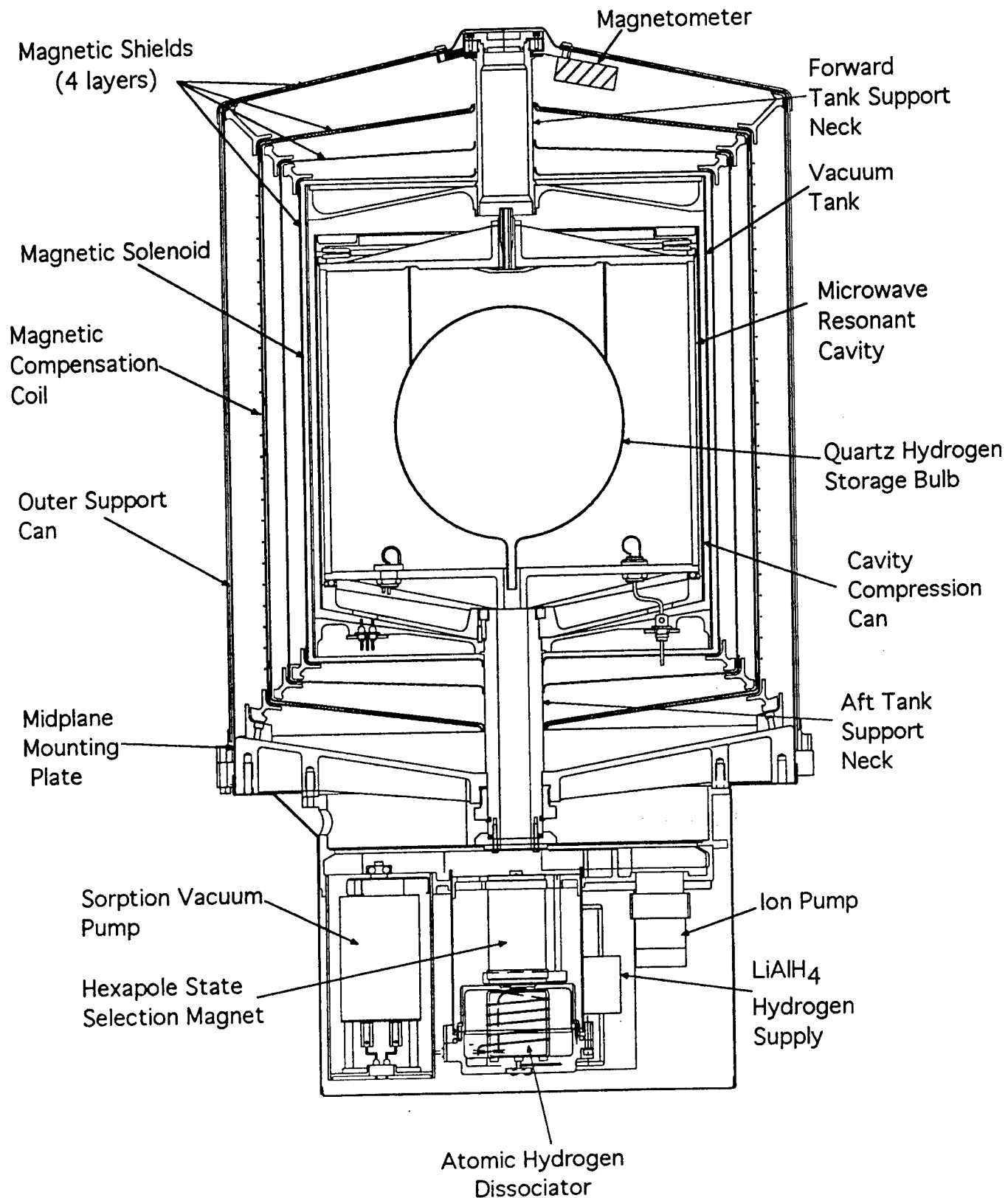


Figure 1. HMC maser - major components

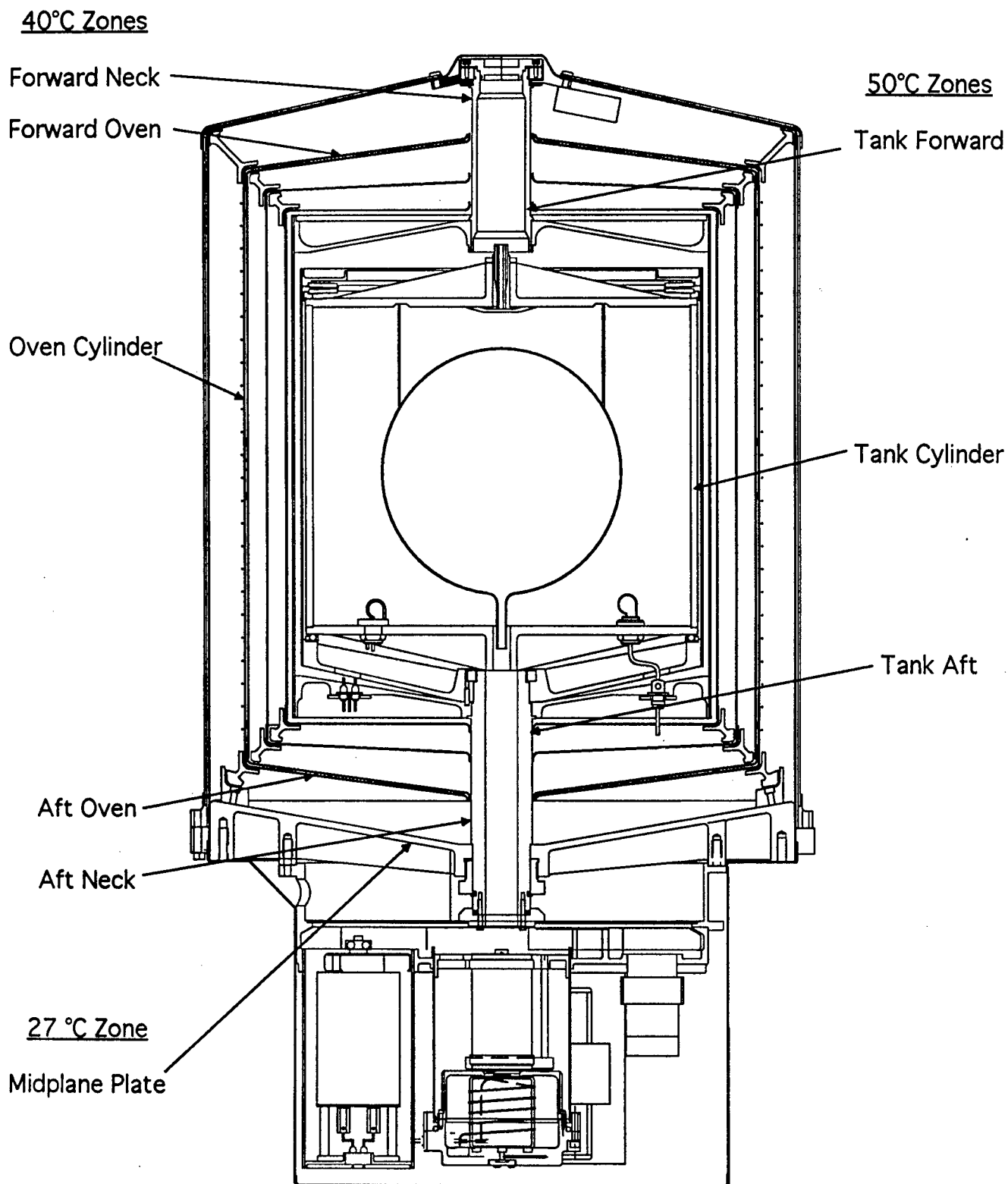


Figure 2. Thermal Control Zone Locations

SPACECRAFT-SPACECRAFT DOPPLER TRACKING AS A XYLOPHONE INTERFEROMETER DETECTOR OF GRAVITATIONAL RADIATION

Massimo Tinto
Jet Propulsion Laboratory
California Institute of Technology
4800 Oak Grove Drive
Pasadena, California 91109, USA

Abstract

We discuss spacecraft-spacecraft Doppler tracking as a detector of gravitational radiation, in which one-way and two-way Doppler data recorded onboard the two spacecraft are time-tagged and telemetered back to Earth. By linearly combining the four Doppler data sets^[1], we derive a method for reducing by several orders of magnitude, at selected Fourier components, the frequency fluctuation due to the clocks onboard the spacecraft. The nonzero gravitational wave signal remaining at these frequencies makes this spacecraft-spacecraft Doppler tracking technique the equivalent of a xylophone interferometer detector of gravitational radiation.^[2,3] In the assumption of calibrating the frequency fluctuations induced by the interplanetary plasma, a strain sensitivity of 3.7×10^{-19} at 10^{-3} Hz is estimated.

Experiments of this kind could be performed by future interplanetary multi-spacecraft missions planned by the National Aeronautics and Space Administration (NASA).

MOTIVATIONS

- The New Millenium Program is planning to launch multi-spacecraft missions.
- Doppler/ranging measurements between spacecraft can potentially decrease reliance on ground-based tracking.^[4]
- Possible backup option for space-based laser interferometers in case of failure.

WHAT IS A XYLOPHONE?

- A detector displaying a significantly enhanced sensitivity at selected Fourier components!
- How can we make a "narrowband" detector out of Doppler tracking?^[5]

TWO-WAY DOPPLER RESPONSE

$$\begin{aligned} \frac{\Delta\nu}{\nu_0}(t) = & \frac{(\mu-1)}{2} h(t) - \mu h(t-(1+\mu)L) + \frac{(1+\mu)}{2} h(t-2L) \\ & + C_E(t-2L) - C_E(t) + T(t-2L) + T(t) + 2B(t-L) \\ & + A_E(t-2L) + A_{sc}(t-L) + TR_{sc}(t-L) + EL_{E_2}(t) + P_{E_2}(t) \end{aligned}$$

where:

$$\mu = \cos(\theta) \quad ; \quad h(t) = h_+(t) \cos(2\phi) + h_-(t) \sin(2\phi)$$

(Estabrook and Wahlquist^[6]).

$$\begin{aligned} \widetilde{\frac{\Delta\nu}{\nu_0}}(f) = & \left[\frac{(\mu-1)}{2} - \mu e^{2\pi i f(1+\mu)L} + \frac{(1+\mu)}{2} e^{4\pi i fL} \right] \widetilde{h}(f) \\ & + \widetilde{C}_E(f) [e^{4\pi i fL} - 1] + \widetilde{T}(f) [e^{4\pi i fL} + 1] + 2 \widetilde{B}(f) e^{2\pi i fL} \\ & + \widetilde{A}_E(f) e^{4\pi i fL} + \widetilde{A}_{sc}(f) e^{2\pi i fL} + \widetilde{TR}_{sc}(f) e^{2\pi i fL} + \widetilde{EL}_{E_2}(f) + \widetilde{P}_{E_2}(f) \end{aligned}$$

(Armstrong^[7]).

XYLOPHONE INTERFEROMETER

The two one-way Doppler data are linearly combined to minimize the rms noise level.^[5]

$$y_{1a}(t) = y_{1a}^0(t) + C_b(t-L) - C_a(t) + B_b(t-L) + B_a(t) + A_b(t-L) + EL_{1a}(t)$$

$$y_{1b}(t) = y_{1b}^0(t) + C_a(t-L) - C_b(t) + B_a(t-L) + B_b(t) + A_a(t-L) + EL_{1b}(t)$$

By taking the Fourier transform of the following two linear combinations:

$$y_+(t) = (y_{1a}(t) + y_{1b}(t))/2$$

$$y_-(t) = (y_{1a}(t) - y_{1b}(t))/2$$

we derive the following expressions in the Fourier domain:

$$\begin{aligned}
\widetilde{y}_+(f) &= \frac{1}{4} \left[(\mu - 1) (1 - e^{2\pi i(\mu+1)fL}) + (\mu + 1) (1 - e^{2\pi i(\mu-1)fL}) e^{2\pi i f L} \right] \widetilde{h}(f) \\
&+ \frac{1}{2} \left[\widetilde{C}_a(f) + \widetilde{C}_b(f) \right] (e^{2\pi i f L} - 1) + \frac{1}{2} \left[\widetilde{B}_a(f) + \widetilde{B}_b(f) \right] (e^{2\pi i f L} + 1) \\
&+ \frac{1}{2} \left[\widetilde{A}_a(f) + \widetilde{A}_b(f) \right] e^{2\pi i f L} + \frac{1}{2} \left[\widetilde{E L}_{1a}(f) + \widetilde{E L}_{1b}(f) \right] \\
\widetilde{y}_-(f) &= \frac{1}{4} \left[(\mu - 1) (1 - e^{2\pi i(\mu+1)fL}) - (\mu + 1) (1 - e^{2\pi i(\mu-1)fL}) e^{2\pi i f L} \right] \widetilde{h}(f) \\
&+ \frac{1}{2} \left[\widetilde{C}_a(f) - \widetilde{C}_b(f) \right] (e^{2\pi i f L} + 1) + \frac{1}{2} \left[\widetilde{B}_a(f) - \widetilde{B}_b(f) \right] (e^{2\pi i f L} - 1) \\
&+ \frac{1}{2} \left[\widetilde{A}_b(f) - \widetilde{A}_a(f) \right] e^{2\pi i f L} + \frac{1}{2} \left[\widetilde{E L}_{1a}(f) - \widetilde{E L}_{1b}(f) \right]
\end{aligned}$$

$\widetilde{y}_+(f)$, $\widetilde{y}_-(f)$ assume the following form at the Xylophone frequencies f_{2k} , f_{2k-1}

$$f_{2k} = \frac{2k}{2L} \pm \frac{\Delta f}{2}$$

$$f_{2k-1} = \frac{2k-1}{2L} \pm \frac{\Delta f}{2}; \quad k = 1, 2, 3, \dots$$

$$\begin{aligned}
\widetilde{y}_+(f_{2k}) &= \frac{1}{2} \mu \left[1 - e^{2\pi i k \mu} \right] \widetilde{h}(f_{2k}) \pm \frac{1}{2} \left[\widetilde{C}_a(f_{2k}) + \widetilde{C}_b(f_{2k}) \right] (\pi i \Delta f L) \\
&+ \left[\widetilde{B}_a(f_{2k}) + \widetilde{B}_b(f_{2k}) \right] + \frac{1}{2} \left[\widetilde{A}_a(f_{2k}) + \widetilde{A}_b(f_{2k}) \right] + \frac{1}{2} \left[\widetilde{E L}_{1a}(f_{2k}) + \widetilde{E L}_{1b}(f_{2k}) \right] \\
\widetilde{y}_-(f_{2k-1}) &= \frac{1}{2} \mu \left[1 + e^{\pi i (2k-1) \mu} \right] \widetilde{h}(f_{2k-1}) + \left[\widetilde{B}_b(f_{2k-1}) - \widetilde{B}_a(f_{2k-1}) \right] \\
&+ \frac{1}{2} \left[\widetilde{A}_a(f_{2k-1}) - \widetilde{A}_b(f_{2k-1}) \right] \frac{1}{2} \left[\widetilde{E L}_{1a}(f_{2k-1}) - \widetilde{E L}_{1b}(f_{2k-1}) \right] \\
&\pm \frac{1}{2} \left[\widetilde{C}_a(f_{2k-1}) - \widetilde{C}_b(f_{2k-1}) \right] (\pi i \Delta f L)
\end{aligned}$$

If $L = 1$ AU, and $\Delta f = 3 \times 10^{-7}$ Hz

$$\frac{\pi \Delta f L}{c} = 4.7 \times 10^{-4}$$

$L = 1$ AU, $f = 5 \times 10^{-4}$ Hz, and $\Delta f = 3 \times 10^{-7}$ Hz, imply:

$$\Delta L = 1.0 \times 10^5 \text{ km}$$

$$\sigma(f_k) = \sqrt{S_y(f_k) \Delta f}$$

$S_y(f_k)$ = One-sided Power Spectral Density of the remaining noise sources at the Xylophone frequencies f_k .

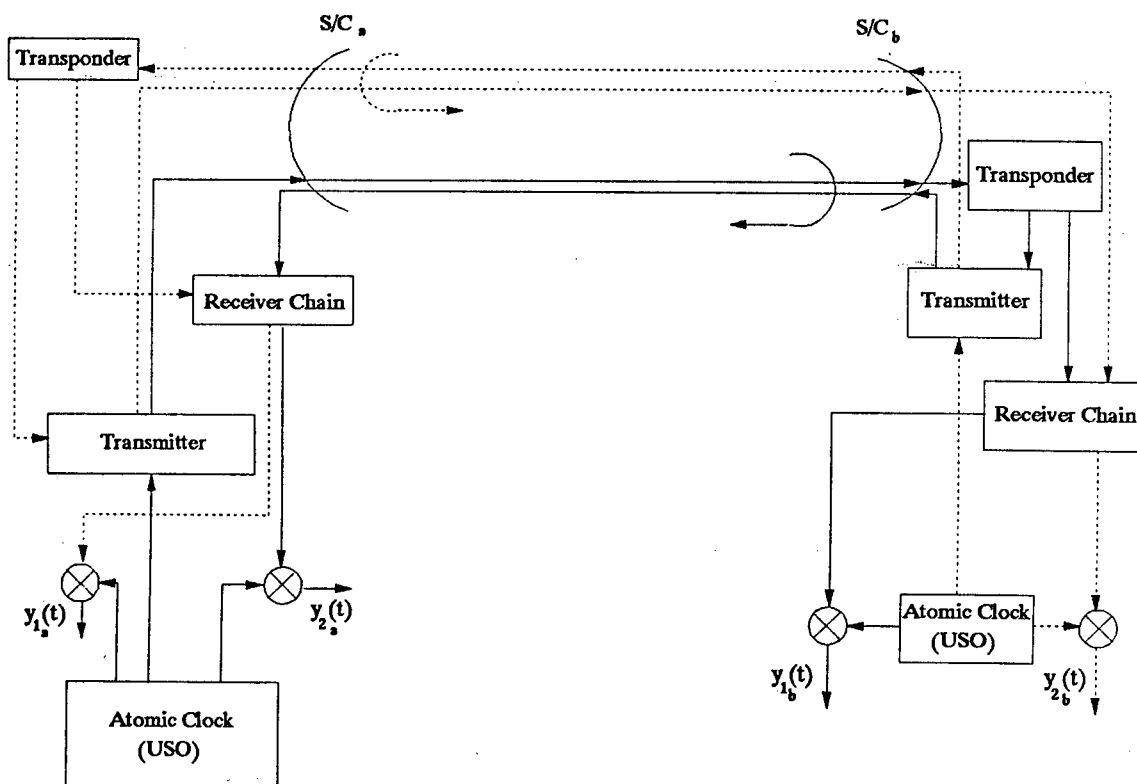
CONCLUSIONS

- We have shown how frequency fluctuations due to the onboard clocks can be reduced by several orders of magnitude at selected Fourier components (*Xylophone Interferometer*)
- We will investigate how this technique can be extended to other tests of relativistic gravity.

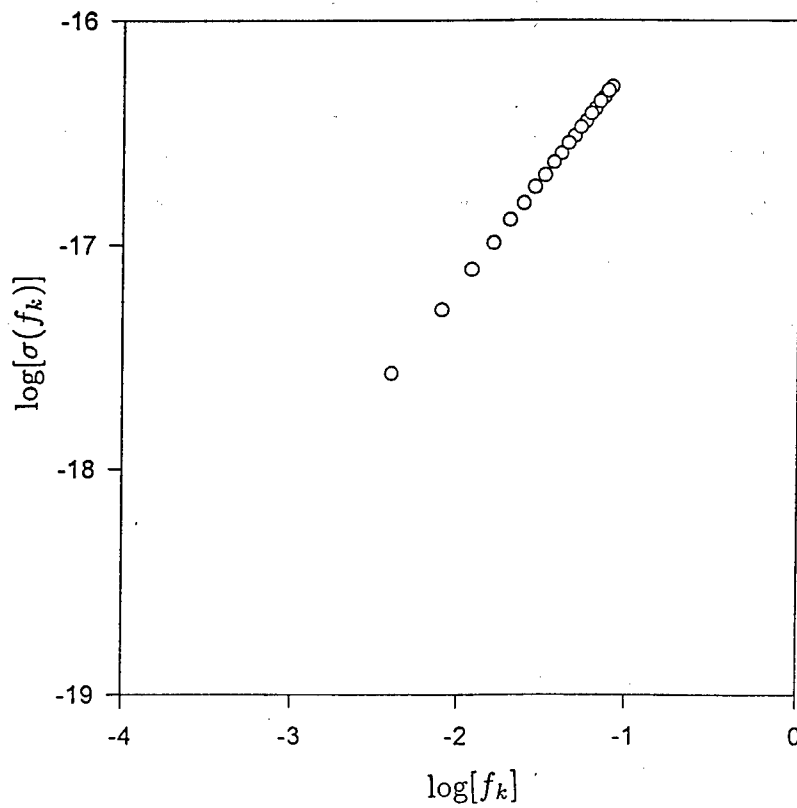
REFERENCES

- [1] R.F.C. Vessot, and M.W. Levine, 1979, **General Relativity and Gravitation**, 10, 181.
- [2] M. Tinto 1996, **Physical Review**, D53, 5354.
- [3] M. Tinto, **Physical Review**, D, submitted.
- [4] R.D. Kahn, S. Thurman, and C. Edwards 1994, "*TDA Progress Report 42-17*," 15 May 1994.
- [5] M. Tinto 1996, "*Spacecraft Doppler tracking as a xylophone detector*," Proceedings of the 27th Annual Precise Time and Time Interval (PTTI) Applications and Planning Meeting, 29 November-1 December 1995, San Diego, California, USA (NASA CP-3334), pp. 467-478.
- [6] F.B. Estabrook, and H.D. Wahlquist 1975, **General Relativity and Gravitation**, 6, 439.
- [7] J.W. Armstrong 1987, **Gravitational Wave Data Analysis**, ed. B.F. Schutz (Kluwer, Dordrecht, Netherlands).

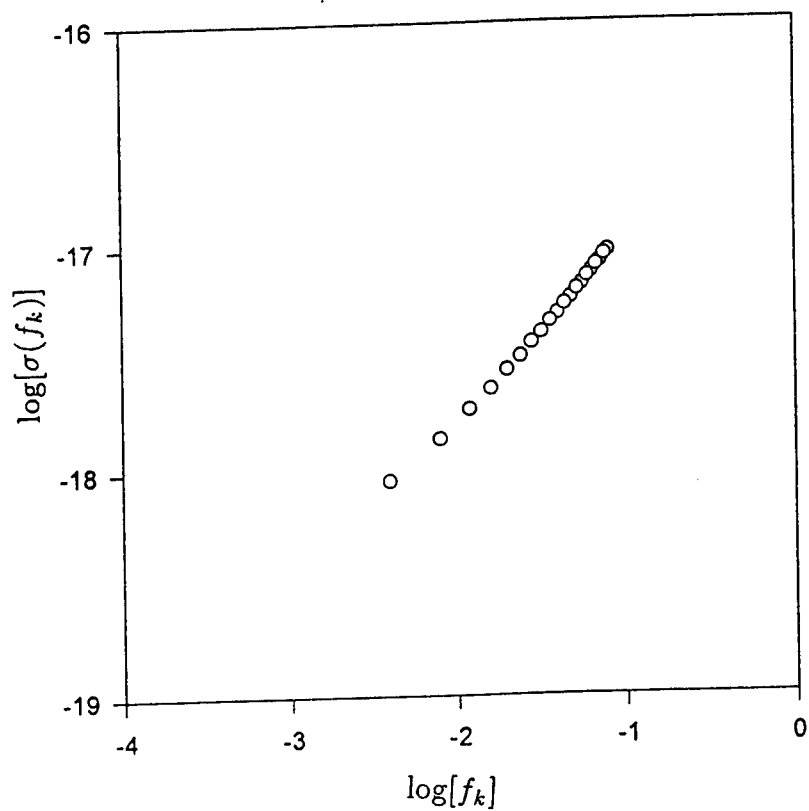
4-Links (Vessot's) Method



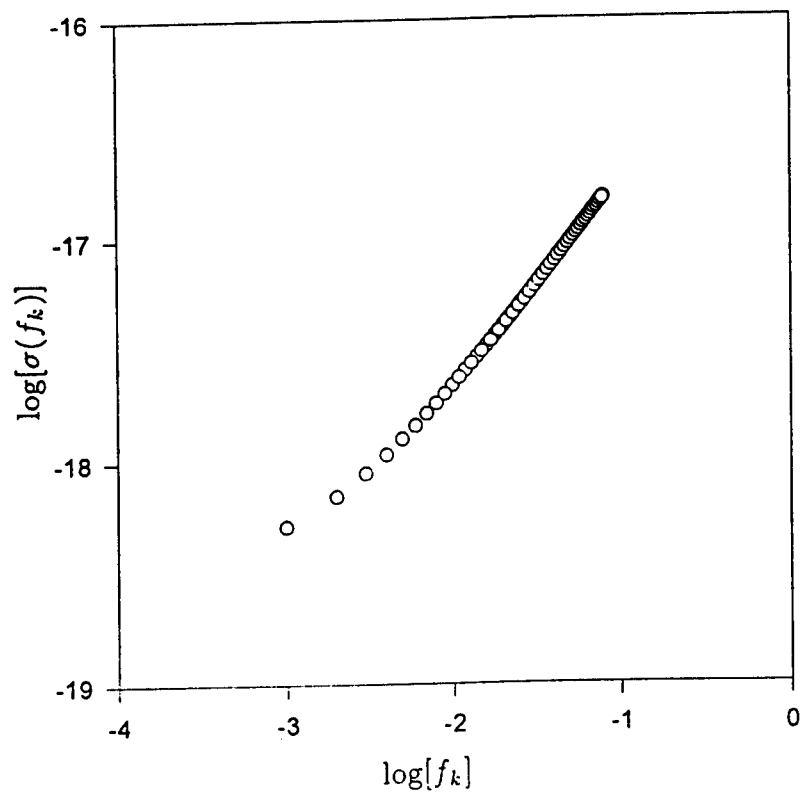
L = 1/4 AU - 1 m HGA



L = 1/4 AU - 4 m HGA



L = 1 AU - 4 m HGA



PHARAO: A SPACE CLOCK WITH COLD CESIUM ATOMS

Ph. Laurent¹, E. Simon¹, G. Santarelli¹, A. Clairon¹, Ch. Salomon²,
P. Lemonde², P. Petit³, N. Dimarcq³, C. Audoin³, F. Gonzalez⁴, and
F. Jamin Changeart⁴

¹BNM-Laboratoire Primaire du Temps et des Fréquences, 61, Av. de l'Observatoire 75014 Paris, France

²Laboratoire Kastler Brossel, École Normale Supérieure, 24 rue Lhomond 75231 Paris, France

³Laboratoire de l'Horloge Atomique, Bat. 221, Université Paris-Sud, 91405 Orsay, France

⁴Centre National d'Études Spatiales, 18, Av. Edouard Belin, 31055 Toulouse, France

Abstract

We describe a cold atom clock designed for operating in microgravity, the PHARAO project. Preliminary results have already been obtained on earth and the prototype will be tested in the reduced gravity of aircraft parabolic flights in the beginning of 1997. The PHARAO prototype is an extension of the work done at the BNM-LPTF on a cesium atomic fountain, which presents a resonance linewidth of 700 millihertz, a frequency stability of $1.5 \cdot 10^{-13} \tau^{-1/2}$ where τ is the integration time in seconds. The accuracy of the fountain clock is presently $2 \cdot 10^{-15}$, more than three times better than previously achieved with uncooled conventional devices. The expected relative stability of the PHARAO cesium clock in space is about $3 \cdot 10^{-14}$ at one second or 10^{-16} per day. Because the reduced gravity environment allows a mode of operation of the clock different from earth fountains, the accuracy of PHARAO should surpass that of fountains and be in the 10^{-17} range. The PHARAO frequency standard could be a key element in future space missions in fundamental physics such as SORT (Solar Orbit Relativity Test), detection of gravitational waves, or for the realization of a global time scale and a new generation of positioning system.

1 INTRODUCTION

Today, the most stable frequency standards are cesium clocks, hydrogen masers, and trapped ion clocks. The unit of time, the second, is defined using the hyperfine transition $F=3$ to $F=4$ of atomic cesium. In a cesium clock, the atoms pass through a microwave cavity where they undergo the hyperfine transition. The microwave frequency, generated by a local oscillator, is frequency-locked on the atomic resonance. Cesium clocks have the best long-term frequency stability.^[1] ($\sim 10^{-14}$ from 1,000 s to several years) and accuracy ($\sim 10^{-14}$), while hydrogen masers present the best short-term stability ($\sim 10^{-15}$ from 1,000 to 10,000 s).^[2] A hydrogen maser has flown in space for two hours in 1976 in the NASA Gravity Probe experiment (GPA) and current

plans exist to fly hydrogen masers again on board the Mir space station before the end of this century.^[2,3] Several tens of cesium clocks (as well as less precise rubidium clocks) are now in continuous operation in GPS satellites orbiting at 20,000 km above the earth.

The conventional cesium clocks use a ~ 400 Kelvin thermal atomic beam of cesium atoms (beam velocity ~ 100 m/s and velocity distribution width ~ 50 m/s). Nowadays, laser cooling techniques can very easily produce a dense gas of cold cesium atoms at a temperature of $2.5 \mu\text{K}$ corresponding to atoms with an rms velocity of 12 mm/s.^[4] These small velocities allow interaction times between the atoms and the electromagnetic field approaching one second on earth as compared to a few milliseconds when using a conventional cesium clock.^[5,6,7,8] As the atomic resonance linewidth in cesium clocks is inversely proportional to the interaction time, an improvement of two orders of magnitude in the frequency stability and accuracy over conventional devices is expected. A first frequency standard using cold atoms in a fountain configuration has been constructed at the BNM-LPTF. The interaction time in this atomic fountain can reach 700 ms, leading to a 0.7 Hz resonance linewidth. The frequency stability is $1.5 \cdot 10^{-13} \tau^{-1/2}$ and reaches $1.5 \cdot 10^{-15}$ at $\tau = 10^4$ s. For longer integration times, the stability is limited by the hydrogen maser used as a reference oscillator. The accuracy of the fountain clock has been recently improved over the value reported in [5] to $2 \cdot 10^{-15}$. These are the best results ever obtained with cesium frequency standards. We are at present constructing a second cesium fountain in order to measure the stability over one day. The expected accuracy is in the 10^{-16} range.

It is predicted that microgravity conditions should enable a further factor of 10 improvement in the interaction time with a simple and compact device.^[9] The objective of the PHARAO project is to develop a space clock using cold cesium atoms. Such a frequency standard opens the way to a new generation of experiments.

2 PHARAO PROJECT

In 1994, the French space agency (CNES) decided to support a preliminary research program on a space frequency standard using cold atoms. Three laboratories, the BNM-LPTF, the ENS-LKB, and the LHA, have cooperated to construct a prototype that will be tested in aircraft parabolic flights. Simultaneously, studies on local oscillators, frequency synthesis chains, microwave cavity modeling, and time-frequency transfer are being performed.

The Microgravity Clock Prototype

The main progress in laser cooling were achieved in the last few years. Although well understood and quite easily reproduced in laboratories with the recent development of diode lasers, these experiments are far from being compatible with space requirements. The weight of the BNM-LPTF atomic fountain is about 2 tons, with some hundreds of optical components. The device has to operate in a quiet environment.

The main point of the PHARAO project is the construction of a much smaller, reliable, and automatic prototype which will be tested in aircraft parabolic flights in the beginning of 1997. We want to record the microwave resonance fringes ($\nu \sim 9.2$ GHz) during the reduced gravity of the parabolic flights to prove the reliability of the prototype in a hostile environment. This device is also designed to be transformed later into a high performance transportable fountain frequency standard.

The experimental setup is shown in Fig. 1. As in the atomic fountain^[5], the prototype operates

in a pulsed mode driven by a computer. In a vacuum tube, the cesium atoms are cooled and launched, experience a microwave interaction in a cylindrical TE₀₁₃ cavity, and are finally optically detected. Due to the absence of gravity, only a single pass in the cavity is possible. With a low velocity of 5 cm/s, the resonance linewidth can be as low as 0.1 Hz, a factor of 10 narrower than on earth. All the laser beams are generated on a separate optical bench and connected to the tube chamber by optical fibers. A frequency chain synthesizes the 9.19... GHz microwave field from a 10 MHz BVA quartz oscillator.

Optical Bench

The optical setup generates the laser beams (~852 nm) for cooling and detecting the atoms. A narrow linewidth diode laser, frequency locked on the $F=4-F'=5$ transition of the cesium D₂ line, provides the two detection beams. Two different diode lasers will be tested in the aircraft: an extended cavity diode laser and a DBR diode laser spectrally narrowed with a weak optical feedback and a fast electronic servo-lock. Both have a linewidth in the 100 kHz range, a value much lower than the cesium D₂ natural linewidth (5.3 MHz). A narrow laser linewidth is required for the atom detection in order not to add noise to the fluorescence signal.^[10] After double-pass through an acousto-optic modulator (AOM) which sets the molasses detuning, the beam of this laser is also used to inject two slave diode lasers which provide the cooling beams. The two slave lasers deliver each 200 mW of optical power. Each beam is divided in three and coupled into polarizing optical fibers after a double pass in an AOM. The laser intensity (a few mW per beam) is controlled in each fiber by means of variable retarder plates. The AOM detunes the laser to launch the atoms and allows quick turning off of the laser light. To avoid any parasitic excitation of the atoms during the microwave interaction, mechanical shutters insure a complete extinction of the laser beams. An additional DBR diode laser pumps the atoms in the upper hyperfine state ($F=4$) during the cooling process and at the detection of the atoms in $F=3$. The linewidth is 3 MHz, and the frequency is locked to the $F=3-F'=4$ of the cesium D₂ line. The whole optical bench, designed with standard optical components, has the following dimensions: 65×65×15 cm. Eight optical fibers link the optical bench to the vacuum tube: six for cooling, two for detection.

Vacuum Tube

The cooling region contains a low pressure cesium vapor (10^{-6} Pa). The 10 mW output of each of the six optical fibers are expanded to a 1 cm waist and are distributed in three orthogonal pairs of counterpropagating beams. Each beam is tilted from the vertical direction. With this geometry, the cold atoms are launched in the (1,1,1) direction with the moving molasses technique.^[7] The launch velocity can be adjusted up to 8 m/s. The pressure in the interaction and detection regions is $\sim 10^{-8}$ Pa to avoid collisions and parasitic background fluorescence in the detection region. The chamber is pumped by a 20 l/s ion pump and a graphite tube cesium getter.

The microwave cavity is a 20-cm-long TE₀₁₃ cavity which has a loaded quality factor of several thousands. The duty cycle (interaction time over cycle time) is around 0.5. A highly homogeneous static magnetic field (2 mG) is produced with a long solenoid and a mu-metal magnetic shield around the cavity. Two compensation coils and three additional magnetic shields ensure the direction homogeneity of the magnetic field along the experiment. The axial shielding factor is larger than 10^5 over the cavity lengths. In addition, an external active compensation system will improve this figure by another factor of 10.

After the atoms pass through the cavity, the populations of both hyperfine levels are inde-

pendently measured by fluorescence in the detection region. The atoms in the $F=4$ level are first detected with a standing wave tuned 2 MHz below the $F=4-F'=5$ transition of the D2 line. They are then pushed away by the radiation pressure of a traveling wave tuned at the same frequency. The remaining atoms in the $F=3$ level are optically pumped to $F=4$ by the repumping beam and detected with the same procedure. Condenser lenses collect about 3% of the fluorescence emitted by the atoms.

Frequency Chain

The output of a 10 MHz reference oscillator is frequency multiplied to 100 MHz. The 100 MHz signal is bandpass filtered and then routed to a $\times 92$ multiplier. The output power is 10 dBm. The 9.2 GHz and the 7.3 MHz of a RF synthesizer are mixed in a single sideband mixer with better than about 25 dB image and carrier rejection. The resulting signal at the interrogation frequency is then level controlled by an active microwave attenuator.

The acceleration variations in the plane are 2 g. This sets strong constraints on the accelerometric sensitivity of the reference oscillator. The projected atomic resonance linewidth is in the hertz range. To scan this resonance without introducing errors greater than a few percent, the frequency retrace from one parabola to the other must be a few 10^{-12} . The duration of a parabola (20 s) forbids long measurement averaging. The short-term stability of the frequency chain must, therefore, be a few 10^{-13} at one second. The typical static g-sensitivity of a high performance commercial quartz is a few 10^{-11} , with a frequency stability of $3\text{--}6 \cdot 10^{-13}$ between 1 and 10 seconds. The LCEP at Besançon has provided a quartz oscillator with an acceleration sensitivity of $\sim 4 \cdot 10^{-12}/\text{g}$.

The performances of the aircraft clock prototype will also be evaluated on earth and compared to the atomic fountain. The long-term stability measurement of the fountain being now limited by the H-maser, this comparison will test both the fountain and the prototype. A relative stability of 10^{-16} per day is expected. The accuracy of the prototype will also be evaluated.

3 PRELIMINARY RESULTS

The prototype is being tested on earth in the scope of the future parabolic flights. The atoms are launched vertically with a velocity of 4 m/s in order to reach the detection region. In preliminary experiments we recently obtained a microwave resonance with a central fringe having a width of 10 Hz (Fig. 2). The signal-to-noise ratio is presently 350 for a one second cycle time. We expect large improvements of the S/N in the near future. During 1997 we will compare the PHARAO prototype to the atomic fountain. An accuracy and stability evaluation of PHARAO as a high performances compact and transportable frequency standard will then be carried out.

4 INTEREST OF MICROGRAVITY ENVIRONMENT

Operating in space with longer interaction times should lead to an improvement, in terms of accuracy and long-term stability. Indeed, most of the systematic effects are reduced with the atomic velocity.

The short-term stability depends on both the atomic interrogation scheme and the local oscillator. If we assume a perfect local oscillator, the fractional frequency stability is given by:^[5]

$$\sigma_{at}(\tau) \cong \frac{\Delta\nu}{\pi\nu} \frac{1}{\sqrt{N_{at}}} \sqrt{\frac{T_c}{\tau}} \quad (1)$$

where ν is the frequency of the clock transition, T_c is the cycle duration, about twice the interaction time T_i , and $\Delta\nu$ is the resonance linewidth varying as $1/T_i$. N_{at} is the number of detected atoms per cycle.

One way to improve the short-term stability is to increase N_{at} . Yet, for an accuracy in the 10^{-16} range, the density, averaged over the flight time, cannot exceed 10^6 atoms/cm³. As a matter of fact, the dominant uncertainty is that of a shift proportional to the atomic density, which is due to collisions between the cold atoms.^[8,11] In the BNM-LPTF fountain, this shift is typically $1 \cdot 10^{-15}$ with a $0.5 \cdot 10^{-15}$ uncertainty. It is presently a serious limitation to the performances of cold atom clocks on earth and it also dominates the design of the microgravity clock. In space, as the launching velocity is much smaller, several clouds of cold atoms can be prepared before the first one enters the cavity. This allows the increase of the number of detected atoms with the same average density. This improves the short-term stability without increasing the cold collision shift.

The radius of the cold atom cloud expands as $((V_{rms} T_i)^2 + r_0^2)^{1/2}$, where V_{rms} is the transverse velocity of the atoms and r_0 the initial cloud radius. To optimize the stability for a given initial number of cold atoms, the interaction time must be equal to r_0/V_{rms} . With the typical parameters (a rms velocity of 1 cm/s and an r_0 of 1 cm), the optimum T_i is around 1 s. Thus, in the PHARAO prototype with one cm diameter holes in the cylindrical microwave cavity, a transverse temperature of 1 μ K, an interrogation time of 0.5 second and a cycle time T_c of 1 second, we detect $4 \cdot 10^5$ atoms in mF=0 per cycle for a stability of $3 \cdot 10^{-14} \tau^{-1/2}$ or 10^{-16} per day. Using three successive clouds of cold atoms loaded in ~ 300 ms, the collisional shift is $3 \cdot 10^{-16}$. Assuming 5-10% fluctuation in the average atomic density will lead to a stability floor of $1.5 \cdot 3 \cdot 10^{-17}$. A second interesting case is to assume transverse cooling or transverse selection of the atoms to a temperature so low that all the atoms entering in the microwave cavity do contribute to the signal after an interaction time of 10 seconds. With sub-recoil laser cooling techniques^[12,13,14], the atomic transverse velocity can be reduced below 1 mm/s. This corresponds to an optimum T_i of 10 s, which would lead on earth to a fountain height of 100 m. In space this is realizable with a compact device. Assuming an ideal local oscillator, the Ramsey fringe width is 0.05 Hz and the short-term stability is $10^{-14} \tau^{-1/2}$ with the same collisional shift of $2 \cdot 3 \cdot 10^{-16}$. The stability floor of $1 \cdot 2 \cdot 10^{-17}$ will then be reached after about 3 days of integration time. As pointed out by K. Gibble, it might well turn out that rubidium atoms would ultimately lead to still better performances if the cold collision shift is smaller than that of cesium.

However, the short-term stability performances also depends on the local oscillator: for a pulsed operation, an aliasing phenomenon downconverts the local oscillator noise at all the harmonics of the sampling frequency. This can bring a strong limitation to the short-term stability of the frequency standard. Over a time around T_c , if the flicker frequency noise dominates (for instance with a quartz crystal oscillator), the stability of the frequency standard is expressed by:^[15,16]

$$\sigma^2(\tau) \approx 0.25 \sigma_{LO}^2 \frac{T_c}{\tau} + \sigma_{at}^2(\tau) \quad (2)$$

where σ_{LO} is the flicker floor stability of the local oscillator. For the present BNM-LPTF atomic fountain, $\sigma_{at}(\tau) = 7 \cdot 10^{-14} \tau^{-1/2}$, $\sigma_{LO} = 2 \cdot 3 \cdot 10^{-13}$ at one second and the measured stability is

$1.5 \cdot 10^{-13} \tau^{-1/2}$. Development is being carried out to improve the stability of the quartz oscillator. As long as the short-term stability is limited by the flicker noise floor of the local oscillator, the degradation of the stability increases with the interaction time. With present state-of-the-art quartz oscillator technology, a local oscillator stability of $7 \cdot 10^{-14}$ at 1 s is available. Thus, the PHARAO clock in space can readily reach the fractional frequency stability of $3 \cdot 10^{-14} \tau^{-1/2}$ with 1 s interaction time. For a 10-second interaction time, an H-maser or a cryogenic oscillator are good candidates as local oscillator.

Depending on the requirements of each use of the clock (stability over a few hours or accuracy), a compromise between the different parameters discussed above will be determined: the choice of the local oscillator, the interaction time, the atom number, and velocity.

5 SPACE APPLICATIONS

Time and Frequency Metrology

A space cold atom clock would be a primary frequency standard accessible from anywhere. It opens the way to frequency comparisons, to dissemination of an international time and to a next generation of navigation and positioning systems. The very low drift of the space clock would also allow frequency comparisons between clocks without the constraint of common view of the satellite.

A Tool for Tests of Fundamental Physics

With clocks having a stability of 10^{-16} over one day, it should be possible to measure with a potential 100-fold improvement over the 1976 GPA experiment^[2] the gravitational redshift (Einstein effect). This general relativity effect was determined at the 10^{-4} level using H-masers having a stability around 10^{-15} over the 2-hour mission duration. With a measurement in the 10^{-6} level, the validity of theory could be assessed up to the second order.

A new measurement of the Shapiro effect is proposed: the SORT project.^[17] It intends to measure the gravitational delay on the travel time of light pulses sent from the earth and differentially detected on two satellites orbiting in the solar system. The signature of the gravitational delay is extracted from the comparison between the arrival times of the light pulses to the satellites. This measurement will lead to a better determination of the post-Newtonian parameter γ which is equal to 1 in general relativity. Yet, a more general class of theories predicts a slightly different value of γ .^[18] The best experimental evaluations so far show no deviation from 1 at the 10^{-3} level.^[19] With the SORT project, we could estimate γ with an accuracy of about 10^{-7} .

Various other tests and measurements can be thought of: direct detection of gravitational waves^[20], isotropy of light velocity.^[21]

First Mission

A first objective of a space experiment is the demonstration of a clock running with laser-cooled atoms and the determination of its performance. In space, we expect in a first stage a stability better than $10^{-13} \tau^{-1/2}$ and an accuracy of about 10^{-16} . The evaluation of these performances would be made either on board or from the earth. On board, the comparison oscillator could be either another cold atom clock, or a frequency standard with a better short-term stability (10^{-15} from 1 hour to 1 day). These include space versions of a hydrogen maser, ion trap, or

cryogenic dielectric resonator. The international space station (ISSA) could be the platform of this first experiment (ACES proposal).

A crucial factor in the use of a space frequency standard is the quality of the frequency comparison between the onboard clock and frequency standards on earth. In order to transfer this space clock performance, a 10^{-16} accuracy is required. Today, the GPS is in the 10^{-14} - 10^{-15} range and two-way links are in the 10^{-15} range.^[22,21] We need at least a one order of magnitude improvement. An optical link using picosecond laser pulses is being developed by the Observatoire de la Côte d'Azur (OCA)^[23], with an expected accuracy of 10^{-16} . However, by contrast to the optical link, the microwave link has the advantage of being independent of weather conditions and can allow a continuous link with the space clock.

The PHARAO project aims at developing a new generation of space clocks. In the beginning of 1997, a prototype will be tested in the reduced gravity of aircraft parabolic flights. It will be the first step toward the construction of a satellite cold atom clock with a stability and an accuracy in the 10^{-17} range. This performance, as well as future time and frequency transfer methods, can be validated on board the international space station. This ambitious program seems realistic with an international cooperation.

ACKNOWLEDGMENTS

The PHARAO project has the financial and logistic support of the French Space Agency (CNES) and of région Ile de France. Laboratoire Kastler Brossel is unité associée au C.N.R.S et à l'université Pierre et Marie Curie. Laboratoire de l'Horloge Atomique is unité propre du C.N.R.S. We acknowledge the assistance of M. Lours, M. Dequin, L. Volodimer, P. Aynié, A.H. Gerard, D. Guitard, and J. Olejnik.

6 REFERENCES

- [1] See, for instance, A. Bauch et al., Proceedings of the 25th Moriond Conference on Dark Matter, Cosmology, Ultra-stable Clocks and Fundamental Tests.
- [2] R. Vessot et al. 1980, *Physical Review Letters*, **45**, 2081.
- [3] R. Vessot 1993, Proceedings of the 28th Moriond Conference.
- [4] C. Salomon, J. Dalibard, W. Phillips, A. Clairon, and S. Guellati 1990, *Europhysical Letters*, **12**, 683.
- [5] A. Clairon, S. Ghezali, G. Santarelli, Ph. Laurent, S.N. Lea, M. Bahoura, E. Simon, S. Weyers, and K. Szymaniec 1996, "*Preliminary accuracy evaluation of a cesium fountain frequency standard*," Proceedings of the 5th Symposium on Frequency Standards and Metrology, 15-19 October 1995, Woods Hole, Massachusetts, USA, ed. J. Bergquist (World Scientific, Singapore), pp. 49-59.
- [6] M. Kasevich, E. Riis, S. Chu, and R. de Voe 1989, *Physical Review Letters*, **63**, 612.
- [7] A. Clairon, C. Salomon, S. Guellati, and W. Phillips 1991, *Europhysical Letters*, **16**, 165.
- [8] K. Gibble, and S. Chu 1993, *Physical Review Letters*, **70**, 177.

- [9] B. Lounis, J. Reichel, and C. Salomon 1993, *Comptes Rendus d'Académie des Sciences, Paris*, **316**, Sér. 2, 739.
- [10] N. Dimarcq, V. Giordano, P. Cerez, and G. Theobald 1993, *IEEE Transactions on Instrumentation and Measurement*, **42**.
- [11] S. Ghezali, Ph. Laurent, S.N. Lea, and A. Clairon 1996, *Europhysical Letters*, **36**, 25-30.
- [12] A. Aspect, E. Arimondo, R. Kaiser, N. Vansteenkiste, and C. Cohen-Tannoudji 1988, *Physical Review Letters*, **61**, 826.
- [13] M. Kasevich, and S. Chu 1992, *Physical Review Letters*, **69**, 1741.
- [14] J. Reichel, F. Bardou, M. Ben Dahan, E. Peik, S. Rand, C. Salomon, and C. Cohen Tannoudji 1995, *Physical Review Letters*, **75**, 4575.
- [15] G.J. Dick, J.D. Prestage, C.A. Greenhall, and L. Maleki 1991, "*Local oscillator induced degradation of medium-term stability in passive atomic frequency standards*," Proceedings of the 22nd Annual Precise Time and Time Interval (PTTI) Applications and Planning Meeting, 4-6 December 1990, Vienna, Virginia, USA (NASA CP-3116), pp. 487-508.
- [16] G. Santarelli, P. Laurent, A. Clairon, G.J. Dick, C.A. Greenhall, and C. Audoin 1996, Proceedings of the 10th European Frequency and Time Forum (EFTF), March 1996, Brighton, UK.
- [17] C. Veillet et al. 1993, TROLL proposal to ESA for M3 mission.
- [18] T. Damour, and K. Nordtvedt 1993, *Physical Review Letters*, **70**, 2217.
- [19] D. S. Robertson et al. 1991, *Nature*, **349**, 6312.
- [20] R.F.C. Vessot 1981, *Journal de Physique*, **C8**, 12, 42.
- [21] P. Wolf 1995, *Physical Review*, **A51**, 5016.
- [22] H. Nau, J. Hahn, and S. Bedrich 1994, "*Study on H-maser in space*," draft final report, German Aerospace Research Establishment, DLR Oberpfaffenhofen, Institute of Radio-frequency Technology, November 1994.
- [23] C. Veillet, and P. Fridelance 1995, "*T2L2 time transfer by laser link*," Proceedings of the 26th Annual Precise Time and Time Interval (PTTI) Applications and Planning Meeting, 6-8 December 1994, Reston, Virginia, USA (NASA CP-3302), pp. 443-454.

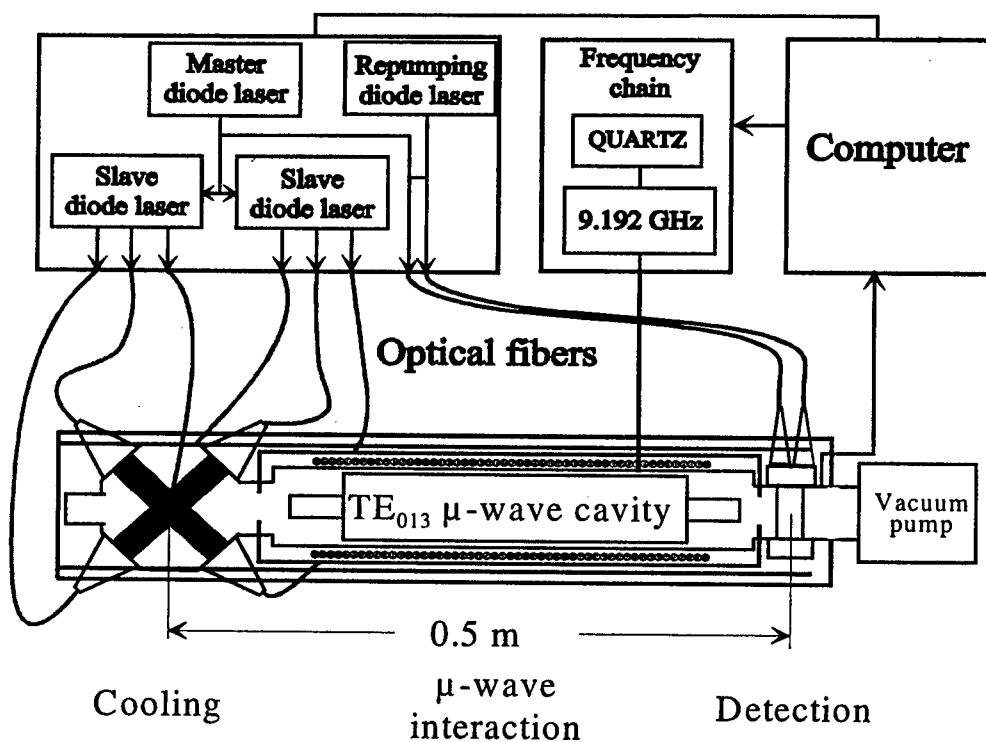


Fig. 1. Scheme of the aircraft clock prototype. The length between the cooling and the detection region is about 50 cm.

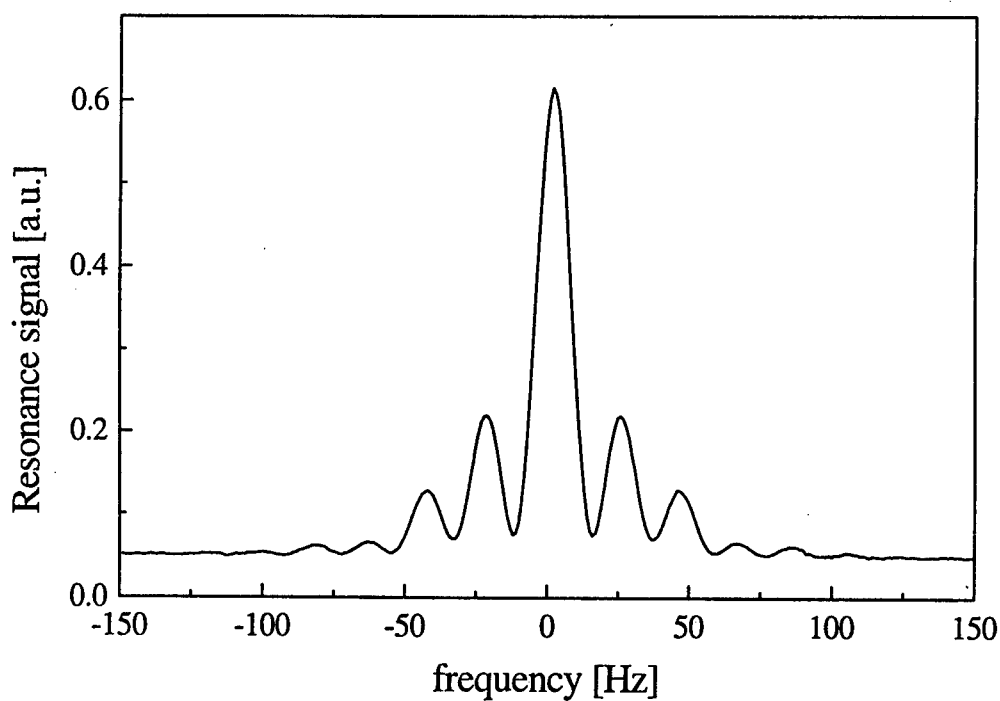


Fig. 2. Experimental microwave resonance fringes in the TE_{013} cavity. Single scan recorded with a 1 Hz frequency step.

PTTI '96

OFFICIAL ATTENDEES' LIST

David W. Allan

Allan's TIME
PO Box 66
Fountain Green, UT 84632
Tel: 805-445-3216
E-mail: 103077.1377@compuserve.com

Carroll O. Alley

University of Maryland
Dept. of Physics
College Park, MD 20742
Tel: 301-405-6102
Fax: 301-314-9525
E-mail: ben@kelvin.umd.edu

Franklin G. Ascarunz

Femtosecond Systems Inc.
440 Wellington Ave.
Lafayette, CO 80026
Tel: 303-497-7432
E-mail: ascarunz@bldrdoc.gov

Mark M. Atkisson

U.S. Naval Observatory
3450 Massachusetts Avenue, NW
Washington, DC 20392-5420
Tel: 202-762-1506
Fax: 202-762-1461
E-mail: atkisson@spica.usno.navy.mil

Michel Baldy

Tekelec Telecom
29 Avenue de a Baltique
Les Ulis 91953
FRANCE
Tel: 33 1 64 46 2069
Fax: 33 1 64 46 4550
E-mail: 100564.3555@compuserve.com

Thomas R. Bartholomew

TASC
131 National Business Pkwy
Annapolis Junction, MD 20701
Tel: 301-483-6000 x2019
Fax: 301-604-0500
E-mail: trbartholomew@tasc.com

Andreas Bauch

Physikalisch Technische Bundesanstalt
Bundesallee 100
D-38116 Braunschweig
GERMANY
Tel: 49 53 15 924 410
Fax: 49 53 15 924 479

Francoise S. Baumont

Observatoire de la Côte d'Azur
(OCA/CERGA)
Avenue Nicolas Copernic
Grasse 06130
FRANCE
Tel: 33 04 93 405331
Fax: 33 04 93 405333
E-mail: gaignebet@obs-azur.fr

Melanie E. Bautista

Lockheed Martin Advanced Technology
1 Federal Street
MS AE3W
Camden, NJ 08102
Tel: 609-338-3987
Fax: 609-338-4144
E-mail: mbautist@atl.lmca.com

Ronald L. Beard

Naval Research Laboratory
4555 Overlook Avenue, SW
Washington, DC 20375
Tel: 202-404-7054
Fax: 202-767-2845
E-mail: beard@juno.nrl.navy.mil

Art Blair

Texas Instruments
6600 Chase Oaks Blvd.
MS 8490
Plano, TX 75023
Tel: 972-575-0421
Fax: 972-575-6809

Martin Bloch

FEI
55 Charles Lindburgh Blvd.
Uniondale, NY 11553
Tel: 516-794-4500
Fax: 516-794-4340
E-mail: marvin@frequelec.com

James N. Bodurtha

AI Associates
56 Hayes Lane
Ridgefield, CT 06877
Tel: 203-438-2392

William V. Bollwerk

U.S. Naval Observatory
Alternate Master Clock
400 O'Malley Ave., Ste 44
Falcon AFB, CO 80912-4044
Tel: 719-567-6740
Fax: 719-567-6763
E-mail: bill@tycho.usnogps.navy.mil

Lee A. Breakiron
U.S. Naval Observatory
3450 Massachusetts Ave., NW
Washington, DC 20392
Tel: 202-762-1092
Fax: 202-762-1511
E-mail: lab@tycho.usno.navy.mil

Carolyn F. Bryant
Naval Research Laboratory
4555 Overlook Avenue, SW
Washington, DC 20375
Tel: 202-404-7063
Fax: 202-767-2845
E-mail: bryant@juno.nrl.navy.mil

James A. Buisson
NRL/AEI
7714 Martel Place
Springfield, VA 22152
Tel: 703-451-3575
Fax: 202-767-2845
E-mail: buisson@juno.nrl.navy.mil

Ed Burkhardt
Burkhardt Monitoring Service
PO Box 1411
Glen Allen, VA 23060
Tel: 804-261-1800

Steven P. Burns
Lockheed Martin Federal Systems
700 N. Frederick Avenue
MS 182/3L110
Gaithersburg, MD 20879
Tel: 301-240-7525
Fax: 301-240-6073
E-mail: steven.burns@imco.com

Giovanni Busca
Observatory of Neuchâtel
Rue de l'Observatoire 58
CH-2000 Neuchâtel
SWITZERLAND
Tel: 41 32 889 68 70
Fax: 41 32 889 62 81
E-mail: schaller@on.unine.ch

Edgar W. Butterline
Telecom Solutions
1461 Carlisle Road
North Brunswick, NJ 08902
Tel: 908-246-7891
Fax: 908-246-7277
E-mail: butterline1@attmail.com

Malcolm D. Calhoun
Jet Propulsion Laboratory
Frequency and Timing Systems
4800 Oak Grove Drive
Pasadena, CA 91109
Tel: 818-354-9763
Fax: 818-393-6773
E-mail: malcolm.d.calhoun@jpl.nasa.gov

James Camparo
The Aerospace Corp.
PO Box 92957
Los Angeles, CA 90009
Tel: 310-336-6944
Fax: 310-336-6801
E-mail: Jim.Camparo@gmailz.aero.org

Ralph W. Carpenter
EG&G Inc.
35 Congress Street
Salem, MA 01970
Tel: 508-745-3209, ext. 201
Fax: 508-741-4923
E-mail: rwc@egginc.com

Harold A. Chadsey
U.S. Naval Observatory
3450 Massachusetts Avenue, NW
Washington, DC 20392-5420
Tel: 202-762-1450
Fax: 202-762-1511
E-mail: hc@planck.usno.navy.mil

Ling Chan
GPS World
859 Willamette St.
Eugene, OR 97401-6806
Tel: 541-343-1200
Fax: 541-344-3514
E-mail: editorial-gps@gpsworld.com

Laura G. Charron
U.S. Naval Observatory
3450 Massachusetts Ave, NW
Washington, DC 220392-5420
Tel: 202-762-1458
Fax: 202-762-1511
E-mail: lgc@spica.usno.navy.mil

Angela Ying Chen
Allied Signal Technical Services Corp.
FTS Group
2500 E. Foothill Blvd.
Suite 400
Pasadena, CA 91107
Tel: 818-584-4502
Fax: 818-584-4480
E-mail: Angela.Chen@cc2mhb.jpl.nasa.gov

Randolph T. Clarke
U.S. Naval Observatory
3450 Mass. Ave., NW
Washington, DC 20392-5420
Tel: 202-762-1500
Fax: 202-762-1511
E-mail: rtc@smart.usno.navy.mil

Franco Cordara

Istituto Elettrotecnico Nazionale G. Ferraris
Electromagnetic and Time and Frequency
Metrology
Corso Massimo d'Azeglio, 42
Torino 10125
ITALY
Tel: 39 11 3919239
Fax: 39 11 346384
E-mail: cordara@tf.ien.it

Michael Costa

Lockheed Martin
1111 Lockheed Way
B/195A, O/48-70
Sunnyvale, CA 94088-3504
Tel: 408-742-8928
Fax: 408-742-4435

Dwin M. Craig

Naval Research Laboratory
4555 Overlook Avenue, SW
Washington, DC 20375
Tel: 202-404-7067
Fax: 202-767-2845
E-mail: craig@juno.nrl.navy.mil

Jeffrey D. Crum

USAF 2 SOPS/DOUAN
300 O'Malley Avenue, Suite 41
Falcon AFB, CO 80912
Tel: 719-567-6396
Fax: 719-567-6307
E-mail: crumjd@fafb.af.mil

Leonard S. Cutler

Hewlett-Packard Co.
Hewlett-Packard Labs
3500 Deer Creek Road
MS 26M-9
Palo Alto, CA 94304
Tel: 415-857-5259
Fax: 415-813-3384
E-mail: len_cutler@hp.com

James Danaher

3S Navigation
23141 Plaza Pointe
Laguna Hills, CA 92677
Tel: 714-830-3777
Fax: 714-830-8411
E-mail: glonassman@aol.com

Theodore C. Dass, III

ITT at Falcon AFB
6974 Los Reyes Circle
Colorado Springs, CO 80918
Tel: 719-567-3928
Fax: 719-567-3927
E-mail: tdass@afmcfafe.af.mil

Gerrit de Jong

NMi Van Swinden Laboratory
PO Box 654
2600 AR Delft
Netherlands
Tel: 31 15 269 1623
Fax: 31 15 261 2971
E-mail: gdejong@NMi.nl

Edoardo Detoma

AlliedSignal Technical Services
Corso Montecucco 95
Torino 10141
ITALY
Tel: 39 11 385-4579
Fax: 39 11 242-0372

James A. DeYoung

U.S. Naval Observatory
Time Service Department
3450 Mass. Ave. NW
Washington, DC 20392-5420
Tel: 202-762-0290
Fax: 202-762-1511
E-mail: dey@herschel.usno.navy.mil

G. John Dick

Jet Propulsion Laboratory
Frequency Standards Laboratory
MS 298-100
4800 Oak Grove Drive
Pasadena, CA 91109
Tel: 818-354-6393
Fax: 818-393-6773
E-mail: jdick@fridge.jpl.nasa.gov

Irvin Diegel

AlliedSignal Technical Services
One Bendix Road
Columbia, MD 21045
Tel: 410-964-7343
Fax: 410-964-7187
E-mail: diegeli@clmmp003.atsc.allied.com

Rick Dielman

TrueTime, Inc.
2835 Duke Court
Santa Rosa, CA 95407
Tel: 707-528-1230
Fax: 707-527-6640
E-mail: truetime@nbn.com

William A. Diener

Jet Propulsion Laboratory
Frequency and Time
4800 Oak Grove Drive
Pasadena, CA 91109
Tel: 818-354-6670
Fax: 818-393-6773
E-mail: bdiener@jpl.nasa.gov

Gary L. Dieter
USAF 2 SOPS/DOUAN
300 O'Malley Avenue, Suite 41
Falcon AFB, CO 80912
Tel: 719-567-6393
Fax: 719-567-6307
E-mail: dietergl@fafb.af.mil

Robert J. Douglas
National Research Council of Canada
1108 Building M-36
Ottawa, K1A 0R6
CANADA
Tel: 613-993-5186
Fax: 613-952-1394
E-mail: rob.douglas@nrc.ca

Robert E. Drullinger
NIST
325 Broadway
Boulder, CO 80303
Tel: 303-497-3183
Fax: 303-497-6461
E-mail: rdrullinger@boulder.nist.gov

Christopher R. Ekstrom
U.S. Naval Observatory
Time Service Department
3450 Massachusetts Ave., NW
Washington, DC 20392-5420
Tel: 202-762-0066
Fax: 202-762-1511
E-mail: ekstrom@spica.usno.navy.mil

Sergey Ermolin
Hewlett-Packard Co.
Santa Clara Division
5301 Stevens Creek Blvd.
MS 51U/23
Santa Clara, CA 95051
Tel: 408/553-2869
Fax: 408/553-6591
E-mail: sermolin@sc.hp.com

Darrell E. Ernst
MITRE
1820 Dolly Madison Blvd.
McLean, VA 22102-3481
Tel: 703-883-5914
Fax: 703-883-1379
E-mail: dernst@mitre.org

Sheila Faulkner
3159 Patrick Henry Drive
Falls Church, VA 22044
Tel: 703-532-6411
Fax: 703-532-6338
E-mail: bopenyan@aol.com

Juan M. Figueroa
CENAM
km 4,5 Carretera a los Cues
Queretaro 76900
MEXICO
Tel: 42 11 05 40
Fax: 42 11 39 04
E-mail: jfigueroa@cenam.mx

Henry F. Fliegel
The Aerospace Corp.
2350 El Segundo Boulevard
El Segundo, CA
Tel: 310-336-1710
Fax: 310-336-5076

D. Earl Fossler
TRAK Systems
4726 Eisenhower Blvd.
Tampa, FL 33634
Tel: 813-884-1411
Fax: 813-884-0981

Kent W. Foster
U.S. Naval Observatory
3450 Massachusetts Avenue, NW
Washington, DC 20392-5420
Tel: 202-762-1538
Fax: 202-762-1461
E-mail: kwf@spica.usno.navy.mil

Sally L. Frodge
Dept. of Transportation
5703 Shropshire Ct.
Alexandria, VA 22315
Tel: 202-336-4894
Fax: 202-366-7206
E-mail: sally.frodge@ost.dot.gov

Yigen Fu
BIRMM
Ministry of Foreign Affairs
Beijing
PEOPLE'S REPUBLIC OF CHINA
Tel: 687 62 839
E-mail: time@pulbic3.bta.net.cn

Ivan J. Galysh
Naval Research Laboratory
4555 Overlook Avenue, SW
Washington, DC 20375
Tel: 202-404-7060
Fax: 202-767-2845
E-mail: galysh@juno.nrl.navy.mil

R. Michael Garvey
Frequency and Time Systems, Inc.
34 Tozer Road
Beverly, MA 01915
Tel: 508-927-8220
Fax: 508-927-4099
E-mail: admin@ftsdatum.com

Al Gifford

U.S. Naval Observatory
3450 Massachusetts Avenue, NW
Washington, DC 20392-5420
Tel: 703-808-2606
E-mail: giffordal@aol.com

Raymond H. Godin

Chief of Naval Operations (N096)
U.S. Naval Observatory
3450 Massachusetts Avenue, NW
Washington, DC 20392
Tel: 202-762-0255
Fax: 202-762-1018
E-mail: godin@ocean.usno.navy.mil

Clive R. Green

Quartzlock UK Ltd.
Gothic, Plymouth Rd.
Totnes Devon TQ9 SLH
Tel: 44 1803 862062
Fax: 44 1803 867962
E-mail: clivegreen@quartzlock.com

Joe C. M. Green

AlliedSignal Technical Services Corporation
(ATSC)
Frequency and Timing
2500 Foothill Blvd.
Pasadena, CA 91107-3464
Tel: 818-584-4472
Fax: 818-584-4480
E-mail: joseph.c.green@jpl.nasa.gov

Charles A. Greenhall

Jet Propulsion Laboratory
4800 Oak Grove Drive
Pasadena, CA 91109
Tel: 818-393-6944
Fax: 818-393-6773
E-mail: cgreen@horology.jpl.nasa.gov

Richard E. Griffin

Texas Instruments
125 Simmons Dr.
Lewisville, TX 75019
Tel: 972-462-2598
Fax: 972-462-4568

Joerg Hahn

DLR Oberpfaffenhofen, Germany
Institut fuer Hochfrequenztechnik
Postfach 1116 D-82230
Wessling
GERMANY
Tel: +49-8153-282335
Fax: +49-8153-281135
E-mail: joerg.hahn@dlr.de

Robert L. Hamell

Jet Propulsion Laboratory
Telecommunications Division
4800 Oak Grove Drive
Pasadena, CA 91109
Tel: 818-354-4944
Fax: 818-393-6773
E-mail: Robert.L.Hamell@jpl.nasa.gov

Bill Harron

Datum Inc./FTS
4545 Pilgrim Lane
Boothwyn, PA 19061
Tel: 610-485-9506
Fax: 610-485-9516
E-mail: bharron@aol.com

Rex Heller

TrueTime, Inc.
2835 Duke Court
Santa Rosa, CA 95407
Tel: 707-528-1230
Fax: 707-527-6640
E-mail: truetime@nbn.com

Helmut W. Hellwig

SAF/AQR
1919 South Eads Street
Suite 100
Arlington, VA 22202-3053
Tel: 703-602-9301
Fax: 703-602-4845
E-mail: hellwig@af.pentagon.mil

Gildas Herman

Tekelec Telecom
29 Avenue de a Baltique
Les Ulis 91953
FRANCE
Tel: 33 1 64 46 2007
Fax: 33 1 64 46 4550
E-mail: 100564.3555@compuserve.com

Stephanie S. Hills

Adroit Systems Inc.
209 Madison Street
Ste 500
Alexandria, VA 22314
Tel: 703-684-2900
Fax: 703-836-7411
E-mail: sstot@alexandria.adroit.com

Douglas W. Hogarth

20241 194th Place, NE
Woodinville, WA 98072-8889
Tel: 500-4GPSUTC or 206-788-1507
E-mail: DougHo@internetMCI.com

Christina Howe
Telecom Solutions
85 West Tasman Drive
San Jose, CA 95134-1703
Tel: 408-428-7926
E-mail: chowe@telecom.com

Steven T. Hutsell
U.S. Naval Observatory
Alternate Master Clock (AMC)
400 O'Malley Ave., Ste 44
Falcon AFB, CO 80912-4044
Tel: 719-567-6740
Fax: 719-567-6763
E-mail: hutsellst@fafb.af.mil

Michito Imae
Communications Research Laboratory
Standards and Measurements Division
4-2-1, Nukukita
Koganei, Tokyo 184
JAPAN
Tel: 81-423-27-7566
Fax: 81-423-27-6686
E-mail: imae@crl.go.jp

Jeffrey S. Ingold
ATSC
1 Bendix Road
Columbia, MD 21045
Tel: 410-964-7188
E-mail: jsingold@atscv1.atsc.allied.com

Marilynn S. Ison
National Imagery & Mapping Agency
USAF SMC/CZD
2435 Vela Way, Ste. 1613
Los Angeles AFB, CA 90245-5500
Tel: 310-363-2284
Fax: 310-363-0643
E-mail: isonms@gps1.laafb.af.mil

Calvin L. James
AlliedSignal Aerospace
1 Bendix Rd.
Columbia, MD 21045
Tel: 410-964-7726
Fax: 410-964-7725

Andrew C. Johnson
U.S. Naval Observatory
Time Service Department
3450 Massachusetts Ave., NW
Washington, DC 20392-5420
Tel: 202-762-1427
Fax: 202-762-1511
E-mail: acj@spica.usno.navy.mil

Donald F. Johnson
ARINC
2250 E. Imperial House
El Segundo, CA 90245-5500
Tel: 310-363-5140

Kenneth J. Johnston
U.S. Naval Observatory
3450 Massachusetts Avenue, NW
Washington, DC 20392-5420
Tel: 202-762-1513
Fax: 202-762-1461
E-mail: kjj@astro.usno.navy.mil

Edward C. Jones
Naval Research Laboratory
4555 Overlook Avenue, SW
Washington, DC 20375-5354
Tel: 202-767-0590
Fax: 202-767-2845
E-mail: jones@juno.nrl.navy.mil

Sarunas K. Karuza
The Aerospace Corporation
PO Box 92957
M1-111
Los Angeles, CA 90009
Tel: 310-336-6837
Fax: 310-336-6225

Richard E. Keating
U.S. Naval Observatory
3450 Massachusetts Ave., NW
Washington, DC 20392-5420
Tel: 202-762-1444

Sonia U. Kim
3S Navigation
23141 Plaza Pointe Dr.
Laguna Hills, CA 92653
Tel: 714-830-3777
Fax: 714-830-8411
E-mail: nav3s@aol.com

Wendy L. King
U.S. Naval Observatory
3450 Massachusetts Ave, NW
Washington, DC 20392-5420
Tel: 202-762-1577
Fax: 202-762-1511
E-mail: wendy@newton.usno.navy.mil

Dieter Kirchner
Technical University Graz
Inffeldgasse 12
Graz A8010
AUSTRIA
Fax: 43 316 46 3697

William J. Klepczynski
Innovative Solutions International
8500 Leesburg Pike, Ste. 608
Vienna, VA 22182
Tel: 703-883-8088
Fax: 703-883-9180
E-mail: WKlepczyns@aol.com

William M. Klipstein
National Institute of
Standards and Technology
Physics A167
Gaithersburg, MD 20899
Tel: 301-975-4208
Fax: 301-975-3038
E-mail: william.klipstein@nist.gov

Douglas E. Koch
Naval Space Command
5280 Fourth St.
Dahlgren, VA 22448
Tel: 540-653-6190
Fax: 540-653-6148

Paul A. Koppang
U.S. Naval Observatory
3450 Massachusetts Avenue, NW
Washington, DC 20392-5420
Tel: 202-762-0913
Fax: 202-762-1511
E-mail: pak@tycho.usno.navy.mil

Paul F. Kuhnle
Jet Propulsion Laboratory
4800 Oak Grove Drive
Pasadena, CA 91109-8099
Tel: 818-354-2715
Fax: 818-393-6773
E-mail: Paul.F.Kuhnle@jpl.nasa.gov

Francois Lahaye
Natural Resources, Canada
(NRCan)
Geodetic Survey Division
615 Booth Street
Ottawa, Ontario K1A 0E9
CANADA
Tel: 613-995-4488
Fax: 613-995-3215
E-mail: lahaye@geod.emr.ca

G. Paul Landis
Naval Research Laboratory
4555 Overlook Avenue, SW
Washington, DC 20375
Tel: 202-404-7051
Fax: 202-767-2845
E-mail: landis@juno.nrl.navy.mil

Marie M. Largay
Naval Research Laboratory
4555 Overlook Avenue, SW
Washington, DC 20375
Tel: 202-767-9133
Fax: 202-767-2845
E-mail: largay@juno.nrl.navy.mil

Albert Leong
The Aerospace Corporation
PO Box 92957
M1-111
Los Angeles, CA 90009
Tel: 310-336-6444
Fax: 310-336-6225
E-mail: leong@courier6.aero.org

Sigfrido M. Leschiutta
Istituto Elettrotecnico Nazionale Galileo Ferraris
Corso M. d'Azeglio n. 42
Torino 10125
ITALY
Tel: 39 11 3919713
Fax: 39 11 6507611
E-mail: pres@amm.ien.it

Judah Levine
National Institute of
Standards and Technology
325 Broadway
Boulder, CO 80303
Tel: 303-497-3903
Fax: 303-497-6461
E-mail: jlevine@boulder.nist.gov

Wlodzimierz Lewandowski
BIPM
Pavillon de Breteuil
92312 Sèvres Cedex
FRANCE
Tel: 33 145 07 7070
Fax: 33 1 145 34 2021
E-mail: wlewandowski@bipm.fr

Funming Li
Datum/Efratom
3 Parker
Irvine, CA 92630
Tel: 714-770-5000
Fax: 714-770-9289

Frank Lifsey
Kaman Sciences
2560 Huntington Avenue
Alexandria, VA 22303
Tel: 202-767-5371

Chuck Little
Hewlett-Packard Co.
Santa Clara Division
5301 Stevens Creek Blvd.
Santa Clara, CA 95052
Tel: 408-553-2506
Fax: 408-553-2058
E-mail: chuck_little@hp.com

Gene E. Long
Odetics Telecom
PO Box 260
Ridge, MD 20680
Tel: 301-872-4453
Fax: 301-872-4489
E-mail: gel@odetics.com

Victoria Molina López
National Metrology Center
km. 4.5 carr. a los Cués
El Marqués, Querétaro 76900
MEXICO
Tel: 52 42 166576
Fax: 52 42 153904
E-mail: vmolina@cenam.mx

Douglas R. Lowrie
EG&G
35 Congress St.
Salem, MA 01970
Tel: 508-745-3200
Fax: 508-741-4923

Carl F. Lukac
U.S. Naval Observatory
3450 Massachusetts Ave., NW
Washington, DC 20392-5420
Tel: 202-762-1456
Fax: 202-762-1511
E-mail: cfl@spica.usno.navy.mil

George H. Luther
U.S. Naval Observatory
3450 Massachusetts Avenue, NW
Washington, DC 20392-5420
Tel: 202-762-1527
Fax: 202-762-1511

Phu V. Mai
U.S. Naval Observatory
3450 Massachusetts Avenue, NW
Washington, DC 20392
Tel: 202-762-1593
Fax: 202-762-1511
E-mail: phu@tycho.usno.navy.mil

Demetrios N. Matsakis
U.S. Naval Observatory
3450 Massachusetts Avenue, NW
Washington, DC 20392
Tel: 202-762-1587
E-mail: dnm@orion.usno.navy.mil

Edward Mattison
Smithsonian Observatory
60 Garden Street
Cambridge, MA 02130
Tel: 617-495-7265
Fax: 617-496-7690
E-mail: emattison@cfa.harvard.edu

Dennis D. McCarthy
U.S. Naval Observatory
Directorate of Time
3450 Massachusetts Ave., NW
Washington, DC 20392-5420
Tel: 202-762-1837
Fax: 202-762-1563
E-mail: dmc@maia.usno.navy.mil

Tim McCauley
Kaman Sciences
2560 Huntington Avenue
Alexandria, VA 22303
Tel: 202-767-5379

Angela D. McKinley
U.S. Naval Observatory
3450 Massachusetts Avenue, NW
Washington, DC 20392
Tel: 202-762-1457
Fax: 202-762-1511
E-mail: amd@tycho.usno.navy.mil

Jack McNabb
TRAK Systems
4726 Eisenhower Blvd.
Tampa, FL 33634
Tel: 813-884-1411
Fax: 813-884-0981

Marvin Meirs
FEI
55 Charles Lindburgh Blvd.
Uniondale, NY 11553
Tel: 516-794-4500 ext. 5013
Fax: 516-794-4340
E-mail: marvin@frequelec.com

Debbie Melnick
Meetings Verbatim
PO Box 941221
Atlanta, GA 31141
Tel: 770-414-5677
Fax: 770-938-1918

Francisco J. G. Mendoza
Real Observatorio de la Armada
Seccion de Hora
Cecilio Pujazon s/n
San Fernando, Cadiz 11.100
SPAIN
Tel: +34 56 59 92 86
Fax: +34 56 59 93 66
E-mail: jgalindo@roa.cica.es

Jeff Miller
Texas Instruments
6600 Chase Oaks Blvd.
MS 8490
Plano, TX 75023
Tel: 972-575-0426
Fax: 972-575-6809

David L. Mills
University of Delaware
Electrical Engineering Department
102 Evans Hall
Newark DE 19716
Fax: 302-831-4316
E-mail: mills@udel.edu

Mihran Miranian
U.S. Naval Observatory
Time Service Department
3450 Massachusetts Ave., NW
Washington, DC 20392-5420
Tel: 202-762-1452
Fax: 202-762-1511
E-mail: mm@tycho.usno.navy.mil

Gilles Missout
HydroQuebec
1800 Montee Ste Julie
Varenes J3X 151 Quebec
CANADA
Tel: 514-652-8084
Fax: 514-652-8435
E-mail: missout@ireq.ca

H. Shawn Mobbs
USAF 2 SOPS/DOUAN
300 O'Malley Avenue, Suite 41
Falcon AFB, CO 80912
Tel: 719-567-2529
Fax: 719-567-6307
E-mail: mobbshs@fafb.af.mil

Thomas B. Moore
Kaman Sciences
2560 Huntington Avenue
Alexandria, VA 22303

David Munton
Applied Research Laboratory
University of Texas
10000 Burnet Road
Austin, TX 78713
Tel: 512-835-3831
E-mail: dmunton@arlut.utexas.edu

James A. Murray
SFA Inc.
1100 McCormick Dr.
Largo, MD
Tel: 202-404-2057
Fax: 202-767-2845
E-mail: murray@juno.nrl.navy.mil

Omar Namoos
U.S. Air Force
Global Positioning System JPO
2435 Vela Way
Ste 1613
Los Angeles AFB, CA 90245-5500
Tel: 310-363-6922
Fax: 310-363-3844
E-mail: namoosom@gps1.laafb.af.mil

Lisa M. Nelson
NIST
Time and Frequency Division
325 S. Broadway
Mailstop 847.4
Boulder, CO 80303-3328
Tel: 303-497-3378
Fax: 303-497-3228
E-mail: lnelson@boulder.nist.gov

John R. Norrington
USAF 50LSS/SCT
6078 Navstar, Ste 78
Falcon AFB, CO 80912
Tel: 719-567-7418
Fax: 719-567-7402
E-mail: norrington@fafb.af.mil

Karen F. O'Donoghue
Naval Surface Warfare Center
Dahlgren Division
Code B35
17320 Dahlgren Road
Dahlgren, VA 22448-5100
Tel: 540-653-1567
Fax: 540-653-8673
E-mail: kodonog@nswc.navy.mil

Timothy Oakley
Sigma Tau Standards Corporation
1711 Holt Road
Tuscaloosa, AL 35404
Tel: 205-553-0038
Fax: 205-553-2768

Orville J. Oaks
Naval Research Laboratory
4555 Overlook Avenue, SW
Washington, DC 20375
Tel: 202-767-1434
Fax: 202-767-2845
E-mail: oaks@juno.nrl.navy.mil

Lisa M. Orr
DISA DSCS Network Management
D3411
701 S. Courthouse Road
Arlington, VA 22204-2199
Tel: 703-607-6639
Fax: 703-607-4240
E-mail: orrl@ncr.disa.mil

Terry N. Osterdock
Absolute Time Corp.
800 Charcot Ave.,
Suite 110
San Jose, CA 95131
Tel: 408-383-1520
Fax: 408-383-0706
E-mail: terry@absolutetime.com

H. Bryan Owings
Sigma Tau Standards Corporation
1711 Holt Road
Tuscaloosa, AL 35404
Tel: 205-553-0038
Fax: 205-553-2768

Juan Palacio
Real Observatorio de la Armada
Seccion de Hora
Cecilio Pujazon s/n
San Fernando, Cadiz 11.100
SPAIN
Tel: +34 56 599286
Fax: +34 56 599366
E-mail: jpalacio@roa.cica.es

Peter Z. Paulovich
NISE EAST (ATG)
Bldg. 165
PO Box 1376
Norfolk, VA 23501-1376
Tel: 757-396-0287
Fax: 757-396-0518

James C. Perry
NASA GSFC
Code 531
Greenbelt Road
Greenbelt, MD 20771
Tel: 301-286-3471
Fax: 301-286-1724
E-mail: jperry@strfleet.gsfc.nasa.gov

Harry E. Peters
Sigma Tau Standards Corporation
1711 Holt Road
Tuscaloosa, AL 35404
Tel: 205-553-0038
Fax: 205-553-2768

Long Pham
Efratom
3 Parker
Irvine, CA 92618
Tel: 714-770-5000
Fax: 714-770-9289
E-mail: lpham@efratom.com

David H. Phillips
2901 Accokeek Road, West
Accokeek, MD 20607
Tel: 301-283-2747

Timothy R. Plunkett
Naval Surface Warfare Center
Dahlgren Division
Code B35
17320 Dahlgren Road
Dahlgren, VA 22448-5100
Tel: 540-653-1090
Fax: 540-653-8673
E-mail: tplunke@nswc.navy.mil

Ted Pollard
Absolute Time Corporation
800 Charcot Avenue
San Jose, CA 94303
Tel: 408-383-1518
Fax: 408-383-0706

Robert E. Price
Allied Signal Aerospace
One Bendix Road
Columbia, MD 21045
Tel: 410-964-7437
Fax: 410-964-7187
E-mail: pricer@clmmp003.atasc.allied.com

Elza K. Redman
5936 Trotter Rd.
Clarksville, MD 21029
Tel: 410-531-6885
Fax: 301-854-3583

Wilson G. Reid
Naval Research Laboratory
4555 Overlook Avenue, SW
Washington, DC 20375
Tel: 202-404-4015
Fax: 202-767-2845
E-mail: reid@juno.nrl.navy.mil

Lauren J. Reuger
Rueger Enterprises
1415 Glen Allen Avenue
Silver Spring, MD 20902
Tel: 301-942-7733

William J. Riley
EG&G
335 Congress St.
Salem, MA 01970
Tel: 508-745-3200
Fax: 508-741-4923
E-mail: riley@delphi.com

Dave Robinson
Datum Inc.
Bancomm-Timing Division
6781 Via Del Oro
San Jose, CA 95119-1360
Tel: 408-578-4161
Fax: 408-578-4165
E-mail: dcr@datum.com

Ron Roloff
Datum Inc.
Frequency & Time Systems
8005 McKenstry Drive
Laurel, MD 20723
Tel: 301-725-3636
Fax: 301-953-0246
E-mail: rroloff@clark.net

Michael H. Rudy
Lockheed Martin
7100 Standard Drive
Hanover, MD 21076
Tel: 202-762-1488
Fax: 202-762-1489
E-mail: voyager07@worldnet.att.net

Giorgio Santarelli
BNM - LPTF
61 Av. de L'Observatoire
75016 Paris
FRANCE
Tel: 33 1 40512225
Fax: 33 1 43255542
E-mail: giorgio.santarelli@obspm.fr

Wolfgang Schäfer
TimeTech GmbH
Technologiezentrum
Nobelstraße 15 D-70569 Stuttgart
GERMANY
Tel: 49 0711 67808-0
Fax: 49 0711 67808-99

Lara S. Schmidt
U.S. Naval Observatory
Time Service Department
3450 Massachusetts Ave., NW
Washington, DC 20392
Tel: 202-762-0289
Fax: 202-762-1511
E-mail: lss@ramsey.usno.navy.mil

Richard E. Schmidt
U.S. Naval Observatory
3450 Massachusetts Avenue, NW
Washington, DC 20392-5420
Tel: 202-762-1578
Fax: 202-762-1511
E-mail: res@tuttle.usno.navy.mil

Willi G. Schwarz
Physical Sciences Inc.
5705-A General Washington Drive
Alexandria, VA 22312
Tel: 703-341-0495
Fax: 703-341-5993
E-mail: schwarz@psicorp.com

Noel R. Sewall
LLNL
PO Box 808, L-493
Livermore, CA 94550
Tel: 510-422-4887
Fax: 510-422-1930

Timothy F. Sheridan
SPAWAR
2451 Crystal Dr.
Arlington, VA
Tel: 703-602-7039
Fax: 703-602-1535
E-mail: sheridan@smtp-gw.spawar.navy.mil

Robert W. Smid
ITT A/CD
Space Systems Engineering
100 Kingsland Rd.
Clifton, NJ 07014-1993
Tel: 201-284-3530
Fax: 201-284-3394
E-mail: rsmid@avionics.itt.com

Gary Smith
Brandywine Communications
3197-C Airport Loop Drive
Costa Mesa, CA 92626
Tel: 714-755-1050
Fax: 714-755-1070

Luke R. Smith
Sigma Tau Standards Corporation
1711 Holt Road
Tuscaloosa, AL 35404
Tel: 205-553-0038
Fax: 205-553-2768

William E. Smith
Datum Inc.
Efratom Division
3 Parker
Irvine, CA 92618
Tel: 714-770-5000, ext. 245
Fax: 714-770-2463
E-mail: besmith@efratom.com

Armin Soering
Deutsche Telekom AG
Am Kavalleriesand 3
64245 Darmstadt
GERMANY
Tel: 49 615 183 4549
Fax: 49 615 183 3834
E-mail: soering@mnh.telekom.de

Sarah B. Stebbins
Naval Research Laboratory
4555 Overlook Avenue, SW
Washington, DC 20375
Tel: 202-404-4821
Fax: 202-767-2845
E-mail: stebbins@juno.nrl.navy.mil

Samuel R. Stein
Timing Solutions Corp.
1025 Rosewood Ave., #200
Boulder, CO 80304
Tel: 303-937-8481
Fax: 303-443-5152
E-mail: srstein@ibm.net

David A. Stowers
Jet Propulsion Laboratory
Frequency and Timing
4800 Oak Grove Drive
MS 298-100
Pasadena, CA 91109
Tel: 818-354-7055
Fax: 818-393-6773
E-mail: dstowers@jpl.nasa.gov

Richard L. Sydnor
Jet Propulsion Laboratory
California Institute of Technology
Telecommunications Division
4800 Oak Grove Drive
Pasadena, CA 91109-8099
Tel: 818-354-2763
Fax: 818-393-6773
E-mail: sydnor@horology.jpl.nasa.gov

Philip E. Talley
1022 Eagle Crest
Macon, GA 31211
Tel: 912-745-3415
E-mail: Petalley@aol.com

Claudine Thomas
Bureau International des
Poids et Mesures
Pavillon de Breteuil
92312 Sèvres Cedex
FRANCE
Tel: 33 1 4507 7073
Fax: 33 1 4507 7059
E-mail: cthomas@bipm.fr

Massimo Tinto
Jet Propulsion Laboratory
California Institute of Technology
Telecommunications Division
4800 Oak Grove Drive
MS 161-260
Pasadena, CA 91109-8099
Tel: 818-354-0798
Fax: 818-393-4643
E-mail: Massimo.Tinto@jpl.nasa.gov

Robert L. Tjoelker
Jet Propulsion Laboratory
Time and Frequency
MS 298-100
4800 Oak Grove Drive
Pasadena, CA 91109
Tel: 818-354-1873
Fax: 818-393-6773
E-mail: tjoelker@fridge.jpl.nasa.gov

Mike Tope
TrueTime, Inc.
2835 Duke Court
Santa Rosa, CA 95407
Tel: 707-528-1230
Fax: 707-527-6640
E-mail: truetime@nbn.com

M. J. Van Melle
Rockwell - Boeing
5505 Flintridge Dr.
Colorado Springs, CO 80918
Tel: 719-567-2705
Fax: 719-567-2664
E-mail: vanmellemj@afmcfa.fb.af.mil

Francine M. Vannicola
U.S. Naval Observatory
Time Service Department
3450 Massachusetts Avenue, N.W.
Washington, DC 20392-5420
Tel: 202-762-1455
Fax: 202-762-1511
E-mail: fmv@cassini.usno.navy.mil

Robert F. C. Vessot
Smithsonian Astrophysical Observatory
60 Garden Street
Cambridge, MA 02138
Tel: 617-495-7276
Fax: 617-496-7690
E-mail: rvessot@cfa.harvard.edu

John R. Vig
Army Research Lab
AMSRL-SE-RE
Ft. Monmouth, NJ 07703
Tel: 908-427-4275
Fax: 908-427-4805
E-mail: j.vig@ieee.org

Frank J. Voit
The Aerospace Corporation
PO Box 92957
M1-111
Los Angeles, CA 90009
Tel: 310-336-6764
Fax: 310-336-6225
E-mail: voit@courier8.aero.org

James D. Voss
Spectracom Corporation
101 Despatch Drive
East Rochester, New York 14445
Tel: 716-381-4827
Fax: 716-381-4998
E-mail: JamesDVoss@aol.com

Warren F. Walls
Femtosecond Systems
690 Arbutus Street
Golden, CO 80401
Tel: 303-462-0799
Fax: 303-462-0766
E-mail: 53124.514@compuserve.com

Ben C. Wang
University of Maryland
Dept. of Physics
College Park, MD 20742
Tel: 301-405-6102
Fax: 301-314-9525
E-mail: ben@kelvin.umd.edu

S. Clark Wardrip
ATSC
726 Foxenwood Drive
Santa Maria, CA 93455-4221
Tel: 805-937-6448
Fax: 805-937-9601
E-mail: skyclark@aol.com

Kevin A. Waters
DoD
2N30 Hercules Dr.
Annapolis, MD 20701
Tel: 301-688-7526

Werner Weidemann
Datum/Efratom Division
3 Parker
Irvine, CA 92618
Tel: 714-770-5000
Fax: 714-770-2463
E-mail: wwiedemann@efratom.com

Marc A. Weiss
NIST
325 Broadway
Boulder, CO 80303
Tel: 303-497-3261
Fax: 303-497-6461
E-mail: MWeiss@boulder.nist.gov

Scott Weiss
TrueTime, Inc.
2835 Duke Court
Santa Rosa, CA 95407
Tel: 707-528-1230
Fax: 707-527-6640
E-mail: truetime@nbn.com

Paul J. Wheeler
U.S. Naval Observatory
3450 Massachusetts Avenue, NW
Washington, DC 20392
Tel: 202-762-1581
Fax: 202-762-1511
E-mail: paul@tsee2.usno.navy.mil

Joseph D. White
Naval Research Laboratory
4555 Overlook Avenue, SW
Washington, DC 20375
Tel: 202-767-5111
Fax: 202-767-2845
E-mail: white@juno.nrl.navy.mil

Jay D. Wiedwald
LLNL
PO Box 808, L-493
Livermore, CA 94550
Tel: 510-422-1338
Fax: 510-422-1930

Gernot M. R. Winkler
Innovative Solutions International
8500 Leesburg Pike, Ste. 608
Vienna, VA 22182
Tel: 703-883-8088
Fax: 703-883-9180
E-mail: gw@fermi.usno.navy.mil

Andy Wu
The Aerospace Corporation
4452 Canoga Dr.
Woodland Hills, CA 91364
Tel: 310-336-0437
Fax: 310-336-5076
E-mail: wu@carrier3.aero.org

Jun Ye
University of Colorado
JILA, Campus Box 440
Boulder, CO 80309
Tel: 303-492-0667
Fax: 303-492-5235
E-mail: ye@jila.colorado.edu